Hemodynamic Monitoring Using Echocardiography in the Critically Ill

Daniel De Backer
Bernard P. Cholley
Michel Slama
Antoine Vieillard-Baron
Philippe Vignon
Editors

DVD-ROM
INCLUDED

Springer

Hemodynamic Monitoring Using Echocardiography in the Critically Ill

Daniel De Backer • Bernard P. Cholley
Michel Slama • Antoine Vieillard-Baron
Philippe Vignon
(Editors)

Hemodynamic Monitoring Using Echocardiography in the Critically Ill

Springer

Editors
Daniel De Backer
Department of Intensive Care
Erasme University Hospital
Université Libre de Bruxelles
Route de Lennik 808
1070 Brussels
Belgium
ddebacke@ulb.ac.be

Michel Slama
Unité de Réanimation Médicale
Service de Néphrologie
CHU Sud
80054 Amiens Cedex 1
France
slama.michel@chu-amiens.fr

Philippe Vignon
Medical-surgical ICU
and
Clinical Investigation Center INSERM
0801, CHU Dupuytren
2 Ave. Martin Luther King
87000, Limoges, France and
Université de Limoges, 2 rue du
Dr. Marcland, 87000 Limoges
France
philippe.vignon@unilim.fr

Bernard P. Cholley
Service d'Anesthésie-Réanimation
Hôpital Européen Georges Pompidou
20 rue Leblanc
75908 Paris, cedex 15
France
bernard.cholley@egp.aphp.fr

Antoine Vieillard-Baron
Intensive Care Unit
University Hospital Ambroise Paré
Assistance Publique Hôpitaux de Paris
9 avenue Charles de Gaulle
92104, Boulogne Cedex
France
antoine.vieillard-baron@apr.aphp.fr

ISBN 978-3-540-87954-1 e-ISBN 978-3-540-87956-5
DOI 10.1007/978-3-540-87956-5
Springer Heidelberg Dordrecht London New York

Library of Congress Control Number: 2011921524

Cover design: eStudioCalamar, Figueres/Berlin

Printed on acid-free paper

Springer is part of Springer Science+Business Media (www.springer.com)

Preface

Echocardiography in the Critically Ill: Not Just a Diagnostic Tool!

Over the past decade, Doppler echocardiography has established itself as an essential element in evaluating hemodynamically unstable patients in intensive care units, operating rooms, and emergency departments. Why has echocardiography become such an important clinical tool in the hemodynamic evaluation of unstable patients?

First, echocardiography is a unique imaging modality that provides both anatomical and functional information about the heart and central circulation at the bedside. No other monitoring system currently allows visual and quantitative assessment online of central hemodynamics. This approach integrates physiology and offers a better understanding of interventricular and heart–lung interactions, especially in mechanically ventilated patients. Accordingly, critical care echocardiography has progressively supplanted the use of invasive, yet blind, hemodynamic monitoring devices, such as right heart catheterization, in an increasing number of institutions.

Second, multiple scientific publications in peer-reviewed journals have validated echocardiography for the evaluation of patients with circulatory and respiratory failure.

Third, improvements in technology and engineering have resulted in the recent emergence of full-feature, compact systems, which are highly portable for optimal use in crowded care units. Echocardiography is also perfectly suited to prolonging the physical examination at the bedside, which has led to the development of the ultrasound stethoscope. Accordingly, most institutions currently have dedicated systems available for around-the-clock assessment of critical illnesses.

Fourth, numerous intensivists and anesthesiologists have progressively become self-sufficient in performing and interpreting echocardiographic examinations as part of the acute management of critically ill patients. It is important to recognize that critical care echocardiography performed by intensivists and anesthesiologists should not be regarded as competing with a thorough echocardiographic evaluation undertaken by cardiologists. In many instances, critical care echocardiography focuses on findings frequently neglected by cardiologists (e.g., heart-lung interactions), while the precise evaluation of complex cardiac diseases (e.g., chronic valvulopathy, endocarditis, source of systemic emboli) still requires the expertise of cardiologists. Since a close collaboration among intensivists, anesthesiologists, and cardiologists is mandatory on clinical grounds in many countries, scientific societies and academic boards have organized national training programs dedicated to critical care echocardiography. These programs are focused on the hemodynamic evaluation of critically ill patients. In some countries, such as France, courses are organized jointly by cardiologists and intensivists.

Critical care echocardiography is performed and interpreted by the intensivist at the bedside to examine the mechanism of cardiopulmonary compromise and help guide the management of critically ill patients. It has specific requirements that demand training on the part of intensivists. Critical care echocardiography has to be available on a 24-h basis since it needs to be performed at the time of the clinical deterioration to provide optimal and clinically relevant information for immediate patient management. The medical history, clinical scenario, and ongoing treatments, including heart–lung interactions and ventilator settings, have to be incorporated into the medical assessment. Valid indices should be used to provide an adequate assessment of central hemodynamic status and offer effective therapy. Finally, serial evaluations should be performed to evaluate rapidly the efficacy and tolerance of these therapeutic interventions.

For all these reasons, competence in critical care echocardiography relies on a specific training and curriculum to achieve professional efficiency. This book is aimed at helping frontline physicians in developing competence in critical care echocardiography, regardless of their personal background. It provides an in-depth, up-to-date, state-of-the-art review of the capabilities and limitations of echocardiography in the specific settings of critical care medicine. As such, the present book should be regarded as a valuable tool for intensivists and anesthesiologists who wish to develop their proficiency in using critical care echocardiography in their daily practice for the benefit of the severely ill. The international panel of authors who contributed to this book reflects the close collaboration and large consensual approach of scientific and medical communities in Europe, North and South America, Australia, and Asia for promoting critical care echocardiography.

France and Belgium

Bernard P. Cholley
Daniel De Backer
Michel Slama
Antoine Vieillard-Baron
Philippe Vignon

Contents

Echocardiography in the Critically Ill: An Overview

1

Philippe Vignon and Paul Mayo

Contents

In recent years, bedside ultrasonography has gained wide acceptance for the assessment of critically ill patients. As opposed to "blind" monitoring systems, which frequently rely on invasive techniques (e.g., pulmonary artery catheter), echocardiography Doppler allows real-time imaging of the heart and great vessels, thereby proving unparalleled anatomical and functional information. Because of its versatility, safety, and instantaneous diagnostic capability, bedside ultrasonography is ideally suited for the evaluation of unstable patients in the intensive care unit (ICU). This overview will examine the utility of critical care echocardiography and the current field of use of transthoracic echocardiography (TTE) and transesophageal echocardiography (TEE) in the ICU. Cardiac output monitoring by esophageal Doppler [1, 2] and noncardiac ultrasonography [3] are purposely excluded from this overview. Training issues are discussed elsewhere (see Chap. 21).

1.1 Historical Perspective

Whereas hemodynamic assessment of ICU patients was predominantly invasive in the 1980s and 1990s, the current approach tends to be less invasive, more functional, and to integrate heart-lung interactions in the diagnostic process. During the last decade, right heart catheterization (RHC) has been progressively supplanted by bedside echocardiography in numerous ICUs [4]. Since its introduction in 1970 [5], RHC has been utilized widely by intensivists for the management of patients with circulatory failure. Therapeutic algorithms based upon RHC rely on pressure, flow, and metabolic measurements. Concordant publications clearly showed a lack of benefit and potential

P. Vignon (✉)
Medical-surgical ICU, and
Clinical Investigation Center INSERM 0801, CHU Dupuytren,
2 Ave. Martin Luther King, 87000, Limoges, France and
Université de Limoges, 2 rue du Dr Marcland,
87000, Limoges, France
e-mail: philippe.vignon@unilim.fr

P. Mayo
Division of Pulmonary, Critical Care and Sleep Medicine,
Long Island Jewish Medical Center, 410 Lakeville Road,
New Hyde Park, 11040, New York, USA and
Albert Einstein College of Medicine, Bronx, New York, USA

D. De Backer et al. (eds.), *Hemodynamic Monitoring Using Echocardiography in the Critically Ill*,
DOI: 10.1007/978-3-540-87956-5_1, © Springer-Verlag Berlin Heidelberg 2011

harm associated with the routine use of RHC [6–11]. In addition, clinically relevant discrepancies between RHC and bedside echocardiography in the evaluation of patients with circulatory failure have been published [12–20] and attributed to intrinsic limitations of RHC [21]. As a result, some intensivists have come to regard bedside ultrasonography as a superior alternative to RHC for the hemodynamic assessment of ICU patients [22, 23].

The early pioneers of critical care echocardiography used TTE and emphasized the superiority of bedside echocardiography over RHC [24–26]. The development of TEE accelerated the diffusion of ultrasonography into some ICUs since surface echocardiography was often limited by inadequate image quality in the ICU environment. TEE yielded good image quality in virtually all ventilated patients and allowed assessment of deep anatomical structures, which were otherwise not accessible to TTE [27–41].

Table 1.1 Technological landmarks in echocardiography

Technological development[a]
First reported use of echocardiography in clinical practice (Edler. 1954)
Time-motion mode allows identification of cardiac condition (Joyner. 1963)
Real-time two-dimensional imaging opens window to the beating heart from the surface of the chest (Bom. 1973)
Spectral Doppler allows an assessment of hemodynamics (Hatle. 1979)
Transesophageal echocardiography yields new information and increases the diagnostic capabilities of cardiac ultrasound, especially in mechanically ventilated patients (Schluter. 1983)
Tissue Doppler provides new insights into intrinsic ventricular properties (Isaaz. 1989)
Three-dimensional echocardiography, initially based on off-line reconstructions of two-dimensional images, is progressively performed in real time, using volumetric ultrasound data acquired by matrix-array transducers
Hand-held echocardiography leads to the development of the ultrasound stethoscope and contributes to the diffusion of ultrasonography in the noncardiology community
Miniaturized full-feature imaging systems and real-time quantitative three-dimensional transesophageal echocardiography become commercially available clinical tools

[a]Years are indicative of breakthrough reports showing the clinical value of the echocardiographic tools, rather than the time of their first description

In addition, TEE became the first-line diagnostic procedure recommended officially for the assessment of circulatory failure complicating the perioperative course or occurring in ICU ventilated patients [42–44]. In the past decade, progress in machine design has allowed the development of smaller, more powerful echocardiography systems with increased TTE diagnostic capabilities (Table 1.1).

1.2 Specificities of Critical Care Echocardiography

As opposed to conventional echocardiography, which is performed by cardiologists on a consultative basis in the echocardiography laboratory, critical care echocardiography is carried out and interpreted by the intensivist at the bedside of the ICU patient. Critical care echocardiography allows the frontline clinician to establish diagnosis and guide management of hemodynamic failure. Critical care echocardiography has specific requirements that cannot be met by consultant cardiologists and that support the need for training intensivists in the use of this technique in the ICU (Table 1.2).

Table 1.2 Specifics of critical care echocardiography

Requirements
Availability of a trained operator and a dedicated platform on a 24-h basis (the intensivist performs and interprets the echocardiographic examination at bedside)
Background in critical care medicine including the use of echocardiography as an adjunct to sound medical reasoning
Integration of heart–lung interactions in the interpretation of echocardiographic studies[a]
Integration of the ventilator settings in the interpretation of echocardiographic studies[b]
Specific diagnostic algorithms based on validated echocardiographic indices to assess central hemodynamic status
Presentation of echocardiographic findings in the clinical scenario to evaluate their relevance
Online interpretation of echocardiographic studies to optimize direct therapeutic impact, including reintervention after cardiac surgery
Immediate evaluation of the efficacy and tolerance of acute therapy (monitoring tool)

[a]Especially in mechanically ventilated patients
[b]Especially in patients ventilated for acute respiratory distress syndrome

Critically ill patients require nonscheduled management and care. Critical care echocardiography must therefore be available on a 24-h basis. A key requirement is that a capable machine be immediately available to the intensivist in the ICU. By definition, critical care echocardiography is performed personally by the frontline intensivist, the study is interpreted at the bedside of the critically ill patient, and the results are used for immediate diagnosis and management. In contrast to conventional echocardiography performed in stable patients presenting with chronic cardiac disease, critical care echocardiography has optimal diagnostic ability when performed at the time of the clinical deterioration. When performed after the initiation of a treatment that rapidly alters the hemodynamic profile (e.g., diuretics in decompensated congestive heart failure, afterload reduction in mitral regurgitation), echocardiography may be less informative [45].

The current approach to hemodynamic assessment using bedside echocardiography has to integrate heart and lung interactions [46, 47]. This requires a specific background in critical care medicine [48]. Whereas positive-pressure ventilation has long been recognized as a potential confounding factor for hemodynamic assessment using RHC [21, 49], Doppler echocardiography allows a better understanding of the complex effects of volume-controlled ventilation on central hemodynamics [47]. Over the last decade, several echocardiographic indices using heart-lung interactions produced by positive-pressure ventilation in the presence of a clinically relevant hypovolemia have been validated for predicting fluid responsiveness [50–54]. Recently, passive leg-raising has allowed echocardiographic indices to predict responders to a fluid challenge in patients with spontaneous breathing activity [55, 56]. These simple yet robust indices of fluid responsiveness allow intensivists to use echocardiography routinely in deciding when to proceed with volume resuscitation.

Heart-lung interactions are influenced not only by the volume status of the mechanically ventilated patient, but also by the lung compliance and ventilator settings [57]. This is especially relevant in patients who are on ventilatory support for acute respiratory distress syndrome (ARDS). Specifically, inappropriate ventilator settings may directly impede right ventricular ejection and contribute to the development of circulatory failure [58]. Early recognition of the negative effects of mechanical ventilation on central hemodynamics is crucial as circulatory failure is a leading cause of death with ARDS [59].

The findings provided by an imaging modality have to be interpreted in light of the clinical scenario and patient history. Accordingly, critical care echocardiography results always need to be interpreted within the clinical context. The intensivist who is directly in charge of the management of a case is best equipped to do this. Operator experience is crucial in order to integrate echocardiography results correctly with the clinical presentation. The results of critical care echocardiography are immediately interpreted by the attending intensivist, and so they may often substantially alter workup and therapy.

1.3 Indications and Safety of Echocardiography in ICU Patients

1.3.1 Indications for Critical Care Echocardiography

Indications for echocardiography have long been defined in the cardiology community [43, 44]. According to these guidelines, hemodynamically unstable patients and patients sustaining severe chest or multisystem trauma represent the main indications for performing echocardiography in the ICU setting. Societies of anesthesiologists have also defined specific indications of TEE in the perioperative period [42]. In contrast, indications for performing Doppler echocardiography in ICU patients have not yet been established by critical care societies. Recent recommendations describe echocardiography as an alternative to right-heart catheterization for the measurement of cardiac output in septic patients [60]. There is compelling evidence that leads us to propose bedside ultrasonography as the first-line diagnostic tool in the ICU for the assessment of patients presenting with circulatory failure (i.e., hypotension, shock), respiratory failure, or both [12–41, 61, 62].

Shock has recently been defined by an international consensus conference as clinical evidence and/or a biological marker of inadequate tissue perfusion – e.g., decreased central venous oxygen saturation ($ScvO_2$) or mixed venous oxygen saturation (SvO_2), increased blood

lactate, increased base deficit, and low pH – considering that hypotension could be inconsistent [63]. Respiratory failure usually refers to the conjunction of dyspnea and potential muscular fatigue, hypoxemia, and radiographic infiltrates. In these clinical settings, Doppler echocardiography provides rapid and comprehensive evaluation of the hemodynamics (e.g., hypovolemia, left or right ventricular failure, vasoplegia, elevated filling pressures) and also allows for immediate critical diagnoses (e.g., severe valve failure, central pulmonary embolus, thrombus in transit, pericardial effusion). When compared with blind and more invasive traditional monitoring techniques, echocardiography has the unparalleled advantage of directly depicting certain mechanisms of hemodynamic embarrassment that otherwise would be undetectable, including ventricular interdependence, pericardial constraints, regional wall-motion abnormalities, impaired relaxation, dynamic left ventricular outflow obstruction, and acute valvular regurgitation. In addition to the major indication for echocardiography in the ICU, which is cardiopulmonary failure, other standard indications apply, such as assessment of blunt chest trauma patients at high risk of cardiovascular injury, searching for a cardiac embolic source, endocarditis [64], and intracardiac shunt (Table 1.3).

1.3.2 TTE Versus TEE

Traditionally, it is assumed that TTE is the first-line approach owing to its versatility, tolerance, and availability [44, 62]. TTE has certain advantages over TEE, including a better Doppler beam alignment with intracardiac flows and a broader field of examination of relatively superficial anatomical structures (Table 1.4). In general, TEE is appropriately used as an adjunct or subsequent test to TTE when surface examination is nondiagnostic (e.g., poor imaging quality, inaccessibility of deep anatomical structures). ICU patients present challenges when assessed by means of TTE since hyperinflation related to mechanical ventilation or chronic obstructive pulmonary disease, obesity, edema, chest wall wounds or dressings, tubings, or surgical emphysema frequently interfere with ultrasound transmission and result in inadequate image quality [43, 62]. This explains why previous studies conducted in the ICU consistently reported a superior diagnostic capability of TEE compared with TTE [12, 15, 28, 30, 32, 33, 36]. When serial hemodynamic assessment is required to monitor acute therapeutic changes in unstable patients, reproducible tomographic imaging planes are frequently more easily obtained with TEE than with TTE. Although recent-generation miniaturized echocardiography machines have excellent image quality and surface echocardiography may be diagnostic in hemodynamically unstable patients [65], TTE remains difficult to perform in certain patient populations. In these cases, TEE may be required. Visualization of specific anatomical structures for accurate diagnoses and assessment of ventilated patients in perioperative settings are other main indications for performing a primary TEE examination [44, 62] (Table 1.4). In North America, TEE is not yet widely performed by intensivists, whereas it is routinely used by frontline intensivists in several European countries.

1.3.3 Tolerance of TEE

TEE can be performed safely in patients with critical illness. The rate of serious complication is very low. Patients are generally on mechanical ventilatory support, with the airway secured by tracheal intubation. Respiratory complications are therefore very rare. Injury to the esophagus (esophageal abrasion, perforation, or bleeding) is always a possibility. This can be avoided by appropriate patient selection and by minimizing rotational movement of the endoscope tip while it is under flexion. A full history has to be obtained that addresses the risk of esophageal injury from TEE. TEE is contraindicated in the setting of esophageal varices, strictures, bleeding, recent surgery, tumors, diverticuli, or other significant esophageal pathology. Coagulopathy or thrombocytopenia are relative contraindications to TEE. Risks associated with sedation, such as airway compromise and transient hypotension, are similar to those with other endoscopic procedures.

In a summary review of 2,504 TEE studies performed in the ICU, there was a 2.6% overall complication rate (discounting inadvertent dislodgement of a nasogastric tube), and no procedure-related deaths were reported [66]. Unsuccessful TEE probe insertion is rare when using laryngoscopic guidance in adequately sedated patients on ventilatory support. In spontaneously breathing patients, the major risk of TEE is related to the development of an acute respiratory failure secondary to the esophageal intubation [67, 68]. TEE should be

Table 1.3 Main indications of critical care echocardiography

Common indications in ICU environment	Raised clinical questions
Circulatory failure (hypotension, shock):	
Persistent shock despite initial therapy	Main mechanism(s) of shock[a]
Complicated AMI	RWMA, LV dysfunction, RV involvement, mechanical complications[b]
Complicated acute aortic syndrome	Tamponade, acute aortic regurgitation, LV dysfunction
Massive pulmonary embolism	Acute cor pulmonale, in-transit or entrapped embolus[c]
Cardiac tamponade	Circumferential compressive pericardial effusion (guidance for pericardiocentesis), compressive mediastinal hematoma
Unexplained hypotension or shock after cardiac surgery	Surgical complication requiring rapid reoperation or medical mechanism(s)[a]
Cardiac arrest (during or after successful resuscitation)	Treatable cause of cardiac arrest[d]
Acute respiratory failure:	
Cardiogenic pulmonary edema vs. ARDS	Elevated LV filling pressure, acute cor pulmonale
Weaning failure from the ventilator	Cardiac cause of weaning failure[e]
Decompensated chronic respiratory failure	Cardiac cause of decompensation, chronic cor pulmonale, pulmonary hypertension
Unexplained hypoxemia	Intracardiac shunt (patent foramen ovale)
Other clinical settings	
Severe blunt chest trauma, penetrating trauma	Cardiovascular injury
Suspected infective endocarditis	Duke criteria and functional consequences of infection-related injuries[f]
Suspected cardiovascular source of systemic embolism	Cardiac or aortic source of systemic embolism (including patent foramen ovale)
Cardiac evaluation in brain-dead patients	Evaluation of potential heart donors

[a]Includes persistent hypovolemia, right ventricular failure (e.g., acute cor pulmonale), left ventricular failure, vasoplegia, low cardiac output unrelated to decreased contractility (e.g., valvulopathy, dynamic outflow obstruction, pericardial constraints)
[b]Includes acute free-wall rupture, septal rupture, papillary muscle rupture
[c]Embolus may be entrapped in proximal pulmonary arteries or in the foramen ovale
[d]Includes tamponade, massive pulmonary embolism, and tension pneumothorax
[e]Includes elevated left ventricular filling pressure, worsened mitral regurgitation, new RWMA, dynamic LV outflow tract obstruction
[f]Duke echocardiographic major diagnostic criteria include the presence of vegetation, abscess, or new partial dehiscence of a prosthetic valve [64], and functional consequences are valvular insufficiencies or anatomical shunts with associated ventricular volume overload
Abbreviations: AMI, acute myocardial infarction; RWMA, regional wall-motion abnormality; LV, left ventricle; RV, right ventricle; ARDS, acute respiratory distress syndrome

discouraged in unstable patients who are not on ventilatory support, especially when a tamponade or a massive pulmonary embolism is suspected, because the procedure may precipitate circulatory or respiratory compromise (Table 1.5). In ambulatory patients examined in the echocardiography laboratory, a large cardiological series of over 10,000 consecutive TEE examinations reported an incidence of complications as low as 0.88% [69] and a rate of hypopharyngeal or esophageal perforation of 0.03% [70]. There are no known mechanical complications with TTE.

1.4 Therapeutic Impact of Critical Care Echocardiography

Owing to its excellent diagnostic capability, TEE has a therapeutic impact that is consistently superior to that of TTE when ventilated ICU patients are evaluated with both procedures [12, 15, 28, 30, 32, 33, 36]. Critical care echocardiography has documented a direct impact on therapy in up to 50% of ICU patients [12, 15, 17, 20, 28, 31, 33–37, 39–41]. TEE has been shown to prompt cardiac surgery in up to 20% of examined patients,

Table 1.4 Indications of transthoracic and transesophageal echocardiography

TTE	TEE
General screening, overall evaluation	Non-diagnostic TTE
Evaluation of cardiac function	Circulatory failure in ventilated patients[a]
Suspected pericardial disease Guidance of pericardiocentesis	Suspected extracardiac tamponade (mediastinal hematoma) or loculated compressive pericardial effusion[b]
Evaluation of left-sided valvulopathy or prosthetic valve	Mechanism and quantification of mitral regurgitation or prosthetic-valve dysfunction
Suspected LV outflow-tract obstruction	Diagnosis and management of infective endocarditis
Evaluation of pulmonary artery pressure	Identification of embolus-in-transit or proximal pulmonary embolism[c]
Suspected thrombus of LV apex	Identification of intracardiac shunt
Inferior vena cava examination	Identification of a cardiac or aortic source of systemic embolism
Penetrating chest trauma	Suspected acute condition of the thoracic aorta (e.g., spontaneous dissection, traumatic aortic injuries)
Contraindications for TEE	Guidance of invasive procedures (other than TEE during cardiac surgery)[d]

[a]Especially in the perioperative period
[b]In ventilated patients, after cardiac surgery or chest trauma
[c]In ventilated patients
[d]For example, guidance of patent foramen ovale closure or aortic stenting, assessment of mechanical circulatory assistance
Abbreviations: TTE, transthoracic echocardiography; TEE, transesophageal echocardiography

according to the type of ICU recruitment [17, 20, 27, 29, 31–35, 37–41]. By accurately identifying the mechanism of shock or acute respiratory failure, critical care echocardiography allows the intensivist to change therapeutic strategy and reduce the risk of inefficient or harmful therapy. It frequently corrects initial diagnosis derived from conventional hemodynamic monitoring [12–20]. In unstable patients, acute therapy (e.g., fluid challenge, initiation of inotropic support, ventilator settings) may result in a rapid variation of the hemodynamic profile. Accordingly, the hemodynamic assessment is best performed early in the course of organ failure and serial echocardiographic examinations provide real-time monitoring of both the efficacy and tolerance of therapeutic interventions in ICU patients. The anticipated efficacy of therapeutic changes related to critical care echocardiography is closely related to the severity of patient presentation, its benefit being maximal in the most unstable patients at the time of examination.

1.5 Conclusions

Echocardiography should be the primary diagnostic tool for the evaluation of ICU patients with circulatory or respiratory failure. Critical care echocardiography requires that a capable machine be immediately available on a 24-h basis in the ICU. The frontline intensivist who uses echocardiography to guide the management of the critically patient must be competent in image acquisition, image interpretation, and application of the results to the clinical situation. Both TTE and TEE offer strong utility in the ICU. TEE may be required where TTE image quality is inadequate to answer the clinical

Table 1.5 Tolerance of transesophageal echocardiography in critically ill patients

Good	Questionable	Contraindications
Ventilated patients	Spontaneously breathing unstable patients[b]	Esophagogastric surgery
Adequate sedation[a]	Shock potentially related to tamponade or massive pulmonary embolism in the absence of mechanical ventilation	Any relevant esophageal disease Excessive risk of bleeding Unstable neck fracture Mediastinal radiation therapy

[a]Muscle relaxation may be necessary to facilitate TEE probe insertion under laryngoscopic examination
[b]Especially when acute aortic syndrome is highly suspected

question, but the use of TEE may also be curtailed by its limited availability in some ICUs. TEE has an excellent safety record in the ICU. The intensivist should regard echocardiography as a key area in which to acquire cognitive and technical skills for optimal management of patients with cardiopulmonary failure.

References

1. Cholley BP, Singer M (2003) Esophageal Doppler: noninvasive cardiac output monitor. Echocardiography 20:763–769
2. Dark PM, Singer M (2004) The validity of transesophageal Doppler ultrasonography as a measure of cardiac output in critically ill adults. Intensive Care Med 30:2060–2066
3. Beaulieu Y, Marik PE (2005) Bedside ultrasonography in the ICU (part 2). Chest 128:1766–1781
4. Vieillard-Baron A, Slama M, Cholley B, Janvier G, Vignon P, for the ECHO-in-ICU group (2008). Echocardiography in the intensive care unit: from evolution to revolution? Intensive Care Med 34:243–249
5. Swan HJ, Ganz W, Forrester J, Marcus H, Diamond G, Chonette D (1970) Catheterization of the heart in man with use of a flow-directed balloon-tipped catheter. N Engl J Med 283:447–451
6. Connors AF, Speroff T, Dawson NV, Thomas C, Harrell FE, Wagner D, Desbiens N, Goldman L, Wu AW, Califf RM, Fulkerson WJ, Vidaillet H, Broste S, Bellamy P, Lynn J, Knaus WA (1996) The effectiveness of right heart catheterization in the initial care of critically ill patients. JAMA 276:889–897
7. Richard C, Warszawski J, Anguel N, Deye N, Combes A, Barnoud D, Boulain T, Lefort Y, Fartoukh M, Baud F, Boyer A, Brochard L, Teboul JL (2003) French Pulmonary Artery Catheter Study Group. Early use of the pulmonary artery catheter and outcomes in patients with shock and acute respiratory distress syndrome: a randomized controlled trial. JAMA 290:2713–2720
8. Rhodes A, Cusack RJ, Newman PJ, Grounds RM, Benett ED (2002) A randomized, controlled trial of the pulmonary artery catheter in critically ill patients. Intensive Care Med 28:256–264
9. Sandham JD, Hull RD, Brant RF, Knox L, Pineo GF, Doig CJ, Laporta DP, Viner S, Passerini L, Devitt H, Kirby A, Jacka M (2003) Canadian Critical Care Clinical Trials Group. A randomized, controlled trial of the use of pulmonary-artery catheters in high-risk surgical patients. N Engl J Med 348:5–14
10. Harvey S, Harrison DA, Singer M, Ashcroft J, Jones CM, Elbourne D, Brampton W, Williams D, Young D, Rowan K (2005) PAC-Man study collaboration. Lancet 366:472–477
11. Binanay C, Califf RM, Hasselblad V, ÓConnor CM, Shah MR, Sopko G, Stevenson LW, Francis GS, Leier CV, Miller LW, ESCAPE investigators and ESCAPE study coordinators (2005) Evaluation study of congestive heart failure and pulmonary catheterization effectiveness: the ESCAPE trial. JAMA 294:1625–1633
12. Reichert CLA, Visser CA, Koolen JJ, Van den Brink RBA, Van Wezel HB, Meyne NG, Dunning AJ (1992) Transesophageal echocardiography in hypotensive patients after cardiac operation. J Thorac Cardiovasc Surg 104:321–326
13. Jardin F, Valtier B, Beauchet A, Dubourg O, Bourdarias JP (1994) Invasive monitoring combined with two-dimensional echocardiographic study in septic shock. Intensive Care Med 20:550–554
14. Kaul S, Stratienko AA, Pollock SG, Marieb MA, Keller MW, Sabia PJ (1994) Value of two-dimensional echocardiography for determining the basis of hemodynamic compromise in critically ill patients: a prospective study. J Am Soc Echocardiogr 7:598–606
15. Poelaert JI, Trouerbach J, De Buyzere M, Everaert J, Colardyn FA (1995) Evaluation of transesophageal echocardiography as a diagnostic and therapeutic aid in a critical care setting. Chest 107:774–779
16. Benjamin E, Griffin K, Leibowitz AB, Manasia A, Oropello JM, Geffroy V, DelGiudice R, Hufanda J, Rosen S, Goldman M (1998) Goal-directed transesophageal echocardiography performed by intensivists to assess left ventricular function: comparison with pulmonary artery catheterization. J Cardiothorac Vasc Anesth 12:10–15
17. Harris KM, Petrovic O, Davila-Roman VG, Yusen RD, Littenberg B, Barzilai B (1999) Changing patterns of transesophageal echocardiography use in the intensive care unit. Echocardiography 16:559–565
18. Wake PJ, Ali M, Carroll J, Siu SC, Cheng DCH (2001) Clinical and echocardiographic diagnoses disagree in patients with unexplained hemodynamic instability after surgery. Can J Anesth 48:778–783
19. Costachescu T, Denault A, Guimond JG, Couture P, Carignan S, Sheridan P, Hellou G, Blair L, Normandin L, Babin D, Allard M, Harel F, Buithieu J (2002) The hemodynamically unstable patient in the intensive care unit: hemodynamic vs. transesophageal echocardiographic monitoring. Crit Care Med 30:1214–1223
20. Colreavy FB, Donovan K, Lee KY, Weekes J (2002) Transesophageal echocardiography in critically ill patients. Crit Care Med 30:989–996
21. Jardin F, Bourdarias JP (1995) Right heart catheterization at bedside: a critical view. Intensive Care Med 21:291–295
22. Vignon P (2005) Hemodynamic assessment of critically-ill patients using echocardiography Doppler. Curr Opin Crit Care 11:227–234
23. Vieillard-Baron A, Prin S, Chergui K, Dubourg O, Jardin F (2003) Hemodynamic instability in sepsis: bedside assessment by Doppler echocardiography. Am J Respir Crit Care Med 168:1270–1276
24. Ozier Y, Guéret P, Jardin F, Farcot JC, Bourdarias JP, Margairaz A (1984) Two-dimensional echocardiographic demonstration of acute myocardial depression in septic shock. Crit Care Med 12:596–599
25. Jardin F, Gueret P, Dubourg O, Farcot JC, Margairaz A, Bourdarias JP (1985) Two-dimensional echocardiographic evaluation of right ventricular size and contractility in acute respiratory failure. Crit Care Med 13:952–956
26. Jardin F, Brun-Ney D, Auvert B, Beauchet A, Bourdarias JP (1990) Sepsis-related cardiogenic shock. Crit Care Med 18:1055–1060
27. Oh JK, Seward JB, Khandheria BK, Gersh BJ, Mc Gregor CGA, Freeman WK, Sinak LJ, Tajik AJ (1990) Transesophageal echocardiography in critically ill patients. Am J Cardiol 66:1492–1495

28. Pavlides GS, Hauser AM, Stewart JR, ÓNeill WW, Timmis GC (1990) Contribution of transesophageal echocardiography to patient diagnosis and treatment: a prospective analysis. Am Heart J 120:910–914
29. Pearson AC, Castello R, Labovitz AJ (1990) Safety and utility of transesophageal echocardiography in the critically ill patient. Am Heart J 119:1083–1089
30. Font VE, Obarski TP, Klein AL, Barlett JC, Nemec JJ, Stewart WJ, Salcedo EE (1991). Transesophageal echocardiography in the critical care unit. Cleveland Clin J Med 58:315–322
31. Foster E, Schiller NB (1992) The role of transesophageal echocardiography in critical care: UCSF experience. J Am Soc Echocardiogr 5:368–374
32. Hwang JJ, Shyn KG, Chen JJ, Tseng YZ, Kuan P, Lien WP (1993). Usefulness of transesophageal echocardiography in the treatment of critically ill patients. Chest 104:861–866
33. Vignon P, Mentec H, Terré S, Gastinne H, Guéret P, Lemaire F (1994) Diagnostic accuracy and therapeutic impact of transthoracic and transesophageal echocardiography in mechanically ventilated patients in the ICU. Chest 106:1829–1834
34. Khoury AF, Afridi I, Quinones MA, Zoghbi WA (1995) Transesophageal echocardiography in critically ill patients: feasibility, safety and impact on management. Am Heart J 127:1363–1371
35. Sohn DW, Shin GJ, Oh JK, Tajik AJ, Click RL, Miller FA, Seward JB (1995). Role of transesophageal echocardiography in hemodynamically unstable patients. Mayo Clin Proc 70:925–931
36. Heidenreich PA, Stainback RF, Redberg RF, Schiller NB, Cohen NH, Foster E (1995) Transesophageal echocardiography predicts mortality in critically ill patients with unexplained hypotension. J Am Coll Cardiol 26:152–158
37. Slama M, Novara A, Van De Putte P, Diebold B, Safavian A, Safar M, Ossart M, Fagon JY (1996) Diagnostic and therapeutic implications of transesophageal echocardiography in medical ICU patients with unexplained shock, hypoxemia, or suspected endocarditis. Intensive Care Med 22:916–922
38. Alam M (1996) Transesophageal echocardiography in critical care units: Henry Ford hospital experience and review of the literature. Prog Cardiovasc Dis 38:315–328
39. McLean AS (1998) Transesophageal echocardiography in the intensive care unit. Anaesth Intensive Care 26:22–25
40. Schmidlin D, Schuepbach R, Bernard E, Ecknauer E, Jenni R, Schmid ER (2001) Indications and impact of postoperative transesophageal echocardiography in cardiac surgical patients. Crit Care Med 29:2143–2148
41. Bruch C, Comber M, Schmermund A, Eggebrecht H, Bartel T, Erbel R (2003) Diagnostic usefulness and impact on management of transesophageal echocardiography in surgical intensive care units. Am J Cardiol 91:510–513
42. Practice guidelines for perioperative transesophageal echocardiography (1996) A report by the American Society of Anesthesiologists and the Society of Cardiovascular Anesthesiologists Task Force on Transesophageal Echocardiography. Anesthesiology 84:986–1006
43. ACC/AHA guidelines for the clinical application of echocardiography (1997) A report of the American College of Cardiology/American Heart Association Task Force on Practice guidelines (Committee on Clinical Application of Echocardiography). Circulation 95:1686–1744
44. Douglas PS, Khandheria B, Stainback RF, Weissman NJ (2007) ACCF/ASE/ACEP/ASNC/SCAL/SCCT/SCMR 2007 appropriateness criteria for transthoracic and transesophageal echocardiography. J Am Coll Cardiol 50: 187–204
45. Vignon P (2008) Assessment of critically-ill patients with acute heart failure syndrome using echocardiography Doppler. In: Mebazaa A, Gheorghiade M, Zannad FM, Parillo JE (eds) Aute heart failure. Springer, London, pp 424–445
46. Vignon P (2004) Evaluation of fluid responsiveness in ventilated septic patients: back to venous return [Editorial]. Intensive Care Med 30:1699–1701
47. Vieillard-Baron A, Chergui K, Augarde R, Prin S, Page B, Beauchet A, Jardin F (2003) Cyclic changes in arterial pulse during respiratory support revisited by Doppler echocardiography. Am J Respir Crit Care Med 168:671–676
48. Mayo PH, Beaulieu Y, Doelken P, Feller-Kopman D, Harrod C, Kaplan A, Oropello J, Vieillard-Baron A, Axler O, Lichtenstein D, Maury E, Slama M, Vignon P (2009) American College of Chest Physicians/La Société de Réanimation de Langue Française statement on competence in critical care ultrasonography. Chest 135:1050–1060
49. Raper R, Sibbald WJ (1986) Misled by the wedge? The Swan-Ganz catheter and left ventricular preload. Chest 89:427–434
50. Feissel M, Michard F, Mangin I, Ruyer O, Faller JP, Teboul JL (2001). Respiratory changes in aortic blood velocity as an indicator of fluid responsiveness in ventilated patients with septic shock. Chest 119:867–873
51. Slama M, Masson H, Teboul JL, Arnout ML, Susic D, Frohlich E, Andrejak M (2002) Respiratory variations of aortic VTI: a new index of hypovolemia and fluid responsiveness. Am J Physiol Heart Circ Physiol 283: H1729–H1733
52. Vieillard-Baron A, Chergui K, Rabiller A, Peyrouset O, Page B, Beauchet A, Jardin F (2004) Superior vena cava collapsibility as a gauge of volume status in ventilated septic patients. Intensive Care Med 30:1734–1739
53. Barbier C, Loubières Y, Schmit C, Hayon J, Ricôme JL, Jardin F, Vieillard-Baron A (2004) Respiratory changes in inferior vena cava diameter are helpful in predicting fluid responsiveness in ventilated septic patients. Intensive Care Med 30:1740–1746
54. Feissel M, Michard F, Faller JP, Teboul JL (2004) The respiratory variation in inferior vena cava diameter as a guide to fluid therapy. Intensive Care Med 30:1834–1837
55. Lamia B, Ochagavia A, Monnet X, Chemla D, Richard C, Teboul JL (2007) Echocardiographic prediction of volume responsiveness in critically ill patients with spontaneously breathing activity. Intensive Care Med 33:1125–1132
56. Maizel J, Airapetian N, Lorne E, Tribouilloy C, Massy Z, Slama M (2007) Diagnosis of central hypovolemia using passive leg rising. Intensive Care Med 33:1133–1138
57. Reuter DA, Bayerlein J, Goepfert MS, Weis FC, Kilger E, Lamm P, Goetz AE (2003) Influence of tidal volume on left ventricular stroke volume variation measured by pulse contour analysis in mechanically ventilated patients. Intensive Care Med 29:476–480
58. Vieillard-Baron A, Jardin F (2003) Why protect the right ventricle in patients with acute respiratory distress syndrome? Curr Opin Crit Care 9:15–21

59. Monchi M, Bellenfant F, Cariou A, Joly LM, Thebert D, Laurent I, Dhainaut JF, Brunet F (1998) Early predictive factors of survival in the acute respiratory distress syndrome. Am J Respir Crit Care Med 158:1076–1081
60. Hollenberg SM, Ahrens TS, Annane D, Astiz ME, Chalfin DB, Dasta JF, Heard SO, Martin C, Napolitano LM, Susla GM, Totaro R, Vincent JL, Zanotti-Cavazzoni S (2004) Practice parameters for hemodynamic support of sepsis in adult patients: 2004 update. Crit Care Med 32:1928–1948
61. Price S, Nicol E, Gibson DG, Evans TW (2006) Echocardiography in the critically ill: current and potential roles. Intensive Care Med 32:48–59
62. Beaulieu Y, Marik PE (2005) Bedside ultrasonography in the ICU (part 1). Chest 128:881–895
63. Antonelli M, Levy M, Andrews PJD, Chastre J, Hudson LD, Manthous C, Meduri GU, Moreno RP, Putensen C, Stewart T, Torres A (2007) Hemodynamic monitoring in shock and implications for management. Intensive Care Med 33:575–590, International consensus conference, Paris, France, 27–28 Apr 2006
64. Li JS, Sexton DJ, Mick N, Nettles R, Fowler VG, Ryan T, Bashore T, Corey GR (2000) Proposed modifications to the Duke criteria for the diagnosis of infective endocarditis. Clin Infect Dis 30:633–638
65. Joseph MX, Disney PJS, Da Costa R, Hutchison SJ (2004) Transthoracic echocardiography to identify or exclude cardiac cause of shock. Chest 126:1592–1597
66. Hüttemann E, Schelenz C, Kara F, Chatzinikolaou K, Reinhart K (2004) The use and safety of transoesophageal echocardiography in the general ICU – a minireview. Acta Anaesthesiol Scand 48:827–836
67. Gendreau MA, Triner WR, Bartfield J (1999) Complications of transesophageal echocardiography in the ED. Am J Emerg Med 17:248–251
68. Vignon P, Mentec H, François B, Gastinne H, Gay R (1996) Tolérance de l'échocardiographie transoesophagienne en réanimation. Réan Urg 5:3–8
69. Daniel WG, Erbel R, Kasper W, Visser CA, Engberding R, Sutherland GR, Grube E, Hanrath P, Maish B, Dennig K, Schartl M, Kremer P, Angermann C, Illiceto S, Curtius JM, Mugge A (1991) Safety of transesophageal echocardiography. A multicenter survey of 10, 419 examinations. Circulation 83:817–821
70. Min JK, Spencer KT, Furlong KT, DeCara JM, Suseng L, Ward RP, Lang RM (2005) Clinical features of complications from transesophageal echocardiography: a single-center case series of 10,000 consecutive examinations. J Am Soc Echocardiogr 18:925–929

Part I

Principles of Ultrasounds and Principal Views

Transthoracic Echocardiography: Normal Two-Dimensional and Doppler Imaging

2

Susanna Price

Contents

S. Price
Consultant Cardiologist and Intensivist,
Royal Brompton Hospital, Sydney Street,
SW3 6NP, London, UK
e-mail: s.price@rbht.nhs.uk

Transthoracic echocardiography (TTE) provides the intensivist with a tool that has potential to give a rapid, noninvasive assessment of the hemodynamic status of the critically ill patient at the bedside. Information obtained may be used to assess cardiac anatomy and physiology. TTE may operate as a monitoring device and be employed to investigate the response to therapeutic intervention. Although TTE images in the critically ill may be suboptimal compared with those in the outpatient setting, the use of harmonic imaging and new upper-end echocardiographic platforms have improved two-dimensional imaging [1–6], and they are usually sufficient for diagnosis, particularly when assessing hemodynamics. Where images are nondiagnostic, transesophageal echocardiography (TEE) should be performed.

There is increasing support for both comprehensive and focused TTE in the investigation, management, and monitoring of the critically ill patient. Given the accessibility of the technique and the lack of risk to the patient (other than misinterpretation of the findings), TTE should be considered the first echocardiographic modality in the intensive care unit (ICU). Recent technological advances have allowed progressive miniaturization of machines. The capabilities vary from fully comprehensive to those capable only of two-dimensional imaging with limited facility for measurements and Doppler function [7–9]. For use in ICU settings, the ultrasound system must have electrocardiographic (ECG), high-quality, two-dimensional imaging, all Doppler-mode capacities, and facilities for recording and subsequent review of scans, ideally in a digital format. In this chapter, the ECG modalities with their respective indications for use in the ICU will be described. The stages involved in performing a TTE study will be

D. De Backer et al. (eds.), *Hemodynamic Monitoring Using Echocardiography in the Critically Ill*,
DOI: 10.1007/978-3-540-87956-5_2, © Springer-Verlag Berlin Heidelberg 2011

explained together with practical tips for optimizing imaging quality.

2.1 Knobology

2.1.1 Ultrasound

Ultrasound is generated by piezoelectric crystals that vibrate when compressed and decompressed by an alternating current applied across the crystal. The same crystals can act as receivers of returning, reflected ultrasound where the vibrations induced by the ultrasound pulse are then used to generate images on the ultrasound machine. Ultrasound can be refracted, reflected, or attenuated, allowing us to image structures owing to its differential interaction with adjacent media. Thus, where adjacent structures have similar acoustic properties, ultrasound may not be able to differentiate between them (an example is hematoma of the liver).

Ultrasound is a sound wave, comprising waves of compression and decompression of the transmitting medium (e.g., air and water) traveling at a fixed velocity. As a longitudinal wave, ultrasound is described by its amplitude, wavelength, and cycle duration. Some of these features are key to understanding how to set up an ultrasound machine for optimal imaging and explain some of the artifacts that may confound the inexperienced user. One of the important differences between ultrasound and audible sound is that at higher frequencies, ultrasound tends to move more in straight lines, like electromagnetic beams, and be reflected and focused like light beams. Ultrasound is reflected by small objects (because of its shorter wavelengths) and does not propagate easily in gaseous media. This is clinically relevant in echocardiography since the heart shares the thoracic cavity with the lungs. Accordingly, there are only certain "windows" where the heart may be visualized easily with ultrasound. Although ultrasound and audible sound differ in some important physical properties, the basic principles are the same. The relationship between the wavelength, velocity, and frequency is shown in the equation below, where λ is the wavelength, V the velocity of ultrasound through tissues, and *f* the frequency of the transducer:

$$\lambda = V/f$$

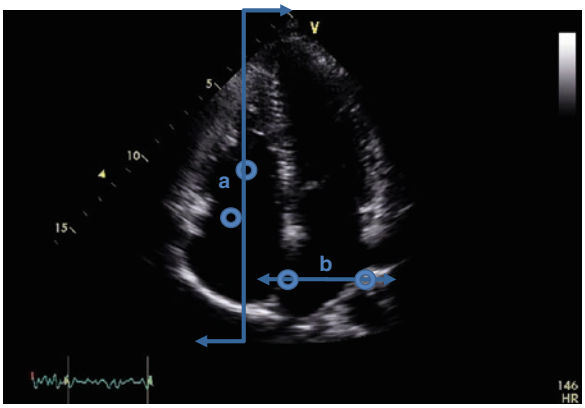

Fig. 2.1 Axial and lateral resolution in transthoracic echocardiography (apical fourchamber view). Axial resolution (**a**) is the ability to discern two structures parallel to the ultrasound beam, and lateral resolution (**b**) is the ability to discern two structures perpendicular to the beam. Axial resolution is optimal with high-frequency short-wavelength ultrasound, whereas lateral resolution is optimized by focusing the ultrasound beam to the zone of interest

As the velocity of ultrasound is relatively fixed in soft tissues, the resolution (ability to distinguish accurately between two points) of the images is determined by manipulation of the other two factors. Thus, a higher-frequency probe will result in shorter wavelength and better axial resolution. However, owing to its interaction with tissues, a higher frequency will be more attenuated and reduce penetration of the ultrasound beam. Spatial (axial and lateral) and temporal resolution (discerning discrete events in time in a moving image) determine the image quality. The principles of axial and lateral resolution are shown in Fig. 2.1. Axial resolution cannot be better than two wavelengths, in practice approximately 0.5 mm using TTE. Temporal resolution is determined by the frame rate and, in turn, by the number of pulses per scan line, the number of scan lines per sector, and the sector depth and width. Thus, reducing the depth and width of the scan will improve the temporal resolution.

2.1.2 Basic Settings

The main challenges are to select the correct probe, adjust the settings, and optimize image quality in order to provide the best resolution for the imaging performed.

1. Probe selection: select the highest-frequency cardiac probe that will enable imaging of the heart with adequate resolution given the depth required (usually 3.5 MHz in an adult).
2. Set the depth according to what needs to be imaged (e.g., the subcostal view may need increased depth, particularly in obese patients), but avoid wasted depth as this will reduce the temporal resolution (Fig. 2.2).
3. Set the sector width as narrow as possible to allow appropriate interrogation of the image (Fig. 2.3).
4. Focus: to maximize lateral resolution, focus on the zone of interest (indicated by dot/mark on the side of the sector).
5. Optimize the gain: imaging in the critical care environment can mean that ambient lighting is high. This results in inappropriately high gain settings for optimal image acquisition since high gain will reduce the resolution (Fig. 2.4). The usual range is 50–70.
6. Time-gain compensation: attenuation of more distant structures means that the gain for these will need to be increased using the time-gain compensation controls. Newer machines already take this into account, and no adjustment is required.
7. Compression: this refers to the logarithmic manipulation of the dynamic range of received signal amplitude. Increasing compression gives a reduced dynamic range of amplitudes (and a "softer" image), whereas reduced compression leads to a wider range of amplitudes and a more contrasted image.

2.1.3 Artifacts

An artifact is a misrepresentation of anatomy or physiology either as a result of poor setting of the ultrasound

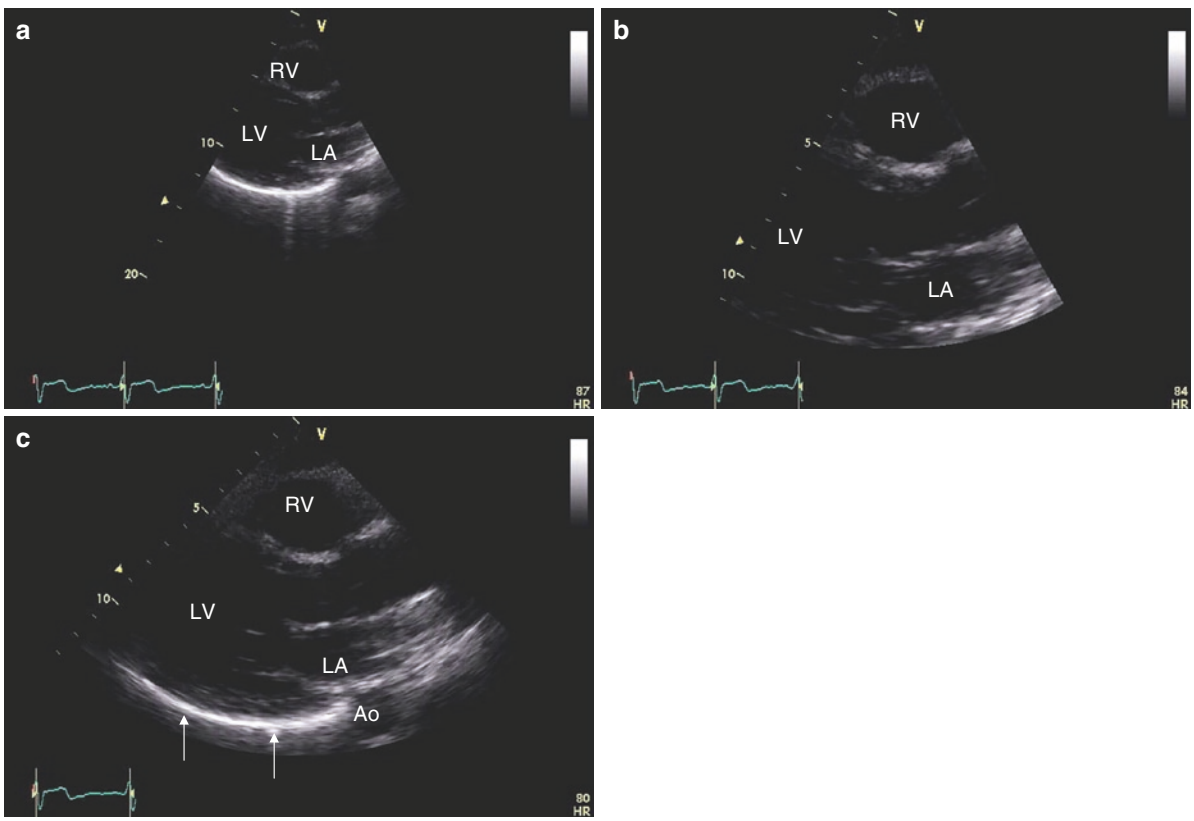

Fig. 2.2 Effects of depth setting on image acquisition. (**a**) The depth setting is excessive, and so the image is small, occupying only half of the available sector. In addition, the focus (yellow arrow to the left of the imaging sector) is set beyond the acquired image, thus limiting the lateral resolution of the image. (**b**) The depth is inadequate. Here, the image extends beyond the sector, which means that the posterior wall of the left ventricle and the descending aorta are not visible. It would not be possible to exclude a pericardial collection from this image, as the pericardial space is not visualized. (**c**) The depth setting is correct, and the whole of the available cardiac image is seen in the imaging sector, including the pericardium (*arrows*) and descending aorta (Ao). Abbreviations: RV, right ventricle; LV, left ventricle; LA, left atrium

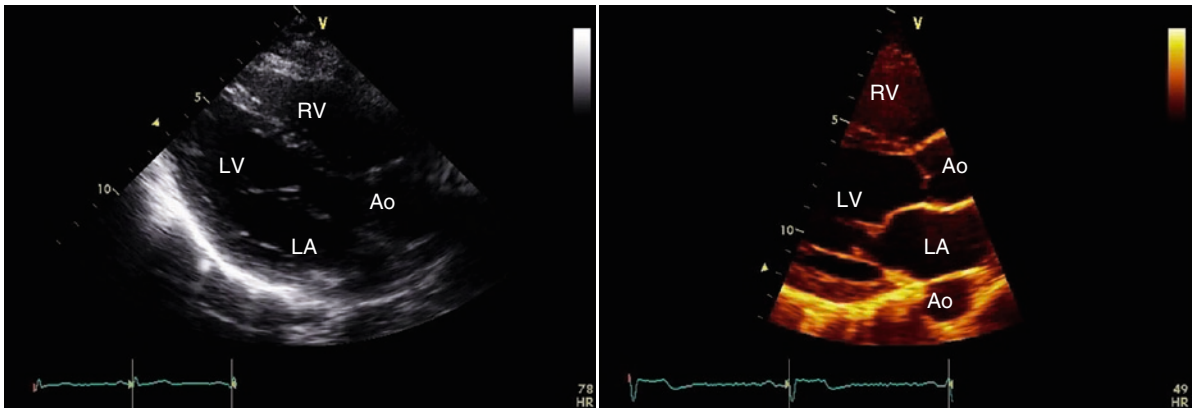

Fig. 2.3 Effects of sector width and colorization on image resolution. In the image on the left (*parasternal long-axis view*) the sector width is maximal, taking in most of the cardiac structures visible from this view. In the image on the right, sector width has been reduced, thus improving resolution. Further colorization improves the ability to discern tissues, particularly where the acoustic properties are similar. Abbreviations: RV, right ventricle; LV, left ventricle; LA, left atrium; Ao: thoracic aorta

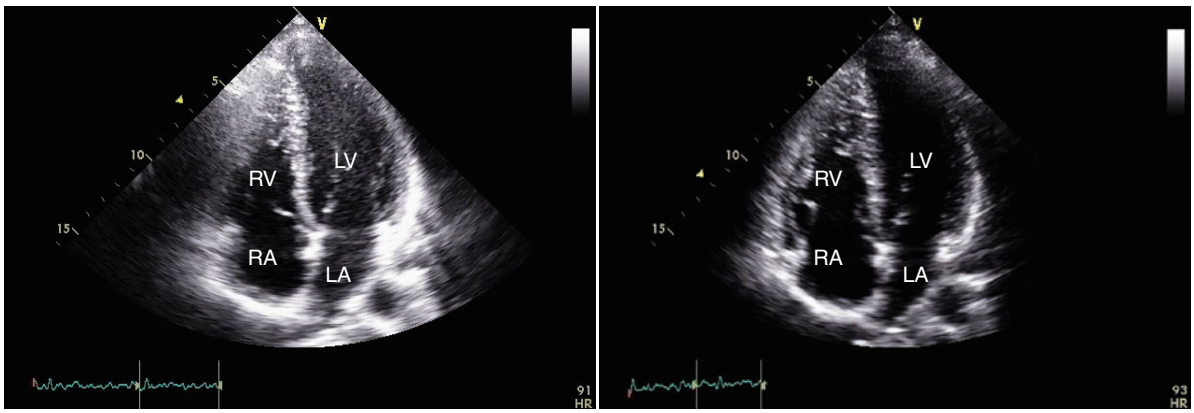

Fig. 2.4 Effects of gain setting on image acquisition. In the image on the left, the borders between black and white (and hence resolution) are difficult to discern as the gain settings are too high. In the image on the right, the gain settings allow better definition and, hence, resolution. Abbreviations: RV, right ventricle; LV, left ventricle; LA, left atrium; RA, right atrium

machine or as a result of the intrinsic properties of the ultrasound. The major artifacts experienced are as follows: echo dropout due to excessive reflection (Fig. 2.5), reverberation, mirror/duplication, gain, and side-lobe artifacts.

2.2 Ultrasound Modalities

Different ultrasound modalities can be utilized (Table 2.1). Although there is a tendency to move toward newer imaging techniques, the challenges in obtaining adequate images in the ICU patient mean that often older techniques may provide more robust data since the potential for artifacts is lessened. In the following sections, the ECG modalities will be described, together with examples from the critical care setting.

2.2.1 M-Mode Echocardiography

The most basic ECG modality still used in the critically ill is M-mode (motion-mode). M-mode is derived by displaying the A-mode (amplitude-mode) images over time (Fig. 2.6). The temporal resolution of this

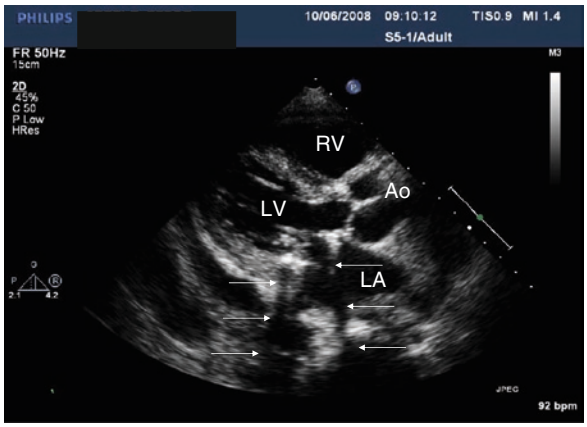

Fig. 2.5 Artifact from acoustic hyper-reflectivity/high density. In this parasternal long-axis view, a mitral annuloplasty ring has been placed, resulting in high echo reflectivity. As a result, little or no ultrasound passes behind, resulting in black, echo-free areas (*arrows*). Abbreviations: RV, right ventricle; LV, left ventricle; LA, left atrium; Ao: ascending aorta

modality means it is superior in demonstrating rapidly moving structures and timing events accurately within the cardiac cycle (Fig. 2.7). M-mode is mostly used for measuring the wall thickness and chamber size of the left ventricle (LV) as well as LV fractional shortening (Fig. 2.8). It also allows measurement of the systolic displacement of the tricuspid valve annulus used as a parameter of right ventricular (RV) function (Fig. 2.9).

2.2.2 Two-Dimensional Echocardiography

To display a two-dimensional representation of the heart, repeated sweeps of M-mode scans are performed electronically or mechanically, and these are reconstructed to provide real-time two-dimensional images of the scanned anatomical structures. Since each sector scan forms one frame, the temporal resolution is limited by the depth of scanning and the number of scan lines (sector width) because the speed of ultrasound in the tissue is usually fixed. Thus, temporal resolution of two-dimensional imaging is less than that provided with M-mode echocardiography.

2.2.3 Doppler Echocardiography

Doppler ultrasound is used to determine the velocity and direction of blood (or tissue) toward or away from the ultrasound probe, first by measuring the Doppler shift. The Doppler shift (F_d) is the difference between the originating (F_o) and received (F_r) ultrasound frequency:

$$F_d = F_r - F_o$$

Thus, where blood flows toward the transducer, the frequency of the returning signal is increased, and when blood flows away the frequency is reduced. From the Doppler shift (F_d), the velocity (c) is calculated as follows (F_o, originating ultrasound frequency, cosθ cosine of the angle of incidence):

$$F_d \times c / 2 \times F_o \times \cos\theta$$

In order to minimize error in recording velocities of the targets (red blood cells, myocardial tissue), the probe should be as parallel as possible to the target being measured because the higher the angle of incidence, the greater the error. Practically, the velocity can only be underestimated. There will be no signal with a crossing angle of 90°, the error being < 6% if the crossing angle is < 20° (Fig. 2.10).

2.2.3.1 Continuous-Wave Doppler

Here, two separate elements of the probe continuously emit and receive ultrasound, with a miniaturized image available to help the practitioner orientate the ultrasound beam. Continuous-wave (CW) Doppler will therefore measure all the velocities along the selected length of the cursor, from highest to lowest, and the peak measured will be the peak velocity along the length chosen (Fig. 2.11). Thus, CW Doppler has excellent resolution of velocity, but not position. The commonest use for CW Doppler in the critically ill is in estimation of peak pulmonary artery pressure (Fig. 2.12), using the simplified Bernoulli equation and a measure of the right atrial pressure (either from invasive monitoring, clinical assessment, or ultrasound assessment of the inferior vena cava).

Table 2.1 Modalities of echocardiography and their applications in the intensive care unit

	M-mode	Two-dimensional echocardiography	Pulsed-wave Doppler	Continuous-wave Doppler	Color Doppler
LV	Dimensions (cavity, wall thickness; parasternal LAX) Systolic function (FS, RWMA; parasternal LAX)	Remodeling RWMA Pericardial collection Thrombus	Filling pressures (mitral Doppler; A4C) TDI: systolic function (S wave; A4C)	VSD	VSD
RV	Dimensions (wall thickness; parasternal LAX) Function (TAPSE; A4C) Diastolic collapse (tamponade; A4C and subcostal views)	Dimensions (cavity; A4C) Thrombus Pericardial collection	TDI: systolic function (S wave; A4C)	Systolic pressure evaluated from maximal velocity of tricuspid regurgitation (A4C)[a]	VSD
LA	Dimensions (end-diastolic diameter, parasternal LAX)	Thrombus, spontaneous contrast (CVA) ASD/PFO (A4C and subcostal views) Pericardial collection	Filling pressures (pulmonary vein Doppler; A4C)		ASD/PFO
RA	–	Thrombus (PE; A4C and subcostal views) ASD/PFO Pericardial collection			ASD/PFO
AoV	Premature closure (parasternal LAX)	Valvular pathology	Sub-aortic velocity (A5C) Cardiac output Fluid responsiveness	AS/AR Estimated LAP (IVRT)	AS/AR Perforations, circulating abscess (complications of IE)
MV	–	Valvular pathology	LV filling pressures (A4C) Severity of MR	Severity of MR (A4C)	MS/MR Perforations, circulating abscess (complications of IE)
TV	–	Valvular pathology	–	Severity of TR (A4C) PASP	Severity of TR
PV	–	Valvular pathology	Cardiac output Indirect sign of pulmonary hypertension	PASP	–
IVC	Dimensions (subcostal view) Filling pressures Fluid responsiveness Assessment of tamponade	Dimensions (subcostal view) Filling pressures Assessment of tamponade	Differentiation constriction vs. restriction (subcostal view)	–	Severity of TR

[a]Reflecting pulmonary artery systolic pressure in the absence of pulmonary valvular stenosis, when adding central venous pressure

Abbreviations: LV, left ventricle; LAX, long-axis view; FS, fractional shortening; RWMA, regional wall-motion abnormality; A4C, apical four-chamber view; TDI, tissue Doppler imaging; VSD, ventricular septal defect; RV, right ventricle; TAPSE, tricuspid annular plane systolic excursion; LA, left atrium; CVA, cerebrovascular accident; ASD, atrial septal defect; PFO, patent foramen ovale; RA, right atrium; PE, pulmonary embolism; AoV, aortic valve; A5C, apical five-chamber view; AS, aortic stenosis; AR, aortic regurgitation, LAP, left atrial pressure; IVRT, isovolumic relaxation time; IE, infective endocarditis; MV, mitral valve; MR, mitral regurgitation; MS, mitral stenosis; TV, tricuspid valve; TR, tricuspid regurgitation; PASP, pulmonary artery systolic pressure; PV; pulmonary valve, IVC, inferior vena cava

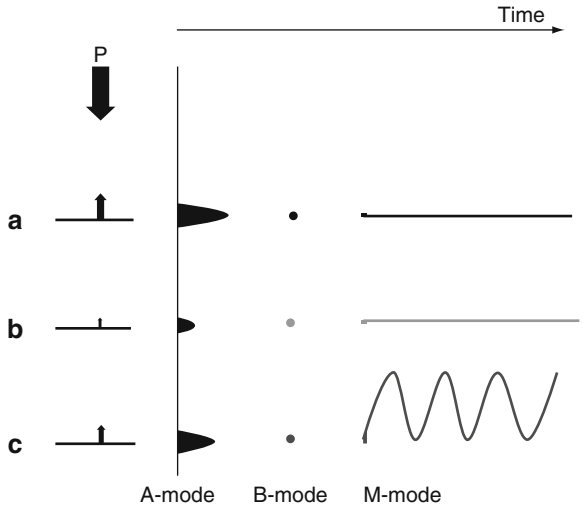

Fig. 2.6 The left of the figure represents the ultrasound pulse (P), which is then reflected from tissues at three different distances – *a*, *b*, and *c* (which is oscillating) – and two different echogenicities ($a = c > b$). Of note, the reflected ultrasound is dependent on the incident ultrasound and also the echogenicity of the tissues. Hence, the reflected pulse from c is of smaller amplitude than that from a, despite identical echogenicity. A-mode (*amplitude mode*) displays the reflected impulse in terms of an amplitude; B-mode (*brightness mode*) displays this on a gray scale; when this is displayed over time; M-mode (*motion mode*) presents the oscillatory movement of c as a wave (adapted from Stoylen with permission)

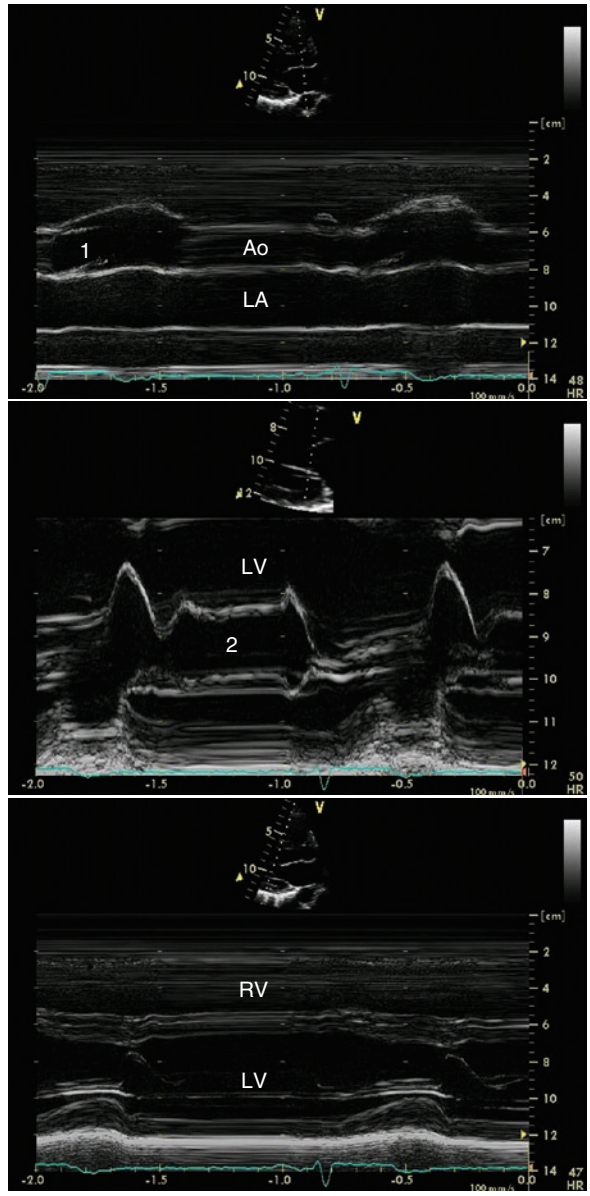

Fig. 2.7 M-mode recordings of a normal heart obtained in the parasternal long-axis view. A minaturized two-dimensional image is seen at the top of each panel. The *x*-axis is time (sweep speed 100 mm/s) and the *y*-axis distance (cm). From the base to the apex of the heart, M-mode allows precise examination of anatomical structures along the scanning line: the left atrium and ascending aorta (*upper panel; 1, opening of the aortic valve*); the mitral valve and basal portion of the left ventricle (*middle panel; 2, opening of the mitral valve*); the two ventricles (*lower panel*). Abbreviations: RV, right ventricle; LV, left ventricle;LA, left atrium; Ao, ascending aorta

2.2.3.2 Pulsed-Wave Doppler

Here, the Doppler pulse is sent from the probe, and the Doppler shift measured at a set time, which determines the depth at which sampling occurs. As the Doppler shift is small compared with the ultrasound frequency, multiple repetitions of Doppler pulses are sent in the same direction. This ensures depth resolution, but at half the pulse-repetition frequency, the signal direction becomes ambiguous (Nyquist limit). Accordingly, pulsed-wave (PW) Doppler is not useful at measuring high-velocity signals, but it is ideally suited for measuring relatively low-velocity signals at the level of specific anatomical locations, as required for the determination of stroke volume for example (Fig. 2.13).

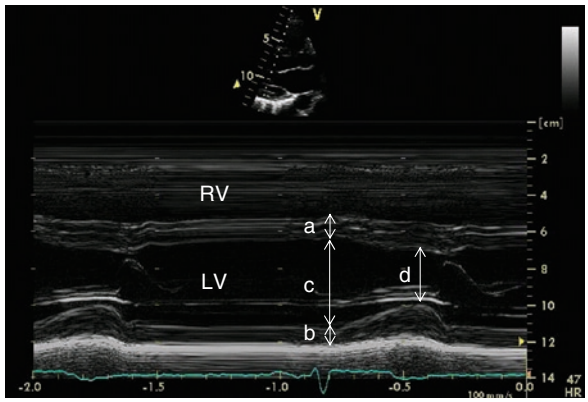

Fig. 2.8 M-mode measurements of the left ventricular cavity and wall thickness of a normal heart in the parasternal long-axis view. The scanning line is positioned perpendicular to the left ventricular walls, immediately below the mitral valve. Measurements are performed using the leading edge-to-leading edge technique. Most frequently performed measurements are the end-diastolic thickness of the interventricular septum (**a**) and posterior wall (**b**), and the end-diastolic diameter (**c**) and end-systolic diameter (**d**) of the left ventricular cavity. Fractional shortening is calculated as end-diastolic minus end-systolic left ventricular diameter divided by end-diastolic diameter. Abbreviations: RV, right ventricle; LV, left ventricle

2.2.3.3 Color Doppler

Color Doppler is based on PW Doppler technology, using multiple sample volumes along multiple planes and color mapping for velocity/direction data. The color map may be changed, but usually the BART (blue away, red toward) scale is used to represent the mean velocity and direction of circulating blood flow for that area. Color Doppler mapping is superimposed on each two-dimensional frame, allowing visual estimation in real time of both the velocity and direction of blood flow within the region of interest (Fig. 2.14). Where the two-dimensional images are poor, color Doppler will be unreliable. As with PW Doppler, aliasing occurs when the Nyquist limit is exceeded. This appears on two-dimensional images as a mosaic of colors. Provided that the Nyquist limit is adequately set, the presence of extended aliasing usually reflects high-velocity and turbulent flows secondary to an underlying cardiac abnormality (Fig. 2.15).

2.3 TTE Views

There are five standard views used in TTE (Fig. 2.16). All are usually easy to obtain in most patients, and where one view is challenging, often another view will provide excellent images. The common order of TTE views when systematically screening a patient is as follows: parasternal long- and short-axis views, apical four- and five-chamber views, and subcostal view of the heart and examination of the inferior vena cava. The suprasternal view is rarely used in critically ill

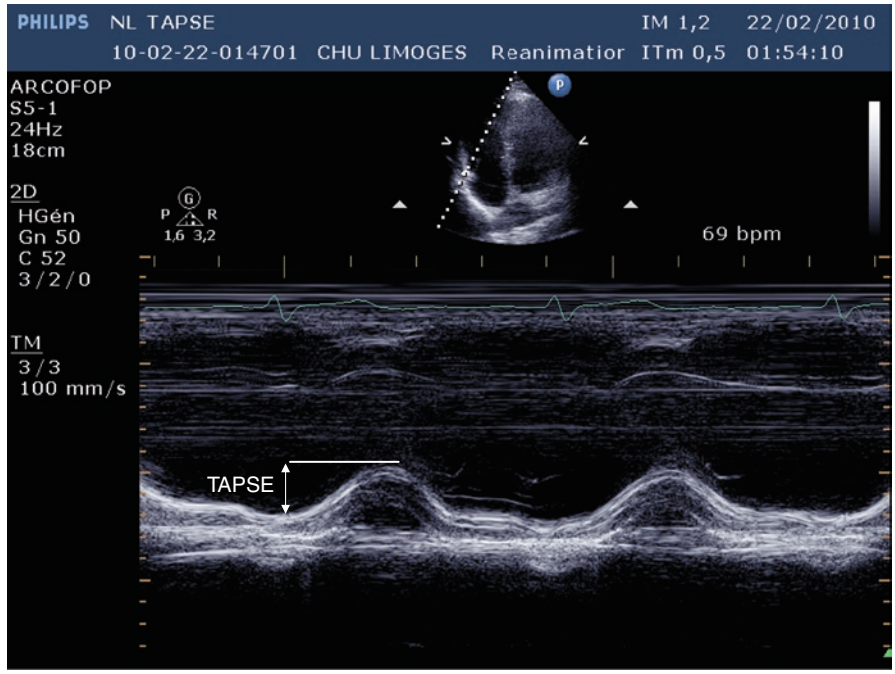

Fig. 2.9 M-mode of the long-axis function of the lateral wall of the right ventricle taken across the tricuspid annulus from the apical four-chamber view. The total excursion (magnitude) is known as tricuspid annular plane systolic excursion (TAPSE)

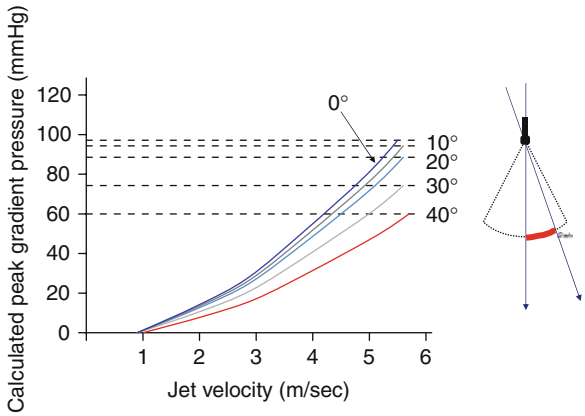

Fig. 2.10 Effect of incident angle of ultrasound probe on velocity. On the left of the figure, the relationship between measured velocity (m/s) and calculated peak gradient pressure (mmHg) is shown. To the right of the figure, the incident angle between the ultrasound and the tissue being interrogated is shown in *red* (reproduced from Stoylen with permission). Thus, where the incident angle increases, the inaccuracy of the calculation of peak gradient pressure also increases, and its value is progressively underestimated (Modified from Feigenbaum et al. [10] with permission)

patients. The order or number of views may change, however, depending upon the circumstances of the echocardiogram. For example, during resuscitation, only the subcostal view may be performed in order to facilitate chest compressions.

In the outpatient setting, the patients are normally turned to their left side, with the left hand placed behind the head in order to move the heart forward and increase the intercostal distance, thus facilitating positioning of the probe between the rib spaces. In the critically ill, this is often impractical, and the patient usually has to be imaged lying supine. Further challenges are presented by the presence of drains, dressings, intercostal and mediastinal tubes, surgical wounds, positive-pressure ventilation, pulmonary pathology, and a rapidly changing pathophysiological environment. Where inadequate views are obtained or for specific indications, TEE should be considered (see Chaps. 1 and 3).

2.3.1 Parasternal Long-Axis View

The transducer is placed in the second left intercostal space, close to the sternal border, with the marker pointing to the patient's right shoulder (Fig. 2.17). This long-axis view of the heart allows evaluation of the LV size and systolic function, regional motion of both the septal and posterior LV walls, size of the left atrium, mitral and aortic valves with the initial portion of the ascending aorta, and anterior and posterior pericardium (Fig. 2.17). Ideally, the interventricular septum should be aligned horizontally to allow accurate measurement of chamber dimensions using

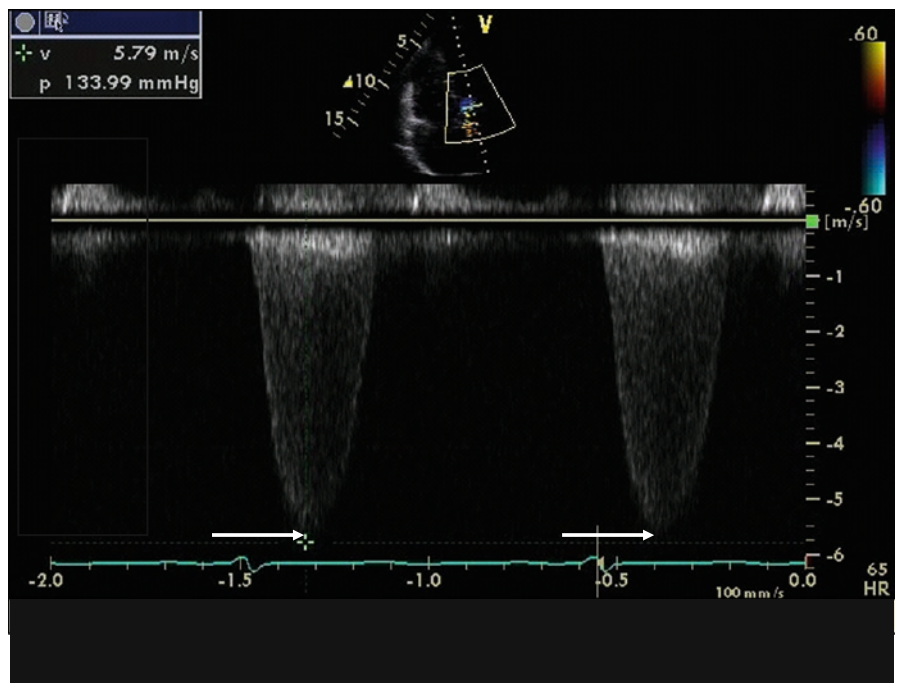

Fig. 2.11 Continuous-wave (CW) Doppler across the left ventricular outflow tract and aortic valve. The flow is high velocity and moving from the left ventricle to the ascending aorta, down, away from the probe. Peak velocity is arrowed, and using the modified Bernoulli equation, the peak pressure drop from the left ventricle to the aorta has been calculated (*top left of figure*) and corresponds to 134 mmHg. Velocity is shown on the y-axis in meters/second. A miniaturized two-dimensional reference image is shown at the top of the figure, demonstrating the correct positioning of the Doppler beam

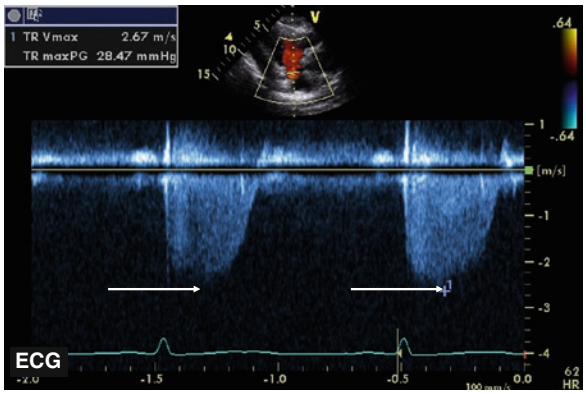

Fig. 2.12 CW Doppler with the Doppler positioned across the tricuspid valve in the apical four-chamber view to measure the maximal velocity of the jet of the tricuspid regurgitation. The flow is high velocity and moving from the right ventricle to the right atrium during systole, away from the probe. The peak velocity between the right ventricle and atrium is arrowed. Velocity is shown (m/s) on the *y*-axis. Using the modified Bernoulli equation, the echo machine converts this maximal velocity to a pressure difference (*seen in top left-hand corner*). In the absence of pulmonary stenosis, systolic right atrioventricular pressure gradient directly reflects the systolic pulmonary artery pressure. A miniaturized two-dimensional reference image is shown at the top of the figure, demonstrating the correct position of the CW Doppler beam

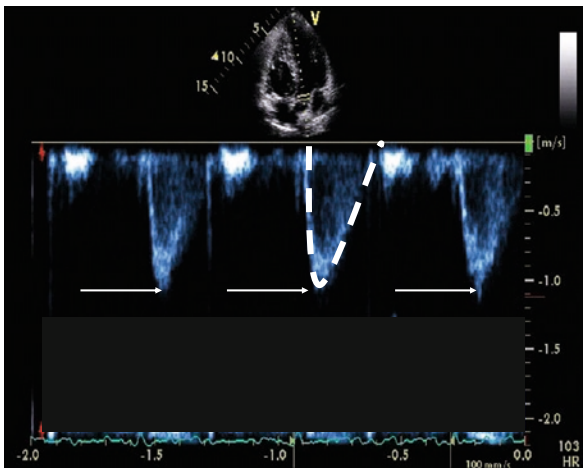

Fig. 2.13 Pulsed-wave (PW) Doppler with the sample volume positioned in the left ventricular outflow tract, just below the aortic valve. The flow is laminar and moving from the left ventricle to the ascending aorta, down, away from the probe. Peak velocity is arrowed, and tracing around the Doppler envelope (for example, in measurement of velocity–time integral) is shown as a dashed white line. A miniaturized two-dimensional reference image appears at the top of the figure, demonstrating the correct positioning of the PW Doppler

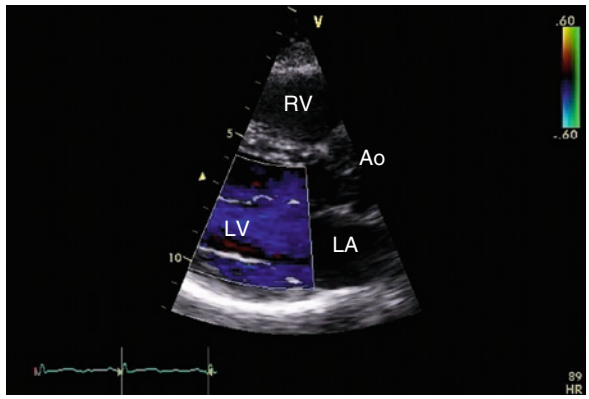

Fig. 2.14 Two-dimensional parasternal long-axis view of a normal heart with color Doppler oriented over the mitral valve during diastole. Note the blue laminar flow across the mitral valve to the left ventricle. Abbreviations: RV, right ventricle; LV, left ventricle; Ao: ascending aorta; LA, left atrium

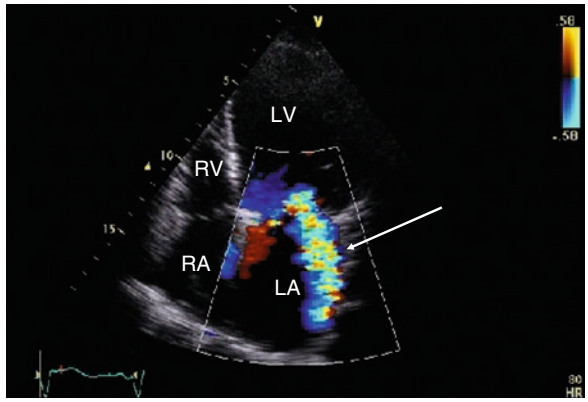

Fig. 2.15 Apical four-chamber view in a patient with postacute myocardial infarction, using color Doppler over the mitral valve and left atrium. With a Nyquist limit set at 58 cm/s, a mosaic of colors indicates the presence of a high-velocity regurgitant jet consistent with a relevant mitral regurgitation (*arrowed*). Abbreviations: RV, right ventricle; RA, right atrium, LV, left ventricle; LA, left atrium

M-mode (Figs. 2.17 and 2.18). Where this is not possible, care must be taken in obtaining measurements of chamber dimensions, most often using electronic calipers on a freeze frame and ensuring measurement strictly perpendicular to the cardiac walls. Finally, color Doppler mapping of the aortic and mitral valves is used to demonstrate any significant valvular regurgitation.

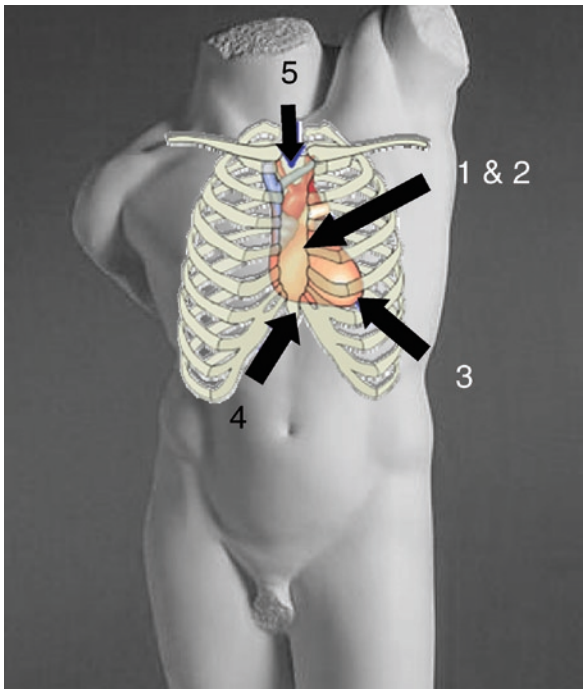

Fig. 2.16 The basic five transthoracic echocardiography views. 1: parasternal long-axis view; 2: parasternal short-axis view; 3: apical four-chamber view; 4: subcostal view; 5: suprasternal view

2.3.2 Parasternal Short-Axis View

From the parasternal long-axis position, with the aortic valve in the center of the image, the probe is rotated clockwise such that the marker is now pointing toward the left shoulder of the patient (Fig. 2.18). Angling up shows the aortic valve and allows pulmonary PW, CW, and color Doppler to be performed (Fig. 2.19). Mild pulmonary regurgitation is common and almost always seen where a pulmonary artery catheter is placed. By tilting the probe perpendicular to the chest wall, more inferior angulation allows for a short-axis view of the mitral valve (Fig. 2.20) and a more apically angled probe enables the LV dimensions to be imaged (Fig. 2.21).

2.3.3 Apical four- and Five-Chamber Views

The probe is positioned at the apex of the heart (judged by palpation and echo imaging) with the marker pointing to the patient's left axilla (Fig. 2.22). Ideally, on viewing the image, the septum should be aligned down the center, and the LV and atrium will be seen to the right, and the RV and atrium to the left (Fig. 2.22). From this position, the ventricular inlet dimensions can be measured and PW Doppler used to assess ventricular filling (see Chap. 16). It should be noted that good Doppler information may be obtained even in the presence of suboptimal two-dimensional images. CW Doppler should then be used to assess atrioventricular valve regurgitation. This should be performed even in the absence of regurgitation on color Doppler mapping since CW Doppler is more sensitive. Where tricuspid

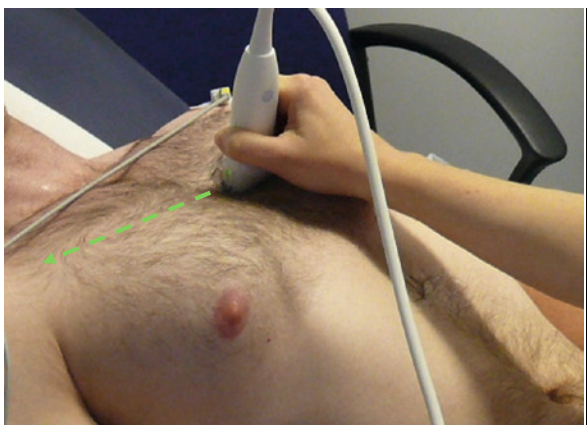

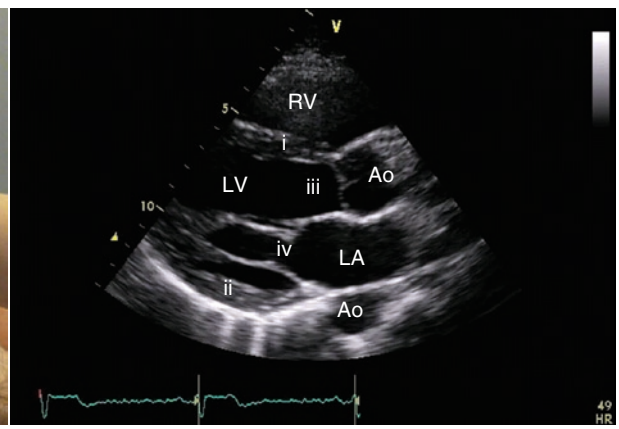

Fig. 2.17 Parasternal long-axis view. Hand and probe positioning are shown for a patient in the supine position (*left panel*). The probe is in the second intercostal space, just lateral (*left*) to the sternal border, with the indicator pointing toward the right shoulder of the patient (*arrowed*). The corresponding two-dimensional image provides valuable information on left cardiac cavities and valves (*right panel*). Abbreviations: RV, right ventricle; LV, left ventricle; Ao: thoracic aorta; LA, left atrium; i, interventricular septum; ii, posterior wall; iii: aortic valve; iv, mitral valve (modified from FEEL-UK with permission)

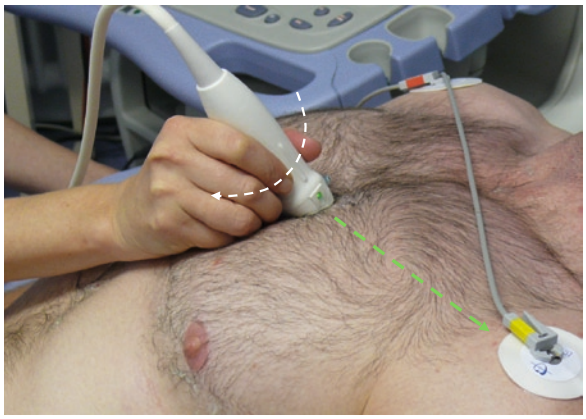

Fig. 2.18 Hand and probe positioning for the parasternal short-axis view in a supine patient. The probe is in the second intercostal space, just lateral (*left*) to the sternal border, with the green indicator light pointing toward the left shoulder of the patient (*arrowed in green*). To move between short-axis views of the aortic valve, mitral valve, and left ventricle, the probe is angled as shown (*white broken arrow*) (modified from FEEL-UK with permission)

regurgitation is detected, the measurement of its maximal velocity may be used to estimate the peak pulmonary artery pressure (Fig. 2.12). Finally, color Doppler should be used to interrogate the two atrioventricular valves in order to detect the presence of an underlying valvulopathy (Fig. 2.15).

Tilting the probe superiorly will reveal the LV outflow tract and aortic valve in the center of the image, giving the five-chamber view (Fig. 2.22). Color Doppler allows the identification of turbulent flow associated with an aortic valvular disease or an LV outflow tract obstruction. In the absence of relevant aortic valvulopathy, PW Doppler should be performed immediately below the valve (Fig. 2.13) to measure LV stroke volume (see Chap. 5). Where aortic stenosis is suspected, CW Doppler may be used to measure peak velocities and velocity–time integral as a reflection of maximal and mean transvalvular gradients, respectively.

2.3.4 Subcostal View

The probe is positioned in the subcostal area with the marker pointing to the right and with the operator's hand on top of the transducer to allow horizontal access to the heart through the subcostal window (Fig. 2.23). Where other views have not been optimal, the subcostal view may provide good image quality, particularly in patients with respiratory disease and those with positive-pressure ventilation. Counterclockwise rotation will open up the inferior vena cava (Fig. 2.23). The vessel has to be visualized in a true long axis together

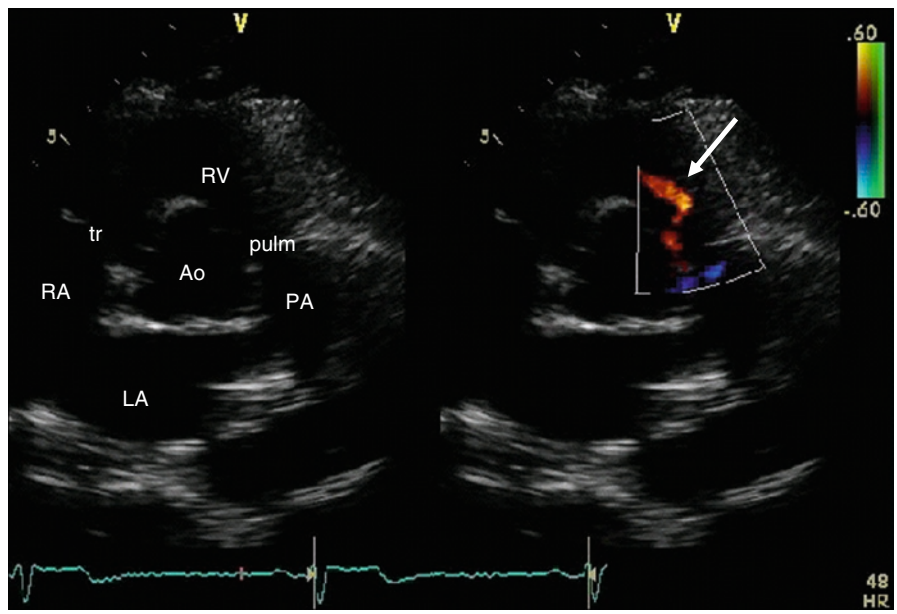

Fig. 2.19 Two-dimensional parasternal short-axis echocardiographic view of the heart. The probe is angled to image the base of the heart with the aortic valve and right ventricular inflow and outflow tracts (*left panel*). Color Doppler over the pulmonary valve reveals a small diastolic jet of pulmonary regurgitation (*right panel, arrow*). Abbreviations: Ao, aortic valve; tr, tricuspid valve; RV, right ventricular outflow tract; pulm, pulmonary valve; PA, main pulmonary artery; LA, left atrium; RA, right atrium

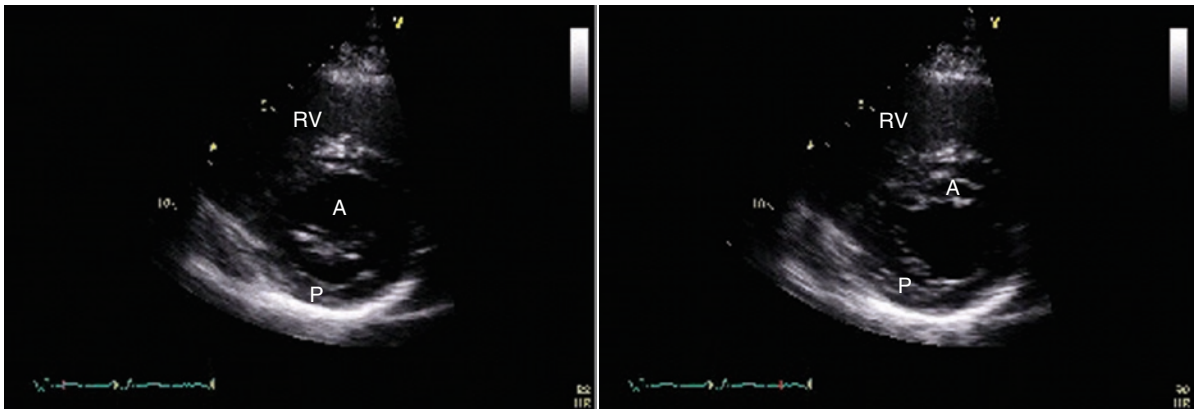

Fig. 2.20 Two-dimensional parasternal short-axis view angled at the level of the mitral valve. The two leaflets of the mitral valve are shown closing during systole (*left panel*) and fully opened at end diastole. Abbreviations: A, anterior leaflet of the mitral valve; P, posterior leaflet of the mitral valve; RV, right ventricle

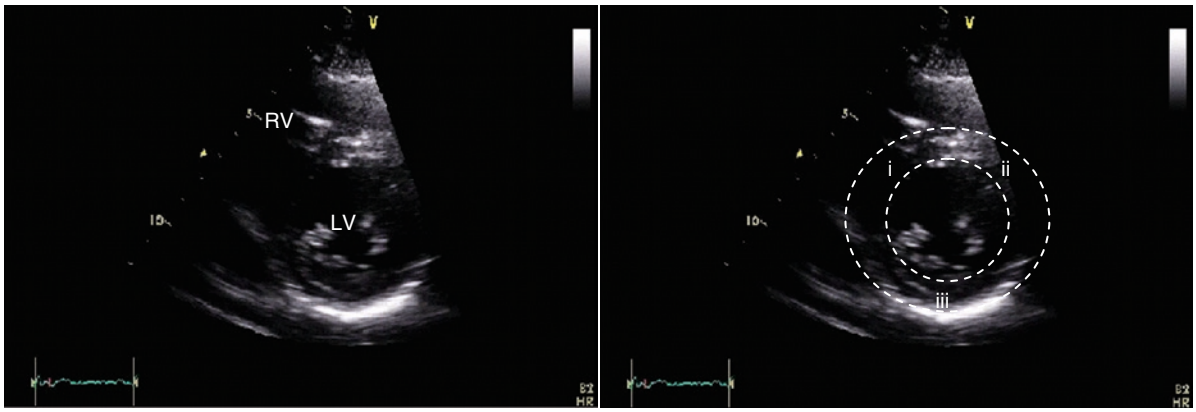

Fig. 2.21 Two-dimensional parasternal short-axis view angled at the level of the left ventricular papillary muscles. The two ventricles are shown in their short axis and the ventricular septum is well depicted (*left panel*). This view allows the analysis of regional wall motion of the left ventricular walls supplied by the three main coronary arteries (*right panel; the endocardial and epicardial borders are outlined*). Abbreviations: LV, left ventricle; RV, right ventricle; i, interventricular septum; ii, anterolateral wall; iii, posterior wall

with the inferior vena cava/right atrial junction. The abdominal aorta may also be imaged from this view.

2.3.5 Additional Echocardiographic Views

In some examinations, additional information is required that necessitates further views. In the echocardiography laboratory, these views are generally performed on all patients, but they are infrequently required and obtained in the ICU setting.

2.3.5.1 Suprasternal View

To examine the aortic arch (for example, in aortic dissection), the probe may be positioned in the suprasternal notch, with the patient's neck slightly extended and the marker toward the right shoulder (Fig. 2.24). The probe should be kept as horizontal as possible to allow access

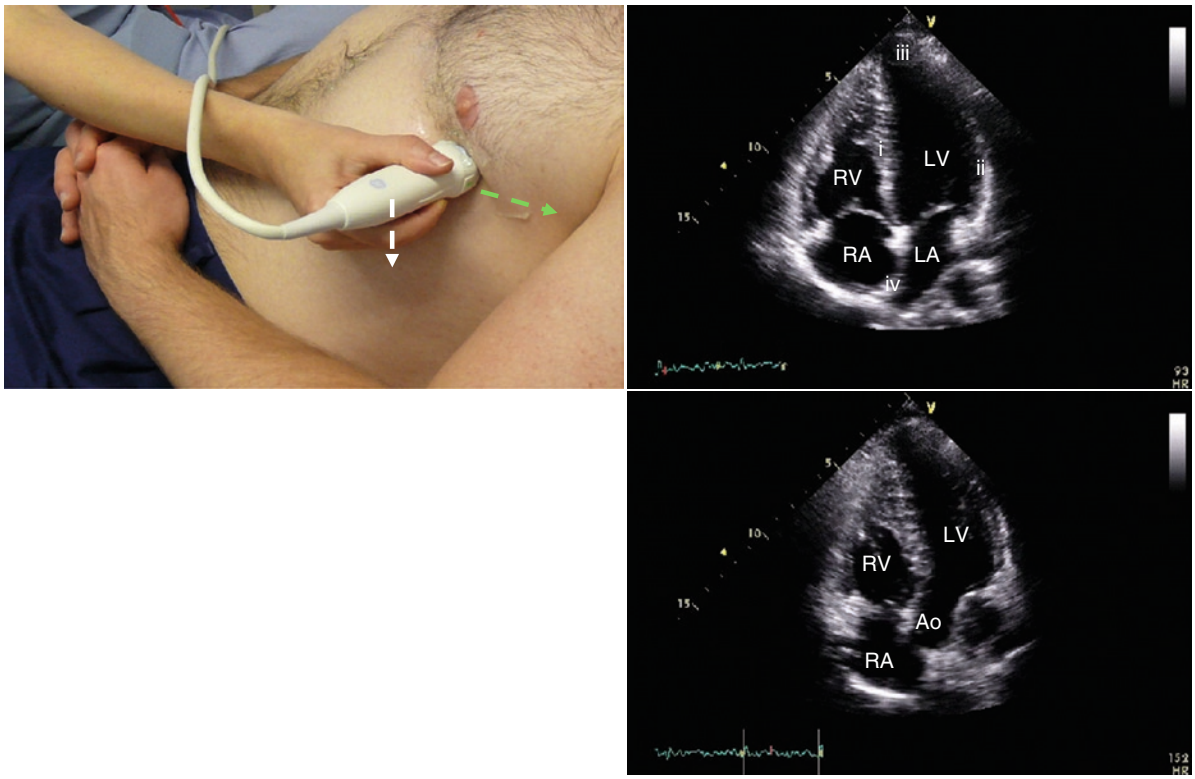

Fig. 2.22 Apical four-chamber view obtained in a supine patient. The probe is positioned at the apex of the heart, with the green indicator pointing toward the left axilla of the patient (*left panel, arrow*). To view the left ventricular outflow tract and aortic valve, the probe is angled so the ultrasound beam is directed superiorly (*white, broken arrow*). The two-dimensional apical four-chamber view depicts the two ventricles and atria (upper right panel), while the apical five-chamber view also includes the left ventricular outflow tract and aortic valve (lower right panel). Abbreviations: LV, left ventricle; RV, right ventricle; LA, left atrium; RA, right atrium; Ao, aortic valve; i, interventricular septum; ii, lateral wall; iii, apex; iv, interatrial septum (modified from FEEL-UK with permission)

to the retrosternal window. Color, PW, and CW Doppler are useful to confirm direction of flow, exclude holodiastolic flow reversal in the descending aorta, and exclude coarctation (Fig. 2.25). This view may, therefore, be performed in all patients with dissection, aortic regurgitation, and congenital heart disease. The aortic arch may not be seen in patients who are intubated owing to interposition of the endotracheal tube. Here, images may be obtained from either the left or right supraclavicular areas and angling accordingly.

2.3.5.2 Apical two- and Three-Chamber Views

These views are obtained by a counterclockwise rotation of the probe when positioned in the apical four-chamber view. They allow evaluation of the inferior, lateral, and anterior walls of the LV. The views are useful in evaluating regional wall-motion abnormalities and in detailed evaluation of the mitral valve.

2.4 Practical Use in the ICU Setting

In the ICU, echocardiography may be used as a diagnostic tool for monitoring the response to interventions or therapeutic maneuvers [11,12], as an extension to the clinical examination [13–15], and as an adjunct to investigation and diagnosis in the periresuscitation period [16,17].

Although many authorities propose that a full study should be performed as important new findings might be missed, under certain circumstances, focused should be

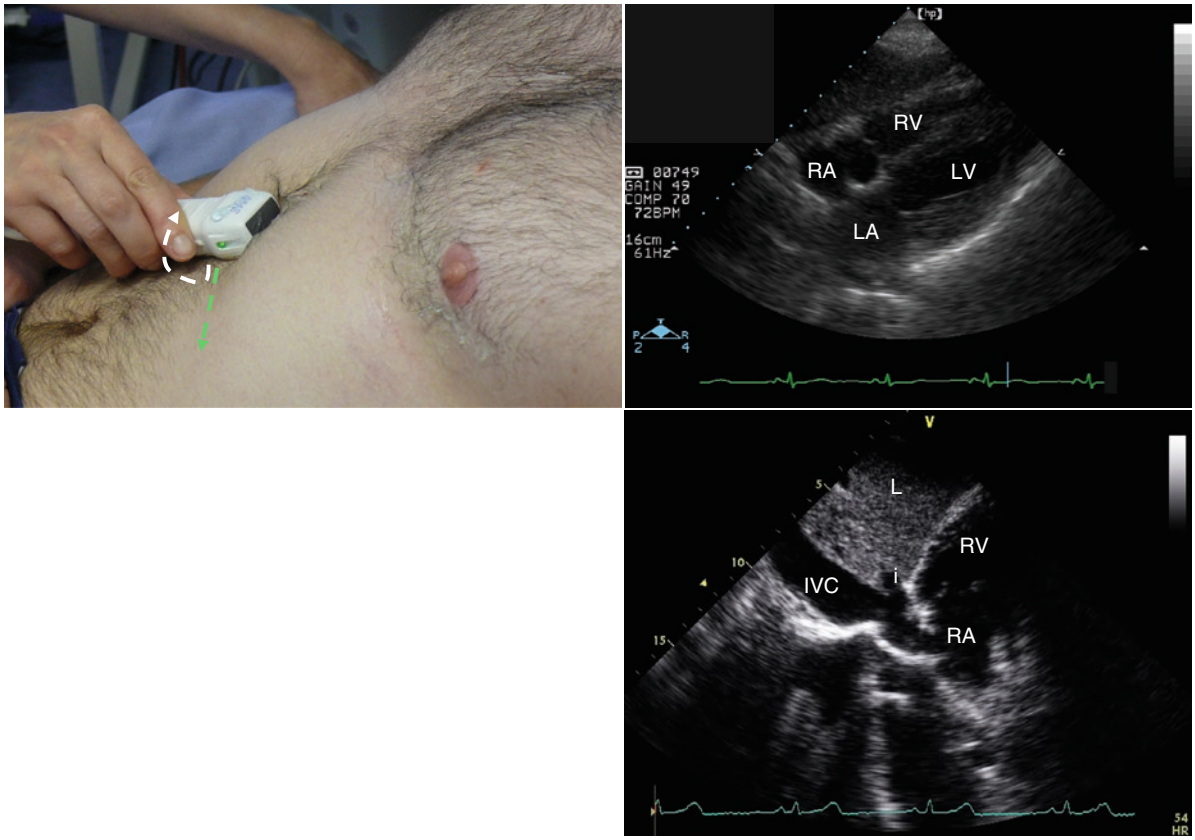

Fig. 2.23 Subcostal view. To obtain the subcostal view, the hand is positioned on top of the probe to allow the ultrasound beam to be directed superiorly, under the ribs toward the heart, with the green indicator pointing to the left upper quadrant of the patient (*left panel, arrow*). Careful positioning of the probe allows depiction of the four chambers of the heart (*upper right panel*). To visualize the inferior vena cava, the probe is rotated counterclockwise such that the green indicator light is pointing upward (*left panel, white broken arrow*). This allows imaging of the inferior vena cava in its long axis and the junction with the right atrium (*lower right panel*). Abbreviations: RA, right atrium; RV, right ventricle; LV, left ventricle; LA, left atrium; IVC, inferior vena cava; L, liver; i, suprahepatic vein (modified from FEEL-UK with permission)

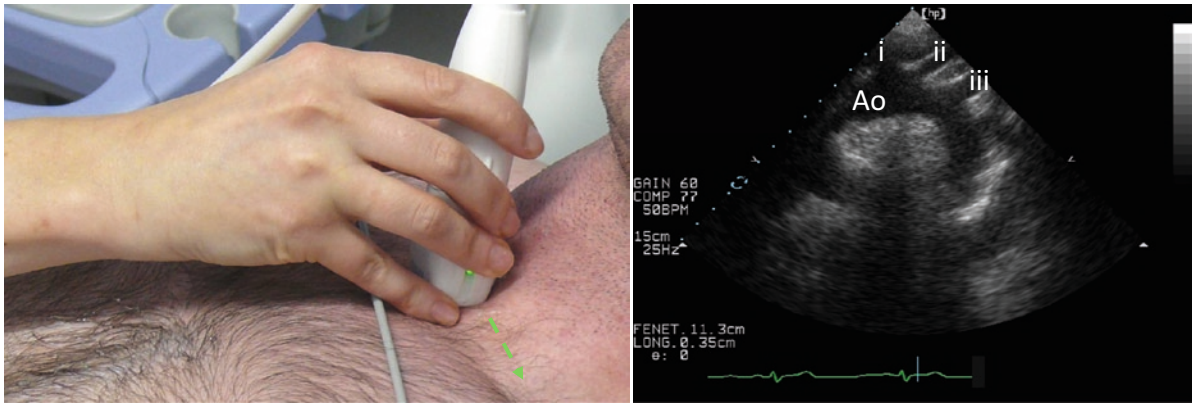

Fig. 2.24 Suprasternal view. The probe is positioned in the suprasternal notch, angled so the ultrasound beam is lined up with the aortic arch, and with the indicator pointing toward the right shoulder of the patient (*left panel, arrow*). This views depicts the aortic arch and the takeoff of supraaortic vessels. Abbreviations: Ao, aortic arch; i, inominate artery, ii, left carotid artery; iii, left subclavian artery

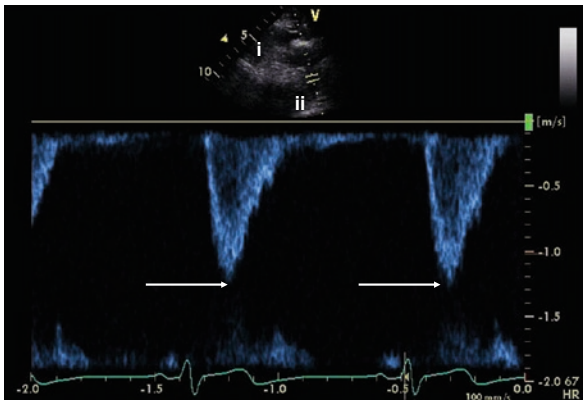

Fig. 2.25 Suprasternal view with the PW Doppler sample volume positioned in the descending aorta. The flow is laminar and moving down, away from the probe. Peak velocity is arrowed. A minaturized two-dimensional reference image is shown at the top of the figure, demonstrating the correct positioning of the PW Doppler. Abbreviations: i, ascending aorta; ii, descending aorta

considered. For example, during cardiopulmonary resuscitation, a comprehensive ECG study is usually not feasible. Here, focused studies designed to exclude obvious treatable causes for the periarrest state may be performed without interference using advanced life-support protocols. These findings may lead to a significant change in immediate management and possibly survival [16]. In the periresuscitation period, a limited ECG study may be performed to exclude obvious pathology, assess ventricular wall thickness and contractility, assess chamber dimensions, and image the pleura in a systematic manner [8,15]. In certain centers, such focused studies are used as an extension to the daily physical examination in the ICU; where an abnormality is seen, a comprehensive study is requested [18].

Echocardiography may be used to answer relatively simple hemodynamic questions in a noninvasive manner, both for diagnosis and in the monitoring of any therapeutic intervention [19]. The indications and main modalities in hemodynamic assessment of the critically ill are shown in Table 2.2.

2.5 Limitations of TTE in the ICU Setting

The limitations of TTE in the ICU relate to the patient, the pathology, and the ability of the operator (both technical and in interpreting the study). Patient factors include immobility, the effects of positive-pressure ventilation, the presence of dressings and drains, and obesity – all of which limit the diagnostic windows and increase the challenge to the operator. Pathological factors include those related to ICU support: changing hemodynamics, inotropic support, sedation, oxygen and carbon dioxide tensions, and those related to confounding factors from the underlying disease process

Table 2.2 Hemodynamic assessment using transthoracic echocardiography

Assessment	View	Modality	Measurement
Filling status	A4C	2D	LV area/volume
Fluid responsiveness	Subcostal	2D	IVC dimensions[a]
	A5C	PW Doppler	Respiratory variations of Doppler LVOT velocity in mechanically ventilated patients
LV filling pressures	A4C	PW Doppler	Mitral and pulmonary vein Doppler indices
		TDI	Diastolic velocity of mitral annulus (TDI)
CO	PLAX and	2D	LVOT diameter
	A4C	PW Doppler	LVOT Doppler VTI
PASP	PSAX and A4Ch	CW Doppler	TR peak velocity
PVR	PSAX	PW Doppler PA	Pulmonary acceleration time

[a]Including respiratory variations

Abbreviations: A4C, apical four-chamber view; 2D, two-dimensional echocardiography; LV, left ventricle; A5C, apical five-chamber view; PW, pulsed-wave; IVC, inferior vena cava; LVOT, left ventricular outflow tract; TDI, tissue Doppler imaging; CO, cardiac output; PLAX; parasternal long axis view; VTI, velocity–time integral; PASP, pulmonary artery systolic pressure; PSAX; parasternal short-axis view; CW, continuous-wave; TR, tricuspid regurgitation; PVR, pulmonary vascular resistance; PA, main pulmonary artery

(i.e., tamponade postcardiac surgery or endocarditis on a prosthetic valve). The greatest limitation, however, is the competence of the operator in adequately acquiring and interpreting TTE images.

In the ICU setting, performing a high-quality TTE is challenging and, as such, should not be regarded as somehow easier than TEE. With the transesophageal approach, obtaining images is simpler and the quality of images superior. Accordingly, image interpretation may be less challenging. There is, however, a risk associated with performing TEE, and the sedation/anesthesia required may change the hemodynamic findings significantly (for example, in mitral regurgitation). Thus, all intensivists should be able to perform TTE as a first-line ECG investigation. With both TTE and TEE come the challenges of interpretation of echocardiography in the context of the critically ill patient. The majority of research regarding ventricular function and valvular pathology derives from the non-ICU setting, and the relevance therefore to the critically ill is questionable. Further, many normal values may not, in fact, be normal in the context of the ICU patient.

2.6 Conclusion

TTE provides noninvasive, real-time, bedside assessment of the critically ill patient, offering unparalleled anatomical and hemodynamic information. Although images are often not perfect, the ability of echocardiography to yield accurate hemodynamic Doppler data, even in the presence of suboptimal image quality, means it is extremely useful in the ICU setting. Although gaining expertise in ICU echocardiography is both time-consuming and challenging and there is the potential for findings to change rapidly, the advantages of having a noninvasive window on cardiac function are undeniable.

References

1. Costa JM, Tsutsui JM, Nozawa E, Morhy SS, Andrade JL, Ramires JF, Mathias W Jr (2005) Contrast echocardiography can save nondiagnostic exams in mechanically ventilated patients. Echocardiography 22:389–94
2. Gunda M, Mulvagh SL (2001) Recent advances in myocardial contrast echocardiography. Curr Opin Cardiol 16:231–9
3. Monaghan MJ (2000) Second harmonic imaging: a new tune for an old fiddle? Heart 83:131–2
4. Nash PJ, Kassimatis KC, Borowski AG, Martin MG, Reynolds KM, Garcia CA, Morehead AJ, Thomas JD (2004) Salvage of nondiagnostic transthoracic echocardiograms on patients in intensive care units with intravenous ultrasound contrast. Am J Cardiol 94:409–11
5. Reilly JP, Tunick PA, Timmermans RJ, Stein B, Rosenzweig BP, Kronzon I (2000) Contrast echocardiography clarifies uninterpretable wall motion in intensive care unit patients. J Am Coll Cardiol 35:485–90
6. Yong Y, Wu D, Fernandes V, Kopelen HA, Shimoni S, Nagueh SF, Callahan JD, Bruns DE, Shaw LJ, Quinones MA, Zoghbi WA (2002) Diagnostic accuracy and cost-effectiveness of contrast echocardiography on evaluation of cardiac function in technically very difficult patients in the intensive care unit. Am J Cardiol 89:711–8
7. Mondillo S, Maccherini M, Galderisi M (2008) Usefulness and limitations of transthoracic echocardiography in heart transplantation recipients. Cardiovasc Ultrasound 11:6–2
8. DeCara JM, Lang RM, Spencer KT (2003) The hand-carried echocardiographic device as an aid to the physical examination. Echocardiography 20:477–85
9. Liang D, Schnittger I (2003) Accuracy of hand-carried ultrasound. Echocardiography 20:487–90
10. Feigenbaum H, Armstrong WF, Ryan T (eds) (2005) Feigenbaum's echocardiography, 6th edn. Lippincott Williams & Wilkins, Philadelphia, PA
11. Price S, Nicol E, Gibson DG, Evans TW (2006) Echocardiography in the critically ill: current and potential roles. Intensive Care Med 32:48–59
12. Cholley BP, Vieillard-Baron A, Mebazaa A (2006) Echocardiography in the ICU: time for widespread use! Intensive Care Med 32:9–10
13. Schiller NB (2001) Hand-held echocardiography: revolution or hassle? J Am Coll Cardiol 15(37):2023–4
14. Vignon P, Chastagner C, François B, Martaillé JF, Normand S, Bonnivard M, Gastinne H (2003) Diagnostic ability of hand-held echocardiography in ventilated critically ill patients. Crit Care 7:R84–91
15. Manasia AR, Nagaraj HM, Kodali RB, Croft LB, Oropello JM, Kohli-Seth R, Leibowitz AB, DelGiudice R, Hufanda JF, Benjamin E, Goldman ME (2005 Apr) Feasibility and potential clinical utility of goal-directed transthoracic echocardiography performed by noncardiologist intensivists using a small hand-carried device (SonoHeart) in critically ill patients. J Cardiothorac Vasc Anesth 19(2):155–8
16. Breitkreutz R, Walcher F, Seeger FH (2007 May) Focused echocardiographic evaluation in resuscitation management: concept of an advanced life support-conformed algorithm. Crit Care Med 35(5 Suppl):S150–61
17. Vignon P, Dugard A, Abraham J, Belcour D, Gondran G, Pepino F, Marin B, François B, Gastinne H (2007 Oct) Focused training for goal-oriented hand-held echocardiography performed by noncardiologist residents in the intensive care unit. Intensive Care Med 33(10):1795–9
18. Sloth E (Aug 2006) Echocardiography in the ICU. Intensive Care Med 32(8):1283; Jensen MB, Sloth E, Larsen KM, Schmidt MB (Sept 2004) Transthoracic echocardiography for cardiopulmonary monitoring in intensive care. Eur J Anaesthesiol 21(9):700–707
19. Vignon P (2005 Jun) Hemodynamic assessment of critically ill patients using echocardiography Doppler. Curr Opin Crit Care 11(3):227–34

Transesophageal Echocardiography: Principal Views

3

Jan Poelaert

Contents

Although echocardiography has developed as the most common imaging tool for evaluation of the heart and great vessels, the transthoracic approach has important limitations with respect to visualizing the different structures. In the early 1960s, several investigators started mounting single-element transducers on a catheter [1,2] or single- or dual-element constructions on a standard gastroscope [3], providing continuous-wave Doppler flow velocities within the heart. Only with the introduction of electronic scanners in the early 1980s could a definitive breakthrough with the transesophageal approach be achieved [4,5]. Transesophageal echocardiography (TEE) opened another window to the heart [6], providing an alternative in those situations where good cardiac ultrasound signals through the chest wall were difficult to obtain (Table 3.1). TEE is able to provide optimal images where transthoracic echocardiography (TTE) sometimes cannot. Subsequently, the development of higher-frequency transducers improved construction techniques [7,8], and the implementation of two-phased-array transducers perpendicular to each other led to imaging capabilities in both transverse and longitudinal planes [5]. A few years later, multiplane technology, providing an infinite number of planes between 0° and 180°, was a major development [9]. TEE became essential as both a diagnostic and monitoring tool for many critically ill patients [10]. Smaller units allow easier access for intraoperative or intensive care unit (ICU) monitoring [11].

3.1 Specifics of TEE Systems

A phased-array transducer is mounted onto the tip of a commercially available gastroscope or bronchoscope, with a length of 70–110 cm, connected to an echocardiograph. The shaft is subdivided in 10-cm intervals.

J. Poelaert
Department of Anesthesiology and Perioperative Medicine, Acute and Chronic Paintherapy, Flemish University Hospital of Brussels, Laarbeeklaan 101, 1090, Brussels, Belgium
e-mail: jan.poelaert@uzbrussel.be

D. De Backer et al. (eds.), *Hemodynamic Monitoring Using Echocardiography in the Critically Ill*,
DOI: 10.1007/978-3-540-87956-5_3, © Springer-Verlag Berlin Heidelberg 2011

Table 3.1 Shortcomings and advantages of transthoracic and transesophageal echocardiography

	Transthoracic	Transesophageal
Ease of approach	Rapid	Needs preparation
Visualization	Sometimes poor	Most often very good
indications	Not all structures can be seenSome structures partly visualized: valve prostheses	Some structures are solely/better visualized byTEE: LAA Great vessels Valve prostheses Ventricular function + hypoxemia Major thoracic trauma Local tamponade (esp. LA)

LAA, left atrial appendage; LA, left atrium; TEE, transesophageal echocardiography

The normal guidance controls are retained, providing anteroposterior mobility of the tip of at least 90° in each direction and a minimal lateral mobility of 70°. Imaging is delivered with a sector of 90°. The operating frequency is around 5 MHz. The transducer frequency is available up to 10 MHz [12], and the device can be miniaturized [13] for neonatal indications.

Visualization of transverse planes encompasses structures closest to the esophagus at the top of the screen; structures of the left heart are imaged on the right. Longitudinal views are built up with the most cranial structures visualized on the right.

Safety considerations involve disinfection of the probe, attention to electrical hazards and control of the probe temperature. Several measures for cleaning the TEE probe may be followed since the use of covers [14] and disinfection between investigations may vary according to the guidelines of the manufacturer. Electrical safety is set according to international standards (IEC 601-1). For clinical purposes, it is important to check the probe daily for biting lesions, other damage, and cable disruption. Temperature control is achieved by means of a thermistor mounted at the tip of the transducer. Temperatures above 41°C either cause the transmitting power to be switched off or produce a warning on the echocardiograph screen. Although safety is an important issue, a multicenter study including more than 10,000 TEE investigations revealed a procedural mortality of 0.0098% [15]. Cardiac, pulmonary, or bleeding complications necessitating interruption of the TEE investigation were described in 0.18% of the cases [15]. Also, in a mixed population of ICU patients, retrospective analysis in 108 patients showed a relative contraindication in only 11% [10].

3.2 Two-Dimensional Imaging with TEE

Though initially TEE imaging was limited to transverse planes [16,17], the exponential growth of TEE is attributed to technological improvements, allowing a broad set of imaging modalities: from biplane to three-dimensional scanning, from color and pulsed-wave Doppler to tissue Doppler imaging. All this technology did not make interpretation of the various images and signals any easier. It is essential in correctly interpreting the viewed images to have thorough knowledge of the anatomical landmarks and the relationship between the intrathoracic structures, such as the esophagus, the different cardiac sights, and the great vessels.

The major difference in using the TEE probe between the transverse and longitudinal planes is the manner of handling the probe: the transverse plane necessitates up and down movement of the TEE probe, whereas the longitudinal plane necessitates rotation about the probe's longitudinal axis.

A standard TEE examination should always be performed completely and systematically. Individualization should be guided by specific questions. The following descriptions are in accordance with the guidelines and recommendations of the American Society of Echocardiography [18]. The next sections provide a general guide to assess systematically all structures of the heart. This review is not meant to be complete although it includes the most appropriate TEE views associated with the respective clinical applications.

3.2.1 *Transgastric Short-Axis Views*

In critical care medicine as well as intraoperatively, the transgastric view in a transverse plane is the most important view. The TEE probe is advanced gently into the stomach at about 40 cm from the incisors. Slight anteflexion will provide visualization of both left and right ventricles in a short axis (Fig. 3.1), although the true short-axis view of the right ventricle is located 1–2 cm deeper. Adjustments along the long axis of the shaft of the TEE probe will offer

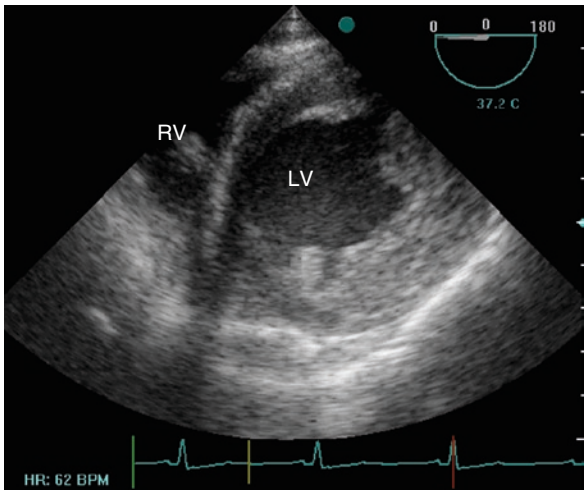

Fig. 3.1 Short-axis view, with the anterior wall in the lower part of the image, the interventircular septum on the left, the posterior wall in the upper part, and the inferolateral wall on the right. RV, right ventricle; LV, left ventricle

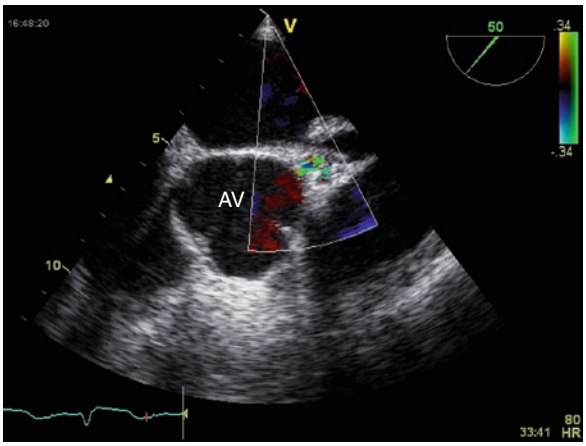

Fig. 3.2 Coronary perfusion at the level of the aortic valve (AV): the left anterior descending coronary artery (LAD) is visualized with color Doppler

better visualization of the left or right ventricle, providing imaging of both papillary muscles in the same plane.

Three major features can be obtained directly from this short-axis view, making it one of the most important images in acute care [19]:

1. Global left and right ventricular systolic function. This view offers the opportunity to delineate easily the boundaries of the blood/myocardial tissue level to obtain end-diastolic and end-systolic areas and thus fractional area contraction, the analogue of ejection fraction.
2. End-diastolic area, though static, is a measure of preload. Kissing walls with end-systolic obliteration have been recognized as an important marker of hypovolemia in the absence of inotropic support [20].
3. This view gives direct insight into the function of the various regional wall segments and thus indicates the efficiency of the coronary perfusion (Fig. 3.2). The left ventricular anterior wall and the anterior first two-thirds of the anteroseptal part are perfused by the left anterior descending coronary artery. The inferoposterior segment obtains blood from the circumflex coronary artery and the posterior part of the left ventricle, including the posterior segment of the interventricular septum; the right ventricular free wall derives blood from the right coronary artery. The appearance of new regional wall-motion abnormalities is an early and sensitive sign of coronary hypoperfusion [21], although many drawbacks and pitfalls should be recognized [22].

From the short-axis view in a transverse plane, use of the multiplane facility provides many other images. An important one is the left ventricular outflow tract view at ±120° (Fig. 3.3), which offers the possibility of estimating stroke volume and cardiac output in addition to functional assessment of the aortic valve.

3.2.2 Deep Transgastric Views

From the short-axis view, the TEE probe can be advanced smoothly into the stomach until contact with the mucosa is lost. Pulling back with anterior flexion and shaft rotation of the probe to the left presents the deep transgastric view in a transverse plane (Fig. 3.4). Blood flow is in alignment with Doppler flow estimations. This is the optimum view for assessing the function of the left ventricular outflow tract and aortic valve.

Rotation of the complete probe to the right will offer right-sided deep transgastric views, particularly of the tricuspid valve; appearing at the top of the screen is the right ventricle, and at the bottom the right atrium (Fig. 3.5).

Deep transgastric views are only indicated when a clear-cut need for the functional assessment of the aortic valve is necessary in terms of exclusion or diagnosis of aortic regurgitation, determination of a pressure gradient in aortic stenosis, or dynamic left ventricular outflow tract obstruction. Care must be taken that the probe is completely deflexed before pulling back into the short-axis view.

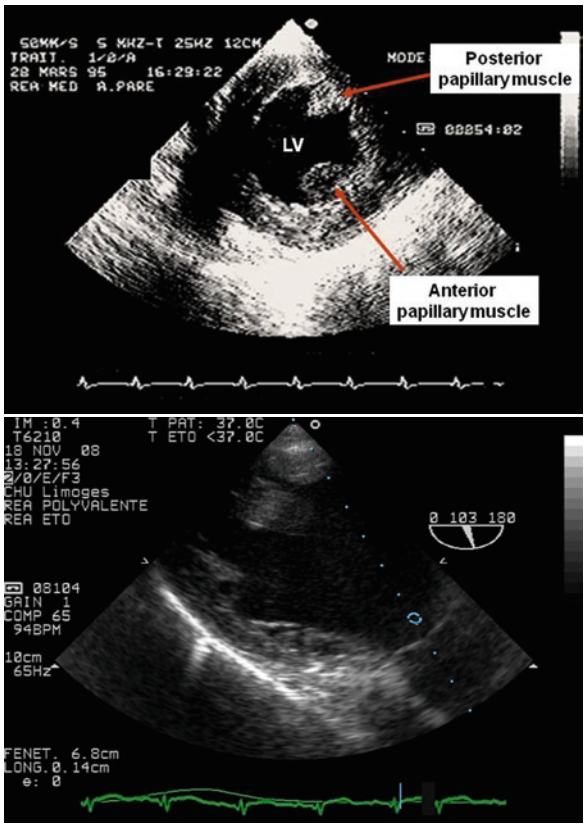

Fig. 3.3 Transgastric Long axis view, obtained by rotating by 100-130° from short axis view, at the level of papillary muscles. It allows perfect alignment of left ventricular outflow tract for cardiac output measurements

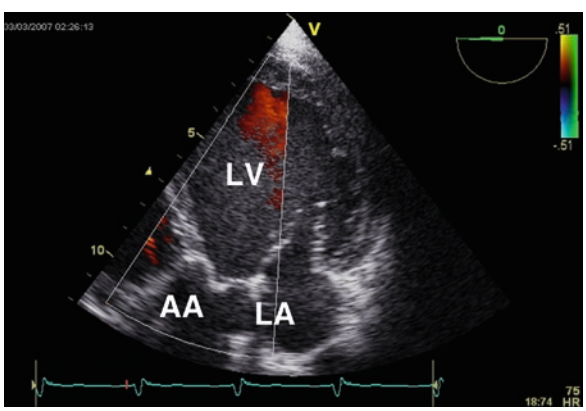

Fig. 3.4 A deep transgastric view with the ascending aorta (AA), left ventricle (LV), and left atrium (LA)

3.2.3 Mid-esophageal Views

Withdrawing the probe from the short-axis view offers a gastroesophageal view in the transverse plane: this is perfect for observing the closure of the mitral valve

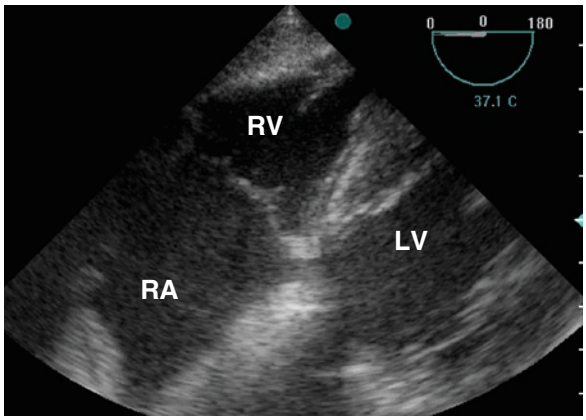

Fig. 3.5 A deep transgastric view of the right heart (RV, right ventricle), with the tricuspid valve. RA, right atrium; LV, left ventricle

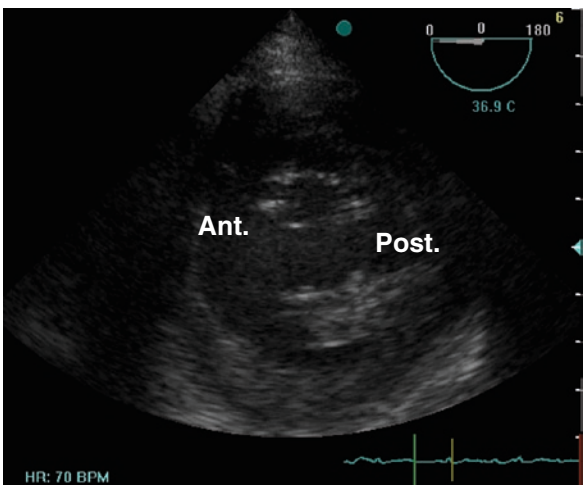

Fig. 3.6 The mitral valve with the anterior leaflet (Ant.) and posterior leaflet (Post.). See text for further details

over the whole rim of the mitral valve leaflets (Fig. 3.6), which is very useful in detecting the localization of the mitral regurgitation.

Various midesophageal views both in the transverse and longitudinal planes, which are located 30–35 cm from the incisors. In the transverse plane, three separate views can be observed:

1. The four-chamber view reveals the four cardiac chambers, including the respective valves after a slight anteflexion (Fig. 3.7). This view permits assessment of coaptation and the degree of closure of both atrioventricular valves. In addition, contraction of the right ventricular free wall can be assessed in conjunction with the motion of the interventricular septum and the *de visu* descent of the tricuspid valve.

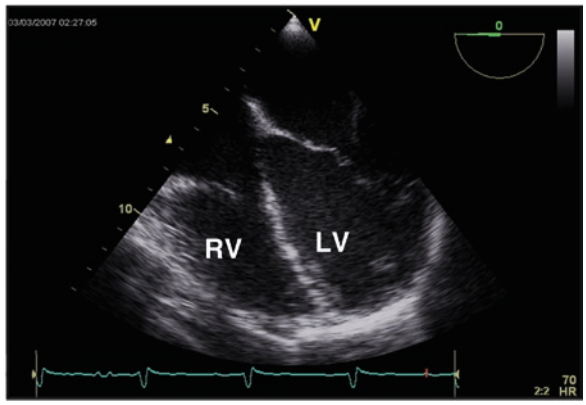

Fig. 3.7 The four-chamber view in a transverse plane. LV, left ventricle; RV, right ventricle

2. A few centimeters deeper from the four-chamber view, the coronary sinus is observed. In this view, the right ventricle is more easily visualized.
3. Alternatively, a few centimeters above the level of the four-chamber view, the five-chamber view appears, revealing the four cardiac chambers and the aortic valve. At this level, the left atrial appendage is also observed on the right of the screen to exclude thrombi.

Rotating the TEE probe toward the longitudinal plane offers the two-chamber view of the left ventricle; when turning the shaft of the TEE probe counterclockwise, visualization of the left atrial appendage may allow exclusion of thrombi. Further manipulation of the TEE probe in counterclockwise fashion reveals the inlet of the left upper pulmonary vein.

Clockwise manipulation of the TEE probe provides consecutively the following images:

1. Two-chamber view of the left ventricle; this view provides insight as to the degree of coaptation, typically of the posterior leaflet (P1, most anterior; P3, most posterior) at the border and the anterior leaflet in the middle.
2. The left ventricular outflow tract and aortic valve with the noncoronary and right coronary cusp; also, the right ventricular outflow tract and pulmonary valve can often be visualized (Fig. 3.4).
3. The aortic valve (as in 2) and initial 5–7 cm of the ascending aorta (Fig. 3.8).
4. The tricuspid valve and right atrium in an optimal position to perform Doppler assessment, as appropriate (Figs. 3.3 and 3.9).
5. The inflow tract of the right heart with the superior caval vein on the right and inferior caval vein on the left. This is the bicaval view (Fig. 3.10). Here, the interatrial septum is shown, perpendicular to the Doppler beam. Hence, the integrity of this structure can be ascertained.

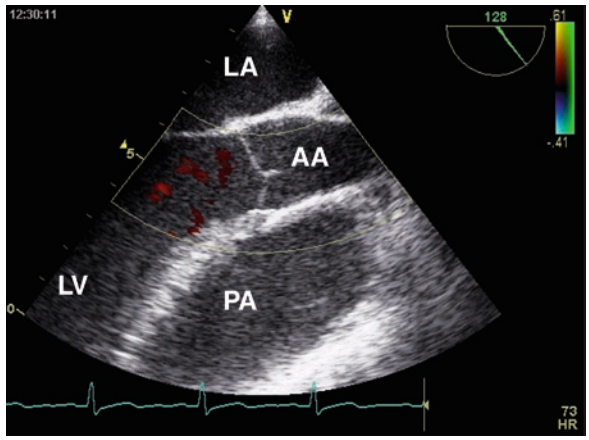

Fig. 3.8 The left ventricular (LV) outflow tract at 120°; on the right, the ascending aorta (AA) is visualized. LA, left atrium; PA, pulmonary artery

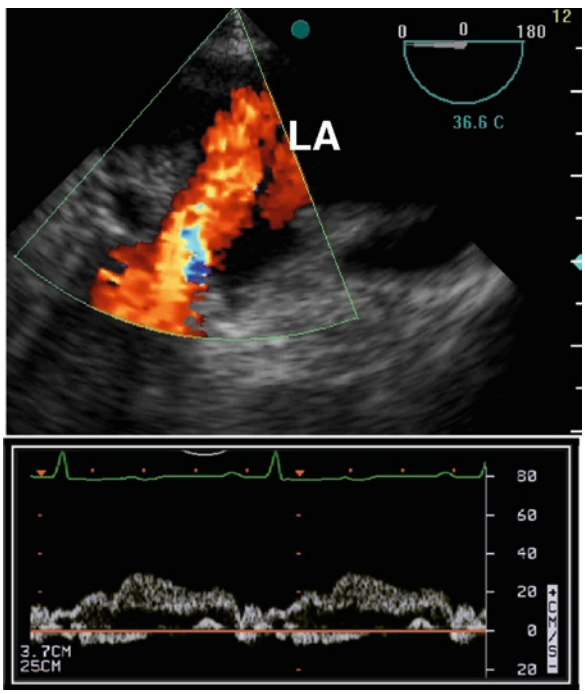

Fig. 3.9 The right lower pulmonary vein (*upper level*) entering the left atrium (LA). In the lower panel, a typical pulmonary vein pulsed-Doppler pattern is shown

3.2.4 Upper Esophageal Views

After withdrawal of the TEE probe to a distance of 27–33 cm from the incisors in a transverse plane, the

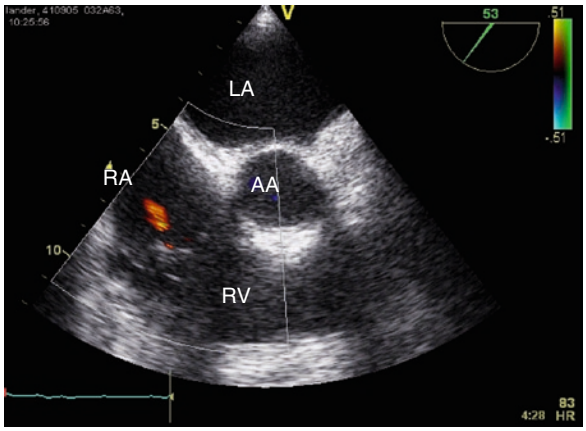

Fig. 3.10 The tricuspid valve, right atrium (RA), and right ventricle (RV). AA, ascending aorta; LA, left atrium

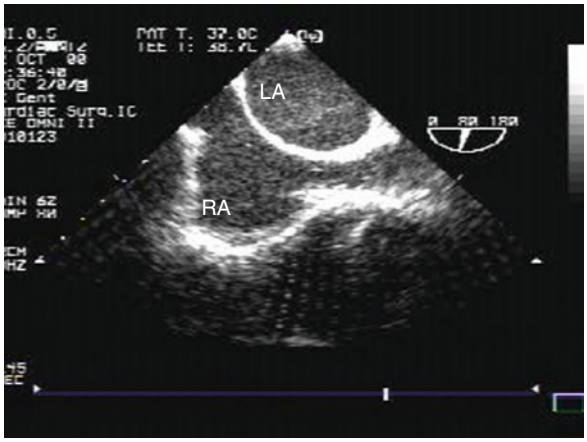

Fig. 3.11 The bicaval view with, on the right, the superior caval vein inlet and, on the left, the inferior caval vein inlet into the right atrium (RA). The left atrium (LA) is separated from the RA by the interatrial septum

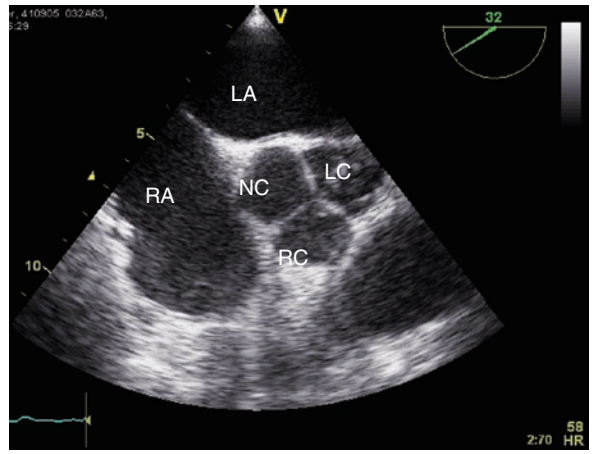

Fig. 3.12 An aortic valve with the typical star image, illustrating the three cusps of the aortic valve: the noncoronary cusp (NC), right coronary cusp (RC), and left coronary cusp (LC). LA, left atrium; RA, right atrium

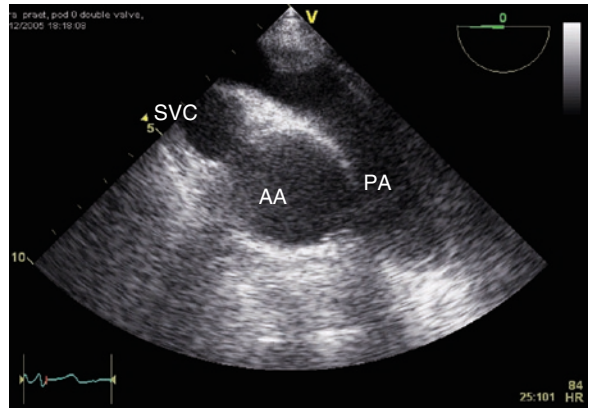

Fig. 3.13 The great vessels of the superior mediastinum: ascending aorta (AA), pulmonary artery (PA), and superior caval vein (SVC)

aortic valve appears, including the left ventricular outflow tract. Progressively rotating the TEE probe toward a longitudinal plane will depict the complete aortic valve, including the three cusps (Fig. 3.11). At the right upper level, the left main coronary artery is often seen and can be followed until the bifurcation into the left anterior descending and circumflex coronary artery (Fig. 3.12). Less frequently, the right coronary artery at the left lower level of this view is observed.

Back to the transverse plane and less than 0.5 cm above this level, the pulmonary trunk appears and further withdrawal depicts the bifurcation. Further retraction of the TEE probe displays particularly the right pulmonary artery as the left part disappears behind the trachea and pulmonary parenchyma.

Rotating the shaft of the TEE probe to the right images the right upper and lower pulmonary veins. By means of color Doppler, the veins can be easily located (Fig. 3.13) and the Doppler sample volume correctly placed. Sometimes, adjustment with the multiplane facility is necessary to obtain proper visualization.

3.2.5 Aortic Views

The initial section of the ascending aorta can be observed at the superior mediastinal level. The upper part of the ascending aorta, however, cannot be seen owing to the interference of the main bronchus. Pulling back the probe and turning the shaft of the TEE probe to the left offers imaging of the distal part of the aortic arch. Turning the probe posteriorly and pushing it more deeply depicts the descending aorta:

- Transversely in the short axis
- Longitudinally in the long axis

In an intermediate plane, between 40° and 70°, the left subclavian artery can be seen on the right. This is an important view as it can provide information on the correct localization of an intra-aortic balloon catheter [23].

3.3 Conclusion

A TEE investigation should be performed in a consistent and systematic manner. Utilizing the technique as a goal-directed tool implicates the start of each investigation with the short-axis view in a transverse plane: this provides the examiner immediately with significant clinical information on global left and right systolic function, static preload assessment, and the presence or absence of segmental wall-motion abnormalities.

Thereafter, the four-chamber view in the transverse plane should be evaluated, followed by the views in the longitudinal plane at the same depth. Deep transgastric views are only indicated when clear evidence is present following the evaluation of the different valves.

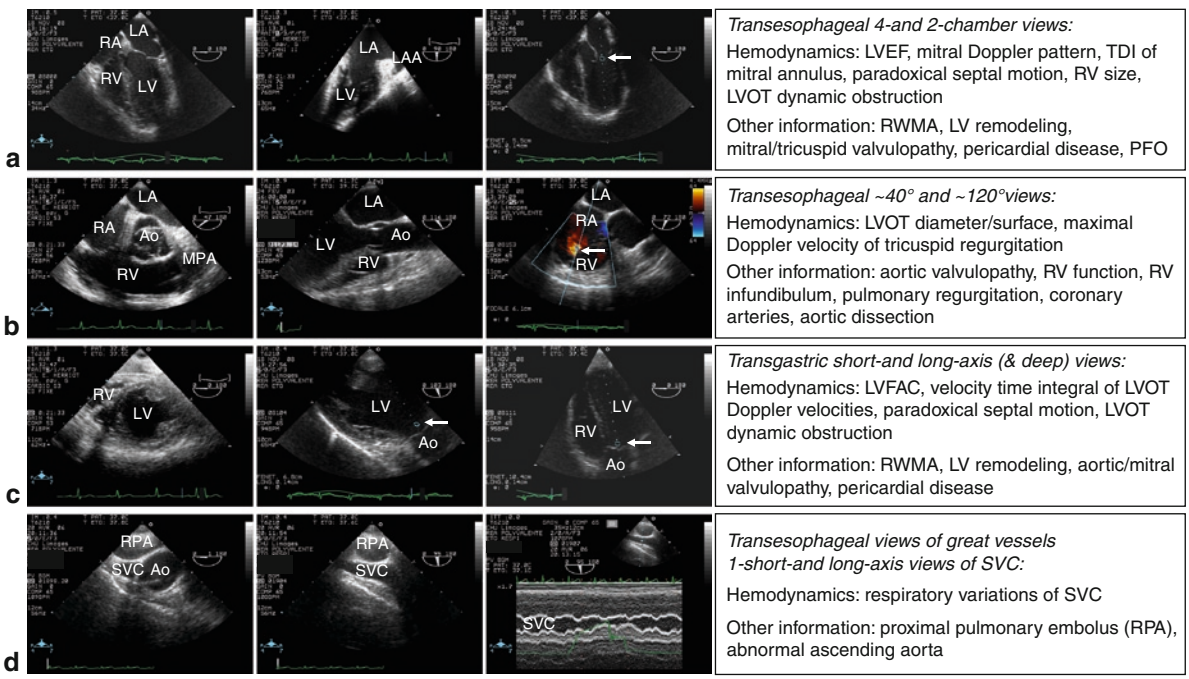

Main transesophageal echocardiographic views and corresponding indices and information routinely used for the hemodynamic assessment of patients in the intensive care unit. Panels (**A**). Transesophageal four-chamber view (*left panel*) is mainly used to visually assess or measure left ventricular (LV) ejection fraction (EF) and record mitral Doppler velocity profile (*right panel, arrow*). Transesophageal two-chamber view (*middle panel*) is mainly used to assess LVEF (biplane Simpson's rule) and identify the presence of regional wall motion abnormality (RWMA). Panels (**B**). Transesophageal intermediate views include the 40 to 70° plane that allows evaluating right ventricular (RV) size and function and aortic valve morphology (*left panel*) and the ~ 120° plane disclosing the LV outflow tract (OT) and ascending aorta (*middle panel*). Using such intermediate plane in conjunction with color Doppler mapping may help aligning the continuous was Doppler beam with the regurgitant tricuspid jet to infer information on the systolic pulmonary artery pressure (*right panel, arrow*). Panels (**C**). Transgastric views are essential to evaluate LV systolic function and the presence of a paradoxical septal motion in the short axis plane (*left panel*). It also allows the measurement of velocity-time integral of LVOT Doppler profile either in the ~ 120° view (*middle panel, arrow*) or in the deep 0° transgastric view (*right panel, arrow*).Panel (**D**). Transesophageal views of the great vessels provides information on respiratory variations of the superior vena cava (SVC) in ventilated patients, in both the transversal (*left panel*), and longitudinal views (*middle panel*). M-mode of the SVC in its long-axis plane precisely discloses respiratory variations of the vessels within the respiratory cycle in mechanically ventilated patients (*right panel*).

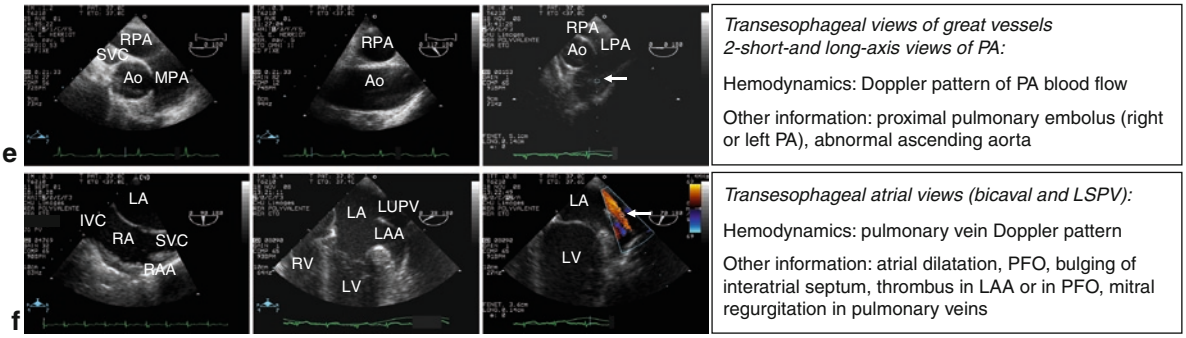

Panel (**E**). Transesophageal views of the great vessels may also be centered on the main pulmonary artery (MPA) and ascending aorta (*Ao*) in both the transverse (*left panel*) and longitudinal views (*middle panel*). In the transverse view, the pulse wave Doppler sample may be precisely positioned in the MPA, immediately downstream the pulmonary valve to display pulmonary artery Doppler pattern (*right panel*, *arrow*). Panel (**F**). Transesophageal atrial views provide morphological information on the left (LA) and right (RA) atria and precisely depict the foramen ovale, especially in the longitudinal plane that is also referred as "bicaval view" (*left panel*). The ~40° view centered on the LA depicts the left atrial appendage (LAA) and the left upper pulmonary vein (LUPV) (*middle panel*). Using color Doppler mapping, the electronic rotation of the probe is set to image the LUPV in its long axis (in this patient in the 70° plane) and to locate the pulse wave Doppler sample to measure pulmonary vein blood flow velocities (*right panel, arrow*). Abbreviations: *RPA*, right pulmonary artery; *LPA*, left pulmonary artery; *RAA*, right atrial appendage; *IVC*, inferior vena cava; *LVFAC*, left ventricular fractional area change; *TDI*, tissue Doppler imaging; *PFO*, patent foramen ovale; *PA*, pulmonary artery. (by the courtesy of Pr P Vignon, Limoges, France)

References

1. Cieszynski T (1960) Intracardiac method for the investigation of structure of the heart with the aid of ultrasonics. Arch Immunol Ther Exp (Warsz) 8:551–7
2. Bom N, Lancee CT, Van Egmond FC (1972) An ultrasonic intracardiac scanner. Ultrasonics 10(2):72–6
3. Side CD, Gosling RG (1971) Non-surgical assessment of cardiac function. Nature 232(5309):335–6
4. Schluter M et al (1982) Transoesophageal cross-sectional echocardiography with a phased array transducer system. Technique and initial clinical results. Br Heart J 48(1):67–72
5. Souquet J et al (1982) Transesophageal phased array for imaging the heart. IEEE Trans Biomed Eng 29(10):707–12
6. Frazin L et al (1976) Esophageal echocardiography. Circulation 54(1):102–8
7. de Jong N et al (1985) Transducers in medical ultrasound: Part Two. Vibration modes, matching layers and grating lobes. Ultrasonics 23(4):176–82
8. Lancee CT et al (1985) Transducers in medical ultrasound: Part One. Ferro-electric ceramics versus polymer piezoelectric materials. Ultrasonics 23(3):138–42
9. Daniel WG, Pearlman AS, Hausmann D (1993) Initial experience and potential applications of multiplane echocardiography. Am J Cardiol 71:358–61
10. Poelaert JI et al (1995) Evaluation of transesophageal echocardiography as a diagnostic and therapeutic aid in a critical care setting. Chest 107(3):774–9
11. Vignon P et al (2003) Diagnostic ability of hand-held echocardiography in ventilated critically ill patients. Crit Care 7(5):R84–91
12. Bruce CJ et al (1999) Feasibility study: transesophageal echocardiography with a 10F (3.2-mm), multifrequency (5.5- to 10-MHz) ultrasound catheter in a small rabbit model. J Am Soc Echocardiogr 12(7):596–600
13. Bruce CJ et al (2002) Miniaturized transesophageal echocardiography in newborn infants. J Am Soc Echocardiogr 15(8):791–7
14. Fritzsche D et al (1994) Effect of an anabolic steroid (Metenolon) on contractile performance of the chronically stimulated latissimus dorsi in sheep. Eur J Cardiothorac Surg 8(4):214–9
15. Daniel WG et al (1991) Safety of transesophageal echocardiography. A multicenter survey of 10,419 examinations. Circulation 83:817–21
16. Seward JB et al (1988) Transesophageal echocardiography: technique, anatomic correlations, implementation, and clinical applications. Mayo Clin Proc 63(7):649–80
17. Visser CA, Koolen JJ, Dunning AJ (1988) Transesophageal echocardiography: technique and clinical applications. J Cardiothorac Anesth 2:74–81
18. Shanewise J et al (1999) ASE/SCA guidelines for performing a comprehensive intraoperative multiplane transesophageal echocardiographic examination: recommendations of the American Society of Echocardiography Council for intraoperative echocardiography and the Society of Cardiovascular Anesthesiologists task force for certification

in perioperative transesophageal echocardiography. J Am Soc Echocardiogr 12:884–900
19. Poelaert JI, Schupfer G (2005) Hemodynamic monitoring utilizing transesophageal echocardiography: the relationships among pressure, flow, and function. Chest 127(1): 379–390
20. Leung JM, Levine EH (1994) Left ventricular end-systolic cavity obliteration as an estimate of intraoperative hypovolemia. Anesthesiology 81:1102–9
21. Shah PM et al (1991) Utility of biplane transesophageal echocardiography in left ventricular wall motion analysis. J Cardiothorac Vasc Anesth 5(4):316–9
22. Seeberger M et al (1997) Acute hypovolemia may cause segmental wall motion abnormalities in the absence of myocardial ischemia. Anesth Analg 85:1252–7
23. Nishioka T et al (1996) Usefulness of transesophageal echocardiography for positioning the intraaortic balloon pump in the operating room. Am J Cardiol 77:105–106

Part II

Hemodynamic Assessment

Heart–Lung Interactions in Mechanical Ventilation

4

Antoine Vieillard-Baron

Contents

4.1 Introduction

A chapter on heart–lung interactions may not seem an obvious choice in a book on the use of echocardiography in intensive care. But it is knowledge of the mechanisms promoting such interactions that allows us to understand why and how to use echocardiography in the most critical clinical situations, such as in ventilated patients with shock or acute respiratory distress syndrome (ARDS). This knowledge also helps us understand the concept of functional hemodynamic monitoring proposed a few years ago [1]. The present chapter therefore provides the physiological support for other chapters in this book mainly devoted to hemodynamic monitoring using echocardiography. Readers especially interested in heart–lung interactions will see that echocardiography is the most efficient method because of its ability to show cardiac structures directly and their changes throughout the respiratory cycle.

4.2 Physiological Background

Three pressures are generated by the presence of air in the respiratory system and vary during respiration (Fig. 4.1). *Alveolar pressure* is the pressure in the lung. It depends in part on compliance of the respiratory system (lung plus chest wall). In spontaneous ventilation, it is zero at end expiration, provided the patient has reached functional residual capacity, and also in end inspiration; but it is negative during inspiration and positive during expiration. In mechanical ventilation, alveolar pressure becomes positive throughout the respiratory cycle. It is maximal at end inspiration, and this is the plateau pressure. *Intrathoracic pressure*

A. Vieillard-Baron
Intensive Care Unit, University hospital Ambroise Paré,
Assistance Publique Hôpitaux de Paris,
9 avenue Charles de Gaulle, 92104,
Boulogne Cedex, France
e-mail: antoine.vieillard-baron@apr.aphp.fr

D. De Backer et al. (eds.), *Hemodynamic Monitoring Using Echocardiography in the Critically Ill*,
DOI: 10.1007/978-3-540-87956-5_4, © Springer-Verlag Berlin Heidelberg 2011

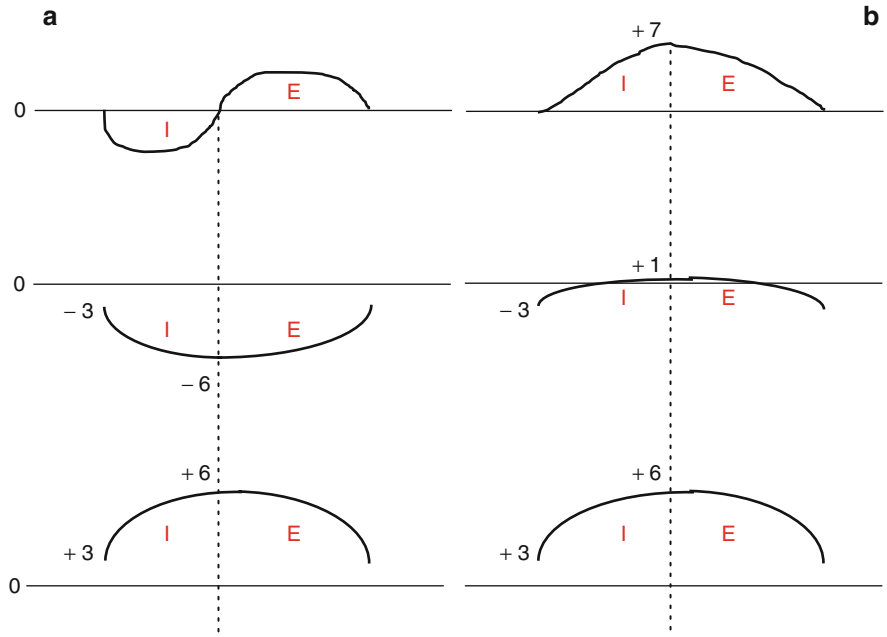

Fig. 4.1 Changes in alveolar (*top*), intrathoracic (*middle*), and transpulmonary (*bottom*) pressures during the respiratory cycle in spontaneous ventilation (**a**) and mechanical ventilation (**b**). I, inspiration; E, expiration

depends in part on compliance of the chest wall. It is usually negative throughout the respiratory cycle in spontaneous ventilation, thus representing the driving pressure for inspiration and facilitating the systemic venous return. In mechanical ventilation, it becomes positive throughout much of the respiratory cycle, especially when a positive end-expiratory pressure (PEEP) is applied. Finally, *transpulmonary pressure* (TPP) depends in part on lung compliance. It represents the distending pressure of the lung and is calculated as alveolar pressure minus intrathoracic pressure. It acts on the pulmonary capillaries.

For a long time, heart–lung interactions have been studied using measurement of intracardiac pressures. But, two types of pressure have to be distinguished. *Intravascular pressure* is the absolute value of the pressure measured by a catheter placed in a cardiac cavity, the right atrium for instance. Intravascular pressure gradients generate blood flow. *Transmural pressure* is the distending pressure of a heart chamber. For a given compliance of a heart chamber, it thus depends on the amount of blood in this chamber. It is calculated as the intravascular pressure minus the surrounding pressure, i.e., the intrathoracic pressure for the heart chambers. This difference between the intravascular and transmural blood pressures is important and has been well illustrated in two clinical situations where these two pressures differ markedly: cardiac tamponade and mechanical ventilation (Fig. 4.2).

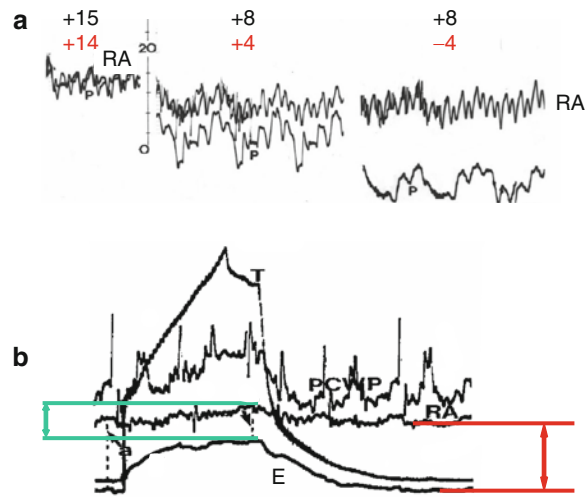

Fig. 4.2 Difference between intravascular and transmural right atrial pressures in cardiac tamponade (**a**) and mechanical ventilation (**b**). In cardiac tamponade, intravascular pressure (*in black*) is initially elevated, whereas transmural pressure is almost zero because of the large increase in pericardial pressure (*in red*). During fluid removal, intravascular pressure decreases, whereas transmural pressure increases (reflecting an increase in systemic venous return) because of the fall in pericardial pressure. In mechanical ventilation, tidal ventilation induces an increase in intrathoracic pressure, as reflected by an increase in esophageal pressure (E). Whereas intravascular right atrial pressure increases, transmural pressure decreases because of the decrease in systemic venous return. RA, intravascular right atrial pressure; P, pericardial pressure; E, esophageal pressure; PCWP, pulmonary capillary wedge pressure; red arrow, transmural right atrial pressure during expiration; green arrow, transmural right atrial pressure during inspiration

4.3 Reverse Pulsus Paradoxus

Hemodynamic reflections of heart–lung interactions in a mechanically ventilated patient were described in 1976 by Massumi et al. and termed reverse pulsus paradoxus [2]. Reverse pulsus paradoxus is defined as an increase in systolic arterial pressure during tidal ventilation and a decrease during expiration (Fig. 4.3). It reflects in part similar changes in left ventricular stroke volume (LVSV). Using an end-expiratory pause, these changes in arterial pressure can be separated into a component called dDown (absolute fall in pressure and so, in LVSV, during expiration) and a component called dUp (absolute increase in pressure and so, in LVSV, during tidal ventilation) (Fig. 4.3) [3]. dDown and dUp are mediated by alterations in transpulmonary and intrathoracic pressures that occur during tidal ventilation, acting on left and right ventricular (RV) functions.

4.3.1 dDown Component

The left ventricle is directly filled by the pulmonary venous return and not by the systemic return. So any change in the amount of blood in the pulmonary circulation will immediately have an effect on left ventricular (LV) preload and then on LVSV [4]. The normal amount of blood in the pulmonary circulation is around 500 mL: 80 mL in the pulmonary arteries, 120 mL in the pulmonary capillaries, and 300 mL in the pulmonary veins [5]. During tidal ventilation, increases in intrathoracic and TPP will induce a fall in right ventricular stroke volume (RVSV), leading to emptying of the pulmonary circulation described as "low tide" by Versprille [6]. A few heartbeats later, during expiration, this will result in a decrease in LV preload and finally a decrease in LVSV (Fig. 4.4).

Decrease in RVSV during tidal ventilation is promoted by two very different mechanisms: a decrease in systemic venous return and an increase in (RV) afterload. In an experimental study, Scharf et al. demonstrated that application of a positive intrathoracic pressure, without any change in TPP, induced a fall in cardiac output related to a decrease in systemic venous return, as shown by a decrease in transmural right atrial pressure [7]. In the same study, an increase in TPP also induced a fall in cardiac output, though this was related to an increase in RV afterload, as shown by an increase in transmural right atrial pressure.

4.3.1.1 Decrease in Systemic Venous Return

During tidal ventilation, intrathoracic pressure increases. By transmission, it induces an increase in intravascular right atrial pressure (Fig. 4.2b),

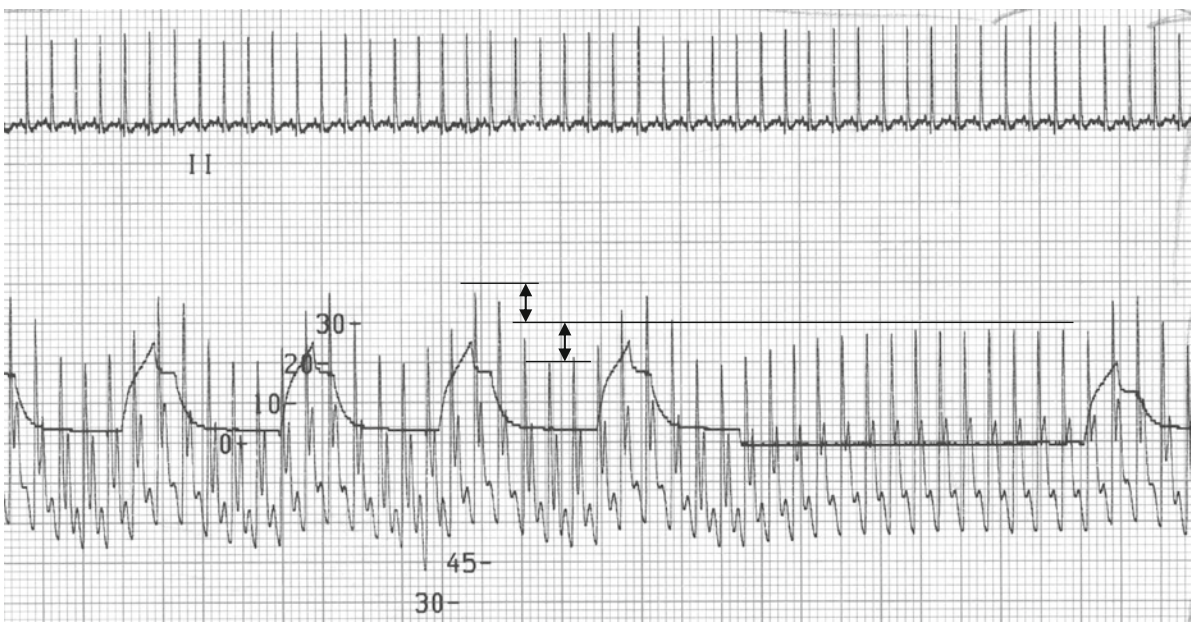

Fig. 4.3 Invasive arterial pressure recorded by a radial catheter in a mechanically ventilated patient. Systolic arterial pressure increases during inspiration and decreases during expiration. The end-expiratory pause distinguishes the dDown from the dUp effect (*black arrows*)

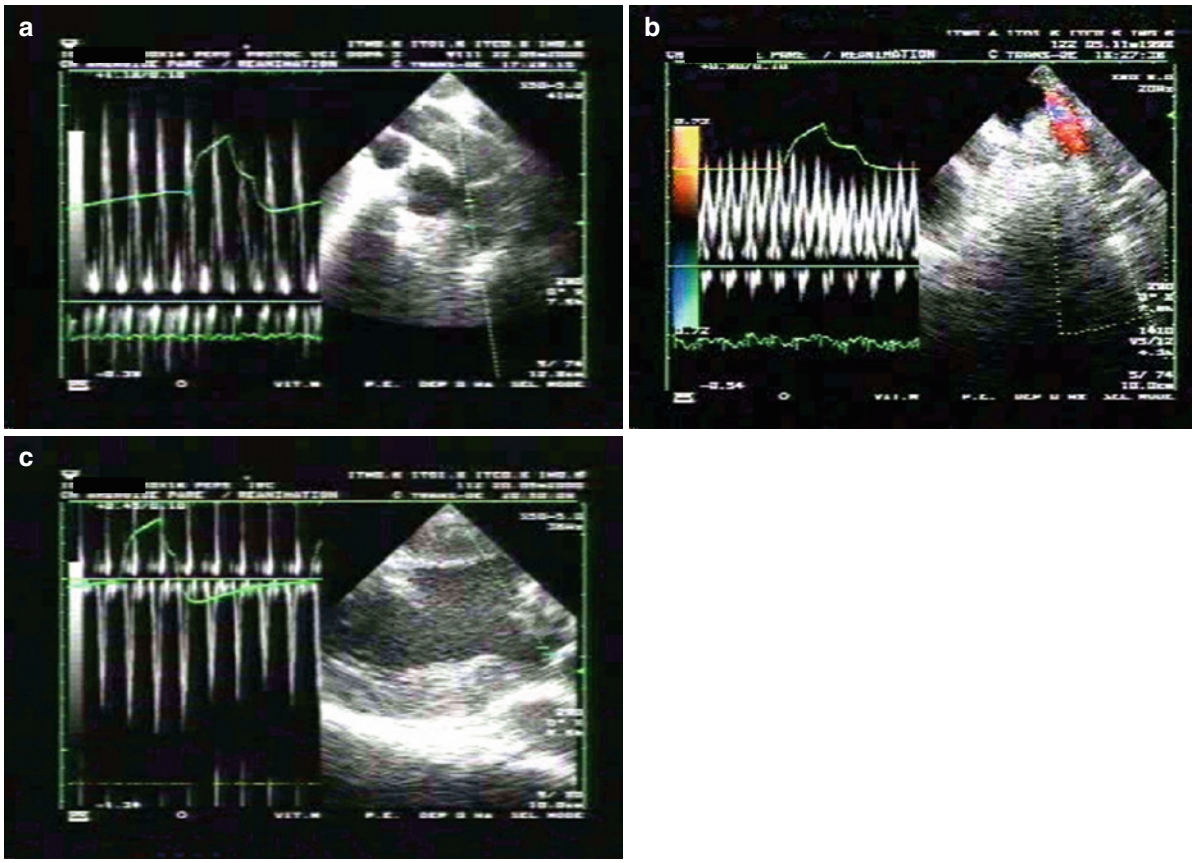

Fig. 4.4 Transesophageal echocardiography in a mechanically ventilated patient. Recording of right ventricular ejection flow (**a**), pulmonary venous flow (**b**), and left ventricular ejection flow (**c**) using pulsed Doppler. A fall in right ventricular ejection, occurring from the beginning of inspiration, was responsible for a decrease in left atrial filling at the beginning of expiration and finally for a fall in left ventricular ejection. This fall is maximal at the end of expiration

leading to a decrease in systemic venous return related to a decrease in the driving pressure gradient for venous return (Fig. 4.5a) [8]. Decrease in systemic venous return then induces a decrease in RV preload, reflected by a decrease in transmural right atrial pressure (Fig. 4.2b), and so a fall in RVSV (Fig. 4.5b) [9].

Recently, another mechanism has been proposed to explain the decrease in systemic venous return during tidal ventilation – collapse of the superior vena cava (Fig. 4.6) [10]. Because this vessel is subject to intrathoracic pressure, it can collapse in certain conditions, such as hypovolemia [11], and this collapse is correlated with dDown [12]. Transesophageal echocardiography easily visualizes the superior vena cava [11].

4.3.1.2 Increase in RV Afterload

During tidal ventilation, TPP increases and impedes circulation in the pulmonary capillaries. Whittenberger et al. in 1960 reported a nonlinear relationship between TPP and pulmonary vascular resistance [13]. From a certain pressure, any slight additional increase is responsible for a large increase in resistance [13]. This phenomenon is related to changes in West's zones [14]. When the alveolar pressure becomes higher than the pulmonary venous pressure (zone 2), and also higher than the pulmonary artery pressure (zone 1), it induces a partial or complete collapse of the pulmonary capillaries [14]. This is what happens in certain parts of the lung in mechanically ventilated patients. Because of the sensitivity of the right ventricle to any

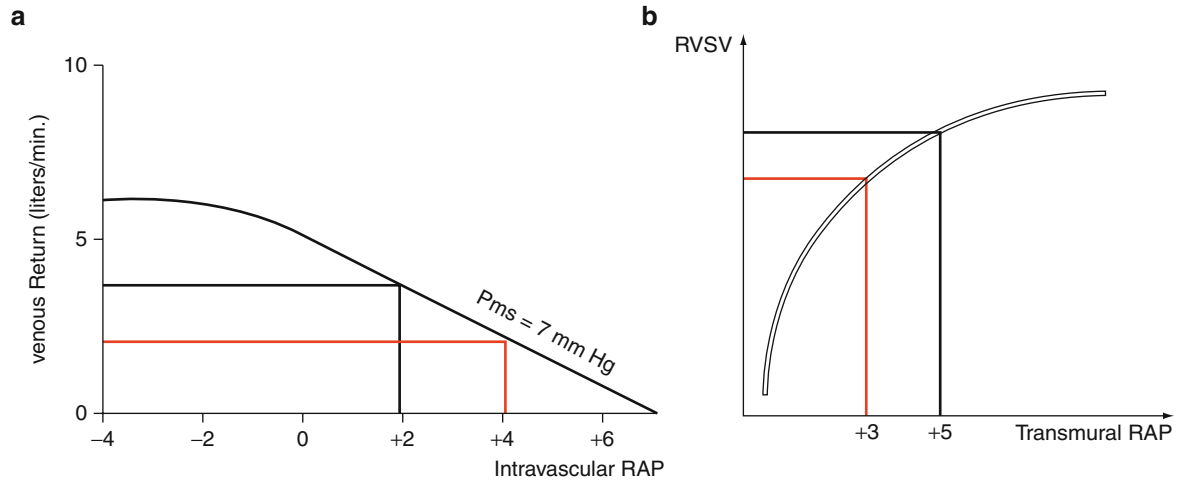

Fig. 4.5 Guyton's curve of systemic venous return (**a**) and Frank–Starling's curve of right ventricular systolic function (**b**). During tidal ventilation, an increase in intrathoracic pressure induces an increase in intravascular right atrial pressure from 2 to 4 mmHg by transmission, leading to a decrease in the driving pressure gradient (**a**) and so to a decrease in systemic venous return. The consequence is a decrease in transmural right atrial pressure, from 5 to 3 mmHg for instance, leading to a decrease in right ventricular stroke volume (**b**). Pms, mean systemic pressure; RAP, right atrial pressure; RVSV, right ventricular stroke volume

acute change in its afterload, cyclic increase in pulmonary vascular resistance during tidal ventilation will induce a fall in RVSV. This was well demonstrated using the pulmonary artery catheter and later by echocardiography [15,16]. It allows us to understand the high sensitivity of the right ventricle to any increase in plateau pressure in ARDS, for instance [17].

4.3.1.3 Hemodynamic Effect of Mechanical Ventilation: Right Ventricular Preload or Afterload Effect?

How the RV preload or afterload effect of mechanical ventilation predominates depends on hemodynamic conditions and the respiratory mechanics of the patient. Decrease in systemic venous return will predominate in patients with hypovolemia with a normal or only slightly decreased lung compliance. In this situation, change in intrathoracic pressure during tidal ventilation represents almost 50% of the change in alveolar pressure [18]. Conversely, increase in RV afterload will predominate in a patient with a suitable plasma volume and a significantly decreased lung compliance. In this situation, alveolar pressure generated by tidal ventilation is higher and TPP represents a large part of it, whereas intrathoracic pressure accounts for less than 30% [19].

Finally, it is crucial to understand that these two mechanisms lead to the same result, i.e., a decrease in RVSV during tidal ventilation, and thus a dDown effect, but that their management greatly differs. Whereas volume expansion can be indicated in the case of a preload effect, when ventilation has clinical consequences for the patient, it is not indicated and is even potentially deleterious in the case of afterload effect. In this situation, correct management is simply to decrease RV afterload by limiting TPP.

4.3.2 dUp Component

Applying a positive pressure to the lung will crush the pulmonary capillaries and so have effects upstream on the right ventricle. But it will also have consequences downstream by pushing blood from the capillaries to the left ventricle, improving LV filling, increasing LVSV, and so promoting the dUp effect [12,19]. By recording blood flow into the pulmonary veins and evaluating left atrial size, echocardiography is especially useful in characterizing this phenomenon (Fig. 4.7), which can be visualized providing the pulmonary circulation is normally filled, i.e., in a patient with a normal plasma volume or even more so in a patient with volume overload.

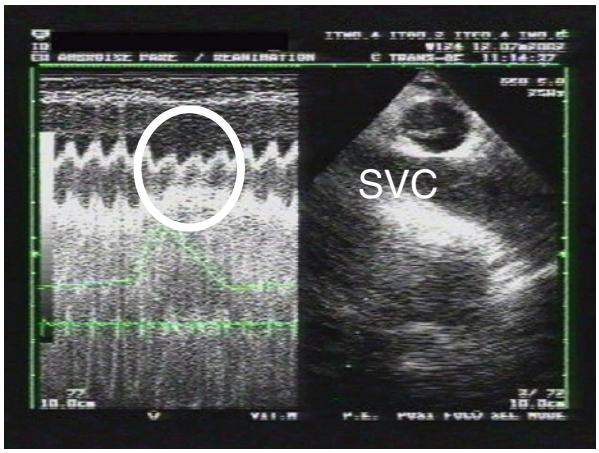

ZEEP

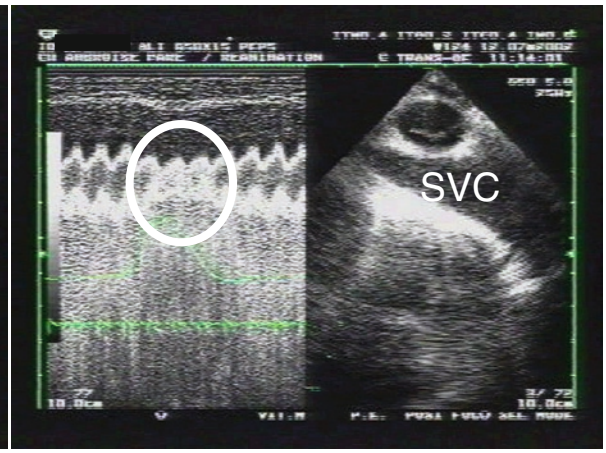

PEEP 5 cmH_2O

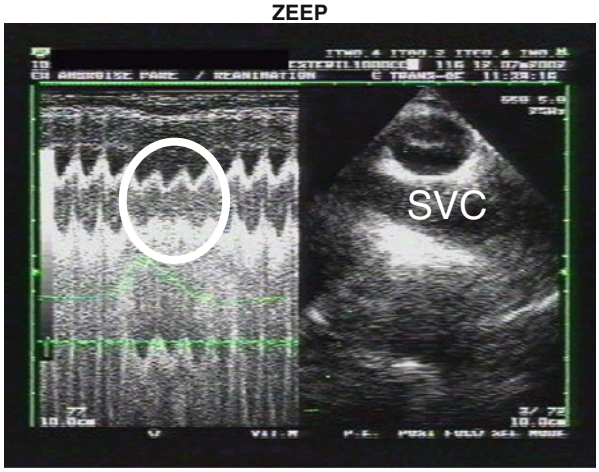

PEEP 5 cmH_2O
Volume expansion

Fig. 4.6 Longitudinal view of the superior vena cava (SVC) by the transesophageal route in a mechanically ventilated patient, using motion mode coupled with the two-dimensional mode. With zero end-expiratory pressure, tidal ventilation induces a partial collapse of the vessel, whereas with 5 cm H_2O positive end-expiratory pressure (PEEP) tidal ventilation induced a complete collapse of the vessel, corrected after 500 mL of fluid infusion. ZEEP, zero end-expiratory pressure

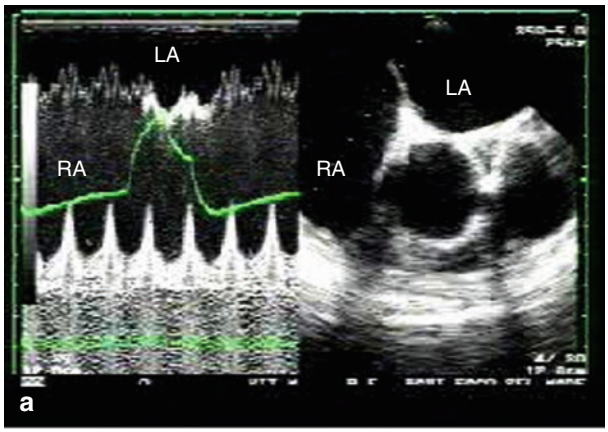

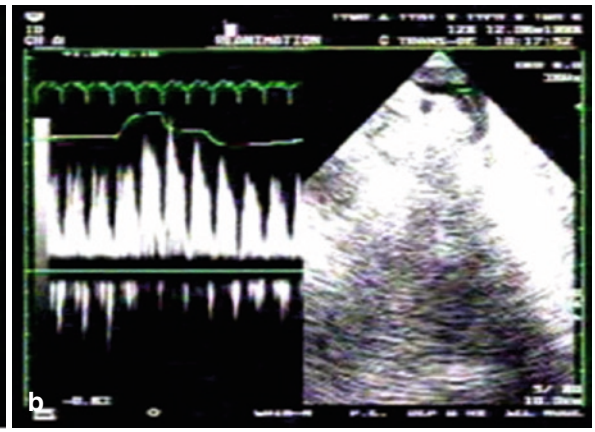

Fig. 4.7 Transesophageal echocardiography in a mechanically ventilated patient. (**a**) Motion mode through the interatrial septum. Inspiration was responsible for an increase in left atrial size. (**b**) In the same patient, pulsed Doppler in the right and upper pulmonary vein showed blood boosted from the pulmonary circulation to the left atrium. LA, left atrium; RA, right atrium; interatrial septum

Decrease in LV afterload is also thought to explain improvement in LV ejection during tidal ventilation [20,21]. It could be related to an increase in intrathoracic pressure [22]. It has, in particular, been reported in patients with a failed afterload-dependent left ventricle [23].

4.4 Conclusion

Knowledge of heart–lung interactions is essential for correct use of recent techniques of hemodynamic monitoring, as echocardiography. It sheds light on the value and limits of hemodynamic indices developed in recent years. It also helps us to understand the consequences of various ventilatory strategies, especially in ARDS.

References

1. Pinsky MR, Payen D (2005) Functional hemodynamic monitoring. Crit Care 9:566–72
2. Massumi R, Mason D, Zakauddin V, Zelis R, Otero J, Amsterdam E (1976) Reversed pulsus paradoxus. N Engl J Med 289:1272–1275
3. Perel A, Pizov R, Cotev S (1987) Systolic blood pressure variations is a sensitive indicator of hypovolemia in ventilated dog subject to graded hemorrhage. Anesthesiology 67:498–502
4. Milnor W, Jose A, McGaff C (1960) Pulmonary vascular volume, resistance and compliance in man. Circulation 22:130
5. Roughton F (1945) Average time spent by blood in the human lung capillary and its relation to the rates of CO uptake and elimination in man. Am J Physiol 143:621
6. Versprille A (1990) The pulmonary circulation during mechanical ventilation. Acta Anaesthesiol Scand 34:51–62
7. Scharf SM, Caldini P, Ingram RH (1977) Cardiovascular effect of increasing airway pressure in the dog. Am J Physiol 232:H35–43
8. Guyton A, Lindsey A, Abernathy B, Richardson T (1957) Venous return at various right atrial pressures and the normal venous return curve. Am J Physiol 189:609–615
9. Sarnoff SJ, Berglund E (1954) Ventricular function. I. Starling's law of the heart studied by means of simultaneous right and left ventricular function curves in the dog. Circulation 9:706–18
10. Vieillard-Baron A, Augarde R, Prin S, Page B, Beauchet A, Jardin F (2001) Influence of superior vena caval zone conditions on cyclic changes in right ventricular outflow during respiratory support. Anesthesiology 95:1083–1088
11. Jardin F, Vieillard-Baron A (2006) Ultrasonographic examination of the venae cavae. Intensive Care Med 32: 203–6
12. Vieillard-Baron A, Chergui K, Augarde R, Prin S, Page B, Beauchet A et al (2003) Cyclic changes in arterial pulse during respiratory support revisited by Doppler echocardiography. Am J Respir Crit Care Med 168:671–6
13. Whittenberger JL, McGregor M, Berglund E, Borst HG (1960) Influence of state of inflation of the lung on pulmonary vascular resistance. J Appl Physiol 15:878–882
14. West J, Dollery C, Naimark A (1964) Distribution of blood flow in isolated lung; relation to vascular and alveolar pressures. J Appl Physiol 19:713–724
15. Jardin F, Brun-Ney D, Cazaux P, Dubourg O, Hardy A, Bourdarias JP (1989) Relation between transpulmonary pressure and right ventricular isovolumetric pressure change during respiratory support. Cathe Cardiovasc Diagn 16:215–20
16. Vieillard-Baron A, Loubières Y, Schmitt JM, Page B, Dubourg O, Jardin F (1999) Cyclic changes in right ventricular output impedance during mechanical ventilation. J Appl Physiol 87:1644–1650
17. Jardin F, Vieillard-Baron A (2007) Is there a safe plateau in ARDS? The right heart only knows. Intensive Care Med 33:444–7
18. Jardin F, Genevray B, Brun-Ney D, Bourdarias JP (1985) Influence of lung and chest wall compliances on transmission of airway pressure to the pleural space in critically ill patients. Chest 88:653–8
19. Jardin F, Farcot JC, Gueret P, Prost JF, Ozier Y, Bourdarias JP (1983) Cyclic changes in arterial pulse during respiratory support. Circulation 68:266–274
20. Buda A, Pinsky M, Ingels N, Daughters G, Stinson E, Alderman E (1979) Effect of intrathoracic pressure on left ventricular performance. N Engl J Med 301:453–459
21. Pinsky M, Summer W, Wise R, Permutt S, Bromberger-Barnea B (1983) Augmentation of cardiac function by elevation of intra-thoracic pressure. J Appl Physiol 54:950–955
22. McGregor M (1979) Pulsus paradoxus. N Engl J Med 301:480–482
23. Pizov R, Ya'ari Y, Perel A (1989) The arterial pressure waveform during acute ventricular failure and synchronized external chest compression. Anesth Analg 68:150–6

Measurement of Stroke Volume and Cardiac Output Using Echocardiography and Doppler

5

Bernard P. Cholley

Contents

B.P. Cholley
Service d'Anesthésie-Réanimation,
Hôpital Européen Georges Pompidou,
20 rue Leblanc, 75908, Paris cedex 15, France
e-mail: bernard.cholley@egp.aphp.fr

Echocardiography and Doppler provide an easy way to estimate systemic blood flow, i.e., stroke volume or cardiac output, in a noninvasive manner. The purposes of this chapter are (1) to emphasize why flow measurement is so central to hemodynamic management, (2) to describe how to perform cardiac-output measurement using echocardiography and Doppler, and (3) to illustrate the use of such measurements in quantifying the effects of therapeutic interventions in clinical practice.

5.1 Rationale for Measuring Stroke Volume or Cardiac Output in Critically Ill Patients

5.1.1 Tissue Perfusion

One of the central problems in the management of critical illness is to correct cardiovascular dysfunction in order to maintain adequate tissue perfusion. The concept of adequate tissue perfusion is rather vague, and there is neither a clear definition of it, nor a simple way to assess perfusion. The cardiovascular system aims at delivering oxygen and various substances that are necessary for cell metabolism and, at the same time, clearing out the by-products of cell metabolism (H^+ ions, carbon dioxide, etc.) throughout the organs. This process requires a complex association between hydrodynamic factors (flow and pressure) and biological conditions for the delivery of oxygen (i.e., appropriate hemoglobin concentration, oxygen availability, serum pH) and other substrates (i.e., adequate serum levels for glucose and various metabolites). It is therefore the task of an intensive care unit (ICU) physician to optimize all these factors to facilitate healing of failing organs and to prevent further damage that could result from prolonged inappropriate perfusion.

D. De Backer et al. (eds.), *Hemodynamic Monitoring Using Echocardiography in the Critically Ill*,
DOI: 10.1007/978-3-540-87956-5_5, © Springer-Verlag Berlin Heidelberg 2011

5.1.2 Why are Stroke Volume or Cardiac Output Infrequently Monitored?

There is a sharp contrast between the attention that is paid to maintain systemic arterial pressure within an acceptable range and the relative indifference toward flow. This difference may be explained in part by the fact that mean arterial pressure provides a numerical end point for resuscitation: values that are beyond admitted thresholds prompt well-defined therapeutic responses [1]. Unlike pressure, cardiac output value is not used as a therapeutic end point in resuscitation algorithms. Indeed, based on numerical value alone, it is virtually impossible to determine which cardiac output achieves adequate perfusion for a given patient. For this reason, many physicians consider biological markers of inadequacy of systemic blood flow, i.e., mixed venous oxygen saturation (SvO_2) and serum lactate, the only parameters worthy of attention. This, combined with technical difficulties associated with flow measurement, has prompted a large proportion of intensive care physicians to discard cardiac output from the panel of information that they use to conduct resuscitation. Although the usefulness of SvO_2 and lactate is absolutely uncontroversial, these markers can reflect only a gross discrepancy between oxygen demand and delivery. Flow variations that are not great enough to result in increased oxygen extraction (low SvO_2), anaerobic metabolism (increased lactate), or reduced mean arterial pressure will remain undetected if stroke volume or cardiac output are not monitored. The reflexes aiming at maintaining tissue perfusion keep mean arterial pressure within a narrow range, sometimes at the expense of flow. Unlike arterial pressure, flow is allowed to vary over a wide range of values. The lack of tight reflex adjustments for flow explains why cardiac output is affected by any alteration of the cardiovascular system. Flow is thus more suitable than mean arterial pressure in providing an early warning about circulatory disturbances. It is, therefore, entirely appropriate for an ICU physician to measure systemic flow in conjunction with arterial pressure and biological parameters in assessing the adequacy of oxygen delivery.

5.1.3 Venous Return Determinants

Flow is frequently altered during the time course of critical illness, and most therapeutic interventions commonly performed in ICU patients do affect cardiac output, often to a greater extent than pressure. To understand the great sensitivity of flow to all perturbations occurring in a critically ill patient, it is useful to focus on the determinants of venous return (VR), i.e., the amount of blood returning to the right ventricle, necessarily equal to cardiac output in the absence of shunt. Using a Poiseuillean approach, Guyton et al. provided a straightforward description of the determinants of VR [2, 3]. They stated that VR is proportional to the averaged pressure gradient between the small venules (origin of the veins) and the right atrium (where all venous blood is drained) and is inversely related to the resistance of the veins (Rv) [4, 5]. The driving pressure for VR (averaged pressure within the small veins) is termed mean systemic pressure (MSP). The backpressure opposing VR is right atrial pressure (RAP) [2, 6]. Therefore, the equation governing VR can be written as follows:

$$VR \approx (MSP - RAP)/Rv$$

The venous reservoir can be schematically depicted as in Fig. 5.1 [7]: a large bucket (roughly two-thirds of the blood volume is located within the veins) with variable capacitance (according to the degree of venous constriction or dilatation) and with a side vent. The height of this vent determines two compartments within the bucket: the fluid located below the vent cannot generate any flow and is termed unstressed volume. Conversely, fluid located above this vent is called stressed volume and determines the flow through the vent. The height of the vent above the bottom of the reservoir is proportional to RAP: the lower the vent (i.e., RAP), the easier the VR (and vice versa). The total height of liquid within the reservoir is proportional to MSP. It is

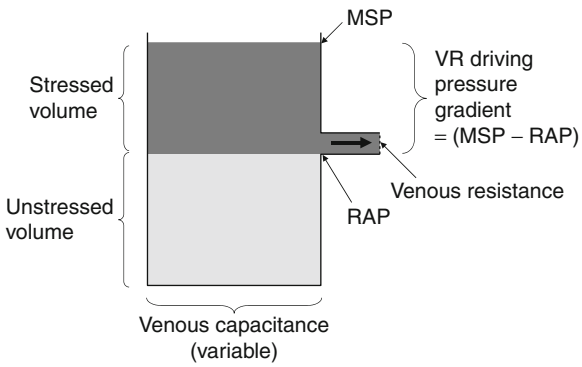

Fig. 5.1 The venous reservoir (see text). MSP, mean systemic pressure; RAP, right atrial pressure

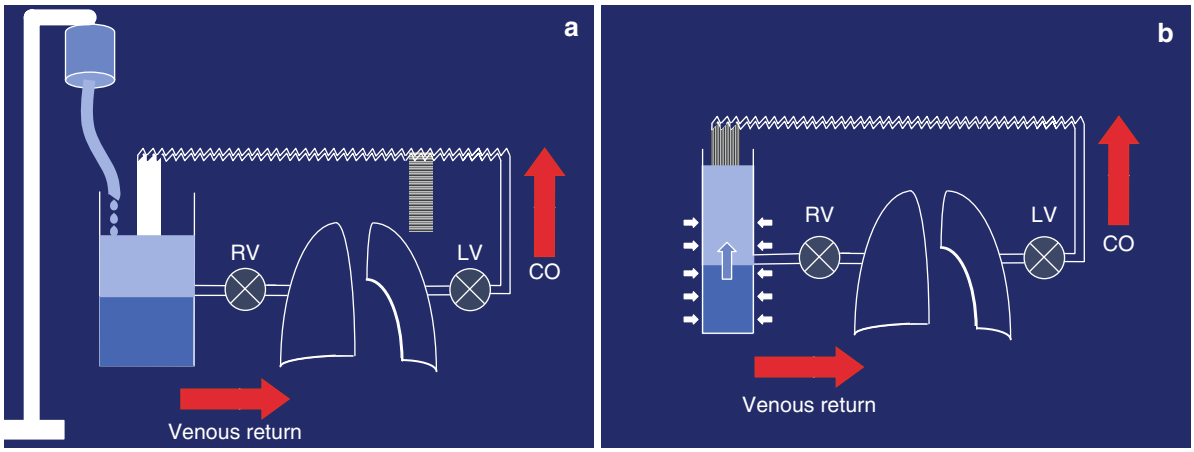

Fig. 5.2 Effect of two common therapeutic interventions on venous return and cardiac output. In (**a**) intravenous fluids increase venous return by increasing stressed volume (represented as liquid above the level of the vent) in the venous reservoir. In (**b**) vasoconstrictors also increase stressed volume at the expense of unstressed volume (represented as liquid under the level of the vent) and increase venous return and cardiac output. Note that both right and left ventricles need to be preload-dependent for venous return and cardiac output to increase in response to these maneuvers. RV, right ventricle; LV, left ventricle

obvious that VR is governed by the height of liquid above the vent, namely the pressure gradient between MSP and RAP. It is also obvious that this gradient can be manipulated either by changing the amount of fluid within the bucket or by changing the size of the bucket (venous constriction or dilatation) (Fig. 5.2).

5.1.4 Stroke Volume or Cardiac Output?

Cardiac output is the product of stroke volume and heart rate, but it is important to determine whether a change in cardiac output is due to a change in heart rate (proportional to myocardial oxygen consumption) or a change in beat-to-beat ejection performance (stroke volume). A reduction in stroke volume may be compensated by an increase in heart rate, which maintains cardiac output. However, this change undoubtedly reflects a less advantageous situation because the energetic cost for the myocardium has increased. Conversely, a fluid challenge may increase stroke volume, but not cardiac output, owing to the concomitant reduction in heart rate. Nevertheless, this is a beneficial result because the same systemic perfusion is achieved at lower energetic expense. In addition, beat-to-beat variations in stroke volume provide an insight into cardiopulmonary interactions and should not be neglected. For these reasons, techniques that provide mean cardiac output (l/min) are less relevant than those providing direct measurement of stroke volume (mL).

5.2 Stroke Volume Measurement Using Echocardiography and Doppler

Several methods have been described for stroke volume measurement, but the most widely accepted and easily applicable in practice is to use the left ventricular (LV) outflow tract diameter and flow velocity by combining transthoracic two-dimensional echocardiography and pulsed-wave Doppler [8, 9].

5.2.1 Step-By-Step Procedure

1. Obtain a parasternal long-axis view of the heart. Ensure there is no aortic stenosis by observing the free motion of the aortic cusps.
2. Freeze the image in systole, while the aortic cusps are fully opened and measure left ventricular outflow tract (LVOT) diameter by placing calipers at the insertion of the cusps (Fig. 5.3).
3. Obtain an apical five-chamber view of the heart.
4. Place the pulsed-wave Doppler window (width, 2–4 mm) in the LVOT, just below the aortic valve (Fig. 5.4).

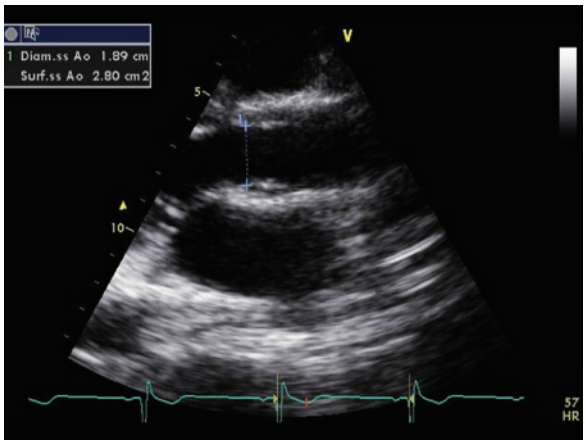

Fig. 5.3 Parasternal long-axis view with a zoom on the left ventricular outflow tract (LVOT). Measurement of LVOT diameter at the insertion of the aortic valves

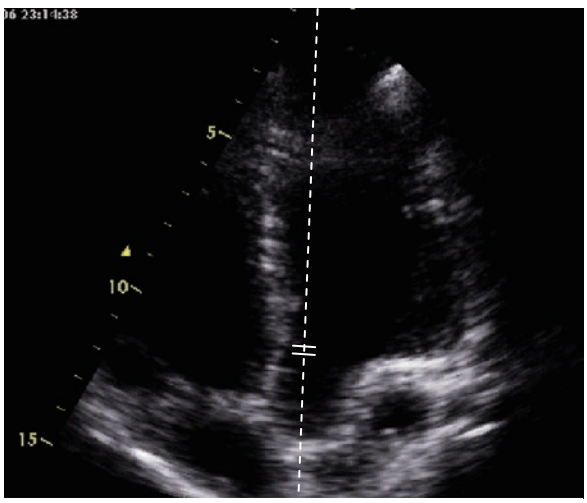

Fig. 5.4 Five-chamber view of the heart from the apex, showing the placement of the Doppler window in the left ventricular outflow tract

5. Record blood flow velocity in the LVOT, freeze the recording, and trace the envelope of maximal velocities. The machine computes the aortic velocity-time integral (VTI, cm), which represents the stroke distance or displacement of the red blood cells during systole. This stroke distance is multiplied by the LVOT cross-sectional area (calculated from aortic diameter and assuming the LVOT to be a cylinder) to obtain stroke volume (Fig. 5.5). Repeat this measurement on three to five consecutive beats (one respiratory cycle) and calculate the averaged stroke volume value. Taking exclusively end-expiratory cycles will not account for the respiratory variability but will reflect changes that are not biased by cyclic changes in VR.
6. Multiply the averaged stroke volume (mL/beat) by heart rate (beat/min) to obtain mean cardiac output (ml/min) (Fig. 5.6).

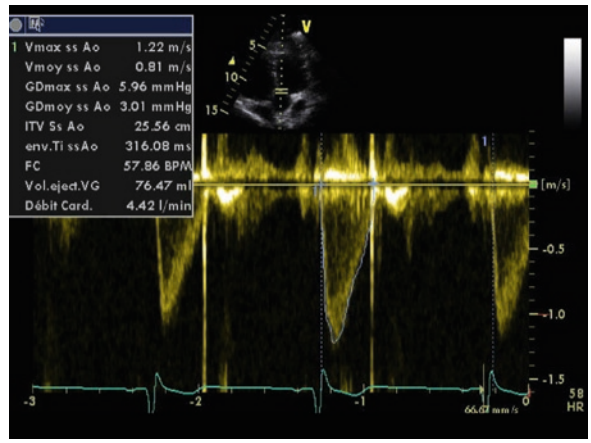

Fig. 5.5 Pulsed Doppler signal obtained at the level of the left ventricular outflow tract (LVOT). Note the characteristic shape of this envelope, consisting of a narrow line (slightly larger after peak systole), indicating that all red blood cells move at the same speed through the LVOT. The closing click of the aortic valve is visible. The maximal velocities have been delineated manually to compute the aortic velocity time interval (VTI)

Doppler measurements are very reproducible [10]. The main source of inaccuracy occurs in measuring the LVOT diameter. Any error in diameter measurement will be squared when computing the cross-sectional area, resulting in under- or overestimation of stroke volume. Variations in aortic VTI are strictly proportional to stroke volume variations because the LVOT cross-sectional area remains unchanged even when flow and pressure are modified. For this reason, variations in aortic VTI can precisely reflect the changes in flow that result from a therapeutic intervention or occur spontaneously. Values for aortic VTI in normal adults at rest are usually 20 ± 3 cm, with peak velocity values ranging from 0.7 to 1.1 m/s [11].

Pulsed-wave Doppler allows velocity measurements precisely at the site where the LVOT diameter is measured. However, in the absence of stenosis at the valvular or subvalvular level, continuous-wave Doppler can also be used since the LVOT is the narrowest chamber along the Doppler trajectory where the maximal velocity is recorded [12] (Fig. 5.7).

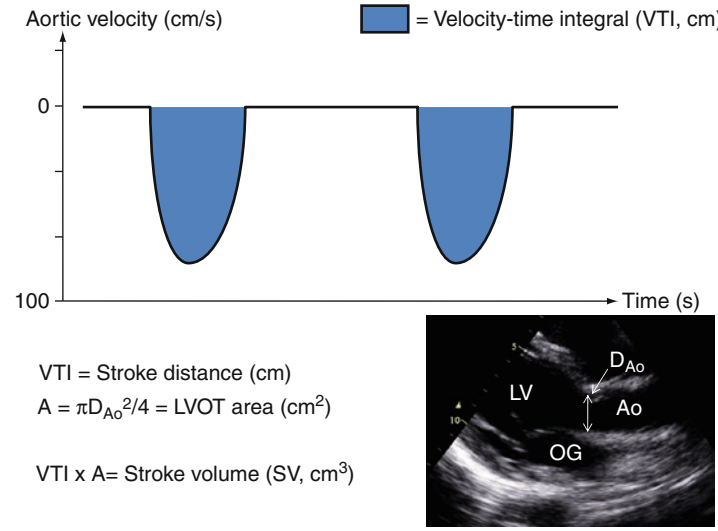

Fig. 5.6 Stroke volume is calculated as the product between aortic velocity-time interval (VTI; or stroke distance, cm) and aortic cross-sectional area (A, cm^2). The latter is calculated using the left ventricular outflow tract (LVOT) diameter (D_{Ao}, cm) measurement and assuming it has the shape of a disk

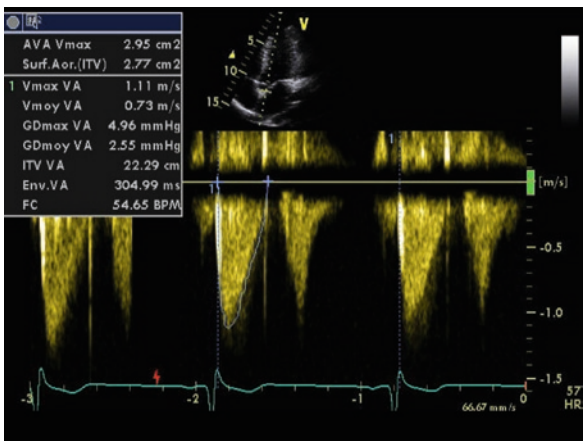

Fig. 5.7 Continuous-wave Doppler signal obtained at the level of the left ventricular outflow tract (LVOT). This envelope differs from the pulsed-wave Doppler envelope because it is "full," attesting that lower velocities are measured along the Doppler beam. However, the shape and calculated velocity-time interval (VTI) are exactly the same to those obtained with pulsed-wave Doppler because maximal velocities occur in the LVOT

The same technique can be applied to the transesophageal approach using continuous-wave [13, 14] or pulsed-wave Doppler [15, 16]. Measuring the LVOT diameter is usually more reliable using transesophageal echocardiography (TEE) [17], but aortic flow-velocity measurement requires careful probe positioning. To obtain the best alignment of the Doppler beam with aortic blood flow, one needs to visualize the LVOT (Fig. 5.8) either with a deep, transgastric, five-chamber view at 0°or a modified transgastric view at 120–130°.

5.2.2 Limitations of this Method

Aortic valvular stenosis and subaortic obstruction preclude the applicability of the procedure since the VTI of maximal velocities may not represent the stroke distance at the level of the LVOT, but rather at the level of stenosis. Atrial fibrillation requires the averaging of several consecutive aortic VTIs in order to obtain a reliable average value owing to beat-to-beat variability (see Chap. 9). Finally, this method overestimates the true forward flow in patients with aortic regurgitation because the regurgitant diastolic flow is not taken into account.

5.2.3 Other Possibilities for Stroke Volume or Cardiac Output Estimation Using Echocardiography and Doppler

Estimation of stroke volume at the level of the mitral or pulmonary valves has also been proposed, but measuring annular diameters is much less reliable than at the aortic level, resulting in greater variability in the calculated values [8]. Determining LV volumes from systolic and diastolic dimensions also offers a possibility to estimate stroke volume. However, whatever the algorithm (Teichholz, Simpson), minimal inaccuracies in dimensions will be magnified and affect the precision of stroke volume estimation [18].

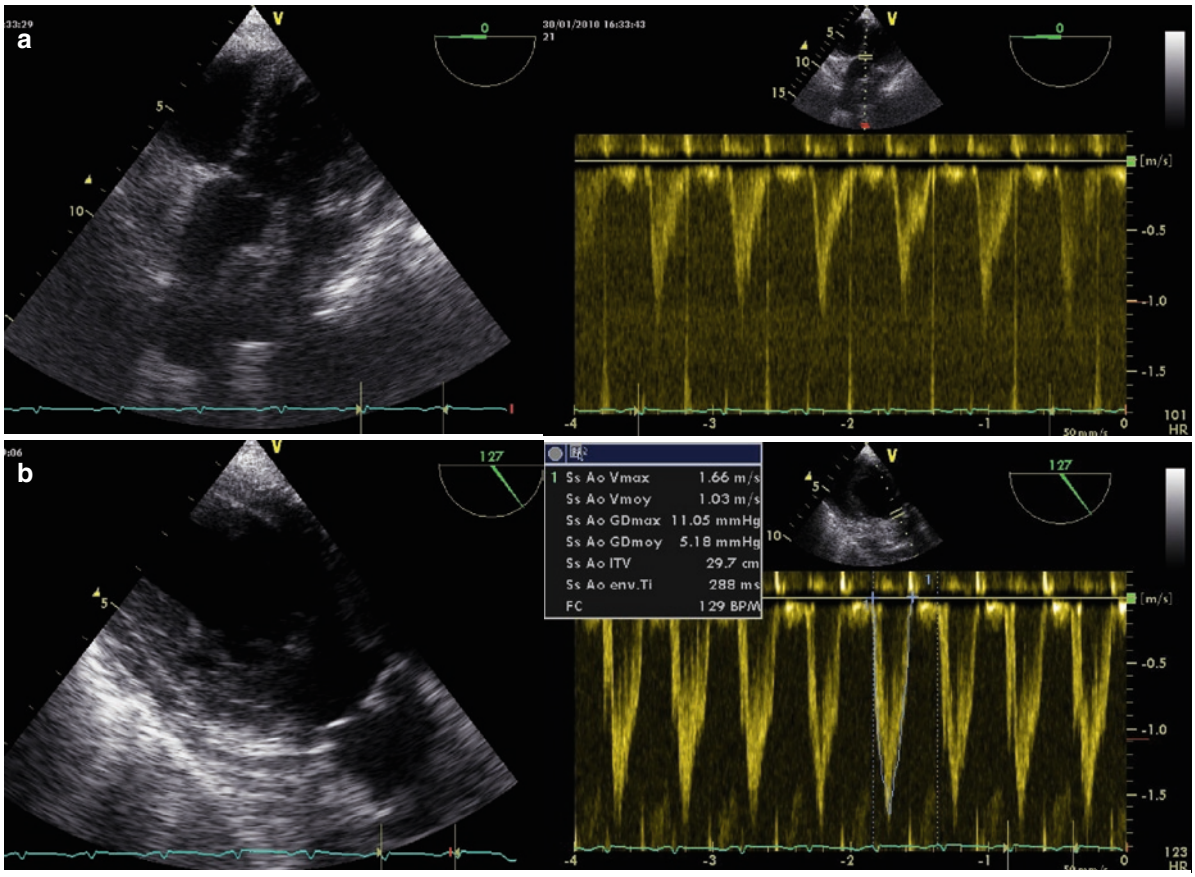

Fig. 5.8 Using the transesophageal approach, the left ventricular outflow tract (LVOT) flow velocity can be measured from two different views: (**a**) five-chamber view obtained at 0° from a deep transgastric window; (**b**) modified "long-axis" view obtained at 120°–130° from a transgastric window. Both provide a fair alignment between Doppler beam and LVOT flow

5.3 Scenarios Where Stroke Volume Measurement Can Assess Effects of Therapeutic Maneuver

5.3.1 Fluids

At the time of intravenous administration, fluid will be distributed in the vascular system. More than two-thirds of this fluid will increase the stressed volume in the venous reservoir (Fig. 5.2a) and reduce venous resistance by dilating the veins. As a consequence, VR and stroke volume will increase immediately, provided that both ventricles operate in the preload-dependent portion of their function curve. According to the type of fluid administered, the stroke volume increase will be maintained for a variable amount of time: prolonged for red blood cells and colloid solutions, shorter for crystalloids [19]. Monitoring stroke volume has two-fold benefits:

1. Stroke volume measurements before and after fluid administration allow the effect of administration to be quantified. In the example shown in Fig. 5.9, 250 mL of fluids were administered in a patient with hypotension (75/55 mmHg) and a heart rate of 94/min. The LVOT diameter could not be measured and an absolute value for the stroke volume was not calculated. This fluid challenge resulted in a 100% increase in aortic VTI (from 10 to 20 cm, Fig. 5.9) and stroke volume. At the same time, a 25% increase in systolic blood pressure (from 75 to 95 mmHg) was observed, and the heart rate remained unchanged. This example shows that even a small amount of fluid can have a large effect on flow.

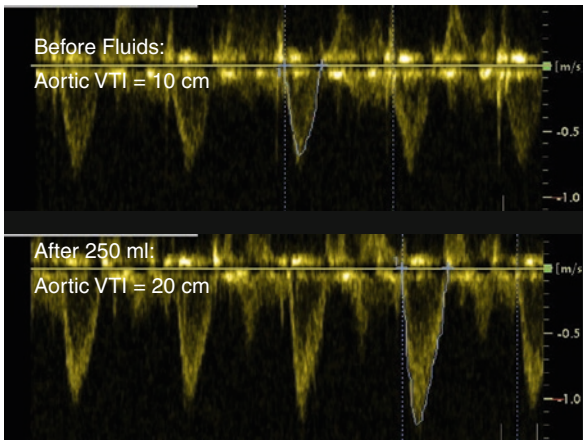

Fig. 5.9 Aortic velocity time interval (VTI) measurement before and after a fluid challenge of 250 mL of normal saline. An increase of 100% was noted, reflecting the increase in stroke volume. At the same time, arterial pressure increase was much less (25%)

2. Stroke volume measurement reduces the risk of excess of blood-volume expansion, which can lead to venous congestion. Repeating the same fluid challenge (250 mL) in the example shown in Fig. 5.9 did not yield further increase in LV stroke volume, attesting that the plateau of the cardiovascular function curve had been reached. This information is crucial because it informs the physician that more fluid will not improve perfusion but will result in venous congestion upstream from the weaker ventricle. Using a small volume for the challenge (or a passive leg-raising maneuver) and quantifying its effect on the stroke volume is the most reliable method to avoid excess fluid administration [5]. Unlike methods based on respiratory variations of systolic pressure, pulse pressure, or stroke volume, the direct quantification of stroke volume (or aortic VTI) after each fluid challenge does not suffer such limitations as pulmonary hypertension, right ventricular failure, or inappropriate settings of the ventilator [20–23]. It is therefore very safe provided that fluids are administered by titrating small volumes and interrupted as soon as there is no more stroke volume increase.

5.3.2 Nitric Oxide Inhalation

In another example, the effect of nitric oxide administration was evaluated in a young patient on day 1 after bilateral lung transplantation for cystic fibrosis. Nitric oxide administration had been interrupted an hour before, and as this was well tolerated the patient was extubated. However, a few minutes after extubation, the patient became tachypneic and peripheral oxygen saturation (SpO_2) dropped to 85%. Bilateral infiltrates were present in the chest X-ray. Aortic VTI was measured as 12.6 cm (Fig. 5.10), but stroke volume could not be calculated owing to poor imaging of the LVOT. Nitric oxide was reintroduced in the nasal prongs. Within the following minutes, SpO_2 increased to 95% and aortic VTI to 14.6 cm (+15%). Reducing right ventricular afterload improved right ventricular ejection and, subsequently, systemic blood flow, which may, in part, explain the reduction in oxygen extraction.

5.3.3 Inotropes/Vasodilators

A 60-year-old man with advanced ischemic cardiomyopathy underwent mitral and tricuspid annuloplasties and a coronary artery bypass graft of the left anterior descending coronary artery for severe ischemic mitral regurgitation. Forty-six days after surgery, it was not possible to wean him from dobutamine and from the ventilator. Baseline measurements while the patient was receiving dobutamine (12 μg/kg/min) showed an ejection fraction of around 30% and a stroke volume fluctuating between 25 and 40 mL owing to multiple premature beats. In an attempt to facilitate weaning from dobutamine, levosimendan was infused (0.1 μg/kg/min). After introducing this inotropic/vasodilating agent, we were able to taper and finally stop dobutamine and wean the patient from the ventilator. On day 3 after the introduction of levosimendan and with dobutamine having been reduced to only 3 μg/kg/min, echocardiography and Doppler documented the improvement in circulatory status (Fig. 5.11). Systemic arterial pressure was unchanged, ejection fraction was mildly affected (≈35%), but the average stroke volume had increased by more than 60%. This case emphasizes that in end-stage heart failure, a therapeutic intervention may have minimal effects on systemic arterial pressure and parameters of LV function, but at the same time improve systemic blood flow to a great extent.

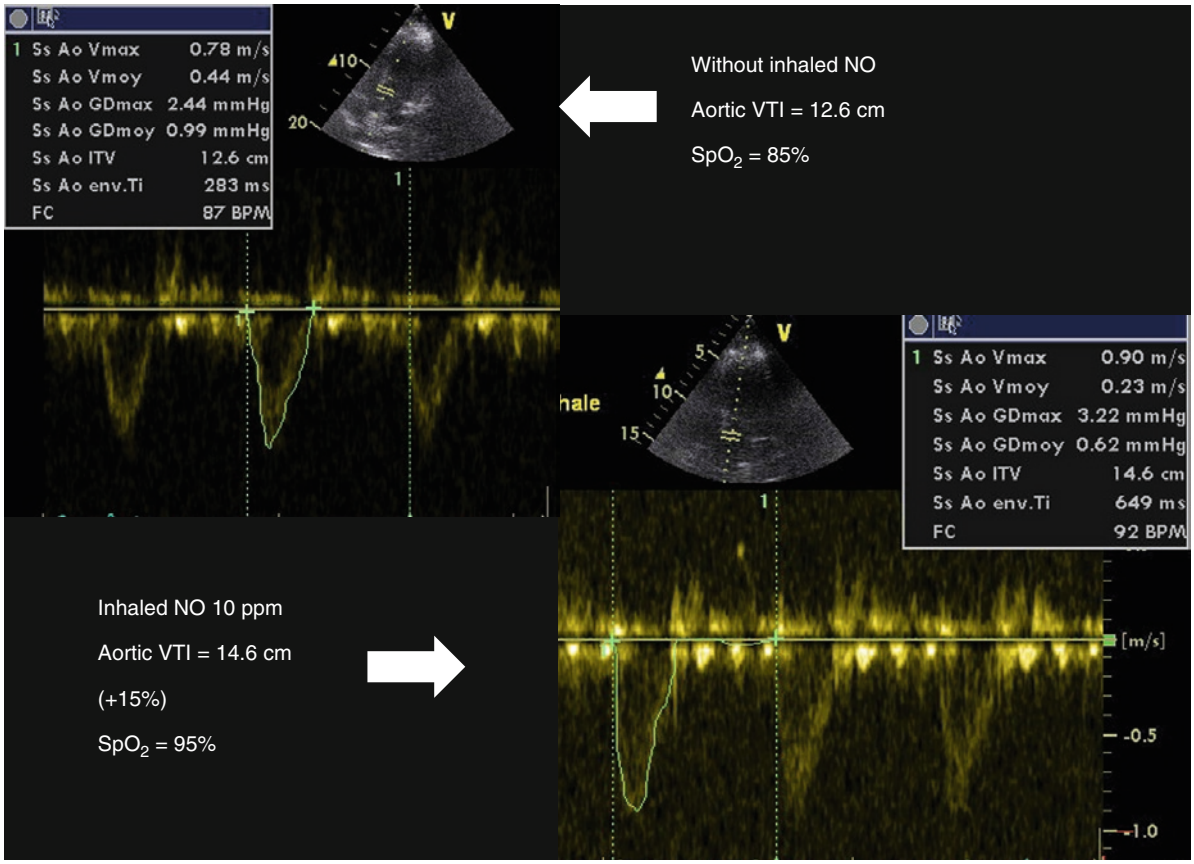

Fig. 5.10 Aortic velocity-time interval (VTI) measurement before and after adjunct inhaled nitric oxide (NO). Note a 15% increase in stroke volume and a concomitant improvement in peripheral oxygen saturation (SpO_2): from 85% to 95%

5.4 Conclusions

Echocardiography and Doppler offer an easy way to assess stroke volume and cardiac output. Since the vast majority of therapeutic interventions in the ICU aim at improving tissue perfusion, it is clearly meaningful to assess their effect on flow. In addition, a lack of response to a small fluid challenge (or a passive leg-raising maneuver) attests that the patient is no longer fluid-responsive, will not benefit from more volume, and may develop congestion if this therapy is not discontinued.

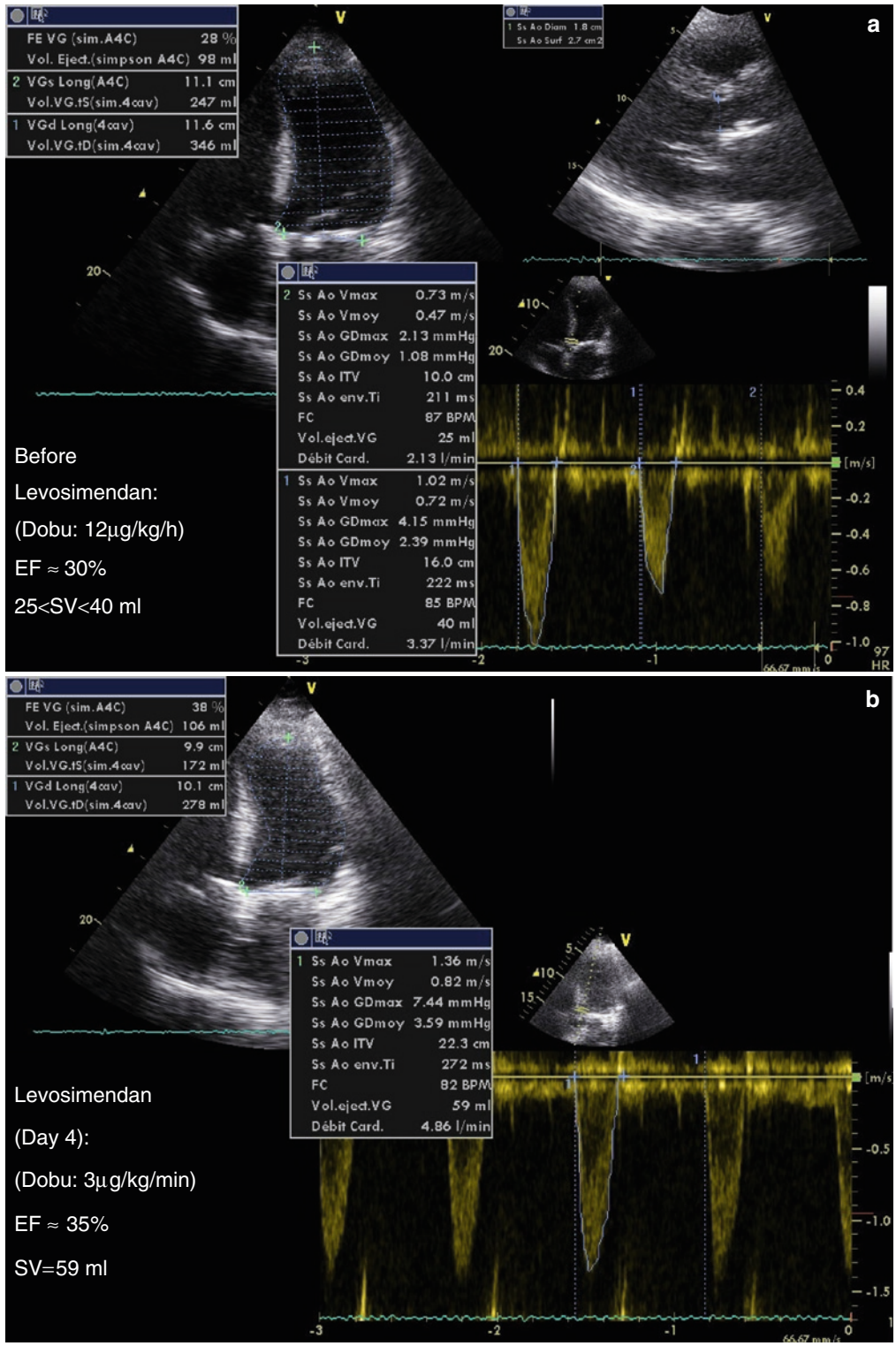

Fig. 5.11 Stroke volume and ejection fraction (EF) measurement before (**a**) and after (**b**) treatment with levosimendan. Note the spectacular increase in stoke volume (SV) despite a reduction in dobutamine (Dobu) infusion, while EF tends to increase slightly

References

1. Dellinger RP, Carlet JM, Masur H et al (2004) Surviving Sepsis Campaign guidelines for management of severe sepsis and septic shock. Crit Care Med 32:858–73
2. Guyton AC, Lindsey AW, Abernathy B, Richardson T (1957) Venous return at various right atrial pressures and the normal venous return curve. Am J Physiol 189:609–15
3. Guyton AC, Guyton AC (1992) Overview of the circulation; medical physics of pressure, flow, resistance, and vascular compliance. In: Human physiology and mechanisms of disease. Saunders, Philadelphia, pp 110–6
4. Guyton AC, Abernathy B, Langston JB, Kaufmann BN, Fairchild HM (1959) Relative importance of venous and arterial resistances in controlling venous return and cardiac output. Am J Physiol 196:1008–14
5. Cholley BP (2008) Fluids: replace or restrict? In: Kuhlen R, Moreno R, Ranieri M, Rhodes A (eds) Controversies in critical care. Medizinisch Wissenschaftliche Verlagsgesellschaft, Berlin, pp 457–3
6. Magder S (2006) The classical Guyton view that mean systemic pressure, right atrial pressure, and venous resistance govern venous return is/is not correct. J Appl Physiol 101:1533
7. Sylvester JT, Goldberg HS, Permutt S (1983) The role of the vasculature in the regulation of cardiac output. Clin Chest Med 4:111–26
8. Lewis JF, Kuo LC, Nelson JG, Limacher MC, Quinones MA (1984) Pulsed Doppler echocardiographic determination of stroke volume and cardiac output: clinical validation of two new methods using the apical window. Circulation 70:425–31
9. Moulinier L, Venet T, Schiller NB, Kurtz TW, Morris RC Jr, Sebastian A (1991) Measurement of aortic blood flow by Doppler echocardiography: day to day variability in normal subjects and applicability in clinical research. J Am Coll Cardiol 17:1326–33
10. Robson SC, Murray A, Peart I, Heads A, Hunter S (1988) Reproducibility of cardiac output measurement by cross sectional and Doppler echocardiography. Br Heart J 59:680–4
11. Weyman AE, Griffin B (1994) Left ventricular outflow tract: the aortic valve, aorta, and subvalvular outflow tract. In: Weyman AE (ed) Principles and practice of echocardiography. Lea & Febiger, Philadelphia, pp 498–574
12. Huntsman LL, Stewart DK, Barnes SR, Franklin SB, Colocousis JS, Hessel EA (1983) Noninvasive Doppler determination of cardiac output in man: clinical validation. Circulation 67:593–602
13. Katz WE, Gasior TA, Quinlan JJ, Gorcsan J 3rd (1993) Transgastric continuous-wave Doppler to determine cardiac output. Am J Cardiol 71:853–7
14. Darmon PL, Hillel Z, Mogtader A, Mindich B, Thys D (1994) Cardiac output by transesophageal echocardiography using continuous-wave Doppler across the aortic valve. Anesthesiology 80:796–805, discussion 25A
15. Stoddard MF, Prince CR, Ammash N, Goad JL, Vogel RL (1993) Pulsed Doppler transesophageal echocardiographic determination of cardiac output in human beings: comparison with thermodilution technique. Am Heart J 126:956–62
16. Descorps-Declere A, Smail N, Vigue B et al (1996) Transgastric, pulsed Doppler echocardiographic determination of cardiac output. Intensive Care Med 22:34–8
17. Shiran A, Adawi S, Ganaeem M, Asmer E (2009) Accuracy and reproducibility of left ventricular outflow tract diameter measurement using transthoracic when compared with transesophageal echocardiography in systole and diastole. Eur J Echocardiogr 10:319–24
18. Axler O, Megarbane B, Lentschener C, Fernandez H (2003) Comparison of cardiac output measured with echocardiographic volumes and aortic Doppler methods during mechanical ventilation. Intensive Care Med 29:208–17
19. Chappell D, Jacob M, Hofmann-Kiefer K, Conzen P, Rehm M (2008) A rational approach to perioperative fluid management. Anesthesiology 109:723–40
20. De Backer D, Heenen S, Piagnerelli M, Koch M, Vincent JL (2005) Pulse pressure variations to predict fluid responsiveness: influence of tidal volume. Intensive Care Med 31:517–23
21. Mahjoub Y, Pila C, Friggeri A et al (2009) Assessing fluid responsiveness in critically ill patients: false-positive pulse pressure variation is detected by Doppler echocardiographic evaluation of the right ventricle. Crit Care Med 37:2570–5
22. De Backer D, Taccone FS, Holsten R, Ibrahimi F, Vincent JL (2009) Influence of respiratory rate on stroke volume variation in mechanically ventilated patients. Anesthesiology 110:1092–7
23. Muller L, Louart G, Bousquet PJ et al (2009) The influence of the airway driving pressure on pulsed pressure variation as a predictor of fluid responsiveness. Intensive Care Med 22:22

Assessment of Fluid Requirements: Fluid Responsiveness

6

Michel Slama and Julien Maizel

Contents

6.1 Introduction

In many clinical situations, such as hypotension, shock, renal failure, oliguria, and clinical and/or laboratory signs of dehydration, hypovolemia may be suspected. Hypovolemia can be both absolute and relative. Absolute hypovolemia is defined as a reduction of the total circulating blood volume, which may be related to blood or plasma loss. Relative hypovolemia is defined as an inadequate distribution of blood volume between the central and peripheral compartments. In septic shock patients, absolute and relative hypovolemia are both involved in genesis of shock.

Two different approaches are adopted by intensivists to manage patients with clinically suspected hypovolemia: performing a fluid challenge [1] or predicting fluid responsiveness [2, 3]. When performing a fluid challenge, the attending (or frontline) intensivist infuses fluids and analyzes the clinical effect in terms of increase in blood pressure, cardiac output, static pressure, such as central venous pressure (CVP) or pulmonary artery occlusion pressure (PAOP), and signs of shock and tissue perfusion improvement (see Chap. 7). Thus, the response is given a posteriori. In contrast, with the fluid-responsiveness approach, intensivists analyze and record some indicators before fluid infusion to predict the effect in term of increasing cardiac output. Echocardiography is a noninvasive method that has created interest in intensive care units, particularly in France and other parts of Europe, and is increasingly used, not only as an imaging modality, but also as a hemodynamic tool [4–8]. It helps in establishing the diagnosis, in developing a therapeutic plan, and then in monitoring the results of therapeutic intervention in patients with hemodynamic failure.

M. Slama (✉)
Unité de réanimation médicale, service de néphrologie, CHU Sud, 80054, Amiens Cedex 1, France
e-mail: slama.michel@chu-amiens.fr

J. Maizel
INSERM, ERI 12, Université Jules Verne, France
e-mail: maizel.julien@chu-amiens.fr

D. De Backer et al. (eds.), *Hemodynamic Monitoring Using Echocardiography in the Critically Ill*,
DOI: 10.1007/978-3-540-87956-5_6, © Springer-Verlag Berlin Heidelberg 2011

This technique may assist the intensivist in identifying the volume responsiveness in patients with hemodynamic failure.

In this chapter, we describe the echocardiographic parameters for assessing fluid responsiveness. These indices are especially useful in complex situations, such as in septic shock after initial resuscitation, and not obvious clinical situations, such as hemorrhagic shock or severe hypovolemic shock, in which fluid infusion or blood transfusion should not be delayed.

6.2 Frank–Starling Relationship

The Frank–Starling curve for the heart consists of two portions: [1] a steep first portion with linear preload and related to SV. On this portion, any change in preload is accompanied by a significant change in SV: the patient is preload dependent; [2] a second flat portion, in which modifications of ventricular preload are associated with almost no change in SV: the patient is preload independent (Fig. 6.1).

Hypovolemia results in a decrease in cardiac preload, and both ventricles are then operating on the steep portion of the Frank–Starling curve. Determination of preload dependency is a critical issue for the patient in shock. Low preload often means that fluid infusion by increasing venous return may increase SV, cardiac output, and peripheral tissue perfusion. By contrast, because many Frank–Starling curves are possible, according to the heart systolic function, a given preload may be placed for one patient on the steep portion (preload dependent) or on the flat portion of the Frank–Starling curve for another (preload independent) (Fig. 6.1). Therefore, fluid responsiveness cannot be predicted by an absolute value of the preload. To assess fluid responsiveness, the heart should be tested by transient modification of preload. This is effected during a fluid challenge, and it can be predicted using the effects of mechanical ventilation on the systemic venous return [9, 10].

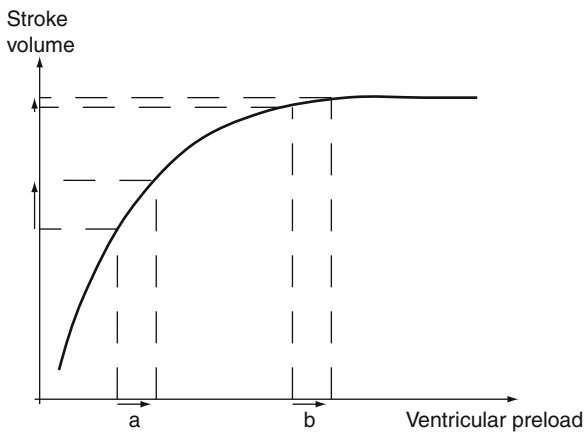

Fig. 6.1 Frank–Starling curve. (**a**) Steep portion of the curve. Any preload modification leads to an increase in SV (preload reserve or dependency). (**b**) Flat portion of the curve. An increase in left ventricular preload does not change the SV (no preload reserve or preload independency)

6.3 Static Parameters

A static parameter is measured under a single ventricular loading condition and is presumed to provide a reliable estimate of the preload of one or both ventricles. This estimation of the preload can then be used to evaluate the probability of responsiveness to ventricular filling by assuming that lower preload increases the probability of response to volume expansion.

The CVP may be assessed by measuring the size of the inferior vena cava (IVC) by transthoracic echocardiography [11], which allows the diameter to be gauged at end expiration. If the patient is on mechanical ventilation, the correlation between IVC size and CVP is low (Fig. 6.2) [11–14]. Feissel et al. have demonstrated that, in general, absolute IVC size as well as CVP failed to predict fluid responsiveness in patients under mechanical ventilation in septic shock; however, an IVC diameter of less than 10 mm may predict a positive response to fluid infusion [15]. In contrast, a congestive IVC with a large diameter (>20 mm) often excluded any fluid responsiveness (figure avec IVC virtuel et IVC congestive) (Fig. 6.2).

Echocardiography may be used to determine PAOP noninvasively by Doppler indices derived from mitral flow (E/A ratio), pulmonary venous flow, tissue Doppler (E/Ea ratio), and color-coded Doppler (E/Vp ratio) [16, 17]. In general, PAOP fails

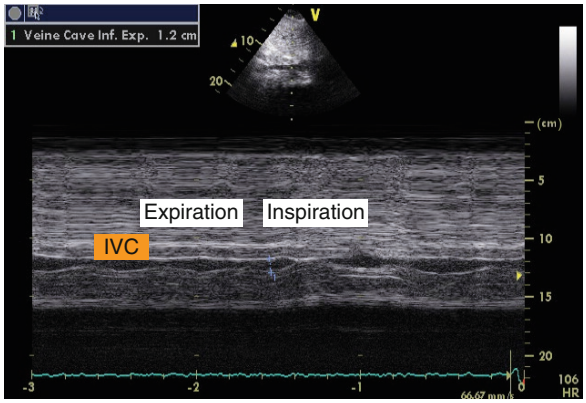

Fig. 6.2 Inferior vena cava (IVC) in M-mode. The IVC is almost virtually collapsed during inspiration in this spontaneously breathing patient

to demonstrate any relationship with increase in cardiac output after fluid expansion and is therefore not useful in predicting fluid responsiveness [1]. However, a restrictive pattern of the mitral flow, when present, is very suggestive of fluid unresponsiveness since it reflects high left ventricular (LV) filling pressures.

The right ventricular (RV) as well as LV diastolic diameter, area, and volume are reliable parameters of preload. Tavernier et al. and Feissel et al. have shown that LV size is a useful predictor of fluid responsiveness in patients on mechanical ventilation only if the left ventricle is very small and hyperkinetic (Fig. 6.3) [18, 19]. This corresponds to a very low preload and therefore predicts a positive response to fluid infusion. In other situations, preload responsiveness cannot be predicted by LV size, except in the operating room. Indeed, providing that LV size is recorded at baseline, any significant decrease in LV size during surgery is suggestive of the need for fluids.

In a study by Kumar et al. on healthy volunteers, static indices of ventricular preload (CVP, PAOP, LV end-diastolic volume index, RV end-diastolic volume index) and cardiac performance indices (cardiac index, SV index) were measured before and after 3 L of normal saline loading [20]. There was no correlation between changes in CVP and PAOP and variations in cardiac performance indices (cardiac index, SV index). As well, no relationship was observed between baseline measurements of static indices and variations in cardiac performance indices after fluid loading.

In conclusion, standard indices of preload are not useful in predicting volume responsiveness except in patients with very low preload. Therefore, dynamic parameters of volume responsiveness are the best available alternative.

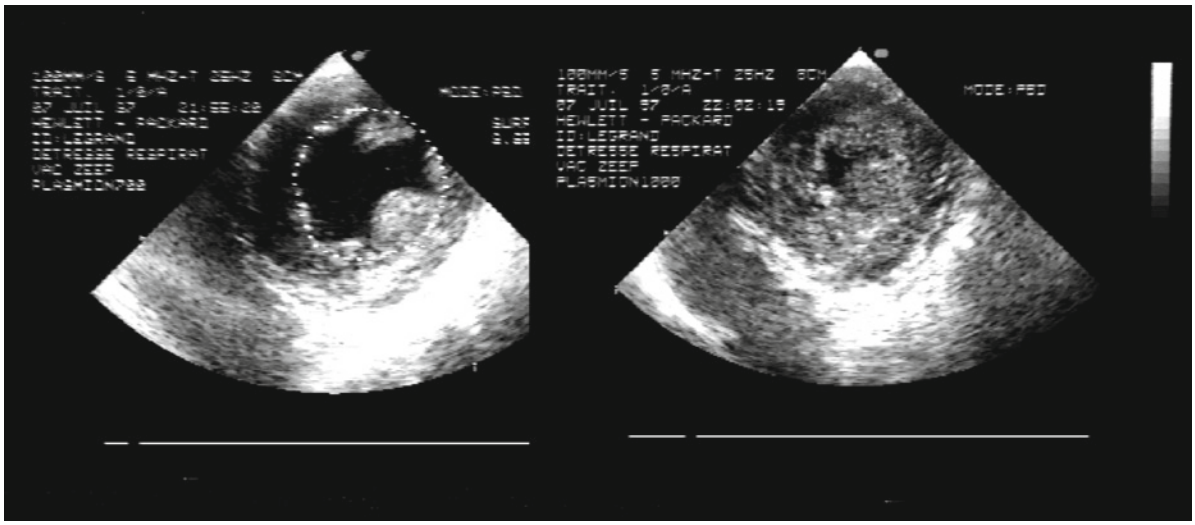

Fig. 6.3 Left ventricle in the short axis. Left, diastole; right, systole. The left ventricle is small and hyperkinetic

6.4 Dynamic Parameters

Dynamic parameters are used to determine whether the patient is on the ascending or flat portion of the Frank–Starling curve. Several approaches can be used to ascertain on what portion of the preload/SV relationship the ventricle is functioning in order to establish the diagnosis of preload dependence or independence. The effect of mechanical ventilation and passive leg-raising on the Frank–Starling relationship was tested to predict fluid responsiveness in ICU patients, particularly in those with septic shock.

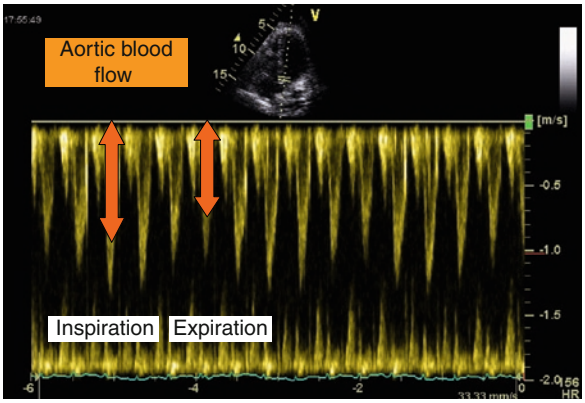

Fig. 6.4 Aortic blood flow recorded using pulsed Doppler at the level of the aortic annulus. There is a large respiratory change. This patient will respond to fluid infusion if the cardiac output is increased

6.4.1 Effect of Mechanical Ventilation

The effect of mechanical ventilation on intrathoracic pressures and SV is the basis for many of the dynamic measurements that are useful in determining volume responsiveness. They are presented in detail elsewhere (see Chap. 4). Briefly, cyclic changes in intrathoracic pressures induced by mechanical ventilation induce cyclic changes in LV preload that will induce cyclic changes in SV if the patient is on the ascending part of the Frank–Starling curve (fluid responsive).

6.4.2 Dynamic Parameters in Patients on Mechanical Ventilation

Analysis of the respiratory changes of LV SV during mechanical ventilation provides a dynamic evaluation of preload dependence. The respiratory changes in SV can be estimated by transesophageal echocardiography (TEE) or transthoracic echocardiography (TTE). In a patient without spontaneous inspiratory effort, the SV of the left ventricle increases during inspiration and decreases during expiration. Slama et al. demonstrated in animals that progressive blood withdrawal is closely related to increased respiratory variation in aortic blood flow [3]. In clinical studies, maximal aortic blood flow velocity or velocity–time integral (VTI) changes measured with TEE predicted with high sensitivity and specificity, and predictive values increase in cardiac output after fluid infusion in patients with shock (Fig. 6.4). A cutoff value of 12% for maximal velocity and 20% for respiratory-cycle changes of aortic VTI discriminated responder from nonresponder patients [21].

IVC and superior vena cava (SVC) diameter changes during mechanical ventilation have also been proposed as a means of predicting fluid responsiveness. IVC diameter was analyzed from a longitudinal subcostal view and recorded using M-mode (Fig. 6.5) [15]. The SVC was recorded from the TEE longitudinal view at 90–100° (Figs. 6.6 and 6.7) [22]. In a patient without spontaneous inspiratory effort, the IVC dilates during inspiration (maximal diameter) and decreases during expiration (minimal diameter), whereas the SVC may collapse during inspiration (minimal diameter) and increase during expiration (maximal diameter). The distensibility index of the IVC may predict fluid responsiveness. A cutoff value of 12% (using max–min/mean value) and 18% (by using max–min/min) has been proposed. The collapsibility index of the SVC may also predict fluid responsiveness. A cutoff value of 36% (sensitivity 90%, specificity 100%; max–min/max) was found to distinguish accurately between fluid responders and nonresponders [15, 22, 23].

Very importantly, there is a close relationship between all of the described parameters and an increase in cardiac output after fluid infusion. Therefore, large respiratory changes may predict a large increase in cardiac output after fluid infusion.

Dynamic approach has significant methodological limitations. Firstly, all patients have to be on

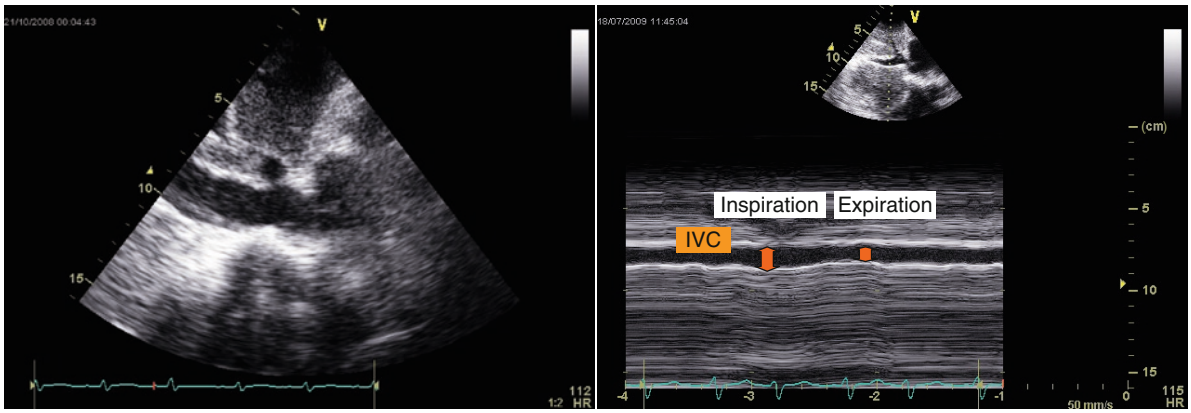

Fig. 6.5 Left, inferior vena cava (IVC) in bidimentional (BD); *right*, IVC in M-mode. The IVC diameter increases during mechanical insufflation. By measuring the smallest and largest dimensions, the collapsibility index can be calculated

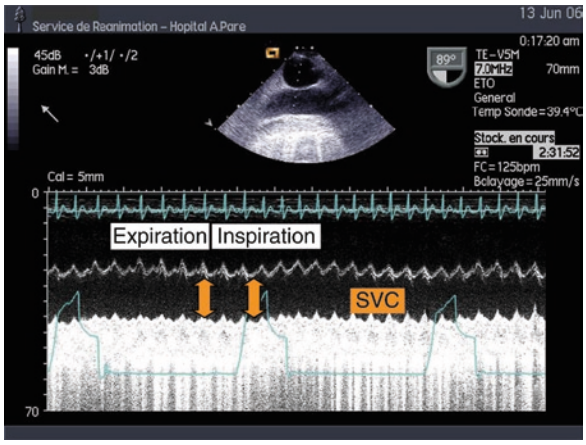

Fig. 6.6 Superior vena cava (SVC). There is no change during mechanical insufflation. The distensibility index is lower than 36%, indicating the patient would

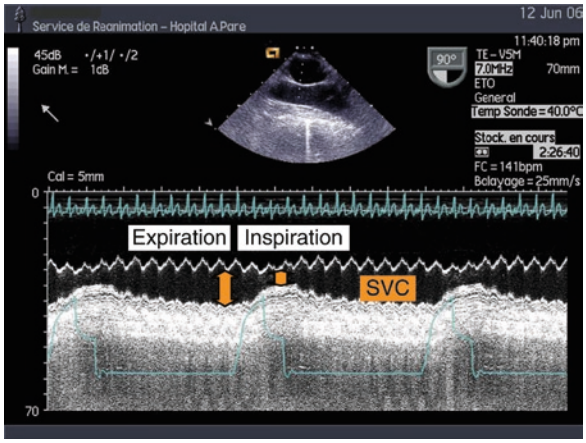

Fig. 6.7 Superior vena cava (SVC). The large diameter changes during mechanical insufflation indicate a responder patient

mechanical ventilation and passive in their interaction with the ventilator without spontaneous breathing effort during the measurement. They have also to be in sinus heart rhythm (except for IVC and SVC variations).

Moreover, some studies have suggested that patients ventilated for acute respiratory distress syndrome (ARDS) with a tidal volume lower than 7 mL/kg could be responsible for false negatives, based on the fact that tidal ventilation is then inadequate to induce significant changes in heart preload [24]. A recent study has proposed adjusting respiratory changes by alveolar driving pressure [alveolar pressure minus total positive end-expiratory pressure (PEEP)] so as to provide a more accurate assessment of fluid responsiveness [24].

Finally, these methods have been studied in patients with sepsis, but they have not been extensively examined in patients with concurrent heart disease. This is of particular concern in patients with RV dysfunction. Such patients may show false-positive respiratory changes in SV [25]. Respiratory changes in SV appear to be due to RV afterload changes and do not reflect a need for fluid resuscitation.

Technical problems have also been described. There are pitfalls with IVC and SCV measurements. In addition to the need to obtain a good-quality image, translational artifacts may be a problem. As the respiratory cycles, it displaces the liver and the adjacent IVC. The IVC may appear to change in size when it simply shifts out of the ultrasound beam plane. In such cases, there is no actual change in IVC size, even though that is how it appears. Additionally, during measurement of

aortic blood flow, Doppler sample volume may move and thereby lead to a false indication of respiratory changes in aortic blood flow.

6.4.3 Dynamic Parameters in Spontaneously Breathing Patients

All previously described parameters failed to predict fluid responsiveness in spontaneously breathing patients. Recently, the passive leg-raising (PLR) test has been proposed as an alternative to the fluid-challenge test to predict preload dependence (Fig. 6.8) [26–29]. This maneuver rapidly mobilizes about 300 mL of blood from the lower limbs to the intrathoracic compartment and reproduces the effects of volume expansion. It is reversible and devoid of any risk of volume expansion. The test consists of raising the lower limbs elevated at 45° from the 45° semirecumbent position while measuring SV and cardiac output before and approximately 1 min after the PLR maneuver. It is readily accomplished by measuring the VTI of the aortic outflow velocity-with TTE.

In two recent studies, aortic VTI, SV, and cardiac output were recorded using transthoracic echocardiography in spontaneously breathing patients during PLR. Lamia et al. demonstrated in 24 patients that PLR induced an increase in SV of 12.5% or more predicted an increase in SV of 15% or more after volume expansion with a sensitivity of 77% and a specificity of 100% [28]. In this study, static indices of preload, such as LV end-diastolic area and E/Ea, did not predict volume responsiveness. Patients were intubated with spontaneous breathing movements. In the study of Maizel et al., 34 patients were spontaneously breathing without a tracheal tube [27]. An increase in cardiac output or SV by 12% or more during PLR was highly predictive of central hypovolemia. Sensitivity and specificity values were 63% and 89%, respectively, for cardiac output and 69%, and 89% for SV. A close correlation was observed between cardiac output changes during leg-raising and changes in cardiac output after fluid expansion. Of particular note is that these studies have demonstrated that PLR may be used to predict volume responsiveness in patients with atrial fibrillation. PLR also achieves good accuracy in patients under mechanical ventilation.

In several situations, the PLR test may give false-negative results. In profound hypovolemia, there is almost no blood in the legs, and thus the very small amount of mobilized blood is insufficient to test heart preload sensitivity. Similarly, leg bandages that exert pressure on the veins may lead to false-negative findings with this maneuver. In any event, this test should be performed by changing the position of the bed and not simply by carrying out a PLR. Initially, the patient should be in a semirecumbent 45° position and the bed shifted such that the patient is in a supine position with the legs elevated at 45° (Fig. 6.9). Larger preload changes were demonstrated during this position change when compared with moving the bed, such that the patient went from a semirecumbent to supine position

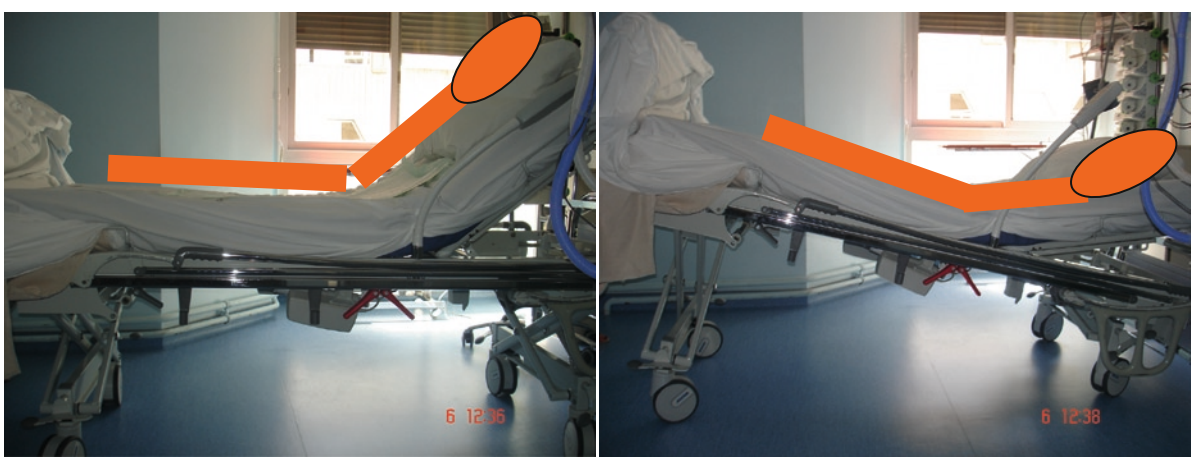

Fig. 6.8 Passive leg-raising maneuver

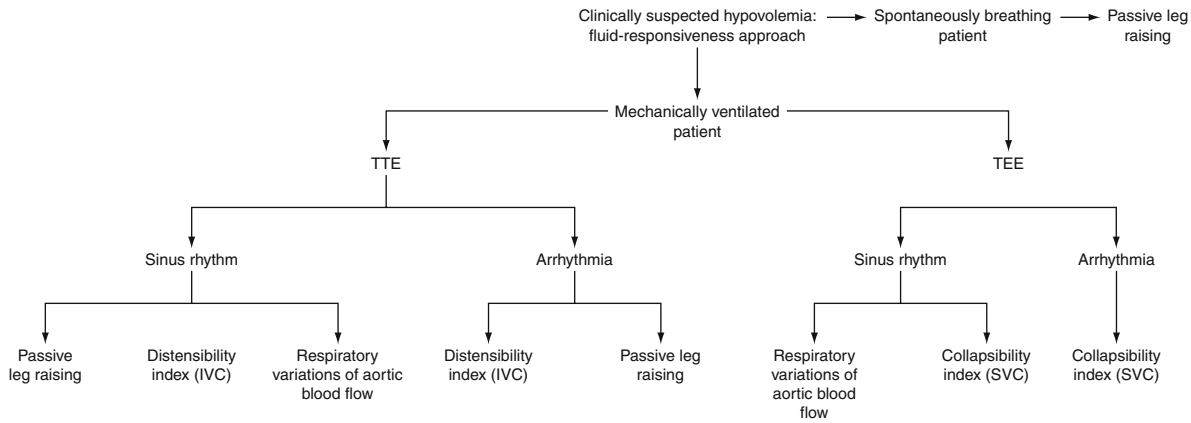

Fig. 6.9 Fluid responsiveness. TTE, transthoracic echocardiography; TEE, transesophageal echocardiography; IVC, inferior vena cava; SVC, superior vena cava

[30]. This study would appear to demonstrate that when a patient is moved from a semirecumbent 45° to a supine position with the legs at a 45° elevation, mobilized blood comes from both the legs and the abdomen. Simple PLR is an insufficient test for fluid responsiveness. It has been our experience that the higher the intra-abdominal pressure, the lower the response to the PLR maneuver.

6.5 Clinical Application

It has to be emphasized that echocardiography is only useful within the overall clinical context. Normal individuals without hemodynamic compromise exhibit volume responsiveness: they are on the steep preload-dependent portion of the Frank–Starling curve. Patients who show echocardiographic evidence of preload dependence should receive volume resuscitation only if there is evidence of clinically significant hemodynamic failure. Echocardiography should always be integrated within the overall clinical picture. Therefore, echocardiographic evidence of fluid responsiveness does not warrant volume resuscitation unless the clinician identifies hemodynamic failure, which may improve by augmenting cardiac output (Fig. 6.9).

In certain clinical situations, the need for immediate volume resuscitation is manifest, such as massive hemorrhage, severe dehydration due to gastrointestinal disease, major third-space losses, and obvious septic shock. The clinical context and physical examination allow the recognition of severe central hypovolemia, where immediate volume resuscitation is appropriate. Initial resuscitation is generally accomplished to some extent before transfer to the ICU.

Norepinephrine infusion is widely used in patients with shock. This may influence dynamic variables of fluid responsiveness and decrease SV variations [31, 32].

The intensivist then has to address the question of whether to continue volume resuscitation. A balance has to be struck between the patient's needs and the potential harmful effects of fluid infusion. In this regard, indices of volume responsiveness, as well as PAOP evaluation using the E/Ea ratio, may help the clinician in managing the patient.

6.6 Conclusion

Echocardiographic methods may help the intensivist to determine the need for fluid infusion in patients with hemodynamic failure. Very low static parameters are usually associated with fluid responsiveness: a small IVC or small hyperdynamic LV corresponds to profound hypovolemia with immediate need for fluid infusion. But most of the time, these static parameters fail to predict a positive response in patients with suspected hypovolemia. Dynamic parameters should, therefore, be preferred. The clinician with basic critical care echocardiography skills may use respiratory

variation of IVC diameter to identify the preload-dependent patient. The intensivist with more advanced skills may use respiratory variation of the SVC, aortic blood flow, or SV determined by echocardiography and changes in SV or aortic VTI following the PLR maneuver to identify volume responsiveness.

References

1. Dellinger RP, Levy MM, Carlet JM, Bion J, Parker MM, Jaeschke R, International Surviving Sepsis Campaign Guidelines Committee, American Association of Critical-Care Nurses, American College of Chest Physicians, American College of Emergency Physicians, Canadian Critical Care Society, European Society of Clinical Microbiology and Infectious Diseases, European Society of Intensive Care Medicine, European Respiratory Society, International Sepsis Forum, Japanese Association for Acute Medicine, Japanese Society of Intensive Care Medicine, Society of Critical Care Medicine, Society of Hospital Medicine; Surgical Infection Society, World Federation of Societies of Intensive and Critical Care Medicine et al (2008) Surviving sepsis campaign: international guidelines for management of severe sepsis and septic shock. Crit Care Med 36:296–327
2. Michard F, Teboul JL (2002) Predicting fluid responsiveness in ICU patients: a critical analysis of the evidence. Chest 121:2000–8, Review
3. Slama M, Masson H, Teboul JL, Arnout ML, Susic D, Frohlich E, Andrejak M (2002) Respiratory variations of aortic VTI: a new index of hypovolemia and fluid responsiveness. Am J Physiol Heart Circ Physiol 283:H1729–33
4. Cholley BP, Vieillard-Baron A, Mebazaa A (2006) Echocardiography in the ICU: time for widespread use! Intensive Care Med 32:9–10
5. Mayo PH, Beaulieu Y, Doelken P, Feller-Kopman D, Harrod C, Kaplan A, Oropello J, Vieillard-Baron A, Axler O, Lichtenstein D, Maury E, Slama M, Vignon P (2009) American College of Chest Physicians/La Société de Réanimation de Langue Française statement on competence in critical care ultrasonography. Chest 135:1050–60
6. Vieillard-Baron A, Slama M, Cholley B, Janvier G, Vignon P (2008) Echocardiography in the intensive care unit: from evolution to revolution? Intensive Care Med 34:243–9
7. Slama MA, Novara A, Van de Putte P, Diebold B, Safavian A, Safar M, Ossart M, Fagon JY (1996) Diagnostic and therapeutic implications of transesophageal echocardiography in medical ICU patients with unexplained shock, hypoxemia, or suspected endocarditis. Intensive Care Med 22:916–22
8. Vignon P, Mentec H, Terré S, Gastinne H, Guéret P, Lemaire F (1994) Diagnostic accuracy and therapeutic impact of transthoracic and transesophageal echocardiography in mechanically ventilated patients in the ICU. Chest 106:1829–34
9. Monnet X, Teboul JL (2007) Volume responsiveness. Curr Opin Crit Care 13:549–53
10. National Heart, Lung, and Blood Institute Acute Respiratory Distress Syndrome (ARDS) Clinical Trials Network, Wiedemann HP, Wheeler AP, Bernard GR, Thompson BT, Hayden D, deBoisblanc B, Connors AF Jr, Hite RD, Harabin AL (2006) Comparison of two fluid-management strategies in acute lung injury. N Engl J Med 354:2564–75
11. Jardin F, Vieillard-Baron A (2006) Ultrasonographic examination of the venae cavae. Intensive Care Med 32:203–6
12. Mintz GS, Kotler MN, Parry WR, Iskandrian AS, Kane SA (1981) Real-time inferior vena caval ultrasonography: normal and abnormal findings and its use in assessing right-heart function. Circulation 64:1018–25
13. Brennan JM, Blair JE, Goonewardena S, Ronan A, Shah D, Vasaiwala S, Kirkpatrick JN, Spencer KT (2007) Reappraisal of the use of inferior vena cava for estimating right atrial pressure. J Am Soc Echocardiogr 20:857–61
14. Jue J, Chung W, Schiller NB (1992) Does inferior vena cava size predict right atrial pressures in patients receiving mechanical ventilation? J Am Soc Echocardiogr 5:613–9
15. Feissel M, Michard F, Faller JP, Teboul JL (2004) The respiratory variation in inferior vena cava diameter as a guide to fluid therapy. Intensive Care Med 30:1834–7
16. Vignon P, AitHssain A, François B, Preux PM, Pichon N, Clavel M, Frat JP, Gastinne H (2008) Echocardiographic assessment of pulmonary artery occlusion pressure in ventilated patients: a transoesophageal study. Crit Care 12:R18
17. Combes A, Arnoult F, Trouillet JL (2004) Tissue Doppler imaging estimation of pulmonary artery occlusion pressure in ICU patients. Intensive Care Med 30:75–81
18. Tavernier B, Makhotine O, Lebuffe G, Dupont J, Scherpereel P (1998) Systolic pressure variation as a guide to fluid therapy in patients with sepsis-induced hypotension. Anesthesiology 89:1313–21
19. Feissel M, Michard F, Mangin I, Ruyer O, Faller JP, Teboul JL (2001) Respiratory changes in aortic blood velocity as an indicator of fluid responsiveness in ventilated patients with septic shock. Chest 119:867–73
20. Kumar A, Anel R, Bunnell E, Habet K, Zanotti S, Marshall S, Neumann A, Ali A, Cheang M, Kavinsky C, Parrillo JE (2004) Pulmonary artery occlusion pressure and central venous pressure fail to predict ventricular filling volume, cardiac performance, or the response to volume infusion in normal subjects. Crit Care Med 32:691–9
21. Feissel M, Michard F, Mangin I, Ruyer O, Faller JP, Teboul JL (2001) Respiratory changes in aortic blood velocity as an indicator of fluid responsiveness in ventilated patients with septic shock. Chest 119:867–73
22. Vieillard-Baron A, Chergui K, Rabiller A, Peyrouset O, Page B, Beauchet A, Jardin F (2004) Superior vena caval collapsibility as a gauge of volume status in ventilated septic patients. Intensive Care Med 30:1734–9
23. Barbier C, Loubières Y, Schmit C, Hayon J, Ricôme JL, Jardin F, Vieillard-Baron A (2004) Respiratory changes in inferior vena cava diameter are helpful in predicting fluid responsiveness in ventilated septic patients. Intensive Care Med 30:1740–6
24. Vallée F, Richard JC, Mari A, Gallas T, Arsac E, Verlaan PS, Chousterman B, Samii K, Genestal M, Fourcade O (2009) Pulse pressure variations adjusted by alveolar driving pressure to assess fluid responsiveness. Intensive Care Med 35:1004–10

25. Mahjoub Y, Pila C, Friggeri A, Zogheib E, Lobjoie E, Tinturier F, Galy C, Slama M, Dupont H (2009) Assessing fluid responsiveness in critically ill patients: false-positive pulse pressure variation is detected by Doppler echocardiographic evaluation of right ventricle. Crit Care Med 37:2570–5
26. Monnet X, Osman D, Ridel C, Lamia B, Richard C, Teboul JL (2009) Predicting volume responsiveness by using the end-expiratory occlusion in mechanically ventilated intensive care unit patients. Crit Care Med 37:951–6
27. Maizel J, Airapetian N, Lorne E, Tribouilloy C, Massy Z, Slama M (2007) Diagnosis of central hypovolemia by using passive leg raising. Intensive Care Med 33:1133–8
28. Lamia B, Ochagavia A, Monnet X, Chemla D, Richard C, Teboul JL (2007) Echocardiographic prediction of volume responsiveness in critically ill patients with spontaneously breathing activity. Intensive Care Med 33:1125–32
29. Monnet X, Rienzo M, Osman D, Anguel N, Richard C, Pinsky MR, Teboul JL (2006) Passive leg raising predicts fluid responsiveness in the critically ill. Crit Care Med 34:1402–7
30. Jabot J, Teboul JL, Richard C, Monnet X (2009) Passive leg raising for predicting fluid responsiveness: importance of the postural change. Intensive Care Med 35:85–90
31. Renner J, Meybohm P, Hanss R, Gruenewald M, Scholz J, Bein B (2009) Effects of norepinephrine on dynamic variables of fluid responsiveness during hemorrhage and after resuscitation in a pediatric porcine model. Paediatr Anaesth 19:688–94
32. Sakka SG, Becher L, Kozieras J, van Hout N (2009) Effects of changes in blood pressure and airway pressures on parameters of fluid responsiveness. Eur J Anaesthesiol 26: 322–7

Assessment of Fluid Requirements: The Fluid Challenge

7

Daniel De Backer

Contents

7.1 Introduction

Administration of fluids is one of the most important therapeutic interventions that we have to perform in critically ill patients [1, 2], especially in sepsis [3–5]. However, fluid administration may be associated with risks of worsening in pulmonary edema, especially in patients with increased permeability, and this may have important implications in the outcome [6]. Elsewhere in this volume (see Chap. 6), we have shown how echocardiography can usefully discriminate patients with a higher likelihood of significantly increased cardiac output in response to fluids from those whose cardiac index is less likely to increase with the same amount of fluids.

However, treating patients with fluids is not simple, and when the physician decides to administer fluids because the index predicts that the patient will respond, the practitioner has to ensure that the patient effectively responds to the administration and tolerates it. Alternatively, when the index predicts that a response to fluids is unlikely, the physician must always consider whether the potential benefits of fluid administration outweigh the risks.

The definition of cutoffs used to separate responders from nonresponders is based on a specific analysis using receiver operative curves (ROC). This analysis characterizes the performances of the test in predicting the response to fluids, computing stepwise pairs of sensitivity and specificity (in fact 1–Specificity) after sequential inclusion of each of the patients classified in an ascending (or descending, depending on the physiological significance) order for the variable to evaluate. The area under the curve should be appreciably higher than 0.5 (a value obtained if chance alone determined the results) and be as close as possible to 1 (Fig. 7.1).

In this analysis, the best cutoff is determined as the point situated on a line drawn from the lower right to

D. De Backer
Department of Intensive Care, Erasme University Hospital, Université Libre de Bruxelles, 808 route de Lennik, 1070 Brussels, Belgium
e-mail: ddebacke@ulb.ac.be

D. De Backer et al. (eds.), *Hemodynamic Monitoring Using Echocardiography in the Critically Ill*,
DOI: 10.1007/978-3-540-87956-5_7, © Springer-Verlag Berlin Heidelberg 2011

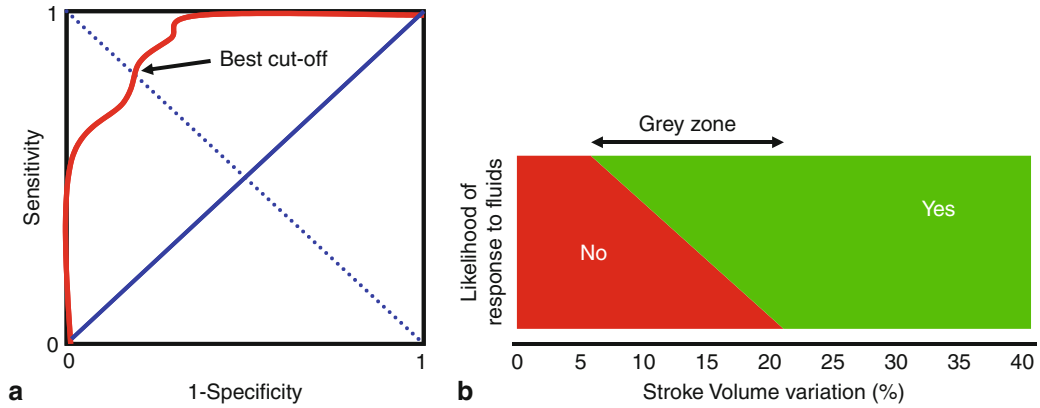

Fig. 7.1 Panel A: Evaluation of a test with a Receiver Operative Characteristics (ROC) curve. The ROC curve plots stepwise pairs of sensitivity versus 1-specificity after sequential inclusion of each of the patients, classified in a ascending or descending order for the variable investigated. The blue continuous line represents the results of chance alone. The area under the curve of the test should be as close as possible to 1 and in any case significantly greater than the area under the curve due to chance alone (0.5). The best cut-off is computed as the value of the variable corresponding to the pair of sensitivity/1-specificity closest to the intersection of dotted blue line and ROC curve (shown by the arrow) Panel B: Likelihood of the response to fluids according to stroke volume variations. A test used to predict fluid responsiveness (here stroke volume variations) seldom gives a dichotomic response, with no response below the cut-off value and a positive response above it. On the contrary, the likelihood of response progressively increases and there is a grey zone around the cut-off value

the upper left angle. This point is considered the best compromise between sensitivity and specificity, and it is usually close to 12–14% for pulse pressure variations [7–9] or stroke volume variations [10, 11]. However, this does not imply that the test is dichotomic, with absolutely no response below the cutoff and a certainty of response above. There is a gray zone around this point, with the likelihood of response progressively increasing when the variable comes closer to the cutoff value and likelihood of nonresponse progressively decreasing above it. Hence, when a value relatively close to the cutoff is found, the physician should always consider whether the potential benefits outweigh the risks of a failed attempt. Conversely, values slightly above the cutoff are still associated with a risk of failure of fluid challenge (false positive). For these reasons, it is important to evaluate whether or not the patient responds to fluid administration.

Another aspect is that irrespective of the index used to predict the response to fluids, there is no certitude that the patient will tolerate it. Indeed, all indices evaluate the position on the Frank–Starling relationship, but the changes in hydrostatic pressure are mostly related to the position and shape of left ventricular pressure/left ventricular volume relationship (Fig. 7.2). Even though patients with very severe hypovolemia show increased end-diastolic volume much more than end-diastolic pressure, this extreme situation is often transient, and most critical patients experience moderate hypovolemia. Accordingly, the changes in hydrostatic pressure may be small or large for a given increase in preload, even when cardiac output increases. Of course, the risks of increased hydrostatic pressure will be more significant in patients with moderate hypovolemia or altered left ventricular (LV) compliance. For these reasons, it is appropriate to check whether pulmonary artery pressure increases during fluid challenge and to define stopping rules.

Finally, when lung permeability is altered, the measurements of pulmonary artery pressure may be falsely reassuring, as pulmonary edema can occur with moderate – and often considered insignificant – increases in pulmonary artery pressure.

The fluid-challenge technique, which was first described in 1979 [12] and recently revised [13], optimizes the benefit/risk ratio of fluid administration, and we will see how echocardiography can help us to conduct a fluid challenge.

7.2 Indications for Fluid Challenge

A fluid challenge is indicated each time one considers that fluid should be administered, based on signs of altered tissue perfusion and reasonable likelihood of response

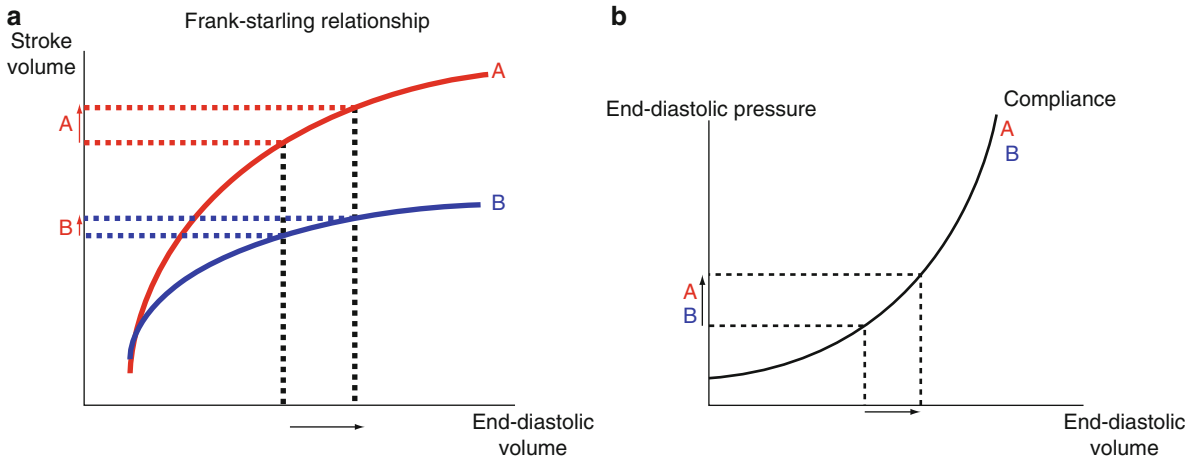

Fig. 7.2 Change in left ventricular stroke volume and end-diastolic volume during fluid challenge. (**a**) A given increase in left ventricular end-diastolic during fluid challenge is associated with an increase in stroke volume in preload-dependent patients (A), but not in preload-independent patients (B). (**b**) This given increase in end-diastolic volume is associated with a similar increase in left ventricular end-diastolic pressure in both types of patient

according to dynamic indices of fluid responsiveness, such as pulse pressure and stroke volume variation, elevated caval index (see Chap.6), or positive response to a passive leg-raising test. However, there is some risk that a fluid challenge may not be tolerated, i.e., in cases of acute respiratory distress syndrome (ARDS), pulmonary edema from any cause, right ventricular (RV) dysfunction, alteration in LV diastolic function. Additionally, there is the risk of failure to respond to fluids (borderline values). When the response is indubitable (i.e., in a patient with hemorrhagic shock with obvious persistent bleeding or in initial resuscitation of a patient with septic shock), administration of fluids without hemodynamic evaluation of the effects is reasonable, but in most other cases the more cautious approach involves performing a fluid challenge, especially when the likelihood of a positive response or good tolerance to fluids may be disputable. The fluid challenge needs to address four areas: type of fluid, rate of administration, safety limits, and evaluation of the effects [13]. This chapter discusses how echocardiography may help in this issue.

7.2.1 Type of Fluid and Administration Rate

Discussion of the nature of fluids is beyond the scope of this chapter; however, it always has to be taken into consideration that there are differences in volume-expansion capacities between colloids and crystalloids [14] and that these substances should not be given in similar amounts and rates. Also, the infusion has to be sufficiently rapid so as to limit the influence of external factors when interpreting the results and to offer rapidly the benefits of volume expansion (limit exposure to hypovolemia-related tissue hypoperfusion) to the patient. Though variable volumes have been detailed in the literature, it is generally accepted that 1,000 mL of crystalloids or 500 mL of colloid solutions should be given over a period of 30 min [13, 15]. It should be noted that administration of the full volume of these fluid amounts is not necessary if one of the intermediate evaluations shows that the patient does not tolerate fluids or the therapeutic goals have been achieved. Indeed, hemodynamic optimization may occur by infusing a small amount of fluids. This is because the response to fluids is usually more marked with the initial administration than with subsequent aliquots, in accordance with the Frank–Starling curve, which is steeper at low preload than at higher preload levels.

7.2.2 Evaluation of Tolerance During Fluid Challenge

Whatever the hemodynamic response to fluids, the increase in preload will be accompanied by an increase in hydrostatic pressure and thus may promote pulmonary edema. Of course, the increase in hydrostatic pressure, and hence development of pulmonary edema,

is greater when preload is greater; but it does not depend on the response of stroke volume to fluid administration for a given change in LV end-diastolic volume (Fig. 7.2). Accordingly, even when the likelihood of response to fluids is high according to the measured index of fluid responsiveness, it is advisable to set safety limits during fluid challenge.

Several safety limits can be used: oxygenation, measurement of extravascular lung water (EVLW), pulmonary artery occluded pressure. However, these are not without problems. Oxygenation and EVLW may not be sufficiently sensitive and, more importantly, there may be an important delay between the increase in hydrostatic pressure and the onset of pulmonary edema. Pulmonary artery occluded pressure (PAOP) reflects the hydrostatic pressure, but capillary pressure may be higher than PAOP, especially in ARDS patients. More importantly, there is no direct link between the level of PAOP and pulmonary edema since the level at which edema occurs varies considerably among patients, depending on endothelial permeability and oncotic pressure. Nevertheless, estimation of PAOP is probably the most useful variable to measure. Van der Heiden et al. [16] recently reported that the increase in EVLW in preload-dependent patients was inversely related to the gradient between oncotic pressure and hydrostatic pressure in patients with both normal and increased permeability. Accordingly, it may be appropriate to define a maximal PAOP when performing a fluid challenge. It should be noted that the change in preload (LV volume) is of less relevance, but it can be used to ensure that preload is effectively manipulated during fluid administration.

Echocardiography can be useful in evaluating safety limits during fluid challenge. PAOP can be estimated with echocardiography using different indices (see Chap. 16). In particular, evaluation of mitral inflow (E wave/A wave ratio) or early mitral inflow to mitral annular velocity (E/Ea) may be effective in predicting PAOP in critically ill patients. However, it could be asserted that echocardiographic measurements of PAOP are not sufficiently accurate to detect small changes in PAOP. Indeed, when PAOP estimated by E/Ea is compared with invasively measured PAOP, the limits of agreement may reach up to 5 mmHg [17]: so this measurement is often used semiquantitatively to differentiate low from high PAOP values [18]. These indices can nevertheless be employed to evaluate changes in PAOP.

In critically ill hemodialyzed patients, Vignon et al. [19] reported that the E/A ratio decreased during acute fluid withdrawal. Conversely, Lamia et al. recently reported that the E/A ratio increased during weaning trials, especially with failed attempts [20]. The E/A ratio can also be used to detect hydrostatic changes induced by fluid challenge (Fig. 7.3). Indeed, small changes in the E wave or E/A ratio are mostly related to changes in PAOP, while other factors affecting the E wave or E/A ratio (such as the diastolic properties of the heart) are not affected by preload. However, it is difficult to define a maximal value for the E wave or E/A ratio that can be tolerated during fluid challenge. Accordingly, it is more useful as a gauge of preload manipulation, helping to determine whether fluid challenge fails to increase cardiac index despite significant increase in preload, rather than as a true safety limit.

Echocardiography can also be effective in detecting fluid-induced RV dilation. Indeed, critically ill patients, especially when suffering from ARDS and ventilated with high positive end-expiratory pressure (PEEP) levels, often present RV dysfunction [21]. Acute cor pulmonale may be associated with a false-positive stroke volume variation, but the true status can easily be confirmed by echocardiography [22]. If fluid loading is nevertheless attempted in such patients, an acute increase in RV volume can be detected by an increase in RV to LV area. There is no predefined safety limit that can be recommended, as some patients with acute RV failure may tolerate fluid loading-induced RV dilation [23]. Of note here is that responders usually have moderate RV dilation (RV/LV ratio close to 0.6) rather than severe dilation (ratio close to 1). Nevertheless, fluid challenge should be suspended when RV dilation is not associated with an improvement in aortic velocity–time integral (VTI). Development of paradoxical septal motion should prompt termination of fluid administration.

Finally, the indication to administer fluids should be reassessed at each step. Signs of preload dependency should disappear during fluid administration (Fig. 7.3). When these reach values associated with a limited response to fluids, further fluid administration may be futile and even dangerous.

7.2.3 Evaluation of Reponse to Fluids

When fluids are administered, it is very important to evaluate the response. One may of course assess whether the problem justifying infusion (hypotension,

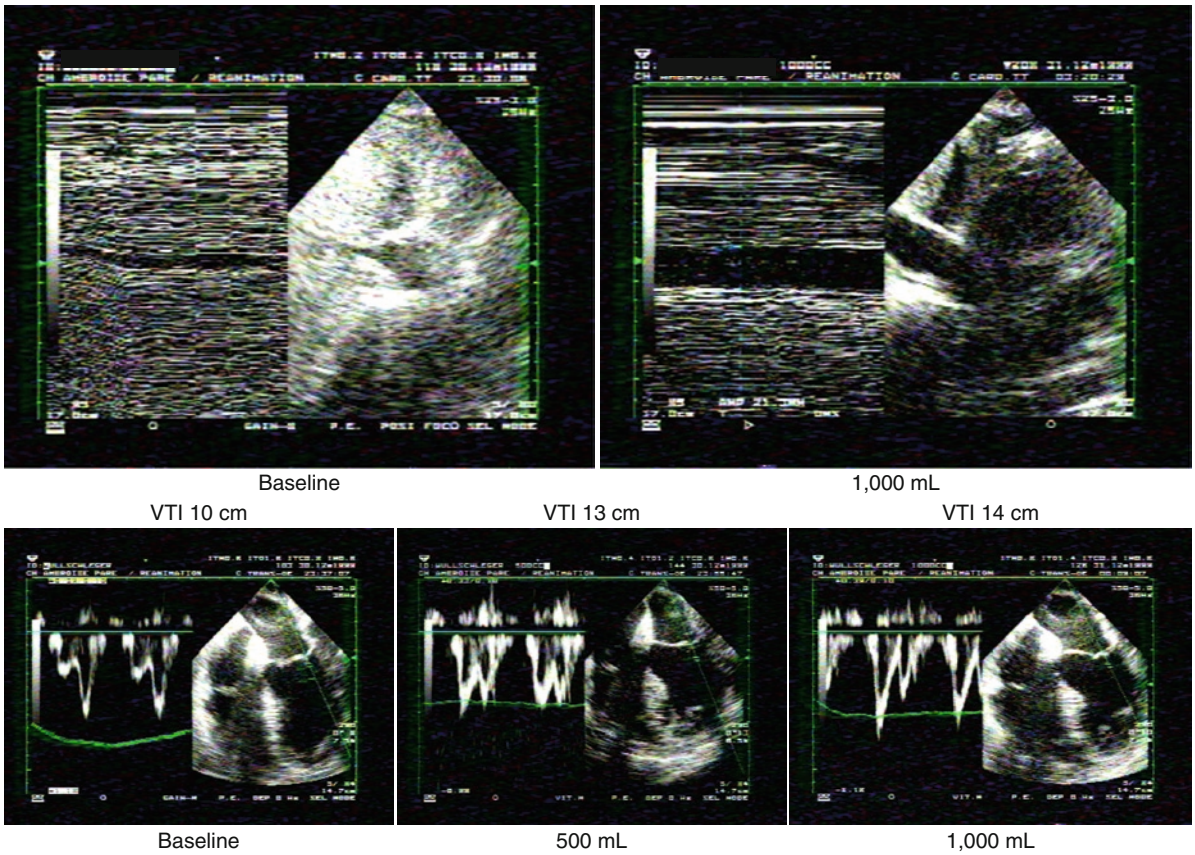

Fig. 7.3 Guidance of fluid challenge using echocardiography. In this preload-dependent patient, fluid challenge is associated with an increase in stroke volume, as reflected by an increase in aortic velocity–time integral (VTI), and resolution of signs of preload dependency (*upper panel*). A progressive increase in hydrostatic pressure is reflected by the progressive increase in mitral flow E/A ratio. Of note, 1,000 mL of saline was given but the increase in VTI was already maximal with a smaller amount of fluids. Ideally, fluid challenge should have been after administration of 500 mL. It is therefore important to check at each step whether indices of fluid responsiveness are still present

oliguria, increased lactate levels) has been resolved. However, these are not particularly sensitive, as an increase in cardiac output may fail to translate into an increase in blood pressure (especially in patients with low systemic vascular resistance), urine output (established renal failure), or blood lactate levels. In addition, the improvement in organ function may take some time, even when tissue perfusion is restored. Accordingly, stroke volume and cardiac output are the best indices of a response to fluids.

Echocardiography is appropriate for this purpose. Measurements of VTI of aortic flow in the left ventricular outflow tract (LVOT; apical four-chamber view in the transthoracic approach, or transgastric view 100–120°; see Chap. 5 for details) are particularly reliable. End-expiration measurements should be used, as respiratory variations of VTI are likely to occur in hypovolemic patients. Changes in end-expiratory aortic VTI of more than 10–15% can be considered a positive response to fluids. Smaller variations may be due to a lack of change in either preload or preload independence (changes in the mitral flow E wave or E/A ratio may help in distinguishing between these two possibilities).

It should be noted that measuring cardiac output is not necessary since changes in the LVOT and aortic annulus are negligible. Even though hypovolemia is often associated with reflex tachycardia, this response is more limited in critically ill patients (owing to the impact of sedation and/or alterations in the autonomic system), and changes in heart rate during fluid challenge are often of limited magnitude.

Other echocardiographic measurements of stroke volume can be used. Dark et al. [24] showed that

echocardiography can be employed in the emergency department to evaluate the response to fluids and to construct individual Frank–Starling curves. Stroke distance, an index of stroke volume, was used to evaluate the response to repeated boluses; stroke volume initially responded to several boluses and then reached a plateau.

7.3 Conclusion

Although several measures can be used to predict the response to fluids, it is reasonable to perform a fluid challenge for effectively evaluating the response to fluid administration. This is especially true when risks associated with this procedure may be high, such as in patients with associated respiratory failure.

Fluid challenge consists of infusing a calibrated volume of fluids over a short period and evaluating the effects. The response to fluid challenge can be categorized as follows:

1. Positive response: increase in aortic VTI by more than 10–15%, which signifies an increase in stroke volume
2. Negative response: increase in mitral flow E or E/A by more than 10% and changes in aortic VTI of less than 10%, which signifies a lack of change in stroke volume despite significant changes in preload
3. Indefinite response: increase in mitral flow E or E/A and changes in aortic VTI of less than 10%, which signifies a lack of change in stroke volume and absence of change in preload

References

1. Chytra I, Pradl R, Bosman R et al (2007) Esophageal Doppler-guided fluid management decreases blood lactate levels in multiple-trauma patients: a randomized controlled trial. Crit Care 11:R24
2. Brienza N, Giglio MT, Marucci M, et al (2009) Does perioperative hemodynamic optimization protect renal function in surgical patients? A meta-analytic study. Crit Care Med 37:2079–2090
3. Hollenberg SM, Dumasius A, Easington C et al (2001) Characterization of a hyperdynamic murine model of resuscitated sepsis using echocardiography. Am J Respir Crit Care Med 164:891–895
4. Zanotti-Cavazzoni SL, Guglielmi M, Parrillo JE et al (2009) Fluid resuscitation influences cardiovascular performance and mortality in a murine model of sepsis. Intensive Care Med 35:748–754
5. Rivers E, Nguyen B, Havstadt S et al (2001) Early goal-directed therapy in the treatment of severe sepsis and septic shock. N Engl J Med 345:1368–1377
6. Wiedemann HP, Wheeler AP, Bernard GR et al (2006) Comparison of two fluid-management strategies in acute lung injury. N Engl J Med 354:2564–2575
7. Michard F, Boussat S, Chemla D et al (2000) Relation between respiratory changes in arterial pulse pressure and fluid responsiveness in septic patients with acute circulatory failure. Am J Respir Crit Care Med 162:134–138
8. Hofer CK, Muller SM, Furrer L et al (2005) Stroke volume and pulse pressure variation for prediction of fluid responsiveness in patients undergoing off-pump coronary artery bypass grafting. Chest 128:848–854
9. De Backer D, Heenen S, Piagnerelli M et al (2005) Pulse pressure variations to predict fluid responsiveness: influence of tidal volume. Intensive Care Med 31:517–523
10. Feissel M, Michard F, Mangin I et al (2001) Respiratory changes in aortic blood velocity as an indicator of fluid responsiveness in ventilated patients with septic shock. Chest 119:867–873
11. Slama M, Masson H, Teboul JL et al (2004) Monitoring of respiratory variations of aortic blood flow velocity using esophageal Doppler. Intensive Care Med 30:1182–1187
12. Weil MH, Henning RJ (1979) New concepts in the diagnosis and fluid treatment of circulatory shock. Thirteenth annual Becton, Dickinson and Company Oscar Schwidetsky Memorial Lecture. Anesth Analg 58:124–132
13. Vincent J-L, Weil MH (2006) Fluid challenge revisited. Crit Care Med 34:1337
14. Verheij J, van Lingen A, Beishuizen A et al (2006) Cardiac response is greater for colloid than saline fluid loading after cardiac or vascular surgery. Intensive Care Med 32:1030–1038
15. Dellinger RP, Levy MM, Carlet JM et al (2008) Surviving sepsis campaign: international guidelines for management of severe sepsis and septic shock: 2008. Intensive Care Med 34:17–60
16. van der Heijden M, Verheij J, Nieuw Amerongen GP, et al (2009) Crystalloid or colloid fluid loading and pulmonary permeability, edema, and injury in septic and nonseptic critically ill patients with hypovolemia*. Crit Care Med 37:1275–1281
17. Combes A, Arnoult F, Trouillet JL (2004) Tissue Doppler imaging estimation of pulmonary artery occlusion pressure in ICU patients. Intensive Care Med 30:75–81
18. Vignon P, AitHssain A, Francois B et al (2008) Echocardiographic assessment of pulmonary artery occlusion pressure in ventilated patients: a transoesophageal study. Crit Care 12:R18
19. Vignon P, Allot V, Lesage J et al (2007) Diagnosis of left ventricular diastolic dysfunction in the setting of acute changes in loading conditions. Crit Care 11:R43
20. Lamia B, Maizel J, Ochagavia A et al (2009) Echocardiographic diagnosis of pulmonary artery occlusion pressure elevation during weaning from mechanical ventilation. Crit Care Med 37:1696–1701

21. Vieillard-Baron A, Schmitt JM, Augarde R et al (2001) Acute cor pulmonale in acute respiratory distress syndrome submitted to protective ventilation: incidence, clinical implications, and prognosis. Crit Care Med 29:1551–1555
22. Vieillard-Baron A, Chergui K, Rabiller A et al (2004) Superior vena caval collapsibility as a gauge of volume status in ventilated septic patients. Intensive Care Med 30:1734–1739
23. Mercat A, Diehl JL, Meyer G et al (1999) Hemodynamic effects of fluid loading in acute massive pulmonary embolism. Crit Care Med 27:540–544
24. Dark PM, Delooz HH, Hillier V et al (2000) Monitoring the circulatory responses of shocked patients during fluid resuscitation in the emergency department. Intensive Care Med 26:173–179

Evaluation of Left Ventricular Systolic Function

8

Daniel De Backer

Contents

D. De Backer (✉)
Department of Intensive Care, Erasme University Hospital, Université Libre de Bruxelles, 808 route de Lennik, B-1070, Brussels, Belgium
e-mail: ddebacke@ulb.ac.be

8.1 Introduction

Evaluation of left ventricular (LV) systolic function is of paramount importance in the management of critically ill patients, not only to analyze the mechanism of inadequate tissue perfusion or respiratory failure but also to adjust the therapeutic response accordingly. In patients with acute circulatory failure, a decreased LV function may suggest cardiogenic shock or myocardial depression in septic shock. But measurement of LV function alone can be misleading, and it has to be considered with other indices for the proper identification of hemodynamic disorders. In cardiogenic shock, LV dysfunction is associated with low cardiac output and high filling pressures or severe dilation, whereas in septic shock it is often associated with preserved cardiac output and normal filling pressures. Similarly, an alteration in LV function in a patient with respiratory failure suggests a cardiac participation in pulmonary edema. More importantly perhaps, the observation of an altered LV function will also be helpful in guiding therapy, indicating inotropic therapy in patients with inadequate cardiac output in patients with circulatory failure or in patients with pulmonary edema.

The evaluation of systolic function (Table 8.1) is more complicated than might be expected. Ejection fraction, the most widely used index of systolic function, depends not only on contractility but also on preload, afterload, and heart rate. Ideally, contractility, which reflects the intrinsic ability of myocardial fibers to shorten at a given preload and afterload, is the variable we should assess with echocardiography. Simple indices of systolic function, which are easy to implement at the bedside, are markedly affected by preload, afterload, and heart rate. More sophisticated

D. De Backer et al. (eds.), *Hemodynamic Monitoring Using Echocardiography in the Critically Ill*,
DOI: 10.1007/978-3-540-87956-5_8, © Springer-Verlag Berlin Heidelberg 2011

indices have been developed, and these are reported to be relatively independent of loading conditions; however, these indices are difficult to use in daily practice and are mostly restricted to research purposes.

8.2 Evaluation of Ejection Fraction and Related Indices

Ejection fraction, defined as stroke volume divided by LV end-diastolic volume, is the most frequently determined index of LV function. It can be established by iodine contrast cineangiography during left heart catheterization or noninvasively with radionuclide cineangiography and magnetic resonance imaging (MRI). The recently developed real-time three-dimensional echocardiography is ideal for the determination of LV ejection fraction, and it has excellent correlation with MRI [1, 2, 3]. However, this imaging technique is available only on the most recent (and expensive) ultrasound platforms. In addition, this technique is solely feasible using the transthoracic approach and requires excellent acoustic access to the heart and minimal movements of the chest wall, which limits its use in ICU patients. Two-dimensional and M-mode echocardiography are widely available and can be used to evaluate LV ejection fraction (LVEF) or surrogates of LVEF obtained from two-dimensional images or simple diameter measurements. Their principal limitation is that LV volume is estimated based on geometrical models using LV diameter or area measurements performed in one or two orthogonal planes. These estimations rely on the assumption that the left ventricle has a spherical or elliptical shape and a homogenous contraction, which is not the case in patients with cardiac disorders.

8.2.1 *Unidimensional Approach Using M-Mode (Fig. 8.1)*

LV diameter shortening fraction can be calculated as the difference between end-systolic and end-diastolic diameters divided by end-diastolic diameter. These diameters are measured from the transthoracic approach in the parasternal long-axis or short-axis view using M-mode. Here, it is important to put the cursor perpendicular to the ventricular walls, close to papillary muscles. This measurement evaluates contractility of the basal part of the anteroseptal and inferior regions. In using this index to reflect global systolic function, one has to assume that contractility is homogenous and that anteroposterior shortening is

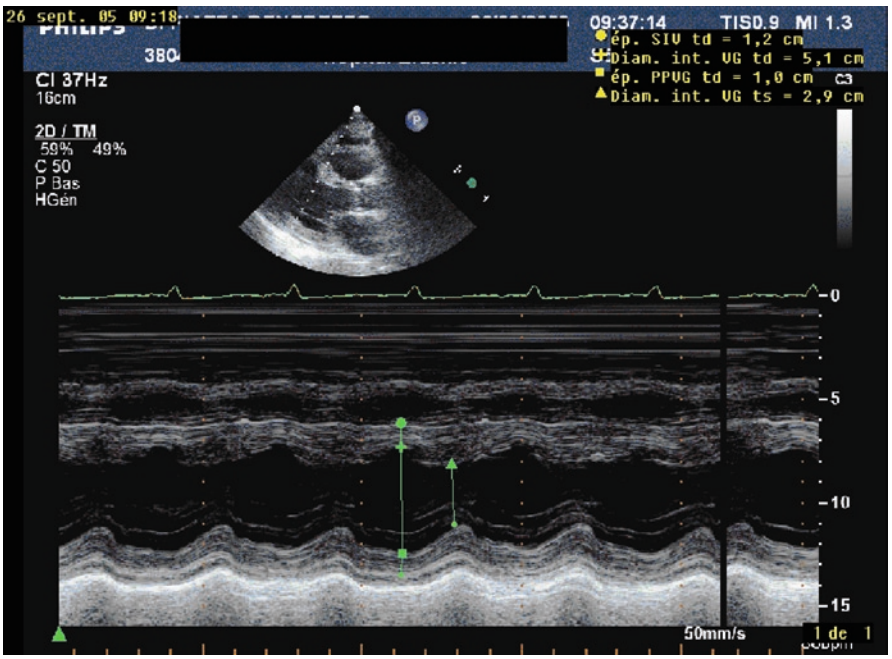

Fig. 8.1 Measurement of left ventricular ejection fraction using M-mode (shortening fraction). Parasternal long-axis view, sampler set at insertion of papillary muscles and perpendicular to interventricular septum. Shortening fraction is computed as (end-diastolic minus end-systolic diameter) divided by end-diastolic diameter: (51 – 29)/51 = 22/51 = 43%

Table 8.1 Normal values of most frequently used indices of left ventricular function

Method	Normal values
Ejection fraction	
Shortening fraction (diameter)	24–36%
Shortening fraction (area)	38–60%
Ejection fraction (volumes)	>60%
Ejection fraction (eyeball)	>60%
Circumferential fibers shortening	1.2 ± 0.2 circ/s
Cardiac power	NA (W)
dP/dt using mitral regurgitation	800–1,200 mmHg/s

uniform along the LV long axis. This is far from being the case even in normal conditions since LV-diameter shortening increases from the base toward the apex. This is reflected in shortening fraction by normal values (25–40%) that are far below ejection fraction values (60–70%) measured by radionuclides, ventriculography, or MRI. One of the first estimations of LVEF using echocardiography was obtained using LV-diameter measurements and the Teichholz formula, assuming that the LV had a spherical shape. This calculation is available on most echocardiographic machines, but it is now widely considered less accurate than more recent methods (Simpson's rule).

8.2.2 Two-Dimensional Approach: LV Short-axis Area Measurements

Fractional area change is measured as the difference between end-systolic and end-diastolic LV short-axis areas divided by the end-diastolic area (Fig. 8.2). These areas are measured from the transthoracic approach using the parasternal short-axis view, or from the transesophageal approach using the transgastric short-axis view. In normal conditions, fractional area change is highly related to ejection fraction since 80% of ventricular stroke volume is related to the circumferential shortening of the ventricular myofibrils. However, as mentioned above, the percentage of LV circumferential shortening increases from the base toward the apex. This method correlates well with the radionuclide ejection fraction, even though limits of agreement are close to 10% [3]. In addition, the interobserver variability is quite limited (less than 5%) [4]. However, this approach may be less accurate when contractility is inhomogeneous. In critically ill patients, contractility is not often homogenous as regional motion abnormalities may occur in ischemic diseases and also in bundle branch blocks or as a consequence of right ventricular dysfunction.

8.2.3 Two-Dimensional Approach: LV Volume Estimation

Finally, ejection fraction can be evaluated from volumetric estimations (Fig. 8.3), using either the area-length formula or Simpson's method. The area-length method considers the heart as an ellipse, while Simpson's method considers it as the sum of multiple thin disks. Simpson's method has been shown to estimate the angiographic ejection fraction more reliably than the area-length method [5]. The LV cavity endocardial border has to be traced in two orthogonal apical views (four- and two-chambers), obtained from the transthoracic approach. The use of a single-plane four-chamber view (transthoracic) or long-axis (transesophageal) is less reliable but simpler and quicker to perform.

A point to be noted here is that all these indices are affected by arrhythmias and the respiratory cycle. It is recommended that they be measured during expiration and averaged over several beats in patients with atrial fibrillation.

8.3 Measuring or Estimating Ejection Fraction

Calculations of shortening fraction or fractional area changes are relatively easy even though they necessitate freezing of the image. Automatic border detection is a modality provided on sophisticated ultrasound platforms that allows continuous automatic computation of fractional area change in transesophageal echocardiography (TEE) using the transgastric view of the LV short axis. It has to be noticed that good identification of the epicardium is mandatory, but that is not always easily obtained in critical care patients [6]. Automatic border detection slightly underestimates

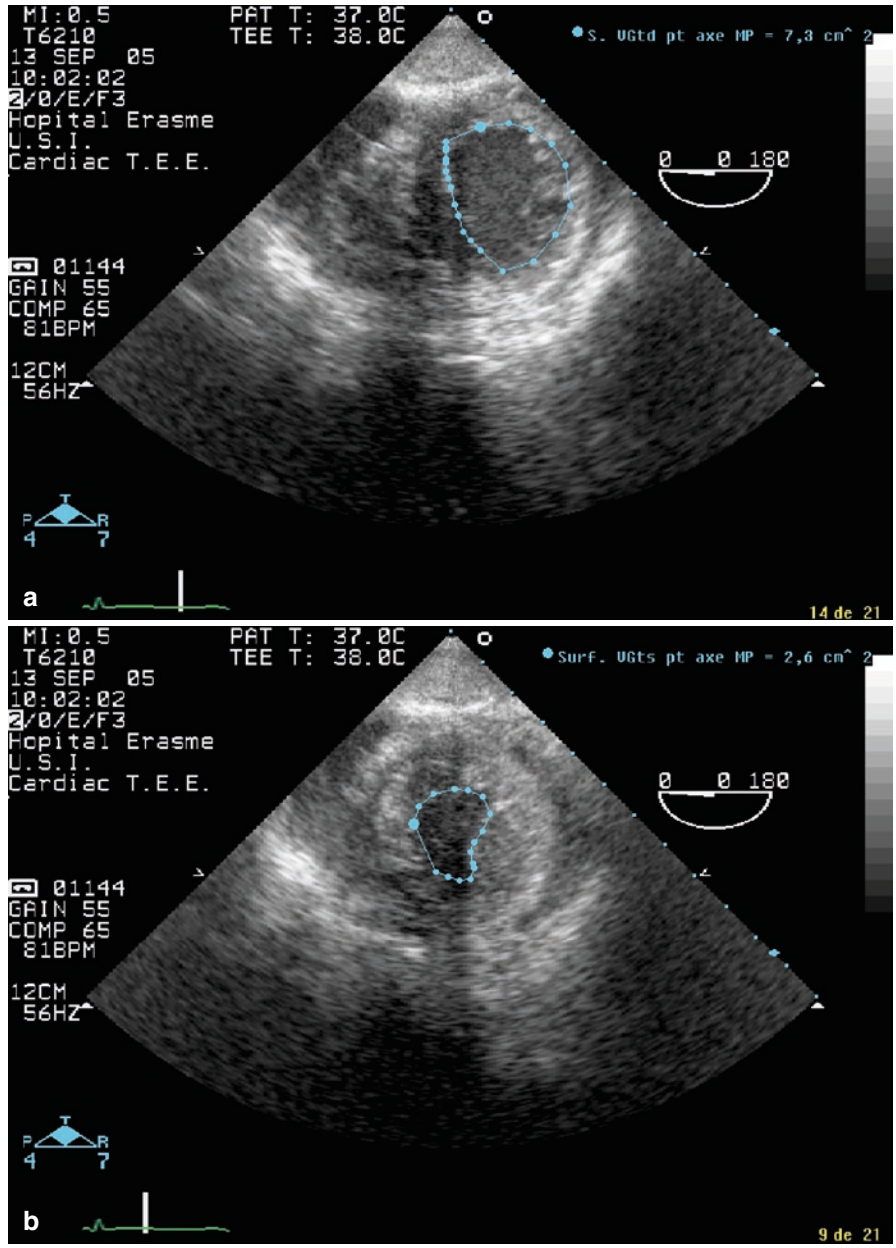

Fig. 8.2 Measurement of left ventricular ejection fraction using left ventricular surfaces (short-axis surface shortening fraction). Parasternal short-axis view at insertion of papillary muscles and perpendicular to interventricular septum. (**a**) diastole; (**b**) systole. Surface shortening fraction is computed as (end-diastolic minus end-systolic surface) divided by end-diastolic surface: $(73-26)/73=47/73=64\%$

manual measurements of fractional area change since mitral papillary muscles are excluded using the automated technique, but not employing manual tracing.

Measurement of the ejection fraction using Simpson's method is quite cumbersome, and one can question its clinical advisability considering the variability in measurements [7]. To reduce intra- or interobserver variability, averaging measurements obtained on several beats is often required, which further limits clinical feasibility unless automatic border detection is used.

In many instances, visual evaluation of the ejection fraction may be satisfactory. In cardiac patients, evaluation of the ejection fraction correctly estimated the measured ejection fraction [8]. In patients with septic shock, Vieillard-Baron et al.[9] recently

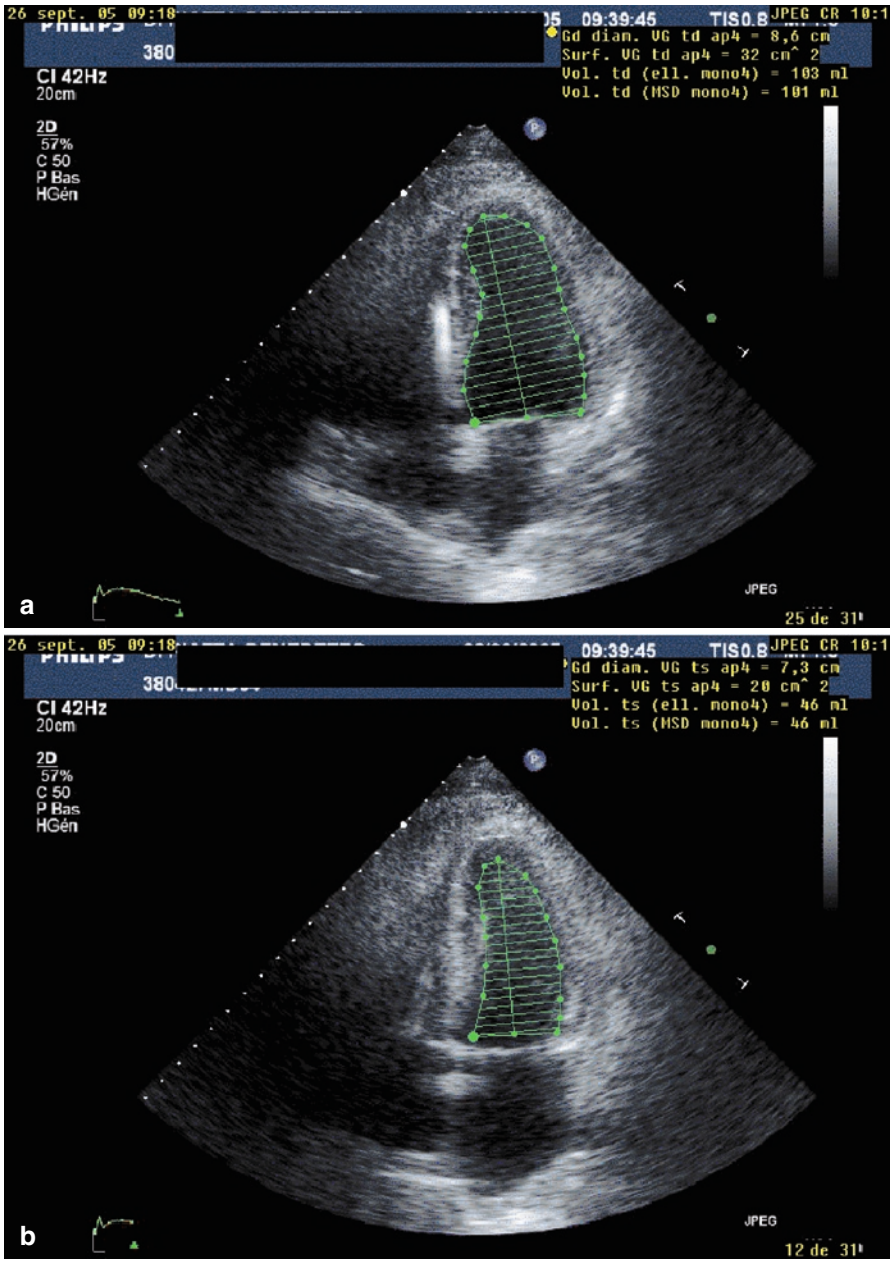

Fig. 8.3 Measurement of left ventricular ejection fraction (LVEF) using volume measurements (Simpson's rule). End-diastolic (**a**; 100 mL) and end-systolic (**b**; 46 mL) volumes were measured. LVEF was calculated as (end-diastolic minus end-systolic volume) divided by end-diastolic volume: (101 − 46)/101 = 55/101 = 54%

reported that semiquantitative classification into normal, moderately depressed, and severely altered correctly classified patients compared with actual measurements of LV ejection fraction by fractional area changes or the area-length method (Fig. 8.4). Interestingly, this semiquantitative approach can be reliably performed with minimal training [10–12].

8.4 Dependence on Loading Conditions: Separating Intrinsic from Extrinsic Alteration in Cardiac Function

Ejection fraction is dependent on contractility, but it is also directly related to preload and inversely related to afterload: ejection fraction = 1–(end-systolic

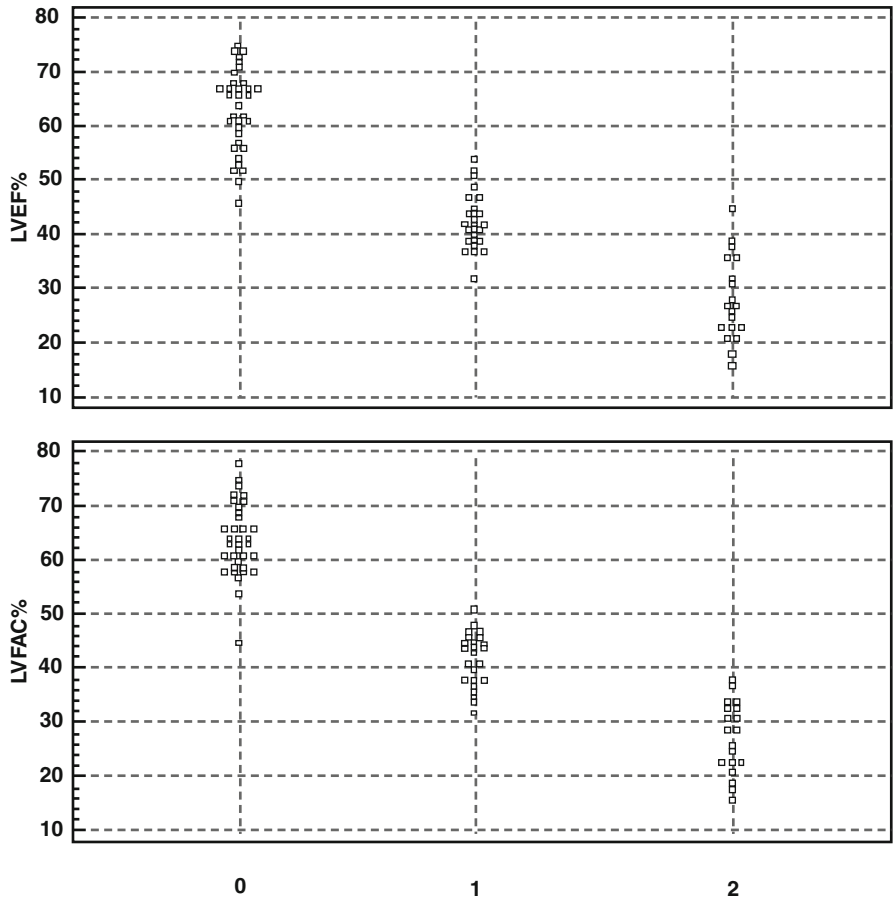

Fig. 8.4 Comparison of visual evaluation and quantification of left ventricular ejection fraction. Eyeball semiquantitative classification into normal, moderately depressed, and severely altered correctly classified patients compared with actual measurements of left ventricular ejection fraction by fractional area changes or area-length method (From Vieillard-Baron et al. [9]). Grade 0 normal systolic function; grade 1 moderately altered systolic function; grade 2 severely altered systolic function. Left ventricular ejection fraction (LVEF) calculated from single-plane area-length formula (long axis); left ventricular fractional area contraction (LVFAC) calculated from surface measurements in short axis

pressure/end-diastolic volume)(1/elastance) [13]. Accordingly, several other indices have been proposed to provide a better description of contractility. These are also more difficult to acquire, requiring specific training and software that is available only on the most sophisticated ultrasound platforms. From a clinical standpoint, there is no need to quantify the intrinsic contractility of the left ventricle, but rather to assess how the heart contracts with given loading conditions. A low ejection fraction can reflect either an intrinsic LV systolic dysfunction or an excessive LV afterload, but in both conditions it reflects the fact that ventriculoarterial coupling is inadequate [13]. Depending on the situation, inotropic agents, vasodilatory agents, or even intra-aortic counterpulsation may be considered [14]. The following indices are therefore to be used mainly for research purposes, when a closer insight into contractility is required to characterize LV function.

8.4.1 Rate-Corrected Velocity of Circumferential Fiber Shortening and LV Wall Stress Relationship

The velocity of circumferential fiber shortening (VCF) during systole is related to myocardial contractility, but it is also affected by LV afterload. Therefore, some authors have suggested using the curve of the relationship between VCF shortening and an index of afterload to obtain an afterload-independent index of contractility.

VCF shortening is calculated as the shortening fraction of LV circumference measured at the level of the papillary muscles in the short-axis view divided by ejection time:

(LV end-diastolic circumference – LV end-systolic circumference) / (LV end-distolic circumference × ejection time)

Ejection time can be measured using pulsed-wave Doppler as the duration of aortic flow on high-speed (>100 cm/s) recordings to increase accuracy. To normalize ejection time with respect to heart rate, it is divided by the square root of the cardiac cycle length (measured as RR interval on the electrocardiogram), according to Bazett's formula.

LV peak systolic wall stress (σ, g/cm^2) is defined as the maximum force opposing to fiber shortening. According to Laplace's law, it is proportional to the pressure and diameter of ventricular cavity but inversely proportional to ventricular wall thickness: where P is systolic arterial pressure, D is end-systolic

$$\sigma = 1.35 \times P \times \left[\frac{D}{4h\left(1 + \frac{h}{D}\right)} \right]$$

diameter, and h end-systolic thickness, the latter two being measured in parasternal long axis using M-mode.

Some authors have used this afterload-independent index of contractility in anesthesia and intensive care [15, 16]. For example, Goertz et al. [15] reported that beta-adrenergic agents had differential effects on myocardial contractility. In children, it has been used to evaluate precisely the severity of sepsis-induced myocardial depression [16].

Nevertheless, the complexity of these computations is obvious. The heart rate has to be very regular since small changes in the ejection time greatly affect the values of VCF shortening. For these reasons, this analysis is not frequently used.

8.4.2 Mean and Maximum Acceleration of Aortic Blood Flow

The mean acceleration of aortic blood flow in the aortic root was forwarded a long time ago as an index of LV contractility [17]. Maximum acceleration calculated over the first 20 ms of aortic ejection was believed to be more closely related to contractility and less affected by loading conditions [18]. Mean acceleration in the left ventricular outflow tract (LVOT) is measured on a pulsed-Doppler envelope and calculated as the ratio of peak aortic velocity divided by the time to peak flow. Using this technique, Bauer et al.[19] reported that the LVOT acceleration time is proportional to LV maximal elastance acquired by conductance catheters under different loading conditions. Even though these results appear persuasive, this index is not widely used since the LVOT acceleration time is sensitive to preload [20] as well as to afterload.

8.4.3 Estimation of dP/dt Max Using Mitral Regurgitation Jet Acceleration Time

One of the very first measures of myocardial contractility used in clinical practice was the peak of the first derivative of LV pressure rise during systole (dP/dt max). This was obtained in the catheterization laboratory by differentiating the LV pressure signal over time. The mitral valve regurgitation jet can be used to estimate dP/dt max noninvasively (Fig. 8.5) [21]. The first step is to measure the time delay required to reach 3 m/s from the time point where mitral regurgitation velocity is only 1 m/s. The pressure rise between these two velocities represents 32 mmHg according to Bernoulli's equation: $(4 \times 3^2) - (4 \times 1^2) = 32$. By dividing 32 mmHg with the time to generate this pressure rise, one obtains an approximation of dP/dt max. The main limitation of this method is that it assumes that left atrial pressure is negligible (which is less likely when LV function is markedly altered). In addition, technical limitations to achieving an optimal tracing make this technique difficult to apply in clinical practice. In patients submitted to cardiac surgery, preoperative measurement of dP/dt was predictive for the use of inotropic agents in the postoperative period [22]. The good correlation of this variable with shortening fraction nevertheless questions the use of this more difficult index compared with more simple measures. This index remains nevertheless particularly interesting in patients with aortic valve regurgitation [23] or mitral valve regurgitation, when LVEF evaluation, as noted above, is often misleading.

8.4.4 LV External Mechanical Power

LV total hydraulic power (measured in watts) represents the amount of energy delivered from the left

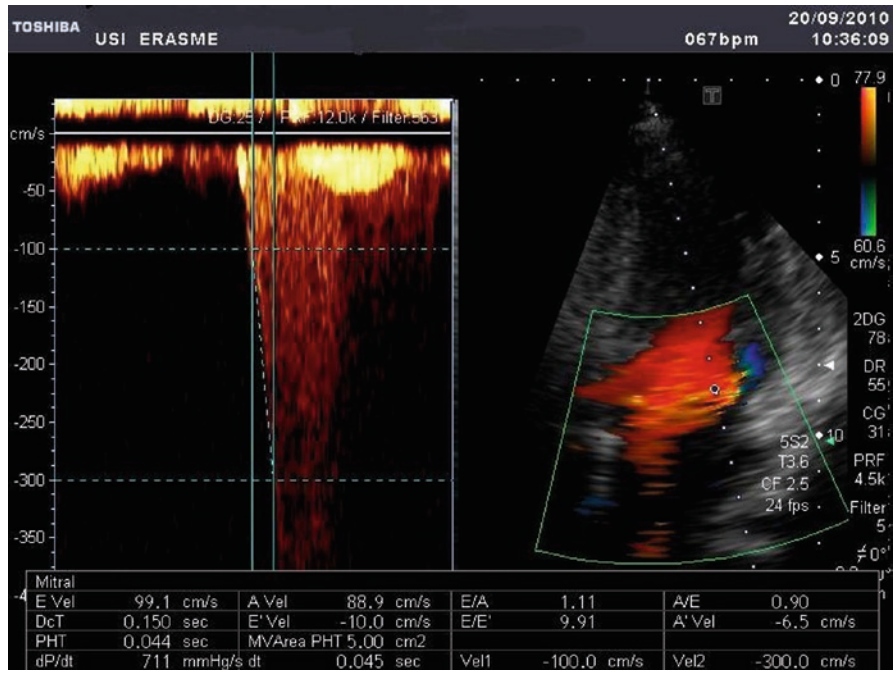

Fig. 8.5 Measurement of left ventricular (LV) contractility using dP/dt on mitral regurgitation. Measurement of maximal acceleration (between 1 and 3 m/s) on mitral regurgitant flow is proportional to LV contractility (expressed in mmHg/s)

ventricle to the peripheral circulation per unit time. It is calculated as the instantaneous product of LV pressure and flow:

where $P(t)$ is instantaneous aortic pressure and $Q(t)$ instantaneous aortic flow.

$$W = \frac{1}{T}\int_0^T P(t)Q(t)dt$$

A simplified approach involves using peak systolic arterial pressure (SAP) and maximum aortic velocity (VAo_{max}) to calculate flow. It can thus be calculated:

where AVA is aortic valvular area.

$$W_{peak} = \mathrm{SAP} \times \mathrm{VAo}_{max} \times \mathrm{AVA} \times 1.333 \times 10^{-4}$$

It has been proposed to normalize cardiac power by LV end-diastolic area or volume [24]. Cardiac power calculation assumes that there is no leak in the system, i.e., no mitral regurgitant flow, but this is often not the case when LVEF is altered, especially when the left ventricle is enlarged. Another problem is that this computation takes into account aortic pressure measured at the aortic root. In critically ill patients, arterial pressure is measured in the femoral or radial arteries, and systolic arterial pressure may be quite different from aortic pressure as a consequence of wave reflection in the arterial tree (especially when radial cannulation is used). Wave-reflection phenomena are affected by arterial mechanical properties and thus by therapeutic interventions affecting them (such as vasopressors or vasodilatory agents) [25] or by disease states (such as sepsis) [26]. Accordingly, cardiac power may not be calculated reliably in these conditions

8.4.5 Maximal Elastance

Maximal elastance is derived by analyzing the LV pressure/volume relationships, and it is defined as the line correlating the various telesystolic pressure/volume points obtained during acute changes in preload. Classically, generating pressure/volume curves requires invasive procedures with volumetric (conductance) and pressure catheters advanced into the ventricular cavity. Echocardiography can replace the conductance catheters, with LV volumes approximated by LV areas measured using automated border-detection techniques. LV systolic pressure is estimated from peripheral arterial pressure. Of course, only the

systolic part of the relationship can be evaluated, since LV diastolic pressure cannot be approximated using peripheral arterial pressure measurements. Respiratory variations in venous return, or changes in positive end-expiratory pressure (PEEP) levels, or infusion of vasodilatory or vasoconstrictive agents can be used to produce preload variations.

Gorcscan et al. [27] demonstrated the feasibility of this technique in anesthetized patients submitted to cardiac surgery. More recently, Cariou et al. [28] reported that end-systolic elastance is transiently altered in patients with sepsis-induced myocardial depression and that the response to dobutamine is blunted for several days.

This technique is far from being widely use, even though it represents the most rigorous approach of contractility. As outlined above, it requires the use of automated border-detection and specific equipment to synchronize echographic and pressure measurements. In addition, peripheral pressure measurements may under- or overestimate true ventricular pressure owing to reflection waves, and these may vary depending on the condition [26] or therapeutic interventions [25], making measurements of end-systolic elastance unreliable.

8.4.6 Speckle Tracking

When regional wall-motion abnormalities occur, measurement of the ejection fraction and many methods requiring area or volume estimates may become less reliable. New techniques estimating regional myocardial strain may provide insight into the myocardial performance, taking into account regional abnormalities in contractility.

Speckle tracking of specific pixels of two-dimensional echocardiographic images in the stable short-axis view (midpapillary level) allows quantification of regional wall-motion abnormalities and helps identifying dyssynchrony. Global strain is proportional to myocardial contractility, while time differences between the earliest and latest segmental strain offer an assessment of cardiac dyssynchrony [29].

This technique is promising, but it requires latest-generation echocardiographic machines and dedicated software. At this stage, it should still be considered an experimental technique.

8.5 Conclusion

Evaluation of systolic LV function can be a complex task, as illustrated by the huge number of methods proposed to evaluate it. For clinical purposes, the measurement of ejection fraction, or of fractional area change in the short-axis view at the level of the papillary muscles, is widely used to characterize a patient. In most cases, a rough visual evaluation of the ejection fraction is sufficient to make a correct hemodynamic evaluation. For research purposes or in specific situations, such as in valvular diseases, other indices may be used to quantify the contractile function more accurately. The complexity of these methods is such that they are not part of clinical routine and are used by a limited number of investigators.

In routine clinical practice, the LV ejection fraction (transthoracic approach, four-chamber view) or fractional area change should be measured (TEE or transthoracic ecocardiography, short-axis view, midpapillary muscle level). Visual evaluation is sufficient in most cases for trained operators. If available, automated border detection may be used to facilitate measurements and reduce inter- and intraobserver variability.

In patients with mitral regurgitation and severe aortic regurgitation, noninvasive dP/dt measurements on mitral regurgitant flow can be used.

For research purposes, one may consider other indices (VCF coupled with wall-stress measurement, LV hydraulic power). The position of end-systolic elastance and the speckle-tracking method remains to be determined.

References

1. Brown J, Jenkins C, Marwick TH (2009) Use of myocardial strain to assess global left ventricular function: a comparison with cardiac magnetic resonance and 3-dimensional echocardiography. Am Heart J 157:102–105
2. Krenning BJ, Voormolen MM, Roelandt JR (2003) Assessment of left ventricular function by three-dimensional echocardiography. Cardiovasc Ultrasound 1:12
3. Naik MM, Diamond GA, Pai T et al (1995) Correspondence of left ventricular ejection fraction determinations from two-dimensional echocardiography, radionuclide angiography and contrast cineangiography. J Am Coll Cardiol 25:937–942
4. Kuecherer HF, Kee LL, Modin G et al (1991) Echocardiography in serial evaluation of left ventricular systolic and diastolic function: importance of image acquisition, quantitation, and physiologic variability in clinical and investigational applications. J Am Soc Echocardiogr 4:203–214

5. Smith MD, MacPhail B, Harrison MR et al (1992) Value and limitations of transesophageal echocardiography in determination of left ventricular volumes and ejection fraction. J Am Coll Cardiol 19:1213–1222
6. Vignon P, Mentec H, Terre S et al (1994) Diagnostic accuracy and therapeutic impact of transthoracic and transesophageal echocardiography in mechanically ventilated patients in the ICU. Chest 106:1829–1834
7. Himelman RB, Cassidy MM, Landzberg JS et al (1988) Reproducibility of quantitative two-dimensional echocardiography. Am Heart J 115:425–431
8. Rahmouni HW, Ky B, Plappert T et al (2008) Clinical utility of automated assessment of left ventricular ejection fraction using artificial intelligence-assisted border detection. Am Heart J 155:562–570
9. Vieillard-Baron A, Charron C, Chergui K et al (2006) Bedside echocardiographic evaluation of hemodynamics in sepsis: is a qualitative evaluation sufficient? Intensive Care Med 32:1547–1552
10. Charron C, Prat G, Caille V et al (2007) Validation of a skills assessment scoring system for transesophageal echocardiographic monitoring of hemodynamics. Intensive Care Med 33:1712–1718
11. Vignon P, Dugard A, Abraham J et al (2007) Focused training for goal-oriented hand-held echocardiography performed by noncardiologist residents in the intensive care unit. Intensive Care Med 33:1795–1799
12. Mayo PH, Beaulieu Y, Doelken P et al (2009) American College of Chest Physicians/La Societe de Reanimation de Langue Francaise statement on competence in critical care ultrasonography. Chest 135:1050–1060
13. Robotham JL, Takata M, Berman M et al (1991) Ejection fraction revisited. Anesthesiology 74:172–183
14. Taccone FS, Lubicz B, Piagnerelli M et al (2009) Cardiogenic shock with stunned myocardium during triple-H therapy treated with intra-aortic balloon pump counterpulsation. Neurocrit Care 10:76–82
15. Goertz AW, Hubner C, Seefelder C et al (1994) The effect of ephedrine bolus administration on left ventricular loading and systolic performance during high thoracic epidural anesthesia combined with general anesthesia. Anesth Analg 78:101–105
16. Feltes TF, Pignatelli R, Kleinert S et al (1994) Quantitated left ventricular systolic mechanics in children with septic shock utilizing noninvasive wall-stress analysis. Crit Care Med 22:1647–1658
17. Ruschmer RF (1964) Initial ventricular implulse: a potential key to cardiac evaluation. Circulation 29:268–283
18. Noble MI, Gabe IT, Trenchard D et al (1967) Blood pressure and flow in the ascending aorta of conscious dogs. Cardiovasc Res 1:9–20
19. Bauer F, Jones M, Shiota T et al (2002) Left ventricular outflow tract mean systolic acceleration as a surrogate for the slope of the left ventricular end-systolic pressure–volume relationship. J Am Coll Cardiol 40:1320–1327
20. Berk MR, Evans J, Knapp C et al (1990) Influence of alterations in loading produced by lower body negative pressure on aortic blood flow acceleration. J Am Coll Cardiol 15: 1069–1074
21. Rhodes J, Udelson JE, Marx GR et al (1993) A new noninvasive method for the estimation of peak dP/dt. Circulation 88:2693–2699
22. Rhodes J, Marx GR, Tardif JC et al (1997) Evaluation of ventricular dP/dt before and after open heart surgery using transesophageal echocardiography. Echocardiography 14:15–22
23. Kang HJ, Kim YJ, Sohn DW et al (2003) Prediction of postoperative left ventricular systolic function with Doppler-derived dP/dt in patients with chronic aortic regurgitation. J Am Soc Echocardiogr 16:1111–1115
24. Poelaert JI, Schupfer G (2005) Hemodynamic monitoring utilizing transesophageal echocardiography: the relationships among pressure, flow, and function. Chest 127:379–390
25. Van den Bos GC, Westerhof N, Randall OS (1982) Pulse wave reflection: can it explain the differences between systemic and pulmonary pressure and flow waves? A study in dogs. Circ Res 51:479–485
26. Bilo HJ, van Schijndel RJ Strack, Schreuder WO et al (1989) Decreased reflection coefficient as a possible cause of low blood pressure in severe septicaemia. Intensive Care Med 15:137–139
27. Gorcsan J III, Denault A, Gasior TA et al (1994) Rapid estimation of left ventricular contractility from end-systolic relations by echocardiographic automated border detection and femoral arterial pressure. Anesthesiology 81:553–562
28. Cariou A, Pinsky MR, Monchi M et al (2008) Is myocardial adrenergic responsiveness depressed in human septic shock? Intensive Care Med 34:917–922
29. Tanabe M, Lamia B, Tanaka H et al (2008) Echocardiographic speckle tracking radial strain imaging to assess ventricular dyssynchrony in a pacing model of resynchronization therapy. J Am Soc Echocardiogr 21:1382–1388

Hemodynamic Evaluation in the Patient with Arrhythmias

9

Julien Maizel and Michel Slama

Contents

9.1 Introduction

In the general population as in patients hospitalized in intensive care units (ICUs), arrhythmia is a common, potentially fatal, condition [1, 2]. Annane et al. showed in a prospective, multicenter, cohort study the high prevalence (12%) and increased mortality of sustained arrhythmias in patients hospitalized in general ICUs [3]. The age, medical history of cardiovascular or endocrine disease, Simplified Acute Physiology Score II (SAPS II), and the need for vasopressor agents or mechanical ventilation were identified as risk factors for arrhythmias during an ICU stay. Because arrhythmias can dramatically alter the hemodynamic state of critically ill patients and limit the use of several echocardiographic variables usually recorded in sinus rhythm, it is necessary to know how to perform hemodynamic assessment with echocardiography in these patients.

In this chapter, we explain why the presence of an arrhythmia can alter the stroke volume and systolic and diastolic functions. We also indicate how echocardiography can be used to evaluate the hemodynamic state of patients with arrhythmias. Since atrial fibrillation (AF) is the most prominent clinical problem, we are focusing on this condition, but most of these considerations also apply in recurrent extrasystoles. Evaluation of the thromboembolic risk is not addressed here.

9.2 Hemodynamic Consequences of AF

A rapid heart rate, loss of atrial contraction, and irregularity of ventricular ejection affect the hemodynamic functions during AF.

J. Maizel (✉) and M. Slama
Unité de réanimation médicale, service de néphrologie, CHU Sud, 80054, Amiens Cedex 1, and
INSERM, ERI 12, Faculté de médecine d'Amiens, Université Jules Verne, France
e-mail: maizel.julien@chu-amiens.fr; slama.michel@chu-amiens.fr

D. De Backer et al. (eds.), *Hemodynamic Monitoring Using Echocardiography in the Critically Ill*,
DOI: 10.1007/978-3-540-87956-5_9, © Springer-Verlag Berlin Heidelberg 2011

9.2.1 Effects on Systolic Function

The irregular transmission of auricular depolarization to the ventricle generates a permanent change in myocardial contractility. Three mechanisms, resulting from the force–interval relationship, are responsible for this change in contractility. The first is the beat-to-beat variation in left ventricular (LV) afterload. During a short cycle or premature contraction, LV ejection begins before pressure in the aorta has completely decreased, and it remains higher than with longer diastoles [4, 5]. The second mechanism is the limited filling of the LV during a short diastole, generating a small LV preload and consequently a smaller stroke volume (in accordance with the Frank–Starling relationship) [5, 6]. The third mechanism relates the duration of diastole preceding ejection with contractility [4, 7]. A long diastole is associated with a higher contractility, a short diastole with a smaller contractility. Moreover, the improvement in contractility following a long diastole is amplified when this diastole is preceded by a shorter diastole [8].

A prolonged diastole is associated with a prolonged filling of the LV, resulting in a higher LV end-diastolic volume and thus a higher contractility according to the tension–length relationship. This relationship between contractility and duration of diastole is a consequence of the intracytoplasmic calcium concentration. The calcium transient is the succession of an intracellular calcium release from the sarcoplasmic reticulum during systole and a calcium reintegration into the sarcoplasmic reticulum during diastole. The calcium reintegration into the sarcoplasmic reticulum is more complete during a long than during a short diastole. The systole that follows a long diastole will be associated with a higher calcium release and consequently improved contractility.

9.2.2 Effects on Diastolic Function

AF is associated with a relative decrease in LV end-diastolic pressure (LVEDP) and an increase in both left atrial and pulmonary artery occlusion pressure (PAOP) [9]. The decrease in LVEDP is due to the short diastole and the loss of left auricular contraction occuring alongside an incomplete draining of the left atrium into the LV. If the left atrium cannot completely drain, a residual volume progressively accumulates with each diastole, resulting in an auricular dilatation [10]. Consequently, during AF, the LV filling is only dependent on the gradient between the left auricle and LV, corresponding to the passive filling period only [11]. This phenomenon is critical in patients with LV diastolic impairment, as LV filling is predominantly dependent on left atrial contraction in these cases, which explains the poor tolerance of AF in this population, whatever the systolic function.

9.2.3 Effects on Cardiac Output

The relative decrease in LVEDP, owing to the shortened diastole and decrease in LV contraction, results in a small stroke volume. However, the small stroke volume is not necessarily associated with a decrease in cardiac output because of the heart-rate acceleration [9, 12]. Tachycardia is associated with a decrease in diastolic time, but the relationship between diastolic time and stroke volume is not completely linear (Fig. 9.1). The first section of this curve is straight, which explains why the stroke volume does not change, though the heart rate increases. During the second part of this curve (>100 beats per min), the stroke volume significantly decreases whereas the heart rate increases. Hence, cardiac output may decrease if the heart rate exceeds 100 beats per min [13]: hence, the poor clinical tolerance of rapid AF. However, a preexistent systolic dysfunction does not seem to increase the risk of

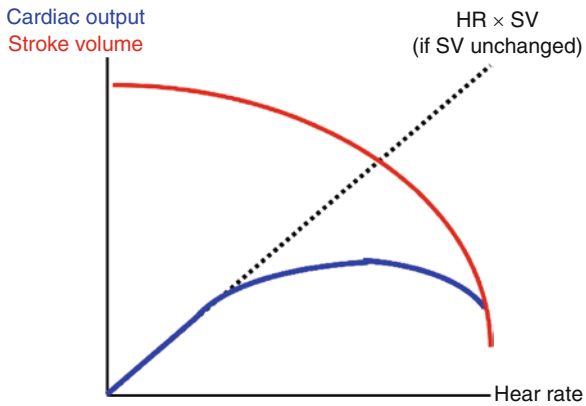

Fig. 9.1 Relationship between heart rate (HR) and stroke volume (SV) or cardiac output

acute cardiac failure during AF [14]. Conversely, a history of ischemic cardiomyopathy can have a negative impact on the prognosis. Indeed, increased oxygen consumption by the myocardium associated with tachycardia can be limited by the existence of coronary artery disease. In such cases, treatment should focus on reducing the heart rate.

9.3 Echocardiographic Evaluation of Patients with Arrhythmia

The hemodynamic evaluation of patients with arrhythmia, and particularly with AF, is not wholly different to that in patients in sinus rhythm, though some specific points should be noted.

9.3.1 Evaluation of Systolic Function

The variations in LV load conditions associated with arrhythmia markedly complicate evaluation of the LV pump function as most of the indices used at the bedside are preload and afterload dependent (see Chap. 8). Two methods are principally used (Table 9.1).

The first is based on the average of several consecutive measures of contractility variables (ejection fraction, shortening fraction). Admittedly, the number of measurements that should be averaged is not clearly established in the literature. This number depends on RR variability, with more measurements being required in the case of high RR variability. However, in most conditions, 10 consecutive measurements would appear to be satisfactory [15]. It is important to emphasize that these beats have to be consecutive since each beat is influenced by the preceding ones.

The second method measures LV contractility in a single beat as representing the mean heart rate, provided that this beat is preceded by two consecutive beats with the same RR interval. This method is based on the relationship between LV contractility and the two preceding RR intervals. The immediately preceding RR interval is termed RR-1, and the one before that RR-2. In an experimental study, the ejection fraction was better estimated using only one measurement preceded by two identical RR intervals (RR-1/RR-2 = 1) than averaging several consecutive measurements [8]. Of note, it is important that the selected beat be representative of the mean heart rate averaged over several beats (it would be meaningless to compute it during atrial acceleration). This method has been validated in humans, but it requires measurement of the ejection fraction in two different cardiac cycles, each of these being characterized by RR-1/RR-2 = 1 and a cycle length >500 ms [18, 19]. The main difficulty is, of course, that of obtaining two identical diastolic times. Theoretically, this requires measurement of the RR interval prior to measurement of the ejection fraction. In practice, visual estimation of the RR interval seems to be satisfactory. It should be noted that this technique has not been validated in patients under mechanical ventilation (or with important changes in pleural pressure during spontaneous ventilation), in whom changes in pleural pressure induce different loading conditions at inspiration and expiration.

Table 9.1 Methods and drawbacks in evaluating left ventricular systolic function in patients with atrial fibrillation

Methods	Drawbacks	References
Average 13 consecutive measures of LVEF	Increase the duration of the test	[15]
Measurement of LVEF over 2 cardiac cycles preceded by 2 equivalent RR intervals (RR-1/RR-2 = 1) >500 ms	Having to repeat RR-interval measurement before measuring LVEF	[8] [16] [17] [18]

Abbreviation: LVEF, left ventricular ejection fraction.

9.3.2 Evaluation of Stroke Volume

With regard to measurement of LV contractility, variability in load conditions generated by the irregular rhythm constitutes the main difficulty in assessing stroke volume reliably. In the first method, several measurements of the velocity–time integral (VTI) in the aortic root with pulsed Doppler are averaged. Dubrey et al. reported that 13 consecutive VTI measurements had to be averaged to produce a reliable estimate of stroke volume [15]. In practice, as noted above, 10 measurements should be sufficient since it appears that the ejection fraction seems can be reliably gauged with this number.

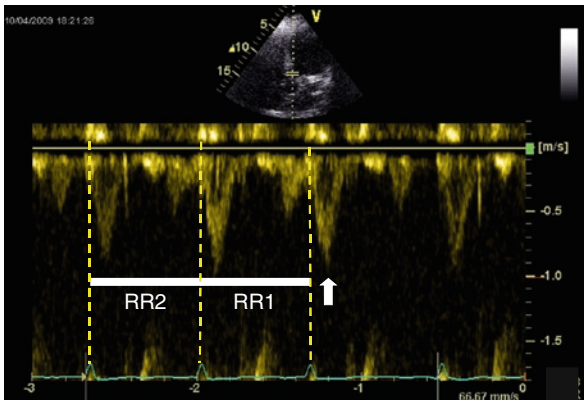

Fig. 9.2 Pulsed Doppler aortic flow in a patient with atrial fibrillation. Velocity–time integral is recorded after RR-1/RR-2 = 1

The second method (as with ejection fraction evaluation) measures VTI during a systole preceded by two similar RR intervals (Fig. 9.2) [8, 16, 17]. As mentioned above, visual estimation of the RR intervals appears to be sufficient, and measurements at a different part of the respiratory cycle need to be obtained. Hence, this method is even more demanding than the first in critically ill patients.

9.3.3 Evaluation of LV Diastolic Pressure

Since chronic AF itself enlarges the left atrium, it is not easy to differentiate the effect of an increased left auricular pressure from the progression of left atrial remodeling. Minimal left atrial volume (measured just before mitral valve closure) has been shown to correlate poorly ($r = 0.55$) with LV filling pressure in AF [20]. Accordingly, left atrial volume cannot be used to estimate left atrial pressure.

Even though there is a good correlation between Doppler measurements and the PAOP in sinus rhythm, many of these measurements may not be utilized in AF owing to the lost of left atrial contraction and irregularity of the RR intervals. The A waves of the mitral and pulmonary inflows disappear, and the S wave of the pulmonary inflow systematically decreases. Moreover, the irregularity of diastolic times is coupled with a variation in LVEDP such that several consecutive measurements should be averaged. However, some Doppler parameters can still be used even with the presence of AF. Doppler measurements have to be recorded over 5–10 cardiac cycles, selected on the quality of the signal, and need not be consecutive [20]. We can also record the Doppler parameters after a unique cycle length (RR interval) between 700 and 1,000 ms (heart rate 60–85 beats per min) (Fig. 9.3) [20–22]. Again, this latter approach will be limited in patients under mechanical ventilation.

According to Nagueh et al., the peak velocity of the early mitral inflow recorded by pulsed Doppler (E) is poorly correlated with the PAOP whatever the systolic function ($r = 0.42$) [20]. The E-wave maximal velocity is dependent on LV relaxation and left atrial pressure. Alteration in LV relaxation decreases E and, conversely, an increase in left atrial pressure increases E.

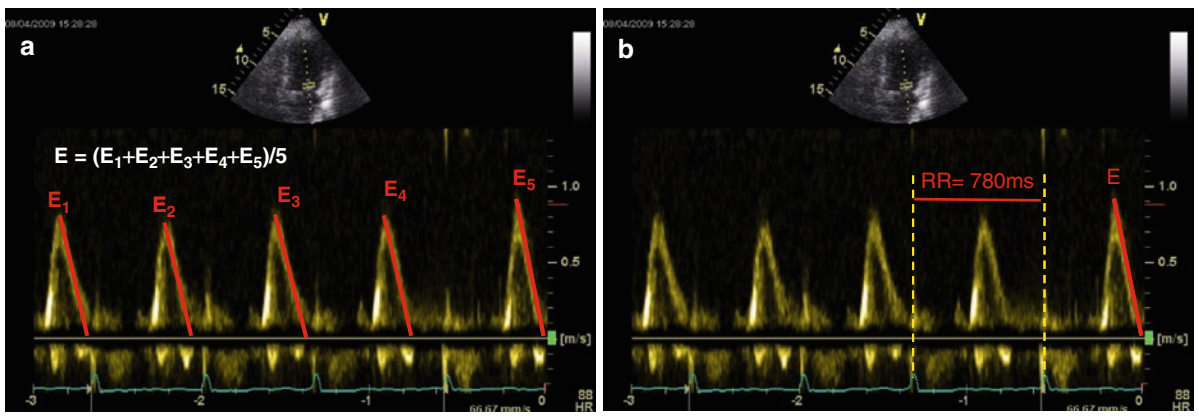

Fig. 9.3 Pulsed Doppler transmitral flow in a patient with atrial fibrillation. Maximal E-wave velocity and time deceleration are recorded (**a**) over five cardiac cycles (not necessarily consecutive, but based on the quality of the signal) or (**b**) after a cycle length >700 ms

This dual dependence affecting the relationship between E and PAOP explains why a young patient with a low left atrial pressure can present a higher E-wave maximal velocity than an older patient with a high left atrial pressure. Nevertheless, for a given patient, changes over a limited period of time may represent changes in PAOP, provided that diastolic function is not also affected.

The E deceleration time correlates well with the PAOP ($r=-0.78$) only in patients with impaired LV contractility: left ventricular ejection fraction (LVEF) <45%. In this population, an E deceleration time ≤150 ms predicts a PAOP >15 mmHg, with a sensibility of 71% and a specificity of 100% [20]. Similarly, Temporelli et al. reported a good correlation ($r=-0.95$) between the E deceleration time and the PAOP in 35 patients with a dilated cardiomyopathy and an altered LVEF [23]. An E deceleration time less than 120 ms predicts a PAOP ≥20 mmHg with a sensibility of 100% and a specificity of 96%.

The isovolumic relaxation time (IVRT) is the period between the beginning of diastole (aortic valve closure) and the beginning of LV filling (basis of mitral inflow). IVRT is recorded using continuous Doppler mode, placing the cursor between the mitral valve and the LV outflow. This duration is known to be related to LV relaxation and compliance, but it is also influenced by the heart rate. IVRT decreases when LV compliance decreases or when the heart rate increases. Conversely, IVRT increases when LV relaxation is impaired. The correlation with PAOP is excellent ($r=-0.76$). A cutoff value of IVRT ≤ 65 ms predicts a PAOP >15 mmHg, with a sensitivity and specificity of 72% and 88%, respectively [20].

Pulmonary venous inflow can also still be used to estimate the LVEDP. A deceleration time of the diastolic pulmonary venous flow >220 ms predicts a PAOP <15 mmHg, with a sensibility and specificity of 100% [21].

Tissue Doppler imaging may be utilized to limit the impact of diastolic function on PAOP measurements. The *E*/Ea ratio (where Ea is the early diastolic velocity recorded from Doppler tissue imaging with the sample cursor placed in the mitral annulus) is a good way of analyzing the LVEDP of patients in AF (Fig. 9.4). Sohn et al. found a correlation between E/Ea and PAOP of $r=0.79$ with a cutoff value of *E*/Ea ≥ 11 to predict a PAOP >15 mmHg, with a sensibility of 75% and a specificity of 93% [24].

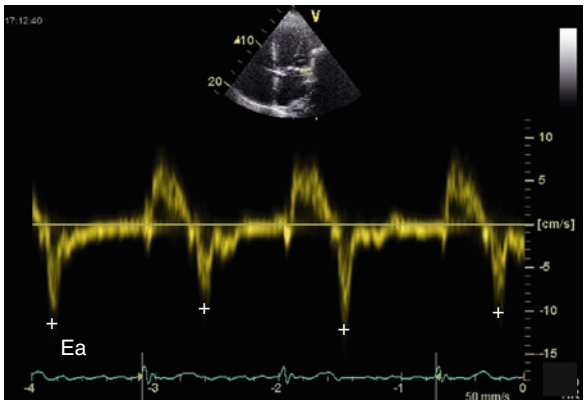

Fig. 9.4 Tissue Doppler assessment of Ea (early diastolic velocity recorded from imaging with the sample cursor placed in the mitral annulus) in a patient with atrial fibrillation

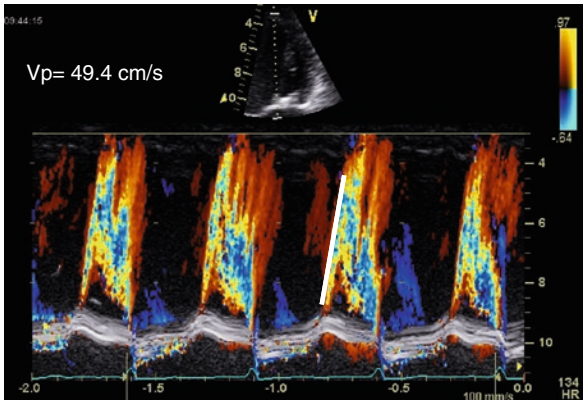

Fig. 9.5 Measurement of color M-mode Vp (slope of the first aliasing velocity of left ventricular inflow extending from the mitral valve to 4 cm distally into the left ventricular cavity) in a patient with atrial fibrillation

Alternatively, progression of mitral flow into the LV with color imaging can be employed. The *E*/Vp ratio (where Vp is the slope of the first aliasing velocity of LV inflow extending from the mitral valve to 4 cm distally into the LV cavity) may still be used to evaluate the PAOP (Fig. 9.5). According to Nagueh et al., the correlation between E/Vp and invasive PAOP is good ($r=0.75$), and an *E*/Vp > 1.4 is predictive of a PAOP >15 mmHg, with a sensitivity of 72% and a specificity of 100% [20]. However, Vp is not easy to record and offers poor reproducibility, particularly for the inexperienced echocardiographist. The different echocardiographic measurements are summarized in Table 9.2.

Table 9.2 Doppler assessment of left ventricular filling pressures in patients with atrial fibrillation

Method	Cutoff	Diagnostic accuracy	limits and drawbacks	References
E-wave deceleration time	≤120 ms	Sensibility 100% and specificity 96% in predicting a PAOP ≥ 20 mmHg	LVEF < 45%	[23]
Deceleration time of diastolic pulmonary venous flow	>220 ms	Sensibility and specificity of 100% in predicting a PAOP ≤ 12 mmHg	Difficulties in recording a pulmonary venous flow with transthoracic echocardiography	[21]
Isovolumic relaxation time	≤65 ms	Sensibility 72% and specificity 88% in predicting a PAOP >15 mmHg	Highly dependent on heart rate	[20]
E/Ea ratio	≥11	Sensibility of 75% and specificity of 93% in predicting a PAOP >15 mmHg	Cinetic perturbation of mitral annulus	[24]
Rapport E/Vp	≥1.4	Sensibility of 72% and specificity of 100% in predicting a PAOP >15 mmHg	High variability of Vp measurement	[20]

Abbreviations: E, maximal velocity of mitral E wave; Ea, early diastolic velocity recorded from Doppler tissue imaging with sample cursor placed in mitral annulus; PAOP, pulmonary artery occlusion pressure; Vp, slope of first aliasing velocity of LV inflow extending from mitral valve to 4 cm distally into LV cavity; TTE, transthoracic echocardiography; LVEF, left ventricular ejection fraction

9.3.4 LV strain and Strain Rate

Left ventricular strain (LVSt) and strain rate (LVStR) are parameters that have been obtained only recently using the latest echocardiographs and off-line analysis. The LV global strain and strain rate correlate well with LV relaxation parameters, and the ratios E/LVSt and E/LVStR have been recently studied in cardiology patients referred to the catheterization room. Wang et al. showed that the ratio E/LVStR (with LVStR measured during the IVRT) is closely correlated with LV filling pressure, irrespective of LVEF. A cutoff value of E/LVStR >236 cm predicts a PAOP >15 mmHg, with a sensitivity of 96% and a specificity of 82% [25]. In 2008, Dokainish et al. confirmed the accuracy of *E*/LVStR (with LVStR measured during peak mitral filling) to predict a PAOP >15 mmHg with a cutoff >115 cm, having a sensitivity of 89% and a specificity of 85% [26]. But these studies were performed only in patients with sinus rhythm. In AF, these measurements have not yet been validated. Measurement of the regional LVStR on a single cardiac beat with RR-1/RR-2 = 1 reliably estimates the average value of multiple cycles [27], but no attempt to correlate it with invasively measured PAOP has been made.

Therefore, strain and strain rate are promising methods to explore LV filling pressure and diastolic function in cardiology patients, but more studies are needed before using the methods in critically ill patients, especially when presenting with AF. The feasibility and simplicity of those measurements have not been compared with those of more conventional parameters.

9.4 Conclusions

Hemodynamic evaluation using echocardiography in a patient with AF is a challenge for the intensivist. Tachycardia, loss of atrial contraction, and irregularity of ventricular ejection affect the hemodynamic functions during AF. Measurements of stroke volume and LV systolic and diastolic functions require the use of appropriate methods and knowledge of their limits.

References

1. Peters NS, Schilling RJ, Kanagaratnam P, Markides V (2002) Atrial fibrillation: strategies to control, combat, and cure. Lancet 359:593–603
2. Trappe HJ, Brandts B, Weismueller P (2003) Arrhythmias in the intensive care patient. Curr Opin Crit Care 9:345–355
3. Annane D, Sébille V, Duboc D, Le Heuzey JY, Sadoul N, Bouvier E, Bellissant E (2008) Incidence and prognosis of

sustained arrhythmias in critically ill patients. Am J Respir Crit Care Med 178:20–25
4. Karliner JS, Gault JH, Bouchard RJ, Holzer J (1974) Factors influencing the ejection fraction and the mean rate of circumferential fibre shortening during atrial fibrillation in man. Cardiovasc Res 8:18–25
5. Belenkie I (1979) Beat-to-beat variability of echocardiographic measurements of left ventricular end diastolic diameter and performance. J Clin Ultrasound 7: 263–268
6. Braunwald E, Frye RL, Aygen MM, Gilbert JW (1960) Studies on Starling's law of the heart. III. Observations in patients with mitral stenosis and atrial fibrillation on the relationships between left ventricular end-diastolic segment length, filling pressure and the characteristics of ventricular contraction. J Clin Invest 39:1874–1884
7. Meijler FL, Strackee J, Van Capelle JL, Du Perron JC (1968) Computer analysis of the RR interval-contractility relationship during random stimulation of the isolated heart. Circ Res 22:695–702
8. Tabata T, Grimm RA, Greenberg NL, Agler DA, Mowrey KA, Wallick DW et al (2001) Assessment of LV systolic function in atrial fibrillation using an index of preceding cardiac cycles. Am J Physiol Heart Circ Physiol 281: H573–H580
9. Alboni P, Scarfò S, Fucà G, Paparella N, Yannacopulu P (1995) Hemodynamics of idiopathic paroxysmal atrial fibrillation. Pacing Clin Electrophysiol 18:980–985
10. White CW, Kerber RE, Weiss HR, Marcus ML (1982) The effects of atrial fibrillation on atrial pressure-volume and flow relationships. Circ Res 51:205–215
11. Mitchell JH, Gilmore JP, Sarnoff SJ (1962) The transport function of the atrium. Factors influencing the relation between mean left atrial pressure and left ventricular end diastolic pressure. Am J Cardiol 9:237–247
12. Lau CP, Leung WH, Wong CK, Cheng CH (1990) Haemodynamics of induced atrial fibrillation: a comparative assessment with sinus rhythm, atrial and ventricular pacing. Eur Heart J 11:219–224
13. Kerr AJ, Simmonds MB, Stewart RA (1998) Influence of heart rate on stroke volume variability in atrial fibrillation in patients with normal and impaired left ventricular function. Am J Cardiol 82:1496–1500
14. Freudenberger RS, Wilson AC, Kostis JB, AFFIRM Investigators and Committees (2007) Comparison of rate versus rhythm control for atrial fibrillation in patients with left ventricular dysfunction (from the AFFIRM Study). Am J Cardiol 100:247–52
15. Dubrey SW, Falk RH (1997) Optimal number of beats for the Doppler measurement of cardiac output in atrial fibrillation. J Am Soc Echocardiogr 10:67–71
16. Sumida T, Tanabe K, Yagi T, Kawai J, Konda T, Fujii Y et al (2003) Single-beat determination of Doppler-derived aortic flow measurement in patients with atrial fibrillation. J Am Soc Echocardiogr 16:712–715
17. Tanabe M, Onishi K, Dohi K, Kitamura T, Ito M, Nobori T, Nakano T (2006) Assessment of left ventricular systolic function in patients with chronic atrial fibrillation and dilated cardiomyopathy using the ratio of preceding to prepreceding R-R intervals. Int J Cardiol 108:197–201
18. Wang CL, Ho WJ, Luqman N, Hsu LA, Kuo CT (2006) Biplane assessment of left ventricular function during atrial fibrillation at beats with equal subsequent cycles. Int J Cardiol 113:54–60
19. Wang CL, Lin KH, Luqman N, Ho WJ, Hsu LA, Chu PH, Kuo CT (2005) Refinement on single-beat determination of left ventricular systolic function in patients with atrial fibrillation. J Am Soc Echocardiogr 18:913–918
20. Nagueh SF, Kopelen HA, Quiñones MA (1996) Assessment of left ventricular filling pressures by Doppler in the presence of atrial fibrillation. Circulation 94:2138–2145
21. Chirillo F, Brunazzi MC, Barbiero M, Giavarina D, Pasqualini M, Franceschini-Grisolia E et al (1997) Estimating mean pulmonary wedge pressure in patients with chronic atrial fibrillation from transthoracic Doppler indexes of mitral and pulmonary venous flow velocity. J Am Coll Cardiol 30:19–26
22. Matsukida K, Kisanuki A, Toyonaga K, Murayama T, Nakashima H, Kumanohoso T et al (2001) Comparison of transthoracic Doppler echocardiography and natriuretic peptides in predicting mean pulmonary capillary wedge pressure in patients with chronic atrial fibrillation. J Am Soc Echocardiogr 14:1080–1087
23. Temporelli PL, Scapellato F, Corrà U, Eleuteri E, Imparato A, Giannuzzi P (1999) Estimation of pulmonary wedge pressure by transmitral Doppler in patients with chronic heart failure and atrial fibrillation. Am J Cardiol 83:724–727
24. Sohn DW, Song JM, Zo JH, Chai IH, Kim HS, Chun HG, Kim HC (1999) Mitral annulus velocity in the evaluation of left ventricular diastolic function in atrial fibrillation. J Am Soc Echocardiogr 12:927–931
25. Wang J, Khoury DS, Thohan V, Torre-Amione G, Nagueh SF (2007) Global diastolic strain rate for the assessment of left ventricular relaxation and filling pressures. Circulation 115:1376–1383
26. Dokainish H, Sengupta R, Pillai M, Bobek J, Lakkis N (2008) Usefulness of new diastolic strain and strain rate indexes for the estimation of left ventricular filling pressure. Am J Cardiol 101:1504–1509
27. Yamanaka-Funabiki K, Onishi K, Tanabe M, Dohi K, Ito M, Ohte N et al (2006) Single beat determination of regional myocardial strain measurements in patients with atrial fibrillation. J Am Soc Echocardiogr 19:1332–1337

Part III

Diagnosis and Management of Circulatory Failure

Diagnosing the Mechanisms of Circulatory Failure

10

Philippe Vignon and Michel Slama

Contents

P. Vignon (✉)
Medical-surgical Intensive Care Unit,
Clinical investigation Centre INSERM 0801,
CHU Dupuytren, 2 Avenue Martin Luther King, 87000,
Limoges and
Université de Limoges, 2rue du Dr. Marcland, 87000,
Limoges, France
e-mail: philippe.vignon@unilim.fr

M. Slama
Faculté de médecine d'Amiens,
Unité de réanimation médicale,
service de néphrologie, CHU Sud,
Amiens, and INSERM, ERI 12,
Université Jules Verne, 80054, Amiens Cedex 1, France

Circulatory failure encompasses a broad range of clinical scenarios, primarily involving the occurrence of shock in critically ill patients with frequently associated comorbidities. The primary goal of acute therapeutic management is to restore rapidly an adequate tissue perfusion and oxygen delivery in order to meet the patient's metabolic demand. If shock persists after initial resuscitation, a comprehensive evaluation of hemodynamic status is crucial in identifying the prime mechanism of circulatory failure and guiding acute care in patients requiring more advanced and prolonged support.

Echocardiography Doppler is an unparalleled technique that provides functional and morphological information about the heart and great vessels [1]. By providing real-time images, it directly depicts the response and tolerance to therapy, which are not accessible using other "blind" technologies [2]. The assessment of circulatory failure and shock constitutes the most frequent indication for performing an echocardiographic study in intensive care unit (ICU) settings. In addition to its diagnostic capability, echocardiography allows for a close monitoring of ultrasound-guided therapeutic changes.

The present chapter describes the use of Doppler echocardiography for the diagnosis and management of circulatory failure and presents an overview of decision algorithms. It is important to note that the algorithms proposed here are unable cover the great complexity and number of different clinical situations. Circulatory failure after cardiac surgery, severe trauma, or associated with the acute aortic syndrome is detailed in a specific section (see Part. 5).

D. De Backer et al. (eds.), *Hemodynamic Monitoring Using Echocardiography in the Critically Ill*,
DOI: 10.1007/978-3-540-87956-5_10, © Springer-Verlag Berlin Heidelberg 2011

10.1 Definitions

Clinical findings suggestive of shock are typically associated with the presence of hypotension together with abnormal heart rate and signs of tissue hypoperfusion, such as altered mental status, decreased urine output, skin mottling, and cold extremities [3]. Shock results from inadequate tissue perfusion and oxygen delivery with respect to organ needs, which ultimately lead to cellular dysoxia. Accordingly, shock has recently been defined by an international consensus conference as a life-threatening, generalized maldistribution of blood flow, resulting in failure to deliver and/or utilize adequate amounts of oxygen, leading to tissue dysoxia [4]. Importantly, the conference recommended that the presence of hypotension (i.e., systolic blood pressure <90 mmHg or decrease of at least 40 mmHg from baseline or mean arterial pressure <65 mmHg) was not required to define shock [4]. Although hemodynamic instability is most frequently present in the development of shock, clinical signs of tissue hypoperfusion and/or biological markers of inadequate tissue perfusion – e.g., decreased central venous oxygen saturation ($ScvO_2$) or mixed venous oxygen saturation (SvO_2), increased blood lactate, increased base deficit, and low pH – can be observed in the absence of hypotension [4].

10.2 Indications of Echocardiography

Recent American guidelines recommend performing a transthoracic (TTE) or transesophageal echocardiography (TEE) to evaluate hypotension or hemodynamic instability of uncertain or suspected cardiac etiology with an appropriateness score [5]. The recent international consensus conference postulates that TTE can be safely considered in patients sustaining persistent shock despite aggressive initial therapy [4]. Using modern upper-end platforms, TTE has been reliably shown to exclude a cardiac source of shock in ventilated critically ill patients [6]. Nevertheless, accumulated experience in ICUs routinely using echocardiography as a first-line imaging technique for the assessment of circulatory failure suggests that TTE frequently fails to provide adequate imaging quality and unambiguous findings in mechanically ventilated patients [7, 8]. In these cases, TEE is the preferred approach [5]. When contraindications are carefully excluded, esophageal intubation is safe in critically ill patients who are mechanically ventilated [9]. TEE provides further insight into central hemodynamics, such as in examining the superior vena cava, which indirectly allows assessment of volume status (see Chap. 4).

10.3 Advantages and Limitations of Echocardiography

Several studies have shown the additional value of echocardiography in patients presenting with circulatory failure who were assessed using right-heart catheterization [10–14] or the single-indicator transpulmonary thermodilution technique (PiCCO system) [15]. This is presumably related to: (1) the limitations of the thermodilution technique for accurate measurement of cardiac output [16, 17] and identification of the failing ventricle in low-flow states [8, 15]; (2) the inability of cardiac filling pressures to predict fluid responsiveness reliably [18]. Whether echocardiography and continuous monitoring technologies should be jointly used in a multimodal approach ultimately to treat these complex patients more effectively remains to be determined (see Chap. 22).

Doppler echocardiography suffers from substantial limitations. As with every imaging modality, cardiac ultrasonography is an intermittent, yet easily repeatable, operator-dependent technique. Adequate image acquisition and interpretation of echocardiographic findings are of utmost importance to ensure diagnostic accuracy and provide a satisfactory guide to therapy in unstable ICU patients. These require a tailored training, especially when performed in the ICU environment by non-cardiologists [19]. Focused, goal-oriented TTE [20] and TEE [14, 21] have proved efficient after limited training to provide adequate answers to simple, limited clinical questions. Nevertheless, the assessment of patients sustaining complex shock requires a more comprehensive hemodynamic evaluation (see Chap. 21).

10.4 Diagnostic Algorithms

To accommodate all nuances of interpretation, the proposed algorithms should be considered within the context of the following important assumptions. First, the

algorithms should be used in light of the clinical situation and are unable to cover the great complexity and number of clinical situations encountered in the ICU environment. Second, the indications of TTE and TEE are assumed to be adequate with regard to their respective diagnostic accuracy (see Chap. 1). Third, the echocardiographic study is performed and interpreted by a trained intensivist, who is aware of the adequate conditions for using this diagnostic modality, as described below.

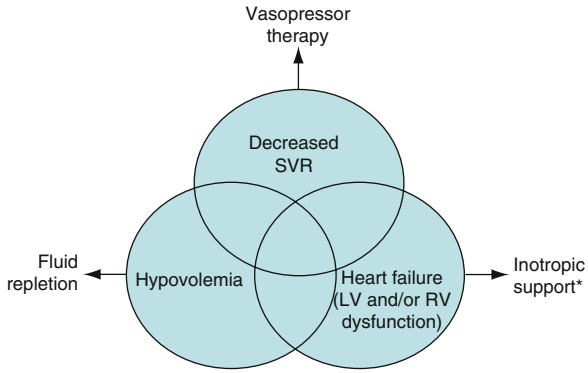

Fig. 10.1 Primary mechanisms of acute circulatory failure. Doppler echocardiography allows identifying the leading mechanism of shock and helps in guiding acute therapy. It also allows prompt diagnosis of mainstream obstruction of blood flow (e.g., cardiac tamponade, massive pulmonary embolism, dynamic left outflow tract obstruction). *: Vasopressors may be indicated in the presence of isolated RV failure. Abbreviations: SVR, systemic vascular resistance; LV, left ventricle; RV, right ventricle

10.4.1 Conditions of Use

Echocardiographic results have to be incorporated within a sound medical framework, which takes into account medical history, current clinical situation, and ongoing therapies (e.g., fluid loading, vasopressor or inotropic support). In the absence of overt echocardiographic abnormalities, concordant abnormal findings or out-of-range indices should be gathered to identify more confidently the leading mechanism of shock. The clinical relevance of fortuitous echocardiographic diagnoses (e.g., underlying chronic cardiomyopathy, or valvulopathy) should carefully be examined in patients assessed for circulatory failure. Since the hemodynamic profile is influenced by both the pathological process and therapeutic interventions, the profile observed in an unstable patient may rapidly change over a short period. For example, transient left ventricular (LV) systolic dysfunction is commonly observed at the acute phase of septic shock and in many other clinical circumstances encountered in ICU patients. The diagnostic algorithms proposed below should be used in the specific clinical context of each patient to prompt diagnosis of the origin of shock and determine the appropriate therapy (Fig. 10.1).

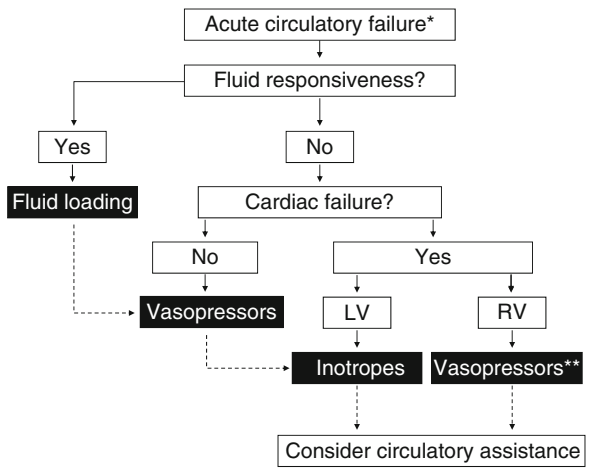

Fig. 10.2 General algorithm illustrating the successive steps followed using echocardiography in the comprehensive assessment of an acute circulatory failure. Dashed arrows indicate second-line or rescue therapies in the absence of efficacy or poor tolerance of initial treatment. *: Cardiac tamponade is usually immediately ruled out; **: inhaled nitric oxide may be used to decrease pulmonary vascular resistance, and inotropic support may be proposed, especially if left ventricular (LV) systolic dysfunction is also present. Abbreviation: RV, right ventricle

10.4.2 General Approach

In a patient with acute circulatory failure, the first step is to determine whether cardiac output – and eventually mean blood pressure – can be significantly improved by fluid repletion, a situation commonly termed fluid or preload responsiveness (Fig. 10.2). Although overt hypovolemia can be immediately diagnosed in the presence of a severely reduced LV cavity size, the measurement of end-diastolic LV area or volume used as surrogates of ventricular preload commonly fails to predict fluid responsiveness

accurately in a given patient [22]. Accordingly, "dynamic" echocardiographic parameters are better suited to evaluate preload responsiveness in ventilated patients who have frequently received variable amounts of fluid during initial resuscitation efforts (see Chaps. 6 and 7). Like other dynamic circulatory indices, respiratory variations of vena cava diameters and aortic Doppler velocities have been validated in septic patients under strict clinical conditions [18].

Table 10.1 Common causes of left ventricular systolic dysfunction in the intensive care unit patient with circulatory failure and associated echocardiographic findings

	Time sequence	Main etiology
Decompensated heart failure	Acute on chronic	Dilated cardiomyopathy Chronic ischemic heart disease Severe left-sided valvulopathy[a]
Acute heart failure	Acute	Acute (extended/complicated) myocardial infarction Acute/fulminant myocarditits Severe myocardial contusion Severe intoxication with cardiac depressant drugs
Sepsis	Acute	Septic shock[b]

[a]With the exception of severe mitral stenosis
[b]In this case, left ventricular filling pressure is not necessarily elevated

In the absence of preload dependence, the second step is to document a potential cardiac failure (Fig. 10.2). Echocardiography allows accurate measurement of LV stroke volume using the Doppler method at the level of the aortic ring/LV outflow tract [23]. In low-flow states, cardiac ultrasonography clearly depicts which is the prominent failing ventricle (see Chap. 5).

Global LV systolic function can be readily quantified using relatively simple geometric assumptions to obtain LV ejection fraction [24] (see Chap. 8). LV systolic dysfunction may be related to a decompensated heart failure secondary to any cardiac disease, the development of an acute heart failure most frequently related to an extended/complicated myocardial infarction, or acute myocarditis; alternatively, it may be associated with septic shock regardless of its origin (Table 10.1). The presence of a significant LV remodeling (e.g., LV cavity enlargement, thin LV walls) usually reflects the presence of an underlying chronic heart disease. Regional wall-motion abnormalities are usually consistent with ischemic heart disease. Assessment of the severity of a mitral or aortic valvulopathy allows the chronic cardiac disease to be integrated into the clinical scenario. Pulmonary hypertension may be severe, especially in chronic cardiac disease. In contrast, acute heart disease is typically characterized by the presence of a normal-sized LV, with moderately elevated pulmonary artery pressures. The presence of LV regional wall-motion

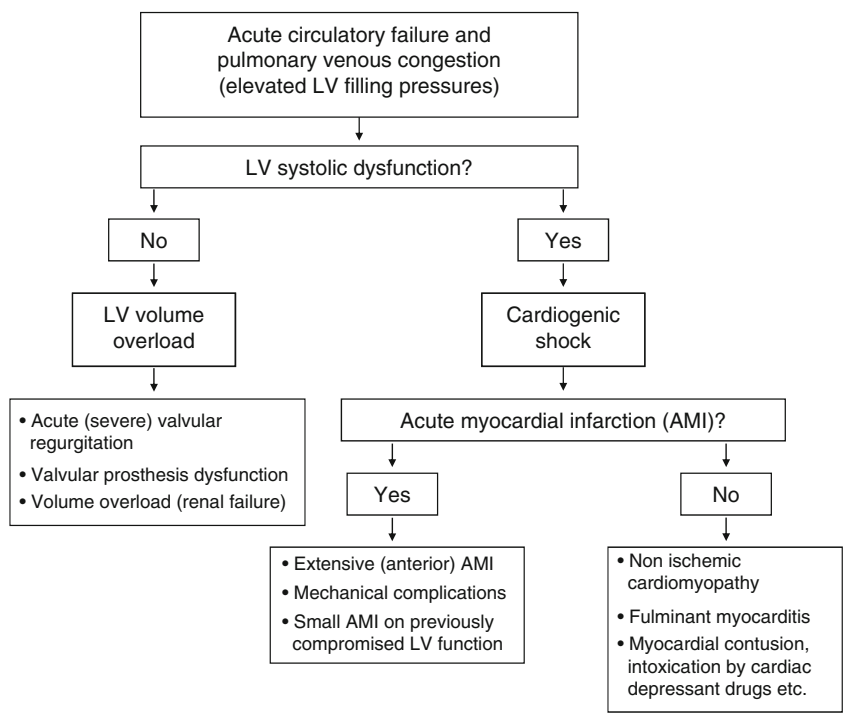

Fig. 10.3 Diagnostic algorithm proposed for assessing acute circulatory failure associated with pulmonary venous congestion, i.e., elevated left ventricular (LV) filling pressures. Acute myocardial infarction is the most frequent cause of cardiogenic shock. Mechanical complications refer to LV wall or papillary muscle rupture. LV volume overload is less common and mainly related to acute valvular diseases. Abbreviation: AMI, acute myocardial infarction

abnormalities is consistent with an acute myocardial infarction, an acute fulminant myocarditis, or it may reflect a severe myocardial contusion after a blunt chest trauma. LV systolic dysfunction associated with septic shock is usually characterized by an anatomically normal ventricle and low to normal filling pressures.

Right ventricular (RV) systolic function is more difficult to quantify precisely than LV systolic dysfunction (see Chap. 13). In most situations in which a failing RV is responsible for shock, its cavity is (markedly) dilated. RV sensitivity to abrupt variations in afterload may exacerbate systolic dysfunction, especially in ventilated patients with respiratory compromise and increased pulmonary vascular resistance (see Chap. 17). The presence of an associated paradoxical septal motion suggests an RV systolic overload [25]. Biventricular failure frequently requires inotropic support, whereas prominent RV systolic dysfunction may be improved by vasopressor therapy aimed at restoring an adequate level of coronary artery perfusion pressure [8]. In addition, protective ventilator settings should be considered to avoid excessive plateau pressure in ventilated patients with an overloaded RV (see Chap. 17).

When both significant hypovolemia and cardiac pump failure have been excluded by echocardiography, vasopressor therapy needs to be considered. In the absence of clinical improvement, LV systolic function should be reassessed echocardiographically. In septic patients, increasing systemic vascular resistance may reveal the underlying myocardial dysfunction, and the increase in LV afterload may be poorly tolerated [26, 27].

Finally, Doppler echocardiography allows the diagnosis of uncommon acute conditions that may result in circulatory failure (e.g., dynamic LV outflow tract obstruction, acute valvular regurgitation) and remain inaccessible to blind monitoring systems.

10.4.3 Acute Circulatory Failure with Pulmonary Venous Congestion

Acute circulatory failure in conjunction with signs of pulmonary venous congestion (pulmonary edema) indicates the presence of a prominent LV failure. Cardiogenic shock is the most severe clinical presentation (see Chap. 12). The leading cause of cardiogenic shock is LV systolic dysfunction secondary to extended acute myocardial infarction. Hemodynamic confirmation relies on the presence of sustained hypotension with adequate or elevated LV filling pressures and reduced cardiac output [28]. Recent guidelines recommend that objective documentation of cardiac dysfunction related to acute heart failure has to be obtained by echocardiography [29]. First, two-dimensional echocardiography allows the identification of low-flow states related to severe LV systolic dysfunction. Second, Doppler examination confirms the presence of typically elevated LV filling pressures (see Chap. 16). Third, echocardiography provides exceptional information regarding the causal cardiomyopathy: LV remodeling and regional wall-motion abnormalities consistent with ischemic heart disease, mechanical complications of acute myocardial infarction (see Chap. 12), or noncoronary cardiac diseases, such as severe cardiomyopathies, extended myocardial contusion, fulminant myocarditis, or massive intoxication by cardiac depressant drugs [30, 31].

The presence of a preserved LV systolic function but elevated filling pressures suggests that an acute LV volume overload could be the origin of the circulatory failure (Fig. 10.3). The absence of dilatation of left cardiac cavities and relatively low levels of pulmonary hypertension are usually consistent with an acute condition [30]. Interestingly, echocardiography may clearly depict the cause of acute LV volume overload (e.g., acute endocarditis, ruptured papillary muscle or mitral chordae, valvular prosthesis dysfunction) and

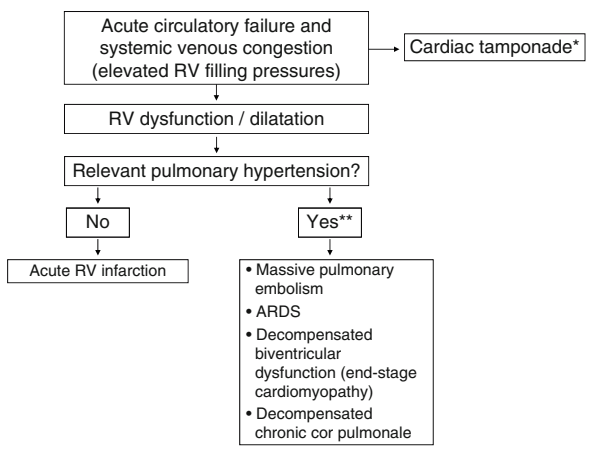

Fig. 10.4 Diagnostic algorithm proposed for assessing an acute circulatory failure with systemic venous congestion, i.e., elevated right ventricular (RV) filling pressures. With the exception of cardiac tamponade, the RV is typically dilated in this clinical scenario. RV failure may be precipitated by increased pulmonary vascular resistance, regardless of its origin. *: Cardiac tamponade is usually diagnosed immediately; **: provided that the RV can generate a substantial systolic pressure. Abbreviation: ARDS, acute respiratory distress syndrome

confirm its severity (see Chaps. 12 and 16). Iatrogenic volume overload is predominantly encountered in anuric patients with renal failure.

10.4.4 Acute Circulatory Failure with Systemic Venous Congestion

Acute circulatory failure in conjunction with signs of systemic venous congestion indicates the presence of a prominent RV failure, or it may reflect a mainstream obstruction of blood flow (e.g., cardiac tamponade, massive pulmonary embolism). Concomitant RV and LV systolic dysfunction associated with biventricular dilatation is usually consistent with a long-standing cardiomyopathy [32]. Patients with right-heart failure typically present with acute-onset dyspnea at rest, physical signs of peripheral congestion, and clear lung fields [29]. In this clinical setting, echocardiography helps identify the severity and origin of RV failure and promptly allows an alternative diagnosis of cardiac tamponade to be made (see Chap. 14).

In a hypotensive patient who presents with an acute coronary syndrome, a dilated RV with marked systolic dysfunction, but no relevant pulmonary hypertension, may be attributed to an RV infarction (Fig. 10.4). RV systolic pressure is not increased, as reflected by a low peak tricuspid regurgitant velocity, and associated regional wall-motion abnormality in the LV inferior wall is frequently observed [33]. In

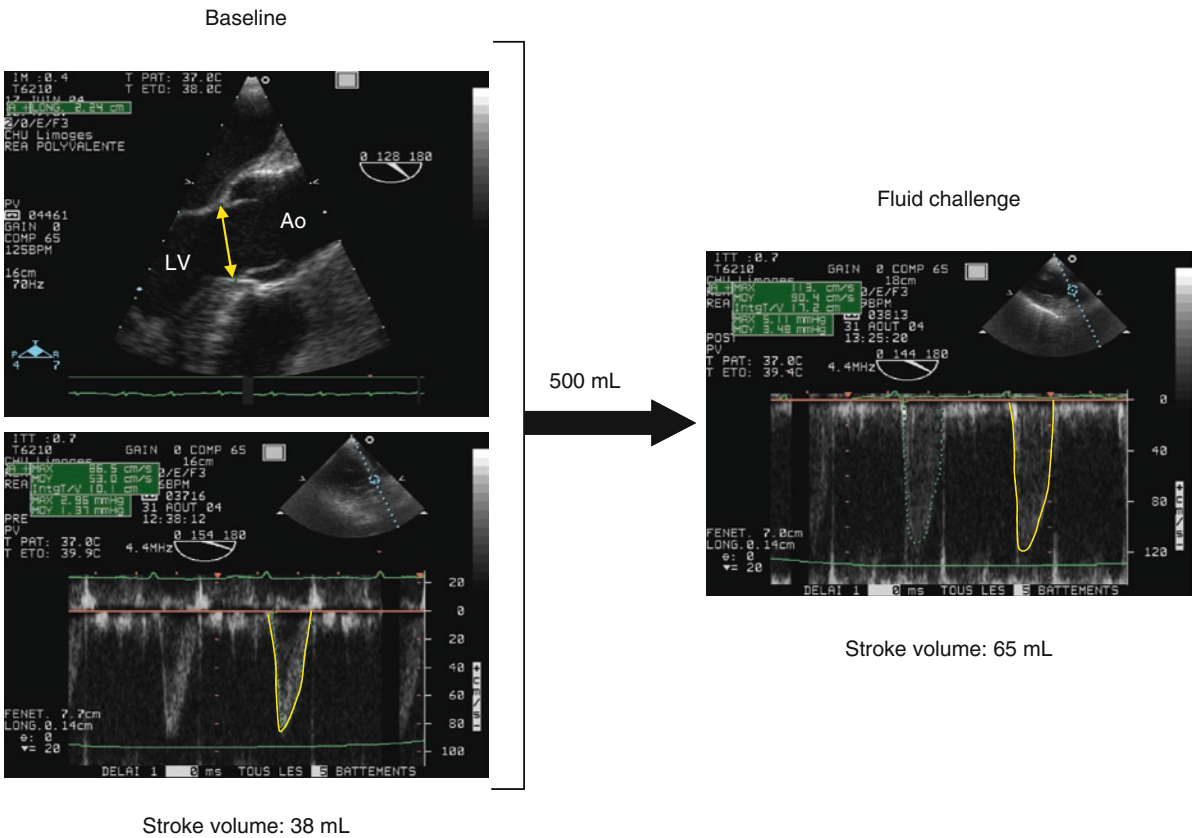

Fig. 10.5 Monitoring of a fluid challenge using transesophageal echocardiography. Real-time iterative measurements of left ventricular stroke volume during volume repletion allow a close tracking of cardiac response to fluid therapy. Prior to the fluid challenge, measurement of both the left ventricular outflow tract diameter (*upper left, yellow double-headed arrow*) and velocity-time integral of Doppler velocity profile (*lower left, yellow line*) allows for determination of stroke volume. After blood volume expansion, the velocity-time integral of the aortic Doppler pattern is solely measured since the surface of the aortic annulus is considered to remain constant (*right panel, yellow line*). In this patient, left ventricular stroke volume increased from 38 to 65 mL after the rapid infusion of 500 mL of colloids

the setting of increased RV output afterload, the conjunction of significant RV dilatation and paradoxical septal motion is suggestive of acute cor pulmonale [25, 34]. RV afterloading is usually reflected by pulmonary hypertension, provided that RV systolic function can still generate a substantial systolic pressure [35]. In this clinical setting, the identification of an embolus-in-transit within right cardiac cavities or the documentation of an entrapped embolus in the proximal pulmonary artery is pathognomonic of massive pulmonary embolism (see Chap. 13). Although TEE has a greater diagnostic accuracy than TTE, it should be performed only in patients who are already ventilated since esophageal intubation may abruptly deteriorate the condition of spontaneously breathing, unstable patients. Importantly, acute cor pulmonale is consistent with massive pulmonary embolism, but it may also be observed in up to 25% of patients with acute respiratory distress syndrome [34].

Exacerbation of chronic heart disease or chronic pulmonary hypertension can also lead to a circulatory failure with systemic venous congestion. In these patients, marked RV free-wall hypertrophy (10 mm or more) in conjunction with a dilated RV cavity is consistent with chronic cor pulmonale [25]. Severe pulmonary hypertension is usually present. Finally, RV volume overload secondary to an atrial septal defect or an organic tricuspid insufficiency (e.g., flail tricuspid leaflet, endocarditis) may contribute to RV failure.

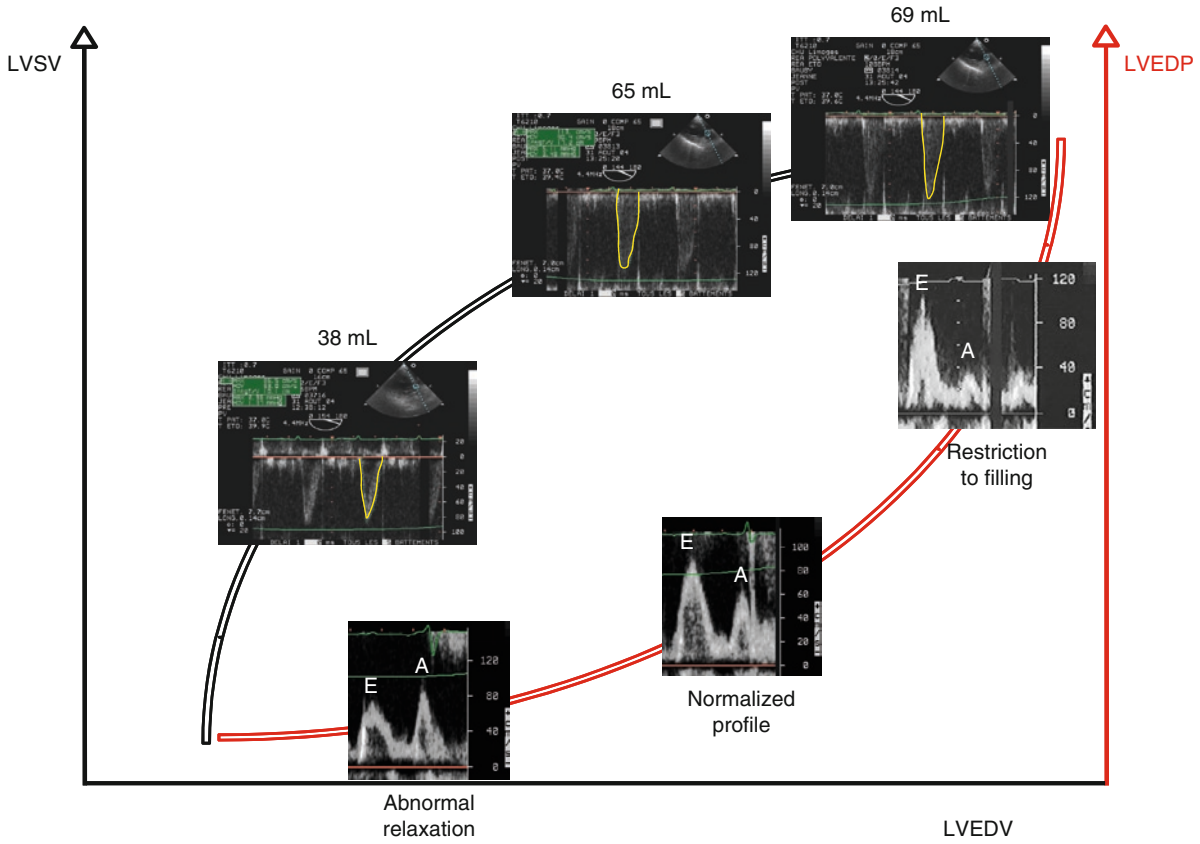

Fig. 10.6 Assessment of the efficacy (stroke volume) and tolerance (left ventricular filling pressures) of blood volume expansion using Doppler echocardiography. With serial echocar-diographic hemodynamic assessments, one can mentally construct the systolic function curve and the diastolic pressure-volume curve of the left ventricle. In this patient, the first fluid challenge resulted in a substantial increase in left ventricular stroke volume (LVSV; 38–65 mL), whereas the second blood volume expansion was unsuccessful (65–69 mL). The mitral Doppler velocity profile grossly reflects both left ventricular diastolic properties and filling pressures; the progressive alteration from "Abnormal relaxation" to "Restriction to filling" is consistent with a gradual increase in left cardiac pressures. Abbreviations: LVEDV, left ventricular end-diastolic volume; LVEDP, left ventricular end-diastolic pressure

10.5 Monitoring Efficacy and Safety of Acute Therapy

The therapeutic impact of echocardiography – defined as changes in therapy directly related to the procedure – is consistently high in critically ill patients assessed for acute circulatory failure [2, 7, 9]. In addition to its diagnostic capabilities, echocardiography provides real-time monitoring of both the efficacy and tolerance of therapeutic interventions derived from the noninvasive comprehensive hemodynamic assessment. Echocardiography allows precise quantification of the variations in LV stroke volume induced by a fluid challenge (Fig. 10.5) and can indirectly track variations in LV filling pressures (Fig. 10.6). When the circulatory failure persists despite the initiation of a vasopressor or inotropic support, a repeated examination may help identify the cause of treatment failure: development of LV failure secondary to increased systemic vascular resistance, dynamic LV outflow tract obstruction revealed or exacerbated by excessive inotropic stimulation, adrenergic-induced extended LV wall-motion abnormality. Echocardiography can also detect the deleterious consequences of aggressive ventilator settings in patients with severely decreased lung compliance and failing RV (see Chap. 17).

10.6 Conclusion

Echocardiography has opened a window to the heart and great vessels. In patients with acute circulatory failure, echocardiography allows swift diagnosis of the leading mechanism of shock and provides a real-time visual assessment of both the efficacy and tolerance of acute therapy. In directly depicting the effects of drugs or assistance devices, including the central circulatory effects of mechanical ventilation, echocardiography is ideally suited for assessing acute circulatory failure in critically ill patients, especially in the ICU environment.

References

1. Vignon P (2005) Hemodynamic assessment of critically-ill patients using echocardiography. Curr Opin Crit Care 11:227–234
2. Price S, Nicol E, Gobson DG, Evans TW (2006) Echocardiography in the critically ill: current and potential roles. Intensive Care Med 32:48–59
3. Weil MH (2005) Defining hemodynamic instability. In: Pinsky MR, Payen D (eds) Functional hemodynamic monitoring. Springer-Verlag, Berlin
4. Antonelli M, Levy M, Andreas PJD, Chastre J, Hudson LD, Manthous C, Meduri GU, Moreno RP, Putensen C, Stewart T, Torres A (2007) International Consensus Conference. Hemodynamic monitoring in shock and implications for management. Intensive Care Med 33:575–590
5. ACCF/ASE/ACEP/ASNC/SCAI/SCCT/SCMR (2007) Appropriateness criteria for transthoracic and transesophageal echocardiography. J Am Coll Cardiol 50:187–204
6. Joseph MX, Disney PJF, Da Costa R, Hutchison SJ (2004) Transthoracic echocardiography to identify or exclude cardiac cause of shock. Chest 126:1592–1597
7. Vignon P, Mentec H, Terré S, Gastinne H, Guéret P, Lemaire F (1994) Diagnostic accuracy and therapeutic impact of transthoracic and transesophageal echocardiography in mechanically ventilated patients in the ICU. Chest 106:1829–1834
8. Vieillard-Baron A, Prin S, Chergui K, Dubourg O, Jardin F (2003) Hemodynamic instability in sepsis. Bedside assessment by Doppler echocardiography. Am J Respir Crit Care Med 168:1270–1276
9. Hüttemann E, Schelenz C, Kara F, Chatzinikolaou K, Reinhart K (2004) The use and safety of transesophageal echocardiography in the general ICU – A minireview. Acta Anaesthesiol Scand 48:827–836
10. Reichert CLA, Visser CA, Koolen JJ, Brink RBA, Van Wezel HB, Meyne NG et al (1992) Transesophageal echocardiography in hypotensive patients after cardiac operations. Comparison with hemodynamic parameters. J Thorac Cardiovas Surg 104:321–326
11. Jardin F, Valtier B, Beauchet A, Dubourg O, Bourdarias JP (1994) Invasive monitoring combined with two-dimensional echocardiographic study in septic shock. Intensive Care Med 20:550–554
12. Kaul S, Stratienko AA, Pollock SG, Marieb MA, Keller MK, Sabia PJ (1994) Value of two-dimensional echocardiography for determining the basis of hemodynamic compromise in critically ill patients: a prospective study. J Am Soc Echocardiogr 7:598–606
13. Poelaert JI, Trouerbach J, De Buyzere M, Everaert J, Colardyn FA (1995) Evaluation of transesophageal echocardiography as a diagnostic and therapeutic aid in a critical care setting. Chest 107:774–779
14. Benjamin E, Griffin K, Leibowitz AB, Manasia A, Oropello JM, Geffroy V et al (1998) Goal-directed transesophageal echocardiography performed by intensivists to assess left ventricular function: comparison with pulmonary artery catheterization. J Cardiothorac Vasc Anesth 12:10–15
15. Combes A, Berneau JB, Luyt CE, Trouillet JL (2004) Estimation of left ventricular systolic function by single transpulmonary thermodilution. Intensive Care Med 30:1377–1383
16. Van Grondelle A, Ditchey RV, Groves BM, Wagner WW, Reeves JT (1983) Thermodilution method overestimates low cardiac output in humans. Am J Physiol 245:H690–H692
17. Cigarroa RG, Lange RA, Williams RH, Bedotto JB, Hillis LD (1989) Underestimation of cardiac output by thermodilution in patients with tricuspid regurgitation. Am J Med 86:417–420
18. Cavallaro F, Sandroni C, Antonelli M (2008) Functional hemodynamic monitoring and dynamic indices of fluid responsiveness. Minerva Anesthesiol 74:123–135

19. Vieillard-Baron A, Slama M, Cholley B, Janvier G, Vignon P (2008) Echocardiography in the intensive care unit: from evolution to revolution? Intensive Care Med 34:243–249
20. Vignon P, Dugard A, Abraham J, Belcour D, Gondran G, Pépino F, Marin B, François B, Gastinne H (2007) Focused training for goal-oriented hand-held echocardiography performed by noncardiologist residents in the intensive care unit. Intensive Care Med 33:1684–1686
21. Charron C, Prat G, Caille V, Belliard G, Lefèvre M, Aegerter P, Boles JM, Jardin F, Vieillard-Baron A (2007) Validation of a skills assessment scoring system for transesophageal echocardiographic monitoring of hemodynamics. Intensive Care Med 33:1712–1718
22. Tousignant CP, Walsh F, Mazer CD (2000) The use of transesophageal echocardiography for preload assessment in critically ill patients. Anesth Analg 90:351–355
23. Zoghbi WA, Quinones MA (1986) Determination of cardiac output by Doppler echocardiography: a critical appraisal. Herz 11:258–268
24. Lang RM, Bierig M, Devereux RB, Flachskampf FA, Foster E, Pellikka PA et al (2006) Recommendations for chamber quantification. Eur J Echocardiogr 7:79–108
25. Jardin F, Dubourg O, Bourdarias JP (1997) Echocardiographic pattern of acute cor pulmonale. Chest 111:209–217
26. Vieillard-Baron A, Caille V, Charron C, Belliard G, Page B, Jardin F (2008) Actual incidence of global left ventricular hypokinesia in adult septic shock. Crit Care Med 36:1701–1706
27. Etchecopar-Chevreuil C, François B, Clavel M, Pichon N, Gastinne H, Vignon P (2008) Cardiac morphological and functional changes during early septic shock: a transesophageal echocardiographic study. Intensive Care Med 34:243–249
28. Reynolds HR, Hochman JS (2008) Cardiogenic shock. Current concepts and improving outcomes. Circulation 117: 686–697
29. Dickstein K, Cohen-Solal A, Filippatos G, McMurray JJV, Ponikowski P, Poole-Wilson PA, Strömberg A, Van Veldhuisen DJ, Atar D, Hoes AW, Keren A, Mebazaa A, Nieminen M, Priori SG, Swedberg K (2008) ESC guidelines for the diagnosis and treatment of acute and chronic heart failure 2008. Eur Heart J 29:2388–2442
30. Vignon P (2008) Assessment of critically ill patients with acute heart failure syndromes using echocardiography Doppler. In: Mebazaa A, Gheorghiade M, Zannad FM, Parrillo JE (eds) Acute heart failure. Springer-Verlag, London
31. Charron C, Mekontso-Dessap A, Chergui K, Rabiller A, Jardin F, Vieillard-Baron A (2005) Incidence, causes and prognosis of hypotension related to meprobamate poisoning. Intensive Care Med 31:1582–1586
32. Vignon P, Weinert L, Mor-Avi V et al (1999) Quantitative assessment of regional right ventricular ventricular function with Color Kinesis. Am J Respir Crit Care Med 159: 1949–1959
33. Kinch JW, Ryan TJ (1994) Right ventricular infaction. N Engl J Med 330:1211–1217
34. Vieillard-Baron A, Prin S, Chergui K et al (2002) Echo-Doppler demonstration of acute cor pulmonale at the bedside in the medical intensive care unit. Am J Respir Crit Care Med 166:1310–1319
35. Weber KT, Janicki JS, Shroff SG et al (1983) The right ventricle: physiologic and pathophysiologic considerations. Crit Care Med 11:323–328

Septic Shock

11

Daniel De Backer and Antoine Vieillard-Baron

Contents

11.1 Introduction

Septic shock is accompanied by profound cardiovascular alterations, including a decrease in vascular tone, hypovolemia, and myocardial depression. Hemodynamic treatment represents a real challenge for intensivists because all these mechanisms of shock may be involved, and at any one time the dominant mechanism can be different. Making the correct diagnosis thus become somewhat complicated, especially with adapted treatment. By its ability to assess the situation in a step-by-step fashion and examine the variables of cardiovascular function separately, echocardiography is particularly suitable in treating septic shock. However, since echocardiography is a noncontinuous monitoring device, it has to be used in this context with a continuous hemodynamic monitoring method.

11.2 Hypovolemia in Septic Shock

Hypovolemia may be either absolute or relative according to the volume of blood in the large-capacitance veins. If not corrected, hypovolemia may lead to a deleterious increase in norepinephrine dosage and finally to an augmentation of organ ischemia. Whereas at the early phase of sepsis, hypovolemia is constant, half of patients respond to fluids only at later stages of sepsis [1]. Recent clinical studies have reemphasized the inability of clinical signs of invasive hemodynamic measurements, such as intravascular pressures (central venous pressure (CVP) and pulmonary artery occlusion pressure (PAOP)) and intravascular volumes (right and left ventricular volumes), to predict the response to

D. De Backer (✉)
Department of Intensive Care, Erasme University Hospital, Université Libre de Bruxelles, 808 route de Lennik, B-1070, Brussels, Belgium
e-mail: ddebacke@ulb.ac.be

A. Vieillard-Baron
Service de Réanimation médicale, CHU Ambroise Paré, Assistance Publique Hôpitaux de Paris, 9 avenue Charles de Gaulle, 92104, Boulogne Cedex, France

D. De Backer et al. (eds.), *Hemodynamic Monitoring Using Echocardiography in the Critically Ill*,
DOI: 10.1007/978-3-540-87956-5_11, © Springer-Verlag Berlin Heidelberg 2011

fluids. This may limit conventional hemodynamic monitoring since it has been suggested that excessive or inadequate fluid infusion exerts a negative impact on oxygenation [2] and on prognosis in septic shock [3]. Strategies based on echocardiography to manage fluid requirement, either by using predicting factors of fluid responsiveness or by monitoring cardiac function during a fluid challenge, have been proposed [4]. These are developed elsewhere in this book (see Chaps. 6 and 7).

11.3 Cardiac Depression in Septic Shock

11.3.1 Incidence

The presence of cardiac dysfunction was initially postulated in the mid-1960s, when investigators were able to show that septic shock may present two distinct patterns: a hyperdynamic pattern, with high cardiac output; and a hypo- or normal-dynamic pattern, associated with a low to normal cardiac output [5]. In the 1970s, radionuclide cineangiography identified that myocardial depression may be present in septic shock, even when cardiac output is high [6, 7]. Parker et al. [6] showed that left ventricular ejection fraction (LVEF) is already altered in septic shock on the day of admission in half of patients and that over time it progressively resolves. At the same time, Jardin et al. made the same observation using transthoracic echocardiography [8, 9]. Many later studies using a fast-response thermistor catheter, radionuclide cineangiography, and echocardiography showed that right ventricular function is also altered [10, 11].

11.3.2 Pathophysiology

Many factors may contribute to cardiac depression. Using in vitro isolated myocardial muscle, Parillo et al. [12] demonstrated that exposure to serum obtained from septic patients leads to a transient decrease in left ventricular (LV) contractility. The circulating myocardial depressant factor was later shown to be related to the inflammatory processes since tumor necrosis factor (TNF) administration can mimic these alterations [13, 14]. The exact factor has not yet been identified, though it would seem that a mixture of various cytokines, either alone or in combination, can promote cardiac depression. Even though hypotension is frequent, coronary hypoperfusion was not observed in patients without a prior history of coronary artery disease [15, 16]; but, of course, patients with coronary disease may behave differently.

Experimental data have demonstrated that microcirculatory alterations may occur [17]. In addition, direct alterations in cellular respiration, especially mitochondrial dysfunction, have been shown to occur in septic hearts [18], though other studies failed to confirm this finding [19]. Alterations in both the microcirculation and in cellular respiration most likely coexist, but the predominance of one over the other and the sequence of occurrence remain to be established.

At the cellular level, troponin phosphorylation leads to calcium uncoupling, while calcium intracellular movements are preserved [19, 20]. Even though the involvement of pro-apoptotic substances has been demonstrated, apoptotic or necrotic cells have rarely been detected. Accordingly, therapies specifically aimed at correcting these factors have not yet been tested. In addition, these are difficult to evaluate at the bedside, and individualizing therapy would present further problems.

11.3.3 Impact of Cardiac Depression on Treatment and Prognosis

The incidence of LV dysfunction during the first 3 days of septic shock is close to 60% [21].

11.3.3.1 Impact on Outcome

In experimental conditions, the severity of myocardial depression has been related to outcome. Implanting various amounts of infected clots in the peritoneal cavity demonstrated that the severity of systolic dysfunction is dose-dependent and associated with outcome [22]. The impact of myocardial depression in patients with sepsis is difficult to evaluate since it would require multivariate analysis in a large series of patients using systematic evaluation of cardiac function with preload-independent markers of heart function at relevant time points. Indirect evidence points to myocardial

depression having a negative impact on outcome. Patients that do not survive septic shock often present a more pronounced tachycardia [23] to compensate for the decreased stroke volume. During a dobutamine test, which evaluates the cardiac reserve of the patient, improvement in LV ejection fraction was associated with a higher survival rate [24]. Together, these data suggest that myocardial dysfunction is associated with an impaired outcome.

11.3.3.2 Impact on Therapy

The impact of LV systolic and diastolic dysfunction will be to limit cardiac output, either directly by a decrease in contractility, or indirectly limiting LV preload. In both cases, this would lead to decreased stroke volume, but this may be compensated by a reflex tachycardia. However, in many instances, this increase in heart rate is insufficient, and cardiac output is inadequate for metabolic requirements. LV systolic dysfunction, when detected, can usually be improved by inotropic agents, such as dobutamine, epinephrine, enoximone, and levosimendan [25, 26]. In the early-goal directed protocol proposed by Rivers et al., infusion of dobutamine was finally recommended, and it may have contributed to the improved outcome [27]. Norepinephrine infusion, by correcting the LV afterload, may unmask or even promote LV systolic dysfunction, as observed in 30% of cases in the study by Vieillard-Baron et al. [21]. Similarly, Loubieres et al. [28] observed that military anti-shock trousers (MAST) decreased stroke volume in several patients with septic shock by increasing the LV afterload.

Many experimental and humans studies have suggested that LV diastolic function can also be impaired and be related with outcome. Recently, Bouhemad et al. [29], using tissue Doppler imaging, reported that early excursion of the mitral annulus (Ea) was impaired in some patients with sepsis. Interestingly, the magnitude of diastolic dysfunction was more pronounced in those patients who also had systolic dysfunction (Ea 6.5 cm/s) than in patients with preserved systolic function (Ea close to 9 cm/s). In some situations, LV compliance may be increased. This phenomenon is apparently observed in cases with depressed LV contractility, in which a slight LV dilation limits the fall in stroke volume. This preload adaptation remains limited, and no echocardiographic study in humans has ever reported a marked LV dilatation. Serial measurements of LV volumes in mice have shown that LV diastolic volume is larger during the severest impairment in systolic function [30]. But in other situations, a decrease in LV compliance may be observed, limiting LV dilation [31]. This specific profile, including a small LV size, an "apparent" LV increased contractility, and a preserved LV stroke volume, has been reported in up to 15–20% of patients and was associated with a very poor prognosis [32]. Jardin et al. [33] and Etchecopar-Chevreuil et al. [31] found using, respectively, transthoracic echocardiography (TTE) and transesophageal echocardiography (TEE) that the LV volume was greater in survivors than in nonsurvivors.

Finally, regarding the right ventricle (RV), a study using radionuclide cineangiography satisfactorily demonstrated that RV failure was the main factor limiting the response to fluids [34]. Moreover, the occurrence of acute cor pulmonale in patients with acute respiratory distress syndrome (ARDS), which is frequently associated with septic shock, may account for an increase in mortality if not adequately taken into account [35].

11.4 Practical Echocardiographic Evaluation of Patients in Septic Shock

Echocardiography should be included in the clinical management of patients with septic shock (Fig. 11.1). It has to be repeated during the first days of the evolution, either because signs of tissue hypoperfusion persist or because of hemodynamic deterioration. Figure 11.1 illustrates how echocardiography can detect in a stepwise fashion the different causes of circulatory failure in septic patients. This is illustrated in a clinical case in Fig. 11.2. Finally, because echocardiography is not a continuous monitoring tool, it has to be used in conjunction with a method that does offer continuous surveillance and indicates to the intensivist when echocardiography should be performed. According to the type of patient, size of the intensive care unit (ICU), and ICU protocol, it can require continuous monitoring of cardiac output, mixed venous oxygen saturation (SVO_2), or only invasive blood pressure (see Chap. 22).

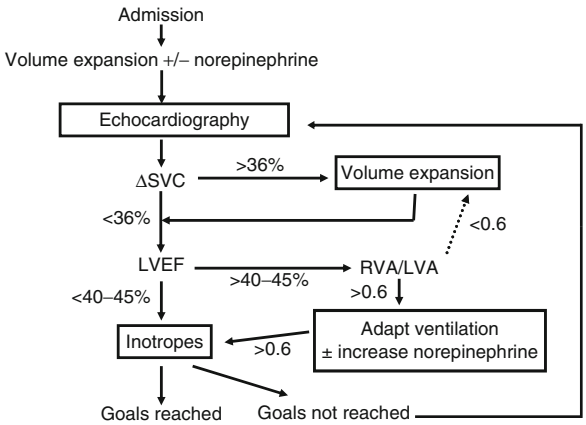

Fig. 11.1 General algorithm for evaluating the patient in septic shock. The approach using transesophageal echography is used as an example. Transthoracic echocardiography can also be used, but then other indices of fluid responsiveness have to be employed (see Chaps. 6 and 7). RVA/RLV represents the ratio between the surfaces of the right and left ventricles. Goals have to be defined by the intensivist (indices of tissue perfusion, such as diuresis, lactate). Abbreviations: RVA/RLV represents the ratio between the surfaces of the right and left ventricles; "d"SVC respiratory changes in superior vena cava diameter; LVEF left ventricular ejection fraction

11.4.1 First Step: Evaluation of Cardiac Output

Cardiac output can be measured by echocardiography (described in detail in Chap. 5), but the question is: should we measure cardiac output in patients with septic shock? Usually, cardiac output is normal or elevated in septic shock, but it can be low in the presence of severe myocardial depression or hypovolemia. More importantly, metabolic needs are also affected by sepsis (fever, inflammatory response) and its therapy (sedative agents and mechanical ventilation decrease metabolic needs, while adrenergic agents increase metabolic requirements). Accordingly, it is crucial to determine whether cardiac output is adapted to metabolic requirements.

Two very different situations support the implementation of echocardiography. The first is when intensivists perform an echocardiography during the course of septic shock for such clinical problems as hypotension, persistent oliguria, and persistent or worsened lactic acidosis associated with a "nonelevated" cardiac output and/or low venous oxygen saturation. This suggests that cardiac output is inadequate. Hence, any echocardiographic abnormalities observed during the examination should be corrected. Ideally, repeated cardiac output measurement should be undertaken to evaluate the response to changes in therapy. Inadequate volemia has to be corrected, depressed LV contractility may require inotropic stimulation, and RV dysfunction should lead to adaptation in volume, drugs, and ventilatory settings.

In the second situation, an echocardiography is routinely performed during the first days of clinical management to monitor cardiovascular function. Here, measurement of cardiac output may assist clinicians in deciding whether to change the treatment. In a large series of 183 patients with septic shock, cardiac output was found to be decreased in one-third of the subjects [36]. But, many patients with an altered ejection fraction had "preserved" cardiac output (Fig. 11.3), which suggests that these patients were unlikely to benefit from inotropic agents. Conversely, if cardiac output is found to be significantly low, it can prompt the physician to infuse inotropic drugs even though otherwise the clinical situation is not judged to be so bad. In any event, measurement of cardiac output can often provide the appropriate warning signals, especially if the hemodynamics is impaired in the first few hours of clinical care.

Finally, in order to facilitate the hemodynamic assessment during echocardiography, we usually prefer to calculate the LV stroke volume alone. A low stroke volume is very indicative of hypovolemia or cardiac dysfunction even when cardiac output is maintained by tachycardia.

11.4.2 Second Step: Evaluating Response to Fluids

Evaluation of the response to fluids is critical in patients with septic shock. The classical hyperdynamic response is usually achieved only after adequate fluid replacement has been achieved [37, 38]. However, the generalized increase in vascular permeability makes this response transient, and repeated fluid boluses are often required. In addition, interstitial edema develops, and this may worsen gas exchange. Furthermore, the increase in cardiac output in response to fluids is less likely to occur at later stages [39]. Hence, the benefits and risks of fluid administration decrease with time and should be evaluated carefully.

The use of echocardiography to predict fluid responsiveness and evaluate the response to the fluid

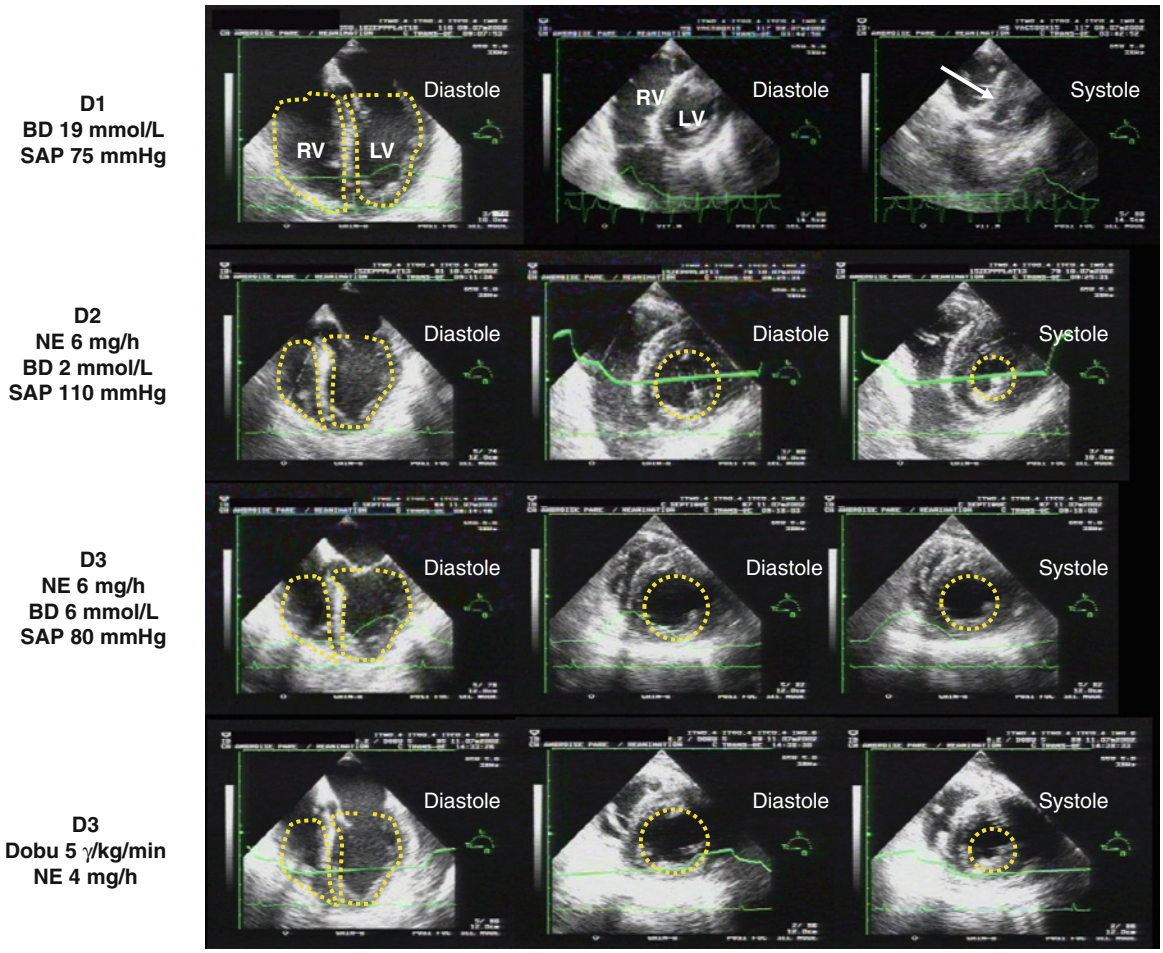

Fig. 11.2 Illustrative clinical case. Patient hospitalized for septic shock of a urinary origin, mechanically ventilated. On day 1 (D1), systolic arterial pressure (SAP) is low with a marked metabolic acidosis (base deficit, BD, 19 mmol/L). Transesophageal echography (TEE) demonstrated an acute cor pulmonale with a right ventricular (RV) dilatation in diastole and a paradoxical septal motion in systole (*arrow*) using a transgastric approach. Left ventricular (LV) contractility was normal. On day 2 (D2), under norepinephrine (NE), shock was corrected as well as metabolic acidosis. Now, TEE demonstrated normalization of RV function. LV contractility was normal. On day 3 (D3), hemodynamic worsening was observed, with a fall in systolic arterial pressure and concomitant metabolic acidosis. TEE now demonstrated a marked decrease in LV contractility. Infusion of dobutamine (Dobu) was able to correct LV contractility and restore normal blood pressure. At the same time, NE dosage was decreased

challenge is described in detail elsewhere (Chaps. 6 and 7). To evaluate the efficacy of a fluid challenge requires only measurement of LV stroke volume just before and after volume infusion. To predict the fluid responsiveness requires using dynamic parameters previously validated in mechanically ventilated patients without any spontaneous effort. Echocardiographic evaluation of cardiac filling pressures in predicting the response to fluids is irrelevant.

However, in patients with septic shock who have altered systolic and diastolic dysfunction, it may be useful to estimate LV filling pressures to evaluate their tolerance to fluids. Whatever the index employed to evaluate PAOP, it is often more reliable when used semiquantitatively [40] than when precise numbers are calculated. Similarly, PAOP determined by echocardiography often correlates well with invasive measurements, but the limits of agreement are too wide (5–7 mmHg [41]) to allow these measurements to be used for fine-tuning therapy. However, it is important to reemphasize that LV filling pressure is usually normal or low in patients with septic shock, even in the presence of LV systolic dysfunction [42].

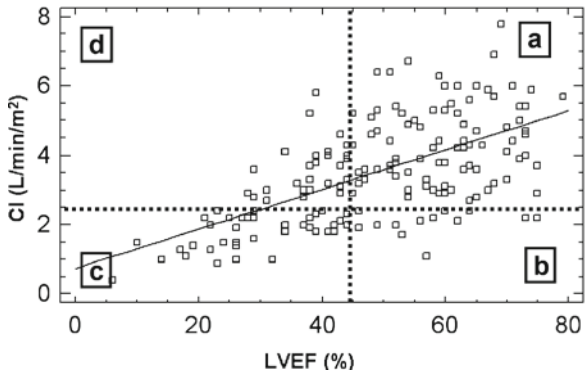

Fig. 11.3 Relationship between left ventricular (LV) ejection fraction and cardiac (CI) index in patients with septic shock. The dotted lines separate the patients into four quadrants. (**a**) Normal cardiac function; (**b**) normal systolic function and low CI related to insufficient LV preload (which can be due to hypovolemia, impaired diastolic function, and/or right ventricular dysfunction); (**c**) symptomatic LV systolic dysfunction: likely to respond to inotropic stimulation; (**d**) decreased LV function but preserved CI: may require inotropic therapy if CI insufficiently elevated, be particularly cautious with norepinephrine use (Adapted with permission from [36])

11.4.3 Third Step: Evaluation of Cardiac Function

When fluids fail to improve cardiac output, the use of inotropic agents should be considered. However, to guide inotropic therapy, it is important to determine cardiac function as several patients may have a low cardiac output but a preserved ejection fraction [36] (Fig. 11.3).

Numerous methods have been developed to evaluate cardiac function (see Chap. 5 for details). In clinical practice, the most accurate way is to use a surrogate of the LVEF, i.e., the left ventricular fractional area contraction (LVFAC) in a short-axis view of the LV (Fig. 11.2). The simplest way of doing this is to perform eyeball determination rather than calculating it, as LV end-diastolic area minus end-systolic area divided by end-diastolic area [43]. In our experience, only decreases in LVEF or LVFAC below 45% are likely to be responsible for hemodynamic deterioration.

These indices are, however, influenced by loading conditions. Accordingly, various authors have proposed several other methods, from the rate of circumferencial shortening, rate of pressure rise, or maximal systolic elastance to more recent stress and strain analysis. These are often less sensitive to loading conditions and are also more difficult to acquire, requiring specific training; sometimes, they can be measured only with the most recent echocardiographic devices. However, it is important to understand that from a clinical point of view, the objective of echocardiography is not to appreciate the intrinsic systolic function of the LV, but to assess how the heart contracts in a given load situation. For example, a low ejection fraction can reflect either an intrinsic LV systolic dysfunction or an excessive LV afterload; the latter, though, is infrequent in septic shock unless a very high blood pressure is attained through excessive doses of norepinephrine. Conversely, a normal ejection fraction can be observed in a patient with an intrinsic LV systolic dysfunction when LV afterload is markedly diminished. In this situation, inotropic drug infusion will never improve hemodynamics and so should not be implemented; but, again, intensivists should keep in mind that LV function has to be rechecked after correcting the afterload by norepinephrine infusion [21].

The most currently used agents are beta-adrenergic agents, especially dobutamine. In septic patients, dobutamine has been shown to reliably increase cardiac output [44]. Recently, isoprenaline has also been proposed for this indication [45]. Unfortunately, the response to adrenergic agents is quite variable, and some patients show increased cardiac output via a rise in heart rate more than through an increase in stroke volume [46]. Measuring the velocity-time interval (VTI) as a surrogate of stroke volume would allow identification of patients who may benefit most from dobutamine administration since raising cardiac output by an increase in heart rate is probably not very efficient. More recently, levosimendan has been introduced. Some preliminary data suggest that this agent may improve cardiac output in patients not responding to dobutamine, by improving contractility and decreasing end-diastolic volume [26]. The impact of this agent on diastolic function in sepsis has yet to be determined.

Finally, to evaluate cardiac function also requires a systematic consideration of RV function (see Chap. 13 and Fig. 11.2), as noted above. Very simply, any RV dilatation reflects RV dysfunction. To assess RV size, the best means is to calculate the ratio between the end-diastolic RV area and end-diastolic LV area in a long-axis view of the LV. Details of the interventricular septum kinetics in a short-axis view of the LV are also informative, and a paradoxical septal motion during systole reflects a systolic overload of the RV. In the case of severe RV dysfunction, which is partly responsible for the persistent shock in septic patients, we

prefer to infuse or increase norepinephrine when LV systolic function appears normal and infuse or increase dobutamine when RV systolic dysfunction is associated with a poor LV function.

11.5 Other Applications of Echocardiography in Septic Shock

In patients with septic shock, special care should be taken to rule out endocarditis. Since patients with septic shock may present bacteremia or fungemia, cautious inspection of the valves should always be performed at each echocardiographic examination. During transesophageal examination, one should also carefully appraise the large veins and catheter tips to exclude the possibility of purulent thrombophlebitis.

11.6 Conclusion

Myocardial depression is common in patients with septic shock, even when cardiac output is maintained. It is characterized by an alteration in systolic function of the LV, associated with variable diastolic dysfunction and RV dysfunction. The echocardiographic evaluation should aim at evaluating fluid responsiveness and contractility, RV function, and the likely response of these to therapeutic interventions.

Echocardiography should be repeated and focus on the following aspects:

- Cardiac output: aortic VTI and heart rate; LV outflow tract should be determined once only
- Fluid responsiveness: respiratory variations in peak aortic flow and/or in superior vena cava
- Ejection fraction: eyeball measurement
- RV function-surfaces ratio and, eventually, septal bowing

Echocardiography could be combined with the following measurements:

- $ScvO_2$ and/or lactate and base deficit to assess adequacy of cardiac output
- Central venous pressure to ensure that preload is effectively increased during a fluid challenge

11.7 Videos Related to this Chapter

1. Patient with severe myocardial dysfunction (apical transthoracic view) at day 0. Eye ball ejection fraction was 40%; cardiac output was 6.2 L/min.m², $ScvO_2$ 69% and lactate 2.9 mmol/L. The patient was treated with norepinephrine 0.6 mcg/kg · min.
2. Same Patient investigated on day 5 (apical transthoracic view). At this time, eye ball ejection fraction was 50%; cardiac output was 4.3 L/min · m², $ScvO_2$ 65% and lactate 1.4 mmol/L. The patient was weaned from vasopressors agents.
3. Severe right ventricular dysfunction.

References

1. Michard F, Teboul JL (2002) Predicting fluid responsiveness in ICU patients: a critical analysis of the evidence. Chest 121:2000–2008
2. Wiedemann HP, Wheeler AP, Bernard GR et al (2006) Comparison of two fluid-management strategies in acute lung injury. N Engl J Med 354:2564–2575
3. Sakr Y, Reinhart K, Vincent JL et al (2006) Does dopamine administration in shock influence outcome? Results of the Sepsis Occurrence in Acutely Ill Patients (SOAP) Study. Crit Care Med 34:589–597
4. Charron C, Caille V, Jardin F et al (2006) Echocardiographic measurement of fluid responsiveness. Curr Opin Crit Care 12:249–254
5. MacLean LD, Mulligan WG, McLean APH et al (1967) Patterns of septic shock in man – a detailed study of 56 patients. Ann Surg 166:543–559
6. Parker MM, Shelhamer JH, Bacharach SL et al (1984) Profound but reversible myocardial depression in patients with septic shock. Ann Intern Med 100:483–490
7. Suffredini AF, Fromm RE, Parker MM et al (1989) The cardiovascular response of normal humans to the administration of endotoxin. N Engl J Med 321:280–287
8. Ozier Y, Gueret P, Jardin F et al (1984) Two-dimensional echocardiographic demonstration of acute myocardial depression in septic shock. Crit Care Med 12: 596–599
9. Jardin F, Brun-Ney D, Auvert B et al (1990) Sepsis-related cardiogenic shock. Crit Care Med 18:1055–1060
10. Parker MM, McCarthy KE, Ognibene FP et al (1990) Right ventricular dysfunction and dilatation, similar to left ventricular changes, characterize the cardiac depression of septic shock in humans. Chest 97:126–131
11. Dhainaut JF, Pinsky MR, Nouria S et al (1997) Right ventricular function in human sepsis: a thermodilution study. Chest 112:1043–1049
12. Parillo JE, Burch C, Shelhamer JH (1985) A circulating myocardial depressant substance in humans with septic shock. J Clin Invest 76:1539–1553

13. Natanson C, Eichenholz PW, Danner RL et al (1989) Endotoxin and tumor necrosis factor challenges in dogs simulate the cardiovascular profile of human septic shock. J Exp Med 169:823–832
14. Hollenberg SM, Cunnion RE, Lawrence M et al (1989) Tumor necrosis factor depress myocardial cell function: results using an in vitro assay of myocyte performance. Clin Res 37:528–534
15. Cunnion RE, Schaer GL, Parker MM et al (1986) The coronary circulation in human septic shock. Circulation 73:637–644
16. Dhainaut JF, Huyghebaert MF, Monsallier JF et al (1987) Coronary hemodynamics and myocardial metabolism of lactate, free fatty acids, glucose, and ketones in patients with septic shock. Circulation 75:533–541
17. Ince C, Ashruf JF, Avontuur JA et al (1993) Heterogeneity of the hypoxic state in rat heart is determined at capillary level. Am J Physiol 264:H294–H301
18. Levy RJ, Piel DA, Acton PD et al (2005) Evidence of myocardial hibernation in the septic heart. Crit Care Med 33: 2752–2756
19. Tavernier B, Mebazaa A, Mateo P et al (2001) Phosphorylation-dependent alteration in myofilament ca2+ sensitivity but normal mitochondrial function in septic heart. Am J Respir Crit Care Med 163:362–367
20. Tavernier B, Li JM, El Omar MM et al (2001) Cardiac contractile impairment associated with increased phosphorylation of troponin I in endotoxemic rats. FASEB J 15:294–296
21. Vieillard-Baron A, Caille V, Charron C et al (2008) Actual incidence of global left ventricular hypokinesia in adult septic shock. Crit Care Med 36:1701–1706
22. Natanson C, Danner RL, Fink MP et al (1988) Cardiovascular performance with E. coli challenges in a canine model of human sepsis. Am J Physiol 254:H558–H569
23. Parker MM, Shelhamer JH, Natanson C (1987) Serial cardiovascular variables in survivors and nonsurvivors of human septic shock: heart rate as an early predictor of prognosis. Crit Care Med 15:923–929
24. Kumar A, Schupp E, Bunnell E et al (2008) Cardiovascular response to dobutamine stress predicts outcome in severe sepsis and septic shock. Crit Care 12:R35
25. Vincent J-L, Roman A, Kahn RJ (1990) Dobutamine administration in septic shock: addition to a standard protocol. Crit Care Med 18:689–693
26. Morelli A, De Castro S, Teboul JL et al (2005) Effects of levosimendan on systemic and regional hemodynamics in septic myocardial depression. Intensive Care Med 31:638–644
27. Rivers E, Nguyen B, Havstadt S et al (2001) Early goal-directed therapy in the treatment of severe sepsis and septic shock. N Engl J Med 345:1368–1377
28. Loubieres Y, Vieillard-Baron A, Beauchet A et al (2000) Echocardiographic evaluation of left ventricular function in critically ill patients: dynamic loading challenge using medical antishock trousers. Chest 118:1718–1723
29. Bouhemad B, Nicolas-Robin A, Arbelot C et al (2008) Isolated and reversible impairment of ventricular relaxation in patients with septic shock. Crit Care Med 36:766–774
30. Zanotti-Cavazzoni SL, Guglielmi M, Parrillo JE et al (2009) Fluid resuscitation influences cardiovascular performance and mortality in a murine model of sepsis. Intensive Care Med 35:748–754, Epub 2008 Dec 9
31. Etchecopar-Chevreuil C, Francois B, Clavel M et al (2008) Cardiac morphological and functional changes during early septic shock: a transesophageal echocardiographic study. Intensive Care Med 34:250–256
32. Vieillard-Baron A, Schmitt JM, Beauchet A et al (2001) Early preload adaptation in septic shock? A transesophageal echocardiographic study. Anesthesiology 94: 400–406
33. Jardin F, Fourme T, Page B et al (1999) Persistent preload defect in severe sepsis despite fluid loading: a longitudinal echocardiographic study in patients with septic shock. Chest 116:1354–1359
34. Schneider AJ, Teule GJ, Groeneveld AB et al (1988) Biventricular performance during volume loading in patients with early septic shock, with emphasis on the right ventricle: a combined hemodynamic and radionuclide study. Am Heart J 116:103–112
35. Osman D, Monnet X, Castelain V et al (2009) Incidence and prognostic value of right ventricular failure in acute respiratory distress syndrome. Intensive Care Med 35:69–76
36. Vieillard-Baron A, Prin S, Chergui K et al (2003) Hemodynamic instability in sepsis: bedside assessment by Doppler echocardiography. Am J Respir Crit Care Med 168:1270–1276
37. Cholley BP, Lang RM, Berger DS et al (1995) Alterations in systemic arterial mechanical properties during septic shock: role of fluid resuscitation. Am J Physiol 269: H375–H384
38. De Backer D, Zhang H, Cherkhaoui S et al (2001) Effects of dobutamine on hepato-splanchnic hemodynamics in an experimental model of hyperdynamic endotoxic shock. Shock 15:208–214
39. Axler O, Tousignant C, Thompson CR et al (1997) Small hemodynamic effect of typical rapid volume infusions in critically ill patients. Crit Care Med 25:965–970
40. Vignon P, AitHssain A, Francois B et al (2008) Echocardiographic assessment of pulmonary artery occlusion pressure in ventilated patients: a transoesophageal study. Crit Care 12:R18
41. Combes A, Arnoult F, Trouillet JL (2004) Tissue Doppler imaging estimation of pulmonary artery occlusion pressure in ICU patients. Intensive Care Med 30:75–81
42. Jardin F, Valtier B, Beauchet A et al (1994) Invasive monitoring combined with two-dimensional echocardiographic study in septic shock. Intensive Care Med 20:550–554
43. Vieillard-Baron A, Charron C, Chergui K et al (2006) Bedside echocardiographic evaluation of hemodynamics in sepsis: is a qualitative evaluation sufficient? Intensive Care Med 32:1547–1552
44. Vincent JL, Roman A, Kahn RJ (1990) Dobutamine administration in septic shock: addition to a standard protocol. Crit Care Med 18:689–693
45. Leone M, Boyadjiev I, Boulos E et al (2006) A reappraisal of isoproterenol in goal-directed therapy of septic shock. Shock 26:353–357
46. Jellema WT, Groeneveld AB, Wesseling KH et al (2006) Heterogeneity and prediction of hemodynamic responses to dobutamine in patients with septic shock. Crit Care Med 34:2392–2398

Cardiogenic Shock Associated with Acute Left-Heart Failure

12

Jina Sohn and Steven M. Hollenberg

Contents

J. Sohn and S.M. Hollenberg (✉)
Division of Cardiovascular Disease and Critical Care Medicine, Cooper University Hospital, One Cooper Plaza, 366 Dorrance, Camden, NJ, 08103, USA
e-mail: hollenberg-Steven@cooperhealth.edu

12.1 Introduction

Hemodynamic instability after myocardial infarction can include hypotension, low cardiac output, pulmonary edema, and cardiogenic shock. Although there is overlap, distinguishing the primary clinical presentation and the pathophysiology of that abnormality has important therapeutic implications.

Cardiogenic shock results from cardiac dysfunction, with cardiac output inadequate to maintain systemic perfusion. The diagnosis of cardiogenic shock is often made on clinical grounds by the presence of systemic arterial hypotension along with clinical signs indicative of poor tissue perfusion, including oliguria, clouded sensorium, and cool, mottled extremities, all in the setting of myocardial dysfunction. A rigorous determination requires hemodynamic confirmation, with sustained systemic hypotension (systolic arterial pressure <90 mm Hg or mean arterial pressure 30 mm Hg or more below basal levels), adequate or elevated left ventricular filling pressures (pulmonary artery wedge pressure >15–18 mm Hg), and a reduced cardiac output (cardiac index <2.2 L/min/m^2) [1]. It is important to document myocardial dysfunction and to exclude or correct such factors as hypovolemia, hypoxia, and acidosis.

In cases of suspected cardiogenic shock, an electrocardiogram should be performed immediately to evaluate for evidence of recurrence of myocardial ischemia and to assess the rhythm. Other initial diagnostic tests usually include a chest radiograph and measurement of arterial blood gases, electrolytes, complete blood count, and cardiac enzymes.

Echocardiography is an excellent tool for sorting through the differential diagnosis, and it should be performed as early as possible. Echocardiography can easily be performed at the bedside, and it is a simple

D. De Backer et al. (eds.), *Hemodynamic Monitoring Using Echocardiography in the Critically Ill*,
DOI: 10.1007/978-3-540-87956-5_12, © Springer-Verlag Berlin Heidelberg 2011

and noninvasive tool to assess the anatomy of the cardiac chambers, ventricular function, valve structure, and function and anatomy of the pericardial space. Echocardiography allows for expeditious evaluation of overall and regional left ventricular performance and can rule out other etiologies of shock. In addition, early use of echocardiography is the technique of choice for rapid diagnosis of mechanical causes of shock, such as acute mitral regurgitation resulting from papillary muscle rupture, acute ventricular septal defect, and free-wall rupture. When transthoracic echocardiographic images are suboptimal – a not uncommon situation in critically ill patients, particularly those who are obese, have chronic lung disease, or are on positive pressure ventilation – transesophageal echocardiogram can be performed safely at bedside and provide better visualization [2].

12.2 Acute Myocardial Infarction

Cardiogenic shock is the most common cause of death in hospitalized patients with acute myocardial infarction. In the SHOCK (SHould we emergently revascularize Occluded Coronaries for cardiogenic shocK) trial registry, myocardial infarction and its complications made up 94.3% of all incidences of cardiogenic shock [3]. Cardiogenic shock usually results from an extensive acute infarction, although a smaller infarction in a patient with previously compromised left ventricular function may also precipitate shock. Cardiogenic shock can also be caused by mechanical complications of infarction (including ventricular septal rupture, ventricular free-wall rupture, pseudoaneurysm, and acute mitral regurgitation due to papillary muscle rupture or ischemia) or by large right ventricular infarctions. Cardiogenic shock is the most common cause of death in hospitalized patients with acute myocardial infarction, and despite advances in reperfusion therapies, shock in the setting of acute myocardial infarction still carries a mortality rate as high as 50–60%. Cardiogenic shock may also result from mechanical complications of infarction. Other important, although less common, causes of cardiogenic shock include fulminant myocarditis, valvular diseases, prolonged cardiopulmonary bypass, and trauma [1].

The predominant cause of cardiogenic shock in the setting of acute myocardial infarction is severe left ventricular (LV) dysfunction. Infarction of approximately 40% of the LV mass will lead to significant loss of pumping capacity, decreasing stroke volume and cardiac output [4]. The myocardial dysfunction resulting from ischemia leads to worsening ischemia, creating a downward spiral. (Fig. 12.1) Compensatory mechanisms that are activated when cardiac output is reduced may become maladaptive and further worsen systolic dysfunction.

Echocardiography is a valuable initial diagnostic tool for assessment of the amount of myocardium at risk, infarct size, hemodynamics, myocardial viability, and for risk stratification [5]. Acute changes in LV regional wall motion can often be more sensitive than electrocardiography (ECG) in detecting significant infarction, and so echocardiography is often useful in the differential diagnosis of suspected ischemia. The amount of myocardium at risk can be estimated by echocardiography, and although resting echocardiography is not the best way to evaluate myocardial viability, evidence of infarcted segments can be seen as thinning of the myocardium [6] (Fig. 12.2). Factors such as left ventricular ejection fraction (LVEF) and mitral regurgitation (MR) at presentation have been shown to predict a poor prognosis in acute myocardial infarction (AMI), and the more extensive regional wall-motion abnormalities predicted greater adverse events [7].

Doppler echocardiography can also be used to assess hemodynamics. Stroke volume may be calculated by measuring the velocity-time integral of left ventricular outflow tract (LVOT) velocity and multiplying by LVOT area. Doppler assessment requires imaging windows that allow for parallel alignment of the Doppler cursor to avoid errors in velocity measurements. Incorrect measurement of the LVOT diameter can lead to large errors in LVOT area calculations and stroke volume. The myocardial performance index, or Tei index, uses Doppler measurements to assess ventricular performance by taking the ratio of the isovolumic contraction plus isovolumic relaxation times divided by the ejection time [8]. The Tei index is relatively independent of heart rate and blood pressure, can be obtained even when the two-dimensional images are inadequate, is not based on any geometric assumptions, and has been shown to be a better prognostic indicator for death than ejection fraction in dilated cardiomyopathy [9].

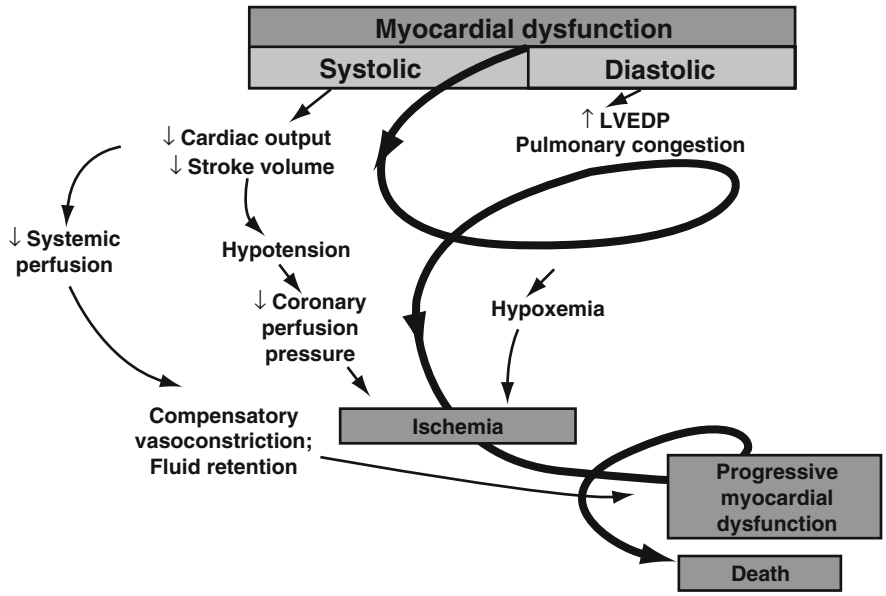

Fig. 12.1 The downward spiral in cardiogenic shock. Left ventricular dysfunction results in a decrease in stroke volume and cardiac output, resulting in hypotension and tachycardia. This in turn causes a reduction in coronary blood flow, along with an increase in ventricular diastolic pressure. Increase in diastolic pressure also causes an increase in wall tension and myocardial oxygen demand. All of these factors combine to worsen ischemia. The decrease in systemic perfusion triggers compensatory mechanisms of sympathetic stimulation and fluid retention to increase preload. These mechanisms can actually worsen cardiogenic shock by increasing myocardial oxygen demand and afterload. Thus, a vicious circle can be established. Abbreviation: *LVEDP*, left ventricular end diastolic pressure (Adapted from [1])

Pulmonary artery systolic pressure can be estimated by measuring the tricuspid regurgitation velocity, using the modified Bernoulli equation ($P = 4 \times V^2$) to calculate the pressure gradient across the tricuspid valve and adding estimated right atrial pressure. Pulmonary artery diastolic pressure can be estimated by similar methods measuring pulmonary valve regurgitation velocity. Right atrial pressure (RAP) can be estimated by measurement of inferior vena cava (IVC) diameter and its collapsibility. This method is not accurate when the patient is mechanically ventilated, but an IVC of <12 mm can be reasonably correlated with RAP of <10 mm Hg [10]. (Table 12.1) Left-sided filling pressures can be estimated by Doppler echocardiography of mitral inflow velocity. Mitral inflow velocities are extremely dependent on the heart rate and loading conditions, but with initial elevation of left-sided filling pressures, early filling (E wave) velocity decreases as the atrial contraction filling (A wave) velocity increases, resulting in an E/A ratio <1 [10]. Addition of tissue Doppler assessment of mitral annular velocity provides a more reliable indicator of elevated left-sided filling pressure. Early mitral inflow velocity (E) to tissue Doppler of mitral annular velocity (E') ratio of >15 indicates an elevated left ventricular end-diastolic pressure (LVEDP) of >15 mm Hg [9]. Details of these methods can be found in recent reviews [10].

12.3 Mechanical Complications of AMI

12.3.1 *Ventricular Septal Rupture*

The frequency of acute rupture of the interventricular septum has decreased in the reperfusion era to an incidence of <1% [11], but this complication still represents about 4% of patients with cardiogenic shock due to AMI. Predisposing factors include hypertension, advanced age, and female gender. It occurs mostly in anteroapical or inferior infarcts, often during the patient's first myocardial infarction (MI) [12]. Patients with ventricular septal rupture (VSR) have abrupt changes in hemodynamics, with severe heart failure or cardiogenic shock, a holosystolic murmur, and a

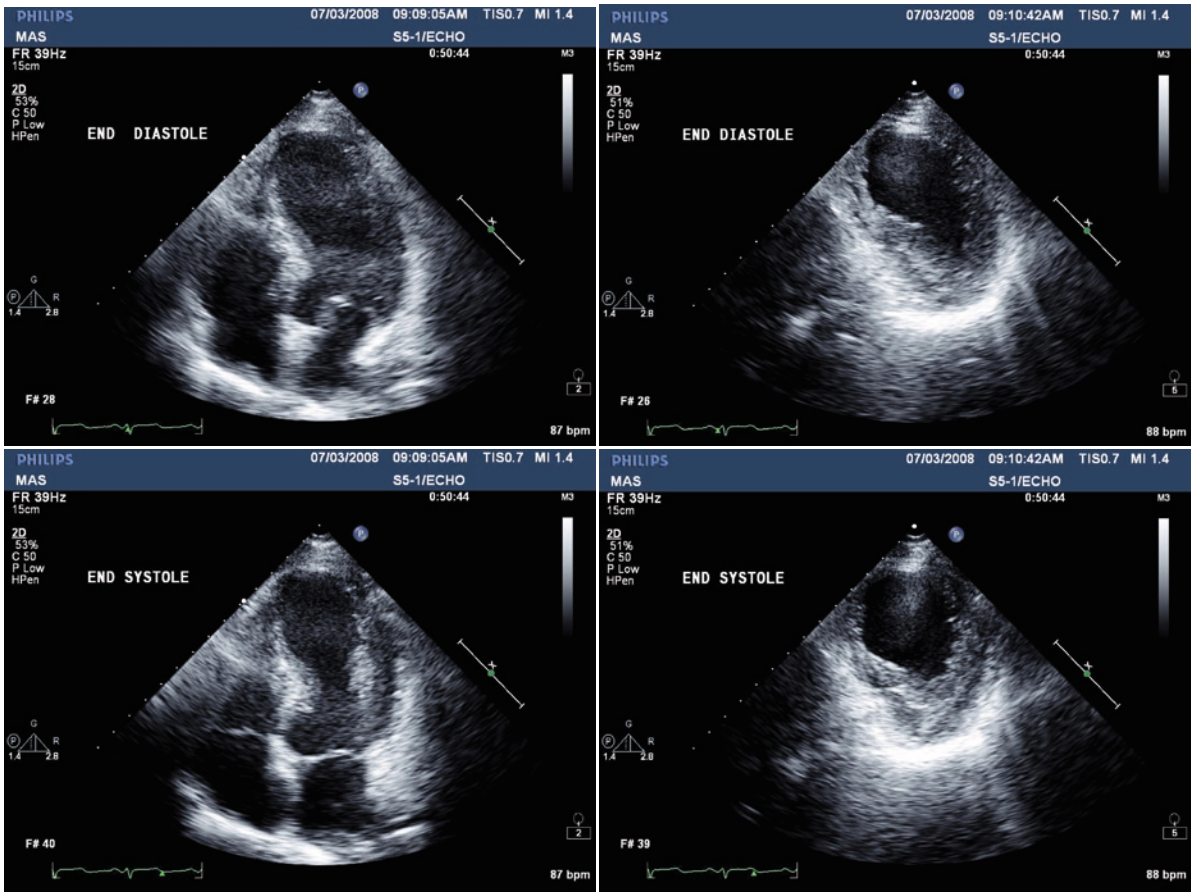

Fig. 12.2 Regional wall-motion dysfunction after acute myocardial infarction. The anteroapical segments are akinetic and thinned in the apical view (*left-side panels*). The short-axis view (*right-side panels*) of the left ventricle shows the severe hypokinesis of the anterior segment and the thinned myocardium

Table 12.1 Estimates of right atrial pressure (RAP) using the IVC size and collapsibility by echocardiogram (Adapted from [9])

IVC Size (cm)	Collapsibility (%)	RAP (mm Hg)
<2	>55	0–5
	30–50	0–10
	<30	Indeterminate
>2	>55	0–10
	30–50	10–15
	<30	10–20

parasternal thrill. Inferoseptal ruptures, although they can occur in smaller infarctions, often also involve right ventricular (RV) failure and carry a poor prognosis. Anteroapical ruptures can likewise involve the LV free wall [5].

Echocardiography is the diagnostic procedure of choice for suspected septal rupture. VSR can be seen by color flow Doppler on the echocardiogram as a left-to-right shunt. The opening defect can be serpiginous and difficult to locate; thus, nonconventional imaging planes may be needed to visualize it. The opening defect is often seen at the thinned myocardium with dyskinetic motion, sometimes with an associated pseudoaneurysm (Fig. 12.3). The peak flow velocity of a left-to-right shunt by continuous-wave Doppler represents the pressure gradient between the LV and RV, and if LV systolic pressure is assumed to be equal to systolic blood pressure, it can be used to estimate RV systolic pressure [13].

Medical therapy consists of mechanical support with an intra-aortic balloon pump and pharmacological measures, including judicious use of inotropes and afterload reducers. Definitive treatment is surgical,

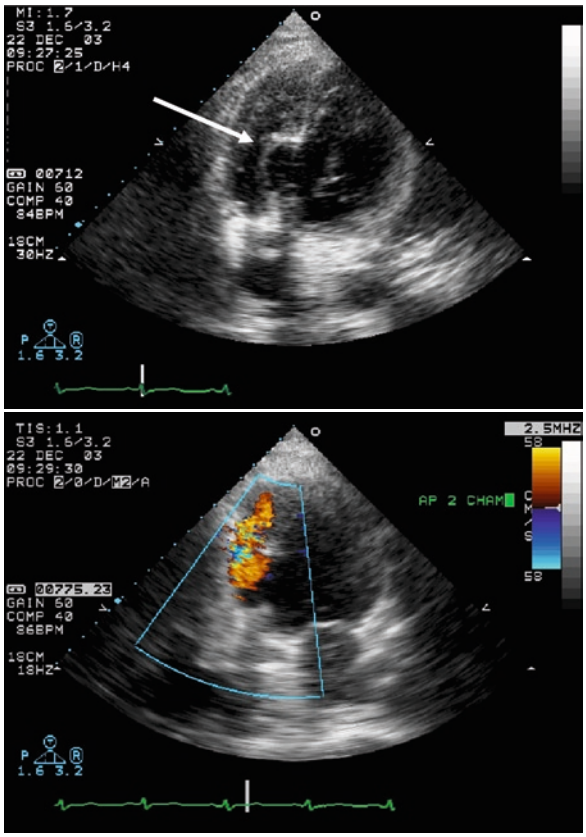

Fig. 12.3 Ventricular septal rupture shown in the apical view. The inferoseptal wall has an aneurysm (*arrow*), with color Doppler showing flow through the septal wall to the right ventricle

although mortality is quite high (20–50%), especially for inferoposterior ruptures, which tend to be serpiginous and less well circumscribed than anteroapical ruptures, and so are harder to repair. The timing of surgery has been controversial, but guidelines now recommend that operative repair be undertaken early, within 48 h of the rupture [14]. Placement of a septal occluding device may be contemplated in selected patients, but experience is limited. Intracardiac echocardiography is frequently useful to guide placement of such devices.

12.3.2 Ventricular Free-Wall Rupture

Ventricular free-wall rupture occurs in less than 1% of AMI cases in the postthrombolytic era. Predisposing factors are large infarct, advanced age, and female gender [15]. Free-wall rupture occurs owing to shearing effects at the peri-infarct area and leads to hemopericardium and tamponade [5]. Patients with frank rupture may present with a catastrophic pulseless rhythm; however, pseudoaneurysms may be more subacute, and patients can present with hypotension and cardiogenic shock [15].

A pericardial effusion may be visualized on the echocardiogram, most often in an area of thinned myocardium [5]. The effusion is seen as layered echo-dense fluid, suggesting blood clots, and can be small and loculated [7]. In the SHOCK trial registry, of the patients who had ventricular free-wall rupture, 75% had pericardial effusion, 67% of which were circumferential and the rest localized. The location of the effusion did not correlate with that of the rupture, and only 39% of the echocardiograms were able to identify the location of the tear [15]. Contrast agents, such as perfluorocarbon-exposed sonicated dextrose albumin (PESDA), can be used to demonstrate extravasation of the contrast agent into the pericardial space, indicative of free-wall rupture. Both contrast agents and color Doppler can aid in identifying ventricular free-wall rupture when the location of the opening is difficult to find [16] (Fig. 12.4).

Pseudoaneurysms represent incomplete ruptures of the ventricular wall that are sealed with pericardium and thrombus. They can often be very large and may present with chest pain, nausea, and restlessness. Echocardiography classically shows a small neck with a communication connecting the LV with the aneurysmal cavity, (Fig. 12.5) as opposed to the typically large neck of a true aneurysm [5].

Pericardiocentesis may be necessary to relieve acute tamponade, ideally in the operating room since the pressure of the pericardial effusion may be tamponading the bleeding. Although mortality after free-wall rupture is very high, salvage is possible with expeditious thoracotomy and repair [17].

12.3.3 Acute MR

Papillary muscle rupture leading to acute MR accounts for 6.9% of cardiogenic shock in patients with AMI and portends a poor prognosis. It is usually associated with inferior MI resulting in ischemia or infarction of the posteromedial papillary muscle, which has a single

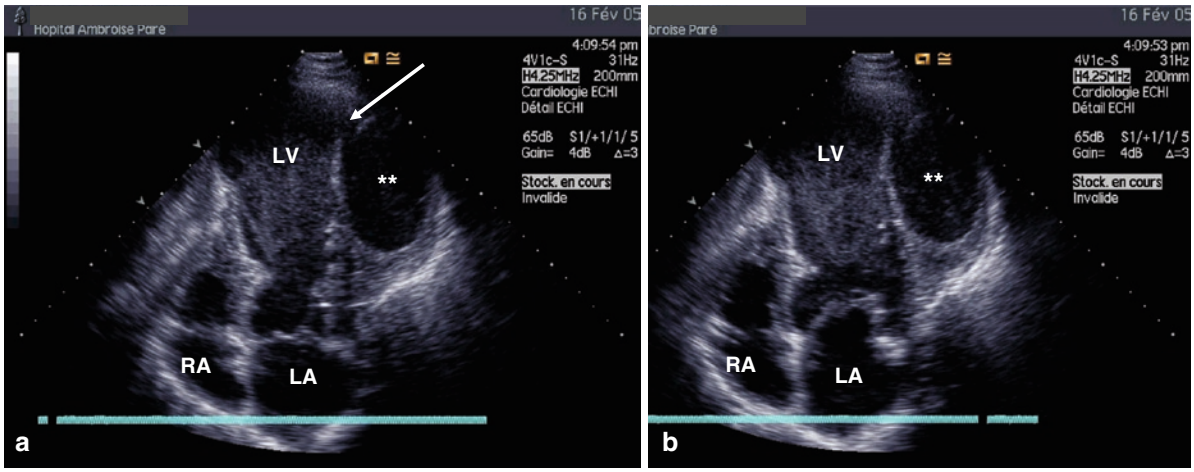

Fig. 12.4 Ventricular free-wall rupture, apical four-chamber view in diastole (**a**) and in systole (**b**) Note the spontaneous contrast into the left ventricle. (By courtesy of Prof. Nicolas Mansencal, Cardiologic Department, University hospital Ambroise Paré, Boulogne, France. *Arrow* free-wall rupture, *asterisk* false aneurysm, *LV* left ventricle, *LA* left atrium, *RA* right atrium)

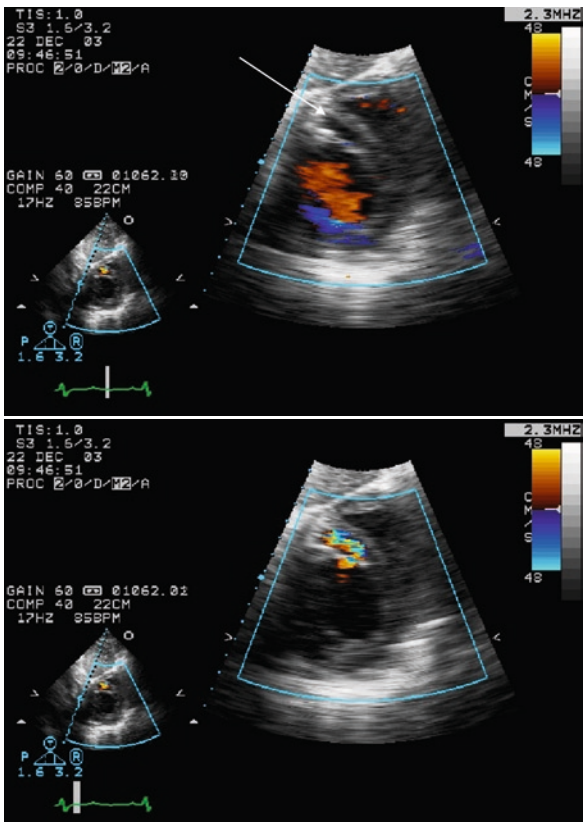

Fig. 12.5 Pseudoaneurysm of the septal wall (*arrow*) in the short-axis view. There is a small neck opening into the pseudoaneurysm, with color Doppler showing flow into the aneurysm

blood supply. Patients present with acute pulmonary edema, hypotension, and a new murmur, which can be soft or inaudible, especially when the cardiac output is low [18]. Papillary muscle rupture is distinct from other etiologies of a new murmur in cardiogenic shock, including mitral annular dilatation due to LV failure, papillary muscle dysfunction, VSR, and systolic anterior motion of the mitral valve leaflet due to LVOT obstruction [5, 7].

Echocardiography is extremely useful in identifying the etiology of new murmurs. MR is seen with color Doppler, and papillary muscle rupture or dysfunction should be suspected in eccentric MR with normal left atrial size. The MR jet is eccentric with a partial flail leaflet and anteriorly directed with complete flail of the posteromedial valve leaflet. Transthoracic echocardiograms (TTE) can readily identify new MR, but transesophageal echocardiography (TEE) may be needed to visualize the ruptured papillary muscle head. TEE may also be necessary to clarify whether MR is due to papillary muscle rupture in the setting of previously existing MR [5, 7] (Fig. 12.6).

The severity of the MR can be evaluated by the size of the regurgitant jet as a percentage of the left atrium (>40% is severe for central jets; this measure can be falsely low with eccentric jets), the size of the vena contracta, the jet area at the mitral orifice (>0.7 cm is

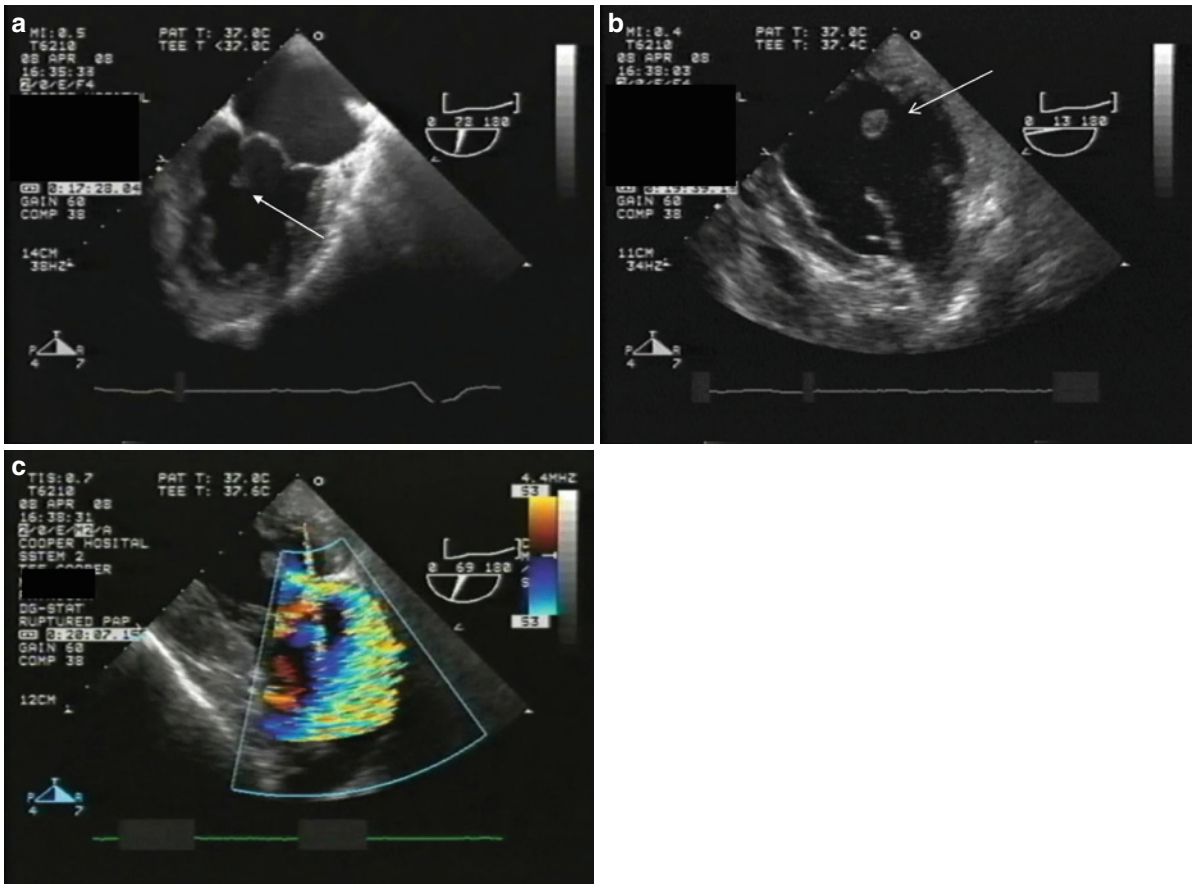

Fig. 12.6 (**a**) Transesophageal echocardiography (TEE) long-axis view of the left ventricle (LV) and mitral valve (MV); the *arrow* shows a mass at the inferior side of the posteromedial MV leaflet, a ruptured papillary muscle head. (**b**) TEE short-axis view of the LV and MV; the *arrow* shows the ruptured papillary muscle head. (**c**) Color Doppler of the short axis of the MV, showing an anteriorly directed eccentric jet of mitral regurgitation

severe), the calculated regurgitant volume (>60 mL is severe), and regurgitant fraction (>50% is severe). The proximal isovolumic surface area (PISA) can be used to calculate the regurgitant orifice area; >0.4 cm^2 is severe. Severe MR is also associated with systolic reversal of pulmonary vein flow and elevated peak early mitral valve filling velocities (>1.2 m/s).

Immediate management includes afterload reduction and intra-aortic balloon pumping as temporizing measures. Inotropic or vasopressor therapy may also be needed to support cardiac output and blood pressure. Definitive therapy, however, is surgical valve repair or replacement. Although mortality with emergency mitral valve replacement is high, ranging from 20% to 40%, survival and ventricular function are improved after surgery compared with medical therapy [19]. Surgery, if indicated, should be undertaken as soon as possible, since clinical deterioration can be sudden.

12.4 Stress Cardiomyopathy

Stress cardiomyopathy, also known as apical ballooning syndrome (ABS) and takotsubo cardiomyopathy, usually results from profound emotional stress. Patients typically present with chest pain or dyspnea with ST elevation on the ECG and elevated cardiac markers. Cardiac catheterization shows no significant coronary obstruction in the anterior territory [20]. The pathogenesis is not entirely clear, but there is evidence of sympathetic activation, with elevated plasma catecholamine levels [21].

Echocardiography findings of ABS show characteristic findings of apical ballooning and compensatory hyperdynamic function of the base of the heart. Overall LV function can be mildly to severely impaired, with ejection fractions ranging from 20% to 50%. Hemodynamic presentations can be similarly variable, from no heart failure to frank cardiogenic shock. The wall-motion abnormalities are distinct and include apical akinesis or dyskinesis and midventricular dysfunction. Hyperdynamic motion of the inferobasal and posterior wall can result in LVOT obstruction [22] (Fig. 12.7). ABS presents acutely, and the LV dysfunction is reversible. Treatment is supportive until recovery occurs, generally within a few days.

12.5 Myocarditis

Myocarditis is defined as inflammation of the heart muscle. There are many different causes, including autoimmune disorders, infections, drugs, and hypersensitivity. Many cases present with a prodrome of a recent flu-like illness and are presumed viral, although precisely how to make the diagnosis of viral myocarditis remains uncertain since different techniques have differing sensitivities and specificities. Acute myocarditis can present as a benign self-limited illness, with either resolution or slow progression, but its onset can also be fulminant with cardiogenic shock. Fulminant myocarditis presents with congestive heart failure and atrial and ventricular arrhythmias, and it requires pharmacological and mechanical support. Giant cell myocarditis is an uncommon cause of fulminant myocarditis that can occur in young people, but deterioration can be rapid, and prognosis without transplantation is generally worse than with other forms of myocarditis [23]. Presentation with conduction system disease along with LV dysfunction should raise the suspicion of giant cell myocarditis. The gold standard for the diagnosis of myocarditis is endomyocardial biopsy.

Echocardiography is helpful in myocarditis, but usually not diagnostic. Echocardiography of myocarditis will typically show severe global hypokinesis, but regional variations may be present, reflecting the focal nature of myocarditis. The distinguishing feature of acute myocarditis, one that may not always be present, is that the LV is not dilated and the wall thickness is often normal or thickened. A trabeculated pattern of wall thickening may be seen if inflammation is substantial. Myocytolysis and cell infiltration in myocarditis can change the acoustic properties of the myocardium [24], and so echocardiographic tissue characterization can also aid in the diagnosis of myocarditis. Echocardiography can likewise detect intracardiac thrombi, functional mitral or tricuspid regurgitation, and pericardial involvement.

A small study demonstrated specific echocardiographic features that help distinguish fulminant and acute myocarditis. Patients with fulminant myocarditis had near-normal LV diastolic dimensions, but increased septal thickness at presentation, while those with acute myocarditis had increased diastolic dimensions, but normal septal thickness [25]. At 6 months, patients with fulminant myocarditis had dramatic improvement in fractional shortening compared with no improvement in patients with acute myocarditis. Thus, the echocardiogram may be a useful tool to assess prognosis of these patients in cardiogenic shock [25].

12.6 Valvular Disease

12.6.1 Acute Aortic Regurgitation

Acute aortic regurgitation (AR) most commonly occurs as a result of infective endocarditis with leaflet destruction or from acute aortic dissection. Acute AR can also occur as a result of spontaneous rupture of a sinus of Valsalva aneurysm or as a result of traumatic injury. In acute AR, the LV does not tolerate the large regurgitant volume, and thus stroke volume and cardiac output fall, and end-diastolic pressure rises. Patients in the acute setting are tachypneic, tachycardic, and have cardiogenic shock. Patients appear ill with tachycardia, tachypnea, and restlessness. The pulse pressure is usually narrow, indicating decreased forward stroke volume, and the bounding pulsations seen with chronic AR are usually absent [26]. The diastolic murmur of acute AR tends to be short, decrescendo, and blowing in quality; it is best heard along the sternal border or at the apex.

Echocardiography in acute AR is an extremely useful tool for the diagnosis of its etiology. Color Doppler will show a sharp regurgitant jet in the parasternal and

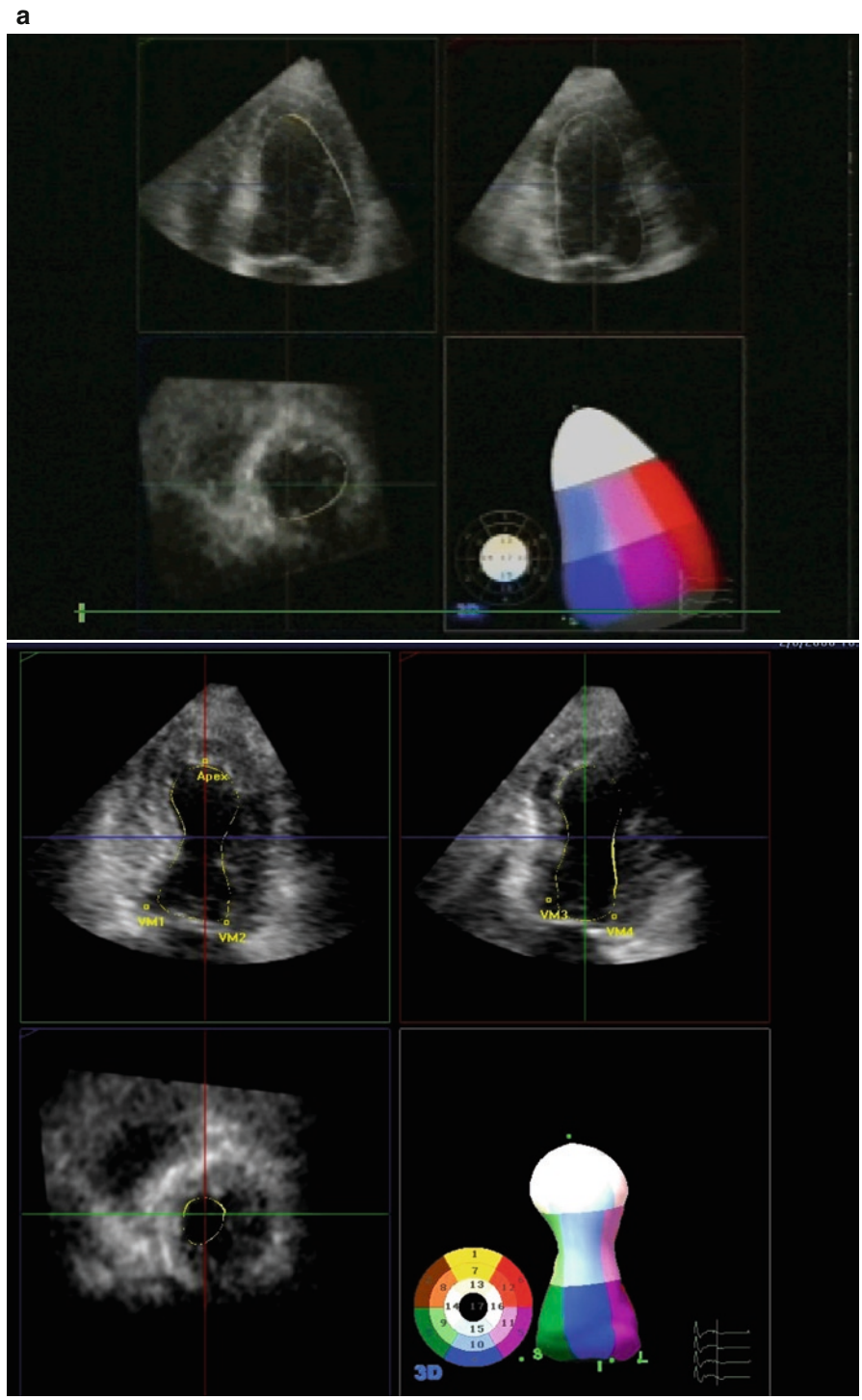

Fig. 12.7 Apical ballooning syndrome (takotsubo cardiomyopathy). (**a**) Diastolic (*top*) and systolic (*bottom*) apical and short-axis view of the left ventricle. (**b**) Transthoracic echocardiography (TTE) images obtained during the acute phase of left ventricular apical ballooning syndrome in apical four-chamber views during diastole (panel **a**) and systole (panel **b**) and apical two-chamber views during diastole (panel **c**) and systole (panel **d**)

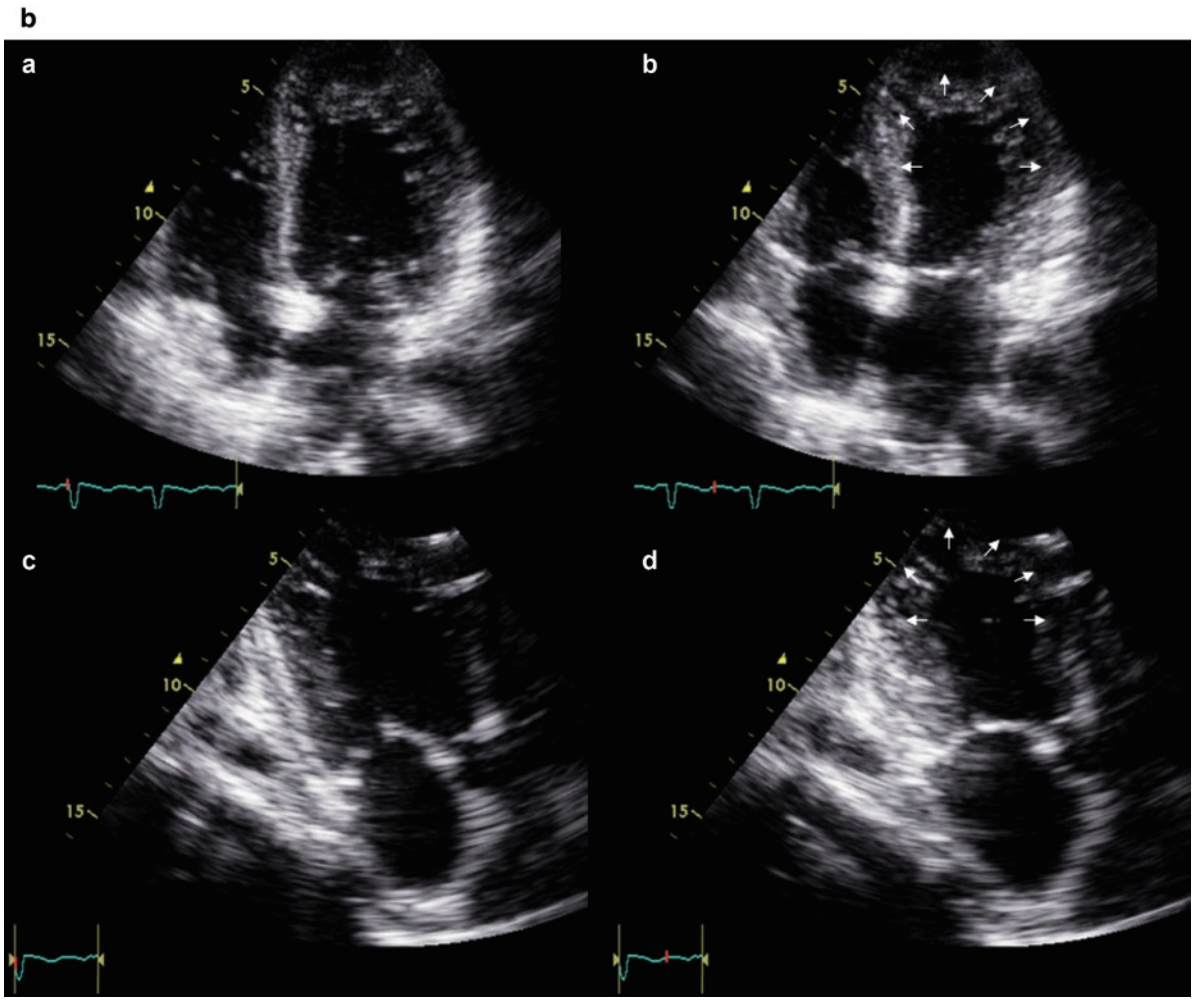

Fig. 12.7 (continued)

apical views. The width of the jet at its origin in relation to the LVOT correlates with the severity of the AR (>0.6 cm is severe) (Fig. 12.8). Continuous-wave (CW) Doppler can help distinguish whether the AR is acute or chronic since the deceleration time of the CW signal (measured as the pressure half-time) is related to the rate at which the LV pressures equilibrate in diastole. In acute severe AR, the deceleration is steep owing to a rapid rise in LVEDP, and the pressure half-time is <200 ms [27] (Fig. 12.9). With severe acute AR, increased LVEDP may cause high-frequency fluttering and even premature closure of the anterior leaflet of the mitral valve, and this can be seen on M-mode [5] (Fig. 12.10).

For the evaluation of aortic dissection, TEE can visualize the ascending aorta, aortic arch, and descending thoracic aorta. An intimal flap that moves toward the false lumen in systole, color Doppler flow in the true and false lumen with identification of the entry site, and thrombosis within the false lumen are all typically seen in TEE [28] (Fig. 12.11). Aortic valve structure may be visualized in this examination as well. TEE may also be useful for visualization of valvular structure and function in infective endocarditis and in identifying potential abscess formation in the fibrous valvular ring.

12.6.2 Aortic Stenosis

Aortic stenosis (AS) typically has a gradual disease course and is not a common cause of cardiogenic shock; however, in settings of increased metabolic

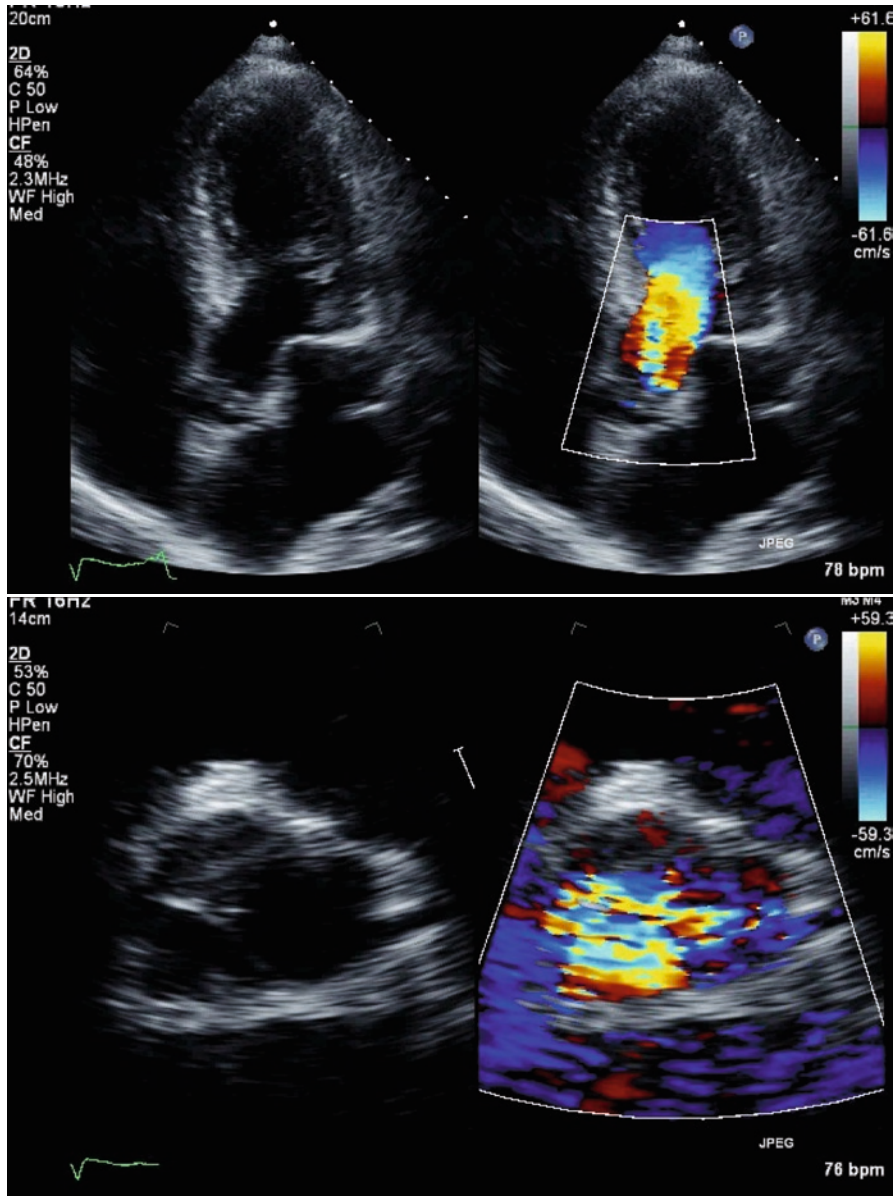

Fig. 12.8 Severe aortic regurgitation (AR) is shown in apical and short-axis views. The color Doppler of the regurgitant jet occupies more than 50% of the left ventricular outflow tract

demands, such as tachycardia and existing LV failure, shock can occur. Patients can present with tachycardia and hypotension, and the murmur of AS may be soft or absent owing to low cardiac output.

Echocardiography will typically show a thickened and calcified AV with restricted leaflet motion (Fig. 12.12). AS severity is best assessed with transvalvular pressure gradients measured by Doppler. Aortic valve area is then calculated using the continuity equation [AV area = AV outflow tract area × (outflow tract velocity–time integral/transvalvular velocity–time integral)]. With severely depressed LV function, as in shock, low cardiac output may reduce valve-opening forces, the transvalvular gradient may be only mildly elevated, and the severity of moderate AS can be overestimated [5] (Fig. 12.13). Increasing cardiac output may be helpful in this setting; if cardiac output increases and the valve gradient is unchanged, then the calculated valve area will increase, indicating pseudostenosis. If cardiac output increases and the valve gradient increases to a commensurate degree, then true AS is confirmed.

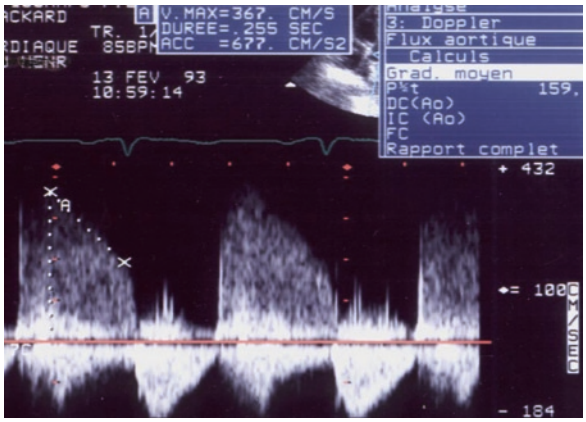

Fig. 12.9 Continuous Doppler in severe aortic regurgitation (AR; apical view). The deceleration half-time of regurgitant flow is lower than 250 ms

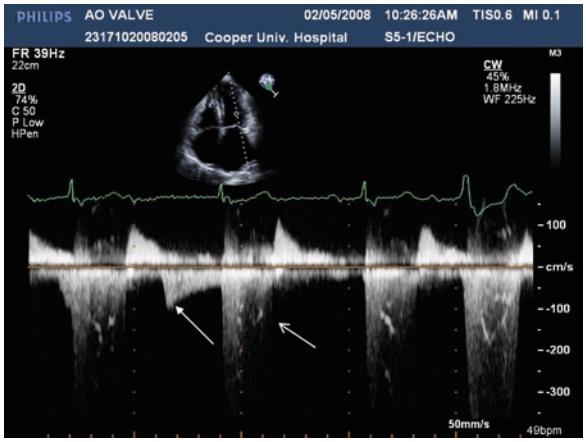

Fig. 12.10 With severe acute aortic regurgitation, premature closure of the mitral valve is seen on continuous-wave Doppler (*closed arrow*) owing to increased left ventricular end-diastolic pressure along with high-frequency fluttering of the anterior leaflet of the mitral valve (*open arrow*)

12.6.3 Mitral Stenosis

Mitral stenosis (MS) usually has a gradual disease course, but severe MS can result in cardiogenic shock when atrial fibrillation, supraventricular tachycardia, thyrotoxicosis, or pregnancy occur. The transmitral diastolic flow duration is inversely related to heart rate and directly related to stenosis severity, an important consideration when metabolic demands exceed the ability to augment cardiac output. Patients present with pulmonary vascular congestion, even though LV function is normal. RV failure is more common, owing to secondary pulmonary hypertension.

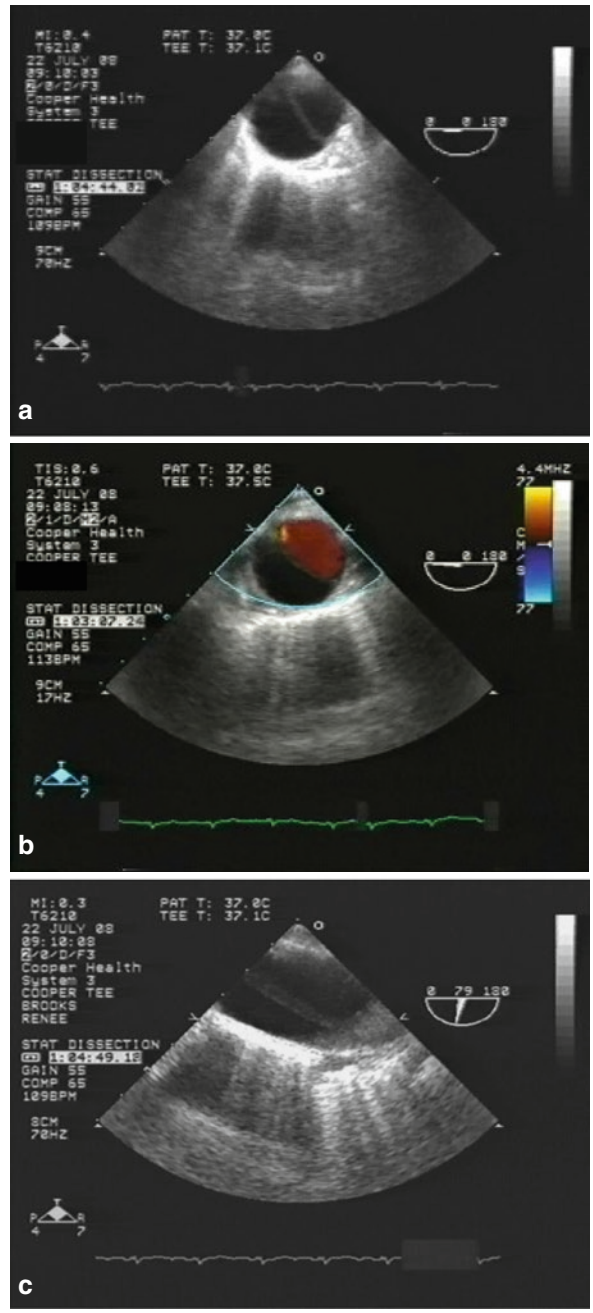

Fig. 12.11 Aortic dissection. Transthoracic echocardiography (TEE) short-axis view of the aorta. A distinct flap is visible with color flow in the true lumen (**a**, **b**). TEE long-axis view of the aorta with the visible flap (**c**)

Virtually all significant MS is rheumatic, although other etiologies include myxoma, endocardial fibrosis, and prosthetic valve dysfunction. Echocardiography shows thickened mitral valve (MV) leaflets with

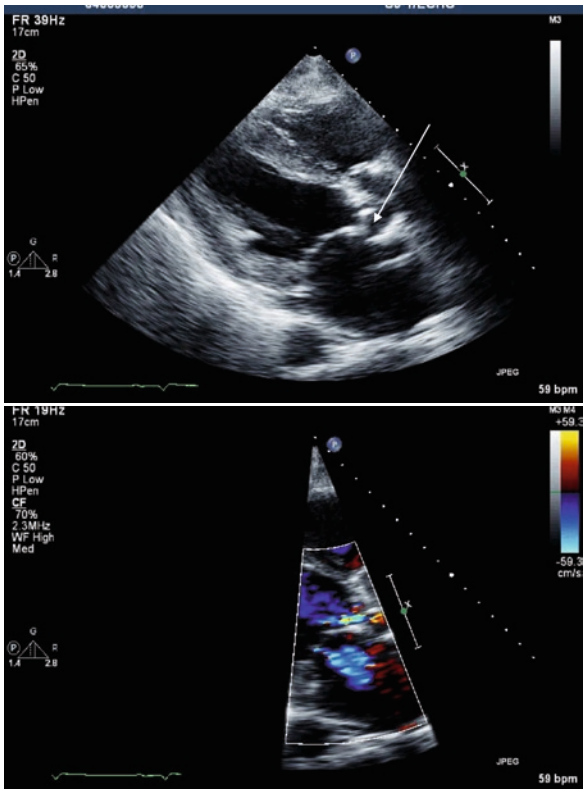

Fig. 12.12 Severe aortic stenosis. A heavily calcified aortic valve with restricted leaflet motion is shown (*arrow*) in the parasternal long-axis view. The color Doppler demonstrates turbulent flow proximal to the valve with a narrow flow through the severely stenotic valve

abnormal and restricted mobility. There is usually doming of the anterior leaflet, described as a "hockey-stick" deformity, in the parasternal long-axis view (Fig. 12.14). The MV area can be measured by direct planimetry when visualized in the parasternal short-axis view (Fig. 12.15). MV area can also be calculated by using Doppler to measure the mitral inflow pressure half-time (MV area = 220/pressure half-time) [13] (Fig. 12.16).

Because tachycardia decreases diastolic filling time and thus increases atrial pressure, the first therapeutic goal is to decrease the heart rate. Cardioversion may be necessary to restore the atrial contribution to filling in the presence of atrial fibrillation. Percutaneous balloon mitral valvuloplasty is equivalent or superior to surgery in patients with favorable valve anatomy, but valve replacement may be required.

12.7 Conclusion

Echocardiography is the cornerstone of cardiogenic shock management. By providing precise cardiac imaging, echocardiography points out the exact cause of cardiogenic shock and provides evaluation of the hemodynamic state. This technique helps the clinician to choose the best therapeutic options.

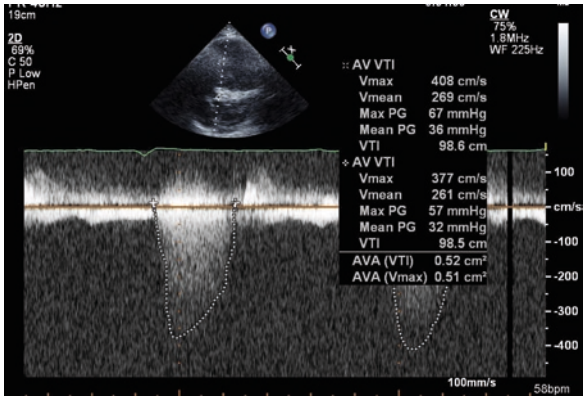

Fig. 12.13 Continuous-wave Doppler of severe aortic stenosis, demonstrating a large transvalvular pressure gradient. The continuity equation is used to calculate the aortic valve area

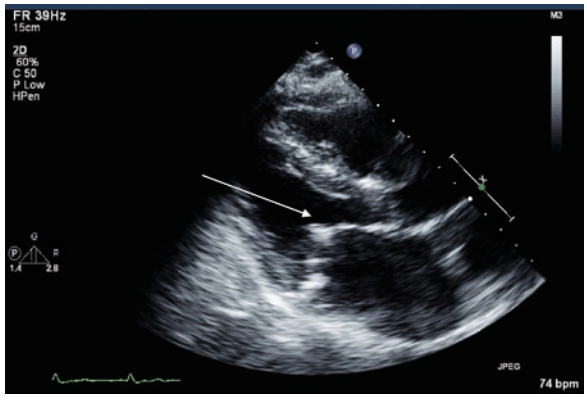

Fig. 12.14 Parasternal long-axis view of the mitral stenosis. The mitral valve leaflets are thickened with the anterior leaflet showing the typical "hockey stick" appearance with restricted motion

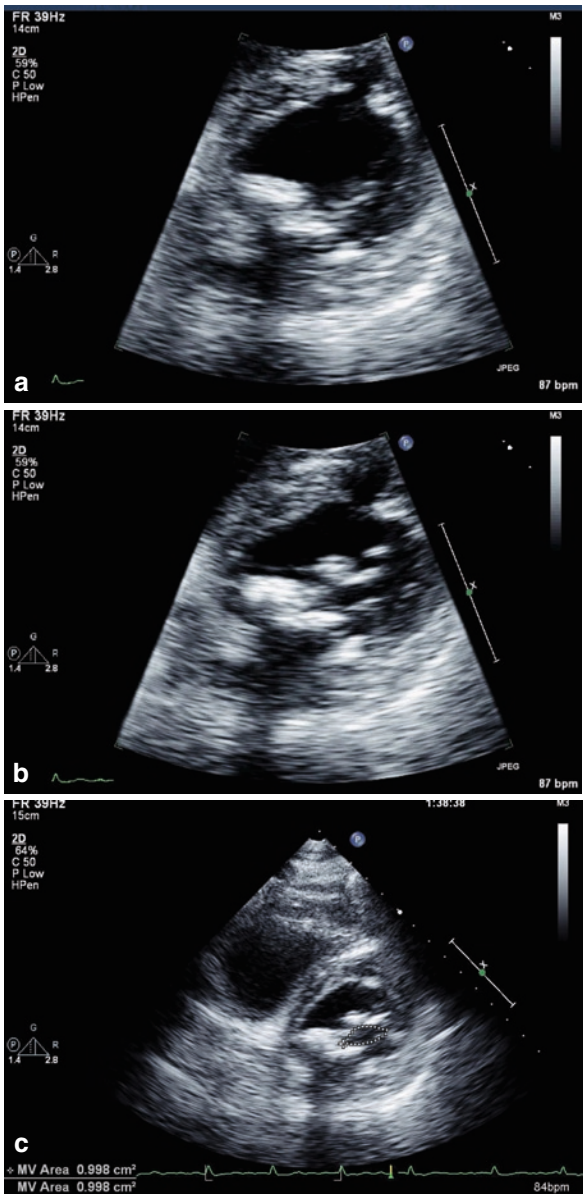

Fig. 12.15 Mitral stenosis. The mitral valve is visualized in the short-axis view of the left ventricle at the parasternal position (**a**, **b**). The mitral valve leaflets are thickened, with an asymmetric opening. Planimetry can be done of the opening area of this stenotic mitral valve (**c**)

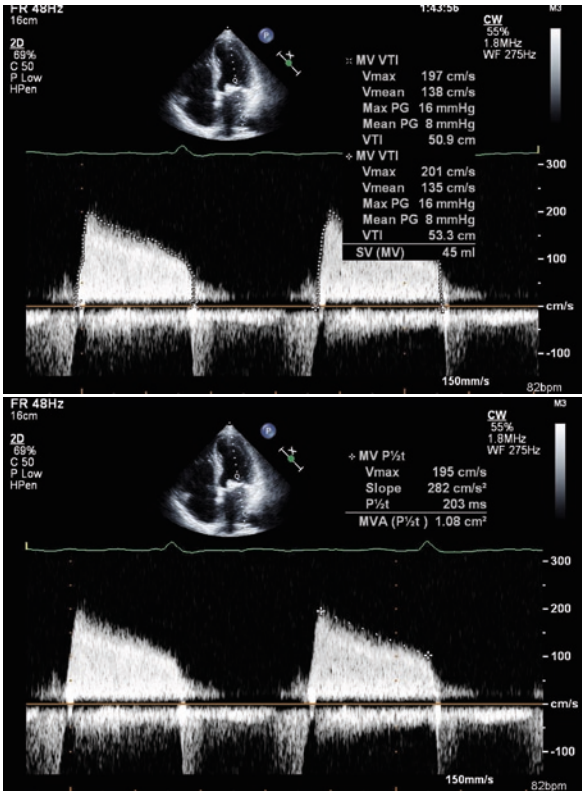

Fig. 12.16 Continuous-wave Doppler of the mitral valve (MV) in the apical view. The stenotic MV has a large pressure gradient. The pressure half-time can be measured to calculate the MV area. The slope of the flow through the MV is not as steep as a normal valve, indicating significant stenosis of the valve

References

1. Hollenberg SM, Kavinsky CJ, Parrillo JE (1999) Cardiogenic shock. Ann Intern Med 131:47–59
2. Nishimura RA, Tajik AJ, Shub C, Miller FA Jr, Ilstrup DM, Harrison CE (1984 Dec) Role of two-dimensional echocardiography in the prediction of in-hospital complications after acute myocardial infarction. J Am Coll Cardiol 4(6):1080–7
3. Hochman JS, Buller CE, Sleeper LA, Boland J, Dzavik V, Sanborn TA et al (2000) Cardiogenic shock complicating acute myocardial infarction - etiologies, management and outcome: a report from the SHOCK Trial Registry. J Am Coll Cardiol 36(3 Suppl A):1063–70
4. Alonso DR, Scheidt S, Post M, Killip T (1973) Pathophysiology of cardiogenic shock. Quantification of myocardial necrosis, clinical, pathologic and electrocardiographic correlations. Circulation 48:588–96
5. Oh JK, Seward JB, Tajik AJ (eds) (2007) The echo manual, 3rd edn. Lippincott, Williams & Wilkins
6. Augoustides JG, Hosalkar HH, Gambone AJ, Berkowitz D, Floyd TF (2005) Rapid and rational echocardiographic-assisted management of cardiogenic shock after coronary artery bypass surgery. J Cardiothorac Vasc Anesth 19:772–4
7. Picard MH, Davidoff R, Sleeper LA, Mendes LA, Thompson CR, Dzavik V et al (2003) Echocardiographic predictors of survival and response to early revascularization in cardiogenic shock. Circulation 107:279–84
8. Tei C, Ling LH, Hodge DO, Bailey KR, Oh JK, Rodeheffer RJ et al (1995) New index of combined systolic and diastolic myocardial performance: a simple and reproducible measure of cardiac function – a study in normals and dilated cardiomyopathy. J Cardiol 26:357–66

9. Kirkpatrick JN, Vanna MA, Narula J, Lang RM (2007) Echocardiography in heart failure. J Am Coll Cardiol 50(5): 381–96
10. Kirkpatrick JN, Lang RM (2008) Heart failure: hemodynamic assessment using echocardiography. Curr Cardiol Rep 10:240–6
11. Birnbaum Y, Fishbein MC, Blanche C, Siegel RJ (2002) Ventricular septal rupture after acute myocardial infarction. N Engl J Med 347:1426–32
12. Menon V, Webb JG, Hillis LD, Sleeper LA, Abboud R, Dzavik V et al (2000) Outcome and profile of ventricular sepal rupture with cardiogenic shock after myocardial infarction: a report from the SHOCK Trial Regsitry. J Am Coll Cardiol 36(3 Suppl A):1110–6
13. Feigenbaum H, Armstrong WF, Ryan TL (eds) (2005) Feigenbaums's echocardiography, 6th edn. Lippincott, Williams & Wilkins
14. Antman EM, Anbe DT, Armstrong PW, Bates ER, Green LA, Hand M et al (2004 Aug) ACC/AHA guidelines for the management of patients with ST-elevation myocardial infarction – executive summary: a report of the American College of Cardiology/American Heart Association Task Force on Practice Guidelines. Circulation 110(10): 588–636
15. Slater J, Brown RJ, Antonelli TA, Menon V, Boland J, Col J et al (2000) Cardiogenic shock due to cardiac free-wall rupture or tamponade after acute myocardial infarction: A report from the SHOCK Trial Registry. J Am Coll Cardiol 36 (3 Suppl A):1117–22
16. Trindade ML, Tsutsui JM, Rodrigues AC, Caldas MA, Ramires JA, Mathias Junior W (2006) Left ventricular free wall impending rupture in post-myocardial infarction period diagnosed by myocardial contrast echocardiography: case report. Cardiovasc Ultrasound 4:7–10
17. Reardon MJ, Carr CL, Diamond A, Letsou GV, Safi HJ, Espada R et al (1997) Ischemic left ventricular free wall rupture: prediction, diagnosis, and treatment. Ann Thorac Surg 64:1509–13
18. Khan SS, Gray RJ (1991) Valvular emergencies. Cardiol Clin 9:689–709
19. Thompson CR, Buller CE, Sleeper LA, Antonelli TA, Webb JG, Jaber WA et al (2000) Cardiogenic shock due to acute severe mitral regurgitation complicating acute myocardial infarction: a report from the SHOCK Trial Registry. SHould we use emergently revascularize Occluded Coronaries in cardiogenic shocK? J Am Coll Cardiol 36(3 Suppl A):1104–9
20. Hanna M, Finkelhor RS, Shaw WF, Bahler RC (2007) Extent of right and left ventricular focal wall-motion abnormalities in differentiating transient apical ballooning syndrome from apical dysfunction as a result of coronary artery disease. J Am Soc Echocardiogr 20:144–50
21. Wittstein IS, Thiemann DR, Lima JA, Baughman KL, Schulman SP, Gerstenblith G et al (2005 Feb 10) Neurohumoral features of myocardial stunning due to sudden emotional stress. N Engl J Med 352(6):539–48
22. Gianni M, Dentali F, Grandi AM, Sumner G, Hiralal R, Lonn E (2006) Apical ballooning syndrome or takotsubo cardiomyopathy: a systemic review. Eur Heart J 27: 1523–29
23. Feldman AM, McNamara D (2000) Myocarditis. N Engl J Med [review] 343(19):1388–98
24. Lieback E, Hardoulin I, Meyer R, Bellach J, Hetzer R (1996) Clinical value of echocardiographic tissue characterization in the diagnosis of myocarditis. Eur Heart J 17:135–42
25. Felker GM, Boehmer JP, Hruban RH, Hutchins GM, Kasper EK, Baughman KL et al (2000) Echocardiographic findings in fulminant and acute myocarditis. J Am Coll Cardiol 36:227–32
26. Braunwald E, Zipes DP, Libby P, Bonow R, (eds) (2007) Heart disease, 8th edn. W.B. Saunders Co
27. Nagueh SF, Peters PJ (2007) Echocardiography. In: Parrillo JE, Dellinger RP (eds) Critical care medicine: principles of diagnosis and management in the adult, 3rd edn. Mosby, St Louis, MO, pp 117–152
28. Nienaber CA, Eagle KA (2003) Aortic dissection: new frontiers in diagnosis and management. Part 1: From etiology to diagnostic strategies. Circulation 108:628–35

Echocardiographic Evaluation and Monitoring of Right Ventricular Function and Pulmonary Artery Pressures

13

Adolfo Kaplan, Antony Mc Lean, and Antoine Vieillard-Baron

Contents

A. Kaplan (✉)
2821 Michaelangelo Drive, Suite 303, Edinburg, TX, 78539
e-mail: akaplan0504@yahoo.com

A. Mc Lean
University of Sydney, Nepean Hospital, Sydney, Australia

A. Vieillard-Baron
Intensive Care Unit, University Hospital Ambroise Paré,
9 avenue Charles-de-Gaulle, 92104, Boulogne Cedex, France
e-mail: antoine.vieillard-baron@apr.aphp.fr

Right ventricular (RV) dysfunction is common in critically ill patients [1–4]. It is associated with multiple clinical scenarios frequently encountered by the intensivist, including acute cor pulmonale, acute RV dysfunction of sepsis, and acute RV infarction. In addition, assessment of right-heart function is essential to assess a subject's preload responsiveness [5]. Echocardiography is the best available method to diagnose and monitor right-heart function at the bedside (Table 13.1). In the critically ill, prompt, accurate, and serial echocardiographic assessments are required to monitor the function of the right heart and its response to implemented therapies.

This chapter first describes normal RV anatomy and function. It then explores echocardiographic techniques to assess RV dysfunction. The second part of the chapter focuses on specific clinical situations associated with RV dysfunction and how to assess preload responsiveness utilizing right-heart echocardiographic indices.

13.1 Normal RV Anatomy and Function

The RV comprises two anatomically and functionally different cavities separated by the crista supraventricularis: an inflow region (the sinus) and an outflow tract (the cone or infundibulum) (Fig. 13.1). The tricuspid valve (TV) and its apparatus plus the heavily trabeculated myocardium form the sinus. Smooth myocardium and the pulmonary valve form the infundibulum. The sinus generates pressure during systole while the infundibulum regulates this pressure by reducing and prolonging it. RV contraction occurs in three different manners: (1) contraction of the sinus along its longitudinal axis; (2) radial contraction of the RV free wall toward

D. De Backer et al. (eds.), *Hemodynamic Monitoring Using Echocardiography in the Critically Ill*,
DOI: 10.1007/978-3-540-87956-5_13, © Springer-Verlag Berlin Heidelberg 2011

Table 13.1 Echocardiographic methods of evaluating PHT and right-heart dysfunction

Pathology/ investigations	Evaluation
RV systolic function	• Right-heart dimensions • Visual inspection of free-wall motion and tricuspid annulus motion • RV fractional area change • TAPSE • TDV • MPI • Evidence of left-heart abnormalities
Right-heart preload and RAP	• IVC collapsibility in patients breathing[a] spontaneously (TTE) • SVC collapsibility in ventilated patients (TEE) • Hepatic vein systolic filling fraction
Pulmonary hypertension	• Right-heart dimension • Estimation of PASP, PAEDP, and MPAP • Estimation of PVR • Look for paradoxical septal motion • IVC diameter and collapsibility • Nepean Index in case of lack of significant TR • LV diastolic function; LVEDP estimation
Pericardial effusion and tamponade	• RA early diastolic collapse • RV early systolic collapse • Fluid status: IVC diameter and collapsibility

[a]Note that a normal or high RAP can be associated with an inspiratory collapse of the IVC in case of deep inspiratory effort. *TAPSE* tricuspid annular plane systolic excursion; *MPI* myocardial performance index; *TDV* tissue doppler velocities; *IVC* inferior vena cava; *SVC* superior vena cava; *PASP* pulmonary artery systolic pressure; *PAEDP* pulmonary artery end-diastolic pressure; *MPAP* mean pulmonary artery pressure; *PVR* pulmonary vascular resistance; *LVEDP* left ventricular end-diastolic pressure

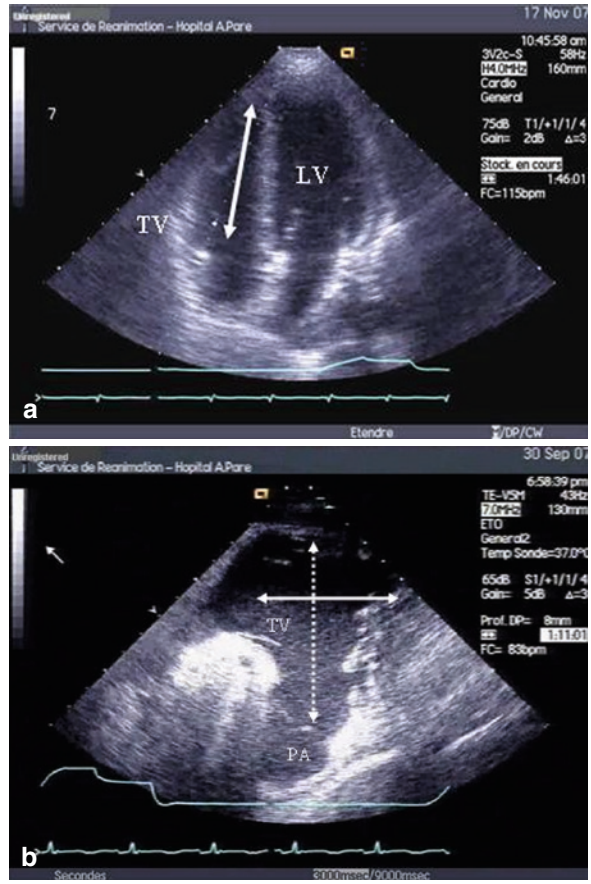

Fig. 13.1 **Panel a**: Apical four-chamber view demonstrating left chambers with the mitral valve to the right, and right chambers with tricuspid valve to the left. Mostly, the more muscular and trabeculated inflow (or sinus) region of the right ventricle can be visualized in this tomographic plane. **Panel b**: Modified short-axis view by a transgastric approach, demonstrating the smooth outflow tract of the right ventricle (*dotted arrow*) as it transitions into the pulmonary artery. This right ventricular portion is also called the cone or infundibulum, has an inferior–superior axis, and is perpendicular to the inflow chamber (*full arrow*). Abbreviations: *TV* tricuspid valve, *PA* pulmonary artery

the interventricular septum (IVS); and (3) torsion of the left ventricle (LV; clockwise rotation of LV base and counterclockwise rotation of its apex), pulling the RV in similar fashion. Overall, the LV contraction contributes 25% of its own stroke work to the generation of the RV stroke work via the IVS. In pulmonary hypertension, this contribution increases to 35% [6].

The normal RV is less muscular than the LV because it pumps into a low-pressure pulmonary vascular resistance system. As demonstrated by the pressure/volume loop technique, the RV isovolumetric contraction time is very short. The ventricle continues to eject blood long after the beginning of its relaxation [7]. Consequently, the RV ejects blood in a quasi-continuous manner into the pulmonary circulation in normal conditions, acting almost like a passive conduit. As a result, it is easily affected by its surroundings and increased afterload [8], and, unlike the LV, it is able to dilate acutely. The effect of increased afterload (pulmonary vascular resistance) has a series of consequences, affecting the functioning of both the right and left heart (Fig. 13.2).

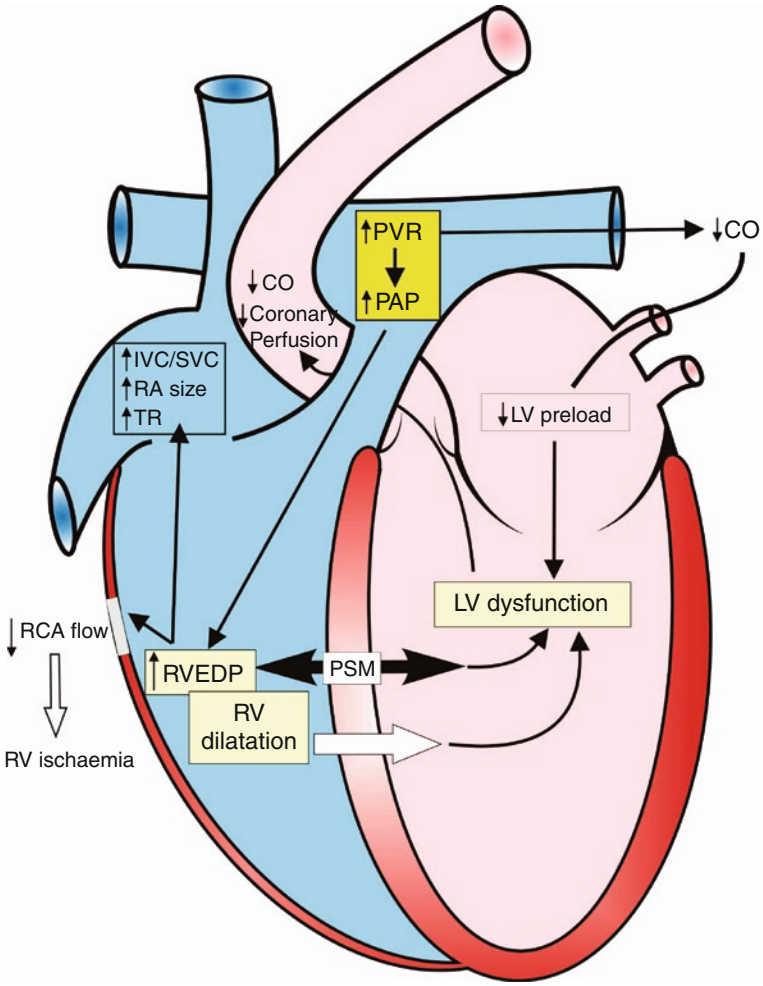

Fig. 13.2 Pathophysiological changes resulting from increased pulmonary vascular resistance. Abbreviations: *CO* cardiac output; *IVC* inferior vena cava; *SVC* superior vena cava; *TR* tricuspid regurgitation; *PAP* pulmonary artery pressure; *RCA* right coronary artery; *RVEDP* right ventricular end-diastolic pressure; *PSM* paradoxical septal motion

The RV myocardium is very sensitive to coronary flow. Contrary to the LV, the RV walls are perfused during both diastole and systole [9]. Therefore, RV function requires maintenance of adequate systemic pressures, particularly if RV pressure overload and failure develop [10].

13.2 Acute Cor Pulmonale

Acute cor pulmonale (ACP) is defined as the clinical setting in which the RV is suddenly afterloaded [11]. Testa was the first to use the term "cor pulmonale" in 1831 to describe the concept of cardiopulmonary interaction [12]. The first description of the clinical features of ACP was performed by McGinn and White in 1935 in patients with pulmonary embolism [13]. Sudden increases in right-heart afterload are frequent in critically ill subjects (Table 13.2). They may result as a consequence of an absolute increase in afterload, as in pulmonary embolism or acute respiratory distress syndrome (ARDS), or a relative increase, such as an unwanted side effect of mechanical ventilation on a failed RV. ACP is characterized by the combination of systolic and diastolic overload. It is diagnosed and characterized by echocardiographic findings.

13.2.1 RV Systolic Overload

Septal dyskinesia is the echocardiographic hallmark of sudden elevations of RV systolic overload. It occurs because of ventricular interdependence. When RV afterload is increased, its contraction is prolonged,

taking longer to complete than the LV systole. Because the RV is still contracting when the LV is beginning to relax at the end of systole, right intraventricular pressure becomes transiently greater than that of the left, pushing the IVS left during that period [14, 15]. Septal dyskinesia can be assessed qualitatively and quantitatively. Simple observation of paradoxical septal motion suffices in most clinical situations (Fig. 13.3). If needed, quantification can be achieved by direct measurement of the systolic eccentricity index (EI) [16] and, indirectly, by analysis of the impedance to flow at the level of the right ventricular outflow tract (RVOT).

Table 13.2 Causes of acute cor pulmonale

Acute cor pulmonale
Acute pulmonary embolism
Acute respiratory distress syndrome (ARDS)
Inappropriately adjusted ventilatory support in a failed right ventricle
Respiratory and metabolic acidosis
Fat emboli
Gas emboli

Quantification of the systolic RV overload can also be achieved by direct measurement of the systolic EI. To do this, the short-axis view of the mid-LV (when both papillary muscles are displayed) is obtained via transthoracic (TTE) or transesophageal (TEE) echocardiography. At end systole, D1 is measured as the

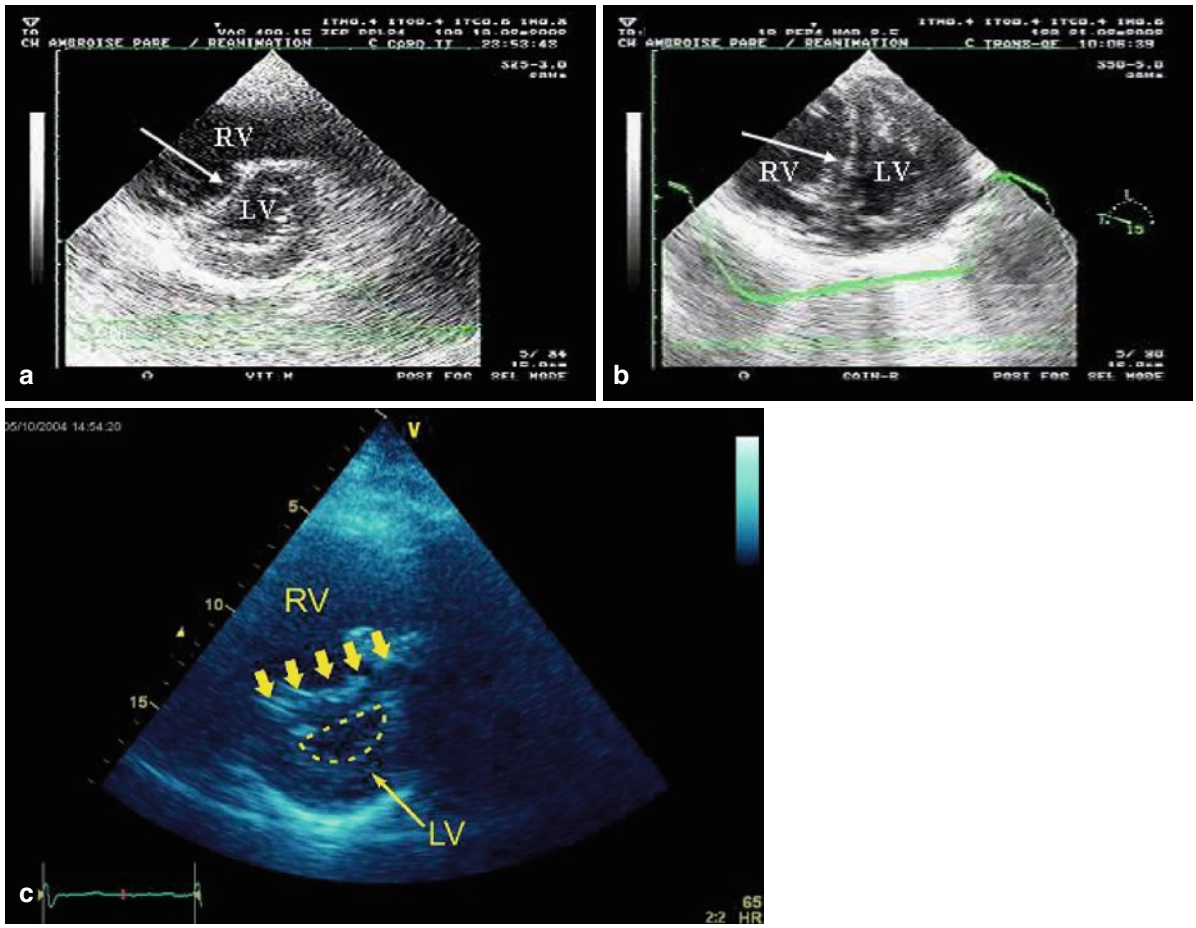

Fig. 13.3 **Panels a, c**: Transthoracic echocardiography in a ventilated patient with an acute respiratory distress syndrome (**a**) and in a patient with massive pulmonary embolism (**c**). Parasternal short-axis interrogation at the left midventricular level shows the interventricular septum deviated toward the center (*arrow*) of the left ventricular (LV) cavity during systole. Notice the dilated, "spherical" right ventricular (RV) silhouette and its size in relation to the LV chamber. **Panel b**: Short-axis view by a transgastric approach in a patient ventilated for severe acute respiratory distress syndrome. It demonstrates septal deviation and bowing (*arrow*) toward the LV center during systole, reflecting the systolic overload of the RV

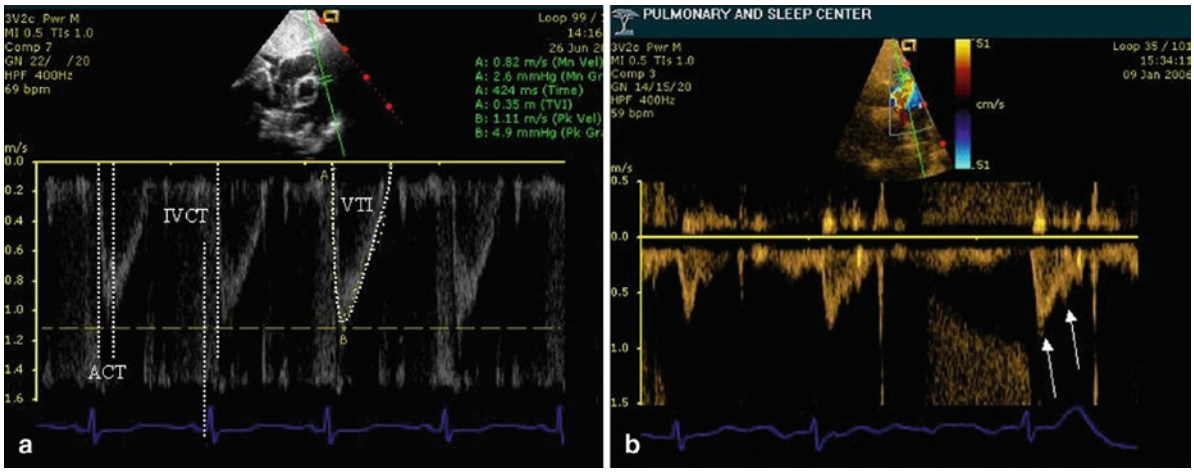

Fig. 13.4 **Panel a**: Normal right ventricular outflow tract (RVOT) spectral Doppler signal determined by pulsed-wave Doppler interrogation. The interrogation box is placed immediately above the pulmonary valve. **Panel b**: Dichromatic RVOT spectral Doppler signal (*arrows*) in a patient with pulmonary arterial hypertension. Abbreviations: *IVCT* isovolumetric contraction time, *VTI* velocity–time integral, *ACT* acceleration time

Table 13.3 Quantitative RV output measurements

	Normal	RV systolic overload
Stroke volume	70–100 mL	<70 mL
RVOT velocity–time integral (VTI)	18 ± 3 cm	<15 cm
Acceleration time	≥120 ms	<100 ms
Ejection time	304 ± 23 ms	<281 ms
Acceleration time/ejection time	>0.34 [2]	<0.34

diameter that bisects the papillary muscles, and D2 is the orthogonal diameter to D1. The systolic EI is D2/D1. A normal systolic EI is 1. Septal dyskinesia will result in an EI >1 [16]. An atrial septal defect could, however, result in a falsely elevated EI [17]. Therefore, a search of intracardiac shunting should always be considered within the right clinical context.

Systolic RV overload can also be indirectly identified by Doppler assessment of the RVOT. RV systolic overload results in increased RV output impedance. It can be assessed by both TTE and TEE using pulsed-wave (PW) Doppler. The PW interrogation box is placed either above the pulmonary valve (by TTE or by TEE using a transgastric view) or just below the valve (view of the great vessels by TEE). A spectral Doppler signal is obtained, allowing both qualitative and quantitative assessment of increased pulmonary vascular impedance. The normal RVOT spectral Doppler signal is easily discriminated from the biphasic pattern that occurs due to the reduction of velocity during midsystole when impedance is increased (Fig. 13.4). The RV mean acceleration time can be calculated as the ratio between peak pulmonary artery flow velocity and acceleration time. This ratio correlates well with RV systolic function (contractility plus afterload) and is decreased in ACP [18]. Multiple quantitative measurements can be obtained. Table 13.3 summarizes normal and pathological measurements derived from analysis of the RVOT spectral Doppler signal. Unfortunately, these measurements suffer from limitations that frequently lead to high interobserver and intraobserver variability. These include the following:

- Poor TTE image quality.
- Misalignment between ultrasound beam and RVOT jet. Even with color Doppler guidance, the spectral Doppler signal may not reflect the spatial distribution of the pulmonary artery jet, which is higher along the inner edge of its natural curvature.
- Misinterpretation of the spectral Doppler signal: only the outer edge of the dark spectral envelope should be used.
- Misinterpretation of the very short time intervals being measured.

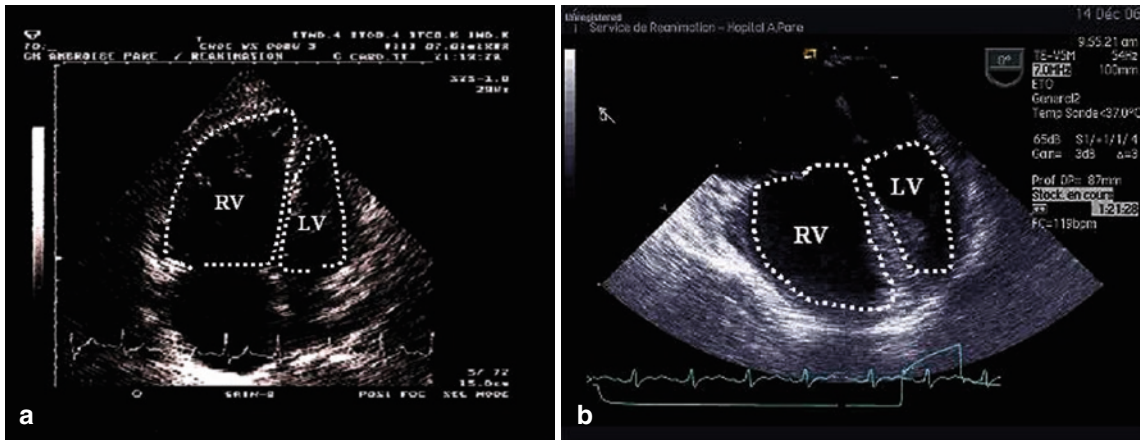

Fig. 13.5 Severe right ventricular (RV) dilation, with right ventricular end-diastolic area to left ventricular end-diastolic area (RVEDA/LVEDA) >1 in a patient with massive pulmonary embolism by transthoracic echocardiography (**a**), and in a patient with severe acute respiratory distress syndrome (ARDS) by transesophageal echocardiography (**b**). Abbreviation: *LV* left ventricle

13.2.2 RV Diastolic Overload

RV diastolic overload is synonymous with RV dilation. There are multiple definitions of right-heart dilation. Ideally, RV volumes should be measured. However, two-dimensional echocardiographic methods are unable to provide an accurate estimate of RV volumes owing to failure of geometric models to reflect the complicated RV anatomy. Three-dimensional echocardiography is more accurate in this regard, but it is not yet readily available and is time consuming. To circumvent this problem, Jardin et al. initially proposed assessing right-heart diastolic overload semiquantitatively [11]. They measured both ventricular areas at end diastole by tracing the endocardium on the apical four-chamber view. When the endocardium was not well visualized, the area was traced to the epicardium (usually not a problem with TEE). They found that the right ventricular end-diastolic area to left ventricular end-diastolic area (RVEDA:LVEDA) ratio correlated well with RV dilation. The normal RVEDA:LVEDA ratio was found to be between 0.36 and 0.6 (0.48 ± 0.12). They defined moderate dilation as a ratio of 0.7–0.9, and severe dilation as a ratio ≥1 (Fig. 13.5). Recently, another group confirmed the prognostic value of end-diastolic (measured at the beginning of the QRS complex) RVEDA:LVEDA in patients with acute pulmonary embolism [19]. In their registry of 1,416 hospitalized patients with acute pulmonary embolism, 31 subjects (3.3%) died. Among patients with systolic blood pressure ≥90 mmHg, the mortality rate was 3.3% for those with an RV/LV ratio ≥0.6, and 1.1% for those with a ratio <0.6. Using mortality ROC curves, an RV/LV ratio ≥0.9 had the best sensitivity (72%) and specificity (58%) to discriminate those patients at higher risk of dying: 6.6% if the ratio ≥0.9, 1.9% if <0.9. Interestingly, Fremont et al. measured chamber size in the parasternal and subcostal views. This is important as the subcostal plane is frequently the most acceptable TTE view in critically ill patients on ventilatory support.

The assessment of RV compared with LV size has many advantages, including its simplicity, avoidance of individual variations in cardiac size, and decreased interobserver and intraobserver variability introduced by quantitative methods [1]. Vieillard-Baron et al. recently evaluated the accuracy of qualitative versus quantitative assessment of several echocardiographic parameters by TEE, as performed by intensivist echocardiographers [20]. They subjectively classified RVED size compared with LVED size in the apical four-chamber view as normal, moderately enlarged, and markedly enlarged. Subjective qualitative observation of chamber size correlated closely with quantitative assessment of the RV/LV ratio. In addition, the interobserver variability was very good [K = 0.74; 95% confidence interval (CI) 0.54–0.94]. Their results indicate that a trained echocardiographer can readily identify RV diastolic overload by visual assessment.

A sudden increase in RV diastolic afterload will result not only in its dilation, but also in a change of its normal configuration. When enlarged, the RV loses its triangular shape and becomes more rounded in apical views. An oval, instead of half-moon-like shape, is observed in both short- and long-axis views.

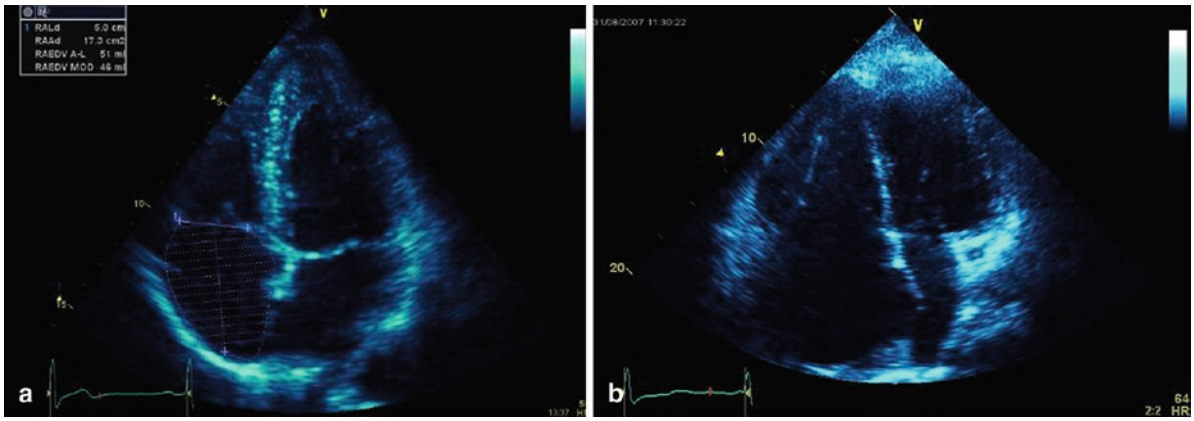

Fig. 13.6 Measurement of right atrial area in the apical four-chamber view: (**a**) a normal size right atrium; (**b**) a dilated right atrium (and right ventricle)

Table 13.4 Recommended ASE/EAE guidelines on RV chamber quantification

	Normal (cm)	Severe dilation (cm)
Basal diameter	≤2.8	≥3.9
Midventricular diameter	≤3.3	≥4.2
Base-to-apex length	≤7.9	≥9.2
RVOT diameter above aortic valve	≤2.9	≥3.6
RVOT diameter above pulmonary valve	≤2.3	≥3.2

RVOT right ventricular outflow track

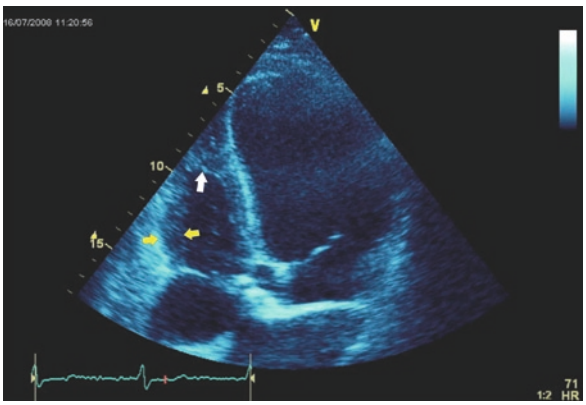

Fig. 13.7 Right ventricular hypertrophy. Note the thickened right ventricular free wall (*yellow arrows*) and the prominent moderator band (*white arrow*)

Both right atrial (RA) areas can also be enlarged in the case of RV dilatation. The RA is best measured in the apical four-chamber view (Fig. 13.6). The normal range of RA area for adults is large, ranging from 8.3 to 19.5 cm^2.

Right-heart dilation results in decreased LV filling. Since the pericardium encloses the heart within a relatively stiff envelope, the right heart can dilate only at the expense of the space normally occupied by the larger LV. This leads to an impairment of LV filling. PW Doppler interrogation of mitral valve inflow displays a spectral signal that reverses when impaired filling is present (E/A < 1).

The American Society of Echocardiography in conjunction with the European Association of Echocardiography recently published guidelines on chamber quantification recommendations, including normal and abnormal right-chamber sizes [21]. They are summarized in Table 13.4. These measurements have limited clinical utility in critical care practice. On the other hand, Jardin's proposed definition of RV dilatation is more appropriate in the intensive care unit (ICU) population since it does not rely on detailed, frequently error-prone measurements in specific chamber landmarks.

13.2.3 Acute Versus Subacute Chronic Cor Pulmonale

There are no definite criteria to distinguish ACP from chronic right-heart failure. Clinical judgment in conjunction with thorough echocardiographic examination should help establish the diagnosis.

When right-heart impedance is chronically elevated, the RV wall becomes hypertrophic relatively rapidly (Fig. 13.7). The RV free-wall thickness is best evaluated in the subcostal view at end diastole.

The normal thickness is 3.3 ± 0.6 mm. After only 48 h of a sudden increase in afterload, the RV free-wall thickness may increase to double this width [11]. In chronic cor pulmonale, the RV free wall may thicken to as much as 10–11 mm. In addition to wall thickening, there may be increased intracavitary muscle trabeculations and, frequently, LV hypertrophy [22]. The level of pulmonary artery pressure calculated by Doppler echocardiography can also provide a clue as to whether the process is chronic. While the pulmonary artery systolic pressure (PASP) in acute conditions is generally <60 mmHg, it can be higher in chronic cor pulmonale. Finally, the confirmation of ACP can be made retrospectively. ACP reverses once the baseline disorder is corrected. The lack of complete reversibility of ACP indicates the presence of chronic cor pulmonale.

13.2.4 Cor Pulmonale and Pulmonary Hypertension

Cor pulmonale is usually associated with elevation of pulmonary arterial pressures. High pulmonary pressures in a patient with findings of ACP correlate with increased impedance. However, if the RV pump function is severely impaired, it may be unable to generate significant cardiac output, resulting in pseudonormal pulmonary artery pressures. Conversely, the clinician will frequently encounter clinical scenarios where elevated pulmonary pressures are present in the absence of ACP. This finding in the critically ill should prompt the physician to rule out "intracardiac" and "intrapulmonary" causes of pulmonary hypertension. Intracardiac etiologies include left-to-right shunts, pulmonary embolism, unsuspected pulmonary valve stenosis, subpulmonary stenosis, and constrictive pericarditis. Pulmonary etiologies of pulmonary hypertension include chronic thomboembolic pulmonary hypertension and lung diseases, such as chronic obstructive pulmonary disease and a variety of interstitial lung processes.

13.3 Echocardiographic Estimates of Pulmonary Artery Pressure

Pulmonary artery systolic, diastolic, and mean pressures can be estimated from the tricuspid and pulmonary regurgitant jets (Fig. 13.8), using the modified Bernouilli equation. The majority of people (>70%) have some degree of tricuspid regurgitation (TR), and hence the utilization of TR to estimate PASP is the most common practice in echocardiography. The TR jet is the easiest to evaluate and, probably, the most reliable. The jet should be interrogated from multiple acoustic windows (apical, parasternal), with careful transducer angulation to obtain a parallel intercept angle between the ultrasound beam and jet.

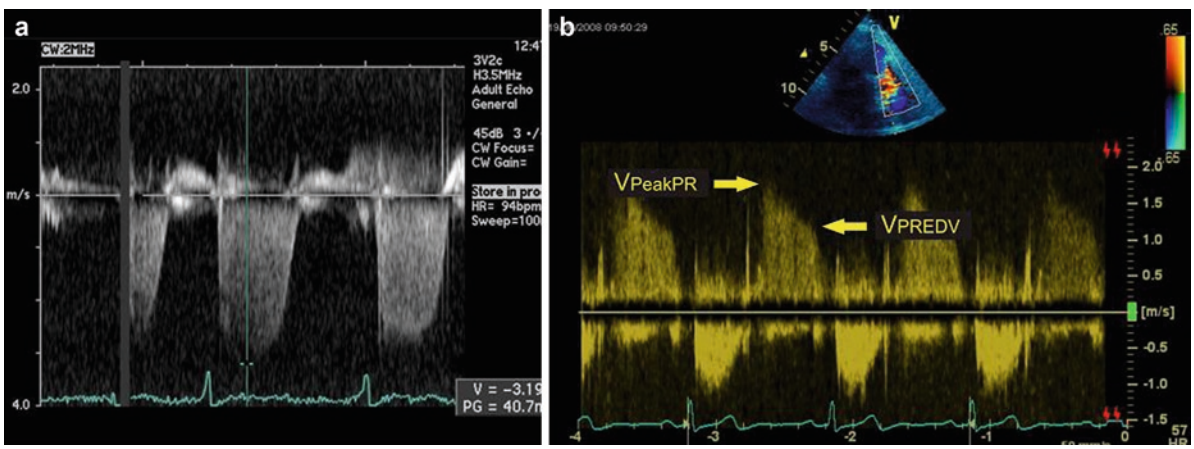

Fig. 13.8 **Panel a**: Spectral Doppler signal of tricuspid regurgitant jet. According to the modified Bernouilli equation and depending on right atrial pressure measurements (range 5–20 mm Hg), one could expect this patient's pulmonary artery systolic pressure to range between 45 and 65 mmHg. **Panel b**: pulmonic regurgitation is frequently present in the population and can be utilized to estimate pulmonary artery end-diastolic pressure as well as mean pulmonary artery pressure

Table 13.5 RAP as estimated by IVC size and dynamic

RAP (mmHg)	IVC size (mm)	IVC contraction (inspiration; %)	Hepatic vein
0–5	<20	>50	Normal
10	<20	<50	Normal
15	>20	<50	Normal
20	>20	<50	Dilated

PASP:

$4 \times (\text{tricuspid regurgitant jet}_{\text{peak velocity}})^2 +$ right atrial pressure (RAP)

Pulmonary artery diastolic pressure:

$4 \times (\text{pulmonary regurgitant}_{\text{end-diastolic velocity}})^2 +$ RAP

Mean pulmonary artery pressure:

$4 \times (\text{pulmonary regurgitant}_{\text{peak velocity}})^2$, or

80 – RVOT acceleration time/2 [23–25]

Numerous factors can affect the accuracy of the estimates. Technically, it may be difficult to obtain an adequate spectral Doppler envelope and/or adequate intercept between the ultrasound beam and the jet. Using estimates of RAP instead of actual measurements can lead to over- or underestimations (Table 13.5). Systemic hypertension, body mass index, and age also have to be accounted for [26], but their role in the critically ill population has never been adequately assessed.

Pulmonary vascular resistance (PVR) can also be determined by Doppler echocardiography using the ratio of peak tricuspid regurgitant flow velocity (TRV) to the RVOT velocity-time integral (VTI_{RVOT}). The TRV/VTI_{RVOT} correlates well with invasive PVR measurements($r = 0.929$; 95% CI = 0.87–0.96), and the regression equation $PVR = TRV/VTI_{RVOT} \times 10 + 0.16$ shows satisfactory limits of agreement. A TRV/VTI_{RVOT} ratio greater than 0.175 has a sensitivity of 77% and specificity 81% to determine PVR > 2WU.

The combination of tissue Doppler velocity of the lateral tricuspid annulus and RV dimensions can be used to identify the presence of pulmonary hypertension (the "Nepean Index") [27]. The Nepean Index is defined as the RV end-diastolic diameter (measured from the atrial four-chamber view) divided by the Tpeak, i.e., the duration between the onset of isovolumic contraction to the peak systolic wave velocity (Sm; Fig. 13.9).

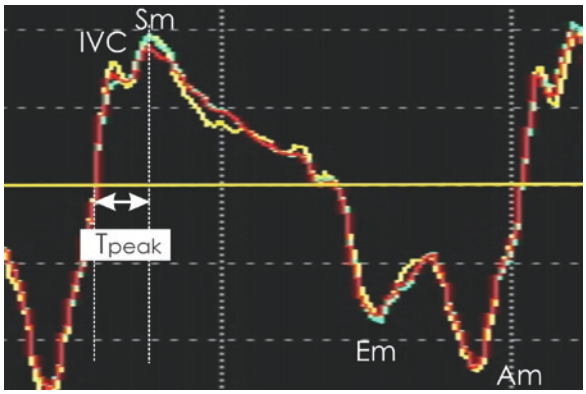

Fig. 13.9 Measurement of Tpeak value for the Nepean Index. The tracing shown is a typical example of right ventricular tissue Doppler imaging (see also Fig 13.11). The Tpeak is the "time-to-peak" duration as measured from the start of isovolumic contraction (IVC) to the peak of the systolic wave (Sm)

13.4 Assessment of RV Systolic Dysfunction Due to Depressed Intrinsic Contractility

Depressed intrinsic RV dysfunction can occur following acute infarction involving the RV as part of a global cardiomyopathy that is either primary (e.g., viral) or reversible such as seen in severe sepsis. Standard echocardiography does not allow the direct measurement of RV contractility. However, it can accurately assess right-heart pump function and the status of its interaction with its circuit. The assessment of RV contractile function can be performed qualitatively and quantitatively. Most frequently, the evaluation of RV systolic function by the intensivist at the bedside is based on qualitative analysis of the RV free wall and IVS endomyocardial thickening and contraction. This is similar to qualitative assessment of LV function. The contractile function of the RV is graded by the examiner as normal, mild, moderate, or severely reduced. This approach is obviously dependent on the skills and experience of the interpreter. There are several quantitative techniques to assess RV contractile function. These include ejection fraction, fractional area of contraction, systolic tissue annular motion by two-dimensional, M-mode, or tissue Doppler, myocardial performance index, and measurement of dP/dt. These interesting measurements are not practical for use by the bedside critical care echocardiographer.

13.4.1 Ejection Fraction

Measurement of RV ejection fraction (EF) is inaccurate because of its configuration and inability to image the entire RV from only one echocardiographic plane, resulting in failure to utilize the biplane methods routinely used in the calculation of LV EF. In addition, the RV is poorly accessible to sonograms since it lies behind the sternum, and its endocardial borders are difficult to track owing to its trabeculation. However, under increased preload or afterload, the RV cavity tends to become more spherical, particularly at end diastole. It may be possible to obtain more accurate RV volumes to estimate EF under these circumstances using the modified Simpson's method to interrogate the RV in the apical four-chamber plane, or alternatively in the subcostal plane. A normal RV EF is 60%.

13.4.2 RV Fractional Area Contraction

The RV area is obtained in the apical four-chamber view. Fractional area contraction (FAC) = (RV end-diastolic area minus RV end-systolic area) divided by RV end-diastolic area × 100. The FAC is supposedly less prone to erroneous estimates than Simpson's method because none of the measurements is squared, however this claim may be questioned. Another variation consists of estimating the RV transverse shortening length: RV end-diastolic transverse axis length minus the RV end-systolic transverse-axis length divided by RV end-diastolic transverse axis length × 100. It is the monodimensional equivalent of EF. In one study [28], the RV FAC correlated with angiographic RV EF (r = 0.79). However, correlation with thermodilution was poorer (r = 0.48) [29]. In addition, there is a large range of normal values: 30–74% [29, 30], with 60% being considered normal by most experts. As previously noted, the RV tends to shorten more in the longitudinal axis than in the transverse dimension. This would explain the range of normal values and questionable correlation with EF. Mean value: 46 ± 7.3%; range: 30–59.5%.

13.4.3 Tricuspid Annular Motion

This method is based on the normal longitudinal motion of the RV sinus region. It can be measured with two-dimensional or M-mode echocardiography (the latter offers better resolution). In the apical four-chamber view, the M-mode cursor is placed through the lateral aspect of the tricuspid annulus such that the annulus moves along the M-mode cursor (Fig. 13.10). The systolic displacement is measured from end diastole to end systole. Tricuspid annular motion (TAM), or tricuspid annular plane systolic excursion (TAPSE), correlates moderately with thermodilution (r = 0.51) [31]. Kaul et al. were able to discriminate groups of patients with normal versus abnormal RV EF [32]. The lower the TAM, the worse the RV pump function was found to be. TAM also helps identify patients with LV dysfunction with a higher mortality due to abnormal RV function [33]. It predicts decreased exercise capacity in patients with RV dysfunction after coronary artery

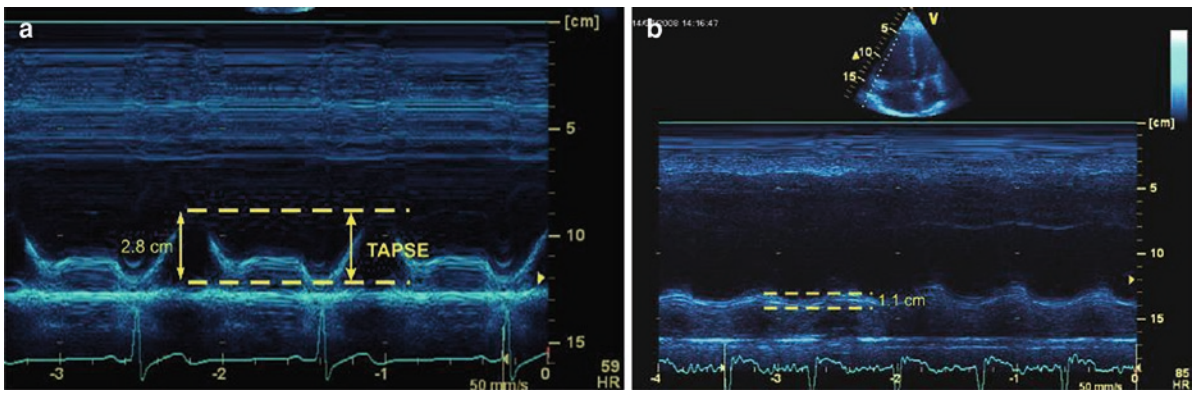

Fig. 13.10 Tricuspid annulus plane systolic excursion (TAPSE). The M-mode is obtained by placing the cursor along the lateral tricuspid annulus. TAPSE is obtained by measuring the peak-to-peak (peak systole to end diastole) distance of the annulus excursion. (**a**) Normal TAPSE; (**b**) reduced TAPSE in a patient with markedly reduced right ventricular function

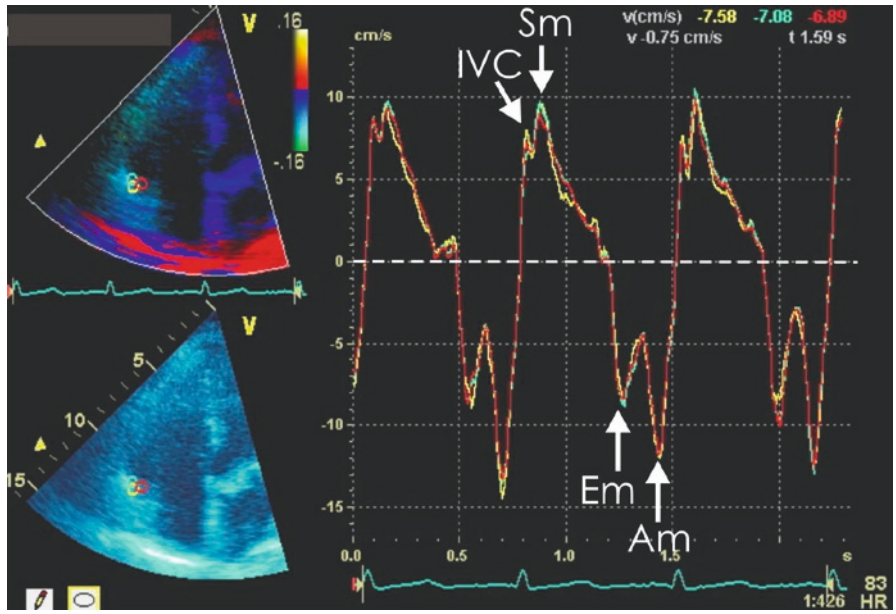

Fig. 13.11 Right ventricular (RV) tissue Doppler imaging (TDI) as measured at the tricuspid annulus. A normal RV TDI trace consists of three major waves: systolic (Sm), early diastole (Em), and late diastole (Am). The isovolumic contraction (IVC), which precedes the Sm, can also be observed

bypass grafting [34]. Normal TAM is considered to be ≥1.4 cm. In a recent study performed in patients with mostly primary pulmonary arterial hypertension [35], TAM >1.8 cm was found to be an excellent predictor of survival. One- and 2-year survival in subjects with TAM >1.8 cm were 94% (95% CI: 65–90%) and 88% (95% CI: 61–97%), respectively, as compared with those with TAM <1.8 cm: 60% (95% CI: 40–75%) for 1-year and 50% (95% CI: 31–66%) for 2-year survival. Importantly, there was a clear inverse correlation with survival: the lower the TAM, the higher the mortality.

13.4.4 Tissue Doppler

The position of the apex during the cardiac cycle is relatively stable. The tricuspid annulus moves toward the apex in systole and away from the apex in diastole as a consequence of contraction/relaxation of longitudinal myocardial fibers. Tissue Doppler imaging (TDI) measures myocardial and annular velocities. A typical TDI profile consists of three distinct waves: (1) an apically directed (upward/positive) systolic wave (Sm); (2) an early diastolic wave directing away from the apex (downward/negative) (Em); and (3) a late diastolic wave (Am). The isovolumic contraction period can be found between the Am and Sm, whereas the isovolumic relaxation period can be found between the Sm and Em (Fig. 13.11).

Tricuspid annular Sm is independent of age [36]. Sm <11.5 cm/s predicts RV EF <45% with a sensitivity of 90% and a specificity of 85% [37]. It is easy to measure and has a low intra- and interobserver variability. It does not correlate with RA pressure, and it has a negative correlation with mean pulmonary artery pressure. In one study of 90 patients with chronic pulmonary hypertension of multiple causes, Sm discriminated the study group from normals (11.7 ± 4 vs 13.5 ± 6 cm/s respectively) [38]. Damage to the RV muscle may affect annular velocities and EF in a different manner. Therefore, analysis of the RV longitudinal function may provide useful additional information that is difficult to obtain by looking at global estimates of its function [39].

13.4.5 dP/dt

This is the rate of RV pressure change during the isovolumic contraction period (dP/dt). The rate of RV pressure rise is reflected by the rate of the TR blood jet moving from the RV into the RA if there is no significant change in RA pressure during the isovolumic contraction period. Thus, TR velocity changes during this period reflect dP/dt. From a continuous-wave spectral Doppler signal of TR, one determines the pressure of the TR jet by placing calipers on the TR jet at 1 and 2 m/s (Fig. 13.12). This is different from LV dP/dt

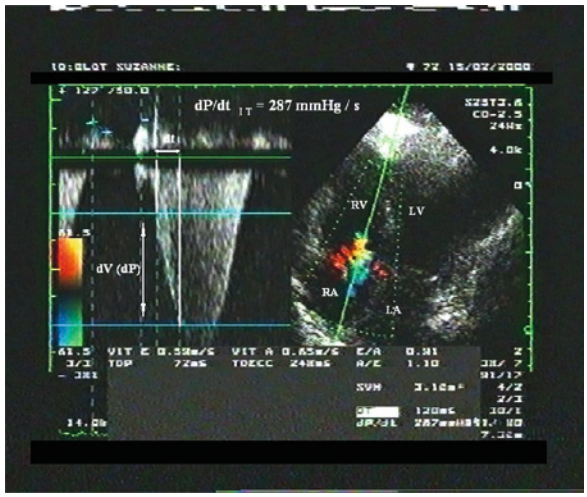

Fig. 13.12 Calculation of dP/dt from the spectral Doppler signal of the tricuspid regurgitant jet. The value of 287 mmHg/s in this patient was very suggestive of right ventricular failure. Abbreviations: *RV* right ventricle, *LV* left ventricle, *RA* right atrium, *LA* left atrium

calculation, where calipers are placed at 1 and 3 m/s. The change in pressure is then calculated by the simplified Bernoulli equation (pressure$^2 \times 4$). The pressure at 1 m/s is $1^2 \times 4 = 4$. The pressure at 2 m/s is $2^2 \times 4 = 16$. The pressure at 2 m/s minus the pressure at 1 m/s is 16 − 4 = 12 mmHg. Thus, dP/dt = 12 mmHg/(TR time$_1$ m/s−TR time$_2$ m/s) [39]. The normal dP/dt in adults is 255 +/− 17.5 mHg/s. dP/dt is undoubtedly the least sensitive index to loading conditions, particularly preload. dP/dt becomes progressively more prolonged as RV function deteriorates. Brecker and collaborators found that patients with severe pulmonary hypertension had a prolonged dP/dt at 673 mmHg/s [40].

13.4.6 Myocardial Performance Index

Myocardial performance index (MPI) is a nongeometric approach for assessing RV function since it does not require volume measurements [41]. It is obtained by measuring the duration of the TR and ROVT jet intervals. RV MPI = isovolumic contraction + isovolumic relaxation times/ejection time. In practice, RV MPI = (TR jet interval – RVOT jet interval)/RVOT jet interval. As myocardial function deteriorates, ejection time is shortened and the preejection and isovolumic relaxation periods are lengthened, resulting in the prolongation of MPI. The normal RV MPI is 0.28 ± 0.05 [42, 43]. The MPI has the advantage of avoiding the limitations of indices that depend on RV geometry and can be obtained in patients with poor quality images. It is a good predictor of survival in patients with pulmonary arterial hypertension [44]; it enables diagnosis of RV dysfunction in cardiac amyloidosis [42] and lengthens in proportion to the grade of RV dysfunction in Ebstein's anomaly [45].

13.5 Specific Clinical Scenarios Leading to ACP: The Diagnostic Role of Echocardiography

We now briefly review specific clinical scenarios frequently encountered by the intensivist and the specific role of echocardiography. Some of these topics are extensively described in other chapters of this book.

13.5.1 Massive Pulmonary Embolism

Pulmonary embolism (PE) may be associated with RV dysfunction. Several authors have defined ACP in the context of acute PE using different criteria [46–48]. Because of its simplicity, the RV/LV ratio definition is the most practical for bedside application. Using this ratio, Vieillard-Baron et al. reported a 61% incidence of ACP in 161 subjects with anatomically massive PE [49]. Whether ACP is an independent prognostic factor of mortality and how it may change treatment (e.g., thrombolysis) remains to be investigated. Occasionally, a thrombus-in-transit will be identified in the right heart. These thrombi are typically mobile and serpiginous; they are of grave clinical concern. A thrombus may be visible in the main and proximal pulmonary arteries in a parasternal short-axis view with TTE. In addition, the main and proximal pulmonary arteries are readily visualized with TEE, and this is a means of rapidly diagnosing PE in critically ill patients who are unable to undergo contrast study [50, 51].

Other indirect echocardiographic signs of acute PE include:

1. McConnell sign: diffuse hypokinesis of the RV free wall, sparing the apex [52]
2. 60/60 sign: RVOT acceleration time <60 ms in association with pulmonary artery systolic pressure <60 mmHg (as estimated by TR regurgitant jet) [53]

Both these signs were described retrospectively. When tested in a prospective study of 100 consecutive patients with proven PE, the sensitivity of McConnell and 60/60 signs ranged only between 19% and 36% [53]. This is likely due to the subjectivity inherent in determining

segmental wall-motion abnormality and the high margin of error when measuring the acceleration time.

13.5.2 Acute Respiratory Distress Syndrome

ACP is frequent in acute respiratory distress syndrome (ARDS). Vieillard-Baron et al. reported an incidence of 25% in patients with ARDS submitted to protective ventilation, defined as a plateau pressure below 30 cm H_2O with a mean positive end-expiratory pressure (PEEP) of 6–7 cm H_2O [54]. Echocardiography can identify patterns of ventilatory support that may result in ACP. Only serial echocardiography can alert the physician to this possibility and allow adjustment of therapies in a sequential, reasonable, and effective manner. If bedside echocardiography demonstrates persistent ACP despite plateau pressure <26 and tidal volumes of 6 mL/kg, intrinsic PEEP should be completely avoided, aggressive intravenous fluids minimized, and extrinsic PEEP and/or tidal volume lowered even further. Intra-abdominal pressures should be monitored and maintained within normal limits. If severe hypoxemia persists, and PEEP or tidal volumes cannot be lowered any further, prone positioning should be considered since it can unload the RV [55]. Conversely, tidal volumes could be increased above 6 mL/kg ideal body weight (IBW; but maintained below 10 mL/kg IBW) if plateau pressure remains between 26 and 28 cm H_2O, there is no evidence of right-heart dysfunction, and respiratory acidosis is present.

13.5.3 Acute RV Failure of Sepsis

Both LV and RV function can become depressed in sepsis [3, 5, 56–58]. In one series, 32% of patients had evidence of RV dysfunction [58]. The cardiomyopathy is usually compensated, and cardiac output is maintained within normal limits with adequate fluid resuscitation. It is maximal on the second day after onset of sepsis and recovers completely in 7–10 days [59]. It may explain the inability of blood volume expansion to increase LV cardiac output [5] and improve the clinical status of some patients. However, RV failure with ACP can become manifest when ventilatory support is applied. By increasing pulmonary vascular resistance, mechanical ventilation can result in ACP in an RV that is dysfunctional from sepsis. If ACP develops, the clinician should adjust ventilator settings to minimize alveolar distension, hypoxemia, and acidosis, restrict intravenous fluid resuscitation, and add vasopressor/inotropic therapy to maintain adequate coronary artery perfusion pressure [4, 11].

13.5.4 RV Infarction

RV infarction occurs predominantly because of occlusion of the right coronary artery. In addition to perfusing the RV free wall, this artery also supplies blood to the inferior aspect of the LV and the inferior IVS through the posterior descending artery. As a result, RV infarction is frequently accompanied by LV inferior wall infarction with corresponding segmental-wall abnormality.

Echocardiography allows assessment of RV segmental-wall abnormality. When myocardial ischemia is present, decreased endomyocardial thickening and wall-motion abnormalities (hypokinesis, akinesis, or dyskinesis) occur. Using TTE, the parasternal long-axis view allows examination of the RV infundibulum; while the parasternal, short-axis view at the midventricular level permits assessment of the anterior, lateral, and a portion of the inferior RV walls. The anterior and inferior free RV walls are also seen in a different plane on inspection of the RV inflow tract axis, while the apical four-chamber view demonstrates the lateral wall and apex. When RV infarction is suspected, the echocardiographer has to assess the subcostal views. The long-axis plane shows the RV inferior free wall, while the short-axis plane brings up part of the inferior wall and the RVOT. Importantly, 20% of RV infarctions may be missed if this plane is not interrogated and the right coronary artery (RCA) occlusion is distal [60].

With proximal RCA occlusion, severe acute RV failure may occur. Unlike in ACP, PA pressures may not be elevated since the cause of the RV failure is acute failure of pump function. A clue to the diagnosis of ischemia is the presence of abnormal endomyocardial thickening and segmental wall-motion abnormality of the inferior LV wall and inferior septum. Dilation of the tricuspid annulus secondary to RV dilation results in acute TR, elevation of RAP, RA enlargement, and inferior vena cava (IVC) dilation.

13.5.5 Preload, Volume Responsiveness and the Right Heart

Dynamic parameters of volume responsiveness have to be evaluated in conjunction with right-heart function. Preload assessment is best assessed with dynamic parameters [61]. Dynamic parameters of volume responsiveness always have to be evaluated within the context of right-heart function. While preload responsiveness evaluation is best assessed with dynamic parameters, all described indices (e.g., change in RA pressure with respiration, ddown, pulse pressure variation, change in peak aortic velocity or stroke volume with respirator cycling or leg elevation) assume a normal RV function. RV failure itself can result in pulse pressure variation during tidal positive-pressure ventilation, independently of the patient's volume status (Fig. 13.13). If RV function is not evaluated, the clinician could erroneously conclude that more volume expansion is necessary if relying on dynamic parameters alone. The presence of ACP with septal dyskinesia contraindicates volume resuscitation, even if dynamic parameters indicate otherwise. Preload assessment utilizing right heart echocardiographic indices is presented in the Chapter 6.

13.6 Conclusion

RV failure is frequent in critically ill patients. Echocardiography is presently the best bedside tool available to identify RV dysfunction and assist adjustment of therapeutic interventions. Competence in advanced critical care echocardiography allows the clinician to perform a wide variety of measurements. However, the most clinically valuable information is routinely obtained with qualitative or semiquantitative evaluation.

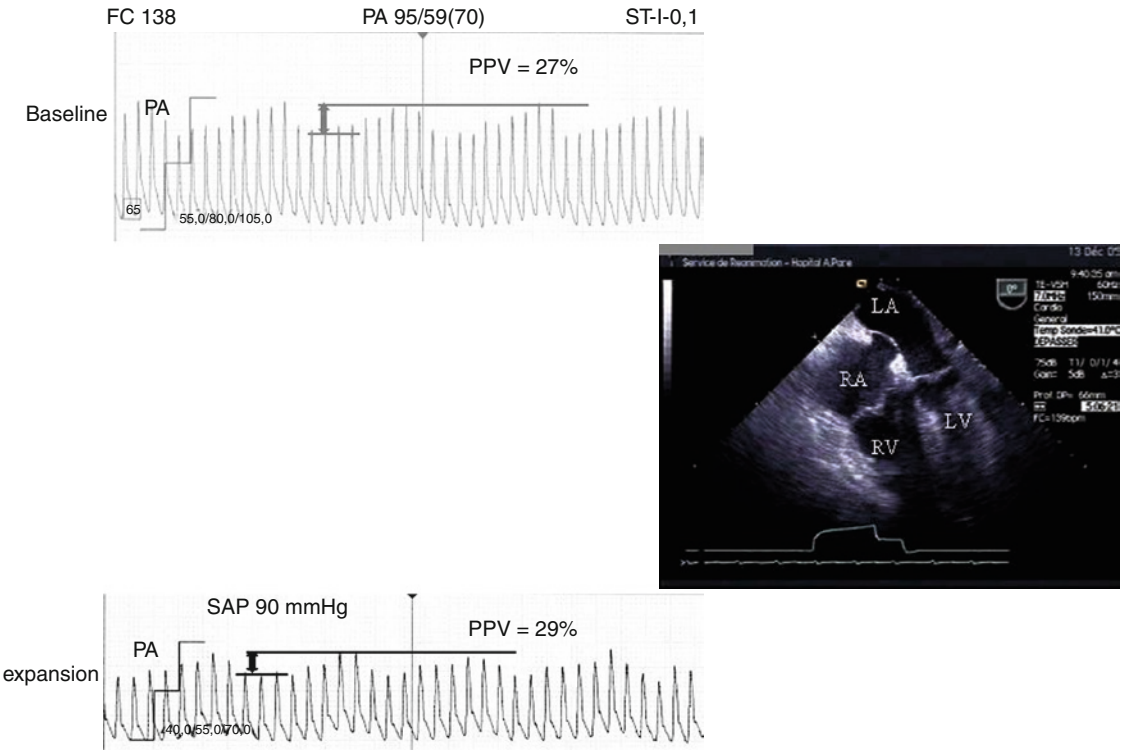

Fig. 13.13 Pulse pressure variations in a patient mechanically ventilated for a severe acute respiratory distress syndrome. At baseline, variations were 27%, suggesting the need for fluids. After fluid expansion, neither systolic arterial pressure nor pulse pressure variations were corrected. The pulse pressure variations were explained in this patient by the presence of a severe acute cor pulmonale, as demonstrated in the long-axis view of the left ventricle. Abbreviations: *SAP* systolic arterial pressure, *PPV* pulse pressure variations, *RV* right ventricle, *LV* left ventricle, *RA* right atrium, *LA* left atrium

Acknowledgement: Assistance in preparation of this chapter from Dr. Stephen Huang noted.

Bibliography

1. Jardin F, Dubourg O, Bourdarias JP (1997) Echocardiographic pattern of acute cor pulmonale. Chest 111:209–217
2. Ozier Y, Gueret P, Jardin F, Farcot JC, Bourdarias JP, Margairaz A (1984) Two-dimensional echocardiographic demonstration of acute myocardial depression in septic shock. Crit Care med 12:596–599
3. Etchecopar-Chevreuil C, François B, Clavel M, Pichon N, Gastinne H, Vignon P (2008) Cardiac morphological and functional changes during early septic shock: a transesophageal echocardiographic study. Intensive Care Med 34: 250–256
4. Vieillard-Baron A, Prin S, Chergui K, Dubourg O, Jardin F (2003) Hemodynamic instability in sepsis: bedside assessment by Doppler echocardiography. Am J Respir Crit Care Med 168:1270–1276
5. Schneider A, Teule G, Groeneveld AB, Nauta J, Heidendal GA, Thijs LG (1988) Biventricular performance during volume loading in patients with early septic shock, with emphasis on the right ventricle: a combined hemodynamic and radionuclide study. Am Heart J 116:103–112
6. Hoffman D, Sisto D, Frater RW, Nikolic SD (1994) Left-to-right ventricular interaction with a noncontracting right ventricle. J Thorac Cardiovasc Surg 107:1496–1502
7. Redington AN, Gray JJ, Hodson ME, Rigby ML, Oldershaw PJ (1988) Characterization of the normal right ventricular pressure-volume relation by biplane angiography and simultaneous micromanometer pressure measurements. Br Heart J 59:23–30
8. Elzinga G, Pienne H, De Jong J (1980) Left and right ventricular pump function and consequences of having two pumps in one heart. A study on isolated cat heart. Circ Res 46:56
9. Cross C (1962) Right ventricular pressure and coronary flow. Am J Physiol 202:12–16
10. Vlahakes GJ, Turley K, Hoffman J (1981) The pathophysiology of failure in acute right ventricular hypertension: hemodynamic and biochemical correlations. Circulation 63:87–95
11. Vieillard-Baron A, Prin S, Chergui K, Dubourg O, Jardin F (2002) Echo-Dopler demonstration of acute cor pulmonale at the bedside in the medical intensive care unit. Am J Respir Crit Care Med 166:1310–1319
12. Testa AG (1831) Delle malattie di cuore. Schieppati, Truffi e Fusi, Milano
13. McGinn S, White P (1935) Acute cor pulmonale resulting from pulmonary embolism. JAMA 104:1473–8
14. Elzinga G, Pienne H, De Jong J (1980) Left and right ventricular pump function and consequences of having two pumps in one heart: a study on isolated cat heart. Circ Res 46:564–574
15. Jardin F, Farcot JC, Boisante L et al (1981) Influence of positive end-expiratory pressure on left ventricular performance. N Engl J Med 304:387–92
16. Ryan T, Petrovic O, Dillon JC, Feigenbaum H, Conley MJ, Armstrong WF (1985) An echocardiographic index for separation of right ventricular volume and pressure overload. J Am Coll Cardiol 5:918–27
17. Nielsen JC, Kamenir SA, Ko HS, Lai WW, Parness IA (2002) Ventricular septal flattening at end-systole falsely predicts right ventricular hypertension in patients with ostium primum atrial septal defects. J Am Soc Echocardiogr 15:247–252
18. Vieillard-Baron A, Loubières Y, Schmitt JM, Page B, Dubourg O, Jardin F (1999) Cyclic changes in right ventricular output impedance during mechanical ventilation. J Appl Physiol 87:1644–1650
19. Frémont B, Pacouret G, Jacobi D, Puglisi R, Charbonnier B, de Labriolle A (2008) Prognostic value of echocardiographic right/left ventricular end-diastolic diameter ratio in patients with acute pulmonary embolism: results from a monocenter registry of 1, 1416 patients. Chest 133:358–362
20. Vieillard-Baron A, Charron C, Chergui K, Peyrouset O, Jardin F (2006) Bedside echocardiographic evaluation of hemodynamics in sepsis: is a qualitative evaluation sufficient? Intensive Care Med 32:1547–1552
21. Lang RM, Bierig M, Devereux RB, Flachskampf FA, Foster E, Pellikka PA, Picard MH, Roman MJ, Seward J, Shanewise JS, Solomon SD, Spencer KF, Sutton MS, Stewart WJ (2005) Recommendations for chamber quantification: a report from the American Society of Echocardiography's Guidelines and Standards Committee and the Chamber Quantification Writing Group, developed in conjunction with the European Association of Echocardiography, a Branch of the European Society of Cardiology. J Am Soc Echocardiogr 18: 1440–1463
22. Jardin F, Gueret P, Prost JF, Farcot JC, Ozier Y, Bourdarias JP (1984) Two-dimensional echocardiographic assessment of left ventricular function in chronic obstructive pulmonary disease. Am Rev Respir Dis 129:135–142
23. Otto CM (ed) (2004) Textbook of clinical echocardiography, 3rd edn. Elsevier Saunders, Philadelphia, PA, pp 259–269
24. Oh JK, Seward JB, Tajik AJ (eds) (1999) The Echo manual, 2nd edn. Lippincott Williams & Wilkins, Philadelphia, PA, pp 181–190
25. Feigenbaum H, Armstrong WF, Ryan T (eds) (2005) Feigenbaum's echocardiography, 6th edn. Lippincott Williams & Wilkins, Philadelphia, PA, pp 255–260
26. Weyman AE, Davidoff R, Gardin J et al (2002) Echocardiographic evaluation of pulmonary artery pressure with clinical correlates in predominantly obese adults. J Am Soc Echocardiogr 15:454–462
27. McLean AS, Ting I, Huang SJ et al (2007) The use of the right ventricular diameter and tricuspid annular tissue Doppler velocity parameter to predict the presence of pulmonary hypertension. Eur J Echocardiogr 8(2):128–136
28. Trowitzsch E, Colan SD, Sanders SP (1985) Two-dimensional echocardiographic estimation of right ventricular area change and ejection fraction in infants with systemic right ventricle (transposition of the great arteries or hypoplastic left heart syndrome). Am J Cardiol 55:1153–1157
29. Ghio S, Raineri C, Scelsi L, Recusani F, D'armini AM, Piovella F, Klersy C, Campana C, Vigano M, Tavazzi L

(2002) Usefulness and limits of transthoracic echocardiography in the evaluation of patients with primary and chronic thromboembolic pulmonary hypertension. J Am Soc Echocardiogr 15:1374–1380
30. Jardin F (1995) L'evaluation hemodynamique non invasive au lit du patient par l'echocardiographie-Doppler. Masson, Paris, p 44
31. Weyman AE (ed) (1982) Cross sectional echocardiography. Lea & Febiger, Philadelphia, PA, pp 501–502
32. Kaul S, Tei C, Hopkins JM, Shah PM (1984) Assessment of right ventricular function using two-dimensional echocardiography. Am Heart J 107:526–531
33. Ghio S, Recusani F, Klersy C, Sebastiani R, Laudisa ML, Campana C, Gavazzi A, Tavazzi L (2000) Prognostic usefulness of the tricuspid annular plane systolic excursion in patients with congestive heart failure secondary to idiopathic or ischemic dilated cardiomyopathy. Am J Cardiol 85:837–842
34. Hedman A, Alam M, Zuber E et al (2004) Decreased right ventricular function after coronary artery bypass grafting and its relation to exercise capacity: a tricuspid annular motion-based study. J Am Soc Echocardiogr 17:126–131
35. Forfia PR, Fisher MR, Mathai SC, Housten-Harris T, Hemnes AR, Borlaug BA, Chamera E, Corretti MC, Champion HC, Abraham TP, Girgis RE, Hassoun PM (2006) Tricuspid annular displacement predicts survival in pulmonary hypertension. Am J Respir Crit Care Med 174:1034–1041
36. Alam M, Wardell J, Andersson E, Samad BA, Nordlander R (1999) Characteristics of mitral and tricuspid annular velocities determined by pulsed wave Doppler tissue imaging in healthy subjects. J Am Soc Echocardiogr 12: 618–628
37. Meluzin J, Spinarova L, Bakala J, Toman J, Krejci J, Hude P, Kara T, Soucek M (2001) Pulsed Doppler tissue imaging of the velocity of tricuspid annular systolic motion; a new, rapid, and non-invasive method of evaluating right ventricular systolic function. Eur Heart J 22:340–348
38. Moustapha A, Lim M, Saikia S, Kaushik V, Kang SH, Barasch E (2001) Interrogation of the tricuspid annulus by Doppler tissue imaging in patients with chronic pulmonary hypertension: implications for the assessment of right-ventricular systolic and diastolic function. Cardiology 95: 101–104
39. Weyman AE, Weyman AE (eds) (1982) Cross sectional echocardiography. Lea & Febiger, Philadelphia, PA, pp 145–146
40. Brecker SJ, Gibbs JS, Fox KM, Yacoub MH, Gibson DG (1994) Comparison of Doppler derived haemodynamic variables and simultaneous high fidelity pressure measurements in severe pulmonary hypertension. Br Heart J 72: 384–389
41. Tei C (1995) New non-invasive index for combined systolic and diastolic ventricular function. J Cardiol 26:135–136
42. Kim WH, Otsuji Y, Yuasa T, Minagoe S, Seward JB, Tei C (2004) Evaluation of right ventricular dysfunction in patients with cardiac amyloidosis using Tei index. J Am Soc Echocardiogr 17:45–49
43. Moller JE, Sondergaard E, Poulsen SH, Appleton CP, Egstrup K (2001) Serial Doppler echocardiographic assessment of left and right ventricular performance after a first myocardial infarction. J Am Soc Echocardiogr 14: 249–255
44. Yeo TC, Dujardin KS, Tei C, Mahoney DW, McGoon MD, Seward JB (1998) Value of a Doppler-derived index combining systolic and diastolic time intervals in predicting outcome in primary pulmonary hypertension. Am J Cardiol 81:1157–1161
45. Eidem BW, Tei C, O'Leary PW, Cetta F, Seward JB (1998) Nongeometric quantitative assessment of right and left ventricular function: myocardial performance index in normal children and patients with Ebstein anomaly. J Am Soc Echocardiogr 11:849–56
46. Kasper W, Meinertz T, Kerstin F, Löllgen H, Limbourg P, Hanjörg J (1980) Echocardiography in assessing acute pulmonary hypertension due to pulmonary embolism. Am J Cardiol 45:567–572
47. Ribeiro A, Lindmaker P, Juhlin-Dannfelt A, Johnsson H, Jorfeldt L (1997) Echocardiography Doppler in pulmonary embolism: right ventricular dysfunction as a predictor of mortality rate. Am Heart J 134:479–487
48. Goldhaber S, Visani L, De Rosa M (1999) Acute pulmonary embolism: clinical outcomes in the International Cooperative Embolism Registry (ICOPER). Lancet 353: 1386–1389
49. Vieillard-Baron A, Page B, Augarde R, Prin S, Qanadli S, Beauchet A, Dubourg O, Jardin F (2001) Acute cor pulmonale in massive pulmonary embolism: incidence, echocardiographic pattern, clinical implications and recovery rate. Intensive Care Med 27:1481–1486
50. Pruszczyk P, Torbicki A, Pacho R, Maciej C, Kuch-Wocial A, Pruszynski B, Gurba H (1997) Noninvasive diagnosis of suspected severe pulmonary embolism: Transesophageal echocardiography vs spiral CT. Chest 112:722–728
51. Vieillard-Baron A, Qanadli SD, Antakly Y, Fourme T, Loubières Y, Jardin F, Dubourg O (1998) Transesophageal echocardiography for the diagnosis of pulmonary embolism with acute cor pulmonale: a comparison with radiological procedures. Intensive Care Med 24:429–433
52. McConnell MV, Solomon SD, Rayan ME, Come PC, Goldhaber SZ, Lee RT (1996) Regional right ventricular dysfunction detected by echocardiography in acute pulmonary embolism. Am J Cardiol 78:469–473
53. Kurzyna M, Torbicki A, Pruszczyk P, Burakowska B, Fijalkowska A, Kober J, Oniszh K, Kuca P, Tomkowski W, Burakowski J, Wawrzyńska L (2002) Disturbed right ventricular ejection pattern as a new Doppler echocardiographic sign of acute pulmonary embolism. Am J Cardiol 90: 507–511
54. Vieillard-Baron A, Schmitt JM, Augarde R, Fellahi JL, Prin S, Page B, Beauchet A, Jardin F (2001) Acute cor pulmonale in acute respiratory distress syndrome submitted to protective ventilation: Incidence, clinical implications, and prognosis. Crit Care Med 29:1551–1555
55. Vieillard-Baron A, Charron C, Caille V, Belliard G, Page B, Jardin F (2007) Prone positioning unloads the right ventricle in severe ARDS. Chest 132:1440–1446
56. Parker MM, McCarthy KE, Ognibene FP, Parrillo JE (1990) Right ventricular dysfunction and dilation, similar to left ventricular changes, characterize the cardiac depression of septic shock in humans. Chest 97:126–131

57. Jardin F, Brun-Ney D, Auvert B, Beauchet A, Bourdarais JP (1990) Sepsis-related cardiogenic shock. Crit Care Med 18:1055–1060
58. Vieillard-Baron A, Schmitt JM, Beauchet A, Augarde R, Prin S, Page B, Jardin F (2001) Early preload adaptation in septic shock? A transesophageal echocardiographic study. Anesthesiology 94:400–406
59. Rabuel C, Mebazaa A (2006) Septic shock: a heart story since the 1960s. Intensive Care Med 32:799–807
60. Gemayel CY, Fram DB, Fowler LAA, Kiernan FJ, Kelsey AM, Gillam LD (2001) The importance of using multiple windows for the echocardiographic identification of right ventricular infarction. JACC 37(Suppl 2):P1110–147
61. Michard F, Teboul JL (2002) Predicting fluid responsiveness in ICU patients: a critical analysis of the evidence. Chest 121:2000–2008

Pericardial Effusion and Cardiac Tamponade

14

Paul H. Mayo

Contents

P.H. Mayo
Long Island Jewish Medical Center, New Hyde Park, NY, USA and
Albert Einstein College of Medicine, Bronx, NY, USA
e-mail: mayosono@gmail.com

Proficiency in the identification and characterization of pericardial effusion is a key component of critical care echocardiography, as pericardial tamponade is a major consideration in the differential diagnosis of the patient with shock. This chapter reviews echocardiographic features of pericardial effusion and potentially associated cardiac tamponade that are relevant to the frontline intensivist, including the ultrasound guidance of pericardiocentesis.

14.1 Anatomy

The pericardium consists of two serous surfaces. The parietal pericardium is a thin, fibrous structure apposed to the pleural surfaces and attached to the diaphragm inferiorly. The visceral pericardium is attached to the surface of both ventricles, including the apex, and extends superiorly to its point of reflection at the pulmonary veins and systemic vessels. At this point of reflection, the parietal and visceral pericardia meet. The pericardial surfaces extend a short distance along the posterior surface of the great vessels to form the transverse sinus. When this is fluid filled, it may cause confusion on transesophageal examination with a periaortic abscess. The pericardial surfaces extend to cover the right atrium (RA) and the RA appendage, with reflections around the superior and inferior vena cava (IVC). As a result, the juxtacardiac portions of the caval vessels, main pulmonary artery, and ascending aorta lie within the pericardial sac, whereas the left atrium (LA) is predominantly extrapericardial. The normal pericardial space contains only 5–10 mL of fluid and is therefore, in health, a potential space.

D. De Backer et al. (eds.), *Hemodynamic Monitoring Using Echocardiography in the Critically Ill*,
DOI: 10.1007/978-3-540-87956-5_14,

14.2 Pathophysiology

As fluid accumulates in the pericardial space, the pressure in the space increases. The pericardial pressure is determined by the interplay between the volume of the effusion and the compliance of the pericardium. Being an elastic structure, the parietal pericardium will distend as the fluid accumulates as long as stretch remains low (close to physiological cardiac volume). As stretch increases, depending on the compliance of the pericardium, further fluid accumulation results in a rapid rise in pressure owing to pericardial constraint [1]. This is especially dangerous where there is rapid accumulation of pericardial fluid. An acute pericardial effusion due to ventricular perforation may be rapidly fatal following a relatively small amount of volume accumulation. This is because the fluid accumulation reaches the limit of the pericardial reserve volume, such that further fluid results in a rapid rise in intrapericardial pressure. On the other hand, a malignant pericardial effusion may develop gradually, allowing slow, adaptive stretch of the pericardium. In this case, massive fluid accumulation occurs without a major rise in intrapericardial pressure or compromise of cardiac function (Fig. 14.1).

Pericardial tamponade physiology occurs when the pressure in the pericardial space exceeds the pressure in the cardiac chambers. When this happens, cardiac filling is impaired. If of sufficient severity, it may result in a shock state. Pericardial tamponade should therefore always figure in the differential diagnosis of shock. With rising pericardial pressure, the lower-pressure atria are affected first, followed by the higher-pressure ventricles. Pericardial pressure may rise to the extent of causing equalization of chamber pressures. In tamponade, ventricular interdependence is exaggerated on account of the increased intrapericardial pressure and limitation on overall cardiac volume. During spontaneous breathing, inspiration causes a disproportionate reduction in left ventricular (LV) filling and increase in right ventricular (RV) filling; the reverse occurs during expiration. This is associated with marked changes in stroke volume (SV) during the respiratory cycle and with an inspiratory reduction and expiratory increase in LV SV [2]. It explains the finding of pulsus paradoxus on physical examination of the patient. The predictable effect of pericardial fluid on chamber size and respiratory variation in RV SV and LV SV are the basis for echocardiographic findings of pericardial tamponade.

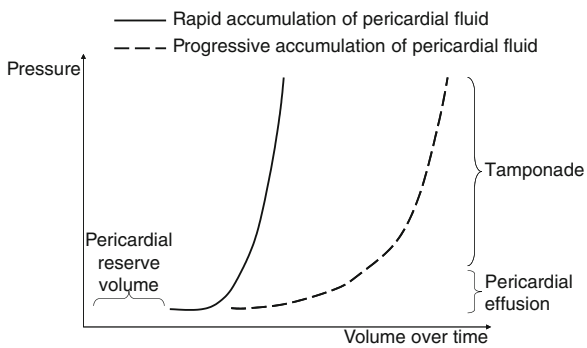

Fig. 14.1 Pericardial pressure versus pericardial volume according to the rapidity of fluid accumulation (Modified from [1]). The rapid constitution of pericardial effusion rather than its absolute volume accounts for the increase in pericardial pressure and the potential development of tamponade physiology

14.3 Identification of Pericardial Effusion

With two-dimensional echocardiography, pericardial fluid appears as a relatively echo-free space adjacent to the heart. Depending on the size of effusion, it may be limited to a dependent small area just posterior to the inferolateral wall of the LV in the parasternal long-axis view. Minimal amounts of fluid detected in this area solely during systole are physiological, whereas pericardial effusions identified during diastole are considered abnormal, regardless of their volume and location. Larger effusions result in a circumferential echo-free space surrounding the heart that may be visible with several of the standard views (Fig. 14.2). Although the accurate identification of tamponade physiology is more relevant than the precise assessment of pericardial fluid volume for the above-mentioned reasons, a semiquantitative evaluation of the pericardial effusion is possible. For the intensivist, it suffices to grade the size of the fluid collection qualitatively as mild, moderate, or large, depending on the distance of separation between the parietal and visceral pericardium: less than 0.5 cm is mild, 0.5–2.0 cm moderate, and greater than 2.0 cm large. Fluid obeys the laws of gravity and favors the dependent position in the pericardial space. At points of

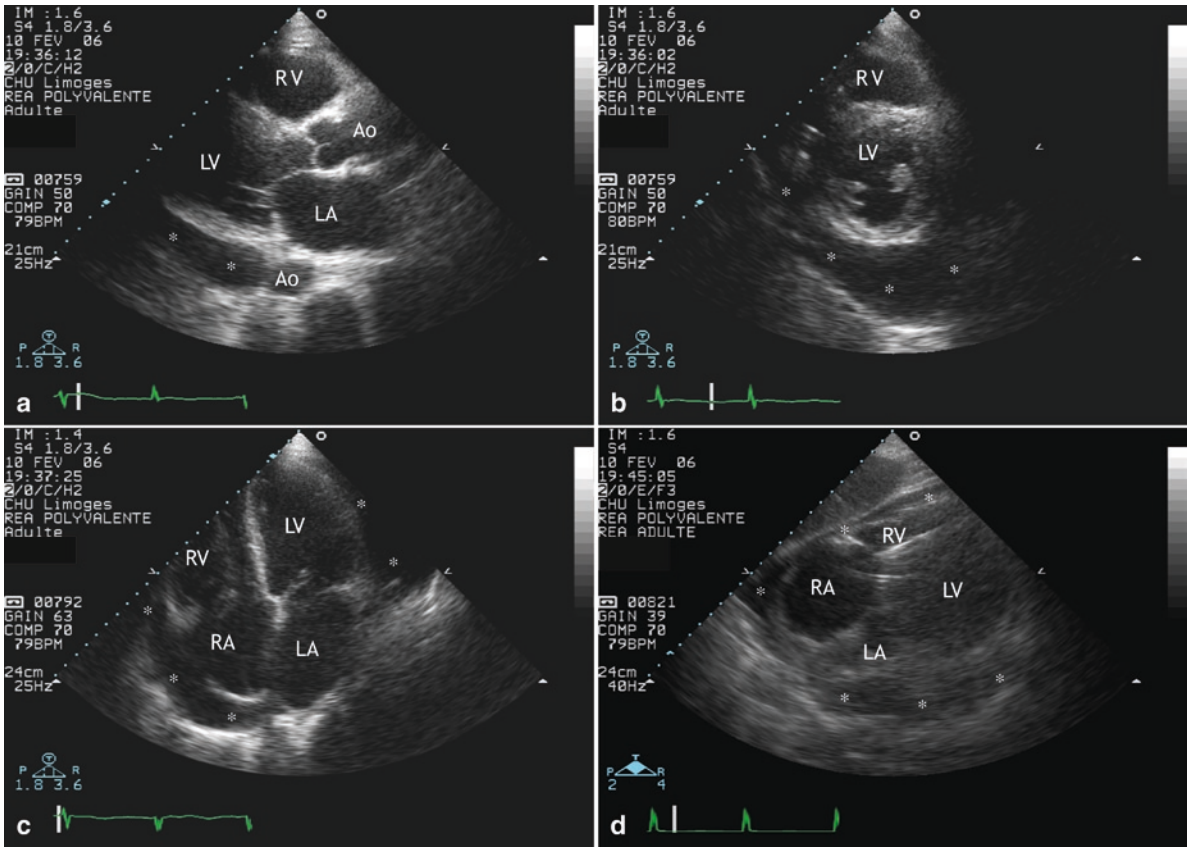

Fig. 14.2 Uncomplicated circumferential pericardial effusion diagnosed using transthoracic echocardiography. In the parasternal long- (**a**) and short-axis views (**b**), apical four-chamber view (**c**), and subcostal view (**d**), the pericardial effusion is identified around the heart (*asterisks*). Note that cardiac cavities are not collapsed in this hemodynamically stable patient without tamponade physiology. Abbreviations: *RV* right ventricle, *LV* left ventricle, *LA* left atrium, *RA* right atrium, *Ao* thoracic aorta

pericardial reflection, the apparent size of the effusion is limited by anatomical constraints. An effusion may appear small around the base of the heart, whereas around the apex the same effusion may appear large. The measurement is made at the largest point of separation since it varies according to the distribution of the fluid in the pericardial space. In the presence of a large pericardial effusion, the heart becomes extremely mobile within the pericardial sac, a finding referred to as "swinging heart." At that stage, cardiac tamponade is frequently present (Fig. 14.3). A pericardial effusion will generally distribute in a predictable circumferential manner and favor a dependent position. However, pericardial adhesions, blood clots, or tumor involvement may result in atypical distribution of pericardial fluid. Loculated pericardial effusions may be difficult to identify with transthoracic echocardiography and require transesophageal echocardiography examination. This is an important consideration when evaluating postcardiac surgery or in chest trauma patients since a loculated pericardial hematoma may cause compression of the LA (Fig. 14.4) or LV (Fig. 14.5), with a localized tamponade effect and hemodynamic compromise [3–6]. Therefore, for purposes of determining the size and location of a pericardial effusion, it is important to obtain multiple echocardiographic views of the heart. Specifically, when cardiac tamponade has to be excluded in postcardiac surgery or chest trauma patients, a negative transthoracic echocardiography requires a transesophageal echocardiographic examination to avoid a potential false-negative result.

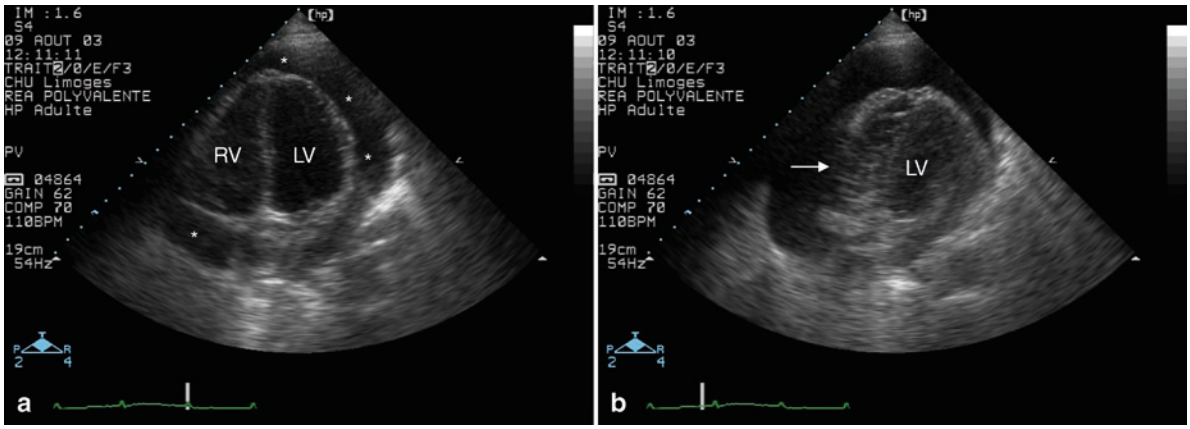

Fig. 14.3 Swinging heart pattern in a spontaneously breathing patient with a cardiac tamponade secondary to a large and progressively constituted malignant pericardial effusion. In the apical four-chamber view, the large circumferential effusion (**a**, *asterisks*) results in wide motions of the heart within the pericardial sac during the respiratory cycle (from right to left panel). Note the transient reduction of right ventricular (*RV*) volume (**b**, *arrow*). Abbreviation: *LV* left ventricle

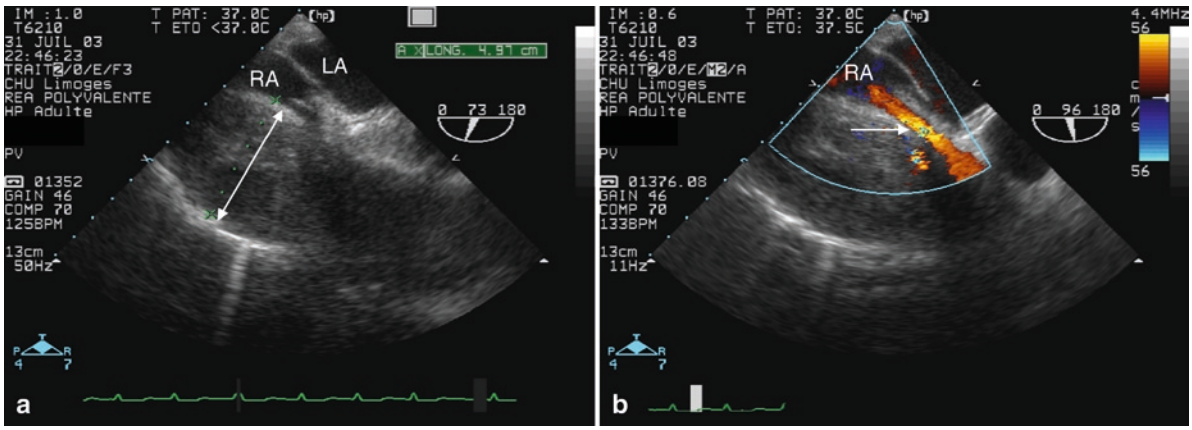

Fig. 14.4 Postoperative right atrial (RA) compression by mediastinal hematoma. In this hypotensive ventilated patient, transthoracic echocardiography was unremarkable, whereas transesophageal examination clearly depicted a 5-cm hematoma collapsing the RA (**a**, *double arrowhead*). Color Doppler mapping confirmed the reduced blood admission by the RA due to tamponade physiology (**b**, *arrow*). Abbreviation: *LA* left atrium

Pericardial fluid may have hyperechoic characteristics. Fibrous stranding is common. Blood and purulent fluid may occur with stranding and loculation. Purulent effusions are often associated with a thickened and shaggy pericardium. Pericardial thrombi appear as discrete hyperechoic masses that may be mobile. A malignant effusion may contain discrete tumor masses that float within the fluid or are attached to the myocardium.

Pericardial fat may be mistaken for pericardial fluid. This may have serious consequence if the clinician attempts pericardiocentesis. Pericardial fat is often anterior in location and therefore seen in parasternal views. It generally has a mild hyperechoic, granular appearance on echocardiography and may move synchronously with the underlying myocardium. This pseudoeffusion is also characterized by the absence of pericardial fluid in the posterior or dependent pericardium. An isolated anterior pericardial effusion is very rare, but it may occur in the context of pericardial scarring that traps the fluid in an unusual position.

Pleural fluid may be confused with pericardial fluid. In the parasternal long-axis view, a left pleural effusion appears as an echo-free space posterior to the

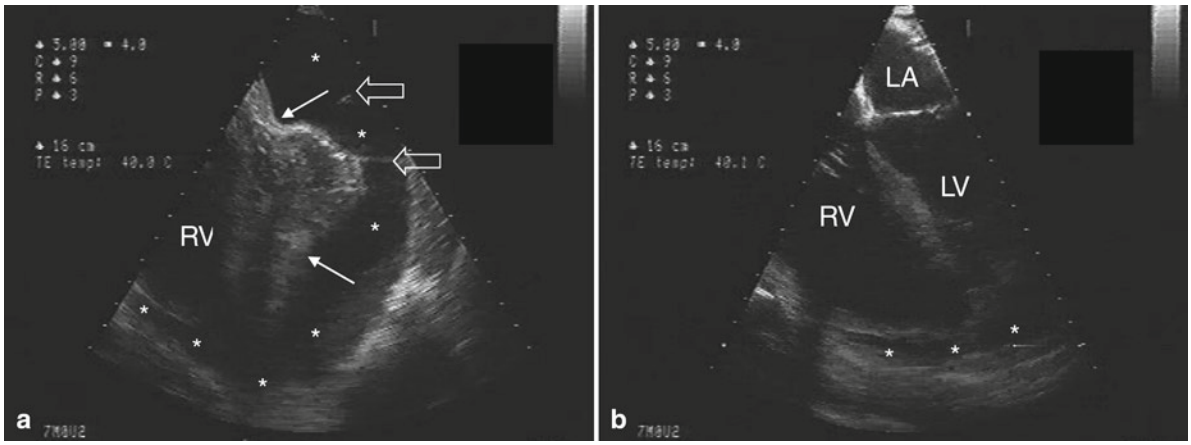

Fig. 14.5 Loculated pericardial effusion responsible for cardiac tamponade after open-heart surgery. In this ventilated hypotensive patient, transthoracic echocardiography was nondiagnostic. Transesophageal echocardiography clearly depicted a large loculated pericardial effusion (**a**, *asterisks*), which effectively caused the collapse of both the left atrium (LA) and ventricle (LV; **b**, *solid arrows*). Note that left-sided cardiac cavities were reduced to a potential space, whereas the right ventricle (RV) was not collapsed by the loculated pericardial effusion. Strands were present in the pericardial space (**a**, *open arrows*). Immediate pericardiotomy performed at bedside allowed the rapid restoration of stable hemodynamics; a small residual pericardial effusion was identified in the apical region (**b**, *asterisks*)

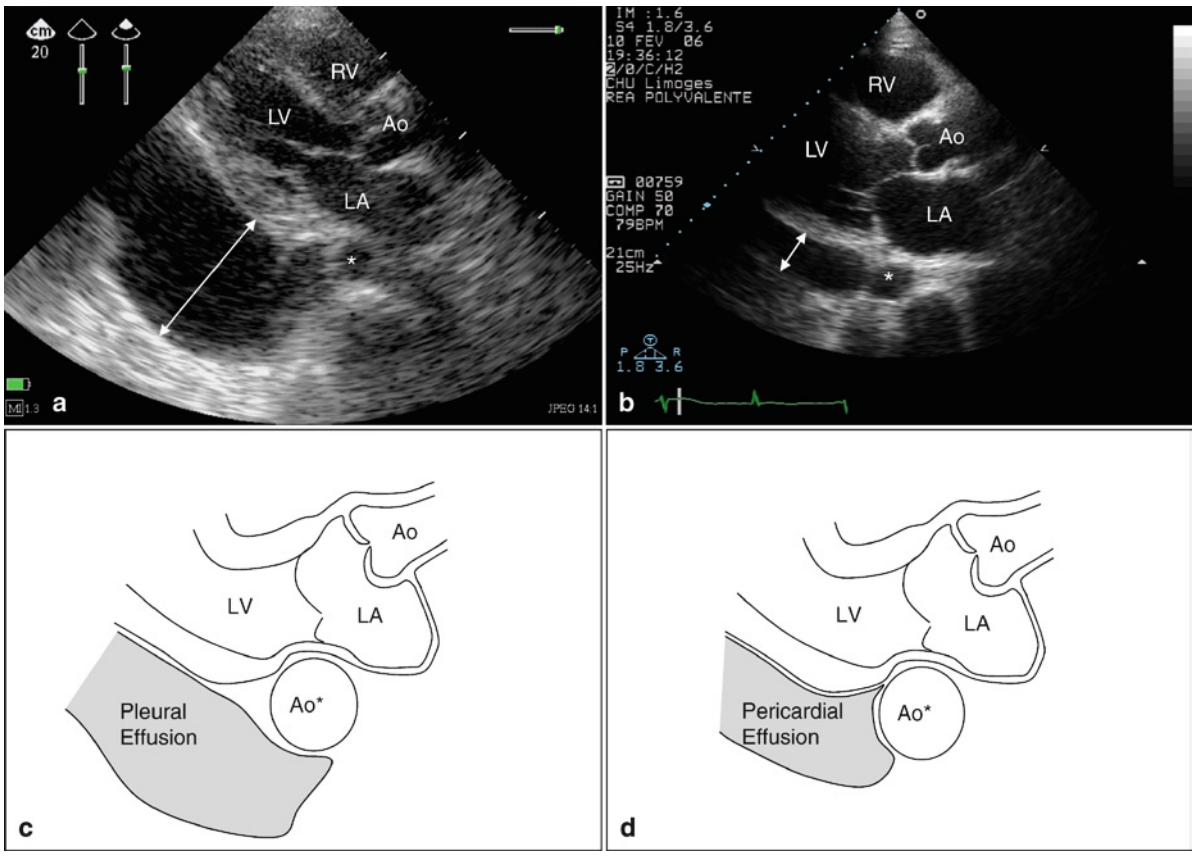

Fig. 14.6 Differential diagnosis between left pleural effusion and pericardial effusion in the parasternal long-axis view. A left pleural effusion appears as an echo-free space posterior to the heart that extends posterior to the descending aorta (**a, c** *asterisk*). In contrast, a pericardial effusion tracks anterior to the descending aorta (**b, d** *asterisks*). Abbreviations: *RV* right ventricle, *LV* left ventricle, *LA* left atrium, *Ao* thoracic aorta

heart similar in position to a pericardial effusion. In this view, a pericardial effusion tracks anterior to the descending aorta, while a left pleural effusion will collect posterior to the descending aorta (Fig. 14.6). Fluid that is located exclusively posterior to the LA is likely to be a pleural effusion, related to the complex pericardial reflections of that area. Distinguishing pleural from pericardial fluid in the apical four-chamber view may be difficult, and ascites can occasionally be mistaken for a pericardial effusion in the subcostal view (Fig. 14.7). A pericardial and pleural effusion may coexist. Echocardiographic examination often identifies the visceral pericardium as a linear structure that separates the two fluid-filled spaces. Importantly, pleural and abdominal ultrasonography allows for prompt differential diagnosis when performed during the same examination (Fig. 14.8). Large pleural effusions have been reported to cause cardiac tamponade [7–9].

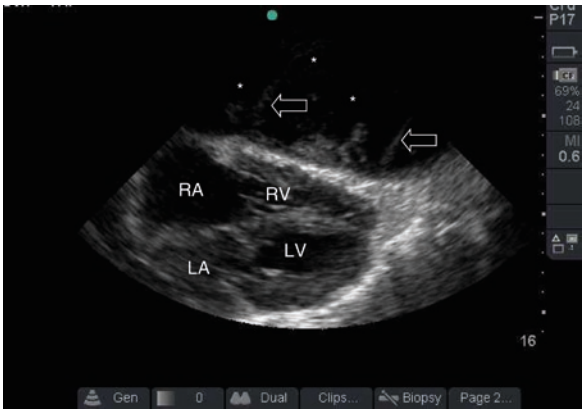

Fig. 14.7 Transthoracic echocardiography performed in a hypotensive patient. On initial screening examination from the subcostal view of the heart, there was concern that the patient had a pericardial effusion. A more comprehensive examination showed this to be complex ascites (*asterisks*) with multiple strands (*arrows*). Abbreviations: *LV* left ventricle, *RV* right ventricle, *LA* left atrium, *RA* right atrium

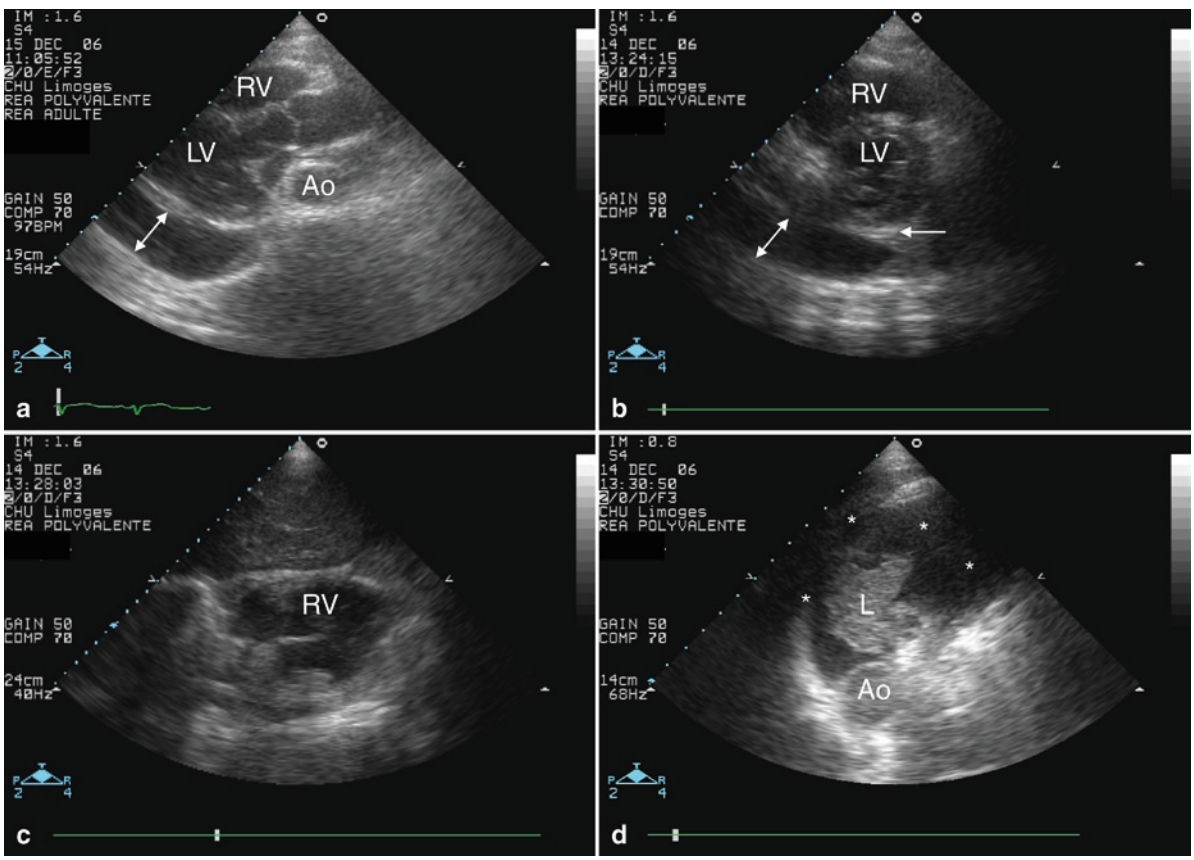

Fig. 14.8 Transthoracic echocardiography performed in a patient referred for a suspected hemopericardium after a blunt chest trauma. The parasternal long-axis view disclosed an echo-free space posterior to the left ventricle (LV; **a**, *double arrowhead*). The parasternal short-axis view confirmed the dependent effusion (**b**, *double arrowhead*), but the pericardial sac remained a potential space (*arrow*). The subcostal view depicted a dry pericardium (**c**). Pleural ultrasonography clearly depicted a large left pleural effusion with a collapsed lung (**d**, *asterisks*). Thoracentesis evacuated a 900-mL left hemothorax. Abbreviations: *RV* right ventricle, *Ao* thoracic descending aorta, *L* left lung

14.4 Echocardiographic Identification of Pericardial Tamponade

14.4.1 Two-Dimensional Echocardiography

If intrapericardial pressure exceeds RA pressure, collapse of the RA wall occurs. This is best seen in the apical four-chamber view (Fig. 14.9). The RA normally reduces in volume at the end of diastole (diastole and systole refer to the ventricular cycle in this discussion), so that the degree and duration of atrial collapse are crucial in determining whether there is compression of the structure by an effusion. Systolic collapse of the RA indicates compression by the pericardial effusion. Inversion of the RA wall for greater than one-third of systole has a high sensitivity and specificity for the diagnosis of pericardial tamponade [10, 11]. Any process that results in elevation of RA pressure will reduce the effect that an elevation of intrapericardial pressure will have on the RA.

Elevated intrapericardial pressures may also cause RV wall collapse [12]. The RV outflow tract is the most compressible part of the RV, so this paradoxical collapse is best visualized in the parasternal long-axis view. It occurs in early diastole. If the collapse extends to the body of the RV, this suggests that intrapericardial pressures are very elevated. Rarely, a localized pericardial effusion causes LA or LV compression that is detected by echocardiography [13]. RV collapse may be attenuated if the RV resists compression due to hypertrophy or infiltrative myocardial disease [14] or when RV pressure is elevated. As a result, RV diastolic collapse is more a specific than sensitive sign of pericardial tamponade.

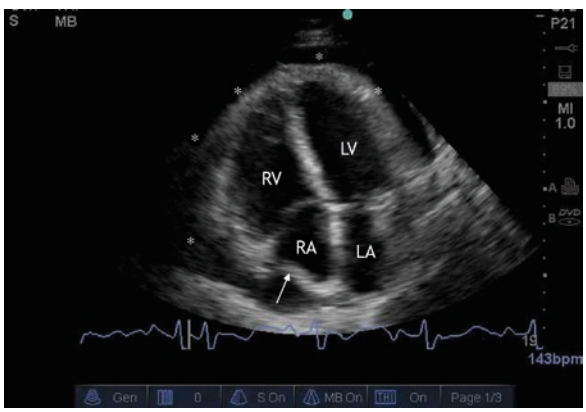

Fig. 14.9 Transthoracic echocardiography performed in a hypotensive patient with a history of metastatic breast cancer. The apical four-chamber view showed a large circumferential pericardial effusion (*asterisks*) with right atrial (RA) collapse during systole (*arrow*). The ECG cursor is seen to be in systole. Pericardiocentesis removed 400 mL of serosanguinous fluid with prompt improvement in hemodynamics. Abbreviations: *LV* left ventricle, *RV* right ventricle, *LA* left atrium

Pericardial tamponade results in a dilated IVC without major size variation during the respiratory cycle [15]. This is a sensitive, but nonspecific, finding. Pericardial tamponade also results in reciprocal respiratory variation in ventricular volumes. The examiner may note marked changes in ventricular size that track the respiratory cycle. During inspiration, the RV increases in size relative to the LV, vice versa during expiration.

14.4.2 Doppler Analysis

Normally, there is a small variation in SV between inspiration and expiration during quiet spontaneous breathing. On the left side, SV falls during inspiration, while on the right SV rises during inspiration. This physiological respiratory variation is accentuated with pericardial tamponade and is the basis for Doppler-based diagnosis of the condition. Rather than measuring actual SV (see Chap. 5), Doppler flow velocity may be used as a surrogate of SV (Fig. 14.10). For example, a reduction in mitral E-wave velocity of greater than 25% during inspiration (in spontaneously breathing patients) is consistent with tamponade physiology [16–18]. Similar measurements may be made at the tricuspid valve and in the hepatic vein.

From the point of view of the frontline intensivist, there are problems with the Doppler-based diagnosis of tamponade. Respiratory variations in SV and flow velocities for the diagnosis of pericardial tamponade have not been validated in patients on mechanical ventilatory support [19]. These measurements can therefore only be applied in patients who are breathing spontaneously. In addition, Doppler velocity measurements are critically dependent on intercept angle and placement of the Doppler sample. The patient with respiratory distress may have marked translational movement of the heart, and cardiac swinging is a feature of patients with pericardial tamponade. In this situation, changes in measured flow velocity may derive from changes in Doppler intercept angle or sample position rather than reflecting true changes in velocity. Finally, a number of disease processes cause respiratory variation in SV that may

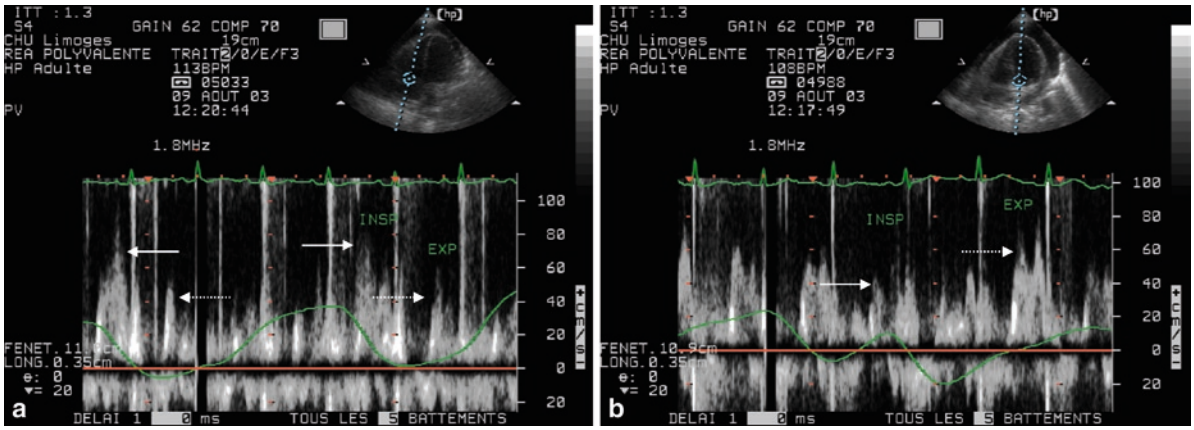

Fig. 14.10 Respiratory variations of spectral Doppler velocities recorded in a spontaneously breathing patient with cardiac tamponade. Tricuspid Doppler velocities are maximal during inspiration (**a**, *arrows*) and minimal during expiration (**a**, *dotted arrows*). Conversely, mitral Doppler velocities are maximal during expiration (**b**, *dotted arrow*) and minimal during inspiration (**b**, *arrow*). Abbreviations: *Insp*. inspiration, *Exp*. expiration

coexist with the pericardial effusion, such as airway obstruction (asthma, chronic obstructive pulmonary disease, upper airway obstruction), pulmonary embolism, RV infarction, and severe hypovolemia.

14.4.3 Clinical Context

Echocardiography is a critical component in diagnosis since it identifies the presence of a pericardial effusion. However, the diagnosis of pericardial tamponade is always a clinical and hemodynamic diagnosis. The presence or absence of chamber collapse or respiratory variations in flow velocities is helpful, but not diagnostic of the condition. This has to be interpreted within the clinical context. Using such findings as the presence of a pericardial effusion and clinical, echocardiographic, or hemodynamic evidence of tamponade, the intensivist has to be proficient in the performance of pericardiocentesis; this may be a life-saving procedure.

14.5 Pericardiocentesis

Pericardiocentesis may be performed safely with echocardiographic guidance. Seward et al. [20] described 1,127 serial pericardiocenteses with a very low complication rate. Echocardiographic-guided pericardiocentesis is so clearly superior to fluoroscopic guidance that the critical care ultrasonographer should develop proficiency as a matter of patient safety.

14.5.1 Overview of Procedure

Echocardiographic guidance of pericardiocentesis is similar to other ultrasound-guided techniques for fluid removal, such as thoracentesis. Identification of the pericardial effusion is followed by selection of a safe site, angle, and depth for needle insertion. Pericardiocentesis has serious potential complications. Laceration of a coronary artery or of the myocardium may cause the death of the patient. Pericardiocentesis is not a procedure for the entry-level ultrasonographer. It requires a high level of proficiency in image acquisition and procedural skill.

14.5.2 Equipment Requirements

This chapter does not discuss in detail the technical aspects of hardware use but concentrates on the use of echocardiography to guide the procedure. Whether the operator uses a commercially available kit or prefers to assemble the equipment as needed, pericardiocentesis is best accomplished using Seldinger's technique. A needle is introduced into the pericardial fluid, followed by a

wire and prompt removal of the needle. The wire can then be used to introduce the appropriate catheter. Some clinicians prefer to introduce a small-bore angiocath (catheter over needle) and then insert the wire through the catheter. In any case, the objective in the same: the needle should be introduced for the shortest time possible. Once the wire is in place and the needle removed, the follow-through hardware is designed to be nontraumatic. Assuming that the operator is skilled in all aspects of wire placement, dilator use, and catheter insertion, the safety of the procedure depends on the echocardiographic determination of a safe site for needle insertion.

14.5.3 Site Selection and Procedural Elements

Using echocardiography, the best site is where the most fluid is found. This may be at any point on the anterior or lateral chest. The subcostal view may be used as well, although the liver may block safe access. Often, the best site is found using the apical four-chamber view. The parasternal view may offer a good approach if the effusion is very large. In the supine patient, the effusion may collect in the dependent posterior pericardium. A change in patient position may distribute the fluid to a more favorable position. Placing the patient in a left lateral decubitus position may shift the fluid for improved apical view, while the semiupright position may improve the subcostal view.

The distance between the heart and the point of needle penetration into the pericardium is a major factor of safety. The heart is a very mobile organ. During the respiratory cycle, the heart is subject to translational movement, which is accentuated if the patient has distressed breathing. Cardiac swinging is a common phenomenon in severe tamponade, and the heart changes in size throughout the contractile cycle. As a result, the apparent thickness of the pericardial effusion may rapidly change to a major extent during cardiac movement. Although there is no definite rule for how much fluid must be present to allow for safe needle insertion, a minimum of at least 1 cm of fluid depth is a reasonable lower limit for the distance between the parietal pericardium and the myocardial surface, taking into account the change in this distance that occurs during cardiac and respiratory cycling.

A key element in site selection is the avoidance of injury to nearby structures. With the subcostal approach, the liver may be injured. Unlike with fluoroscopic guidance in pericardiocentesis, the liver may be readily identified with ultrasonography and therefore avoided when using the subcostal approach. Injury to the lungs may occur during pericardiocentesis. Fortunately, aerated or consolidated lung is readily identified with ultrasonography and therefore easy to avoid. When using the parasternal approach, color Doppler of the proposed needle track is mandatory in order to avoid the internal mammary vessels. A coexisting pleural effusion may block access to the pericardial effusion. In this case, it is best to drain the pleural effusion first and then rescan the patient to establish the best approach to the pericardial effusion. Attempts to insert a needle through a pleural effusion into an underlying pericardial effusion are usually unsuccessful since the needle generally pushes the parietal pericardium inward without penetrating it.

A critical element in safe pericardiocentesis is determination of the depth for needle penetration. The effect of skin compression has to be considered. In the obese or edematous patient, the transducer may be pressed into the skin in order to obtain good image quality. This may indent the skin by several centimeters. The distance for needle penetration is measured during skin compression, such that the depth of needle penetration is underestimated when measured from the machine screen. This may result in an underestimation of the distance required to enter the effusion. Another cause of difficulty is movement of the mark designating the appropriate site for needle insertion owing to the force applied by the operator's hand. Skin is mobile, so the site mark should be made without any traction exerted on the surrounding skin. In addition to determination of site and depth, ultrasonography can be used to ascertain the best angle for needle insertion. The angle at which the transducer is held to obtain the best trajectory is the angle at which the needle is inserted.

Before sterile-field preparation, the site, depth, and angle of needle insertion are determined echocardiographically, and the site is marked. Depth measurement has to include an estimate of skin-compression artifact. The depth of needle penetration is measured using the machine caliper function. The skin is then prepared for sterile procedure and the patient covered with a full body drape. The transducer should be covered with a sterile sleeve and be part of the sterile-field setup.

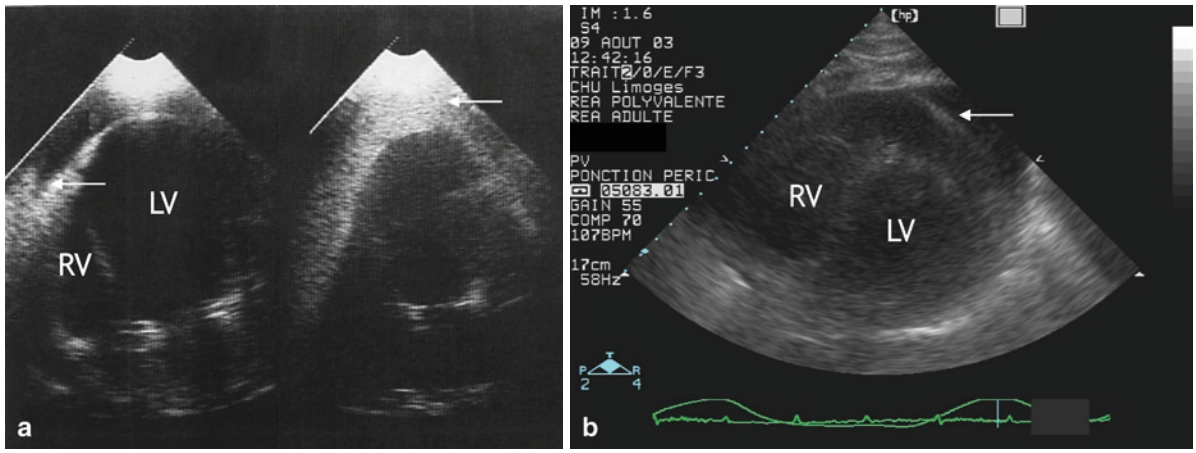

Fig. 14.11 Echocardiographically guided wire insertion for a pericardiocentesis. Injection of agitated saline allows confirmation of adequate needle position within the pericardial sac (**a**, *arrows*). The wire and catheter can subsequently be safely inserted to remove pericardial fluid (**b**). Abbreviations: *RV* right ventricle, *LV* left ventricle

Full sterile preparation and equipment setup should be followed by a final confirmatory scan to check the site, depth, and angle of needle penetration. This angle will be duplicated by the needle/syringe assembly during device insertion. The operator promptly proceeds with needle insertion followed by wire/catheter insertion. No change in patient position is allowed to occur between final scan and needle insertion. Confirmation of device placement may be accomplished by injecting several milliliters of agitated saline into the drainage catheter (Fig. 14.11). Pericardiocentesis does not require real-time guidance with ultrasonography [20]. However, it is essential to have the transducer with sterile cover available in the event of a rescan and to document successful device insertion.

There are several causes for a "dry tap." Skin-compression artifact is a common problem, as noted above. It leads to underestimation of the depth for needle insertion. Inaccurate site marking owing to skin traction or a problem with poor angle duplication are also possibilities. The solution is to rescan the patient to estimate compression artifact more accurately, reassess the site mark, and reestablish the angle for needle insertion. This emphasizes the importance in using a sterile transducer cover as part of routine patient setup. In selecting the angle for needle insertion, it is easier to duplicate a perpendicular transducer angle than one that is acutely angled. The perpendicular transducer angle favors an anterior or lateral chest wall approach since the transducer is often perpendicular to the chest wall when scanning in these areas. The subcostal view requires a more acutely angled approach. An unusual cause of a dry tap is a blocked needle, resulting in overly deep needle insertion. Clotted blood or a skin plug may be responsible. Overly vigorous probing of the anterior costal cartilage (if using a parasternal approach) can also block the needle with cartilage. A large anterior pericardial fat pad may be mistaken for a pericardial effusion by the inexperienced ultrasonographer, with potentially catastrophic consequences to the patient. Pericardial fat has some element of echogenicity, and it moves in synchrony with cardiac contraction. In addition, it is very uncommon for a consequential pericardial effusion to occur anterior to the heart without a significant posterior pericardial effusion also being present.

14.6 Conclusion

Echocardiography allows the frontline intensivist to identify the presence of pericardial fluid. In the patient with hemodynamic failure, the presence of a pericardial effusion raises the possibility of pericardial tamponade. Echocardiography is useful in identifying pericardial tamponade with two-dimensional imaging as well as with Doppler analysis. However, the diagnosis of pericardial tamponade as a cause for shock should be made on clinical and hemodynamic grounds and not rely solely on echocardiographic measurements. Echocardiography permits the safe performance of bedside pericardiocentesis. With careful image

acquisition and interpretation, the frontline intensivist can select a safe site, angle, and depth for needle and device insertion. The critical care ultrasonographer is encouraged to develop competence in echocardiographic guidance of pericardiocentesis as it is superior to subcostal fluoroscopic guidance.

References

1. Spodick DH (1998) Pathophysiology of cardiac tamponade. Chest 113:1372–1378
2. Gonzalez MS, Basnight MA, Appleton CP (1991) Experimental cardiac tamponade: a hemodynamic and Doppler echocardiographic reexamination of the relation of right and left heart ejection dynamics to the phase of respiration. J Am Coll Cardiol 18:243–252
3. Kochar GS, Jacobs LE, Kotler MN (1990) Right atrial compression in postoperative cardiac patients: detection by transeosphageal echocardiography. J Am Coll Cardiol 16:511–516
4. Simpson IA, Munsch C, Smith EEJ, Parker DJ (1991) Pericardial haemorrhage causing right atrial compression after cardiac surgery: role of transesophageal echocardiography. Br Heart J 65:355–356
5. Ananthasubramaniam K, Jaffery Z (2007) Postoperative right atrial compression by extracardiac hematoma: transoesophageal echocardiographic diagnosis in the critically ill patient. Echocardiography 24:661–663
6. Saner HE, Olson JD, Goldenberg IF, Asinger RW (1995) Isolated right atrial tamponade after open heart surgery: role of echocardiography in diagnosis and management. Cardiology 86:464–472
7. Kaplan LM, Epstein SK, Schwartz SL, Cao QL, Pandian NG (1995) Clinical, echocardiographic, and hemodynamic evidence of cardiac tamponade caused by large pleural effusions. Am J Respir Crit Care Med 151:904–908
8. Traylor JJ, Chan K, Wong I, Roxas JN, Chandraratna PAN (2002) Large pleural effusions producing signs of cardiac tamponade resolved by thoracentesis. Am J Cardiol 89:106–108
9. Vaska K, Wann LS, Sagar K, Klopfenstein HS (1992) Pleural effusion as a cause of right ventricular diastolic collapse. Circulation 86:609–617
10. Gillam LD, Guyer DE, Gibson TC, King ME, Marshall JE, Weyman AE (1983) Hydrodynamic compression of the right atrium: a new echocardiographic sign of cardiac tamponade. Circulation 68:294–301
11. Kronzon I, Cohen ML, Winer HE (1983) Diastolic atrial compression: a sensitive echocardiographic sign of cardiac tamponade. J Am Coll Cardiol 2:770–775
12. Armstrong WF, Schilt BF, Helper DJ, Dillon JC, Feigenbaum H (1982) Diastolic collapse of the right ventricle with cardiac tamponade: an echocardiographic study. Circulation 65:1491–1496
13. Chuttani K, Pandian NG, Mohanty PK, Rosenfield K, Schwartz SL, Udelson JE, Simonetti J, Kusay BS, Caldeira ME (1991) Left ventricular diastolic collapse. An echocardiographic sign of regional cardiac tamponade. Circulation 83:1999–2006
14. Leimgruber PP, Klopfenstein HS, Wann LS, Brooks HL (1983) The hemodynamic derangement associated with right ventricular diastolic collapse in cardiac tamponade: an experimental echocardiographic study. Circulation 68: 612–620
15. Himelman RB, Kircher B, Rockey DC, Schiller NB (1988) Inferior vena cava plethora with blunted respiratory response: a sensitive echocardiographic sign of cardiac tamponade. J Am Coll Cardiol 12:1470–1477
16. Appleton CP, Hatle LK, Popp RL (1988) Cardiac tamponade and pericardial effusion: respiratory variation in transvalvular flow velocities studied by Doppler echocardiography. J Am Coll Cardiol 11:1020–1030
17. Leeman DE, Levine MJ, Come PC (1988) Doppler echocardiography in cardiac tamponade: exaggerated respiratory variation in transvalvular blood flow velocity integrals. J Am Coll Cardiol 11:572–578
18. Burstow DJ, Oh JK, Bailey KR, Seward JB, Tajik AJ (1989) Cardiac tamponade: characteristic Doppler observations. Mayo Clin Proc 64:312–324
19. Faehnrich JA, Noone RB, White WD, Leone BJ, Hilton AK, Sreeram GM et al (2003) Effects of positive-pressure ventilation, pericardial effusion, and cardiac tamponade on respiratory variation in transmitral flow velocities. J Cardiovasc Vasc Anesth 17:45–50
20. Tsang TM, Enriquez-Sarano M, Freeman WK, Barnes ME, Sinak LJ, Gersh BJ, Bailey KR, Seward JB (2002) Consecutive 1127 therapeutic echocardiographically guided pericardiocenteses: clinical profile, practice patterns, and outcomes spanning 21 years. Mayo Clin Proc 77:429–436

Echocardiography and Extracorporeal Life Support in Intensive Care Unit

15

Joaquim Calderon and Gérard Janvier

Contents

Cardiac assist devices are used to support patients with circulatory and/or respiratory failure. Most often, cardiac assistance is supposed to provide a bridge to recovery or transplantation. In a few selected patients, it may be used as a "destination therapy," where no recovery can be expected and heart transplantation is not possible. Short-term assistance ordinarily signifies a foreseeable duration of less than 4 weeks, whereas long-term assistance signifies a longer period. They require different types of equipment. Short-term assistance devices are the most commonly used in intensive care units (ICUs) because they are easier to set up and supervise than long-term assistance machines. The most frequent indications for short-term assistance in ICUs include cardiogenic shock as a result of acute myocardial infarction, acute myocarditis, decompensation of chronic cardiomyopathy (with a potentially reversible cause), and intoxication with cardiac depressing drugs. All assist devices require good knowledge of the physiological consequences of their use. Echocardiography is of paramount importance, not only for validating assistance indication and verifying the absence of contraindications, but it is also essential in confirming the correct placement of cannulas and detecting complications. The noninvasive character of ultrasound allows for serial assessments, which helps to assess tolerance to assistance and consider weaning when recovery is sufficient.

15.1 Short-Term Circulatory Assist Devices

Short-term circulatory assistance is increasingly used to treat catecholamine-resistant cardiac failure. This technique was primarily aimed at treating subjects with

J. Calderon (✉) and G. Janvier
CHU de Bordeaux – Université de Bordeaux 2,
Service d'Anesthésie-Réanimation 2,
France
e-mail: joachim.calderon@chu-bordeaux.fr

D. De Backer et al. (eds.), *Hemodynamic Monitoring Using Echocardiography in the Critically Ill*,
DOI: 10.1007/978-3-540-87956-5_15, © Springer-Verlag Berlin Heidelberg 2011

potentially reversible forms of cardiac failure, such as postoperative cardiogenic shock following extracorporeal circulation, shock resulting from acute myocardial infarction, acute myocarditis, intoxications with cardiac depressant drugs, and accidental hypothermia [1]. However, short-term assistance can also be indicated in patients with more dubious prognosis, for example, maintaining flow in non-heart-beating organ donors and as a bridge to long-term cardiac assistance [2]. Different devices are available, and we describe in this chapter the classic intra-aortic balloon pump, intracavitary axial micropumps, and extracorporeal life support or extracorporeal membrane oxygenation.

15.1.1 Intra-aortic Balloon Pump

Counterpulsation using the intra-aortic balloon pump (IABP) is the most widely and extensively used type of left ventricular (LV) assist device. An inflatable balloon mounted on a catheter is introduced percutaneously into the aorta via a femoral artery. The balloon is placed below the emergence of the left subclavian artery and above that of the renal arteries. Cyclic inflation and deflation of the balloon are triggered by echocardiogam (ECG) or aortic-pressure waveform. Helium is used for balloon inflation because it combines very low viscosity, which allows rapid cycling, with high solubility, preventing severe gas embolism in the event of balloon rupture. The balloon inflates (30–50 mL) during diastole, thereby propelling some blood forward and backward, which increases diastolic pressure in the aortic arch. This increase in diastolic pressure improves coronary artery perfusion and, therefore, myocardial oxygen delivery. Balloon deflation during systole results in reduced LV afterload, thereby reducing myocardial wall stress and oxygen consumption. The beneficial effects on myocardial oxygen balance explain why IABP remains the first-line assist device for patients with cardiogenic shock of ischemic origin. However, the circulatory support provided by this technique is limited and will not compensate for very severe LV failure.

15.1.2 Axial Pumps: The Impella® System

Impella assist devices (Impella Abiomed Europe GmbH, Aachen, Germany) consist of electrically driven axial micropumps, designed to support isolated left or right ventricular failure (single ventricle assistance), without concomitant respiratory failure. LV Impella assist devices can be implanted percutaneously via the femoral or subclavian artery, with the help of a guide wire to place them into the LV. Different Impella pump sizes are available. The Impella 2.5 LP generates a flow of up to 2.5 L of blood per minute from the LV into the ascending aorta, actively unloading the heart and reducing oxygen demand [3]. This system can remain in place for up to 5 days. When more assistance is necessary, the Impella 5.0 LP generates a blood flow of 5 L/min and is certified for up to 10 days [4]. This device has to be inserted through a 9Fr introducer because its greatest diameter is 6.4 mm, and removal requires surgical repair of the arterial wound. The Impella RD is designed to assist the right heart, and it has to be implanted via a sternotomy between the right atrium and pulmonary artery to unload the right ventricle. Owing to their limited synthetic surface area, axial micropumps keep damage to the blood to a minimum. However, continuous infusion of unfractioned heparin is necessary to avoid clotting and embolic complications.

15.1.3 Centrifugal Pumps: Extracorporeal Life Support

This technique allows for right-to-left (venoarterial) assistance with extracorporeal oxygenation, and it can maintain systemic oxygen delivery despite cardiopulmonary failure. This type of assistance is termed extracorporeal life support (ECLS) or arteriovenous (AV) extracorporeal membrane oxygenation (ECMO). It can compensate very severe heart failure (sometimes complete asystole) and can also provide support to patients with associated respiratory failure. Venous blood is derived from an extracorporeal circuit, oxygenated, and returned to the arterial circulation by means of a centrifugal pump. The large cannulas can be inserted via a sternotomy into the right atrium and aorta ("central" ECLS); alternatively, they can be inserted into peripheral vessels either surgically (Fig. 15.1) or, more frequently, using a percutaneous Seldinger's technique. Venous blood is suctioned by the centrifugal pump from the venous cannula and is propelled into a membrane oxygenator (Fig. 15.2), which increases oxygen content and removes carbon dioxide. A heater helps maintain physiological blood temperature. Blood is

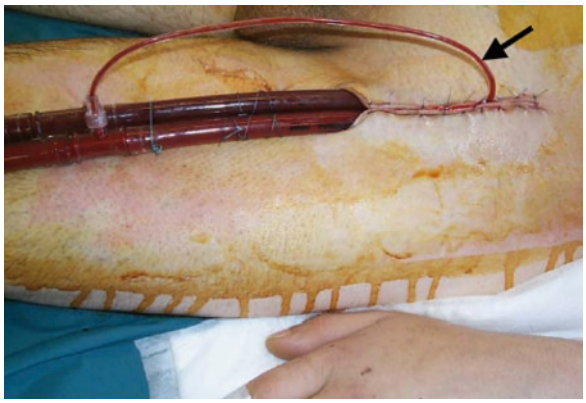

Fig. 15.1 Surgical implantation of peripheral extracorporeal life support (ECLS)/ extracorporeal membrane oxygenation (ECMO). Percutaneous implantation is now possible and recommended. Lower limb reperfusion (*black arrow*) reduces the risk of peripheral ischemia

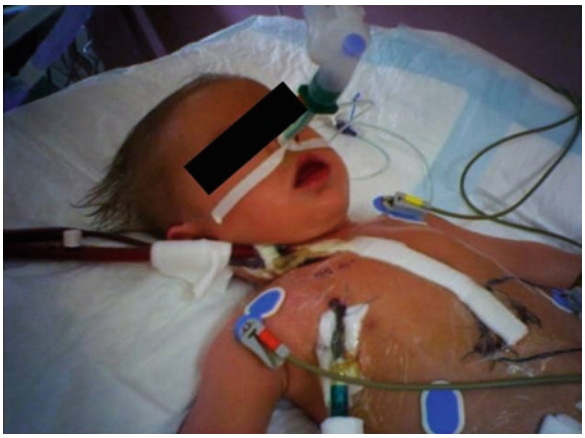

Fig. 15.3 Venoarterial pediatric centrifugal extracorporeal life support (ECLS)/ extracorporeal membrane oxygenation (ECMO) with internal jugular vein and carotid artery cannulation

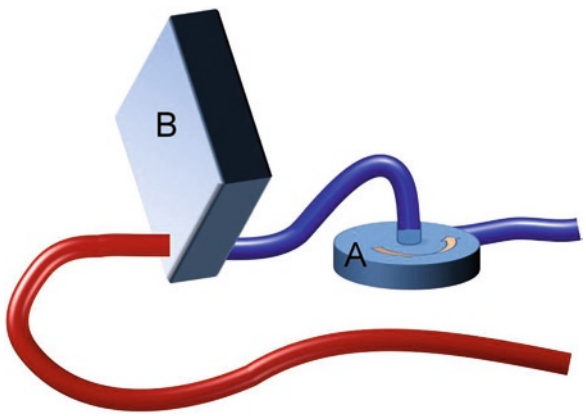

Fig. 15.2 Schematic representation of a centrifugal extracorporeal life support (ECLS) or extracorporeal membrane oxygenation (ECMO) circuit with pump (**a**) and oxygenator (**b**)

reinjected into the arterial system via a femoral artery, or sometimes an axillary or carotid artery (notably in children, Fig. 15.3).

The supra-aortic reinjection sites expose the patient to cerebral edema if excess flow is delivered to the brain. Reinjection via the iliac artery can be complicated by lower-limb ischemia following occlusion of a profunda femoral artery owing to the large diameter of the cannula. Ischemic complications can be reduced by placing a reperfusion catheter into the superficial femoral artery (Fig. 15.1). The diameter of the cannula is the main determinant of ECMO/ECLS flow and accounts for the impossibility of practicing this type of assistance in the newborn. However, partial assistance remains possible in such patients.

The oxygenator also provides support to failing lungs by allowing CO_2 removal and variable improvement in oxygenation, according to the proportion of total flow that is oxygenated. When used in isolated respiratory failure, venovenous cannulation is the most common technique. The simple assembly and management of ECLS/ECMO make it possible to employ this technique outside specialized cardiovascular surgery units. The advent of centrifugal pumps has reduced the numerous hemorrhagic and thrombotic complications associated with roller pumps. Prior to the introduction of centrifugal pumps, prognosis was related more to assistance complications rather than to the underlying pathology. Assistance devices utilizing occlusive roller pumps are inappropriate for ICU deployment and so are not discussed here.

15.2 Role of Echocardiography for Setting Up and Monitoring Assistance

The knowledge of ultrasound principles of circulatory physiology and of the operating principles of the different types of assist devices is mandatory for the proper use of these techniques. Echocardiography is an invaluable aid for physicians at all steps of the process. Certain information is always requisite prior to introducing any type of assist device, and this has to be obtained with echocardiography or general ultrasound techniques.

Table 15.1 Contraindications to assistance requiring intra-aortic (or intra-arterial) devices

Severe aortic regurgitation (>grade 2)	+++
Severe aortic stenosis	+++
Aortic coarctation	+++
Aortic dissection	+++
Severe protruding atheromatous plaques of the aortic arch	+
Aortic aneurysm with intraluminal thrombus (abdominal or thoracic)	+

Aortic conditions that contraindicate the use of assistance involving intra-aortic (or intra-arterial) material (Table 15.1) have to be systematically investigated using echocardiography. Preliminary echocardiographic examination should also assess the arterial puncture site to ensure that the vessel diameter is suitable for device implantation. In addition, all sites of venous cannulation need to be checked for the absence of thrombus. The preimplantation echocardiographic examination also allows initial measurements of cardiac chamber dimensions, indices of ventricular function, stroke volume, and evaluation of valvular (aortic and mitral) regurgitations, which constitute useful yardsticks in assessing ECLS tolerance and ventricular function recovery.

15.2.1 Echocardiography and IABP

The placement of an IABP does not require echocardiography and can be executed blindly, using a percutaneous approach. However, it is not uncommon to perform echocardiography prior to introducing an IABP, especially to rule out severe LV failure, which might require more powerful assistance, or to verify the absence of severe aortic regurgitation. If transesophageal echocardiography (TEE) is employed at the time of IABP introduction, it can easily be used to check the appropriate placement of the catheter tip, i.e., 1–2 cm below the emergence of the left subclavian artery. If the catheter tip is seen at the junction with the horizontal part of the aorta, this signifies that it has been pushed too far, and there is a risk of intermittent obliteration of the left subclavian artery (Fig. 15.4).

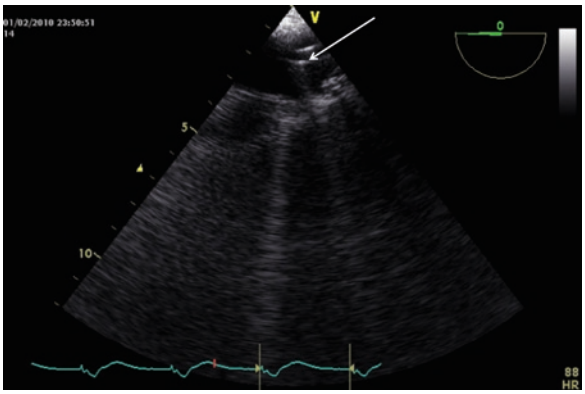

Fig. 15.4 Transesophageal echocardiography (TEE) view of the junction between the descending thoracic aorta and the horizontal part of the aorta. The presence of the catheter tip (*white arrow*) attests that intra-aortic balloon pump has to be retrieved by a few centimeters

15.2.2 Echo and Impella

Since Impella devices provide assistance to a single ventricle, the adequacy of the other ventricular function also has to be carefully verified. In the case of LV assistance, it is essential to analyze the mitral valve and check for preexisting mitral regurgitation [5]. During pump insertion, TEE is used to monitor the progression of the catheter in the aorta, through the aortic valve, and its location in the LV. A large LV cavity (>100–120 mL) facilitates the proper placement of the Impella assist device. Entanglement in the mitral subvalvular apparatus can create or worsen a mitral regurgitation, a complication that demands systematic checks (Fig. 15.5). Correct positioning is attested by the flow readings on the console, but also by the color Doppler analysis, highlighting the aspiration flow in the LV and the reinjection flow approximately 1 cm above the aortic valve (Fig. 15.6). If appropriate discharge of the LV is achieved, the reduction in LV size may be accompanied by a reduction in the severity of mitral regurgitation.

15.2.3 Echo and ECLS

15.2.3.1 ECLS for Circulatory Failure

The choice between central or peripheral ECLS is governed by local technical possibilities (cardiac surgical facility or not), the underlying cardiac condition (especially mitral and aortic competence), as well as the size

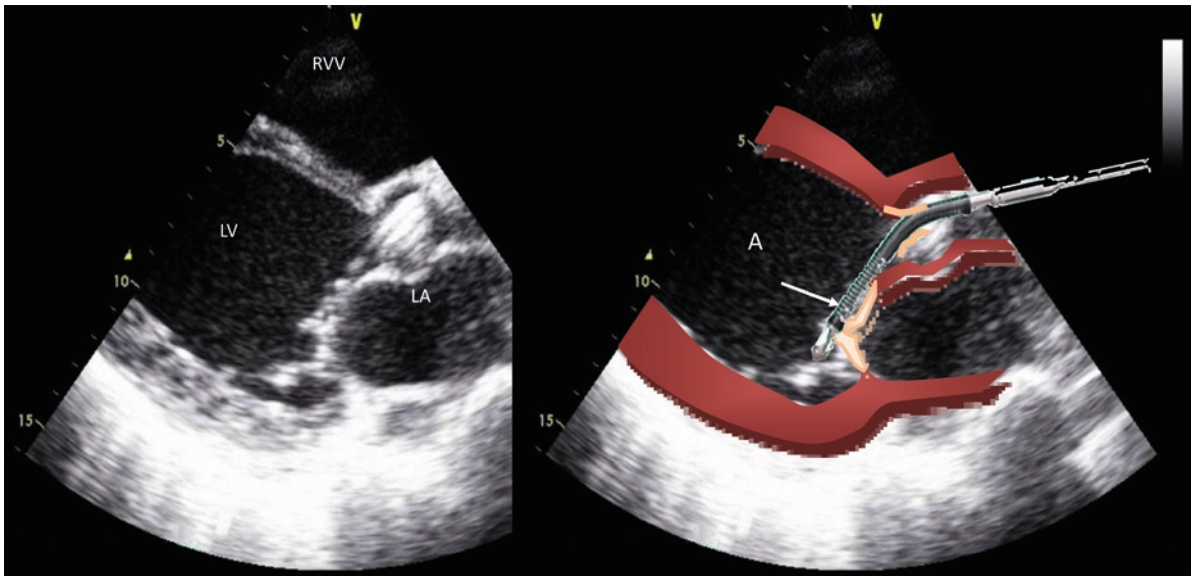

Fig. 15.5 Example of inadequate position of an Impella microaxial pump (*White arrow*) detected using transthoracic echocardiography (TTE; parasternal long-axis view). The probe is entangled with the mitral subvalvular apparatus and obstructs the course of the anterior mitral leaflet. Abbreviations: *RV* right ventricle, *LV* left ventricle, *LA* left atrium

of peripheral arteries (risk of lower limb ischemia). During peripheral ECLS, oxygenated blood is returned to the arterial circulation in a retrograde manner, thereby "competing" with antegrade ventricular ejection and increasing LV afterload. For a severely failing LV, this may be an unacceptable burden, resulting in acute pulmonary congestion. In cases of very severe LV failure, the aortic valve may remain closed during the entire

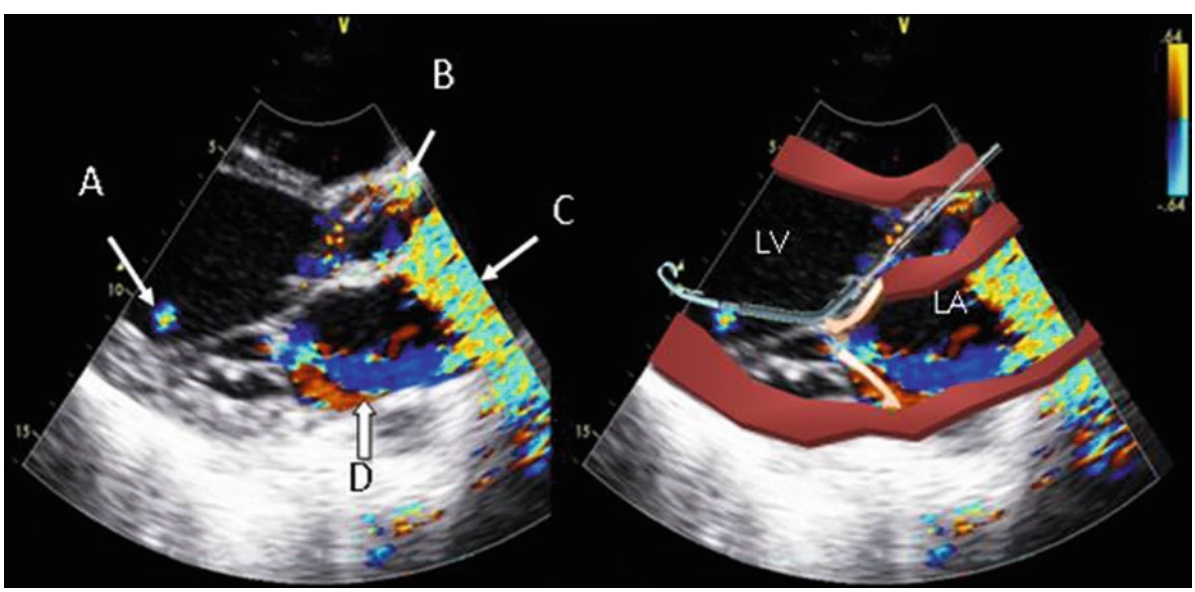

Fig. 15.6 Optimization of Impella micropump placement guided using TTE. The probe is pressing on the anterior mitral leaflet but is not exacerbating the preexisting mitral regurgitation (**a**). Distal aspiration (**b**) and reinfusion (**c**) flows are visible using color Doppler. Color Doppler artifacts (**d**) can be seen when the device is in the imaging plane

cardiac cycle. Aortic regurgitation (preexisting or acquired) will worsen LV dilatation. Mitral regurgitation (MR) will result in pulmonary venous engorgement, acute pulmonary edema, and subsequent right ventricular (RV) overload despite ECLS. In high-risk situations (very severe LV failure with high-grade aortic and/or MR), central ECLS (implying sternotomy) has to be proposed to obtain optimal unloading of the two ventricles, sometimes with the help of a left vent inserted simultaneously for left-heart decompression. Isolated MR due to annular dilatation (Carpentier classification type I) does not contraindicate peripheral ECLS. Indeed, LV size reduction resulting from circulatory improvement (i.e., preload reduction as a consequence of restored renal function) is likely to reduce LV size and improve MR. Hemorrhage is a frequent complication of central ECLS, and repeated echocardiographic examinations are necessary to detect pericardial blood or thrombus and potential atrial tamponade.

A frequent problem with peripheral ECLS is inappropriate unloading of one of the ventricles. Ventricular unloading is inappropriate when dilatation occurs (or fails to regress) despite ECLS. Therefore, ventricular size has to be carefully assessed before (preimplantation examination) and during assistance with ECLS. Aortic retrograde blood flow can sometimes cancel or reverse mitral blood flow (Fig. 15.7). A reversal of pulmonary venous flow can sometimes be demonstrated in patients with very high left atrial pressure (Fig. 15.8) [6]. In the case of persistent or worsening congestion despite ECLS, LV unloading has to be proposed. This can be achieved by placing a left vent via sternotomy or thoracotomy, exposing the patient to hemorrhagic complications. To avoid the surgical approach, various methods of percutaneous left-heart decompression have been described. Transfemoral atrial septostomy has been proposed in pediatric patients [7], transseptal placement of a large (>17Fr) atrial sheath (Fig. 15.9) [8], and even insertion of an Impella LP 2.5 in association with ECLS [9–11] were all able to achieve adequate LV unloading during peripheral ECLS. The association of IABP with ECLS (or with Impella) has also been used in some patients to reduce LV afterload and to increase coronary perfusion while restoring pulsatile aortic flow [12] (Fig. 15.10). A patent foramen ovale offers a natural vent for ventricular unloading; contrast echocardiography should be used to examine for this prior to making a decision regarding the type of assistance to select.

Echocardiography is also useful to detect problems related to venous cannulas: accidental placement in a suprahepatic vein (SHV) or kinking in the right atrium. Catheterization of an SHV results in poor venous drainage, inadequate RV unloading, and limited ECLS flow in addition to hepatic congestion and cytolysis. Sometimes, hepatic venous drainage is impaired despite the normal placement of the cannula. This

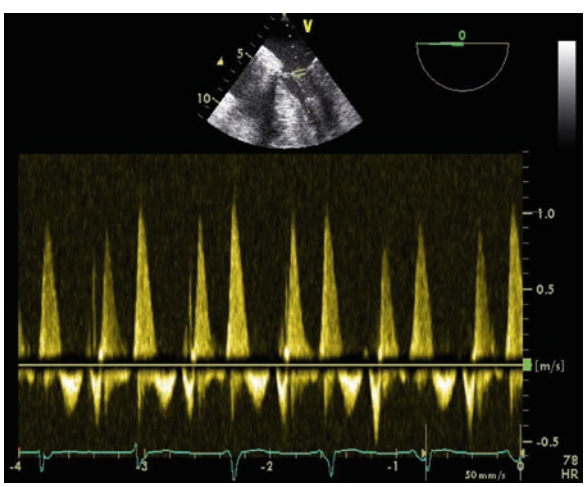

Fig. 15.7 TEE pulsed-Doppler recording of the mitral flow in a patient with peripheral ECLS. Note the biphasic backflow during diastole consistent with inappropriate discharge

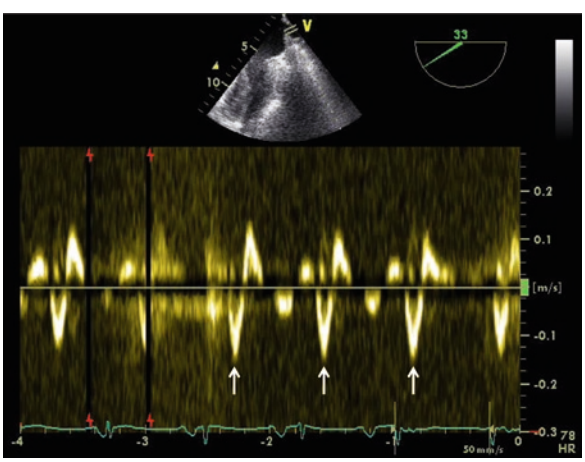

Fig. 15.8 Pulsed-Doppler of the flow of the left superior pulmonary vein recorded using TEE in a patient with severe heart failure supported using peripheral ECMO. The negative systolic wave of the pulmonary venous (*arrows*) flow suggests very high left atrial pressure. Additional LV discharge is necessary

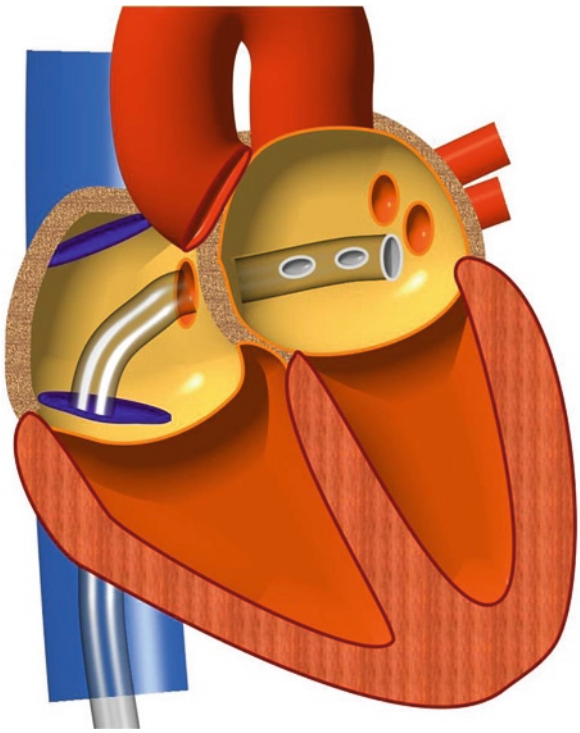

Fig. 15.9 Transseptal unloading of the left atrium

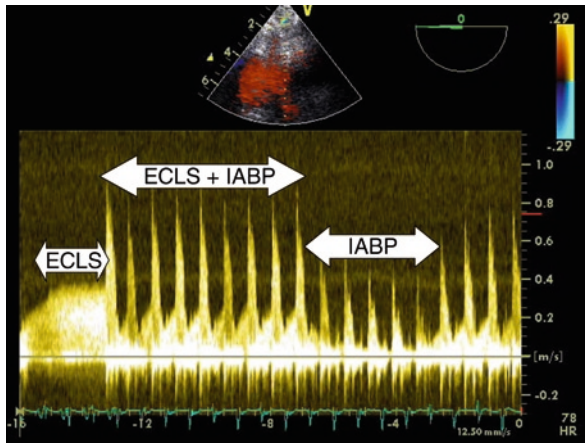

Fig. 15.10 Pulsed Doppler of the left subclavian artery blood flow in a patient with peripheral ECLS and intra-aortic balloon pump (IABP). The continuous flow of the ECLS of ≈0.3 m/s becomes pulsatile with the IABP. When ECLS is stopped, IABP alone only generates a weak pulsed flow compared with ECLS + IABP

complication related to large venous cannulas can be detected by checking the size of the SHV with echocardiography. If the maximum diameter is greater than 10 mm, cannula-related obstruction of SHV has to be suspected. Kinking of the extremity of the cannula can occur in the right atrium with consequences on venous drainage and, hence, limited maximal flow of the ECLS (Figs. 15.11 and 15.12).

Echoes of stasis (spontaneous contrast) in empty heart chambers are indicative of excess discharge

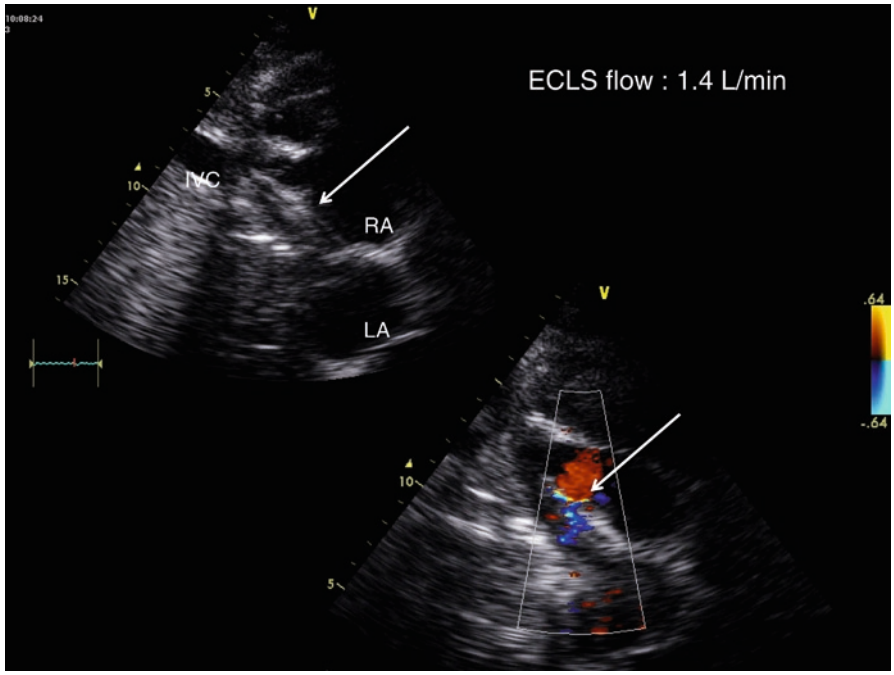

Fig. 15.11 TTE subcostal view showing a kinked cannula in the right atrium (*upper arrow*), with abnormal color flow Doppler, indicating limited inflow through side orifices (*lower arrow*) and aliasing patches coming from the side (rather than from the tip) of the cannula. In this situation, maximal output flow (8,500 rotations/min) was only 1.4 L/min

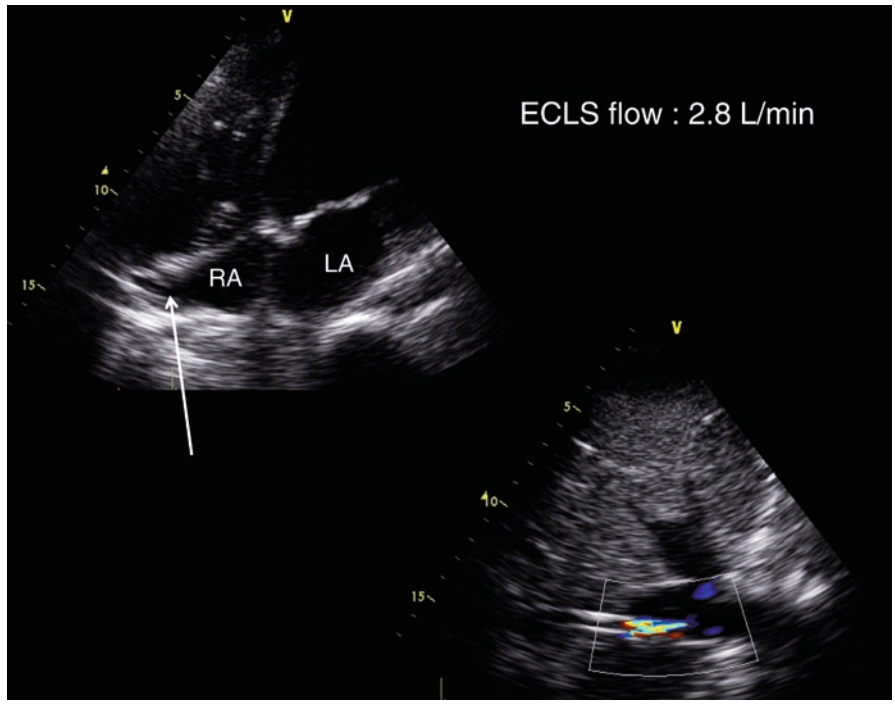

Fig. 15.12 Same patient as in Fig. 15.11 after withdrawing the venous cannula by a few centimeters. The tip is now visible at the junction between the inferior vena cava and right atrium (*arrow*); a large patch of aliased color represents aspiration flow visible at the tip of the cannula. Concomitantly, maximal output flow increased from 1.4 to 2.8 L/min for the same rotation speed of the centrifugal pump (8,500 rotations/min). Abbreviations: *RA* right atrium, *LA* left atrium

and suggest a prethrombotic state. In this situation, it is sometimes necessary to decrease the level of assistance to fill the heart chambers and reinforce inotropism (using catecholamines) in addition to anticoagulation to limit the risk of intracavitary thrombus (Fig. 15.13).

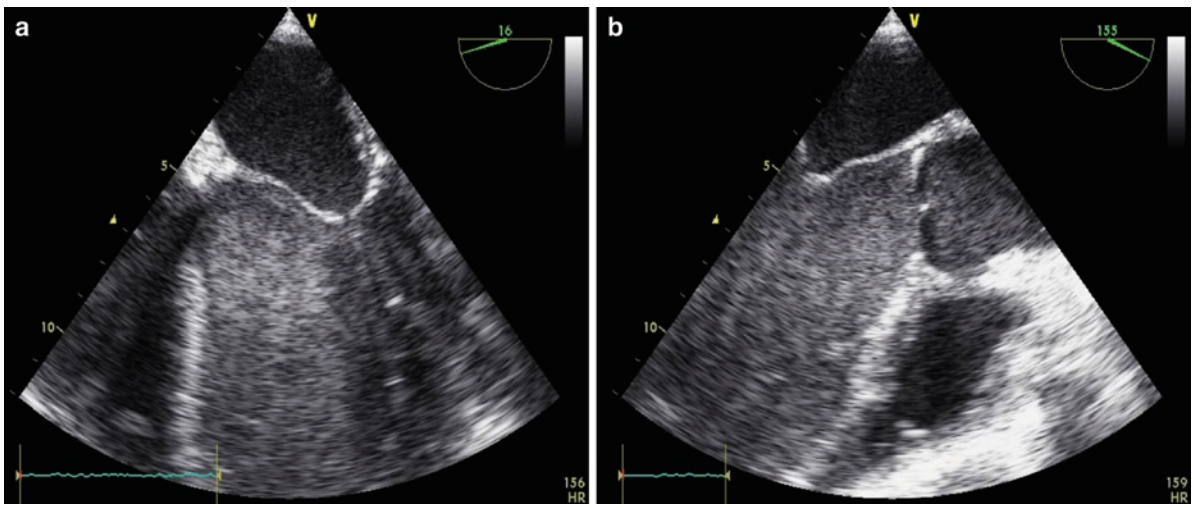

Fig. 15.13 TEE images demonstrating echoes of stasis in the left ventricle (LV; **a**) in a four-chamber view and (**b**) in a view centered on the aortic valve and LV outflow tract (130°). The absence of aortic valve opening and echoes of stasis above the aortic valve attest to a high risk of risk of thrombosis and poor coronary perfusion owing to low flow in the aortic root

15.2.3.2 ECLS for Respiratory Failure Without Associated Cardiac Failure

A preliminary echocardiographic examination is necessary to rule out a cardiogenic origin for the respiratory failure and/or an RV failure resulting from aggressive mechanical ventilation. It is not uncommon that transthoracic echocardiography (TTE) is inadequate owing to lung hyperinflation or other conditions complicating severe respiratory failure (i.e., pneumothorax) and that TEE is the technique of choice. The hallmark of cardiogenic pulmonary edema is elevation of pulmonary capillary wedge pressure (PCWP; >18 mmHg), a condition that may occur despite "normal" systolic LV function. A number of Doppler indices have been developed that can help recognize patients reliably with elevated left atrial pressure and PCWP [13,14] (see Chap. 16). The RV function also has to be examined carefully and quantified using appropriate indices (see Chap. 9).

In the absence of severe RV failure, venovenous ECMO represents the assistance of choice for isolated respiratory failure. Venous blood is aspirated by a long cannula positioned in the inferior vena cava (IVC), and reinjection is performed via a shorter cannula placed in the internal jugular vein. Correct placement of the venous cannula in the right atrium has to be systematically checked by ultrasonography, the only means of visualizing aspiration flow (Fig. 15.12). Again, the absence of hindrance to suprahepatic venous return has to be ascertained by measuring the SHV diameter. Recently, a new type of double-lumen cannula (Avalon Elite™ Bi-Caval Dual Lumen Catheter, AvalonLabs, Compton, USA) has been introduced; it allows for venous blood aspiration and reinjection after oxygenation through a single cannula (Fig. 15.14). It is essential to assess the correct placement of the reinjection port (into the right atrium) using TEE (Fig. 15.15). The greater the proportion of venous return aspirated, the better the improvement in systemic oxygenation. This is mainly determined by the caliber of the cannula. It is very important to check the tolerance of the RV to the venous return generated by the centrifugal pump. Patients with combined circulatory and respiratory failure supported with femorofemoral AV ECLS may have different partial pressure of oxygen in the arterial blood (PaO_2), depending on the site of blood sampling. Indeed, if LV ejection is not completely abolished, blood ejected by the LV is not properly oxygenated by the failing lungs and has a very low PaO_2. On the other hand, blood returning from ECLS in the iliac artery is well oxygenated.

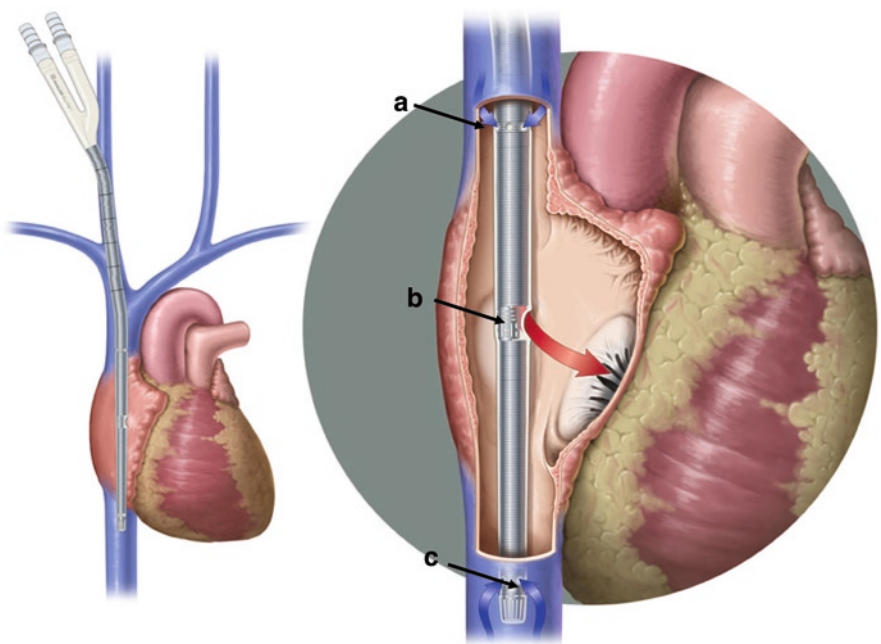

Fig. 15.14 Double-lumen cannula for internal jugular vein catheterization. Ports **a** and **c** are for venous blood aspiration in the superior and inferior vena cava, respectively. Port **b** is for reinjection of oxygenated blood in the right atrium (Source: http://www.avalonlabs.com)

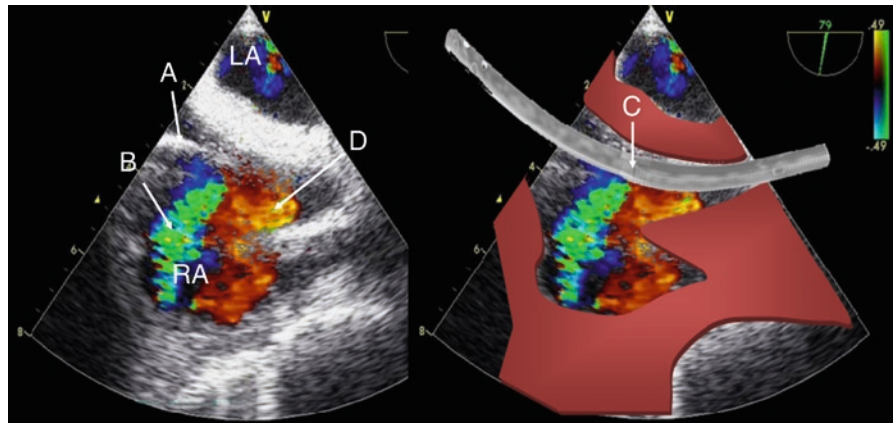

Fig. 15.15 TEE bicaval view (80–90°) showing the optimal placement of a double-lumen cannula (**a**). Oxygenated blood is reinjected (flow **b**) through port **c** into the right atrium (RA). The persistence of flow coming from the superior vena cava (**d**) attests that the cannula is not completely occlusive. Abbreviation: *LA* Left atrium

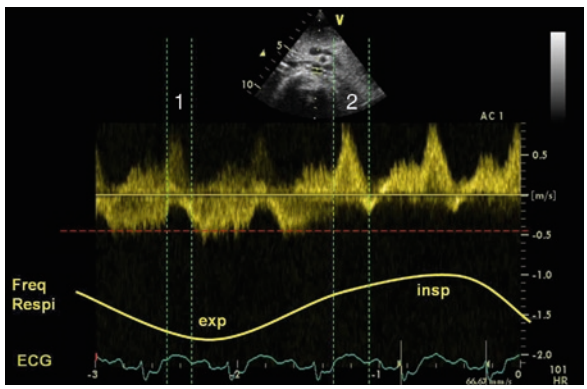

Fig. 15.16 Pulsed-Doppler recording of blood flow velocity in the descending aorta just above the renal arteries, demonstrating the respiratory changes in aortic flow direction in a patient with femorofemoral ECLS. During expiration (exp), aortic flow comes from ECLS and is retrograde (negative) with velocities becoming almost zero during ventricular systole (*vertical dotted lines*, 1). During inspiration (insp), LV ejection is facilitated (afterload reduction) and the flow moves forward during systole (*vertical dotted lines*, 2)

According to where the two competing flows (LV ejection and retrograde ECLS) "interact," coronary arteries, the brain, and upper body may receive blood with low PaO_2, while the lower part of the body is well oxygenated. Since mechanical ventilation facilitates LV ejection during insufflation (reduction in LV afterload), the direction of descending aortic flow varies according to: (1) the balance between LV ejection and retrograde perfusion; (2) the site of measurement in the aorta; and (3) the phase of the respiratory cycle (Fig. 15.16).

15.3 Role of Echocardiography During Weaning from Assistance

Experimentally, it has been shown that discharge of the heart leads initially to favorable myocardial remodeling, followed by pathological myocardial fibrosis 3–4 weeks later [14]. Assessing cardiac recovery using echocardiography during mechanical assistance presents some challenges. An echocardiographic index evaluating discharged hearts has been proposed to evaluate myocardial damage in a model of heterotopic cardiac transplantation [15]. This left ventricular wall area index (LVWAI) derived from the calculation of cardiac mass is calculated as the difference between the "epicardial" and "endocardial" LV short-axis areas measured at end diastole in the short-axis mid-papillary level divided by epicardial area:

$$\text{LVWAI} = \text{Epicardial Area} - \text{Endocardial Area} / \text{Epicardial Area}$$

This index was experimentally correlated with myocardial damage in unloaded hearts. In the context of cardiac assistance, quality of myocardial recovery in discharged hearts is difficult to assess, and no echocardiographic index has been formally validated. It is therefore necessary to perform echocardiographic evaluation while assistance is reduced to a minimum (i.e., flow of 0.5–0.6 L/min/m). If such low flows are to be maintained longer than the period of echocardiographic examination, the risk of clotting is increased and anticoagulation should be reinforced. Under such conditions, the usual parameters of

ventricular function and stroke volume are likely to represent what the heart would do without assistance. The decision to wean the patient from the circulatory assist device relies not only on the absolute performance observed under minimal support, but also on the time course of improvement over several hours or days, indicating that the recovery process is ongoing.

In the future, it is possible that measurements of tissue deformation using strain and strain rate may be useful in evaluating recovery [16] (Figs. 15.17 and 15.18). However, data validating the use of strain rate to quantify myocardial recovery after circulatory assistance is still scarce [17], and the technique has not yet become routine. In our experience, inferobasal wall-motion improvement on echocardiography is an early

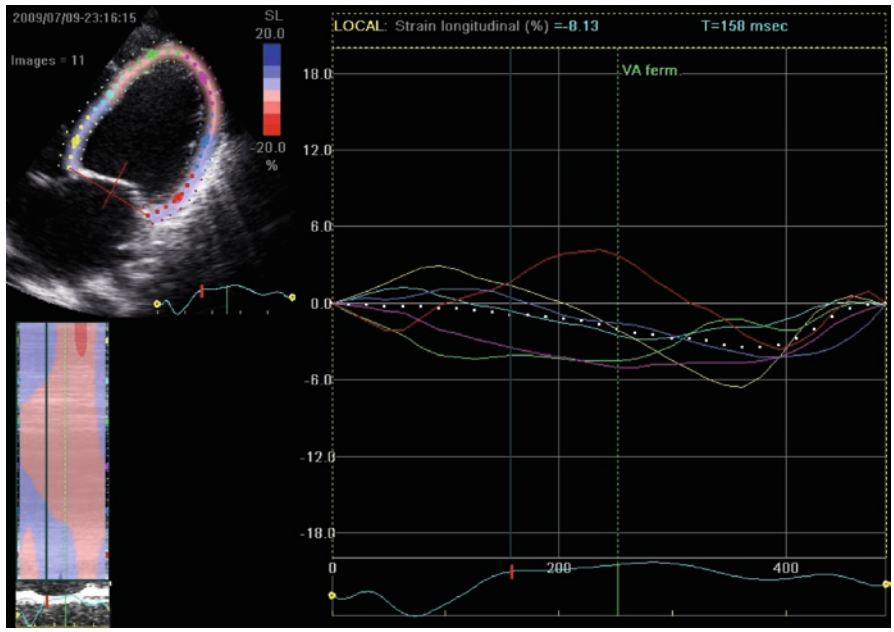

Fig. 15.17 Two-dimensional strain analysis of the LV in a patient with severely dilated cardiomyopathy

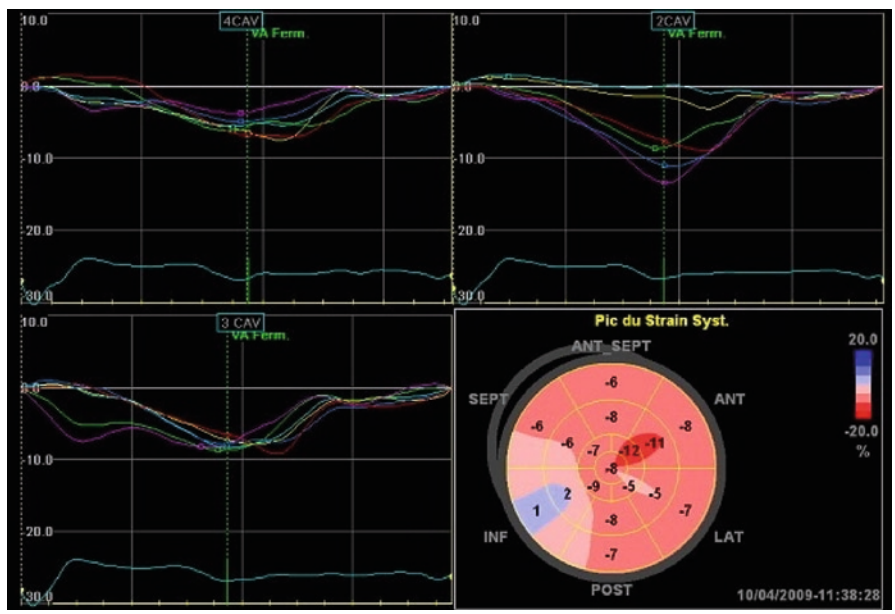

Fig. 15.18 Regional LV systolic strain pattern, showing improvement in systolic function after peripheral assistance

sign of myocardial recovery after initiation of mechanical support. The place of biomarkers in combination with clinical and echocardiographic criteria to assess myocardial recovery is currently being investigated.

15.4 Conclusions

Echocardiography is extremely useful for the management of patients requiring mechanical circulatory and/or respiratory support using short-term assistance. Echocardiography not only helps in recognizing the cause of circulatory failure and quantifying ventricular function and ejectional performance (stroke volume), but it also detects potential contraindications to the use of assist devices. Echocardiography also facilitates device implantation by visualizing vessels at the cannulation sites and proper placement of devices in the aorta and heart chambers. The noninvasive character of ultrasound allows for serial examinations to assess tolerance and proper function of assistance and sometimes to detect complications and guide therapeutic interventions. Finally, echocardiography offers an invaluable safety net prior to weaning the patient from circulatory support.

References

1. Birks EJ, Tansley PD, Hardy J, George RS, Bowles CT, Burke M, Banner NR, Khaghani A, Yacoub MH (2006) Left ventricular assist device and drug therapy for the reversal of heart failure. N Engl J Med 355:1873–84
2. Catena E, Milazzo F (2007) Echocardiography and cardiac assist devices. Minerva Cardioangiol 55:247–65
3. Dixon SR, Henriques JP, Mauri L, Sjauw K, Civitello A, Kar B, Loyalka P, Resnic FS, Teirstein P, Makkar R, Palacios IF, Collins M, Moses J, Benali K, O'Neill WW (2009) A prospective feasibility trial investigating the use of the Impella 2.5 system in patients undergoing high-risk percutaneous coronary intervention (The PROTECT I Trial): initial U.S. experience. JACC Cardiovasc Interv 2:91–6
4. Samoukovic G, Rosu C, Giannetti N, Cecere R (2009) The Impella LP 5.0 as a bridge to long-term circulatory support. Interact Cardiovasc Thorac Surg 8:682
5. Moazami N, Argenziano M, Kohomoto T, Yazdani S, Rose EA, Burkhoff D, Oz MC (1998) Inflow valve regurgitation during left ventricular assist device support may interfere with reverse ventricular remodeling. Ann Thorac Surg 65:628–31
6. Vargas F, Gruson D, Valentino R, Bui HN, Salmi LR, Gilleron V, Gbikpi-Benissan G, Guenard H, Hilbert G (2004) Transesophageal Pulsed Doppler echocardiography of pulmonary venous flow to assess left ventricular filling pressure in ventilated patients with acute respiratory distress syndrome. J Crit Care 19:187–97
7. Koenig PR, Ralston MA, Kimball TR, Meyer RA, Daniels SR, Schwartz DC (1993) Balloon atrial septostomy for left ventricular decompression in patients receiving extracorporeal membrane oxygenation for myocardial failure. J Pediatr 122(6):S95–9
8. Downing SW, Llaneras M, Georgi D, Wood DC, Savage EB, Edmunds LH Jr (1992 Jan) Left ventricular assistance without thoracotomy: mediastinal and transseptal approaches to the left heart. Ann Thorac Surg 53(1):132–8
9. Jouan J, Grinda JM, Bricourt MO, Cholley B, Fabiani JN (2010 Jan) Successful left ventricular decompression following peripheral extracorporeal membrane oxygenation by percutaneous placement of a micro-axial flow pump. J Heart Lung Transplant 29(1):135–6, Epub 2009 Sep 26
10. Lam K, Sjauw KD, van der Meulen J, Symersky P, Biervliet JD, Henriques JP, de Mol BA (2009) A combined surgical and percutaneous approach through the axillary artery to introduce the Impella LP5.0 for short-term circulatory support. Int J Cardiol 134:277–9
11. Gupta A, Allaqaband S, Bajwa T (2009) Combined use of impella device and intra-aortic balloon pump to improve survival in a patient in profound cardiogenic shock post cardiac arrest. Catheter Cardiovasc Interv 74:975–6
12. Vatta M, Stetson SJ, Jimenez S, Entman ML, Noon GP, Bowles NE, Towbin JA, Torre-Amione G (2004) Molecular normalization of dystrophin in the failing left and right ventricle of patients treated with either pulsatile or continuous flow-type ventricular assist devices. J Am Coll Cardiol 43:811–7
13. Vignon P, AitHssain A, Francois B, Preux PM, Pichon N, Clavel M, Frat JP, Gastinne H (2008) Echocardiographic assessment of pulmonary artery occlusion pressure in ventilated patients: a transoesophageal study. Crit Care 12:R18
14. Oriyanhan W, Tsuneyoshi H, Nishina T, Matsuoka S, Ikeda T, Komeda M (2007) Determination of optimal duration of mechanical unloading for failing hearts to achieve bridge to recovery in a rat heterotopic heart transplantation model. J Heart Lung Transplant 26:16–23
15. Gilman G, Hansen WH, Hagen ME, Rosales AG, Bailey KR, McGregor CG, Belohlavek M (2006) An echocardiographic left ventricular wall area index for functional detection of myocardial injury in hemodynamically unloaded hearts. Echocardiography 23:7–13
16. Yildirim A, Soylu O, Dagdeviren B, Zor U, Tezel T (2007) Correlation between Doppler derived dP/dt and left ventricular asynchrony in patients with dilated cardiomyopathy: a combined study using strain rate imaging and conventional Doppler echocardiography. Echocardiography 24: 508–14
17. Havemann L, McMahon CJ, Ganame J, Price J, Fraser CD, Eidem BW, Pignatelli RH (2006) Rapid ventricular remodeling with left ventricular unloading postventricular assist device placement: new insights with strain imaging. J Am Soc Echocardiogr 19:355 e9–355 e11

Part IV

Diagnosis and Management of Acute Respiratory Failure

Pulmonary Edema: Which Role for Echocardiography in the Diagnostic Workup?

16

Philippe Vignon, Frances Colreavy, and Michel Slama

Contents

P. Vignon (✉)
Medical-surgical Intensive Care Unit, Dupuytren Teaching Hospital, 2 Ave. Martin Luther King, 87042, Limoges Cedex, France, and
Clinical Investigation Center (INSERM 0801) Dupuytren Teaching Hospital, 2 Ave. Martin Luther King, 87042, Limoges Cedex, France, and
University of Limoges, 2 Ave. Dr Marcland, 87000, Limoges, France
e-mail: philippe.vignon@unilim.fr

F. Colreavy
Department of Intensive Care, Mater Misercordiae Hospital, Eccles Street, Dublin 7, Ireland
e-mail: fcolreavy@mater.ie

M. Slama
Medical Intensive Care Unit, Nephrology Department, South Teaching Hospital, 80054 Amiens Cedex 1, France, and
INSERM ERI 12 unit, Picardie Jules Verne University, France
e-mail: slama.michel@chu-amiens.fr

Pulmonary edema refers to the presence of excessive fluid in the interstitial spaces and alveoli of the lung. Increased hydrostatic pressure within the pulmonary vascular beds may lead to the efflux of plasmatic water through a normal alveolocapillary membrane and ultimately to a so-called hydrostatic or hemodynamic pulmonary edema. Since the most frequent cause of pulmonary venous congestion is acute heart failure, this type of pulmonary edema is also termed cardiogenic [1]. This clinical entity has to be distinguished from acute respiratory distress syndrome (ARDS), which corresponds to an acute pulmonary edema associated with fairly low pulmonary capillary pressures and severe lesions of the alveolocapillary membrane [2]. Importantly, the absence of relevant left ventricular (LV) systolic dysfunction fails to rule out a hydrostatic pulmonary edema (e.g., acute valvular regurgitation, volume overload, severe diastolic dysfunction, mitral stenosis) [3]. Alternatively, an ARDS may be associated with a significant LV systolic dysfunction (e.g., septic shock) [4, 5]. Consequently, the diagnosis of hydrostatic pulmonary edema relies on the documentation of (markedly) elevated LV filling pressures, regardless of pump function [3].

This introducing chapter reviews principal Doppler parameters employed on clinical grounds for the estimation of LV filling pressures and proposes a diagnostic algorithm for the practical use of echocardiography in the management of patients presenting with an acute respiratory failure secondary to a pulmonary edema.

16.1 Definitions and Pathophysiology

Contraction is the process during systole by which the heart develops pressure and ejects its stroke volume. Relaxation is the process by which the heart

D. De Backer et al. (eds.), *Hemodynamic Monitoring Using Echocardiography in the Critically Ill*,
DOI: 10.1007/978-3-540-87956-5_16, © Springer-Verlag Berlin Heidelberg 2011

returns to its precontractile configuration. Both contraction and relaxation require energy for the activation and inactivation processes (attachment and detachment of actine–myosine cross-bridges, respectively). Compliance refers to a passive property of the heart: the volume/pressure relationship of its chambers during cardiac filling. Accordingly, diastole has two components: relaxation (energy-requiring process) and compliance (passive intrinsic property of the heart). Physiologically, ventricular relaxation begins during the ejection of the stroke volume, when the peak pressure generated by the maximal shortening of the myocardial fibrils is reached, whereas clinically it begins with mitral valve closure [6]. Isovolumetric relaxation and early ventricular filling are influenced by relaxation, while compliance mainly operates at mid- to late diastole, during diastasis and atrial contraction [7]. Diastolic dysfunction refers to the presence of an abnormal diastolic distensibility, filling, or relaxation of the LV. Diastolic heart failure refers to patients with the symptoms and signs of heart failure and LV diastolic dysfunction, but a normal ejection fraction [7]. Diastolic dysfunction may be present in symptomatic or asymptomatic patients, regardless of the value of the ejection fraction or systolic functional state. It is characterized by an impaired, hence prolonged (active), relaxation, with potentially decreased (passive) LV compliance (Fig. 16.1). Marked regional heterogeneity in LV relaxation properties is frequent (Fig. 16.2) [8]. The overall net result is impaired diastolic filling of LV cavity and increased filling pressures. Accordingly, patients with clinical evidence of diastolic heart failure exhibit elevated LV filling pressures – hence, pulmonary venous congestion that may lead to hydrostatic pulmonary edema – resulting from a prolonged LV relaxation and reduced LV compliance [9].

The distinction between systolic and diastolic heart failure is somewhat arbitrary (Table 16.1). Virtually all patients with symptomatic heart failure have LV diastolic dysfunction and most patients with heart failure have both systolic and diastolic dysfunction at rest or during exercise [1]. Similar to patients with systolic heart failure, patients with diastolic heart failure have symptoms initially on exertion and ultimately at rest [10, 11]. Both systolic and diastolic

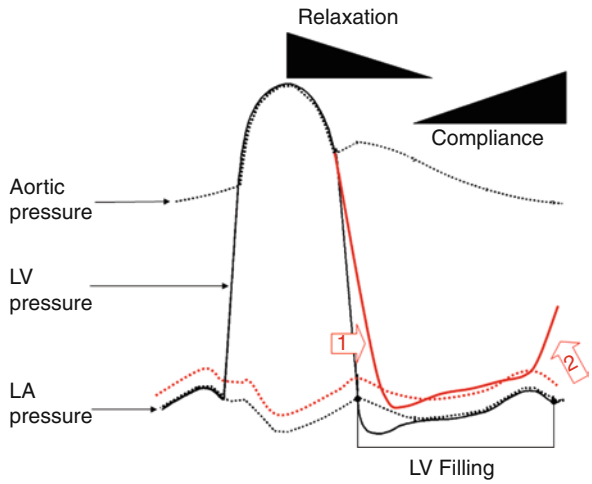

Fig. 16.1 The impact of diastolic dysfunction on left ventricular (LV) filling pressures. Relaxation is an active phenomenon that begins during the ejection phase and is prominent during early diastole, while compliance is a passive property of the LV that is operant during mid- to late diastole. Diastolic dysfunction is characterized by an impaired (i.e., prolonged) relaxation (*arrow* 1), with potentially associated decreased compliance of the LV (*arrow* 2). Overall, LV filling pressures are increased, especially at end diastole (*red solid line*). To maintain the transmitral pressure gradient, left atrial (LA) pressure increases (*red dashed line*)

heart failure result in significantly increased LV filling pressures, which may ultimately lead to hydrostatic pulmonary edema (Fig. 16.3). Subtle LV regional systolic abnormalities (e.g., altered long-axis shortening) have been described in patients with apparently isolated LV diastolic dysfunction using tissue Doppler imaging [12–16]. Precipitating factors triggering congestive failure (e.g., excessive sodium intake, medication noncompliance, volume overload, hypertension, atrial fibrillation) are similar for systolic and diastolic heart failure [17]. Finally, systolic and diastolic heart failure have a common etiology: ischemic cardiomyopathy remains the most frequent cause of heart failure [1]. Systolic heart failure typically associates a decreased myocardial contractility and a dilatation of LV cavity secondary to eccentric remodeling [18]. Diastolic heart failure refers to patients with the symptoms and signs of heart failure, a normal LV ejection fraction, and LV diastolic dysfunction [7]. In these patients, a concentric pattern of LV remodeling secondary to the development of hypertrophy is common (Table 16.1).

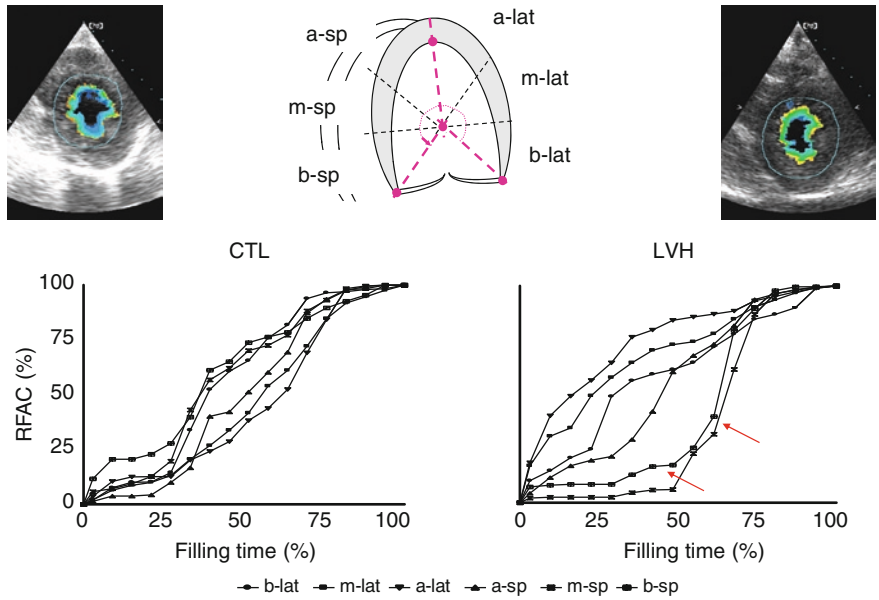

Fig. 16.2 Left ventricular (LV) regional diastolic properties depicted by color kinesis. This technique color-encodes the endocardial displacement on a frame-by-frame basis, such that a single end-diastolic frame provides an integrated display of the timing and magnitude of endocardial wall motion during LV filling (*upper panels*, *left* and *right*). End-diastolic color-encoded images can be divided into segments (*upper panel*, *middle*), in which colored pixel counts are used to calculate regional fractional area change (RFAC), which can be displayed as a function of filling time (*lower panels*). When compared with a normal age-matched subject (CTL, *lower left*), the patient with left ventricular hypertrophy (LVH, *lower right*) and associated diastolic heart failure exhibits regional endocardial motion asynchrony, as reflected by a heterogeneous profile of regional time curves. In this patient, relaxation appears particularly prolonged in the basal and mid-septal LV segments (*lower right*, *red arrows*). This results in a progressive increase of left atrial pressure to maintain LV filling. Abbreviations: *b-lat* basal lateral, *m-lat* mid-lateral, *a-lat* apical lateral, *a-sp* apical septal, *m-sp* mid septal, *b-sp* basal septal

16.2 LV Diastolic Function and Filling Pressures

LV diastolic properties and LV filling pressures are closely linked. Normal diastolic function can be defined as the ability of the LV to fill up to a normal end-diastolic volume without significant increase in left atrial pressure (<12 mmHg) at rest and during exercise. The consequences of LV diastolic dysfunction are threefold. First, prolonged LV relaxation substantially reduces early diastolic filling. Second, the left atrial contribution to LV filling significantly increases to compensate reduced early diastolic filling. Third, filling pressures gradually increase to maintain the transmitral pressure gradient, hence LV filling (Fig. 16.1). As a result, pulmonary venous congestion can develop initially on exertion and ultimately at rest.

16.3 Estimation of LV Filling Pressures with Echocardiography Doppler

Determination of LV filling pressures – but not of LV systolic performance – allows for the distinction between hydrostatic pulmonary edema and ARDS [2, 3]. LV filling pressures are challenging to predict by physical examination alone [19, 20]. Invasive measurement of end-diastolic LV pressure is the gold standard. Unfortunately, this measurement is not routinely accessible on clinical grounds, and measurement of the pulmonary artery occlusion pressure (PAOP) during right-heart catheterization (RHC) is usually used as a surrogate. Echocardiography Doppler appears as a valuable and less invasive alternative modality for serial bedside assessment of LV filling pressures in critically ill patients.

Table 16.1 Structural and functional characteristics of systolic and diastolic left ventricular failure

	Systolic heart failure	Diastolic heart failure
Congestive state (pulmonary edema)[a]	Yes	Yes
Precipitating factors[b]	Yes	Yes
End-diastolic pressure	Increased	Increased
Relaxation	Prolonged	Prolonged
Contractility	Decreased	Normal
Ejection fraction	Decreased	Normal
Left ventricular mass	Increased	Increased
Type of remodeling	Eccentric	Concentric
End-diastolic volume	Increased	Normal to decreased
End-systolic volume	Increased	Normal to decreased
Left atrial size[c]	Increased	Increased

[a]Similar clinical presentation for both conditions
[b]Similar trigger for subacute or acute decompensation of underlying diastolic dysfunction present in both systolic and diastolic heart failure
[c]Left atrial dilatation reflects chronically elevated filling pressure

16.3.1 Principles and Technique of Measurements

The basic principle is that (1) the blood flow that fills the LV is driven by the instantaneous diastolic pressure gradient across the mitral valve, and (2) Doppler accurately measures blood flow velocity. In the absence of significant mitral valvular disease or pericardial constraint, the mitral Doppler velocity profile primarily results from the diastolic pressure gradient between the left atrium (main determinant for pulmonary venous congestion) and the LV (mostly related to its relaxation and compliance) [21]. Pulmonary vein flow Doppler may also be used to evaluate left cardiac filling pressures [22]. Tissue Doppler imaging of the mitral annulus and color M-mode Doppler of early diastolic LV blood inflow have also been proposed to evaluate more precisely both LV relaxation and filling pressures [23].

Pulse-wave Doppler is used to measure blood-flow velocities (Fig. 16.4). In sinus rhythm, the mitral Doppler velocity profile is biphasic with an early diastolic wave (E wave) and a late diastolic wave during atrial contraction (A wave). Pulmonary vein flow comprises a systolic forward wave (S wave), a diastolic forward wave (D wave), which mirrors the mitral E wave, and a reverse wave during atrial contraction (Ar wave). Tissue Doppler imaging and color M-mode Doppler provide further insights into LV relaxation properties (Fig. 16.4). Tissue Doppler imaging allows the measurement of early diastolic mitral annulus velocity (E' or E_a), which is primarily influenced by LV relaxation rate [24]. Color M-mode Doppler propagation velocity of blood flow entering the LV during early diastole (V_p) is closely related to LV relaxation rate [25]. Technical recommendations for adequate Doppler velocity recordings have been detailed elsewhere [26] and are summarized in (Table 16.2).

Numerous Doppler indices derived from transmitral and pulmonary venous flow velocity recordings have been validated to estimate LV filling pressures (Fig. 16.5). The frontline intensivist should routinely use easy-to-measure and reproducible Doppler parameters, such as maximal Doppler velocities and their ratios – *E*/*A* (mitral flow) and *S*/*D* (pulmonary venous flow) – and the systolic fraction of pulmonary venous flow [27]. In contrast, the isovolumic relaxation time, the deceleration time of the mitral E wave and pulmonary vein D wave, and the respective duration of the mitral A wave and pulmonary vein reverse wave during atrial contraction (Ar-A) are more challenging to measure accurately and less reproducible [28]. Normal and pathological values of commonly used Doppler indices are listed in Table 16.3.

Although mitral Doppler velocities are mainly determined by LV diastolic properties and filling pressure, they can also be substantially altered by other confounding factors, such as age, heart rate, and ventricular interactions [29] (Fig. 16.6). Both E_a and V_p reflect the rate of LV relaxation [24, 25]. This has led to normalizing mitral E-wave maximal velocity using these indices to improve the accuracy of Doppler estimation of LV filling pressure [30–32]. E_a appears as a relatively preload-independent tissue Doppler parameter when measured at the lateral mitral ring (as opposed to the septal mitral ring), but not V_p [28]. Whether these indices are minimally or significantly altered by abrupt variations in LV loading conditions remains controversial. E_a appears as a reproducible parameter, whereas V_p needs training to be accurately

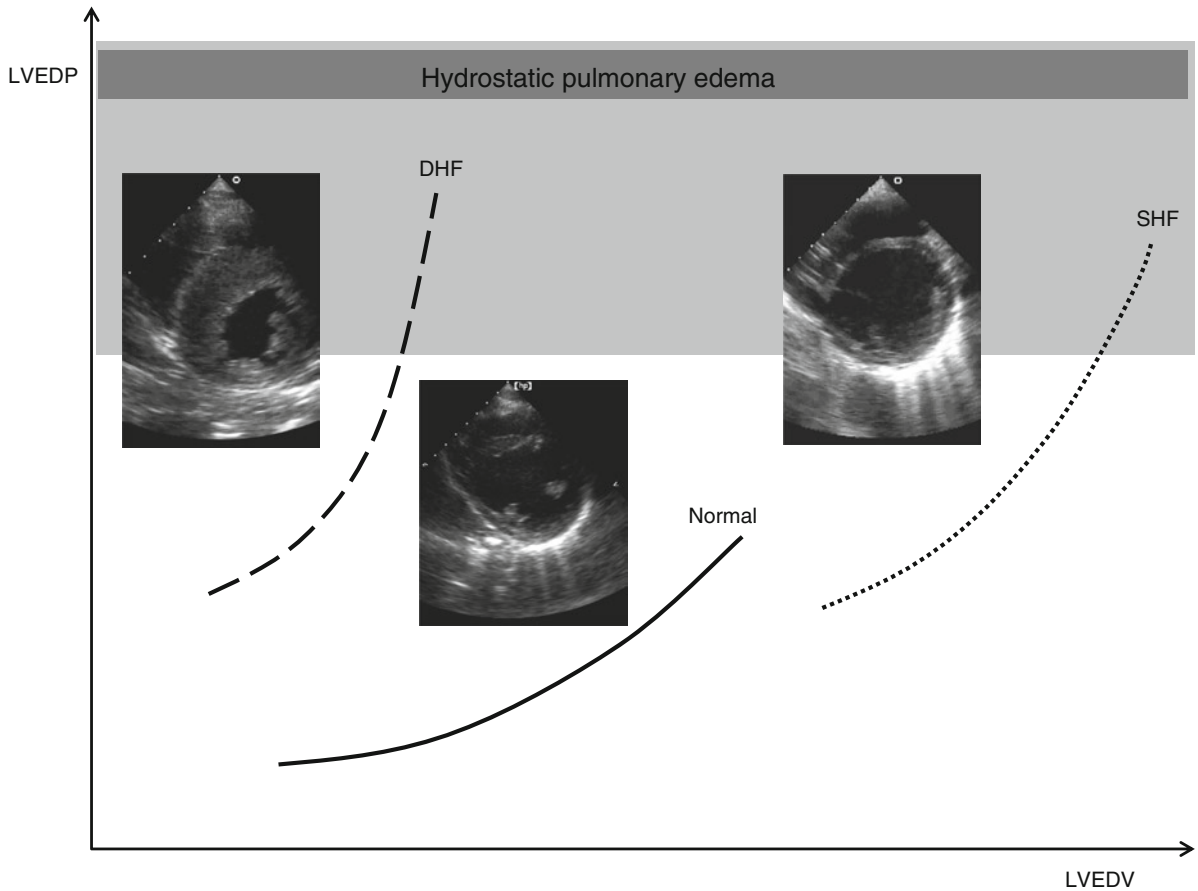

Fig. 16.3 Schematic left ventricular (LV) diastolic pressure-volume curves of a normal heart (*solid line*) and in the presence of diastolic heart failure (DHF, *dashed line*), and systolic heart failure (SHF, *dotted line*). When compared with a normal heart (*middle panel*), diastolic heart failure is typically characterized by an increase in LV diastolic pressure and a frequently decreased cavity volume as a result of concentric remodeling (*left panel*). Systolic heart failure is commonly characterized by an increase in LV diastolic pressure and an increased cavity volume resulting from an eccentric remodeling (*right panel*). Owing to increased LV filling pressure, both systolic and diastolic heart failure may lead to hydrostatic pulmonary edema (*gray area*). Abbreviations: *LVEDP* left ventricular end-diastolic pressure; *LVEDV* left ventricular end-diastolic volume

measured with minimal intraobserver variability [28, 31]. E_a is normally >15 and >10 cm/s when measured at the lateral and septal aspects of the mitral ring, respectively [23]. Decreased E_a velocity <8 cm/s or V_p <45 cm/s are consistent with an underlying LV diastolic dysfunction [23].

16.3.2 Evolution of Doppler Patterns

With the progression of LV diastolic dysfunction, filling pressures gradually increase to maintain stroke volume [33]. This progressively alters mitral Doppler velocity profile (Fig. 16.7). Therapeutic interventions modifying LV loading conditions may also rapidly alter the mitral Doppler pattern (Fig. 16.8). This explains why the diagnostic capacity of echocardiography Doppler is maximal when performed at the time of the acute respiratory failure, prior to the initiation of therapy [3]. With previously mentioned limitations, the frontline intensivist may grossly evaluate the level of LV filling pressure based on the qualitative interpretation of both the mitral Doppler pattern and cardiac two-dimensional examination (Fig. 16.9). LV remodeling (enlarged cavity size), LV concentric hypertrophy, or LV regional wall-motion abnormality consistent with an ischemic cardiomyopathy suggest the presence

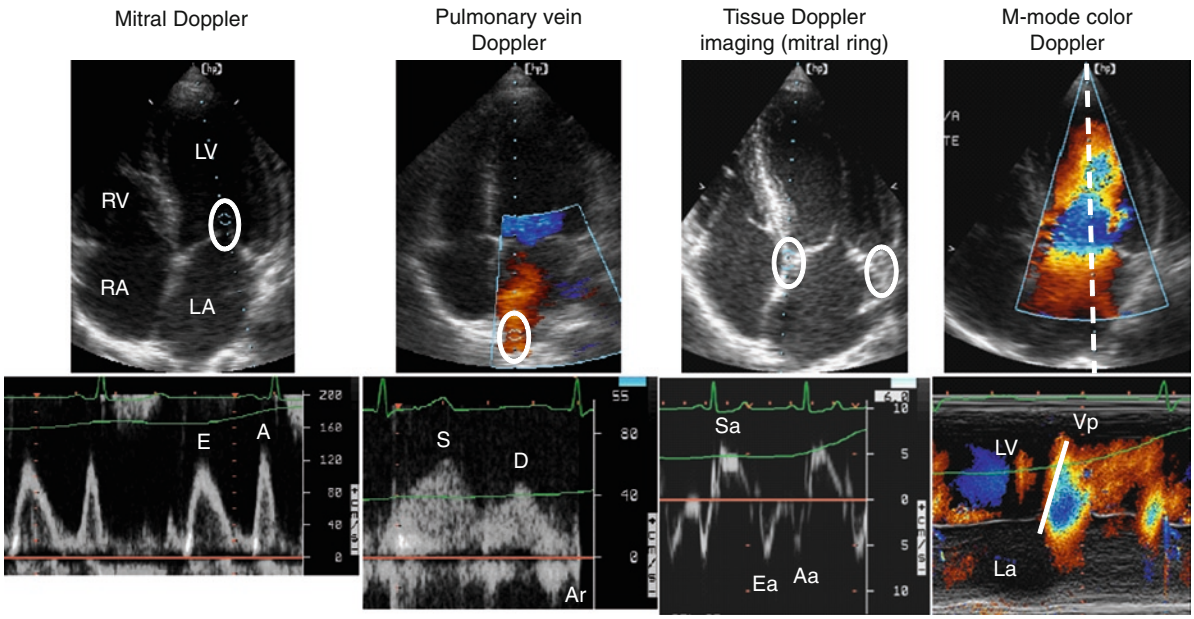

Fig. 16.4 Doppler evaluation of left ventricular (LV) diastolic properties and filling pressures using transthoracic echocardiography (apical four-chamber view). The spatial resolution of pulsed-wave Doppler allows the measurement of blood-flow velocity at the tip of the mitral valve and in the distal pulmonary veins. Tissue Doppler imaging permits the measurement of lower velocities, such as myocardial velocities, which are routinely recorded at the lateral and septal aspects of the mitral ring. Color M-mode Doppler allows the measurement of the propagation velocity of blood flow entering the LV during early diastole. From each velocity profile, various quantitative indices can be measured. Abbreviations: *LA* left atrium, *RV* right ventricle, *RA* right atrium, *Ea* early mitral wave, *A* mitral wave during atrial contraction, *Sa* systolic wave of pulmonary vein flow Doppler pattern, *D* diastolic wave of pulmonary vein flow Doppler pattern, *Ar* reverse wave during atrial contraction, *Sa* systolic wave of tissue Doppler imaging of the mitral ring, *Ea* early diastolic wave of tissue Doppler imaging of the mitral ring, *Aa* late diastolic wave of tissue Doppler imaging of the mitral ring, V_p propagation velocity of blood flow entering the LV during early diastole

of an associated LV diastolic dysfunction. A dilated left atrium with abnormal atrial septal motion (continuous bulging toward the right atrium) reflects the presence of chronically elevated left atrial pressures [34]. This rapid and empirical interpretation can be subsequently confirmed by a quantitative assessment of LV filling pressures (e.g., determination of E/E_a ratio), especially in the presence of an associated cardiopathy.

16.3.3 Validation of Doppler Assessment of LV Filling Pressure

Initial studies have been conducted in the setting of spontaneously breathing cardiac patients presenting with acute heart failure [30, 35–41]. They have uniformly shown that combined Doppler indices fairly predict invasive PAOP. Nevertheless, absolute prediction of RHC-derived PAOP by Doppler appears more accurate for high LV filling pressures [38, 39]. This quantitative approach is cumbersome because it requires multiple tedious measurements combined in complex equations. Therefore, subsequent studies have used a semiquantitative strategy, which tested different threshold values of simple, yet robust, Doppler parameters to predict various levels of invasive PAOP (Table 16.4).

Only a few studies have been conducted in mechanically ventilated patients, all of them using a semiquantitative approach [31, 42–45]. Accurate prediction of a predefined level of invasive PAOP by Doppler indices is of clinical value in ventilated patients presenting with acute respiratory failure since the current

Table 16.2 Technical recommendations for obtaining optimal Doppler recordings of mitral and pulmonary venous flows

Step	Technical recommendations
1	Obtain a true apical (TTE) or transesophageal (TEE) four-chamber view of the heart that excludes the aortic valve
2	Try to reduce the angle between the ultrasound beam and blood flow (visualized with color Doppler mapping) as much as possible (<20°): • Mitral inflow: translate the transducer from the true apical four-chamber view to a slightly more lateral position (TTE) or adjust the depth of the probe into the esophagus or slightly rotate the esophageal probe (TEE) • Pulmonary venous flow: use a slight anterior angulation from the apical four-chamber view to visualize the right upper pulmonary vein (TTE) or slightly withdraw the esophageal probe and rotate the transducer (~20–40°) to obtain a true long-axis view of the left upper pulmonary vein (TEE)
3	Use a small pulsed-wave Doppler sample volume: • Mitral inflow: 1–2 mm • Pulmonary venous flow: 2–3 mm
4	Place the sample volume adequately: • Mitral inflow: between the tips of the mitral leaflets • Pulmonary venous flow: 1–2 cm into the pulmonary vein
5	Use a sweep speed of 50 mm/s (appreciation of the influence of the respiratory cycle on Doppler velocities) or 100 mm/s (measurement of flow duration or deceleration time) Use ECG and respiratory tracings, especially in ventilated patients Set velocity filter as low as possible (200–600 Hz)
6	Perform all measurements at end expiration (or during apnea) to limit the effects of heart–lung interactions on Doppler velocities (select appropriate Doppler velocity profiles with respiratory tracings)
7	Measure Doppler parameters as follows: • *Maximal velocities*: determine the peak velocity of each Doppler wave (mitral E and A waves, pulmonary vein S and D waves) • *Deceleration time*: extend the deceleration slope from the peak wave velocity to the zero-velocity baseline (mitral E wave and pulmonary vein D wave) • *Velocity–time integral*: trace manually the external contour of the spectral display to improve reproducibility (mitral E and A waves, pulmonary vein S and D waves) • *Duration*: perform measurement as close to the zero-velocity baseline as possible from the start of flow at the onset of atrial contraction to the end of flow at mitral valve closure (mitral A wave and pulmonary vein Ar wave)
8	Repeat measurements on nonconsecutive heart beats and respiratory cycles, check for consistency and average ≥3 values
9	Take into account patient's age to interpret obtained Doppler parameters (physiological modification of LV diastolic properties with aging)

Abbreviations: *TTE* transthoracic echocardiography, *TEE* transesophageal echocardiography, *LV* left ventricle
Adapted from [26])

hemodynamic criterion of ARDS relies on the documentation of a pulmonary artery wedge pressure ≤18 mmHg [2]. Concordant results support the use of simple Doppler parameters to satisfactorily predict clinically relevant invasive PAOP levels in ventilated ICU patients (Table 16.5). Interestingly, combined Doppler indices – namely *E/Ea* or *E/Vp* – fail to improve the prediction of LV filling pressures (Table 16.6). Presumably, the influence of impaired LV relaxation minimally alters mitral E-wave maximal velocity in this specific population, thus offsetting the potential additional value of combining this conventional Doppler parameter with a relatively preload-independent Doppler index that better reflects LV diastolic properties [29, 46]. This hypothesis has already been raised in a study of healthy volunteers, where the

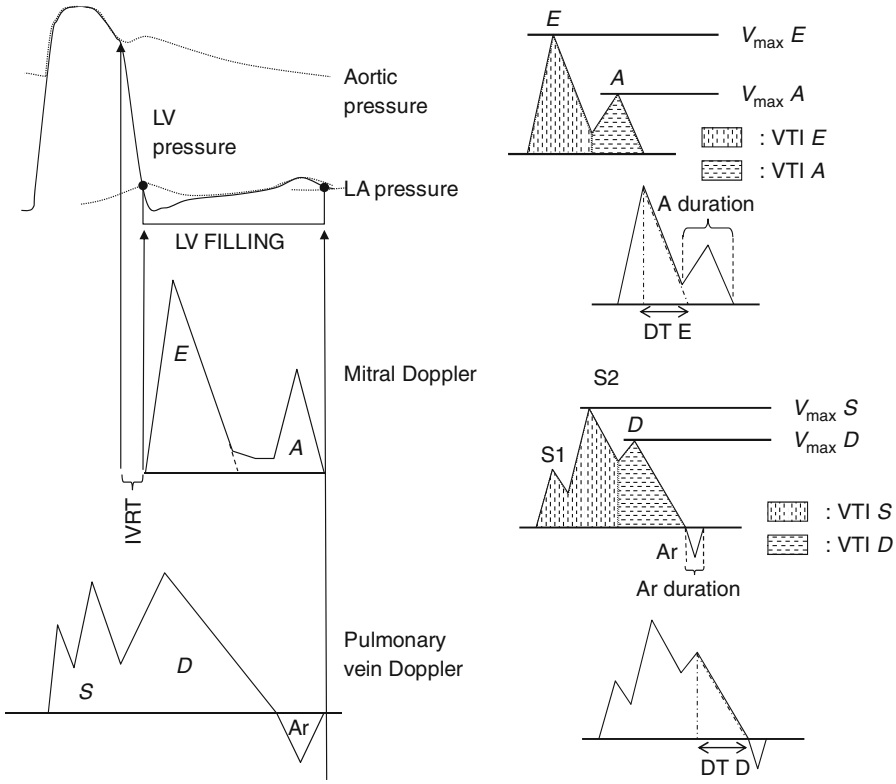

Fig. 16.5 Main pulsed-wave Doppler indices routinely used for the evaluation of left ventricular (LV) diastolic properties and filling pressures. Maximal velocities (V_{max}) and velocity–time integrals (VTI) are fairly easy to measure and are reproducible. Deceleration times (DT) and durations of mitral A wave and pulmonary reverse wave (Ar) are more challenging to measure accurately. Abbreviations: *LA* left atrium, *E* early mitral wave, *A* mitral wave during atrial contraction, *S* systolic wave of pulmonary vein flow Doppler pattern, *D* diastolic wave of pulmonary vein flow Doppler pattern, *Ar* reverse wave during atrial contraction, *IVRT* isovolumic relaxation time

Table 16.3 Normal and pathological values of commonly used Doppler indices

Doppler parameters	Normal	Abnormal relaxation	Normalized profile	Restrictive profile
IVRT (ms)	<100	>100	60–100	<60
Mitral Doppler:				
E/*A*	>1	<1	1–2	>2
DT_E (ms)	<220	>220	150–200	<150
Pulmonary vein Doppler:				
S/*D*	≥1[a]	≥1	<1	<1
Ar (cm/s)	<35	<35	≥35[b]	≥25[b]
TDI of mitral ring:				
Ea (cm/s)	>10–15[c]	<8	<8	<8
Color M-mode Doppler:				
Vp (cm/s)	>45[d]	<45	<45	<45

Abbreviations: *IVRT* isovolumetric relaxation time, *E*/*A* early to late mitral Doppler velocity ratio, DT_E deceleration time of mitral E wave, *S*/*D* systolic to diastolic maximal velocity of pulmonary vein Doppler, *Ar* maximal Doppler velocity of the reverse wave during atrial contraction, *TDI* Tissue Doppler Imaging, *Ea* maximal TDI velocity of mitral ring during early diastole, V_p propagation velocity of blood flow entering the left ventricle during early diastole

[a]<1 in young subjects

[b]Unless atrial contractility is reduced

[c]According to the site of measurement

[d]>55 cm/s in young subjects

Modified from [23]

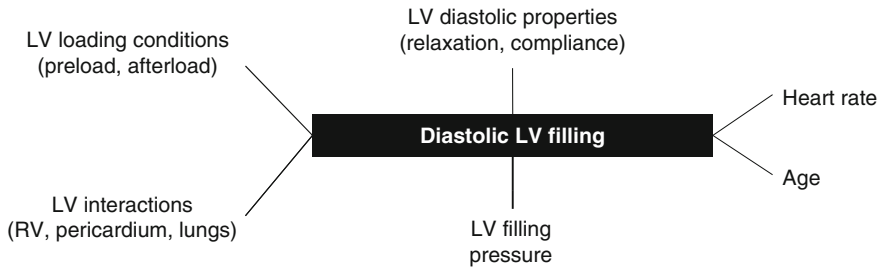

Fig. 16.6 Confounding factors influencing mitral Doppler velocity profile used to assess indirectly left ventricular (LV) diastolic properties and filling pressures. Abbreviation: *RV* right ventricle

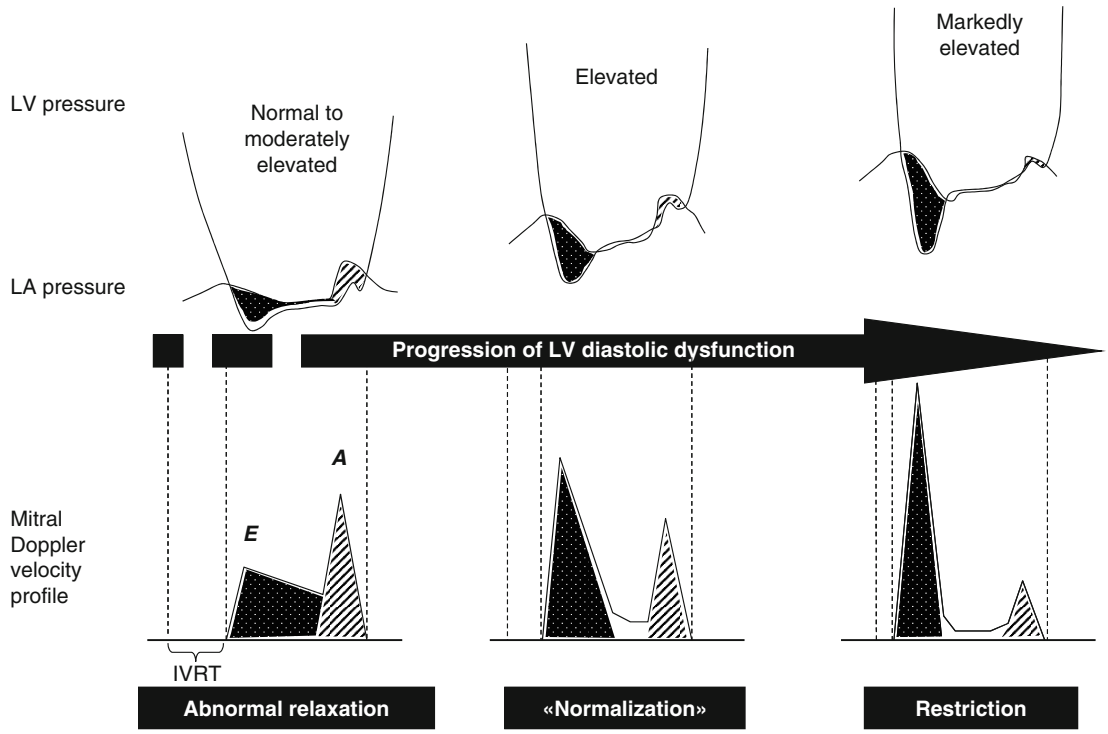

Relaxation	Prolonged	Prolonged	Prolonged
Compliance	Normal	Decreased	Severely decreased

Fig. 16.7 Natural evolution of mitral Doppler velocity pattern. Both the progression of left ventricular (LV) diastolic dysfunction and gradual increase in filling pressures alter the mitral Doppler velocity profile. In the presence of advanced LV diastolic dysfunction, a decrease in LV compliance frequently participates in increasing left atrial (LA) pressure, whereas an abnormal relaxation is uniformly observed during the natural course of diastolic heart failure. Abbreviations: *E* early mitral wave, *A* mitral wave during atrial contraction, *IVRT* isovolumic relaxation time

relationship between mitral E-wave velocity and PAOP was the strongest of all measured Doppler variables, including combined indices *E/Ea* and *E/Vp* [47]. Accordingly, combined Doppler indices appear to be of additional value for estimating LV filling pressure, principally in critically ill patients with underlying cardiac diseases known to alter diastolic properties.

Atrial fibrillation modifies Doppler velocity patterns owing to the variable duration of diastole and the absence of atrial systole. Nevertheless, simple, yet reliable, Doppler indices have been validated to predict semiquantitatively invasive PAOP in spontaneously breathing cardiac patients [48–51] (Table 16.7).

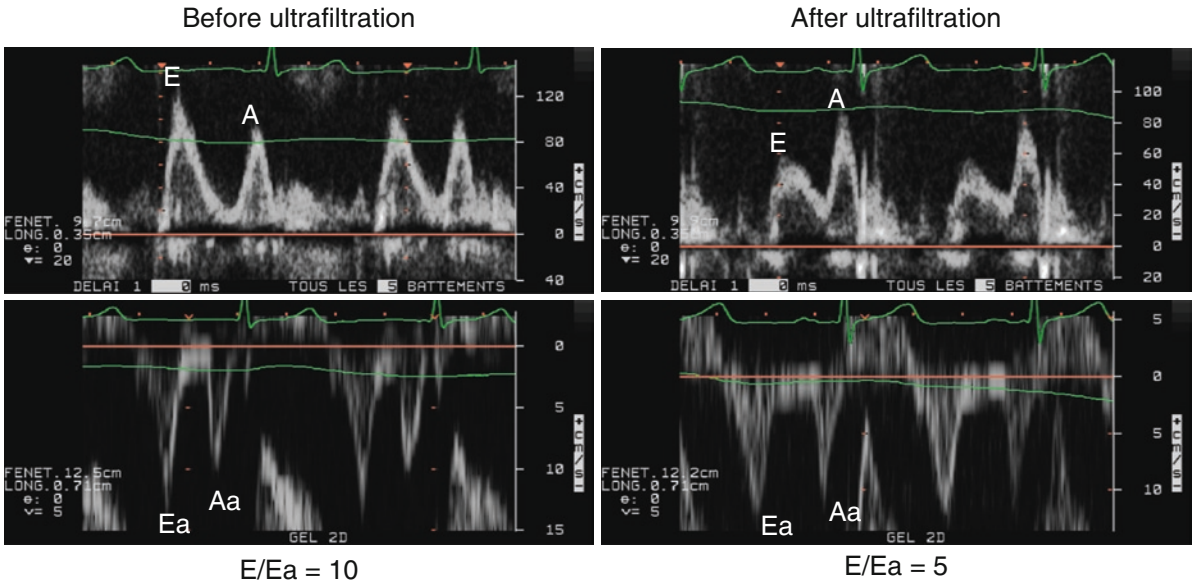

Fig. 16.8 Influence of acute therapy on mitral Doppler velocity profile. This hemodialysis patient was successfully treated for a hydrostatic pulmonary edema secondary to volume overload. A 3-L ultrafiltration resulted in marked left ventricular (LV) preload reduction and decrease in filling pressures. As a result, the spectral Doppler pattern changed from a "normalized" to an "impaired relaxation" profile (*upper panels*). In contrast, tissue Doppler pattern recorded at the lateral mitral ring remained unchanged (*lower panels*). Consequently, the E/E_a ratio markedly decreased, reflecting the reduction in LV filling pressure induced by ultrafiltration

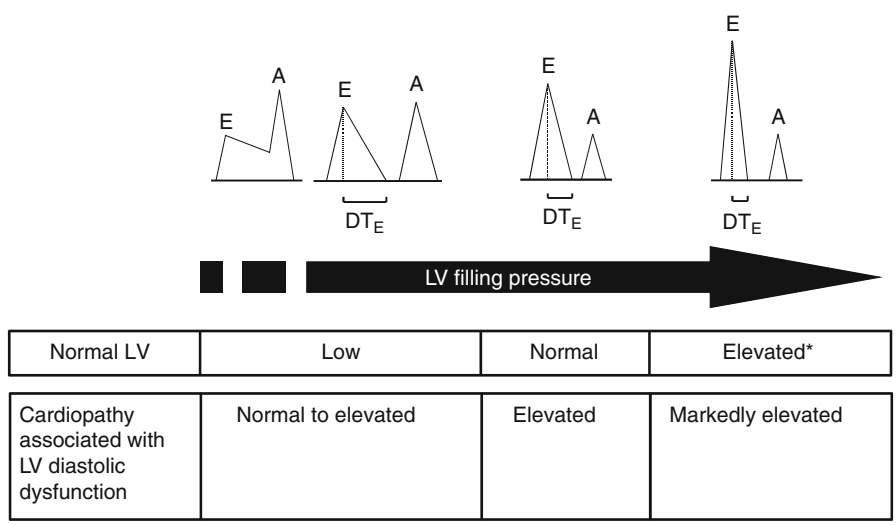

Fig. 16.9 Simplified qualitative interpretation of mitral Doppler pattern to predict the level of cardiac filling pressure according to the presence or absence of a cardiopathy known to be associated with left ventricular (LV) diastolic dysfunction. In the presence of a normal heart, an inverted *E/A* ratio is suggestive of low LV filling pressures. Noticeably, young persons with normal diastolic function and filling pressure in whom LV filling primarily occurs during early diastole owing to a highly compliant ventricle may exhibit a predominant E wave (*). In the presence of two-dimensional findings suggestive of a cardiomyopathy usually associated with LV diastolic dysfunction (e.g., ischemic, hypertrophic, dilated, and infiltrative cardiomyopathy), a qualitative interpretation of mitral Doppler velocity profiles also provides useful information on the level of filling pressures. Nevertheless, more precise evaluation, combining pulmonary vein Doppler assessment and tissue Doppler imaging of the mitral ring, is then necessary. Abbreviation: DT_E deceleration time of mitral E wave

Table 16.4 Threshold values of Doppler indices and predicted level of pulmonary artery occlusion pressure (PAOP) in spontaneously breathing cardiac patients

Doppler parameters	Reference	Threshold values	Predicted PAOP (mmHg)	Sensitivity (%)	Specificity (%)
E/A	[36]	≥2	≥20	43	99
DT E	[36]	<120 ms	≥20	100	99
DurationAr-A	[35]	>0 ms	>15	85	79
	[40]	>0 ms	>19	82	92
Systolic fraction[a]	[35]	<40%	>18	–	–
	[37]	<36%	≥18	90	85
DT D	[41]	≤160 ms	≥18	97	96
E/*E*a	[29]	>10	>15	97	78
E/V_p	[30]	≥2.5	>15	86	85

Abbreviations: *DT E* deceleration time of mitral E wave, *DT D* deceleration time of pulmonary vein D wave, E_a maximal velocity of early diastolic motion of mitral ring measured by tissue Doppler imaging, V_p propagation velocity of blood flow entering the left ventricle during early diastole measured by color M-mode Doppler

[a]Velocity–time integral of pulmonary vein S wave normalized by the velocity–time integral of pulmonary vein S and D waves and expressed as a percentage

Table 16.5 Threshold values of simple mitral and pulmonary vein pulsed-wave Doppler indices currently proposed in mechanically ventilated, critically ill patients to predict an elevated pulmonary artery occlusion pressure (PAOP)

Doppler parameter	Reference	Setting	Threshold value	Predicted PAOP (mmHg)	Sensitivity (%)	Specificity (%)
E/*A* ratio	[42]	ICU	>2	>18	–	–
	[45]	ICU	>1.4	>18	75	100
DT E	[45]	ICU	<100 ms	>18	81	63
S/*D* ratio	[45]	ICU	<0.65	>18	96	100
Systolic fraction[a]	[27]	OR	<55%	>15[b]	91	87
	[42]	ICU	<40%	>18	–	–
	[43]	ICU	<40%	>18	100	100
	[45]	ICU	<44%	>18	92	88

Abbreviations: *DT E* deceleration time of mitral E wave, *ICU* intensive care unit, *OR* operating room

[a]Velocity–time integral of pulmonary vein S wave normalized by the velocity–time integral of pulmonary vein S and D waves and expressed as a percentage

[b]Peroperative assessment of left atrial pressure used as benchmark rather than PAOP

16.4 Pulmonary Edema: Diagnostic Algorithm

In patients admitted to the ICU for an acute respiratory failure associating a severe hypoxemia and bilateral radiological infiltrates, echocardiography Doppler not only allows distinguishing hydrostatic pulmonary edema from ARDS, but also frequently discloses an underlying causal cardiopathy.

16.4.1 Hydrostatic Pulmonary Edema Versus Acute Respiratory Distress Syndrome

The first diagnostic step is to differentiate between a hydrostatic pulmonary edema and an ARDS (Fig. 16.10). Markedly elevated PAOP is suggestive of hydrostatic pulmonary edema, whereas PAOP

Table 16.6 Threshold values of combined Doppler indices currently proposed in mechanically ventilated, critically ill patients to predict an elevated pulmonary artery occlusion pressure (PAOP)

Doppler parameter	Reference	Setting	Threshold value	Predicted PAOP (mmHg)	Sensitivity (%)	Specificity (%)
E/E_a lateral	[31]	ICU	≥7.0	≥13	86	92
	[44]	ICU	>7.5	≥15	86	81
	[45]	ICU	>8.0	>18	83	88
E/E_a septal	[44]	ICU	>9.0	≥15	76	80
E/V_p	[31]	ICU	>2.0	≥13	55	90
	[45]	ICU	>1.7	>18	80	100

Abbreviations: *ICU* intensive care unit, E_a maximal velocity of early diastolic motion of mitral ring measured by tissue Doppler imaging, V_p propagation velocity of blood flow entering the left ventricle during early diastole measured by color M-mode Doppler

Table 16.7 Threshold values of Doppler indices currently proposed in spontaneously breathing patients with atrial fibrillation to predict pulmonary artery occlusion pressure (PAOP)

Doppler parameter	Reference	Threshold value	Predicted PAOP (mmHg)	Sensitivity (%)	Specificity (%)
DT E	[48]	<150 ms	>15	71	100
	[50]	<120 ms	≥20	100	96
DT D	[49]	>220 ms	≤12	100	100
E/E_a	[51]	>10	≥15	75	93
E/V_p	[48]	≥1.4	>15	71	88

Abbreviations: *DT E* deceleration time of mitral E wave, *DT D* deceleration time of pulmonary vein D wave, E_a maximal velocity of early diastolic motion of mitral ring measured by tissue Doppler imaging, V_p propagation velocity of blood flow entering the left ventricle during early diastole measured by color M-mode Doppler

is typically ≤18 mmHg in ARDS patients [2]. The presence of associated structural abnormalities in the left or right cardiac chambers may constitute indirect signs of failing ventricles. A markedly dilated and poorly contracting LV in conjunction with thin walls and enlarged left atrium are indicative of a dilated cardiomyopathy, with chronically elevated LV filling pressure. The presence of an acute cor pulmonale reflecting an afterloaded right ventricle is highly suggestive of associated ARDS [52].

When cardiac abnormalities are less pronounced, the distinction between hydrostatic pulmonary edema and ARDS may be more challenging. Medical history, careful evaluation of LV diastolic properties and filling pressures, and serial echocardiographic examinations performed after therapeutic interventions (e.g., drugs administration, ventilator settings) usually help the clinician in establishing the final diagnosis.

16.4.2 Etiology of Hydrostatic Pulmonary Edema

The second diagnostic step is to identify the origin of a hydrostatic pulmonary edema. Echocardiography may depict the causative underlying decompensated or advanced-stage cardiomyopathy (Table 16.8).

Most frequently, elevated LV filling pressures associated with LV systolic dysfunction are consistent with congestive heart failure (Fig. 16.10). In this case, echocardiography typically depicts a dilated cardiomyopathy or extensive regional wall-motion abnormalities consistent with an ischemic heart disease. When echocardiography discloses a chronic valvulopathy or subtle cardiac abnormalities, their clinical relevance in the setting of acute pulmonary edema may be more difficult to ascertain.

Table 16.8 Main echocardiographic findings associated with cardiomyopathies frequently responsible for hydrostatic pulmonary edema

Cardiomyopathy	Echocardiographic findings
Dilated cardiomyopathy	Marked dilatation of left cardiac cavities (increased end-diastolic and end-systolic dimensions) Uniform reduction of all parameters of LV systolic function Remodeling: spherical LV and thin walls Associated findings: mitral regurgitation (annular dilatation), mural (apical) thrombus, RV enlargement
Hypertrophic cardiomyopathy	Asymmetric septal, or concentric, apical or free LV wall hypertrophy Small LV cavity size Associated findings: systolic anterior motion of the mitral valve with LV outflow tract obstruction and (eccentric) mitral regurgitation
Restrictive cardiomyopathy	Normal LV cavity size and wall thickness Normal or near-normal LV ejection fraction Marked biatrial enlargement Restrictive mitral Doppler pattern

Abbreviation: *LV* left ventricular

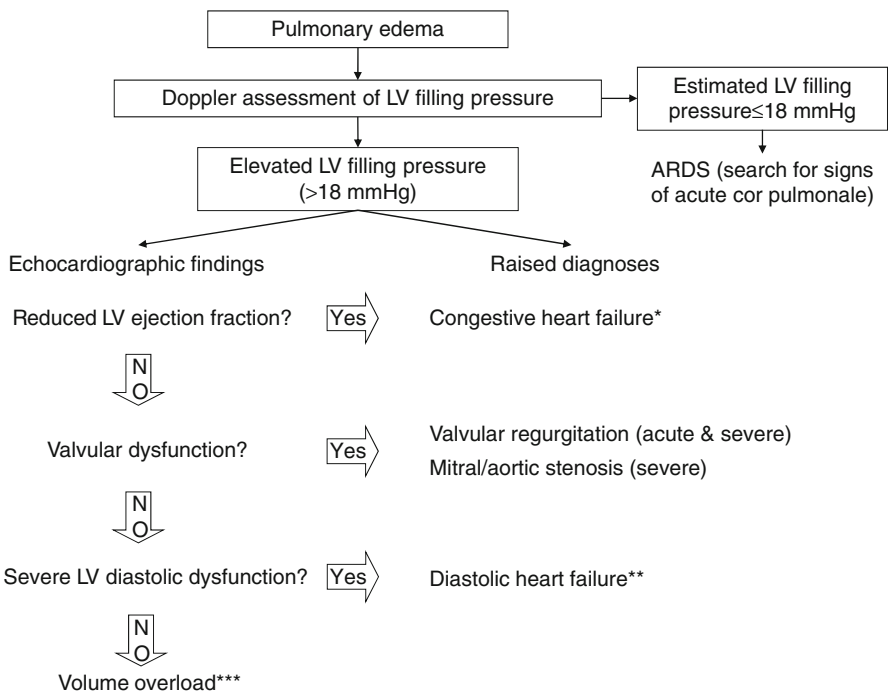

Fig. 16.10 Diagnostic algorithm using echocardiography Doppler for the evaluation of patients with acute respiratory failure secondary to pulmonary edema. Abbreviations: *LV* left ventricular, *ARDS* acute respiratory distress syndrome; * echocardiography also depicts the underlying cardiac disease responsible for congestive heart failure; ** diagnostic criteria have been defined; *** iatrogenic volume overload frequently occurs in the setting of renal failure

In the presence of elevated LV filling pressures but preserved ejection fraction, a severe – and frequently acute – mitral or aortic regurgitation has to be ruled out (Fig. 16.10). Mitral regurgitations may have highly energetic and eccentric jets, which are at times difficult to identify and adequately quantify from the transthoracic approach. In this case, transesophageal echocardiography is more sensitive and accurately depicts both the type and mechanism of the valvular regurgitation. Transesophageal echocardiography is particularly valuable for the identification of an eccentric mitral regurgitation secondary to a systolic anterior motion of the mitral valve with associated dynamic LV outflow tract obstruction (Fig. 16.11). Although LV outflow tract obstruction is frequently secondary to hypertrophic cardiomyopathy, it may also be observed

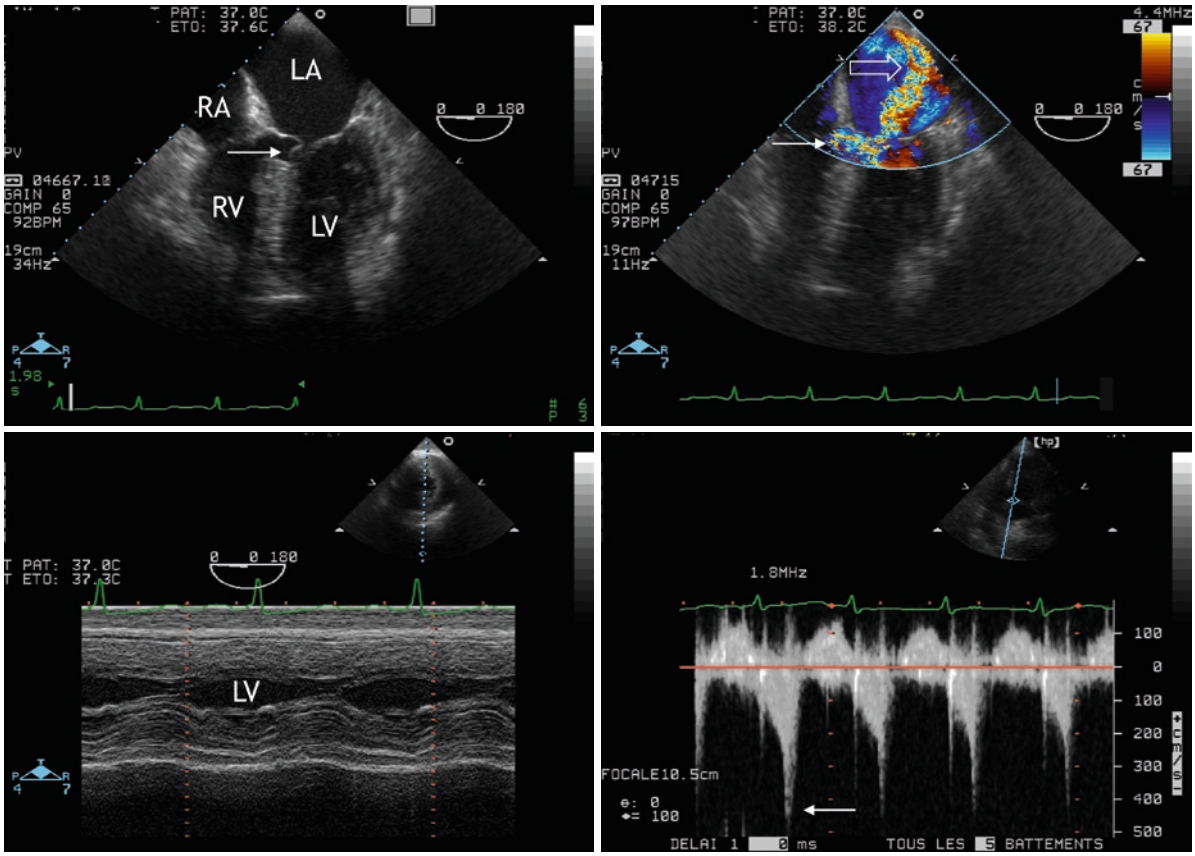

Fig. 16.11 Systolic anterior motion (SAM) of the mitral valve with associated severe eccentric regurgitation observed in a patient mechanically ventilated for an acute pulmonary edema. Transesophageal echocardiography depicted a SAM responsible for a dynamic left ventricular (LV) outflow tract obstruction (*upper left*, *arrow*). As a result, marked blood flow turbulences were observed using color Doppler mapping (*upper right*, *thin arrow*). In addition, the mitral valve distortion resulted in the development of a severe mitral regurgitation directed posterolaterally (*upper right*, *open arrow*). LV wall hypertrophy depicted by the M-mode in the short-axis transgastric view was a predisposing factor (*lower left*). Continuous-wave Doppler performed from the apical five-chamber view showed a dagger-shaped pattern consistent with a dynamic LV outflow tract obstruction (*lower right*, *arrow*). Abbreviations: *LA* left atrium, *RV* right ventricle, *RA* right atrium, *D* diastolic wave of pulmonary vein flow Doppler pattern

in various clinical settings characterized by a hyperdynamic LV (especially basal segments) with a thickened basal interventricular septum. The medical scenario may involve an elderly hypertensive patient who inadequately receives inotropic support, but also a hypovolemic postoperative patient after aortic valve replacement for aortic stenosis. Less frequently, LV outflow tract obstruction may be encountered in patients with acute myocardial infarction or apical ballooning secondary to severe stress who develop a compensatory hyperdynamic contraction of the inferobasal myocardium, which may in turn facilitates a systolic anterior motion of the mitral valve. The absence of LV cavity dilatation is suggestive of an acute valvulopathy. A markedly elevated systolic pulmonary artery pressure is consistent with a subacute or chronic pulmonary hypertension since a nonhypertrophied right ventricle can barely generate systolic pressures above 60 mmHg [53].

When the hydrostatic pulmonary edema with preserved LV ejection fraction has not been ascribed to a severe left-sided valvulopathy, the raised diagnosis is diastolic heart failure (Fig. 16.10). Since LV diastolic properties physiologically deteriorate

with age [33], the prevalence of diastolic heart failure markedly increases beyond the seventh decade [54]. Echocardiography may depict a hypertrophic or restrictive cardiomyopathy (Table 16.8). Cardiac diseases associated with LV diastolic dysfunction and precipitating factors are highly prevalent in patients admitted to the ICU for acute respiratory failure (Table 16.9). The benchmark for defining diastolic dysfunction is left-heart catheterization to document increased LV pressure decay in early diastole due to prolonged relaxation, at rest, and during exercise. Unfortunately, left-heart catheterization is not routinely accessible on clinical grounds for the majority of patients. Accordingly, American guidelines suggest that the diagnosis of diastolic heart failure be based on the presence of symptoms and signs of heart failure in a patient with normal LV ejection fraction and no valvular abnormality on echocardiography [55]. Recent European guidelines underlined the pivotal role of echocardiography for the diagnosis of diastolic heart failure in depicting normal LV ejection fraction and Doppler findings consistent with diastolic dysfunction [1]. Clinically adapted diagnostic criteria of diastolic heart failure have been recently proposed (Table 16.10) [56].

Finally, iatrogenic volume overload frequently occurs in anuric patients with renal failure. In these cases, the heart may appear structurally and functionally normal, but with elevated LV filling pressure owing to significant volume overload (Fig. 16.10).

Table 16.9 Cardiac diseases commonly associated with a left ventricular diastolic dysfunction and main precipitating factors

Cardiac diseases	Precipitating factors
Ischemic heart disease	Markedly elevated blood pressure
Advanced hypertrophy: Long-standing hypertension Aortic stenosis	Tachyarrhythmia (shortened diastolic filling period and loss of atrial contribution to ventricular filling)
Hypertrophic cardiomyopathy	Intravenous infusion of a small volume of fluid
Infiltrative cardiomyopathy	
Restrictive cardiomyopathy	

16.4.3 Influence of Ongoing Therapy

Symptomatic treatment of hydrostatic pulmonary edema rapidly alters mitral Doppler velocity profiles in improving LV loading conditions [3]. Accordingly, the diagnostic value of echocardiography Doppler may be reduced when performed after resolution of hydrostatic pulmonary edema owing to a fall in LV filling pressures (Fig. 16.8). This is especially true in patients with severe LV diastolic dysfunction, in whom a small decrease in LV preload (diuretics, nitrates) markedly decreases LV filling pressure owing to the steepness of the LV diastolic pressure/volume curve (Fig. 16.12). Nevertheless, tissue Doppler indices of intrinsic LV diastolic properties appear less influenced

Table 16.10 Diagnostic criteria for diastolic heart failure[a]

Diagnostic criteria	Objective evidence
1. Congestive heart failure	• Suggestive clinical presentation • Supporting tests (e.g., chest X-ray) • Positive response to diuretics • With or without the documentation of elevated LV filling pressure
2. Normal LV systolic function in proximity to the congestive heart failure event	• LV ejection fraction≥50% within 72 h of the congestive heart failure event
3. LV diastolic dysfunction	• Abnormal LV relaxation, filling, distensibility indices on cardiac catheterization

Abbreviation: *LV* left ventricle

[a]This classification approach is applicable to patients without congestive heart failure attributable to valvular heart disease, cor pulmonale, or a primary volume overload state. Diastolic heart failure is considered as *definite* when all three diagnostic criteria are fulfilled, *probable* when the first two criteria are only present, and *possible* when the first two criteria only are present and preserved ejection fraction has not been documented at the time of the event

Adapted from [56]

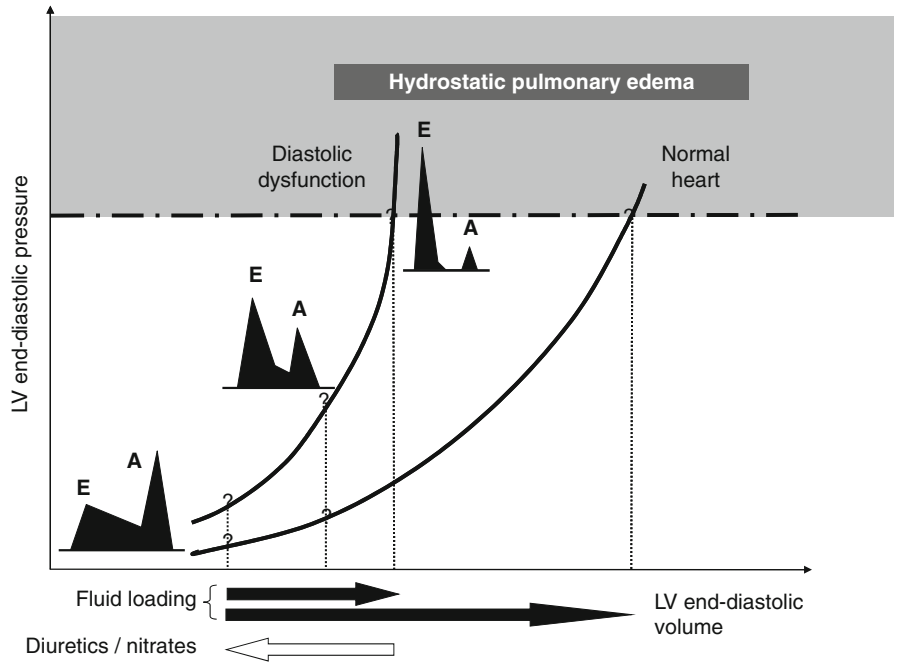

Fig. 16.12 How mitral Doppler velocity profiles may reflect the progressive increase in filling pressures secondary to worsening left ventricular (LV) diastolic dysfunction. In the presence of a severe LV diastolic dysfunction, the risk of iatrogenic hydrostatic pulmonary edema due to excessive fluid loading is high because the diastolic pressure-volume curve is steep and shifted up and left. In these patients, the "curative ratio" of blood volume expansion is markedly low (*short black arrow*) compared with that of normal subjects (*long black arrow*). Note that treatment of hydrostatic pulmonary edema (diuretics, nitrates) may rapidly improve LV loading conditions and modify the mitral Doppler pattern accordingly (*white arrow*). Abbreviations: *E* early mitral Doppler wave, *A* mitral Doppler wave during atrial contraction

by acute variations in LV loading conditions, especially when recorded at the lateral mitral ring [28]. Abnormally low tissue Doppler velocities of diastolic mitral ring motion are informative of LV diastolic dysfunction in this clinical context. Overall, echocardiography should be performed as closely as possible from the occurrence of acute pulmonary edema. When obtained during the acute respiratory failure event, it is best suited for documenting elevated filling pressure, preserved ejection fraction, and diastolic dysfunction of the LV for a definite diagnosis of diastolic heart failure [3, 57].

16.5 Conclusion

Echocardiography Doppler plays a pivotal role in the first-line assessment of patients presenting with acute respiratory failure. The diagnosis of hydrostatic pulmonary edema relies on the identification of elevated LV filling pressures using simple, yet robust, Doppler indices. In contrast, ARDS is characterized by lower LV filling pressures but a frequently afterloaded right ventricle. Importantly, echocardiography Doppler also allows identification of an underlying cardiopathy and serially assessing central hemodynamics after therapeutic interventions in unstable patients.

References

1. Dickstein K, Cohen-Solal A, Filippatos G, McMurray JJV, Ponikowski P, Poole-Wilson PA, Strömberg A, Van Veldhuisen DJ, Atar D, Hoes AW, Keren A, Mebazaa A, Nieminen M, Priori SG, Swedberg K (2008) ESC guidelines for the diagnosis and treatment of acute and chronic heart failure 2008. Eur Heart J 29:2388–2442
2. Bernard GR, Artigas A, Brigham KL et al (1994) The American–European Consensus Conference on ARDS. Definitions, mechanisms, relevant outcomes, and clinical trial coordination. Am J Respir Crit Care Med 149:818–824
3. Vignon P (2008) Assessment of critically ill patients with acute heart failure syndromes using echocardiography

Doppler. In: Mebazaa A, Gheorghiade M, Zannad FM, Parrillo JE (eds) Acute heart failure. Springer-Verlag, London
4. Vieillard-Baron A, Caille V, Charron C, Belliard G, Page B, Jardin F (2008) Actual incidence of global left ventricular hypokinesia in adult septic shock. Crit Care Med 36: 1701–1706
5. Etchecopar-Chevreuil C, François B, Clavel M, Pichon N, Gastinne H, Vignon P (2008) Cardiac morphological and functional changes during early septic shock: a transesophageal echocardiographic study. Intensive Care Med 34: 243–249
6. Brutsaert DL, Rademakers FE, Sys SU (1984) Triple control of relaxation: implications in cardiac disease. Circulation 69: 190–196
7. Aurigemma GP, Zile MR, Gaasch WH (2006) Contractile behaviour of the left ventricle in diastolic heart failure with emphasis on regional systolic function. Circulation 113:296–304
8. Vignon P, Mor-Avi V, Weinert L, Koch R, Spencer KT, Lang RM (1998) Quantitative evaluation of global and regional left ventricular diastolic function with Color Kinesis. Circulation 97:1053–1061
9. Zile MR, Baicu CF, Gaasch WH (2004) Diastolic heart failure – abnormalities in active relaxation and passive stiffness of the left ventricle. N Engl J Med 350:1953–1959
10. Kitzman DW, Higginbotham MB, Cobb FR, Sheikh KH, Sullivan MJ (1991) Exercise intolerance in patients with heart failure and preserved left ventricular systolic function: failure of the Frank–Starling mechanism. J Am Coll Cardiol 17:1065–1072
11. Kitzman DW, Little WC, Brubaker PH, Anderson RT, Hundley WG, Marburger CT, Brosnihan B, Morgan TM, Stewart KP (2002) Pathophysiological characterization of isolated diastolic heart failure in comparison to systolic heart failure. JAMA 288:2144–2150
12. Yu CM, Lin H, Yang H, Kong SL, Zhang Q, Lee SWL (2002) Progression of systolic abnormalities in patients with "isolated" diastolic heart failure and diastolic dysfunction. Circulation 105:1195–1201
13. Yip G, Wang C, Zhang Y, Fung JWH, Ho PY, Sanderson JE (2002) Left ventricular long-axis function in diastolic heart failure: time for a redefinition. Heart 87:121–125
14. Petrie MC, Caruana L, Berry C, McMurray JJV (2002) "Diastolic heart failure" or heart failure caused by subtle left ventricular systolic dysfunction? Heart 87:29–31
15. Nikitin NP, Witte KK, Clark AL, Cleland JGF (2002) Color tissue Doppler-derived long-axis left ventricular function in heart failure with preserved global systolic function. Am J Cardiol 90:1174–1177
16. Yu CM, Zhang Q, Yip GW, Lee PW, Kum LC, Lam YY et al (2007) Diastolic and systolic asynchrony in patients with diastolic heart failure: a common but ignored condition. J Am Coll Cardiol 49:97–105
17. Tsuyuki RT, McKelvie RS, Arnold JM, Avezum A Jr, Barretto AC, Carvalho AC, Isaac DL, Kitching AD, Piegas LS, Teo KK, Yusuf S (2001) Acute precipitants of congestive heart failure exacerbations. Arch Intern Med 161: 2337–2342
18. Kitzman DW, Little WC, Brubaker PH, Anderson RT, Hundley WG, Marburger CT, Brosnihan B, Morgan TM, Stewart KP (2002) Pathophysiological characterization of isolated diastolic heart failure in comparison to systolic heart failure. JAMA 288:2144–2150
19. Connors AF Jr, Mc Caffree DR, Gray BA (1983) Evaluation of right-heart catheterization in the critically ill patient without acute myocardial infarction. N Engl J Med 1983:263–267
20. Eisenberg PR, Jaffe AS, Schuster DP (1984) Clinical evaluation compared to pulmonary artery catheterization in the hemodynamic assessment of critically-ill patients. Crit Care Med 12:549–553
21. Appleton CP, Hatle LK, Popp RL (1988) Relation of transmitral flow velocity patterns to left ventricular diastolic function: new insights from a combined hemodynamic and Doppler echocardiography study. J Am Coll Cardiol 12:426–40
22. Tabata T, Thomas JD, Klein AL (2003) Pulmonary venous flow by Doppler echocardiography: revisited 12 years later. J Am Coll Cardiol 41:1243–1250
23. Garcia MJ, Thomas JD, Klein AL (1998) New Doppler echocardiographic applications for the study of diastolic function. J Am Coll Cardiol 32:865–875
24. Nagueh SF, Sun H, Kopelen HA, Middleton KJ, Khoury DS (2001) Hemodynamic determinants of the mitral annulus diastolic velocities by tissue Doppler. J Am Coll Cardiol 37: 278–285
25. Garcia MJ, Smedira NG, Greenberg NL, Main M, Firstenberg MS, Odabashian J, Thomas JD (2000) Color M-mode Doppler flow propagation velocity is a preload insensitive index of left ventricular relaxation: animal and human validation. J Am Coll Cardiol 35:201–208
26. Appleton CP, Jensen JL, Hatle LK, Oh JK (1997) Doppler evaluation of left and right ventricular diastolic function: a technical guide for obtaining optimal flow velocity recordings. J Am Soc Echocardiogr 10:271–291
27. Kuecherer HF, Muhiudeen IA, Kusumoto FM, Lee E, Moulinier LE, Cahalan MK, Schiller NB (1990) Estimation of mean left atrial pressure from transesophageal pulsed Doppler echocardiography of pulmonary venous flow. Circulation 82:1127–1139
28. Vignon P, Allot V, Lesage J, Martaillé JF, Aldigier JC, François B, Gastinne H (2007) Diagnosis of left ventricular diastolic dysfunction in the setting of acute changes in loading conditions. Crit Care 11:R43
29. Nagueh SF, Middleton KJ, Kopelen HA, Zoghbi WA, Quinones MA (1997) Doppler Tissue Imaging: a noninvasive technique for evaluation of left ventricular relaxation and estimation of filling pressures. J Am Coll Cardiol 30: 1527–1533
30. Gonzalez-Vilchez F, Ares M, Ayuela J, Alonso L (1999) Combined use of pulsed and color M-mode Doppler echocardiography for the estimation of pulmonary capillary wedge pressure: an empirical approach based on an analytical relation. J Am Coll Cardiol 34:515–523
31. Bouhemad B, Nicolas-Robin A, Benois A, Lemaire S, Goarin JP, Rouby JJ (2003) Echocardiographic Doppler assessment of pulmonary capillary wedge pressure in surgical patients with postoperative circulatory shock and acute lung injury. Anesthesiology 98:1091–1100
32. Dokainish H, Zoghbi WA, Lakkis NM, Al-Bakshy F, Dhir M, Quinones MA, Nagueh SF (2004) Optimal noninvasive assessment of left ventricular filling pressures. A comparison of tissue Doppler echocardiography and B-type natri-

uretic peptide in patients with pulmonary artery catheters. Circulation 109:2432–2439
33. Appleton CP, Hatle LK (1992) The natural history of left ventricular filling abnormalities: assessment by two-dimensional and Doppler echocardiography. Echocardiography 9: 437–457
34. Appleton CP, Galloway JM, Gonzalez MS, Basnight MA (1993) Estimation of left ventricular filling pressures using two-dimensional and Doppler echocardiography in adult patients with cardiac disease. Additional value of analysing left atrial size, left atrial ejection fraction and the difference in duration of pulmonary venous and mitral flow velocity at atrial contraction. J Am Coll Cardiol 22:1972–1982
35. Rossvoll O, Hatle LK (1993) Pulmonary venous flow velocities recorded by transthoracic Doppler ultrasound: relation to left ventricular diastolic pressures. J Am Coll Cardiol 21: 1687–1696
36. Giannuzzi P, Imparato A, Temporelli PL, De Vito F, Silva PL, Scapellato F, Giordano A (1994) Doppler-derived mitral deceleration time of early filling as a strong predictor of pulmonary capillary wedge pressure in postinfarction patients with left ventricular systolic dysfunction. J Am Coll Cardiol 23:1630–1637
37. Brunazzi MC, Chirillo F, Pasqualini M, Gemelli M, Franceschini-Grisolia E, Longhini C, Giommi L, Barbaresi F, Stritoni P (1994) Estimation of left ventricular diastolic pressures from precordial pulsed-Doppler analysis of pulmonary venous and mitral flow. Am Heart J 128:293–300
38. Suwa M, Otake Y, Ito T, Moriguchi A, Hirota Y, Kawamura K (1994) Noninvasive estimation of pulmonary capillary wedge pressure from pulmonary venous flow using transesophageal echocardiography. Am J Noninvas Cardiol 8:207–214
39. Vanoverschelde JLJ, Robert AR, Gerbaux A, Michel X, Hanet C, Wijns W (1995) Noninvasive estimation of pulmonary arterial wedge pressure with Doppler transmitral flow velocity pattern in patients with known heart disease. Am J Cardiol 75:383–389
40. Yamamoto K, Nishimura RA, Burnett JC, Redfield MM (1997) Assessment of left ventricular end-diastolic pressure by Doppler echocardiography: contribution of duration of pulmonary venous versus mitral flow velocity curves at atrial contraction. J Am Soc Echocardiogr 10:52–59
41. Yamamuro A, Yoshida K, Hozumi T, Akasaka T, Takagi T, Kaji S, Kawamoto T, Yoshikawa J (1999) Noninvasive evaluation of pulmonary capillary wedge pressure in patients with acute myocardial infarction by deceleration time of pulmonary venous flow velocity in diastole. J Am Coll Cardiol 34:90–4
42. Boussuges A, Blanc P, Molenat F, Burnet H, Habib G, Sainty JM (2002) Evaluation of left ventricular filling pressure by transthoracic Doppler echocardiography in the intensive care unit. Crit Care Med 30:362–367
43. Vargas F, Gruson D, Valentino R, Bui HN, Salmi LR, Gilleron V, Gbikpi-Benissan G, Guenard H, Hilbert G (2004) Transesophageal pulsed Doppler echocardiography of pulmonary venous flow to assess left ventricular filling pressure in ventilated patients with acute respiratory distress syndrome. J Crit Care 19:187–197
44. Combes A, Arnoult F, Trouillet JL (2004) Tissue Doppler imaging estimation of pulmonary artery occlusion pressure in ICU patients. Intensive Care Med 30:75–81
45. Vignon P, Ait Hssain A, François B, Preux PM, Pichon N, Clavel M, Frat JP, Gastinne H (2008) Noninvasive assessment of pulmonary artery occlusion pressure in ventilated patients: a transesophageal study. Crit Care 12:R18
46. Jacques DC, Pinsky MR, Severyn D, Gorcsan J III (2004) Influence of alterations in loading on mitral annular velocity by tissue Doppler echocardiography and its associated ability to predict filling pressures. Chest 126:1910–1918
47. Firstenberg MS, Levine BD, Garcia MJ, Greenberg NL, Cardon L, Morehead AJ, Zuckerman J, Thomas JD (2000) Relationship of echocardiographic indices to pulmonary capillary wedge pressures in healthy volunteers. J Am Coll Cardiol 36:1664–1669
48. Nagueh SF, Kopelen HA, Quinones MA (1996) Assessment of left ventricular filling pressures by Doppler in the presence of atrial fibrillation. Circulation 94:2138–2145
49. Chirillo F, Brunazzi MC, Barbiero M, Giavarina D, Pasqualini M, Franceschini-Grisolia E, Cotogni A, Cavarzerani A, Rigatelli G, Stritoni P, Longhini C (1997) Estimating mean pulmonary wedge pressure in patients with chronic atrial fibrillation from transthoracic Doppler indexes of mitral and pulmonary venous flow velocity. J Am Coll Cardiol 30: 19–26
50. Temporelli PL, Scapellato F, Corra U, Eleuteri E, Imparato A, Giannuzzi P (1999) Estimation of pulmonary wedge pressure by transmitral Doppler in patients with chronic heart failure and atrial fibrillation. Am J Cardiol 83:724–747
51. Sohn DW, Song JM, Zo JH, Chai IH, Kim HS, Chun HG, Kim HC (1999) Mitral Annulus velocity in the evaluation of left ventricular diastolic function in atrial fibrillation. J Am Soc Echocardiogr 12:927–931
52. Vieillard-Baron A, Prin S, Chergui K, Dubourg O, Jardin F (2002) Echo-Doppler demonstration of acute cor pulmonale at the bedside in the medical intensive care unit. Am J Respir Crit Care Med 166:1310–1319
53. Weber KT, Janicki JS, Shroff SG, Likoff MJ, St John Sutton MG (1983) The right ventricle: physiologic and pathophysiologic considerations. Crit Care Med 11:323–328
54. Vasan RS, Benjamin EJ, Levy D (1995) Prevalence, clinical features and prognosis of diastolic heart failure: an epidemiologic perspective. J Am Coll Cardiol 26:1565–1574
55. Hunt SA, Baker DW, Chin MH, Cinquegrani MP, Feldman AM, Francis GS, Ganiats TG, Goldstein S, Gregoratos G, Jessup ML, Noble RJ, Packer M, Silver MA, Stevenson LW, Gibbons RJ, Antman EM, Alpert JS, Faxon DP, Fuster V, Jacobs AK, Hiratzka LF, Russell RO, Smith SC Jr (2001) American College of Cardiology/American Heart Association Guidelines for the evaluation and management of chronic heart failure in the adult: executive summary: a report of the American College of Cardiology/American Heart Association task force on practice guidelines. J Am Coll Cardiol 38:2101–2113
56. Vasan RS, Levy D (2000) Defining diastolic heart failure. A call for standardized diagnostic criteria. Circulation 101:2118–2121
57. Gandhi SK, Powers JC, Nomeir AM, Fowle K, Kitzman DW, Rankin KM, Little WC (2001) The pathogenesis of acute pulmonary edema associated with hypertension. N Engl J Med 344:17–22

Why and How to Use Echocardiography in Acute Respiratory Distress Syndrome

17

Antoine Vieillard-Baron and François Jardin

Contents

A. Vieillard-Baron (✉) and F. Jardin
Intensive Care Unit, University Hospital Ambroise Paré, Assistance Publique Hôpitaux de Paris,
9 avenue Charles de Gaulle, 92104 Boulogne Cedex, France and
Service de Réanimation médicale, Hôpital Ambroise Paré,
9, avenue Charles-de-Gaulle, 92104 Boulogne Cedex, France
e-mail: antoine.vieillard-baron@apr.aphp.fr

17.1 Use of Echocardiography in Acute Respiratory Distress Syndrome

Warren Zapol and colleagues first showed that acute respiratory distress syndrome (ARDS) damages not only the alveoli, but also the pulmonary circulation, with the development of pulmonary hypertension [1, 2]. In the 1970s and 1980s, vascular injury typically resulted in the irreversible destruction of the pulmonary circulation, leading to refractory right ventricular failure and finally death (Fig. 17.1, panels a, b) [3]. This was favored by the use of aggressive mechanical ventilation, which aimed at maintaining the partial pressure of carbon dioxide in arterial blood ($PaCO_2$) within the normal range. Since the advent of tidal volume reduction and strict limitation of airway pressures [4], pulmonary hypertension is becoming reversible. It is no longer related to destruction of pulmonary capillaries, but it results in vascular remodeling, mediated in part by hypoxemia and hypercapnia (Fig. 17.1, panels c, d) [5].

Mechanical ventilation markedly affects the pulmonary circulation, and hence the right ventricle [6]. As noted in Chap. 4, the effect of mechanical ventilation is more pronounced when lung compliance is altered. The use of mechanical ventilation can further exacerbate pulmonary hypertension related to ARDS, especially when overdistension occurs, and it can lead to severe acute cor pulmonale (ACP; Fig. 17.2) [7], whose clinical consequences can be dramatic (Fig. 17.3). Many studies have demonstrated the deleterious impact of right ventricular failure on the prognosis of patients with ARDS [8–10]. Recently, we reported that decreased mortality in ARDS over the last 15 years has been associated with a significant decrease in the incidence of ACP [11].

D. De Backer et al. (eds.), *Hemodynamic Monitoring Using Echocardiography in the Critically Ill*,
DOI: 10.1007/978-3-540-87956-5_17, © Springer-Verlag Berlin Heidelberg 2011

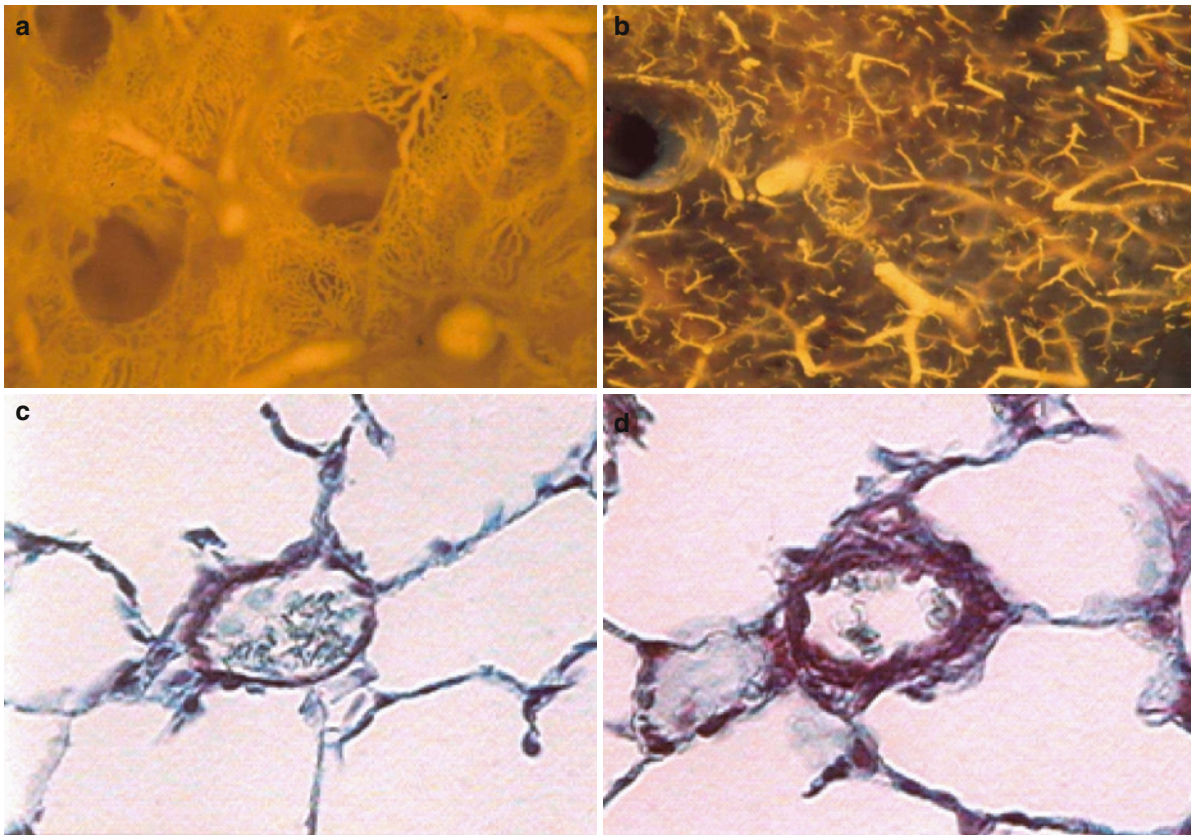

Fig. 17.1 Lung sections in humans (**a**, **b**) and rats (**c**, **d**). (**a**) Lung section seen by electron microscopy in a patient who died without lung injury. Pulmonary circulation in white appears conserved. (**b**) Same view but in a patient who died after a few days of aggressive mechanical ventilation for severe acute respiratory distress syndrome. The pulmonary circulation appears severely impaired with destruction of pulmonary capillaries. (**c**) Lung section of a rat with a normal pulmonary circulation. Pulmonary arteries appear nonmuscularized as normal. (**d**) Lung section of a rat after a few days of hypoxia (FiO_2 0.10). Pulmonary arteries are now abnormally muscularized, reflecting remodeling of the pulmonary circulation (Fig. (a) and (b) graciously provided by Warren Zapol)

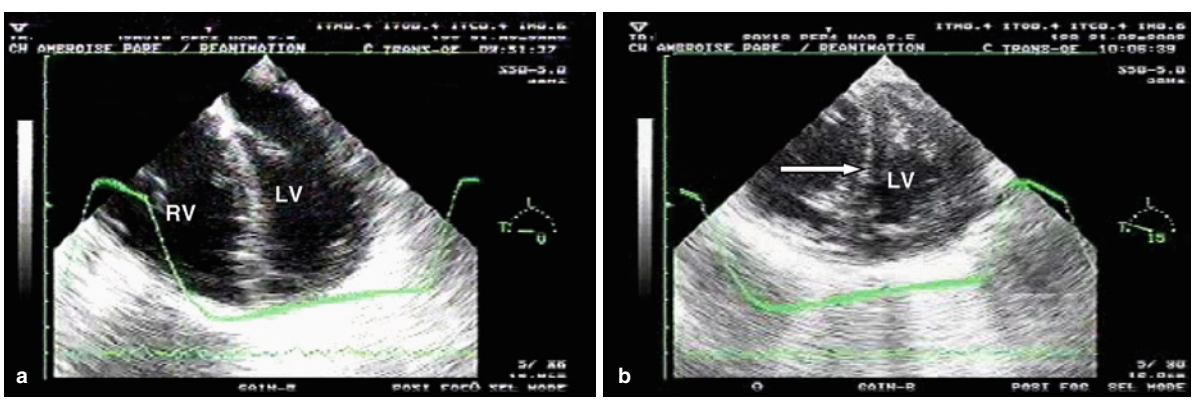

Fig. 17.2 Transesophageal echocardiography (TEE) in a patient mechanically ventilated for 2 days because of severe acute respiratory distress syndrome. TEE showed acute cor pulmonale. (**a**) Long-axis view of the left ventricle (LV), demonstrating dilatation of the right ventricle (RV). (**b**) Short-axis view of the LV demonstrating paradoxical septal motion (*arrow*) at the end of systole

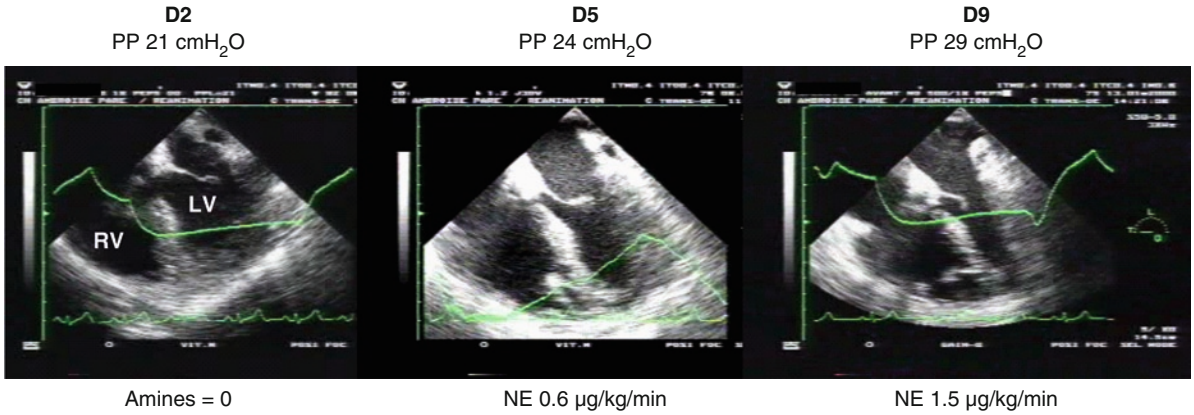

Fig. 17.3 Transesophageal echocardiography after 2 days (D2), 5 days (D5), and 9 days (D9) of mechanical ventilation in a woman hospitalized because of severe acute respiratory distress syndrome related to pneumonia. According to progressive deterioration of respiratory mechanics, we observed an increasingly dilated right ventricle (RV), requiring norepinephrine infusion. On day 9, the left ventricle (LV) was markedly restricted. *NE* norepinephrine, *PP* plateau pressure

It is particularly notable in ARDS that plateau pressure (PP), mainly reflecting transpulmonary pressure, directly affects the pulmonary capillaries. Hence PP has a direct effect on right ventricular function [12]. In 352 ARDS patients, all mechanically ventilated, we reported an ACP incidence of 13% for a PP below 27 cmH_2O, 30% for a PP of 27–35 cmH_2O, and 60% for a PP higher than 35 cmH_2O [12]. The mortality rates in these three PP ranges were 30%, 40%, and 80%, respectively; they were significantly higher in patients who exhibited ACP, except when the PP was below 27 cmH_2O [12]. Applying a high positive end-expiratory pressure (PEEP) also has deleterious effects. It overdistends some parts of the lung [13, 14] and may impact on right ventricular function by overloading the right ventricle during the expiratory phase [15, 16]. This explains why the increased partial pressure of oxygen in arterial blood (PaO_2) induced by PEEP may be associated with an effective decrease in oxygen transport [16]. Finally, limitation of tidal volume, which protects the right ventricle by the induced PP reduction, is responsible for hypercapnia, also called "permissive hypercapnia." Hypercapnia can likewise be deleterious as it induces vasoconstriction of the pulmonary circulation [17] and can thus favor the development of ACP [18]. This hypercapnia thus has to be limited, not by increasing tidal volume, of course, but by reducing instrumental dead space [19] and by increasing the respiratory rate without generating intrinsic PEEP, which is also deleterious to the right ventricle [20].

All of this data points out the need for close monitoring of right ventricular function during the first days of clinical care. This monitoring allows us to appreciate the impact of different ventilatory strategies on the right ventricle and so adapt ventilatory settings to right ventricular function. Adapting ventilatory settings in patients with ARDS may minimize the increased risk of death associated with ACP [18]. Most of these patients had a PP below 27 cmH_2O [18], and we strongly recommend that the PP be maintained below this value. Echocardiography, especially by the transesophageal route, appears to be the most accurate and simplest method of evaluating right ventricular function. It especially has to be used to search for right ventricular dilatation and paradoxical septal motion, which define ACP when associated. Echocardiography should also be employed to detect patent foramen ovale (PFO), a common finding in ARDS patients whose hypoxemia is difficult to control. Recently, a French consensus conference on the management of ARDS recommended the systematic use of echocardiography [21]. The remainder of this chapter uses three clinical cases to illustrate how echocardiographic evaluation allows adaptation of ventilatory strategies.

17.2 How to Use Echocardiography

17.2.1 Case 1: Tidal Volume and PP Adaptation to Right Ventricular Function

A 41-year-old, HIV-positive man was hospitalized in our intensive care unit for acute respiratory failure. His temperature was 38 2°C. Chest X-ray showed bilateral alveolointerstitial syndrome. The final diagnosis was pneumocystis infection.

At admission, oxygen saturation (SpO_2) was 85% with 15 L/min O_2 using a face mask. No signs of shock were detected, and the plasma lactate level was normal. Transthoracic echocardiography showed a hyperkinetic left ventricle and a normal right ventricle, without dilatation or paradoxical septal motion. Owing to worsening gas exchange, the patient was intubated, sedated, and paralyzed a few hours later. Compliance of the respiratory system was calculated as 15 mL/cmH_2O. Ventilatory settings were as follows: tidal volume (TV) 400 mL (5.7 mL/kg), PEEP 5 cmH_2O, respiratory rate (RR) 20/min, fraction of inspired oxygen (FiO_2) 0.6, I/E 0.5. Blood gas analysis showed PaO_2 60 mmHg, $PaCO_2$ 67 mmHg, pH 7.24. The PP was 33 cmH_2O. Thereafter, the patient underwent a fall in systolic arterial pressure (SAP) to 90 mmHg associated with tachycardia [heart rate (HR) 128 beats/min]; transesophageal echocardiography (TEE) indicated ACP (Fig. 17.4). Two solutions were discussed. The first was to administer norepinephrine and/or dobutamine to correct shock without altering ventilatory settings. The second, which was adopted, was to consider mechanical ventilation too aggressive for right ventricular function, even though the PP was below 35 cm_2O and TV below 6 mL/kg. So TV was decreased to 350 mL (5 mL/kg) and PP to 26 cmH_2O; RR increased to 25/min without inducing intrinsic PEEP. Very quickly, the SAP increased to 123 mmHg and HR decreased (112/min). TEE indicated a marked improvement in right ventricular

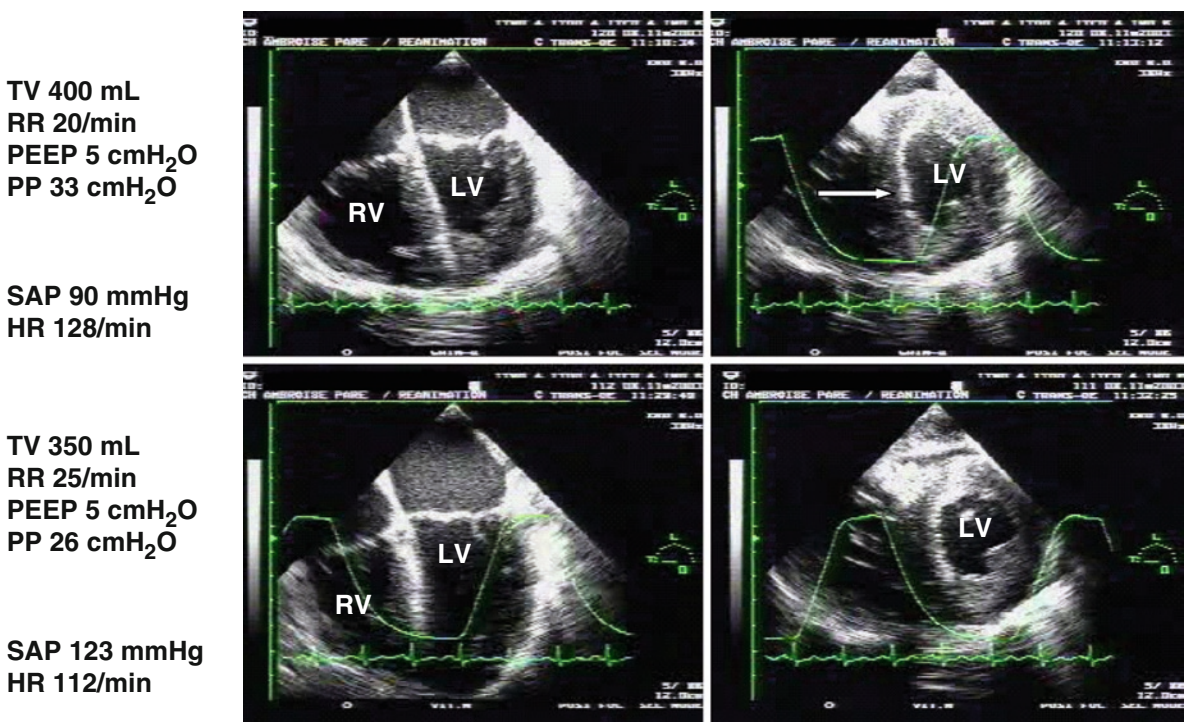

Fig. 17.4 Patient mechanically ventilated because of severe acute respiratory distress syndrome. With a tidal volume (TV) of 400 mL and a plateau pressure (PP) of 33 cmH_2O, transesophageal echocardiography demonstrated acute cor pulmonale with dilatation of the right ventricle (RV; *left*) associated with paradoxical septal motion (*right*, *arrow*). Reduction of TV and PP normalized RV function and improved hemodynamics. *RR* respiratory rate, *PEEP* positive end-expiratory pressure, *SAP* systolic arterial pressure, *HR* heart rate, *LV* left ventricle

function (Fig. 17.4). Blood gas analysis under FiO_2 0.6 showed PaO_2 60 mmHg, $PaCO_2$ 63 mmHg, pH 7.28.

This clinical case is interesting for three reasons:

1. Within a few hours, mechanical ventilation of the patient induced circulatory failure related to ACP. ACP was not present at the first echocardiography performed during spontaneous ventilation. This illustrates the impact of the association between ARDS and mechanical ventilation on pulmonary circulation and, hence, on right ventricular function.
2. The TV and thus PP have to be adapted on a case-by-case basis. Whereas the initial TV was in the recommended range, it was too high in this patient. Conversely, the right ventricle may tolerate ventilation with a TV higher than 6 mL/kg, provided that PP is maintained below 27 cmH_2O and that right ventricular tolerance is good. This avoids excessive hypercapnia.
3. The slight additional limitation of TV, and so of PP, was sufficient to correct right ventricular function without infusing norepinephrine.

17.2.2 Case 2: Monitoring the Effect of PEEP on Right Ventricular Function

A 38-year-old man was hospitalized in our unit for acute respiratory failure related to extensive pneumococcal pneumonia. After 48 h of mechanical ventilation, compliance of the respiratory system was 23 mL/cmH_2O. The patient was sedated, paralyzed, and ventilated with a TV of 500 mL (7.1 mL/kg), an RR of 15/min, a PEEP of 5 cmH_2O, an I/E Inspiration/Expiration time of 0.5, and an FiO_2 of 0.7. The PP was 27 cmH_2O. Blood gas analysis showed a PaO_2 of 61 mmHg, a $PaCO_2$ of 58 mmHg, and pH 7.37. Because of a very low PaO_2/FiO_2, we decided to test the efficacy and tolerance of increased PEEP. TEE was performed just before increasing PEEP, and it indicated a slight increase in right ventricular size without paradoxical septal motion (Fig. 17.5). The SAP was 135 mmHg, HR 100/min. Right ventricular stroke index, calculated by the Doppler method, was 23 mL/m^2. PEEP was increased to 14 cmH_2O and TV decreased to 300 mL

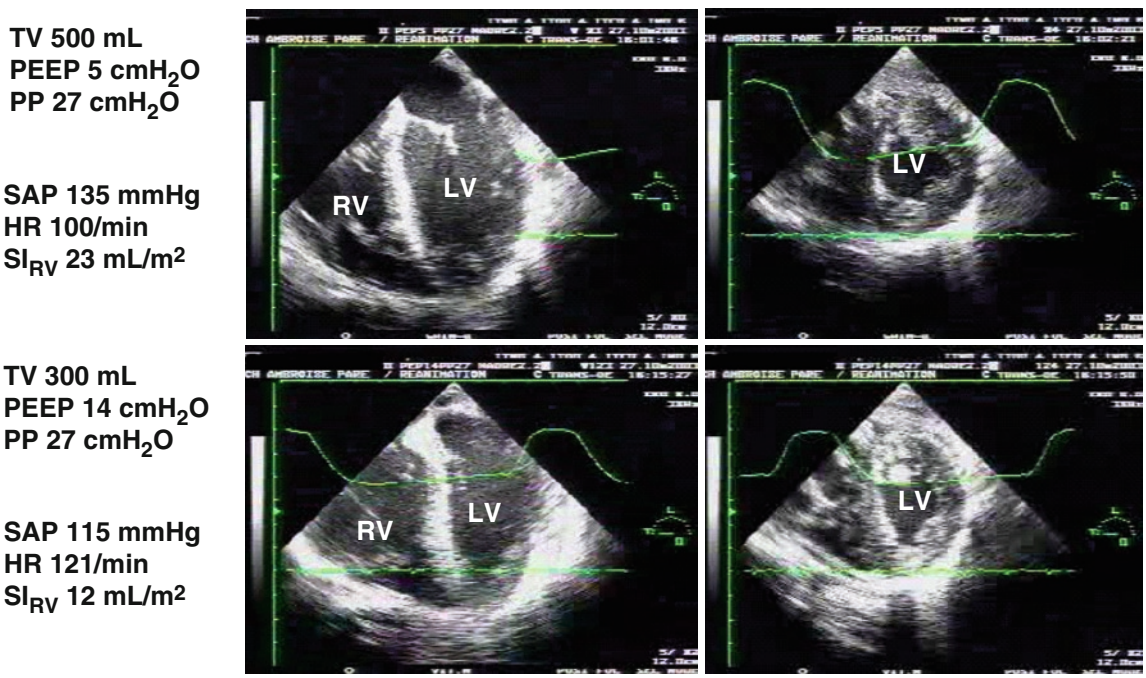

Fig. 17.5 Severe acute respiratory distress syndrome and profound hypoxemia with a positive end-expiratory pressure (PEEP) of 5 cmH_2O. At baseline, right ventricular (RV) function was quite normal with slight dilatation of the RV (*left*), but without paradoxical septal motion (*right*). After applying a PEEP of 14 cmH_2O, with the same plateau pressure (PP), acute cor pulmonale appeared in a few minutes. *TV* tidal volume, *SAP* systolic arterial pressure, *HR* heart rate, SI_{RV} right ventricular stroke index, *LV* left ventricle

(4.3 mL/kg) to maintain PP constant. After 15 min, we observed a decrease in SAP and tachycardia. TEE showed marked dilatation of the right ventricle with the occurrence of a paradoxical septal motion and a fall in right ventricular stroke index to 12 mL/m^2 (Fig. 17.5). Because of the poor tolerance, high PEEP was removed and previous ventilatory settings were restored to normalize right ventricular function. Finally, three periods of prone positioning improved blood gas analysis values and led to patient recovery.

This clinical case is interesting because it clearly demonstrates how a high PEEP can be deleterious despite a strict limitation of PP. It highlights the value of prone positioning, one of whose effects is to correct a profound hypoxemia without overloading the right ventricle. The strict limitation of PP and PEEP in this patient limited organ failure to just one – the lung, whereas high PEEP would probably have induced circulatory failure requiring amine infusion.

17.2.3 Case 3: Role of Prone Positioning in ARDS Management

A 44-year-old woman was hospitalized in our unit for aspiration after drug intoxication. At admission, her temperature was 39°C, respiratory rate 42/min. Chest X-ray showed bilateral alveolar images. Blood gas analysis was performed with 15 L/min of oxygen in spontaneous ventilation and indicated a PaO_2 of 62 mmHg, $PaCO_2$ of 37 mmHg, and pH 7.45. No shock was observed. The patient was quickly sedated and intubated. Ventilatory settings were as follows: TV 450 mL (7.5 mL/kg), RR 18/min, FiO_2 0.8, PEEP 5 cmH_2O. TEE on days 1 and 2 indicated normal cardiac function. On day 3, PaO_2/FiO_2 was 84 mmHg, $PaCO_2$ 52 mmHg, and pH 7.30. PP was 25 cmH_2O, and compliance of the respiratory system was calculated at 23 mL/cmH_2O. TEE now showed ACP, requiring infusion of a small dose of norepinephrine because of hypotension (Fig. 17.6). Association of very poor oxygenation with ACP led us to change our ventilatory strategy, and three successive periods of prone positioning (18 h each) were performed. Ventilatory settings remained unchanged. After the first period, PP had decreased to 21 cmH_2O, reflecting a major improvement in compliance, and right ventricular function was normalized (Fig. 17.6). At the end of the three periods of prone positioning, blood gas analysis indicated a PaO_2 of 114 mmHg, $PaCO_2$ of 45 mmHg, and pH of 7.36.

This case illustrates the importance of prone positioning in the management of severe ARDS. We have previously reported that our main indication to turn the patient to a prone position was a PaO_2/FiO_2 below 100 mmHg after 2 days of mechanical ventilation in the absence of significant hemodynamic impairment [22]. In these patients with severely impaired lung compliance, the prone position improves oxygenation without increasing PEEP, which is deleterious to the right ventricle, as seen in Case 2. Prone positioning not only improves oxygenation, but also induces lung recruitment, improves lung compliance, increases alveolar ventilation, and decreases PP and $PaCO_2$ [23], thus helping to unload the right ventricle. As shown by Case 3, the occurrence of ACP after 2 days of "optimized" ventilation is an indication for prone positioning. We have recently reported normalization of right ventricular function after prone positioning in a series of 21 patients with severe ARDS and ACP [24].

17.3 Conclusion

Evaluation of right ventricular function by echocardiography during the first days of ARDS is essential. It allows optimization of ventilatory strategy: adaptation of TV and PP, monitoring of the cardiac effect of PEEP, and decision-making regarding prone positioning.

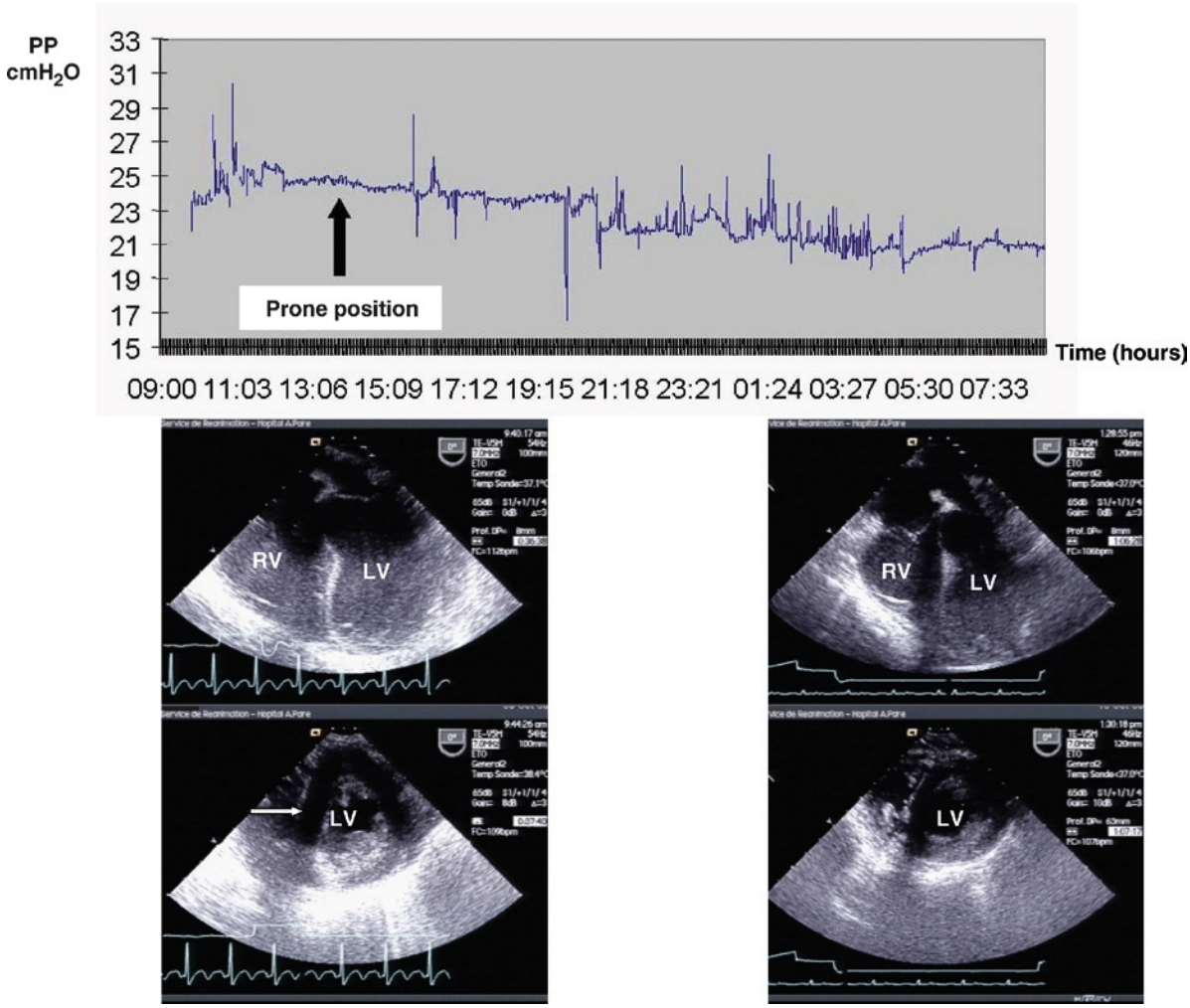

Fig. 17.6 Prone positioning of a patient mechanically ventilated for 48 h because of severe acute respiratory distress syndrome. *Top*, prone positioning significantly decreased plateau pressure in a few hours. Bottom, transesophageal echocardiography before prone positioning (*left*) showed acute cor pulmonale, associating dilatation of the right ventricle (RV) with flattening of the interventricular septum (*arrow*). After 18 h in the prone position (*right*), RV function was normalized. *PP* plateau pressure, *LV* left ventricle

References

1. Zapol W, Jones R (1987) Vascular components of ARDS. Clinical pulmonary hemodynamics and morphology. Am Rev Respir Dis 136:471–474
2. Zapol W, Snider M (1977) Pulmonary hypertension in severe acute respiratory failure. N Engl J Med 296:476–480
3. Jardin F, Gueret P, Dubourg O, Farcot JC, Margairaz A, Bourdarias JP (1985) Two-dimensional echocardiographic evaluation of right ventricular size and contractility in acute respiratory failure. Crit Care Med 13:952–956
4. The National Heart, Lung, and Blood Institute ARDS Clinical Trials Network (2006) Pulmonary-artery versus central venous catheter to guide treatment of acute lung injury. N Engl J Med 354:2213–2223
5. Moloney ED, Evans TW (2003) Pathophysiology and pharmacological treatment of pulmonary hypertension in acute respiratory distress syndrome. Eur Respir J 21: 720–727
6. Jardin F, Vieillard-Baron A (2003) Right ventricular function and positive pressure ventilation in clinical practice: from hemodynamic subsets to respirator settings. Intensive Care Med 29:1426–1434
7. Vieillard-Baron A, Prin S, Chergui K, Dubourg O, Jardin F (2002) Echo-Doppler demonstration of acute cor pulmonale at the bedside in the medical intensive care unit. Am J Respir Crit Care Med 166:1310–1319
8. Monchi M, Bellenfant F, Cariou A, Joly LM, Thebert D, Laurent Y et al (1998) Early predictive factors of survival in the acute respiratory distress syndrome. A multivariate analysis. Am J Respir Crit Care Med 158:1076–1081

9. Squara P, Dhainaut JF, Artigas A, Carlet J (1998) Hemodynamic profile in severe ARDS: results of the European Collaborative ARDS Study. Intensive Care Med 24:1018–1028
10. Osman D, Monnet X, Castelain V, Anguel N, Warszawski J, Teboul JL, Richard C, for the French Pulmonary Artery Catheter Study Group (2008) (2009) Incidence and prognostic value of right ventricular failure in acute respiratory distress syndrome. Intensive Care Med 35:69–76
11. Jardin F, Fellahi JL, Beauchet A, Vieillard-Baron A, Loubières Y, Page B (1999) Improved prognosis of acute respiratory distress syndrome 15 years on. Intensive Care Med 25:936–941
12. Jardin F, Vieillard-Baron A (2007) Is there a safe plateau pressure in ARDS? The right heart only knows. Intensive Care Med 33:444–447
13. Valta P, Takala J, Eissa NT, Milic-Emili J (1993) Does alveolar recruitment occur with positive end-expiratory pressure in adult respiratory distress syndrome patients? J Crit Care 8:34–42
14. Nieszkowska A, Lu Q, Vieira S, Elman M, Fetita C, Rouby JJ (2004) Incidence and regional distribution of lung overinflation during mechanical ventilation with positive end-expiratory pressure. Crit Care Med 32:1496–1503
15. Jardin F, Brun-Ney D, Cazaux P, Dubourg O, Hardy A, Bourdarias JP (1989) Relation between transpulmonary isovolumetric pressure change during respiratory support. Catheter Cardiovasc Diagn 16:215–220
16. Schmitt JM, Vieillard-Baron A, Augarde R, Prin S, Page B, Jardin F (2001) Positive end-expiratory pressure titration in acute respiratory distress syndrome patients: Impact on right ventricular outflow impedance evaluated by pulmonary artery Doppler flow velocity measurements. Crit Care Med 29:1154–1158
17. Viitanen A, Salmenperä M, Heinonen J (1990) Right ventricular response to hypercarbia after cardiac surgery. Anesthesiology 73:393–400
18. Vieillard-Baron A, Schmitt JM, Augarde R, Fellahi JL, Prin S, Page B et al (2001) Acute cor pulmonale in acute respiratory distress syndrome submitted to protective ventilation: Incidence, clinical implications, and prognosis. Crit Care Med 29:1551–1555
19. Prin S, Chergui K, Augarde R, Page B, Jardin F, Vieillard-Baron A (2002) Ability and safety of a heated humidifier to control hypercapnic acidosis in severe ARDS. Intensive Care Med 28:1756–1760
20. Vieillard-Baron A, Prin S, Augarde R, Desfonds P, Page B, Beauchet A et al (2002) Increasing respiratory rate to improve CO2 clearance during mechanical ventilation is not a panacea in acute respiratory failure. Crit Care Med 30:1407–1412
21. Richard JC, Girault C, Leteurtre S, Leclerc F, et le groupe d'experts de la SRLF (2005) Prise en charge ventilatoire du syndrome de détresse respiratoire aiguë de l'adulte et de l'enfant (nouveau-né exclu). Recommandations d'experts de la Société de réanimation de langue française. Réanimation 14:313–322
22. Page B, Vieillard-Baron A, Beauchet A, Aegerter P, Prin S, Jardin F (2003) Low stretch ventilation strategy in acute respiratory distress syndrome: Eight years of clinical experience in a single center. Crit Care Med 31:765–769
23. Vieillard-Baron A, Rabiller A, Chergui K, Peyrouset O, Page B, Beauchet A et al (2005) Prone position improves mechanics and alveolar ventilation in acute respiratory distress syndrome. Intensive Care Med 31:220–226
24. Vieillard-Baron A, Charron C, Caille V, Belliard G, Page B, Jardin F (2007) Prone positioning unloads the right ventricle in severe ARDS. Chest 132:1440–1446

Part V

Specific Situations

Thoracic Trauma

18

Fabio Chirillo

Contents

F. Chirillo
Department of Cardiology, Ca' Foncello Hospital,
Treviso, Italy,
Piazza Ospedale 1, 31100, Treviso, Italy
e-mail: fchirillo@tin.it

18.1 Blunt Chest Trauma

18.1.1 Traumatic Aortic Injury

18.1.1.1 Incidence and Natural History

Blunt chest trauma accounts for 100,000 hospital admissions a year in the United States, and chest injuries are the third-most frequent type of injury following high-speed motor vehicle accidents.

Traumatic aortic injury (TAI) accounts for 10–20% of fatalities in high-speed deceleration accidents, and as a cause of death following automobile accident TAI (5–16%) is second only to head injury (63%)[1].

Each year, approximately 8,000 persons in the US sustain blunt injury to the descending thoracic aorta. The incidence in other industrial countries, such as Western European countries with high death rates from automobile accidents, has not been determined, since autopsies are rarely performed on patients who die at the scene of the accident.

The number of patients with TAI who reach an emergency department alive has risen over recent years because of improved prehospital care, more aggressive resuscitation in the field, and more rapid transportation to appropriate units. Moreover, the safety systems of automobiles have significantly reduced the severity of head, skeletal, and abdominal trauma, but they have no influence on the causative mechanism of TAI in vehicle passengers.

The natural history of TAI was delineated in an autopsy series 50 years ago [2]. In this series, among individuals sustaining a TAI, death was immediate in 80–90%. In the remaining 10–20% of individuals, the mortality rate due to untreated TAI was high: 30% died within 6 h, 40–50% died within 24 h, and 90%

D. De Backer et al. (eds.), *Hemodynamic Monitoring Using Echocardiography in the Critically Ill*,
DOI: 10.1007/978-3-540-87956-5_18,

died within 4 months. Chronic posttraumatic pseudoaneurysms developed in 2–5% of patients with undiagnosed TAI.

With the development of trauma activation systems, rapid transport of victims to trauma centers, large availability of noninvasive and accurate diagnostic methods, and emergent therapeutic surgical and endovascular measures, the survival rate among patients suffering from TAI has significantly increased. In a prospective survey on the activity of 50 trauma centers across North America, Fabian et al. collected 274 patients with TAI [3]. Of those who reached the hospital, 8% arrived in extremis; none of these patients survived. Nine percent of patients died from TAI before treatment; another 8% were considered nonoperative because of severe associated injuries or advanced age. The largest group of patients (75.5%) underwent planned operation, with an overall mortality rate of 31%.

18.1.1.2 Mechanism of Injury

Notwithstanding the large number of published papers, there are no definite answers as to what the main mechanism producing TAI might be. The mechanism of injury in TAI has been explained as being the result of different forces, including horizontal deceleration forces, such as high-speed, head-on vehicular collisions causing shear stress at the isthmus, that is, at the junction of the mobile aortic arch with the less mobile descending thoracic aorta [4]. Among patients sustaining a TAI who reached the hospital alive, 93% have TAI at the isthmus [5]. Such a high level of reproducibility of the site and nature of TAI intuitively suggests that there is a reproducible mechanism of injury. It has been supposed that TAI results from shearing stress (torque and compression) on the thoracic aorta from rapid deceleration. Furthermore, investigators have emphasized the importance of the mobility of the ascending aorta and aortic arch relative to the fixed distal descending aorta (fixed to the thoracic wall by intercostal arteries and to the pulmonary artery by the ligamentum arteriosum) as an important contributory factor. Displacement of the mobile sections of the aorta in a caudal direction would place the isthmus under tension, leading ultimately to rupture. Another mechanism is the "water-hammer" effect, which is an abrupt increase in intra-aortic pressure. This phenomenon is created when the flow of a noncompressible fluid is occluded abruptly, which leads to high-pressure waves being reflected back along the vessel wall. During vehicle impact, the aorta may be occluded at the diaphragmatic hiatus as a result of the abdominal compression; this generates a dramatic pressure pulse in the aorta, and it is expected to be greater at the isthmus on account of the curvature reflecting and intensifying the pressure wave.

Finally severe chest compression might create an "osseous pinch," that is, entrapment of the aorta between the anterior thoracic bony structures (manubrium, clavicle, first rib) and the spine, where the aorta is squeezed, resulting in vessel rupture.

Independent of the underlying mechanism, one should keep in mind that TAI can occur only following high-energy transfer to the aorta. The mechanism of injury remains, therefore, one of the most important factors in establishing the diagnosis: trauma, such as with falls from >5 m, motor vehicle crashes at speeds >50 km/h, unrestrained drivers, ejected passengers, and pedestrians struck by motor vehicles, is usually responsible for TAI, whereas minor blunt chest traumas are not [6, 7]. The nature of the accident remains, therefore, the first clue to the diagnosis.

18.1.1.3 Pathology

Aortic injury following blunt chest trauma is generally represented by a transverse laceration that interrupts the physical integrity of one, two, or all three structural layers of the aorta. The tear varies in depth, with transmural transection being the most severe. The adventitia is intact in about 60% of cases and may serve to contain an incomplete aortic injury, together with the periaortic tissues and the left pleura. The length of the tear ranges from less than 1 mm to a completely circumferential tear, with the majority being nearly circumferential.

According to Parmley et al. [2], the aortic injuries can be classified on the basis of extension in both circumference and depth.

1. *Superficial lesions involving only the intima*. Traumatic tears limited to the aortic intima appear as thin and mobile intraluminal appendages of the aortic wall, usually located at the isthmus. No alterations in either the diameter or external contour of the aorta are present. Mobile wall thrombi within the aortic lumen can be found at the level of the

lesion, probably because the exposed collagen may constitute a nidus for acute thrombus formation.

2. *Intramural hematoma*. The intima and the adventitia are intact, while there is blood accumulation within the media, probably originating from the disrupted vasa vasorum. The aortic wall presents a localized, usually eccentric, thickening; the inner aortic surface is smooth, the aortic lumen partially reduced, and the outer aortic contour unaltered.
3. *Subadventitial aortic rupture involving the intima and media with complete circumferential extension.* A fusiform false aneurysm is produced. The torn intima-media segments are located at the two extremities of the false aneurysm; the inner surface of the aneurysm is smooth (formed by the sole adventitia), the aortic wall is extremely thin and fragile, and the outer surface is pellucid.
4. *Subadventitial aortic rupture involving the intima and media with incomplete circumferential extension.* This is the most frequent lesion in patients with TAI. There is a discrete tear involving the intima and the media. The disrupted aortic wall (intima and media) usually protrudes into the aortic lumen. Through the disrupted wall, the aortic lumen communicates with a cavity (saccular false aneurism), whose wall is constituted by the sole adventia. The inner surface of the aorta presents an abrupt discontinuation, and the outer contour is enlarged and deformed by the presence of an outpouching.
5. *Traumatic aortic dissection.* This can mimic spontaneous dissection, but it has some characteristic features. It is confined to the thoracic aorta (usually the isthmus), fails to create two distinct channels, involves the entire depth of both the aortic intimal and medial layers (being thicker than the classical intimal flap), and it has a direction usually transverse to the longitudinal axis of the aorta.
6. *Lesion of the aortic branches.* Partial or total avulsion, pseudoaneurysm, dissection, and thrombosis have been described as isolated injuries or in association with TAI.

18.1.1.4 Clinical Presentation

The clinical manifestations of TAI depend on the extent and location of the tear and, less commonly, on the involvement of any of the aortic branches (Table 18.1). Possible TAI should be suspected in the case of high-speed deceleration trauma, even in the absence of clinical symptoms or signs [6, 7].

Table 18.1 Signs and symptoms of traumatic aortic injury

Signs
External evidence of thoracic injury
Unexplained hypotension
Difference in pulse amplitude
Paroxysmal upper-limb hypertension
Diminished, delayed, or absent peripheral pulses
Systolic murmur
Symptoms
Chest pain
Dyspnea
Coughing
Hoarseness
Back pain
Dysphagia
Paralysis
Hypovolemia
Asymptomatic (40–50%)

Mediastinal hematoma caused by TAI leads to compression and stretching of mediastinal tissues and may be responsible for retrosternal and interscapular chest pain, dyspnea, hoarseness, and coughing, which are the most frequent symptoms of TAI. Signs include anterior chest wall contusion, unexplained hypotension, upper limb hypertension, acute coarctation syndrome (i.e., decreased lower-limb pulses with normal upper-limb pulses), differences in pulses amplitude, and a systolic harsh murmur audible over the base of the heart or in the interscapular region.

However, symptoms are often absent, and some reports have shown that as many as 50% of individuals with TAI may have no evidence of external injury [8, 9]. A high index of suspicion is therefore required based on the mechanism of injury. Due to the high energy forces causing TAI, associated injuries are common. These include brain, maxillofacial, and chest wall injuries, diaphragmatic, tracheal, lung and heart injuries, laceration of the liver, spleen, bowel, and retroperitoneal organs. Greendyke reported an average of 2.3 visceral lacerations and 3.9 fractures per victim [10]. Pate et al. reported that associated

injuries were present in more than 90% of patients with TAI, and 24% of the patients required major operation before surgical aortic repair [11]. Because of the paucity of reliable signs and symptoms and the frequency of distracting injuries among patients with TAI, emergency clinicians have come to rely on imaging in the management of victims of severe blunt chest trauma.

18.1.1.5 Chest Radiography

Chest radiographic findings suggesting aortic injury (Table 18.2) include the following: mediastinal widening ≥8 cm, loss of the aortic knob, displacement of the nasogastric tube to the right of the T4 spinous process, left apical pleural cap, widened paraspinal lines, widened right paratracheal stripe ≥5 mm, and loss of the descending aorta line [12–14] (Figs. 18.1–18.2). The positive predictive value of an abnormal chest film is as low as 10–20% because most patients with mediastinal widening will not have mediastinal hemorrhage on computed tomography (CT); (78% have normal scans) [15], nor will the vast majority have an aortic injury (>90% will have negative angiograms) [12, 13]. Predicting the presence of mediastinal hemorrhage on supine portable chest films in the setting of trauma is very inaccurate because it depends on the patient's position, depth of inspiration, and X-ray magnification factors [13]. The erect position can improve the positive predictive value of chest film for mediastinal hemorrhage, but this position is impossible to obtain in the vast majority of patients sustaining a severe blunt chest

Table 18.2 Radiological findings indicating traumatic thoracic aortic injury

X-ray sign	Sensitivity (%)	Specificity (%)
>8 cm mediastinal widening	80–100	50–82
Abnormal aortic knob contour	53–100	21–55
Aortopulmonary window opacification	0–100	56–80
Deviation of the nasogastric tube to the right	9–71	90–96
Widened paraspinal stripes	2–83	89–99
Downward (>40° below horizontal line) displacement of left main-stem bronchus	3–30	80–100
Deviation of the left main-stem bronchus	12–53	80–89
Left apical cap	20–63	75–95
Fractured first, second, or third rib	24–41	49–84
Left hemothorax	7–60	55–97
Pneumothorax	12–22	67–93
Right paratracheal stripe thickening	12–30	68–99

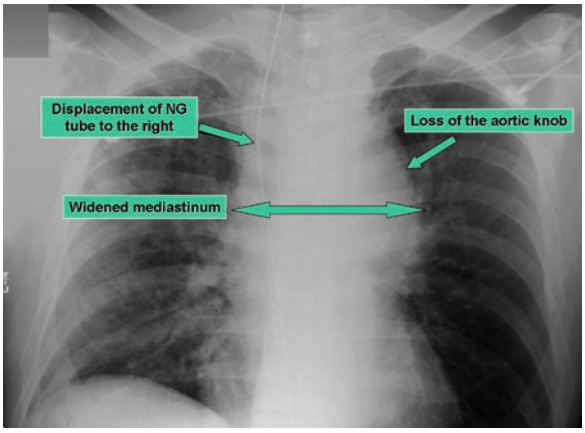

Fig. 18.1 Chest radiograph of a 45-year-old man suffering traumatic aortic injury after a high-speed automobile accident. Note mediastinal widening, deviation of the nasogastric (NG) tube to the right, and blurring of the aortic knob

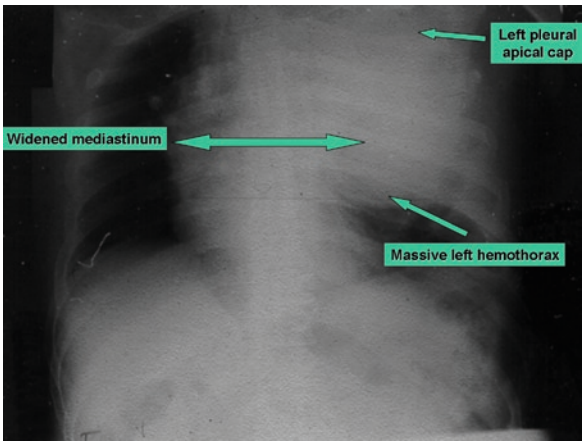

Fig. 18.2 Chest radiograph of a 21-year-old man with traumatic aortic injury (TAI) after an automobile accident. In addition to the widened mediastinum, a massive left hemothorax and an extensive left pleural cap were signs suggestive of TAI

trauma. Moreover, it has to be remembered that most mediastinal hemorrhage in trauma patients is the consequence of a variety of mediastinal or chest wall injuries, including nonaortic vascular injuries (tears and avulsions of the great vessels, internal mammary vessels, or subclavian vessels), sternal fractures, thoracic spine fractures, and esophageal rupture [12–15]. In previous reports, the negative predictive value of a normal chest film has been reported as high as 98%. In trauma patients with a negative chest film, only 3% had occult mediastinal hemorrhage discovered on CT and only 0.4% had an aortic injury [13]. However, in a prospective study Fabian found that up to 25% of trauma victims with TAI had a completely normal chest film [3].

In conclusion, chest X-ray continues to be used to screen trauma patients with blunt chest trauma because it is cheap, readily available, noninvasive, and it can be performed rapidly in the emergency department. It remains a good screening tool, but with variable sensitivity. It requires, therefore, further investigation when it demonstrates a widened mediastinum or other nonskeletal abnormalities and/or there is a high clinical suspicion for TAI and/or a high-risk mechanism of trauma is present.

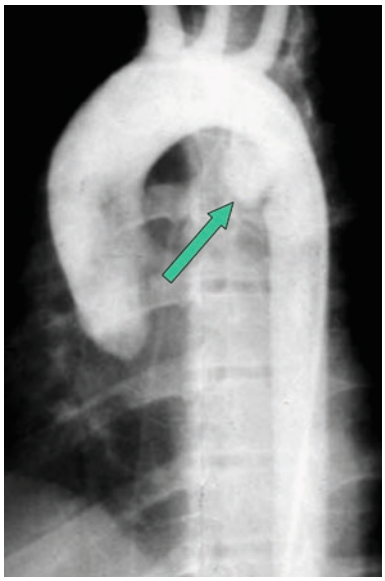

Fig. 18.3 Aortography in left oblique anterior view in a 25-year old male victim of a high-speed car accident. The catheter was introduced through a femoral artery, passed through the injured segment, and contrast medium was injected into the ascending aorta. In the region of the isthmus (*arrow*), multiple filling defects are present and the outer contour of the aorta is deformed, depicting a protruding sac (saccular false aneurysm)

18.1.1.6 Angiography

In the last 3 decades, aortography has played a pivotal role in the rapid and accurate diagnosis of TAI, allowing for emergent therapeutic measures, thus significantly reducing the mortality among victims reaching the hospital alive. With prompt diagnosis and treatment, an 80% survival rate has been reported.

The angiographic diagnosis of TAI is based on the demonstration of an intimal irregularity, a linear defect, or a filling defect caused by a medial flap. The presence of contrast material outside the lumen of the aorta is indicative of a transmural laceration, which may be contained (pseudoaneurysm) or a free extravasation (rupture) [16] (Fig. 18.3). The goal of screening patients with high-energy trauma to the chest is to attain zero nontherapeutic thoracotomies without overlooking any surgically important aortic or brachiocephalic arterial injuries. Because TAI without mediastinal hematoma is rare, the most popular TAI screening algorithms include chest X-ray as first imaging modality because of diffusion, low cost, rapid exam time, and high sensitivity. In patients where there is reasonable suspicion of TAI, immediate aortography is warranted followed by emergency surgery in the presence of angiographic signs of TAI [16].

In recent years, this pragmatic and dogmatic view has changed, first of all because of the number of negative aortographies performed (about 80–85%). One problem with aortography is that it is invasive (possible puncture-site hematoma, the possibility of the guidewire/catheter penetrating the injured aortic wall) and requires injection of iodinated contrast material (possible anaphylaxis or renal problems). The greatest disadvantage, however, is the risk of transferring a potentially unstable patient to the vascular suite (often not on-site), with the problems and risk of transportation of a multiply injured patient and his/her stay for a prolonged period in an environment where not all the life-support facilities are readily available.

In fact, there is great risk to the patient if a TAI is not detected, but considerable time and effort are incurred to exclude its diagnosis. It is now clear that TAI is often not the worst injury that a trauma patient can sustain, and if the attention of the attending

physician is drawn only by the detection of possible TAI, more dangerous and life-threatening injuries may go undetected, with dismal consequences for the patient.

18.1.1.7 Computed Tomography

CT has been now used for more than 30 years in the evaluation of patients with blunt chest trauma. Different values of diagnostic accuracy have been provided, and its use as a screening tool for TAI has been frequently questioned. CT technology has greatly improved in the last 10 years, and when evaluating the diagnostic performance of chest CT in screening for TAI, one should now refer to multislice (at least four slices), helical, CT angiography, using power injectors for intravenous (IV) injection of iodinated contrast material. In spiral or helical CT, the detector array travels in a continuous circle around the patient, so the test takes much less time (usually 15–20 s is sufficient to scan the entire chest), and slices can be obtained more quickly. The movement and respiratory artifacts of the conventional CT are minimized, and the spatial resolution of the technique has greatly increased. Multiple thin slices of the aorta can be obtained to minimize the risk of missing discrete lesions (such as those found in aortic trauma); accurate multiplanar or curved multiplanar displays, maximal intensity projection displays, or shaded-surface displays of the aorta can be obtained, demonstrating with great precision the spatial relationship of the torn aorta with its branches.

Indirect CT signs of TAI include the presence of poorly defined fat planes, mediastinal hemorrhage, and periaortic hematoma, particularly if located near the isthmus [17] (Fig. 18.4). Direct CT signs of TAI

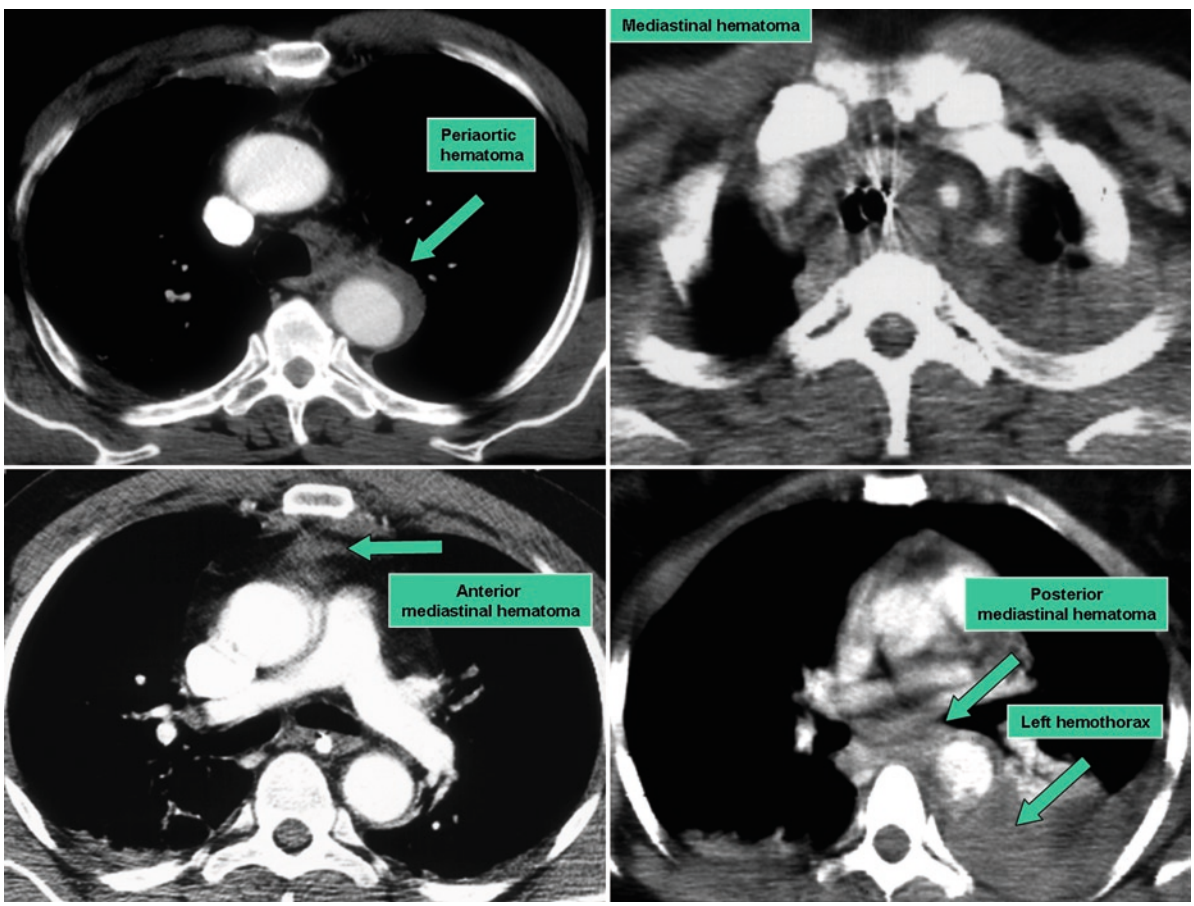

Fig. 18.4 Computed tomography scans with indirect signs of traumatic aortic injury, such as periaortic hematoma, mediastinal hematoma, which can be diffuse or localized to the anterior or posterior mediastinum, and (usually left) hemothorax

include the following: aortic contour deformity, intimal flap, thrombus protruding into the aortic lumen, pseudoaneurysm, abrupt change in caliber of the descending aorta compared with the ascending aorta (pseudocoarctation), and, rarely, contrast extravasation (Fig. 18.5). False positives for mediastinal hemorrhage on CT include as follows: residual thymic tissue, periaortic atelectasis, volume averaging of the pulmonary artery, and pleural effusions adjacent to the descending aorta. Technically deficient examinations also cause problems owing to patient motion, streak artifacts from electrocardiogram (ECG) leads and other monitoring devices, and streak artifacts from dense IV contrast [18]. Atherosclerotic plaques can cause interpretation difficulties; a prominent ductus arteriosus remnant can mimic a traumatic pseudoaneurysm [19]. False-positive diagnoses of intimal flaps have been caused by crossing vessels and volume averaging of the left brachiocephalic vein as it crosses in front of the aortic arch (Fig. 18.6), the left superior intercostal vein, and right bronchial arteries branching from the descending aorta. In conclusion, the improved spatial resolution, ameliorated overall image quality, and supplemental post-processing techniques have led to the recognition of a greater number of normal variants of vascular anatomy and subtler vascular injuries that have to be known in order to avoid pitfalls in diagnosing TAI [20].

Complications associated with CT are directly related to the adverse effects of the IV administration of iodinated contrast material and contrast material extravasation.

The only important contraindication to the CT scan is hemodynamic instability. In fact, the study can be time-consuming, can delay further diagnostic workup or treatment, and removes the patient from an optimal

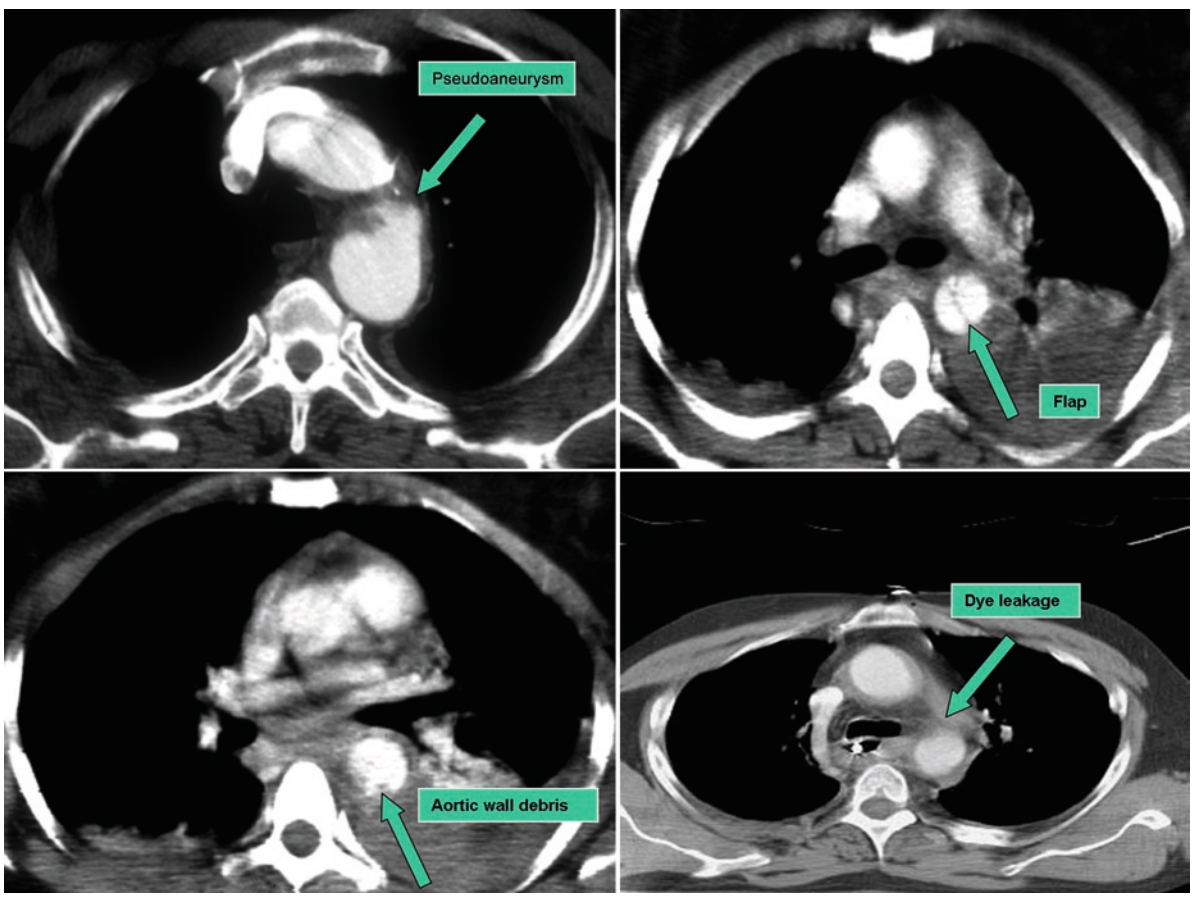

Fig. 18.5 Computed tomography scans with direct signs of traumatic aortic injury, such as saccular pseudoaneurysm, medial flap, aortic wall irregularities, and dye leakage from the aorta into the mediastinum

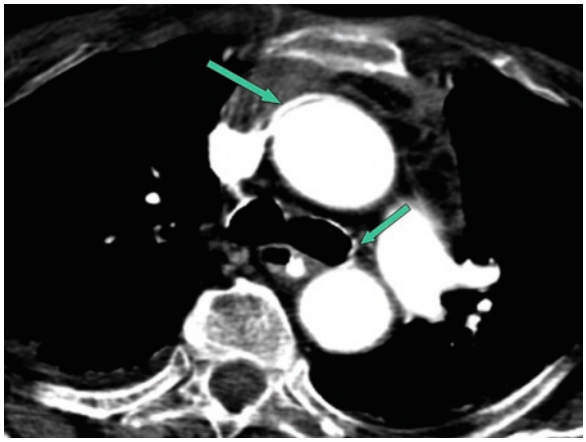

Fig. 18.6 Computed tomography scan in a patient with suspected traumatic aortic injury (TAI), in which the *arrows* indicate irregularities both on the anterior profile of the ascending aorta and the anterior profile of the descending aorta, simulating a TAI. These aspects were due to the presence of partial-volume artifacts from adjacent vessel structures, such as a left brachiocephalic vein (anterior) and right bronchial artery (posterior)

environment for direct clinical observation and support. When the CT scanner suite is at some distance from the patient admission or resuscitation area, the risk to overall patient care is augmented by transport for scanning.

CT scans have become part of the triage of patients suffering severe chest or multisystem trauma because they can provide accurate and rapid diagnostic information on injuries to the head, chest, abdomen, and extremities. Treatment prioritization is frequently based on CT results because the scan can reveal serious and often clinically silent major injuries. A CT scan where there is no evidence of mediastinal hemorrhage has virtually 100% true-negative predictive value for great vessel injury, based on CT studies correlated with angiography [21]. On the other hand, the accuracy of CT in patients with some mediastinal hemorrhage, not related to the aorta and great vessels and with normal appearing aorta and proximal arch vessels, is not yet well established [22].

18.1.1.8 Transesophageal Echocardiography

Because of the close proximity between the esophagus and the descending aorta, transesophageal echocardiography (TEE) provides high-resolution images of the thoracic aorta, representing a potentially ideal technique for imaging TAI. Miniaturization of TEE probes has reduced the discomfort to the patient and increased feasibility. With the development of omniplane transducers, multiple tomographic scan of the aortic arch and isthmus can be obtained in the majority of patients.

Direct TEE signs of TAI include aortic wall hematoma, intimal flap, intraluminal thick stripes, variation in aortic contour and caliber indicative of aneurysm formation, and flow acceleration through the injured aortic segment. These lesions can be combined in different types of TAI (Table 18.3).

In *intimal disruption* (Fig. 18.7), the dimension, outer contour, and thickness of the aorta do not change. The lesion is usually located at the isthmus, and it appears as a limited discontinuity of the inner surface of the aorta, with highly mobile appendages within the vascular lumen, though without evidence for a true medial flap. It does not produce flow acceleration; the color-flow Doppler pattern is, therefore, not altered by the presence of the lesion. There is a paucity of data on the outcome of this limited lesion, but it seems to undergo spontaneous healing. A follow-up using TEE is recommended because this discrete lesion tends to be misdiagnosed using other imaging techniques.

In *intramural hematoma* (Fig. 18.8), the inner surface of the aortic vessels looks unaltered, the outer aortic contour is not deformed, and the aortic wall presents an eccentric localized thickening (circular or semilunar) because of accumulation of blood within the media. The intimal layer is displaced toward the aortic lumen, which looks partially reduced and eccentric. No flow signals can be recorded within the medial hemorrhage. A concomitant pleural or mediastinal hemorrhage may be present. This lesion can be diagnosed using both CT without contrast material and magnetic resonance imaging (MRI; T1-weighted black-blood sequences). Although the aortic wall may be weakened by the hemorrhage, this lesion can usually regress spontaneously.

The characteristics of a *fusiform false aneurysm* (Fig. 18.9) due to circumferentially complete rupture of the intima and media on TEE examination are (1) abrupt change in aortic diameter in serial axial section, (2) smooth inner surface, and (3) loss of elasticity. The torn intima and media can be observed at the proximal and distal end of the false aneurysm, where the aorta caliber returns to be normal.

Table 18.3 Anatomical variants and corresponding echographic aspects of traumatic injuries of the thoracic aorta

Type of lesions	Pathology	TEE aspect
Intimal disruption	Discrete discontinuity of the intimal layer with thin wall appendages present in the aortic lumen; possible overlying thrombus	Discrete discontinuity of the intimal layer, highly mobile appendages within the lumen with neither flap, nor flow acceleration. Dimension and outer contour of the aorta unchanged. Possible thrombus formation
Intramural hematoma	Blood accumulation within the media with localized, usually eccentric (semilunar) wall thickening. The inner aortic surface is smooth; the aortic lumen is partially reduced, and the outer aortic contour is unaltered	Eccentric thickening (>5 mm) of the aortic wall with inner and outer surface of the aorta unchanged. The intima is displaced toward the lumen, which looks partially reduced and eccentric. No flow signals detectable within the hematoma. No flap. Pleural effusion and hemomediastinum usually present
Dissection	The flap is thicker than in classic dissection, being formed by the whole media and intima, has usually a direction transverse to the longitudinal axis of the aorta and fails to create two distinct channels	The flap is less mobile than in classic dissection. The flow velocity is different in the two aspects of the medial flap. The aorta is symmetrically enlarged. Hemomediastinum is usually present
Fusiform false aneurysm	Subadvential aortic rupture involving the whole intima and media with complete circumferential extension. The wall of the aorta is very thin and pellucid (formed by the sole adventia). The torn intima and media are located at the two extremities of the fusiform false aneurysm	Abrupt change in aortic diameter on serial axial sections; smooth inner surface; loss of elasticity; torn intima and media prolapsing into the lumen at the proximal and distal end of the false aneurysm
Saccular false aneurysm	Subadvential aortic rupture involving intima and media with incomplete circumferential extension. There is abrupt discontinuation in the inner surface of the aorta; the outer contour of the aorta is enlarged and deformed by the presence of the saccular false aneurysm; the torn intima and media usually protrude into the lumen	Mobile thick strip in the lumen, usually perpendicular to the major axis of the aorta; large communication with a saccular false aneurysm; to-and-fro low-velocity flow from the aorta to the pseudoaneurysm. If the torn aorta invaginates into the lumen, a flow acceleration and a gradient can be recorded (pseudocoartaction)
Injuries to the aortic branches	Partial or total avulsion, false aneurysm formation, dissection, thrombosis	TEE usually fails to visualize the aortic branches. Utilize linear probes with vascular configuration to investigate the neck vessels

TEE transesophageal echocardiography

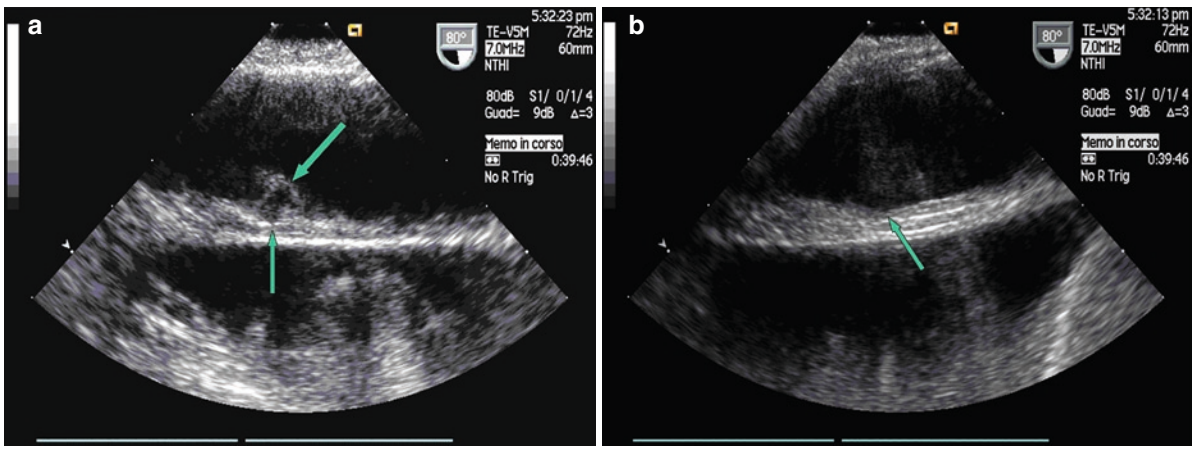

Fig. 18.7 (**a**) Transesophageal echocardiography view in a victim of an automobile accident, demonstrating an intimal disruption. The *small arrow* indicates a discrete discontinuity on the intimal layer, the large arrow the torn intima prolapsing into the lumen. No alteration in either the dimension or the outer contour of the aorta are evident. One week later (**b**), the lesion had undergone spontaneous healing with only a persisting small irregularity on the intimal profile (*arrow*)

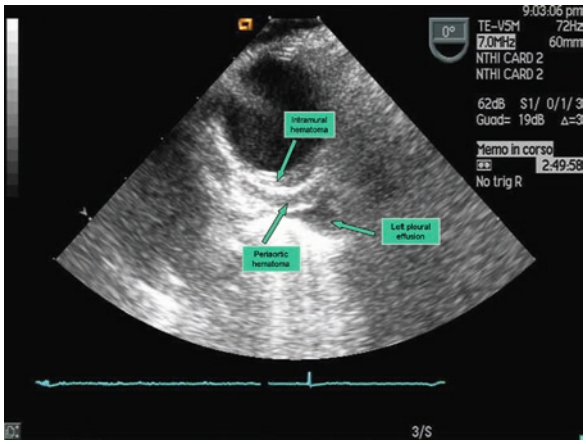

Fig. 18.8 Traumatic intramural hematoma. Transesophageal echocardiography view of the isthmus depicts a semilunar thickening of the posterior aspect of the aorta, indicative of intramural hemorrhage. Posterior to the adventitia, a semilunar periaortic hematoma is visible with an adjacent small left pleural effusion

Saccular false aneurysm is the most frequent type of TAI, and it can be diagnosed by TEE when a circumscribed rupture of the aortic wall (usually confined to the whole intima and whole media) is seen. The torn aortic wall is normally visualized as a thick and protruding intraluminal structure, usually mobile following the heart cycle. This linear structure transverses the entire aortic lumen in a longitudinal fashion perpendicular to the aortic wall (Figs. 18.10–18.11). The communication between the aortic lumen and the false aneurysm is usually large, so no flow acceleration can be detected using color-flow mapping. When the velocity-scale limit is reduced, one can observe a to-and-fro flow from the aorta to the false aneurysm. The outer aortic contour is enlarged and deformed by the presence of the false aneurysm. The torn aortic wall fragments can invaginate into the aortic lumen producing an obstruction to flow. Color-flow interrogation can detect acceleration between the aorta proximal and distal to the lesion, and continuous-wave Doppler can record a significant gradient at the isthmus. This is the only specific (albeit not sensitive) sign of TAI detectable using transthoracic echocardiography and is associated with the so-called pseudocoarctation syndrome (Fig. 18.12).

Potential advantages of TEE include portability, low cost, and low rate of complications. It is minimally invasive and can be performed in 15–20 min. TEE can be easily performed at the bedside, which is particularly useful if the patient is hemodynamically unstable. It can also be performed in the operating room while

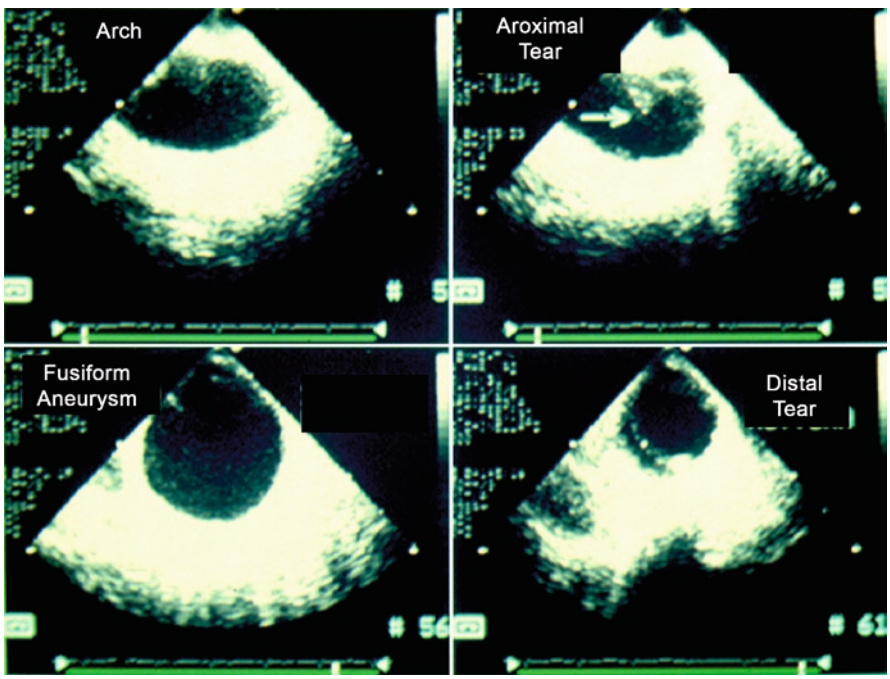

Fig. 18.9 Traumatic aortic injury with circumferentially complete rupture of the intima and media. In serial transesophageal echocardiography tomographic views of the thoracic aorta, the torn intima and media can be observed at the proximal and distal end of the lesion; a fusiform huge false aneurysm is located between these two aortic segments and is characterized by an abrupt change in vessel caliber, smooth inner surface (formed by the sole adventitia), and loss of elasticity

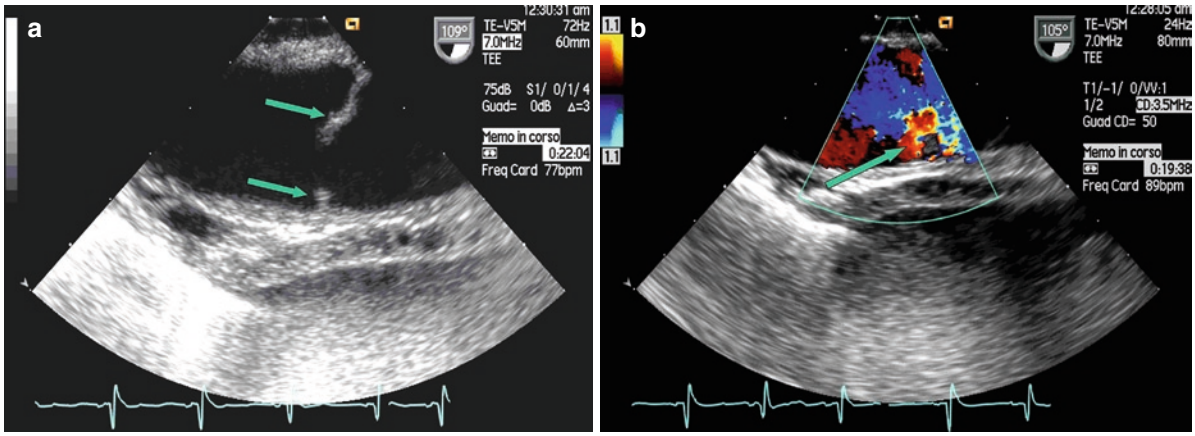

Fig. 18.10 (**a**) Traumatic aortic injury at the isthmus, transesophageal echocardiography view. The *arrows* indicate the torn intima and media partially invaginated into the lumen; (**b**) color-flow interrogation demonstrates flow acceleration (*arrow*) through the injured aortic segment (pseudocoarctation pattern)

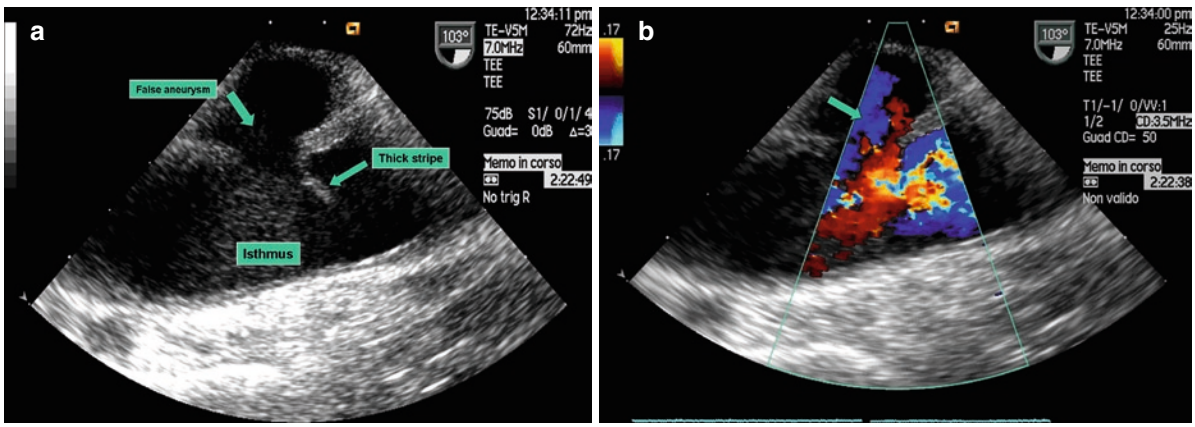

Fig. 18.11 (**a**) Typical transesophageal echocardiography aspect of a posttraumatic saccular false aneurysm at the isthmus. A thick stripe (formed by the torn intima and media) is seen within the aortic lumen; a large discontinuity in the aortic wall is visible, representing the communication between the aorta and the false aneurysm sac. (**b**) By reducing the velocity-scale limits, color-flow interrogation demonstrates (*arrow*) a to-and-fro flow in the false aneurysm

treating life-threatening injuries. TEE is less costly than CT; in addition, TEE requires less time to perform than CT or angiography, which requires a radiological team. Finally, complications have rarely been reported for TEE. TEE is extremely sensitive for aortic injury at the isthmus, and it provides precise evaluation of the nature of TAI, which is very important in planning the vascular intervention, especially in multiple trauma. Moreover, infrequent, but not exceptional, associated cardiac injuries can be easily assessed using TEE.

There are several potential contraindications to TEE. The only absolute contraindication is esophageal pathology, which is relatively unusual in patients with blunt trauma. Relative contraindications to TEE include unstable cervical spine and potential airway problems, such as major facial fractures. In addition, sedation is often required before conducting TEE in patients who are awake and nonintubated. This is a significant concern for patients who have recently eaten, who remain immobilized with spinal precautions, or who are intoxicated. Pharyngeal anesthesia should be avoided because it may increase their risk of aspiration.

Limitations of TEE include the inability to visualize the arch vessels and the distal ascending aorta. In the superior mediastinum, the air-filled trachea and the left mainstem bronchus are interposed between the

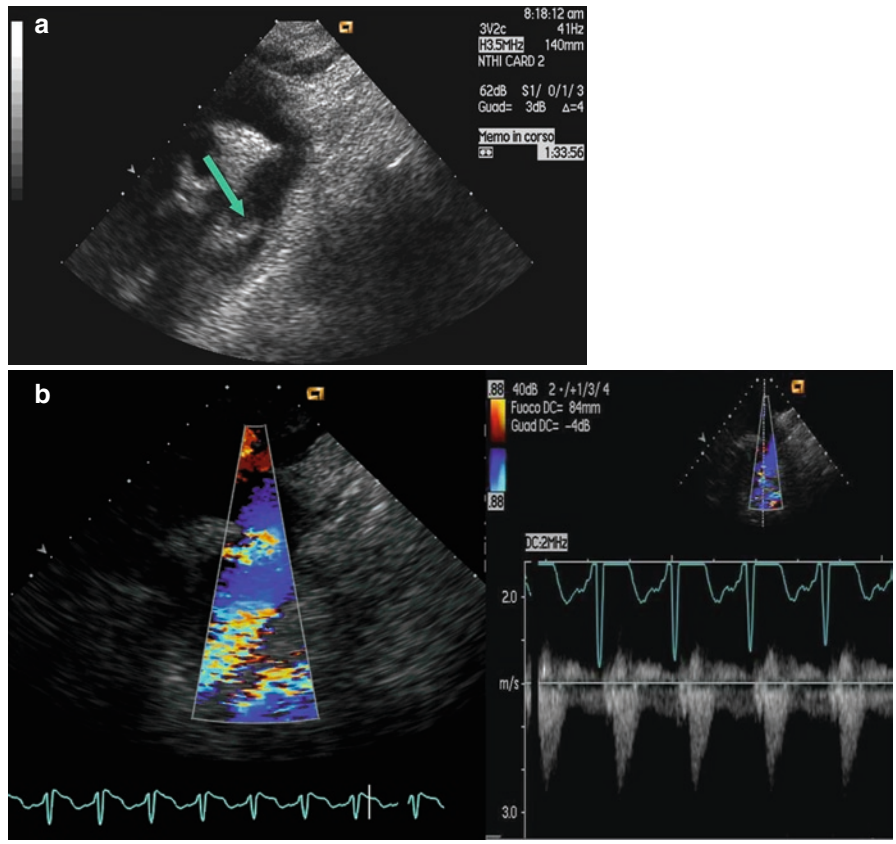

Fig. 18.12 (**a**) Transthoracic echocardiographic view of the region of the isthmus from a suprasternal approach. The *arrow* indicates the torn intima and media, partially invaginated into the lumen; (**b**) Doppler interrogation demonstrates acceleration through the injured aorta with a significant systolic gradient (pseudocoarctation pattern). This is the only specific, albeit little sensitive, echocardiographic sign of traumatic aortic injury obtainable from a transthoracic approach

esophagus and the aorta. The lack of an acoustic window precludes adequate evaluation of the distal ascending aorta and the proximal aortic arch (the so-called TEE blind spot). In addition, despite the use of omniplane transducers, the aortic arch branches cannot be adequately and consistently evaluated by TEE. From a technical standpoint, esophageal intubation is not always successful, and associated injuries, such as pneumomediastinum and pneumopericardium, may interfere with the examination, rendering it nondiagnostic (Fig. 18.13). The technical success rate for the performance of TEE is 98%. TEE requires an experienced and skilled operator for proper intubation and manipulation of the probe and correct acquisition and interpretation of images.

False negatives are generally due to the inability of TEE to detect TAI limited to the distal ascending aorta or the proximal arch, where the interposition of the air-filled trachea and the left bronchus hinders the visualization of the aortic wall. Although a technique to visualize the proximal portion of the supra-aortic vessels using an omniplane TEE probe has been described, the precise evaluation of traumatic injury to arch vessels using TEE remains problematic. In the presence of suspected injury to the aortic arch or to the neck vessels, an angiography should be implemented, especially when there is an important mediastinal hemorrhage and the aortic segments that can be imaged appear unaltered.

There are many possible sources of false positives with TEE. They can be divided into intra-aortic (linear artifacts, mirror artifacts, ulcerated atherosclerotic plaques, pedunculated thrombosis) and extra-aortic (venous-arterial periaortic vessels, left upper lobar atelectasis, dislocation of the aorta due to large mediastinal hematoma).

Linear artifacts are generally encountered when imaging the ascending aorta and can simulate an intimal flap. They are encountered in both the transverse and sagittal planes. They are generally distinguished from intimal flaps by (1) the fuzzy and indistinct borders of the artifact; (2) lack of rapid oscillatory

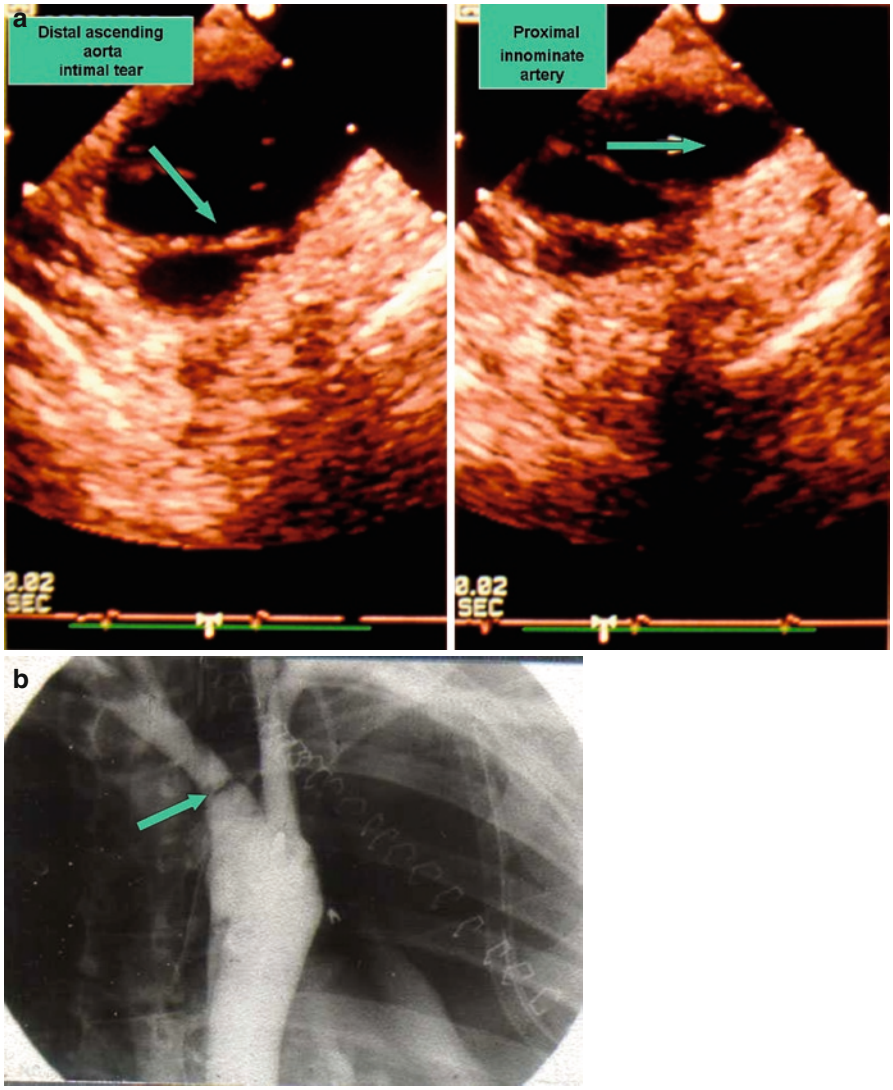

Fig. 18.13 (**a**) Transesophageal echocardiography (TEE) study of a 23-year-old male victim of an automobile accident. The first TEE study was inconclusive because of pneumomediastinum due to lacerated left mainstem bronchus. After surgical transection of the left bronchus, TEE was repeated because of recurrent transient ischemic attack to the right cerebral hemisphere. The TEE investigation of the distal ascending aorta identified an intimal tear (*arrow*) of this segment and a partial avulsion of the innominate artery (*arrow*). Angiography (**b**) confirmed the injury to the innominate artery (*arrow*)

movements generally associated with intimal flaps in acute dissection; (3) extension of the artifact through the aortic wall; (4) no interruption of the flow pattern within the aorta; (5) frequent occurrence when the diameter of the ascending aorta exceeds the left atrial diameter (Figs. 18.14–18.15) [23]. Using M-mode echocardiography, Evangelista et al. described three different types of linear artifacts in the ascending aorta: type A, which were located twice as far from the transducer as the posterior aortic wall; type B, located at the same distance from the posterior aortic wall as the latter was from the right pulmonary posterior wall; type C, located at the same distance from the posterior aortic wall as a reverberation from the right pulmonary artery posterior wall [24]. All these artifacts exhibited a movement parallel to the posterior aortic wall (Fig. 18.15). Linear artifacts originate in multiple-path artifacts secondary to the reflection between two surfaces. In an experimental model, linear artifacts were seen in the chamber distal to the transducer when the diameter of the proximal chamber was less than that of the distal chamber [25]. In clinical practice in patients with intraluminal linear artifacts, the diameter of the ascending aorta consistently exceeds that of the adjacent posterior anatomical structure (left atrium, pulmonary artery). In patients with linear artifacts in the descending aorta, the vessel is consistently shifted anteriorly. This explains the higher incidence of linear artifacts within the descending aorta in patients with severe blunt chest trauma, in whom a traumatic

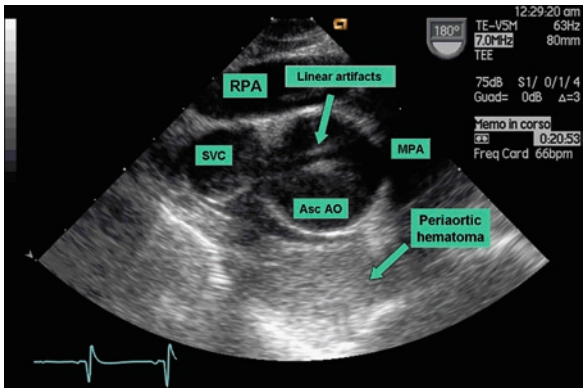

Fig. 18.14 Transesophageal echocardiography transverse view of the base of the heart in an automobile accident victim. A large anterior periaortic hematoma is visible (*arrow*). Within the aortic lumen some linear, fuzzy, and mobile structures are visible, simulating an intimal flap (*arrow*); these were linear artifacts generated from the interface between the right pulmonary artery (RPA) and the ascending aorta (Asc AO). *MPA* main pulmonary artery, *SVC* superior vena cava

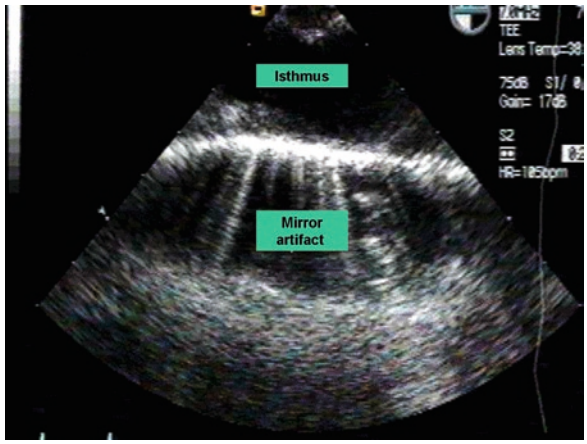

Fig. 18.16 Mirror artifact at the isthmus simulating a double-lumen vessel. The diameter of the "true" and "false" aorta is exactly the same

hemomediastinum, which usually results in an increased distance between the esophageal probe and the anteromedial aortic wall, is frequently observed. Because hemomediastinum is frequently associated with TAI, accurate diagnosis of linear artifacts within the aortic isthmus in the clinical setting is critical to avoid false-positive results.

Mirror artifacts are more frequently observed in the transverse aortic arch and descending aorta; they give the appearance of a double-lumen aorta (the two lumens having the same diameter), with color flow generally visible in the artifactual aorta (Fig. 18.16). They are generated at the level of the aorta-lung interface, which has many properties of an ideal acoustic mirror because

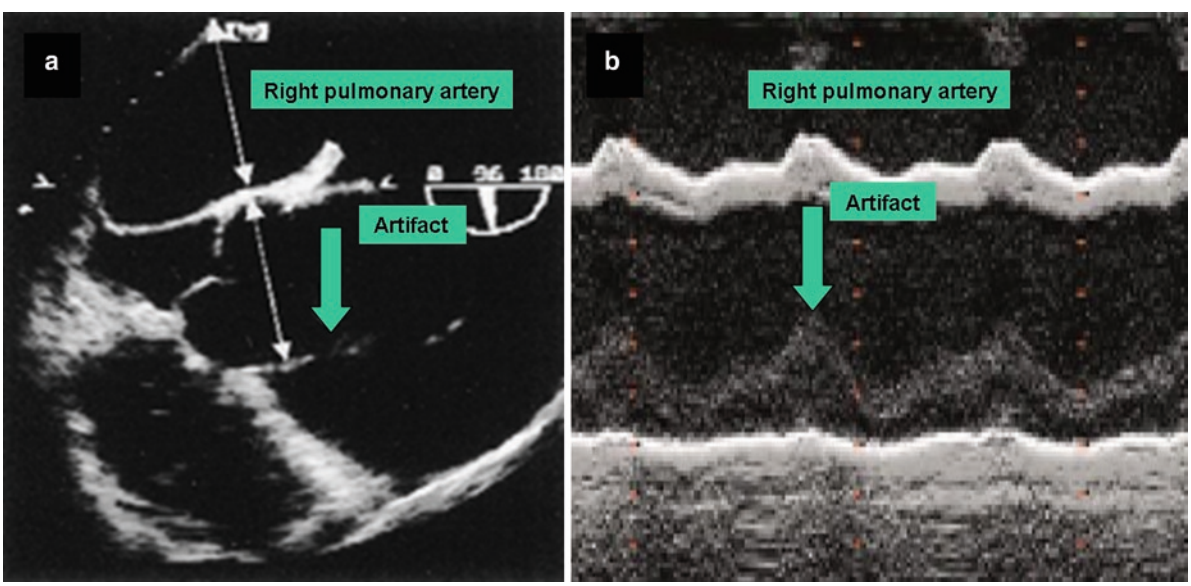

Fig. 18.15 In a longitudinal view (**a**), the artifact has a distinct linear appearance, and it is located twice as far from the transducer as the posterior aortic wall. The artifact exhibits a movement parallel to the posterior aortic wall (**b**)

(1) it is smooth; (2) it is only a few centimeters from the transducer, exposing the reflecting surface to high-energy levels of ultrasound to be reflected; (3) there is little attenuation of the ultrasound by the blood-filled aorta; (4) the aorta-lung interface is flat when the aorta is imaged in the sagittal plane. A mirror artifact is generally easy to distinguish from a true anatomical structure. It occurs at a predictable distance, related to the width of the aorta, and the double-lumen appearance of the aorta disappears when the lung is not adjacent to the aorta (i.e., left pleural effusion).

Extraoartic artifacts may be secondary to the visualization of portions of periaortic structures (vascular structures, mediastinal structures, lung atelectasis, etc.), which can be imaged adjacent to the aortic wall in some views, simulating a discontinuity of the aorta. Particular attention should be given to the left brachiocephalic vein, which has a course often parallel to the aortic arch, simulating an intimal flap, and to the region where the left pulmonary artery and left upper pulmonary vein are in near proximity to the isthmus. In all these cases, multiple views should be utilized and interrogation of the different vascular structures performed using pulsed-wave Doppler to distinguish the characteristic flow patterns (Fig. 18.17).

There have been many studies on the role of TEE in the assessment of injured patients [26–40]. Thirteen studies reported a total of 152 cases of proven thoracic aortic injury among 1,060 patients (Table 18.4). There are major differences in both sensitivity and specificity values reported. These can be due to the use of different TEE probes (single-plane, biplane, or omniplane), but

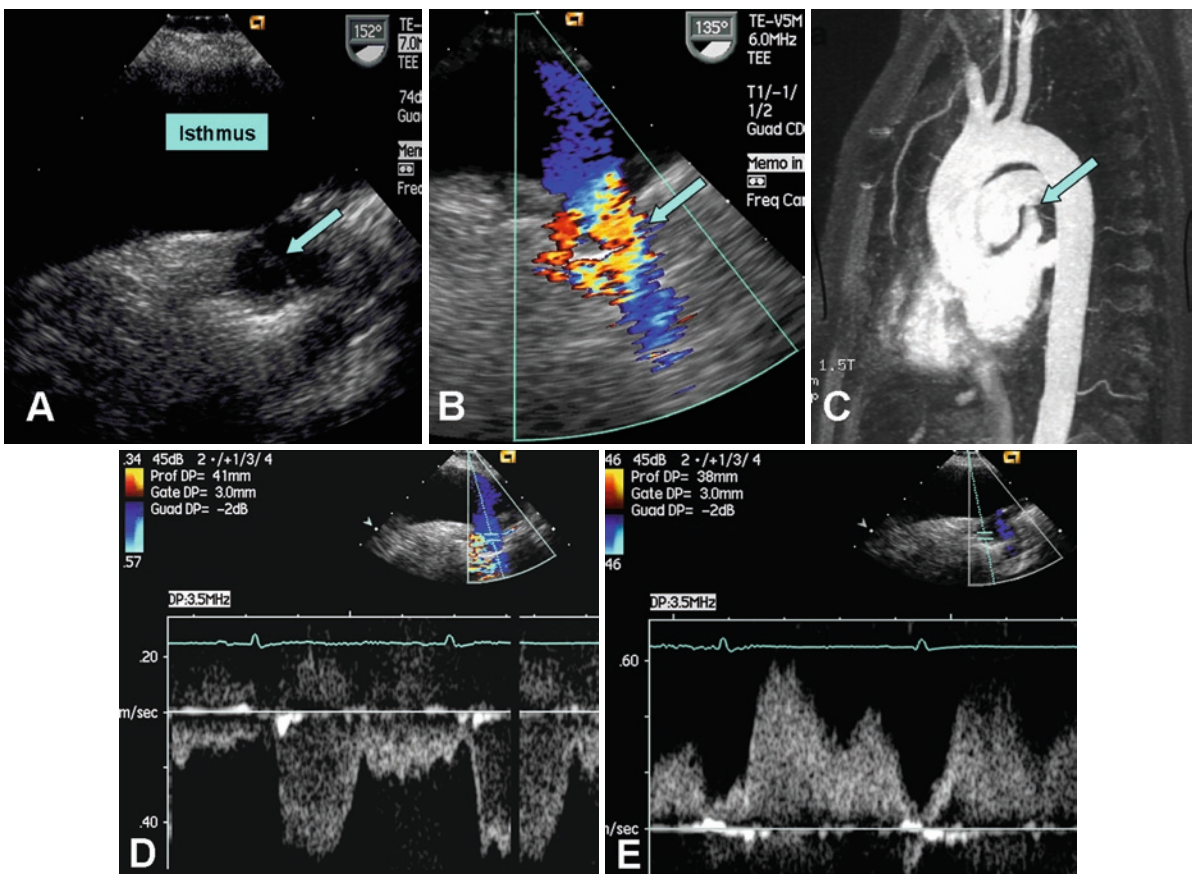

Fig. 18.17 Transesophageal echocardiography imaging of the isthmus in a trauma victim. (**a**) An apparent saccular outpouching is visible on the anterior aspect of the aorta, and a thin linear structure can be imaged within this cavity (*arrow*). (**b**) Color flow interrogation demonstrates the presence of an accelerated flow within this structure, simulating a traumatic false aneurysm. This structure corresponds (**c**) to the region where the left pulmonary artery and the left upper pulmonary vein are in proximity to the isthmus. Pulsed-wave Doppler interrogation of the structure reveals a flow pattern typical for the pulmonary artery (**d**) and pulmonary vein (**e**)

the likelihood is that they are mostly dependent on the different operators' expertise. The 4 studies with the largest study cohorts, collecting a total of 87 incidences of TAI among 566 patients, reported 3 false positives and 1 false negative, with an overall sensitivity of 87% and specificity of 99%. On the other end only one article [33] has reported a very high incidence of false negatives (3/12) and false postives (17/25). In this paper TEE was performed by different operators (cardiologists, anesthesiologists, emergency surgeons) with different expertise in echocardiography. This outlines the importance of a learning curve for operators of TEE in emergency situations in order to achieve optimal images and interpret them correctly, avoiding false positives and negatives.

Although sensitivity and specificity in statistical terms are independent of prevalence, this applies only if we assume uniformity of diagnostic skill, whereby all investigators are on the plateau phase of the learning curve and that the level of diagnostic suspicion does not influence the interpretation of the image. While one should be able to make such a claim for an established laboratory assay, it is unlikely to hold true for TEE in the acutely ill patient, probably performed out of hours in the accident department of a district general hospital.

It is also worth remembering that where there is a degree of uncertainty, there is an element of choice about how we set our criteria. If a test is to be used for screening a population with a low prevalence of a very dangerous condition, the decision threshold is set low, so that sensitivity is high, close to 100%. There are more false positives but fewer missed cases. If, however, you are going to act on that test alone, you must set the decision threshold higher, for fear of operating and finding a normal aorta after an unnecessary thoracotomy. The first approach works if we assume that aortography or MRI will be available as a confirmatory test, either as a policy or in any case where there remains doubt, or there is time to be more certain. The generally high sensitivity of TEE suggests that the test performs well if used in that way. The experience of Saletta et al., who included three patients with negative TEE, but who subsequently had aortic disruption, is out of line with the experience of all others, but it should be noted [33].

Sensitivity and specificity answer the question from one direction only: if the condition exists, can the test detect or exclude it? The indices that help us in that respect are positive and negative predictive values. These are dependent on the prevalence of TAI, and one of the most striking aspects of Table 18.4 is that the prevalence of aortic disruption ranges from 5% to 54%. The likely explanation is that the case mix varies between the studies because of selection bias. In the smallest series, the 11 patients were estimated to be only 25% of the cases with severe blunt

Table 18.4 Diagnostic accuracy of transesophageal echocardiography for the diagnosis of traumatic injury of the thoracic aorta

Year	Author	Patients (n)	TAI (n)	Prevalence of TAI (%)	Sensitivity (%)	False negatives	Specificity (%)	False positives
1991	Shapiro [26]	19	3	16	67	1	100	0
1991	Sparks [27]	11	6	54	50	3	100	0
1992	Brooks [28]	58	3	5	100	0	96	2
1993	Kearney [29]	69	8	11	100	0	100	0
1994	Karalis [30]	20	5	25	100	0	100	0
1994	Buckmaster [31]	160	14	9	100	0	98	2
1995	Smith [32]	93	10	11	100	0	98	1
1995	Saletta [33]	114	8	7	63	3	84	17
1995	Vignon [34]	32	14	43	91	1	100	0
1996	Minard [35]	34	9	26	57	3	91	2
1996	Chirillo [36]	131	14	11	93	1	98	2
2000	Goarin [39]	209	42	20	98	1	100	0
2001	Vignon [40]	110	17	15	93	1	100	0

TAI traumatic aortic injury

chest trauma admitted during the time frame of the study. In the largest series, TEE was used in prospectively designed protocols, which presumably recruited not only more patients, but enrolled a group with a lower pretest probability of aortic injury.

18.1.1.9 Screening for TAI in Patients with Blunt Chest Trauma

The goal of screening patients with high-energy trauma to the chest is to attain zero nontherapeutic thoracotomies without overlooking any surgically important aortic or brachiocephalic arterial injuries. Because TAI without mediastinal hematoma is rare, the most popular TAI screening algorithms include chest X-ray as the first imaging modality because of diffusion, low cost, rapid exam time, and high sensitivity. In patients with reasonable suspicion of TAI, immediate aortography is warranted, followed by emergency surgery in the presence of angiographic signs of TAI.

Recently, this algorithm has undergone some change, primarily because of the number of negative aortographies performed (about 80–85%). In fact, there is great risk to the patient if a TAI is not detected, but considerable time is incurred to exclude TAI deferring the identification of other potentially lethal injuries..

Most reports on TAI have evaluated only patients with a proved injury, and few have examined issues that place aortic injury in the context of total patient care. A review of the treatment of aortic injury may lend the impression that these injuries occur in a vacuum; only recently has the management of multisystem trauma with aortic transection been addressed [40, 41].

With the advent of fast scanning with helical CT, many institutions are screening trauma patients for aortic injuries using chest CT. More than 90% of these patients will not have aortic transections, but other serious, unsuspected injuries are frequently identified on chest CT.

If the transportation of patients to the CT suite does not require much time and does not increase the risk

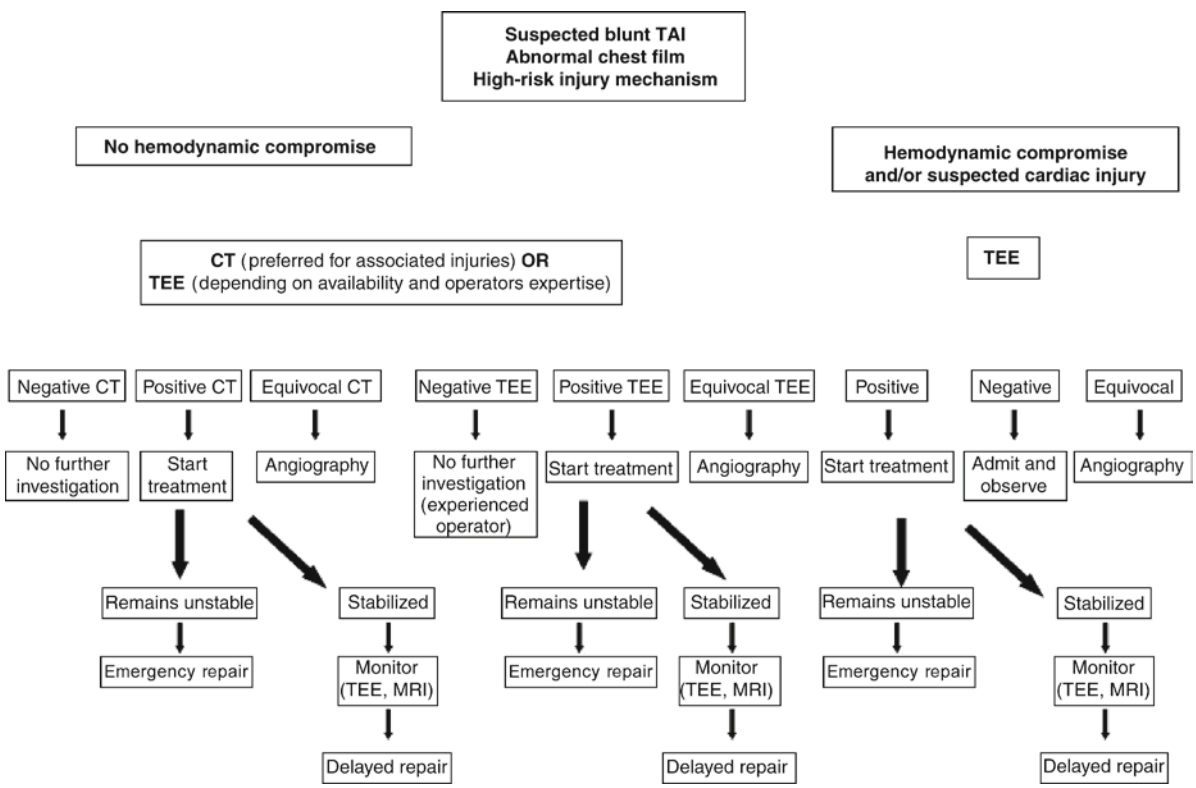

Fig. 18.18 Proposed algorithm for the diagnosis and management of patients with traumatic aortic injury (TAI). *CT* computed tomography, *TEE* transesophageal echocardiography, *MRI* magnetic resonance imaging

for a hemodynamically unstable patient, CT seems a reasonable choice because it can assess multiple injuries in an accurate and rapid way.

If the patient has TAI at the isthmus and a stent-graft repair is planned, CT scan using three-dimensional reconstruction algorithms can provide all the information needed to select the proper graft stent. If surgical repair is indicated, aortography is usually preferred to better delineate the presence of associated vascular injuries. If a traumatic lesion involving the aortic arch or aortic branch vessel is suspected, aortography is the technique of choice.

The patient with multiple trauma in whom CT scan confirms the mediastinal hematoma, but the integrity of the aorta itself remains unclear, demands further investigation. Under these circumstances, a test that reliably excludes aortic rupture, so that we can proceed with other aspects of management, would be extremely helpful. TEE has displayed a 100% negative predictive value in excluding TAI in most series. That seems to be its strength. Moreover, it can be performed at the bedside and appears to be predictive of imminent complete aortic rupture, dictating possible emergent aortic surgery. If TEE provides a reliable negative test on-site, allowing the trauma team to look after the whole patient rather than feeling obliged to concentrate on the aorta, then TEE can be a lifesaver.

TEE seems to be the technique of choice in hemodynamically unstable patients because it can be performed at the bedside without interfering with other ongoing diagnostic and therapeutic procedures; it has a high negative predictive value, it can define the nature of TAI, and it can indicate signs of gravity. All of this is of help in treatment prioritization (Fig. 18.18).

It is not easy to draw some definite conclusion on which imaging modality is best in the diagnosis of blunt aortic injury. Under all conditions, the choice among different techniques will depend on availability, operator expertise, and the level of confidence of the local surgeon to operate on the aorta on the findings of one nonangiographic imaging modality. A recent survey by the American Association for the Surgery of Trauma [42] performed in 18 trauma centers across the USA has demonstrated that the diagnosis of TAI was made by CT scan in 93.3%, aortography in 8.3%, and TEE in 1.0% of patients over the period 2005–2007 compared with 34.8%, 87.0%, and 11.9%, respectively, over the period 1993–1996. The wide acceptance of CT scan as a noninvasive, rapid, largely available, reliable diagnostic method, providing excellent delineation of associated injury in a short time, has brought about the almost complete disappearance of aortography and TEE from the clinical scenario, at least in the USA.

18.1.2 Management

18.1.2.1 Impact of TEE Findings on Patient Management

The accurate determination of the depth of aortic wall tears provided by TEE is crucial in guiding patient management. The high short-term mortality observed in TAI at the isthmus is generally related to the rupture of the wall of the false aneurysm, which is constituted in the case of subadventitial aortic injuries by the sole adventitial aortic layer under tension. There are some signs of gravity that portend a high risk of imminent adventitial rupture. These can be assessed by TEE and are the following: (1) large false aneurysm; (2) large (>10 mm) hemomediastinum; (3) massive left hemothorax; (4) pseudocoarctation pattern.

When these situations are present, patients should undergo immediate repair of the aortic injury [40]. If these aspects are absent, repair of the aortic injury may be delayed. Until few years ago, the extremely high death rate of acute blunt rupture of the thoracic aorta led surgeons to repair the aortic tear as quickly as possible. The overall mortality rate found by Von Oppel et al. in a meta-analysis on 1,492 patients who were hemodynamically stable upon reaching the operating room was 21.3% [43]. It ranged from 0% to 54.2%, with the majority of fatalities occurring in the postoperative period and being often due to associated injuries in other organs. During the early 1970s, Akins et al. [44] and Pate et al. [45] began to delay the surgical repair of TAI in selected patients with other major injuries. With appropriate pharmacological treatment aimed at reducing stress on the aortic wall, TAI could be managed in parallel with other life-threatening injuries. Beta-blockers are the cornerstone of this medical therapy because they simultaneously reduce blood pressure, force of the arterial upstroke, and heart rate. Under these circumstances, other procedures, such as laparotomy for control of intraperitoneal hemorrhage (splenectomy, packing of liver laceration, etc.) and transcatheter embolization of a bleeding

retroperitoneal artery, take precedence over surgical repair of TAI. Certain subgroups of patients may benefit from delayed aortic repair. These include patients with trauma to the central nervous system, contaminated wounds, respiratory insufficiency from lung contusion or other causes, body surface burns, blunt cardiac injury, tears of solid organs that will undergo nonoperative management, established sepsis, retroperitoneal hematoma, age of 50 years or older, and severe medical comorbidities [46, 47]. In these patients, TAI should be monitored at regular intervals, using noninvasive imaging to detect possible enlargement of the aortic caliber or progressive weakening of the aortic wall, anticipating TAI repair. MRI seems to provide the best, most reproducible information and is an ideal tool for this monitoring purpose [48].

In contrast to subadvential disruptions, intimal tears and intramural hematoma can be successfully managed conservatively with serial clinical and TEE follow-up. There is limited experience with these lesions, and the validity of this therapeutic approach needs further confirmation. Importantly, the formation of a false aneurysm or further extension of a previous TAI, especially when signs of fluid extravasation are present, should lead one to consider repair of the TAI.

18.1.2.2 Treatment Prioritization

Notwithstanding the high short-term mortality rate in patients sustaining a blunt injury to the thoracic aorta, it is now clear that TAI is often not the worst injury that a trauma patient can sustain. If the attention of the attending physician is drawn only toward detecting possible TAI, more dangerous and life-threatening injuries may go unidentified and have dire consequences for the patient.

Prioritization of treatment is controversial in patients with multiple organ damage and aortic rupture. Our preference is to discriminate between the hemodynamically stable and unstable patient. If the patient (Fig. 18.18) has a very high operative risk owing to age and severity of other injuries, medical management similar to that employed for acute aortic dissection may have a role, although delayed surgical repair will be required in virtually all cases. In the hemodynamically stable patient without associated injuries, immediate repair of TAI will usually precede other procedures, such as major orthopedic, maxillofacial, or abdominal operations.

In the hemodynamically unstable patient with TAI in whom another source of hemorrhage is identified, the latter should receive attention first, for example, a splenectomy or selective arterial embolization for major retroperitoneal bleeding. If no other bleeding source is obvious, then immediate repair of the aortic injury is indicated.

The issue of isolated intimal injuries to the aorta presents a whole new dimension to the evaluation of aortic injury. The long-term outcome of intimal injury is not known. In anecdotal reports, such lesions seem to have a tendency toward spontaneous healing; however, the potential risk to progression into complete rupture or risk of thromboembolism needs to be evaluated. At the moment, strict follow-up of such lesions seems to be the best policy, especially in the presence of severe associated injuries, which markedly increase the operative morbidity and mortality.

18.1.2.3 Surgery

In the operating room, the positioning of the patient and the choice of incision depend on the distribution of the injuries as depicted by preoperative imaging studies. TAI circumscribed to the isthmus is approached through a left lateral thoracotomy, while involvement of the ascending aorta, aortic arch, or proximal branches requires median sternotomy. Approximately 15% of all TAI can be repaired by primary aortorrhaphy; 85% require graft interposition. The most controversial issue regarding surgical repair of TAI involving the isthmus is the choice of distal perfusion: clamp repair, temporary bypass shunt, centrifugal pump without heparinization, and cardiopulmonary bypass are all acceptable techniques for TAI repair [49, 50]. No currently existing report from a single institution compares these surgical techniques in a prospective, randomized manner. The most serious concerns with surgical repair of TAI are the possible worsening of associated injuries following systemic heparinization and postoperative spinal myelopathy (leading to paraplegia or paraparesis) following intraoperative spinal ischemia. The overall incidence of paraplegia is 5%, with a range from 0% to 15%. Clamp time seems to be one of the most important determinants of postoperative myelopathy. The overall mortality rate is around 15%, with 0–16% rates reported in series greater than 15 [43, 50].

18.1.2.4 Endovascular Repair

Before 1997, patients with TAI were treated with an open repair, but the conventional surgical approach carried high mortality and morbidity rates. Graft interposition and cross-clamping of the aorta were responsible for a high paraplegia rate. Despite the fact that active distal perfusion of the aorta lowers the incidence of neurological deficit, the timing of these extensive procedures in the severely injured multitrauma patient remains problematic. The endovascular repair of a traumatic thoracic aortic rupture has gained rapid acceptance as a better alternative.

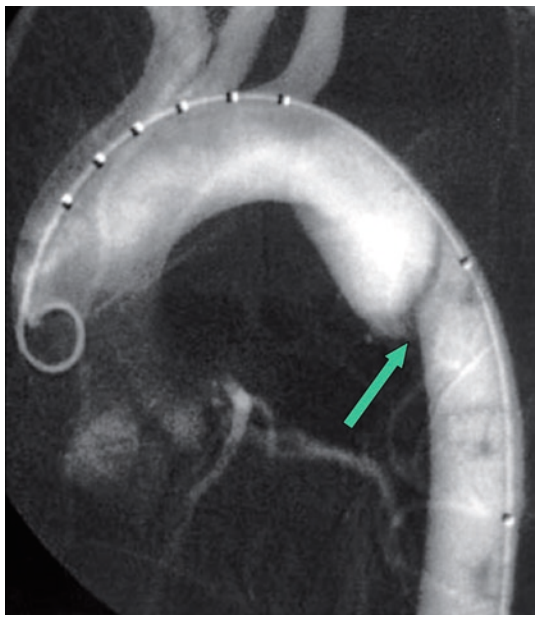

Fig. 18.19 Aortography taken with a calibrated pigtail catheter. The rupture (*arrow*) was identified at the isthmus with a distance between the traumatic aortic injury and the origin of the left subclavian artery of about 2 cm

The procedure is normally performed under angiographic monitoring under general anesthesia. Using a right radial or brachial approach, a pigtail catheter is advanced into the ascending aorta. This catheter allows contrast injection during the procedure and helps to identify the origin of the left subclavian artery, which is an important landmark for proper positioning of the stent graft (Fig. 18.19). In inserting the device, the common femoral artery is surgically exposed. The stent graft is then pushed toward the arch using an ultra-stiff guidewire. The self-expanding endoprosthesis is generally formed by nitinol stent springs, arranged as a tube to conform to the aortic lumen and covered on the outside with a Dacron graft. Precise location of the graft is angiographically assessed; for deployment, the graft is held in position with a pusher while the sheath is withdrawn. The success of the procedure is usually assessed by postoperative angiography, demonstrating full coverage of the lesions by the endoprosthesis with no detectable extravasation of contrast media. Angiography is less accurate than contrast-enhanced spiral CT in detecting endoleaks (Fig. 18.20); if there is a small endoleak despite adequate coverage

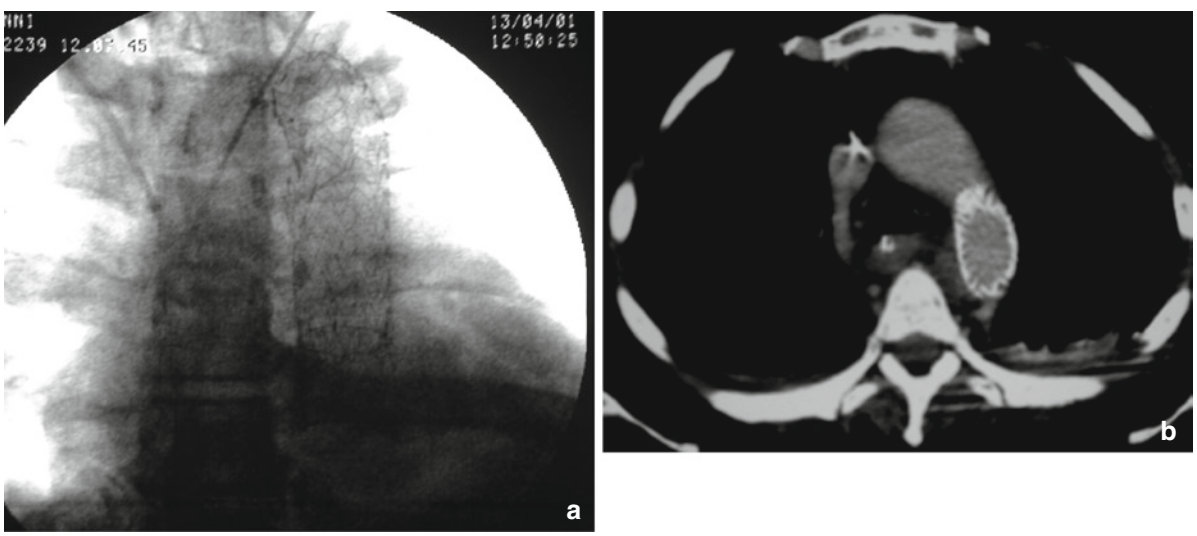

Fig. 18.20. (**a**) The rupture was sealed off by the covered stent. (**b**) Contrast computed tomography scan performed 2 days later showed neither false aneurysm nor leakage of contrast medium outside the aorta

of the TAI, it may be due to residual folding of the graft material and have a tendency to thrombosis spontaneously. In some patients, early extravasation of contrast media through the graft material is generally due to the fact that the porous Dacron mesh requires platelet adhesion and local clot formation to tighten the graft material; these leaks tend to resolve spontaneously in few days. By contrast, incomplete graft apposition (type-I endoleak) is a treatment failure and requires endovascular or open surgical revision in order to hinder the expansion and possible rupture of the false aneurysm.

TEE intraoperative monitoring in expert hands provides an excellent monitoring technique because it is more accurate than angiography in detecting the landing zone of the graft and incomplete apposition of the graft; it can also demonstrate the success of the procedure when a complete thrombus formation is seen within the false aneurysm after graft deployment [51]. If flow to and from the sac is identified by color Doppler or pulsed-wave Doppler and the sac looks only partially obliterated by thrombus, incomplete apposition should be suspected. The stent can then be expanded using a balloon, or a second stent can be implanted (Fig. 18.21). TEE, moreover, reduces the amount of contrast medium and the X-ray dose to the patient.

This minimally invasive procedure has a median operating time of <1 h, and it can be done in the same session in which other life-threatening injuries are repaired. There is no need for a thoracotomy or single lung ventilation, blood loss is minimal, and systemic heparinization is not required. So far, no spinal cord ischemia has been described for the endovascular repair [52–54]. Besides numerous advantages, a few problems can be expected. The narrow aortic diameter in young trauma victims combined with a steep aortic arch sometimes makes the adaptation of the endograft along the inner curvature difficult. Because the

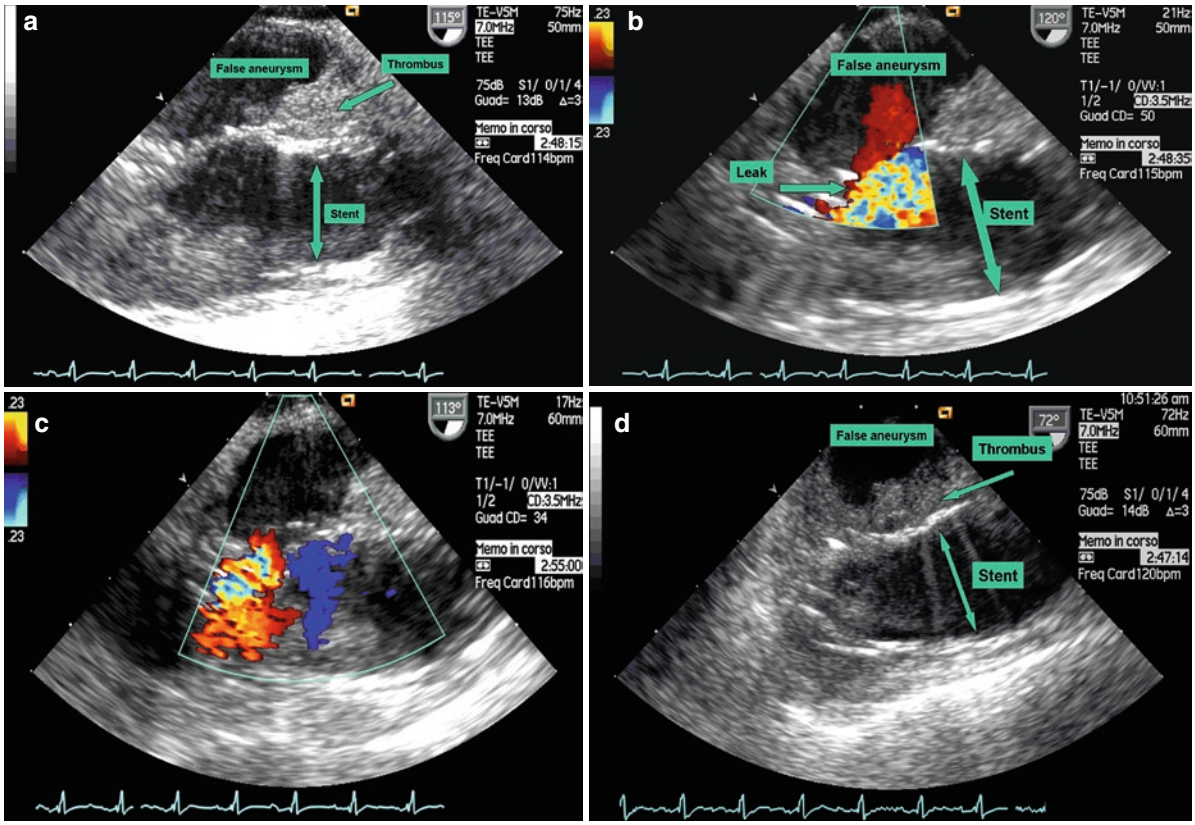

Fig. 18.21 Transesophageal echocardiography monitoring during an endovascular repair of a traumatic false aneurysm. After the stent had been positioned, the false aneurysm looked (**a**) Ather the stent had been only partially filled with thrombus. (**b**) Color Doppler interrogation of the isthmus identified persistent flow from the aorta to the false aneurysm; the stent was therefore dilated using a second balloon. Immediately after stent expansion (**c**), color-flow excluded persistent flow to the false aneurysm, and thrombus began to form within the false aneurysm sac (**d**)

smallest endograft is usually greater than the narrow aortic diameter, only somehow oversized devices can be used, which explains the high rate of type-I endoleak encountered in the published series. No randomized studies are yet available comparing the open with the endovascular technique, but the initial results of endovascular repair seem promising, and lower mortality and morbidity rates have been documented. Data on the long-term outcome is lacking so far, but the durability of the procedure has to be addressed.

In a recent survey of the American Association for the Surgery of Trauma [42], the number of patients treated with endovascular stent grafts increased from 0% in the period 1993–1996 to 64.8% in 2005–2007; the mean time from injury to aortic repair showed an increase over the two periods from 16.5 to 54.6 h, and the overall mortality, excluding patients in extremis, decreased significantly from 22.0% to 13.0% ($p = 0.02$).

18.2 Blunt Cardiac Trauma

Cardiac injury occurs commonly after blunt trauma and has been implicated in 10–76% of deaths in the immediate period following vehicular trauma. The spectrum of blunt cardiac injury is wide, ranging from subtle, subclinical wall-motion or conduction abnormalities detectable after intense investigation to myocardial infarction, life-threatening arrhythmias, and lethal myocardial rupture. Although the terms myocardial contusion and myocardial concussion have been used for several decades, considerable confusion exists over their precise meaning in both clinical and pathological terms. In 1992, Mattox et al. proposed a new classification of cardiac trauma according to the severity of the lesion and diagnostic modality used (Table 18.5) [55]. This classification emphasizes the role of echocardiography in the detection of blunt cardiac injury.

Table 18.5 Specific description of traumatic cardiac injuries

Blunt cardiac injury with septal rupture
Blunt cardiac injury with free-wall rupture
Blunt cardiac injury with coronary artery thrombosis
Blunt cardiac injury with cardiac failure
Blunt cardiac injury with minor echocardiogram or enzyme abnormality
Blunt cardiac injury with complex arrhythmia

According to Mattox et al. [55]

18.2.1 Mechanisms of Injury

The heart is situated in the middle mediastinum, surrounded by the sternum, ribs, and spine. The heart is generally injured by compression against the sternum or between the sternum and the vertebral column as a result of a direct blow to the sternum, as in injuries caused by the steering wheel in automobile accidents or animal kicks. Moreover, because the cardiac base is suspended within the thorax, sudden deceleration in either the anteroposterior or vertical direction can cause the heart to become injured by hitting adjacent structures or rotating on its longitudinal axis, causing torsion and avulsion of the atrial appendages from the atria, the pulmonary veins from the left atrial wall, or the aortic/mitral valves from their annulus. Finally, rapid increases in intrathoracic pressure following transmission of intra-abdominal forces across the diaphragm (the "hydraulic ram" effect), often observed in seat-belt type injuries, can cause significant cardiac lesions [56]. Severe anatomical injuries, such as cardiac rupture, manifest themselves immediately after impact, which accounts for their dramatic clinical presentation and high mortality rate. On the other hand, some other injuries, such as septal defects, valvular incompetence, aneurysm, and pseudoaneurysm formation, may appear at a varying interval (sometimes years) after blunt chest trauma.

It is, therefore, very difficult to generate an adequate clinical index of suspicion for cardiac injury: different algorithms have been proposed to deal with the risk of utilizing many resources to identify a condition that may have no clinical impact on the patient's outcome and generally undergoes spontaneous healing against the risk of not considering cardiac injury responsible for hemodynamic instability in the setting of multiple-system blunt trauma.

18.2.2 Anomalies of Segmental or Global Ventricular Systolic Function

The majority of patients with myocardial injury who are admitted to hospital following blunt trauma have anterior chest wall trauma without myocardial rupture, valve disruption, or coronary injury, but present with one or more of the following: arrhythmias, abnormal cardiac markers levels, abnormal cardiac wall motion, abnormal ECG findings, and apparent small pericardial effusion. Their initial workups, which include ECG, determination of myocardial damage markers, and cardiac imaging, are extensive and expensive, with a very low yield of specific diagnoses. Patients with these abnormalities are frequently admitted to an intensive care unit for extensive monitoring because of fear of missing a potentially lethal condition. In general, these abnormalities do not determine a hemodynamic instability and tend to disappear spontaneously. Only patients with hemodynamic instability that cannot otherwise be explained should be examined for reduced ventricular systolic performance. In these patients, the use of echocardiography (especially TEE because of its larger sensitivity) is indicated.

Due to its location immediately posterior to the sternum, the right ventricle is the most frequently injured chamber. The anterior (free) right ventricular wall may present different degrees of wall-motion impairment (hypokinesia, akinesia, dyskinesia), and the right ventricular cavity is generally dilated. If the pulmonary vascular resistance is increased, the afterload mismatch causes a leftward shift of the interventricular septum, which, in turn, results in decreased left ventricular compliance and stroke volume. The ventricular wall can look thickened and ipo- or hypoechoic or anechoic due to the presence of areas of hemorrhage or interstitial edema. Grossly, there may be a superficial area of cardiac contusion overlying the epicardium that may extend into a larger intramural or transmural area of injury. The pericardium may appear thickened (due to the presence of inflammatory response) or a hemopericardium may develop. The lesion tends to undergo spontaneous healing: however, in some patients the hematic component of the pericardial fluid can organize into a thickened fibrotic and/or calcific layer leading (months to years after trauma) to constriction.

The diagnosis of myocardial contusion is frequently difficult to confirm because well-defined and uniformly accepted diagnostic criteria do not exist. The most frequently used tests are ECG and markers of myocardial damage (CK-MB or troponins). However, the data is often inconsistent because most patients with abnormal ECG and increased troponin levels have normal echocardiograms, and delayed free-wall left ventricular rupture has been observed in the absence of any laboratory or ECG abnormal findings. Moreover, left or right ventricular abnormalities can be the consequences of prolonged hypoxemia, hypovolemia, increased pulmonary resistance, and head trauma associated with intracranial hypertension [56, 57].

18.2.3 Cardiac Rupture

Myocardial laceration and rupture are the most severe cardiac injuries after blunt trauma. These lesions account for over 60% of deaths in large autopsy series but make up only 0.5–2% of admissions for blunt chest trauma [58]. Mechanisms on injury include acceleration-deceleration stresses, direct precordial impact, and compression between the sternum and vertebral column. All four heart chambers rupture with equal frequency, and in up to 30% of patients more than one chamber is affected. The atria are most vulnerable in their appendages, and the interventricular septum at the apex, these being the thinnest portions; the points where the pericardium is tethered (i.e., the sites of entry of the caval and pulmonary veins) may be particularly susceptible to deceleration stresses. The cause of death in patients with cardiac rupture is usually either exsanguination, which occurs if the pericardium is lacerated concomitantly, or cardiac tamponade. Patients suffering from this latter injury frequently die in transit, but they may survive long enough to reach the hospital alive. The diagnosis of cardiac rupture should be suspected in any blunt chest trauma victim who presents with clinical (distended neck vein, hypotension, and distant heart tones – the so-called Beck's triad), electrocardiographic (low voltage, abnormal ventricular repolarization), and radiological signs of cardiac tamponade. However, these signs are not always accurate

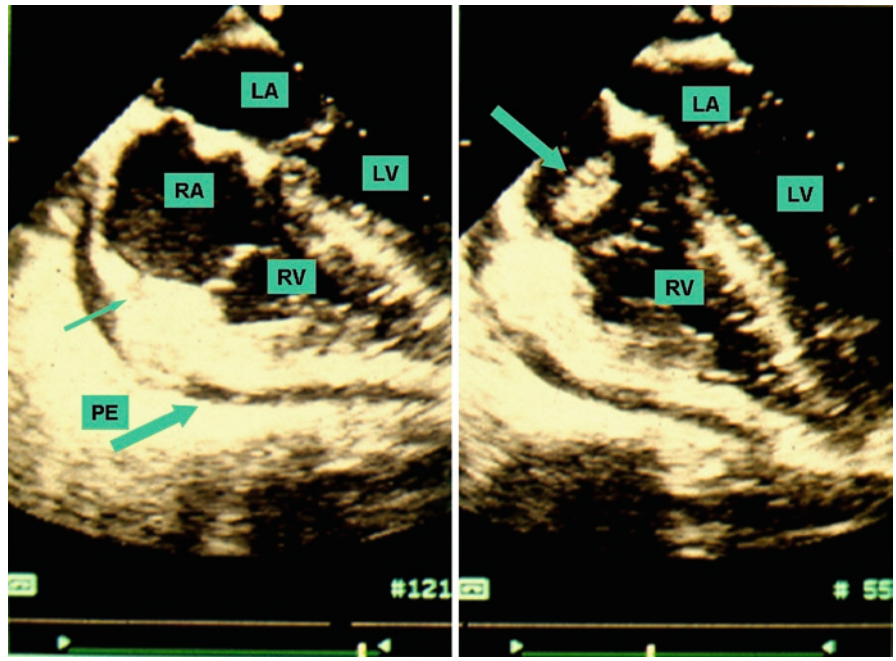

Fig. 18.22 Transesophageal echocardiography four-chamber view in a victim of horse-kick accident presenting with signs and symptoms of cardiac tamponade. A small pericardial effusion (*left panel*, *large arrow*) is evident, and the right ventricle (RV) looks compressed. The *small arrow* indicates a discrete discontinuity in the free right atrial (RA) wall, suggestive of a limited rupture. In a more caudal view (*right panel*), a portion of the torn RA wall is seen within the RA cavity, confirming the diagnosis of ruptured free RA wall. *LA* left atrium, *LV* left ventricle, *PE* pericardial effusion

in patients with traumatic cardiac tamponade because hypovolemia can be responsible for absent venous congestion, and hypotension may be the consequence of many causes in victims of blunt chest trauma. Echocardiography is the technique of choice in identifying cardiac tamponade. Echocardiographic signs of cardiac tamponade include the following: (1) distended inferior and superior vena cava with reduced respiratory excursion; (2) hepatic venous congestion; (3) compressed right atrial or ventricular cavities with reduced or absent diastolic expansion; (4) signs of interventricular interdependence (exaggerated respiratory variation in mitral and tricuspidal velocity-time integral following respiratory phases); (5) reduced right ventricular cavity and normal or exaggerated left ventricular contraction (due to relative hypovolemia). It should be stressed that the amount of pericardial fluid that can determine cardiac tamponade may be very small because rapid accumulation of even a small quantity of fluid does not allow the pericardial sac to distend, determining an acute and critical increase in the intrapericardial pressure.

In some cases, echocardiography can identify the precise location of myocardial rupture, assessing a localized epicardial hematoma or portions of the torn atrial or ventricular wall displaced within the heart cavities or in the pericardial sac (Fig. 18.22).

Pericardiocentesis may assist in confirming the diagnosis and help to provide a brief period of hemodynamic stabilization while the patient is being transported to the operating room. If the patient cannot be stabilized and transported to the operating room, left thoracotomy should be performed in the emergency department to relieve the tamponade or control the hemorrhage.

18.2.4 Septal Defects

Atrial and ventricular septal defect can occur as a result of blunt cardiac injury, although less frequently than free-wall rupture. They may present early or late, and the resultant shunt can be hemodynamically significant. Diagnosis should be suspected in patients with new onset symptoms of pulmonary congestion, refractory hypoxemia, or a new systolic murmur. TEE can be helpful. Most injuries should be repaired, especially when the Qp/Qs ratio is >1.5 (Fig. 18.23)

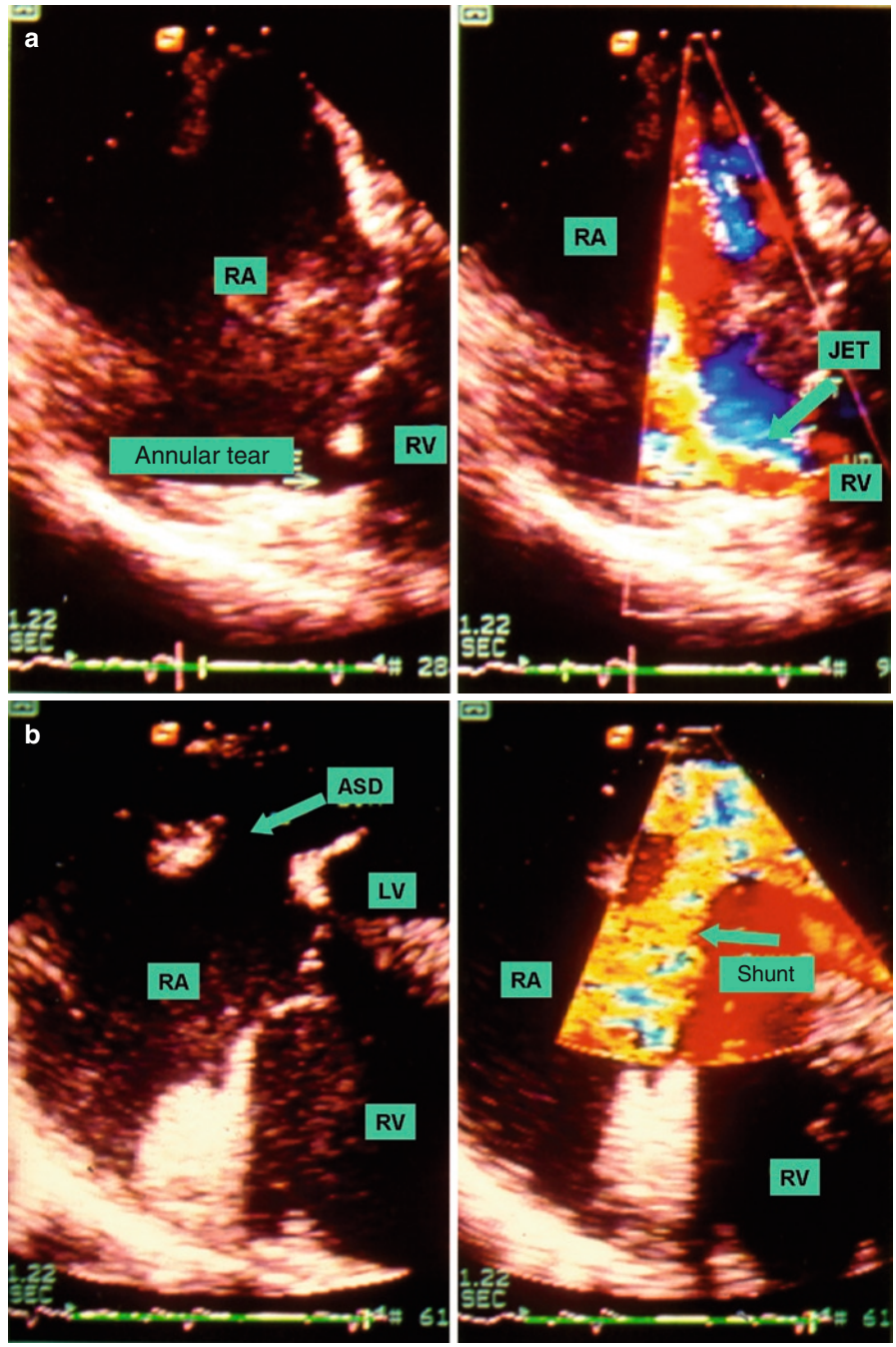

Fig. 18.23 Pedestrian struck by a car with persisting unexplained hypoxemia. (**a**) Transesophageal echocardiography two-chamber view for the right-heart chamber identifies a disrupted tricuspid anterior leaflet with severe tricuspid regurgitation (right panel). (**b**) In a more caudal view, a large atrial septal defect (ASD) is identified, with the eccentric regurgitant tricuspid jet entering the left atrium through this large traumatic septal defect, leading to severe and refractory hypoxemia. *LV* left ventricle, *RA* right atrium, *RV* right ventricle

18.2.5 Valvular Injuries

Valvular injuries due to blunt trauma are not frequent, occurring in less than 5% of patients dying from blunt cardiac injury. The aortic valve is involved most frequently followed by the tricuspid and mitral valves, while traumatic injuries to the pulmonary valve are exceptional.

The mechanism of acute aortic valvular insufficiency is thought to be an abruptly increased intrathoracic pressure as a result of a direct blow to the chest or transmission of intra-abdominal pressure across the diaphragm. This produces a sudden increase in intra-aortic pressure that is transmitted retrograde against the closed aortic valve in diastole, causing disruption of the valve leaflets. The lesions may be associated with TAI. Timing of aortic valve replacement/repair depends on the severity of the regurgitation and the hemodynamic and clinical tolerance of the aortic regurgitation.

Rupture of the mitral and tricuspid valve is thought to occur when the full ventricle in end diastole is suddenly compressed between the sternum and the spine, causing an acute increase in ventricular pressure. This is transmitted to the atrioventricular valves, producing avulsion from the annulus (Fig. 18.24) and injury to the papillary muscles (Fig. 18.25) and/or chordae tendineae, with resultant valvular insufficiency. The anterior position of the right ventricle can be the reason for the relatively higher frequency of traumatic tricuspid valve rupture (Fig. 18.26). In the acute phase, in patients with pulmonary hypertension (following severe lung contusion or pulmonary thromboembolism), the presence of tricuspid regurgitation should be differentiated from functional tricuspid regurgitation due to the pulmonary hypertension. In most cases, the acute tricuspid regurgitation is well tolerated, and it is often identified months to years after trauma on a clinical or echocardiographic basis.

Traumatic mitral regurgitation can be determined by ruptured chordae, ruptured papillary muscle, or avulsion of the mitral leaflets from the annulus. Timing of surgery (replacement or repair) will depend on the hemodynamic consequences of the regurgitant volume and the presence and severity of associated injuries.

18.3 Key Points

TEE provides excellent visualization of the aortic isthmus, where the most TAIs are located, and represents, therefore, an ideal diagnostic technique for this purpose.

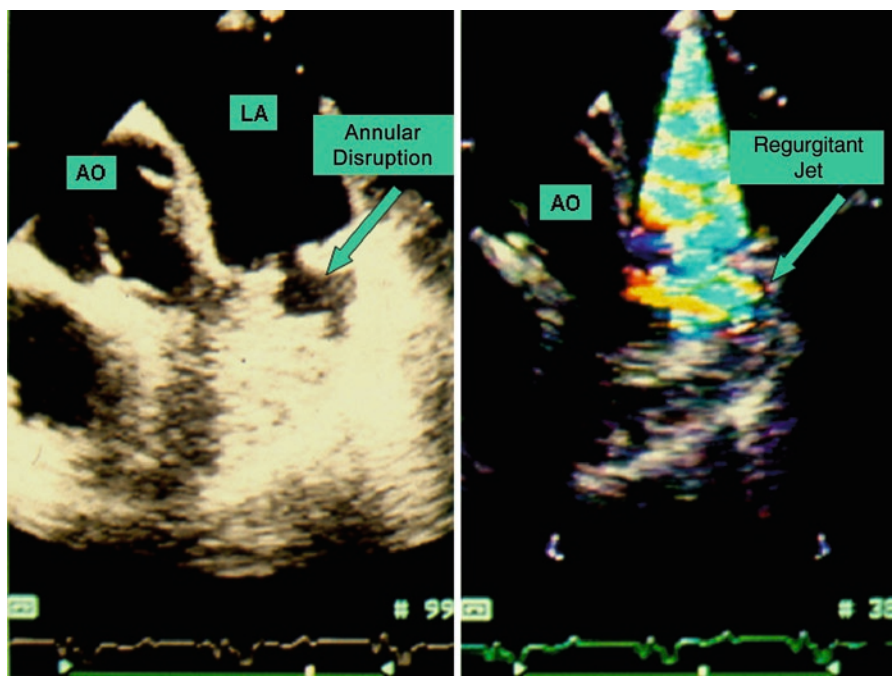

Fig. 18.24 Traumatic mitral regurgitation in a victim of a high-speed automobile accident, in whom transesophageal echocardiography identified a large avulsion of the posterior leaflet from the annulus and a severe "paravalvular" leak (*right panel*). *AO* aorta, *LA* left atrium

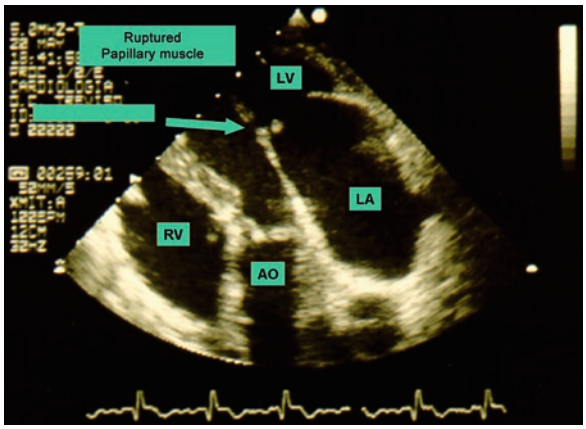

Fig. 18.25 Traumatic mitral regurgitation. Transgastric view demonstrating (arrow) a partially ruptured anterolateral papillary muscle. *AO* aorta, *LA* left atrium, *LV* left ventricle, *RV* right ventricle

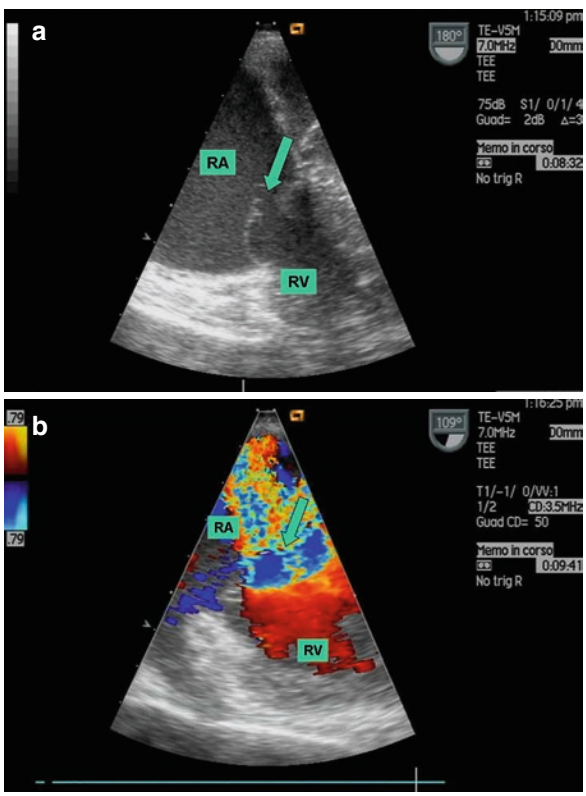

Fig. 18.26 Traumatic tricuspid regurgitation. (**a**) Modified two-chamber view for the right heart shows a flail anterior tricuspid leaflet (*arrow*) with severe regurgitation at color-flow Doppler (**b**). *RA* right atrium, *RV* right ventricle

It can be performed in a short time at the bedside; it does not require the transportation of the patient, and it can identify associated cardiac lesions. However, the technique has some limitations owing to its inability to visualize the distal ascending aorta and the proximal arch because of the interposition of the air-filled trachea and left main bronchus, poor image quality in the presence of pneumomediastinum or pneumothorax, and difficult and potentially dangerous intubation in patients with neck spine instability. The main limitation of TEE is its dependence on the operator's ability since it takes some time to learn how to acquire proper images and provide a correct interpretation; several false positives and false negatives have been reported in the literature. Moreover, TEE cannot identify associated injuries, which are very frequent in patients sustaining a high-energy trauma, such as those with suspected TAI. CT has gained increasing popularity because, utilizing multisliced detectors and helical technology, it can provide accurate imaging of the whole body in a few seconds. TEE is, therefore, indicated especially in hemodynamically unstable patients and in subjects with suspected associated cardiac lesions.

References

1. Kodali S, Jamieson WR, Leia SM, Miyagishima RT, Janusz MT, Tyers GF (1991) Traumatic rupture of the thoracic aorta: a 20-year review – 1969–1989. Circulation 84:140–146
2. Parmley L, Thomas W, Manion W et al (1958) Non penetrating traumatic injury of the aorta. Circulation 17:1086–1101
3. Fabian TC, Richardson JD, Croce MA et al (1997) Prospective study of blunt aortic injury: multicenter trial of the American Association for the surgery of trauma. J Trauma 42:374–380
4. Richens D, Field M, Neale M, Oakley C (2002) The mechanism of injury in blunt traumatic rupture of the aorta. Eur J Cardiothorac Surg 21:288–293
5. Ahrar K, Smith DC (1998) Trauma to the aorta and aortic arch branches. Curr Opin Cardiol 13:355–368
6. Dyer DS, Moore EE, Ilke DN et al (2000) Thoracic aortic injury: how predictive is mechanism and is chest computed tomography a reliable screening tool? A prospective study on 1, 561 patients. J Trauma 48:673–682
7. Katyal D, NcLellan BA, Brenneman FT et al (1997) Lateral impact motor vehicle collisions: significant cause of blunt traumatic rupture of the thoracic aorta. J Trauma 42:769–772
8. Duhaylongsod FG, Glower DD, Wolfe WG (1992) Acute traumatic aortic aneurysm: the Duke experience from 1970 to 1990. J Vasc Surg 15:331–343
9. Mirvis SE, Shanmuganathan K, Miller BH et al (1996) Traumatic aortic injury: diagnosis with contrast-enhanced thoracic CT. Five-year experience at a major trauma center. Radiology 200:413–422

10. Greendyke RM (1996) Traumatic rupture of the aorta: special reference to automobile accidents. JAMA 195: 527–530
11. Pate JW, Fabian TC, Walker W (1995) Traumatic rupture of the aortic isthmus: an emergency? World J Surg 19: 119–126
12. Mirvis SE, Bidwell JK, Buddemeyer EU et al (1987) Value of chest radiography in excluding traumatic aortic rupture. Radiology 163:487–493
13. Woodring JH, King JG (1989) The potential effects of radiographic criteria to exclude aortography in patients with blunt chest trauma. J Thorac Cardiovasc Surg 97:456–460
14. Kram HB, Wohlmut DA, Appel PL et al (1987) Clinical and radiographic indications for aortography in blunt chest trauma. J Vasc Surg 6:168–176
15. Patel NH, Stephens KE, Mirvis SE et al (1998) Imaging of acute thoracic aortic injury due to blunt trauma: a review. Radiology 209:335–348
16. Dart CH, Braitman HF (1976) Traumatic rupture of the thoracic aorta: diagnosis and management. Arch Surg 111: 697–702
17. Parker MS, Matheson TL, Rao AV et al (2001) Making the transition: the role of helical CT in the evaluation of potentially thoracic aortic injuries. Am J Roentg l 76:1267–1272
18. Cleverley JR, Barrie JR, Raymond GS et al (2002) Direct findings of aortic injury on contrast-enhanced CT in surgically proven traumatic aortic injury: a multi-center review. Clin Radiol 57:281–286
19. Downing SW, Sperling JS, Mirvis SE et al (2001) Experience with spiral computed tomography as the sole diagnostic method for traumatic aortic rupture. Ann Thorac Surg 72:495–502
20. Mirvis SE, Shanmuganathan K (2007) Diagnosis of blunt traumatic aortic injury 2007; still a nemesis. Eur J Radiol 64:27–40
21. O'Conor CE (2004) Diagnosing traumatic rupture of the thoracic aorta in the emergency department. Em Med J 21:414–419
22. Scaglione M, Pinto A, Pinto F et al (2001) Role of contrast-enhanced helical CT in the evaluation of acute thoracic aortic injuries after blunt chest trauma. Eur Radiol 11: 2444–2448
23. Vignon P, Spencer KT, Rambaud G et al (2001) Differential transesophageal echocardiographic diagnosis between linear artifacts and intraluminal flap of aortic dissection or disruption. Chest 119:1778–1790
24. Evangelista A, Garcia del Castillo H, Gonzalez-Alujas T et al (1996) Diagnosis of ascending aortic dissection by transesophageal echocardiography: utility of M-mode in recognizing artifacts. J Am Coll Cardiol 27:102–107
25. Appelbe AF, Walker PG, Yeoh JK et al (1993) Clinical significance and origin of artifacts in transesophageal echocardiography of the thoracic aorta. J Am Coll Cardiol 21:754–760
26. Shapiro M, Yanofsky S, Trapp J et al (1991) Cardiovascular evaluation in blunt chest trauma using transesophageal echocardiography (TEE). J Trauma 31:835–839
27. Sparks M, Burchard K, Marrin C et al (1991) Transesophageal echocardiography. Preliminary results in patients with traumatic aortic rupture. Arch Surg 126:711–713
28. Brooks SW, Young JC, Cmolik B et al (1992) The use of transesophageal echocardiography in the evaluation of chest trauma. J Trauma 32:761–768
29. Kearney P, Smith W, Johnson S et al (1993) Use of transesophageal echocardiography in the evaluation of traumatic aortic injury. J Trauma 34:696–703
30. Karalis DG, Victor MF, Davis GA et al (1994) The role of echocardiography in blunt chest trauma: a transthoracic and transesophageal echocardiographic study. J Trauma 36: 53–58
31. Buckmaster M, Keanny P, Johnson S et al (1994) Further experience with TOE in the evaluation of thoracic aortic injury. J Trauma 37:989–995
32. Smith MD, Cassidy M, Souther S et al (1995) Transesophageal echocardiography in the diagnosis of traumatic rupture of the aorta. N Engl J Med 332:356–362
33. Saletta S, Lederman E, Fein S et al (1995) Transesophageal echocardiography for the initial evaluation of the widened mediastinum in trauma patients. J Trauma 39:137–142
34. Vignon P, Gueret P, Vedrinne JM et al (1995) Role of transesophageal echocardiography for the diagnosis of traumatic aortic disruption. Circulation 92:2959–2968
35. Minard G, Schurr MJ, Croce MA et al (1996) A prospective analysis of transesophageal echocardiography in the diagnosis of traumatic disruption of the aorta. J Trauma 40: 225–230
36. Chirillo F, Totis O, Cavarzerani A et al (1996) Usefulness of transthoracic and transesophageal echocardiography in recognition and management of cardiovascular injuries after blunt chest trauma. Heart 75:301–306
37. Goarin JP, Catoire P, Jacquens Y et al (1997) Use of transesophageal echocardiography for diagnosis of traumatic aortic injury. Chest 112:71–80
38. Vignon P, Rambaud G, François B et al (1998) Quantification of traumatic hemomediastinum using transesophageal echocardiography. Impact on patient management. Chest 113:1475–1480
39. Goarin JP, Cluzel P, Gosgnach M et al (2000) Evaluation of transesophageal echocardiography for diagnosis of traumatic aortic injury. Anesthesiology 93:1373–1377
40. Vignon P, Boncoeur MP, François B et al (2001) Comparison of multiplane transesophageal echocardiography and contrast-enhanced helical CT in the diagnosis of blunt traumatic cardiovascular injuries. Anesthesiology 94:615–622
41. Poletti PA, Wintermark M, Schnyder P et al (2002) Traumatic injuries: role of imaging in the management of the polytrauma victim (conservative expectation). Eur Radiol 12: 969–978
42. Demetriades D, Velmahos GC, Scalea TM et al (2008) Diagnosis and treatment of blunt thoracic aortic injuries: changing perspectives. J Trauma 64:1415–1418
43. Von Oppel UO, Dunne TT, DEGroot MK et al (1994) Traumatic aortic rupture: twenty year metaanalysis of mortality and risk of paraplegia. Ann Thorac Surg 58:585–593
44. Akins CW, Buckley MJ, Dagget W et al (1981) Acute traumatic disruption of the thoracic aorta: a ten year-experience. Ann Thorac Surg 31:305–309
45. Pate JW, Gavant ML, Weiman DS et al (1999) Traumatic rupture of the aortic isthmus: program of selective management. World J Surg 23:59–63

46. Maggisano R, Nathens A, Alexandrova N (1991) Traumatic rupture of the thoracic aorta: should one always operate immediately? Ann Vasc Surg 5:491–499
47. Pierangeli A, Turinetto B, Galli R et al (2000) Delayed treatment of isthmic aortic rupture. Cardiovasc Surg 8: 280–283
48. Fattori R, Celletti F, Descovich B et al (1998) Evolution of post-traumatic aortic aneurysm in the subacute phase: magnetic resonance imaging follow-up as a support of the surgical timing. Eur J Cardiothorac Surg 13:582–586
49. Mattox KL, Holzman M, Pickard LR et al (1985) Clamp/repair: a safe technique for treatment of blunt injury to the descending thoracic aorta. Ann Thorac Surg 40:456–463
50. Shorr RM, Crittenden M, Indeck M et al (1987) Blunt thoracic trauma: analysis of 515 patients. Ann Surg 206:200–205
51. Rapezzi C, Rocchi G, Fattori R et al (2001) Usefulness of transesophageal echocardiography monitoring to improve the outcome of stent-graft treatment of thoracic aortic aneurysms. Am J Cardiol 87:315–319
52. Rousseau H, Soula P, Perreault P et al (1999) Delayed treatment of traumatic rupture of the thoracic aorta with endoluminal covered stent. Circulation 99:498–504
53. Marty-Ane CH, Berthet JP, Branchereau P et al (2003) Endovascular repair for acute traumatic rupture of the thoracic aorta. Ann Thorac Surg 75:1803–1807
54. Scheinert D, Krakenberg H, Schmidt A et al (2004) Endoluminal stent-graft placement for acute rupture of the descending thoracic aorta. Eur Heart J 25:694–700
55. Mattox KL, Flint LM, Carrico CJ et al (1992) Blunt cardiac injury. J Trauma 33:649–650
56. Krasna MJ, Flancbaum L (1992) Blunt cardiac trauma: clinical manifestations and management. Sem Thorac Cardiovasc Surg 4:195–202
57. Bansal MK, Maraj S, Chewaproug D et al (2005) Myocardial contusion injury. Redefining the diagnostic algorithm. Emerg Med J 22:465–469
58. Kulshrestha P, Iver S, Sampath KA et al (1987) Cardiac injuries- A clinical and autopsy profile. J Trauma 30:203–207

Hemodynamic Instability in Cardiac Surgical Patients

19

Bernard P. Cholley, Mireille Cherqui, Alain Berrebi, and Jan Poelaert

Contents

B.P. Cholley (✉)
Service d'Anesthésie-Réanimation, Hôpital Européen Georges Pompidou, Université Paris Descartes, 20 rue Leblanc, 75908, Paris cedex 15, France
e-mail: bernard.cholley@egp.aphp.fr

M. Cherqui
Service d'Anesthésie-Réanimation, Hôpital Foch, 40 rue Worth, BP 36, 92150, Suresnes, France

A. Berrebi
Département de Chirurgie Cardio-Vasculaire, Hôpital Européen Georges Pompidou, 20 rue Leblanc, 75908, Paris cedex 15, France

J. Poelaert
Department of Anesthesiology and Perioperative Medicine, Flemish University Hospital, Laarbeeklaan 101, 81090, Brussels, Belgium

Transesophageal echocardiography (TEE) was introduced in the operating room more than 30 years ago [1] and quickly proved to be extremely useful for many types of cardiac interventions [2–11]. During mitral valve repair, TEE is so essential that it is not recommended to perform the procedure if TEE is not available [12–14]. TEE is also undoubtedly the most effective technique to recognize the cause of hemodynamic instability during and after cardiac surgical procedures. Since hemodynamic disorders are frequently encountered in these patients, intraoperative TEE has become routine over the past 15 years in cardiac surgical theaters [15]. The evaluation of patients with hemodynamic instability during cardiac surgery belongs to class I indications for the intraoperative use of TEE according to published guidelines (Table 19.1) [16–18].

19.1 Hemodynamic Instability Prior to Cardiopulmonary Bypass

In patients undergoing elective procedures, acute hemodynamic disorders are usually not a major concern prior to bypass However, even in patients with normal left ventricular (LV) function, induction of anesthesia may be poorly tolerated if drug-induced vasodilatation reduces venous return to a threshold beyond which arterial pressure can no longer be maintained. In such situations, TEE shows small, hyperkinetic heart chambers with end-systolic collapse of the LV (Fig. 19.1). Hypovolemia (absolute or secondary to vasodilatation) is poorly tolerated in patients with hypertrophic cardiomyopathy. In such patients, preload reduction results in poor LV filling and abrupt decrease in cardiac output, leading to collapse [19]. When demonstrating LV hypertrophy with small heart

D. De Backer et al. (eds.), *Hemodynamic Monitoring Using Echocardiography in the Critically Ill*,
DOI: 10.1007/978-3-540-87956-5_19, © Springer-Verlag Berlin Heidelberg 2011

Table 19.1 Recommendations for intraoperative TEE

Class I	Class IIa	Class IIb	Class III
Conditions for which there is evidence and/or general agreement that a given procedure or treatment is useful and effective	Conditions for which there is conflicting evidence and/or a divergence of opinion about the usefulness/efficacy of a procedure or treatment **IIa:** Weight of evidence/opinion is in favor of usefulness/efficacy	Conditions for which there is conflicting evidence and/or a divergence of opinion about the usefulness/efficacy of a procedure or treatment **IIb:** Usefulness/efficacy is less well-established by evidence/opinion	Conditions for which there is evidence and/or general agreement that the procedure/treatment is not useful/effective and in some cases may be harmful
Evaluation of acute, persistent, and life-threatening hemodynamic disturbances in which ventricular function and its determinants are uncertain and have not responded to treatment	Surgical procedures in patients at increased risk of myocardial ischemia, myocardial infarction, or hemodynamic disturbances	Evaluation of suspected cardiac trauma, repair of acute thoracic aortic dissection without valvular involvement, and anastomotic sites during heart and/or lung transplantation	Surgical repair of uncomplicated secundum atrial septal defect
Surgical repair of valvular lesions, hypertrophic obstructive cardiomyopathy, and aortic dissection with possible aortic valve involvement	Evaluation of valve replacement, aortic atheromatous disease, Maze procedure, cardiac aneurysm repair, removal of cardiac tumors, intracardiac thrombectomy, and pulmonary embolectomy	Evaluation of regional myocardial function during and after off-pump coronary artery bypass graft procedures	
Evaluation of complex valve replacement requiring homografts or coronary reimplantation, such as the Ross procedure	Detection of air emboli during cardiotomy, heart transplant operations, and upright neurosurgical procedures	Evaluation of pericardiectomy, pericardial effusions, and pericardial surgery	
Surgical repair of most congenital heart lesions that require cardiopulmonary bypass		Evaluation of myocardial perfusion, coronary anatomy, or graft patency	
Surgical intervention for endocarditis when preoperative testing is inadequate or extension to perivalvular tissue is suspected		Dobutamine stress testing to detect inducible demand ischemia or to predict functional changes after myocardial revascularization	
Placement of intracardiac devices and monitoring of their position during port access and other cardiac surgical interventions		Assessment of residual duct flow after interruption of patent ductus arteriosus	
Evaluation of pericardial window procedures in patients with posterior or loculated pericardial effusions			

According to [17]

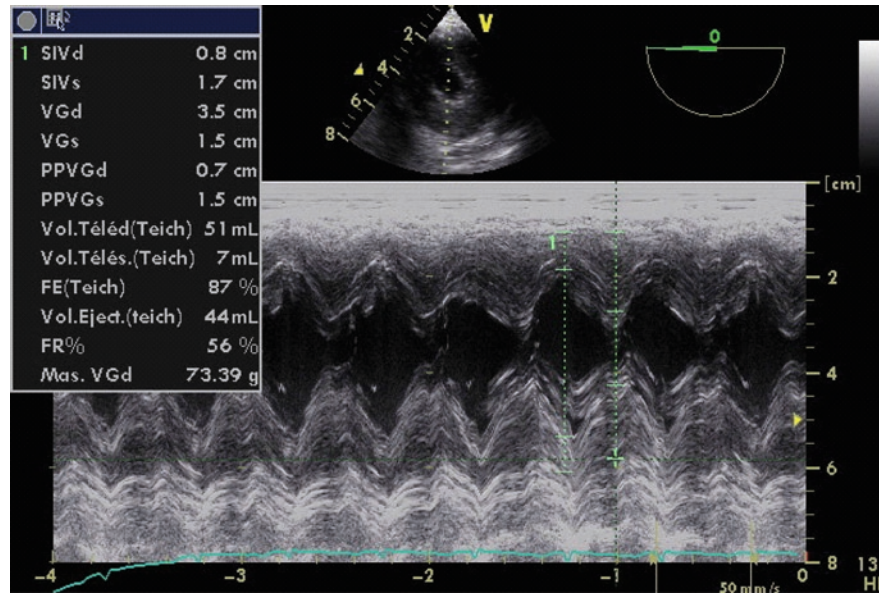

Fig. 19.1 M-mode of the left ventricular short-axis diameter, demonstrating a small hyperkinetic left ventricle as a consequence of severe hypovolemia

chambers, TEE provides immediate clues to the mechanism for refractory hypotension following anesthesia induction. Acute LV failure is unusual prior to cardiopulmonary bypass in patients with previously normal LV function, but it may sometimes be observed as a result of acute myocardial ischemia subsequent to hypotension. In the (rare) example shown, the apical ballooning and akinesia with preserved basal contractility suggested a takotsubo cardiomyopathy (confirmed by ventriculography and normal coronary angiogram) triggered by anesthesia induction. Anesthesia in patients with severe aortic stenosis is considered to put the patients "at risk," and these patients have increased morbidity after noncardiac surgery [20]. The risk of hypotension is well-known, and treatment requires primarily vasoconstrictive agents; TEE might modify this choice for inotropes if LV function appears severely depressed.

On the other hand, emergency surgery is frequently associated with hemodynamic instability even prior to anesthesia induction. In highly unstable patients, it is common practice to perform TEE in the operating room, while the patient is already under general anesthesia to avoid the potential complications inherent to the stress of esophageal intubation in awake subjects. Mechanical complications of myocardial infarction are often associated with shock and can be identified using TEE (cf. Chap. 12) [21]. Ruptured papillary muscle is responsible for massive mitral regurgitation, free-wall rupture is associated with tamponade, and interventricular septum rupture results in acute right ventricular overload. Prompt surgical correction is usually the best option for these situations, even if perioperative mortality is very high.

Acute right ventricular failure is also observed in patients with massive pulmonary embolism requiring surgical embolectomy (Fig. 19.2), and direct visualization of the thrombus within the right pulmonary artery is possible in such cases (Fig. 19.3; cf. Chap. 13). Patients with acute valvular disease or prosthetic valve dysfunction may be in very poor hemodynamic condition prior to bypass. The role of TEE is to analyze the mechanism of valvular dysfunction and to provide as much information as possible to the surgeon in order to target all possible lesions during intervention (Figs. 19.4 and 19.5). This information has to include mobility of the prosthetic leaflets, existence or absence of a paraprosthetic leak and its location, presence or absence of endocarditis and possible underlying abscess.

Aortic dissection involving the ascending aorta (type A) is another situation in which TEE can provide invaluable information with respect to the mechanism of hemodynamic instability [22] (cf. Chap. 20). Again, aortic dissection is a situation where TEE is much safer to perform while the patient is already in the operating room and under general anesthesia. Information obtained from preoperative transthoracic evaluation is usually not sufficiently comprehensive to optimize patient management. Obviously, the presence of pericardial effusion is highly suggestive of hemopericardium and potential

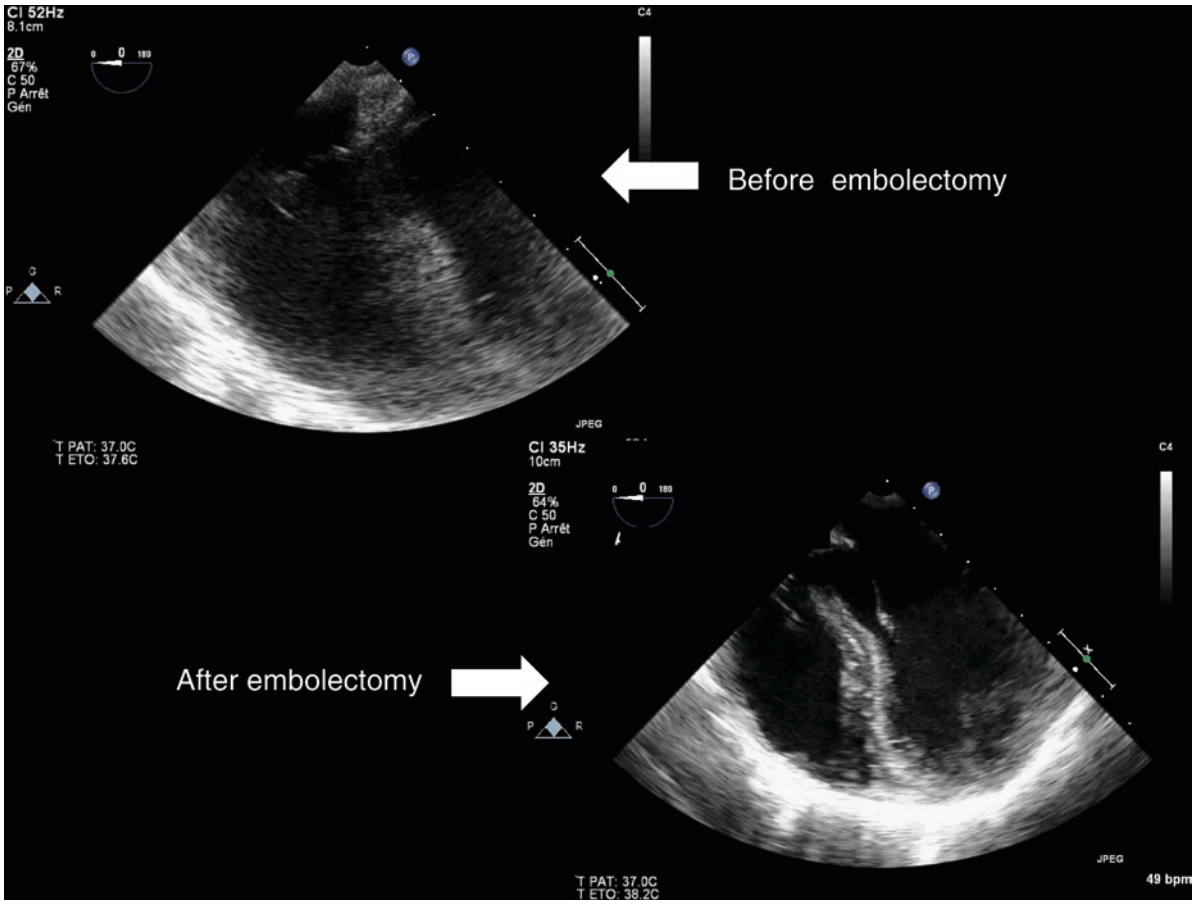

Fig. 19.2 Transesophageal echocardiography four-chamber view, demonstrating acute cor pulmonale before embolectomy in a patient with massive pulmonary embolism and the reduction in right ventricular chamber size following embolectomy

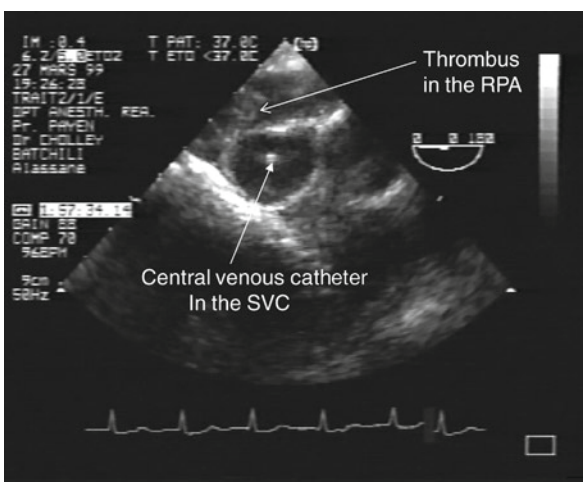

Fig. 19.3 Transesophageal echocardiography view of the great vessels, showing a thrombus in the right pulmonary artery (RPA) and a congested superior vena cava (SVC) with a central venous catheter inside

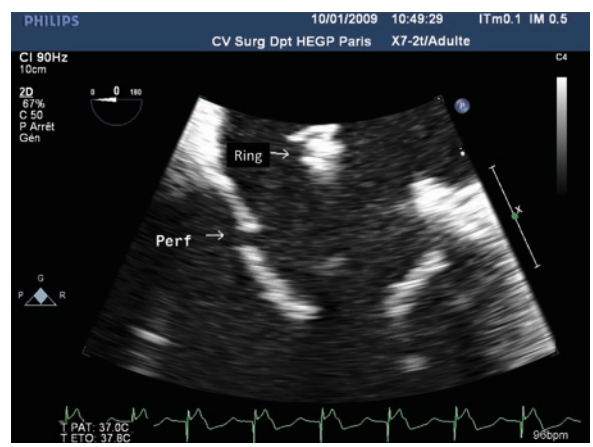

Fig. 19.4 Transesophageal echocardiography zoom on the mitral valve showing a large coaptation defect between the mitral annulus and the prosthetic ring combined with anterior leaflet perforation (Perf) in a patient with massive mitral regurgitation several years after mitral valve repair

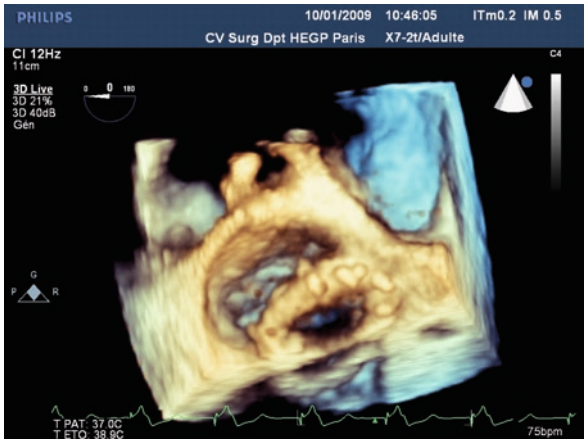

Fig. 19.5 Same patient as in Fig. 19.4. Three-dimensional transesophageal echocardiography atrial view of the mitral valve demonstrating a completely loose prosthetic ring in the left atrium, anchored to the posterior part of the mitral annulus by a few sutures only

tamponade. Massive aortic regurgitation is frequent in aortic dissection, and it is important to understand its precise mechanism: centrovalvular regurgitation results from passive dilation of the aortic annulus and is usually corrected by aortic root replacement alone (Fig. 19.6), while eccentric jets usually result from leaflet prolapse and require that the aortic valve also be replaced. Regional wall-motion abnormalities suggest that extension of the intimal dissection to the coronary artery has resulted in acute myocardial ischemia. Even when TEE has been performed before surgery, it remains very useful during the surgical procedure as it allows one to ensure that arterial cannulation (usually femoral, but sometimes axillary or transventricular) delivers flow to the true lumen of the aorta during bypass [23]. An injection of echo contrast media (saline or gelatin agitated with a small amount of air) can confirm that the cannula is in the true lumen: it expands during systole, and flow is usually faster than in the false lumen (Fig. 19.7). Sometimes, bypass circulation results in acute dilatation of the false lumen, which may induce malperfusion syndromes, requiring an urgent change in cannulation strategy or other specific management (Fig. 19.8).

19.2 Hemodynamic Instability When Weaning from Cardiopulmonary Bypass

Cardiopulmonary bypass (CBP) weaning is a critical step in cardiac procedures. Several factors can account for the difficulties encountered in CBP weaning. Disorders can be separated into dysfunctions related to

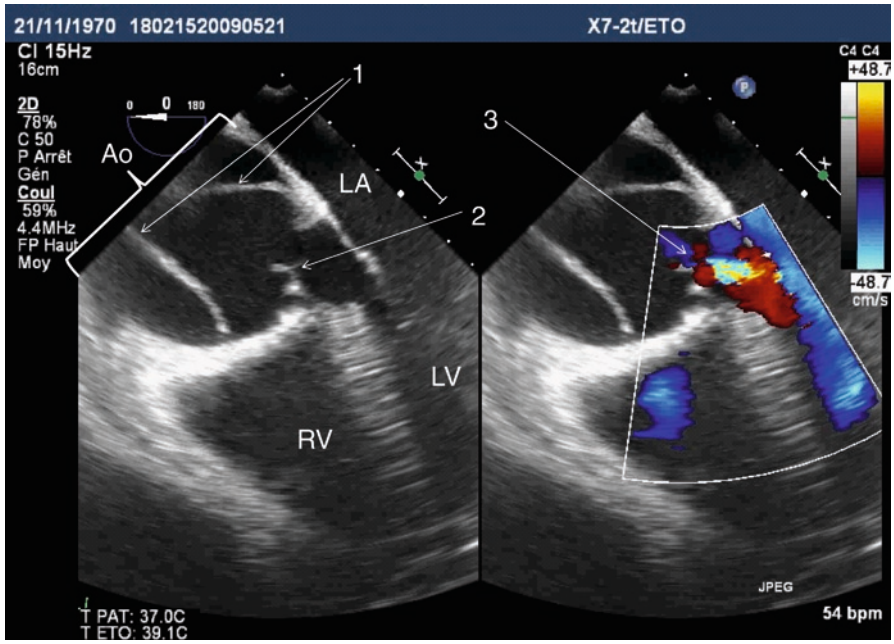

Fig. 19.6 Transesophageal echocardiography 4-chamber view with (*right panel*) and without (*left panel*) color Doppler mapping in a patient with acute aortic dissection (type A). Note the massive enlargement of the ascending aorta (Ao; >50 mm) containing the intimal flap (1) and squeezing the left atrium (LA). The right atrium is not visible as a consequence of massive aortic dilatation. The aortic valve (2) is not severely damaged with a central, grade-2 regurgitation (3) and was preserved during the repair. *LV* left ventricle, *RV* right ventricle

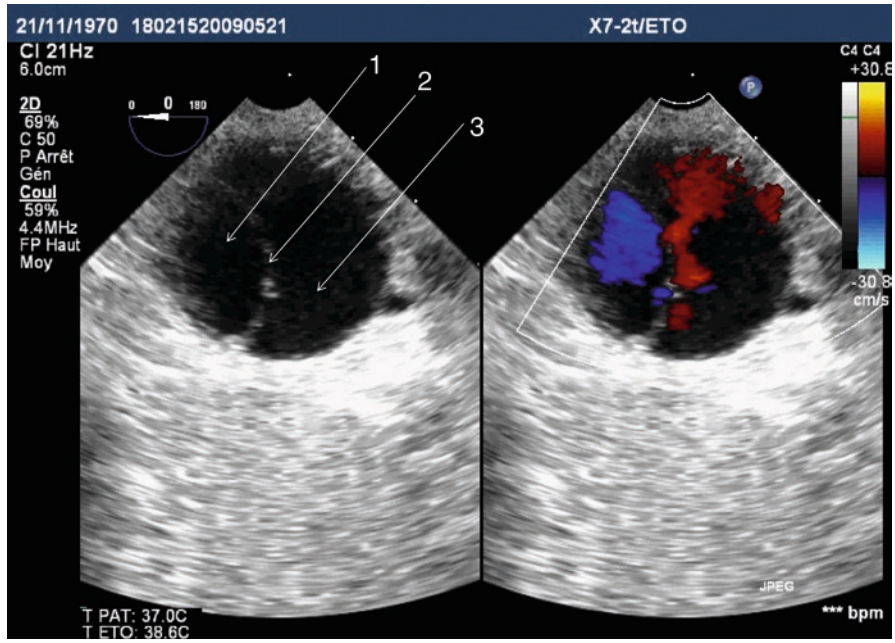

Fig. 19.7 Transesophageal echocardiography short-axis view of the descending thoracic aorta without (*left*) and with (*right*) color Doppler flow mapping showing the true lumen (1), the intimal flap (2) that bulges from the true lumen toward the false lumen, and the false lumen (3), which is usually larger than the true lumen. In this example, the true lumen is not "squeezed" by the false lumen, and there is no malperfusion resulting from bypass circulation

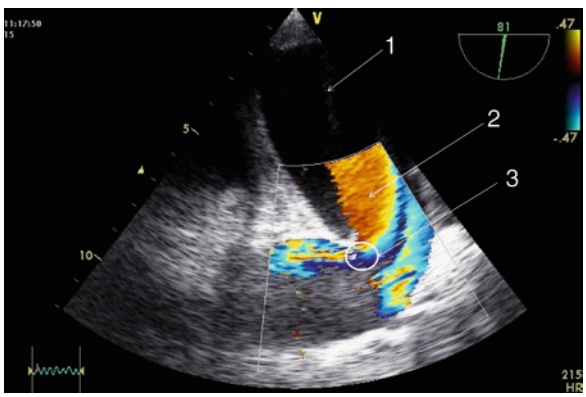

Fig. 19.8 Transesophageal echocardiography longitudinal view of the descending thoracic aorta at the level of the diaphragm with color Doppler flow mapping. The intimal flap (1) and true lumen (2) are evident. The aorta is distorted and exhibits a sharp angle where the true lumen is compressed by the false lumen (3). This "pseudocoarctation" was managed with endovascular stenting

myocardial ischemia and hemodynamic disorders independent of ischemia.

19.2.1 Ischemic Disorders

After cardiac surgery, myocardial ischemia is frequent. It may result from several mechanisms and can affect either the left or right ventricle (or both). After coronary artery bypass graft (CABG) surgery, ischemia may occur if revascularization is inadequate owing to technical surgical problems with the grafts. Surgical mishandling of coronary arteries can also be seen in procedures other than CABG. Ischemia may result from arterial twisting after coronary ostia reimplantation in the Bentall procedure, or if coronary arteries are snared accidentally while performing another repair. A potential cause of myocardial ischemia after cardiac surgery with opening of the cavities or the aorta is air embolism, which deserves specific attention on the part of the echocardiographer and surgeon once it has been detected [24]. Myocardial stunning is very frequent after all kinds of cardiac procedures as a result of inadequate intraoperative protection [25]. In patients with previously normal LV contractility, myocardial dysfunction following bypass is usually transient and returns to normal within approximately 10 min [26]. In patients with previously abnormal hearts, dysfunction may be more pronounced and require specific support according to the severity. When pharmacological support is insufficient to improve ventricular function, the use of a short-term ventricular assist device (intra-aortic balloon pump or arteriovenous extracorporeal membrane oxygenation) may be required [27]. TEE can help identify these problems by demonstrating new regional or global wall-motion abnormalities and

help select the appropriate therapeutic response [28]. Right ventricular dysfunction may also occur following bypass as a result of inadequate protection, especially when retrograde coronary perfusion is used [29]. Right ventricular failure is also a common cause of bypass weaning failure after heart transplantation, and it may be a consequence of myocardial damage secondary to brain death in the donor, preservation inadequacy for the transplanted heart, and/or preexisting pulmonary hypertension in the recipient [30].

19.2.2 Dynamic Left Ventricular Outflow Tract Obstruction After Cardiac Surgery

TEE is the only method that can be used to identify a dynamic obstruction of the left ventricular outflow tract (LVOT) as a cause of difficult bypass weaning. Obstruction results from systolic anterior motion (SAM) of the anterior leaflet of the mitral valve toward the interventricular septum and is responsible for low systemic blood pressure and flow. This phenomenon occurs as a consequence of combined anatomical and hemodynamic conditions. Anatomical risk factors for dynamic LVOT obstruction (Fig. 19.9) include (1) LV concentric hypertrophy or localized septal hypertrophy, (2) a small mitral-aortic angle (<120°), and (3) excess tissue in the mitral valve, especially if the posterior leaflet length exceeds 15 mm [31]. Hemodynamic conditions that may precipitate LVOT obstruction in conjunction with predisposing anatomical factors are hypovolemia [32] and catecholamine infusions [33]. Two mechanisms may participate simultaneously or individually to LVOT obstruction. First, the anterior leaflet is "pushed" toward the septum by the flow that causes the posterior leaflet to coapt and by the posterior leaflet itself when it is too long (Fig. 19.10) or the mitral annuloplasty ring is too small (patients with a high anterior leaflet). Second, flow acceleration through the narrow LVOT produces a pressure drop (Venturi effect) that draws the anterior leaflet toward the septum. This Venturi effect is aggravated by hypovolemia or inotropic agents and can be reversed by correcting these two conditions. Color Doppler shows mitral regurgitation and high-velocity flow in the LVOT (Fig. 19.11). The pressure gradient through the LVOT is proportional to blood-flow

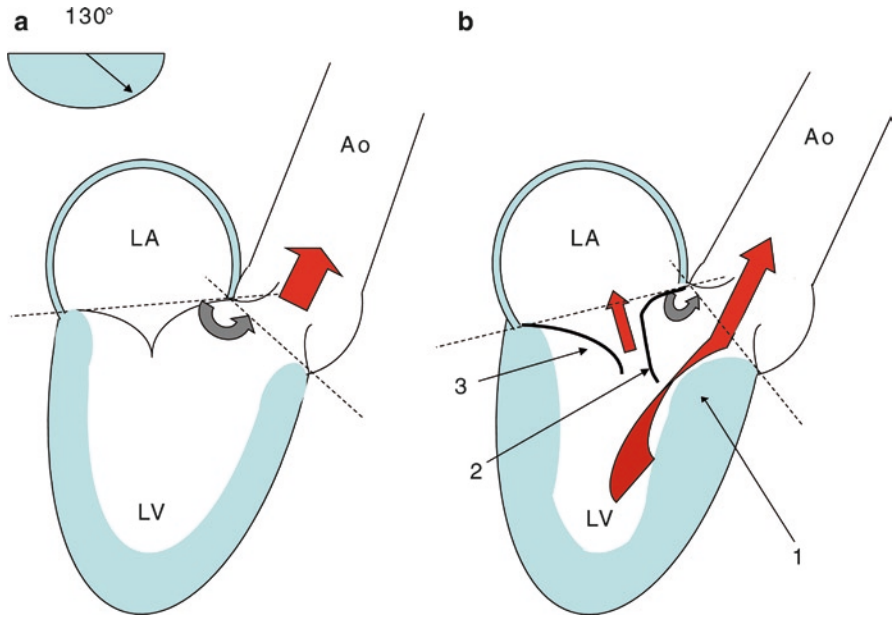

Fig. 19.9 Normal left ventricular outflow tract (LVOT; **a**) as seen using transesophageal echocardiography (130°) during systole and the anatomical variations (**b**) that predispose to systolic anterior motion (SAM). Left ventricular (LV) and, especially, septal hypertrophy (1) are risk factors. A narrow mitral-aortic angle (*dotted lines* delineating aortic and mitral annulus planes; *gray arrows* denoting mitral-aortic angle) and excess tissue in the mitral valve (2 and 3), especially the posterior leaflet (3) after mitral valve repair, also increase the risk of SAM. The resulting effect is mitral valve regurgitation into the left atrium (LA) and LVOT blood flow acceleration. *Ao* aorta

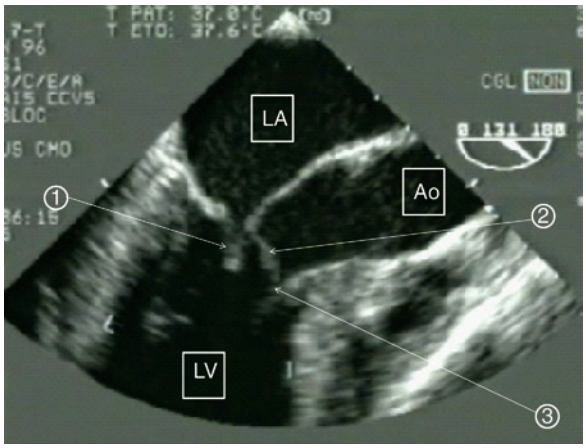

Fig. 19.10 Transesophageal echocardiography view of the left ventricular (LV) outflow tract at 130° showing systolic anterior motion. Note the posterior leaflet (1) pushing the anterior leaflet (2) toward the bulging interventricular septum (3) *LA* left atrium, *AO* aorta

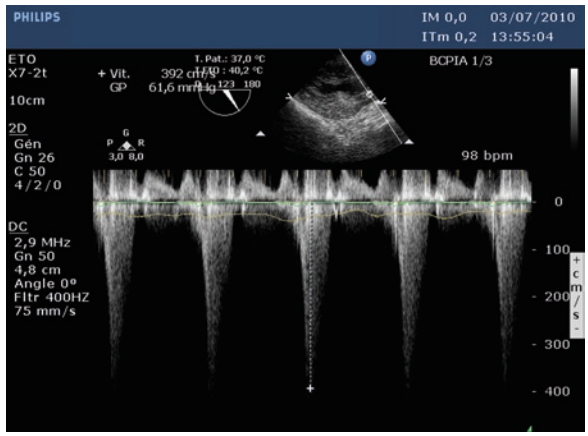

Fig. 19.12 Continuous-wave recording of the blood flow velocity in the left ventricular outflow tract (LVOT) obtained using transesophageal echocardiography from the transgastric view at 120°. Velocities close to 4 m/s correspond to a pressure gradient of ≈ 60 mmHg, attesting to dynamic LVOT obstruction

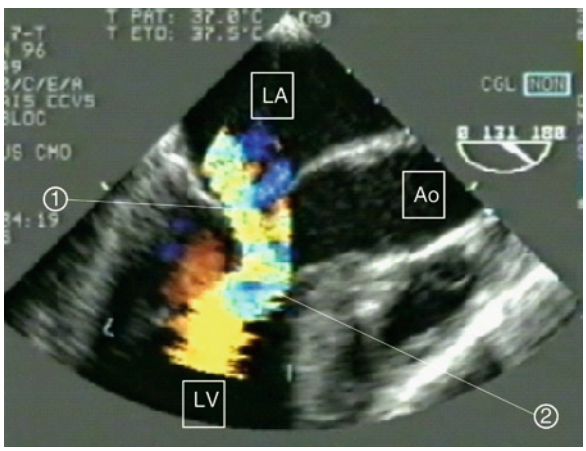

Fig. 19.11 Same view as Fig. 19.10 with color Doppler, demonstrating mitral regurgitation (1) and accelerated blood flow in the left ventricular outflow tract (LVOT; 2) as a consequence of systolic anterior motion. *LA* left atrium, *LV* left ventricle, *AO* aorta

velocity and can be estimated using continuous-wave Doppler (Fig. 19.12). After mitral valve repair, SAM is not uncommon, and it is crucial to understand the precise mechanism in order to propose the right attitude [34]. Once SAM has been recognized, all catecholamine infusions have to be stopped promptly as they can only worsen the situation. Fluid has to be administered using small-volume challenges of 100–200 mL and guided according to stroke volume response. Fluid therapy should be interrupted if no more increase in stroke volume results from additional fluids. Failure to titrate fluids carefully may lead to acute pulmonary edema in those patients who frequently have associated diastolic dysfunction and poor tolerance to excess fluids. Conversely, SAM resulting from excess tissue in the posterior leaflet needs surgical correction, usually a sliding plasty of the posterior leaflet and/or changing the mitral annulus for a larger one [34].

19.2.3 Various Injuries Caused by the Surgical Procedure

A large variety of surgical complications have been described after each cardiac procedure. Systematic intraoperative TEE examination is the most effective way to detect and correct them immediately [2–11, 15]. There is no way to predict who will benefit and who will not from intraoperative TEE, and for this reason some authors suggest that systematic TEE should be performed in each cardiac surgical patient [5, 15]. Mitral valve replacement or repair can be complicated by snaring of the circumflex artery or of the right coronary cusp of the aortic valve, both of which can lead to disastrous complications if not detected right away. In this example, after aortic valve replacement using a bioprosthesis, a noncoronary cusp of the aortic valve was snared during aortic closure, resulting in hyperkinetic LV and massive aortic regurgitation (Figs. 19.13 and 19.14).

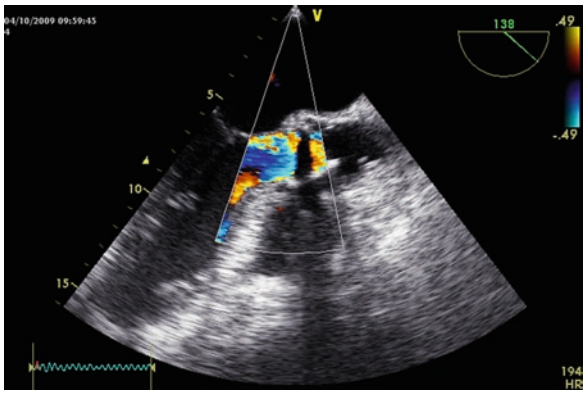

Fig. 19.13 Transesophageal echocardiography view of the left ventricular outflow tract (LVOT; 138°) showing massive aortic regurgitation (color flow jet is as large as the LVOT) following aortic valve replacement with bioprothesis

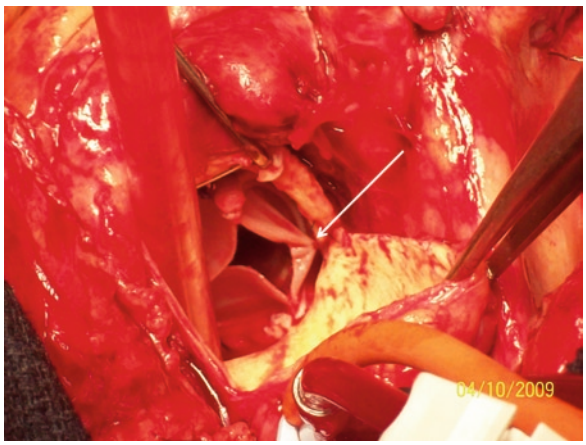

Fig. 19.14 Surgical view demonstrating the snaring of the non-coronary cusp by aortotomy suture (*arrow*)

19.3 Hemodynamic Instability in the Postoperative Period

A large variety of problems can complicate the postoperative course in cardiac surgical patients and result in acute circulatory failure. All problems mentioned above as potential causes for bypass weaning failure (ischemia, dynamic LVOT obstruction, procedure-related damage to the heart) can be encountered in the postoperative period. Among the specific problems in the postoperative period, we would like to mention localized tamponade and mechanical valve thrombosis. Again, these two conditions are electively diagnosed by TEE, when transthoracic echocardiography (TTE) does not provide enough confidence to send the patient back to the operating room.

Localized tamponade should always be suspected when a patient exhibits signs of hypoperfusion (urine output reduction, mottled skin), increased right atrial pressure, low mean arterial pressure, and sometimes acute shock and collapse. TEE should be performed very carefully in an intensive care unit or operating room environment. Tracheal intubation and positive-pressure ventilation are likely to further reduce venous return and aggravate collapse, but TEE should not be performed without airway control and the immediate possibility of surgical decompression in such patients. A sharp contrast between poor TTE and clear TEE images is not uncommon (Figs. 19.15 and 19.16).

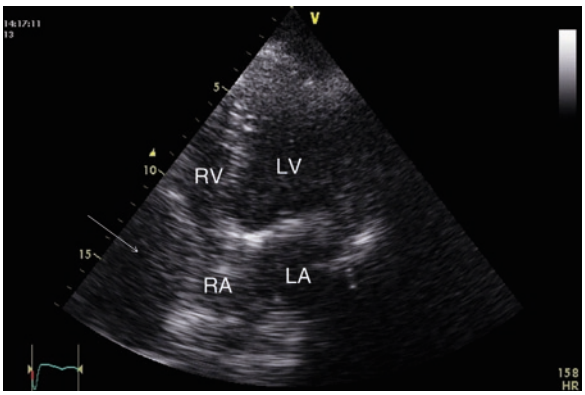

Fig. 19.15 Transthoracic echocardiography four-chamber view suggesting that the right atrium (RA) is compressed by a localized thrombus (*arrow*). *LV* left ventricle, *RV* right ventricle, *LA* left atrium

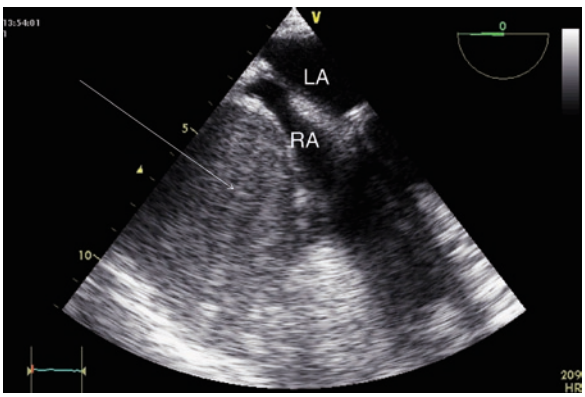

Fig. 19.16 Transesophageal echocardiography (TEE) four-chamber view (0°) demonstrating a large thrombus (*arrow*) squeezing the right atrium (RA). Please note the contrast between transthoracic echocardiography and TEE: a surgical decision is straightforward with TEE images. *LA* left atrium

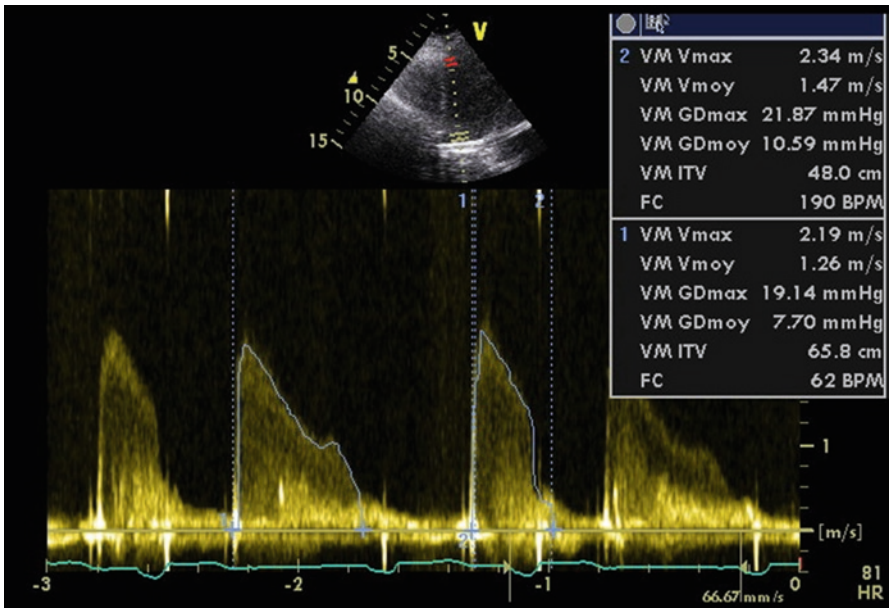

Fig. 19.17 Pulsed-Doppler recording through a mitral mechanical prosthesis indicating recently increased mean diastolic velocities and mean pressure gradient (>10 mmHg), suggesting partial thrombosis

Mechanical valve thrombosis is more likely to involve the mitral rather than the aortic valves owing to lower-flow velocities. Patients can be rapidly deteriorating and are sometimes diagnosed when in shock or pulmonary edema due to low cardiac output and congestion upstream of the mitral valve. Elevated transmitral gradients are highly suggestive and can usually be obtained using TTE (Fig. 19.17). The precise mechanism of prosthetic dysfunction is far better identified using TEE.

19.4 Conclusions

TEE is absolutely essential for the cardiac anesthetist and the intensivist in charge of postoperative care. No other tool permits easy and rapid recognition of so many acute disorders that can be life-threatening in cardiac surgical patients. The benefit/risk-cost ratio is so favorable that a systematic use of TEE for any cardiac procedure is completely justified. In situations where every patient cannot be monitored, the procedure should be prioritized for mitral valve repair and urgent surgery (aortic dissection, mechanical complication of myocardial infarction).

References

1. Matsumoto M, Oka Y, Strom J et al (1980) Application of transesophageal echocardiography to continuous intraoperative monitoring of left ventricular performance. Am J Cardiol 46:95–105
2. Mishra M, Chauhan R, Sharma KK et al (1998) Real-time intraoperative transesophageal echocardiography – how useful? Experience of 5, 016 cases. J Cardiothorac Vasc Anesth 12:625–632
3. Sutton DC, Kluger R (1998) Intraoperative transoesophageal echocardiography: impact on adult cardiac surgery. Anaesth Intensive Care 26:287–293
4. Click RL, Abel MD, Schaff HV (2000) Intraoperative transesophageal echocardiography: 5-year prospective review of impact on surgical management. Mayo Clin Proc 75:241–247
5. Michel-Cherqui M, Ceddaha A, Liu N et al (2000) Assessment of systematic use of intraoperative transesophageal echocardiography during cardiac surgery in adults: a prospective study of 203 patients. J Cardiothorac Vasc Anesth 14:45–50
6. Couture P, Denault AY, McKenty S et al (2000) Impact of routine use of intraoperative transesophageal echocardiography during cardiac surgery. Can J Anaesth 47:20–26
7. Ionescu AA, West RR, Proudman C, Butchart EG, Fraser AG (2001) Prospective study of routine perioperative transesophageal echocardiography for elective valve replacement: clinical impact and cost-saving implications. J Am Soc Echocardiogr 14:659–667
8. Fanshawe M, Ellis C, Habib S, Konstadt SN, Reich DL (2002) A retrospective analysis of the costs and benefits related to alterations in cardiac surgery from routine intraop-

erative transesophageal echocardiography. Anesth Analg 95:824–827, table of contents
9. Qaddoura FE, Abel MD, Mecklenburg KL et al (2004) Role of intraoperative transesophageal echocardiography in patients having coronary artery bypass graft surgery. Ann Thorac Surg 78:1586–1590
10. Gurbuz AT, Hecht ML, Arslan AH (2007) Intraoperative transesophageal echocardiography modifies strategy in off-pump coronary artery bypass grafting. Ann Thorac Surg 83:1035–1040
11. Van Dyck MJ, Watremez C, Boodhwani M, Vanoverschelde JL, El Khoury G (2010) Transesophageal echocardiographic evaluation during aortic valve repair surgery. Anesth Analg 111:59–70
12. Mihaileanu S, el Asmar B, Acar C et al (1991) Intra-operative transoesophageal echocardiography after mitral repair–specific conditions and pitfalls. Eur Heart J 12(Suppl B): 26–29
13. Lambert AS, Miller JP, Merrick SH et al (1999) Improved evaluation of the location and mechanism of mitral valve regurgitation with a systematic transesophageal echocardiography examination. Anesth Analg 88:1205–1212
14. Bridgewater B, Hooper T, Munsch C et al (2006) Mitral repair best practice: proposed standards. Heart 92:939–944
15. Desjardins G, Cahalan M (2009) The impact of routine trans-oesophageal echocardiography (TOE) in cardiac surgery. Best Pract Res Clin Anaesthesiol 23:263–271
16. Practice guidelines for perioperative transesophageal echocardiography (1996) A report by the American Society of Anesthesiologists and the society of cardiovascular anesthesiologists task force on transesophageal echocardiography. Anesthesiology 84:986–1006
17. Cheitlin MD, Armstrong WF, Aurigemma GP et al (2003) ACC/AHA/ASE 2003 guideline update for the clinical application of echocardiography: summary article: a report of the American College of Cardiology/American Heart Association Task Force on Practice Guidelines (ACC/AHA/ASE Committee to update the 1997 guidelines for the clinical application of echocardiography). Circulation 108:1146–1162
18. Practice guidelines for perioperative transesophageal echocardiography (2010) An updated report by the American Society of Anesthesiologists and the Society of Cardiovascular Anesthesiologists Task Force on transesophageal echocardiography. Anesthesiology 112:1084–1096
19. Poliac LC, Barron ME, Maron BJ (2006) Hypertrophic cardiomyopathy. Anesthesiology 104:183–192
20. Kertai MD, Bountioukos M, Boersma E et al (2004) Aortic stenosis: an underestimated risk factor for perioperative complications in patients undergoing noncardiac surgery. Am J Med 116:8–13
21. Reeder GS (1995) Identification and treatment of complications of myocardial infarction. Mayo Clin Proc 70:880–884
22. Hiratzka LF, Bakris GL, Beckman JA et al (2010) ACCF/AHA/AATS/ACR/ASA/SCA/SCAI/SIR/STS/SVM guidelines for the diagnosis and management of patients with Thoracic Aortic Disease: a report of the American College of Cardiology Foundation/American Heart Association Task Force on Practice Guidelines, American Association for Thoracic Surgery, American College of Radiology, American Stroke Association, Society of Cardiovascular Anesthesiologists, Society for Cardiovascular Angiography and Interventions, Society of Interventional Radiology, Society of Thoracic Surgeons, and Society for Vascular Medicine. Circulation 121:e266–e369
23. Shimokawa T, Takanashi S, Ozawa N, Itoh T (2008) Management of intraoperative malperfusion syndrome using femoral artery cannulation for repair of acute type A aortic dissection. Ann Thorac Surg 85:1619–1624
24. Oka Y, Inoue T, Hong Y et al (1986) Retained intracardiac air. Transesophageal echocardiography for definition of incidence and monitoring removal by improved techniques. J Thorac Cardiovasc Surg 91:329–338
25. Leung JM (1993) Clinical evidence of myocardial stunning in patients undergoing CABG surgery. J Card Surg 8: 220–223
26. De Hert SG, Rodrigus IE, Haenen LR, De Mulder PA, Gillebert TC (1996) Recovery of systolic and diastolic left ventricular function early after cardiopulmonary bypass. Anesthesiology 85:1063–1075
27. Noon GP, Ball JW Jr, Short HD (1996) Bio-Medicus centrifugal ventricular support for postcardiotomy cardiac failure: a review of 129 cases. Ann Thorac Surg 61:291–295, discussion 311-293
28. Kato M, Nakashima Y, Levine J, Goldiner PL, Oka Y (1993) Does transesophageal echocardiography improve postoperative outcome in patients undergoing coronary artery bypass surgery? J Cardiothorac Vasc Anesth 7:285–289
29. Baslaim GM, Huynh TT, Stewart JA et al (1998) Assessment of right ventricular function postretrograde cardioplegia by transesophageal echocardiography. J Card Surg 13:32–36
30. Bittner HB, Kendall SW, Chen EP, Davis RD, Van Trigt P 3rd (1995) Myocardial performance after graft preservation and subsequent cardiac transplantation from brain-dead donors. Ann Thorac Surg 60:47–54
31. Mihaileanu S, Marino JP, Chauvaud S et al (1988) Left ventricular outflow obstruction after mitral valve repair (Carpentier's technique). Proposed mechanisms of disease. Circulation 78:I78–I84
32. Leung JM, Levine EH (1994) Left ventricular end-systolic cavity obliteration as an estimate of intraoperative hypovolemia. Anesthesiology 81:1102–1109
33. Mingo S, Benedicto A, Jimenez MC, Perez MA, Montero M (2006) Dynamic left ventricular outflow tract obstruction secondary to catecholamine excess in a normal ventricle. Int J Cardiol 112:393–396
34. Jebara VA, Mihaileanu S, Acar C et al (1993) Left ventricular outflow tract obstruction after mitral valve repair. Results of the sliding leaflet technique. Circulation 88:II30–II34

Acute Aortic Syndrome: Acute Aortic Diseases in Hemodynamically Unstable Patients

20

Isidre Vilacosta, Victoria Cañadas, J. Alberto San Román, and Philippe Vignon

Contents

I. Vilacosta and V. Cañadas
Instituto Cardiovascular. Servicio de Cardiología. Hospital Clínico San Carlos, Madrid, Spain

J.A.S. Román
Instituto de las Ciencias del Corazón. Hospital Universitario de Valladolid, Valladolid, Spain

P. Vignon (✉)
Medical-Surgical ICU, and
Clinical Investigation Center INSERM 0801,
CHU Dupuytren, 2 Ave. Martin Luther King, 87000, Limoges, France and
Université de Limoges, 2 rue du Dr Marcland, 87000, Limoges, France
e-mail: philippe.vignon@unilim.fr

The term acute aortic syndrome (AAS) was coined by us several years ago [1]. This clinical entity is currently widely recognized [2, 3]. Four distinct acute aortic diseases that may result in AAS should be distinguished: classic (i.e., complete) aortic dissection, intramural aortic hematoma (IAH), penetrating aortic ulcer (PAU), and incomplete aortic dissection. Each of these entities has a distinct pathophysiology [2]. Early recognition of AAS is crucial since acute aortic diseases are life-threatening conditions related to the risk of adventitial rupture. Syncope, hypotension, and shock are warning signs, which are commonly indicative for exsanguination or cardiac tamponade related to the involvement of the ascending aorta. Diagnosis of AAS relies on noninvasive imaging modalities. Acute management depends on the aortic segment involved: prompt surgery for the ascending aorta and conservative treatment for the descending aorta. In the absence of surgery, the mortality associated with acute dissection of the ascending aorta is estimated to reach approximately 1% per h during the first 48 h after the onset of symptoms [4].

In this chapter, we describe acute aortic diseases that constitute AAS and initial diagnostic workup. Advantages and limitations of modern imaging modalities, especially echocardiography Doppler, are discussed. Finally, current therapeutic management of patients with AAS is summarized. Aortic inflammatory processes and traumatic aortic injuries are purposely excluded.

20.1 Classifications

AAS encompasses acute aortic diseases that share a common risk of lethal rupture secondary to excessive shearing forces applying on the aortic wall (Fig. 20.1).

D. De Backer et al. (eds.), *Hemodynamic Monitoring Using Echocardiography in the Critically Ill*,
DOI: 10.1007/978-3-540-87956-5_20, © Springer-Verlag Berlin Heidelberg 2011

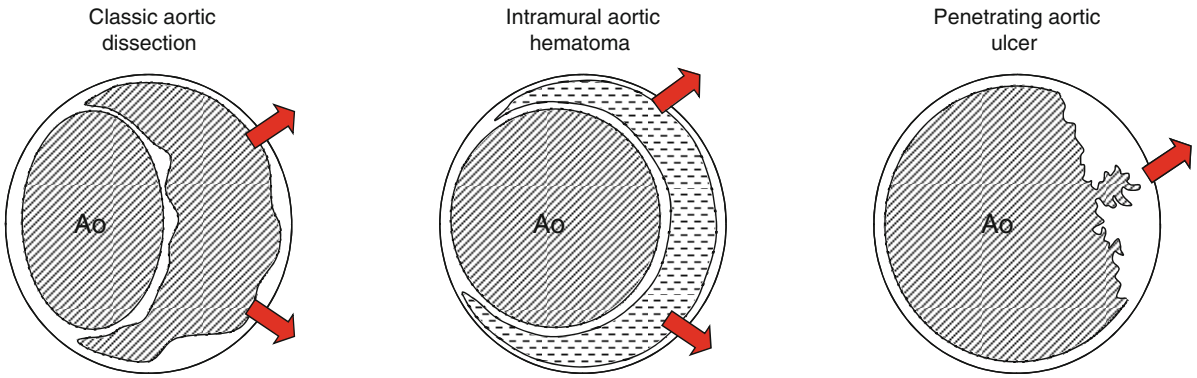

Fig. 20.1 Main conditions constituting acute aortic syndrome. A common risk is abrupt exsanguination secondary to aortic wall rupture. Abbreviation: *Ao* aorta

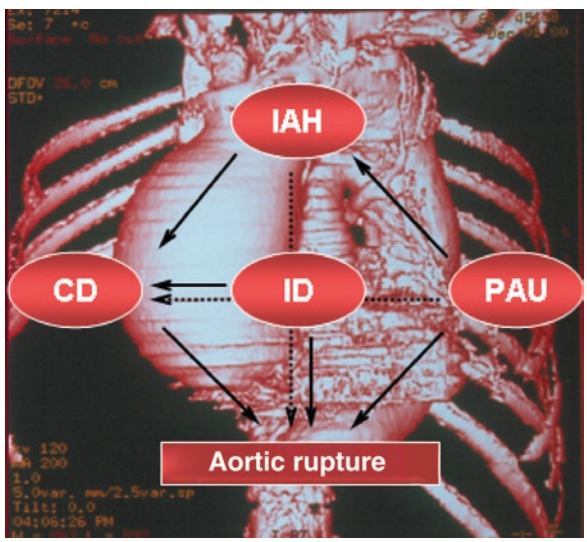

Fig. 20.2 The four acute aortic diseases that constitute acute aortic syndrome. Arrows indicate the possible progression of each of these aortic lesions. Abbreviations: *IAH* intramural aortic hematoma, *CD* classic and complete dissection, *ID* incomplete dissection, *PAU* penetrating aortic ulcer

In some patients, IAH may evolve to a classic aortic dissection. PAU is frequently associated with intramural hemorrhage and may occasionally constitute the entrance tear of a subsequent aortic dissection (Fig. 20.2). Incomplete aortic dissection corresponds to an aortic wall laceration without dissection of the media [5, 6]. It may subsequently evolve to a classic aortic dissection (Fig. 20.2). In certain patients, these acute aortic diseases may succeed each other or coexist. Any of these four components of AAS may rapidly progress to aortic rupture, which can be contained or not [7].

From a surgical and prognostic standpoint, patients with AAS may be classified into two groups, depending on the aortic segment involved: proximal AAS refers to acute aortic diseases involving the ascending aorta and/or the aortic arch, whereas distal AAS implies that the descending aorta is solely involved [1].

Aortic diseases can also be classified according to the duration of symptoms as acute, subacute, or chronic. Acute aortic dissections are diagnosed within 14 days after the onset of symptoms, while subacute aortic dissections are diagnosed between 2 weeks and 2 months of clinical presentation. Patients with symptoms present for more than 2 months at the time of the diagnosis are considered chronic cases [8]. This temporal classification is clinically relevant because 75% of patients presenting with a classic dissection of the ascending aorta die during the acute phase of the disease if left untreated [4], whereas the prognosis of patients who reach the chronic phase is better.

20.2 Identification of Patients at High Risk of AAS and Diagnostic Workup

AAS is the most frequently fatal condition in the spectrum of patients who present to the emergency department with chest pain [9]. AAS and acute coronary syndrome (ACS) are life-threatening cardiovascular emergencies that can be difficult to differentiate, particularly when ACS is the result of an AAS. Accurate and rapid diagnosis will set patient management and prognosis.

Patients are screened for a potential AAS on the basis of a characteristic "aortic pain" associated with a long-lasting history of severe hypertension (Fig. 20.3) [1, 10]. Moderate to severe hypertension is the most frequent risk factor for AAS, regardless of underlying acute aortic disease [11, 12]. Inheritable disorders of elastic tissue also predispose to the development of classic (complete) and incomplete aortic dissections [13, 14]. Aortic pain can be described as a severely intense, acute, tearing or ripping, pulsating and migratory chest pain [10]. As opposed to the more gradual increasing intensity of pain related to ACS, aortic pain associated with AAS is typically sudden and of maximal intensity at the time of onset [10]. Chest pain irradiated to the neck, throat, or jaws indicates that the ascending aorta is presumably involved, whereas back pain or abdominal pain suggests a disease of the descending aorta [10]. The presence of a murmur of aortic regurgitation and pulse differentials can be used as additional diagnostic clues of AAS [15]. Screened patients with clinically suspected AAS have to be further evaluated since delayed diagnosis may be lethal.

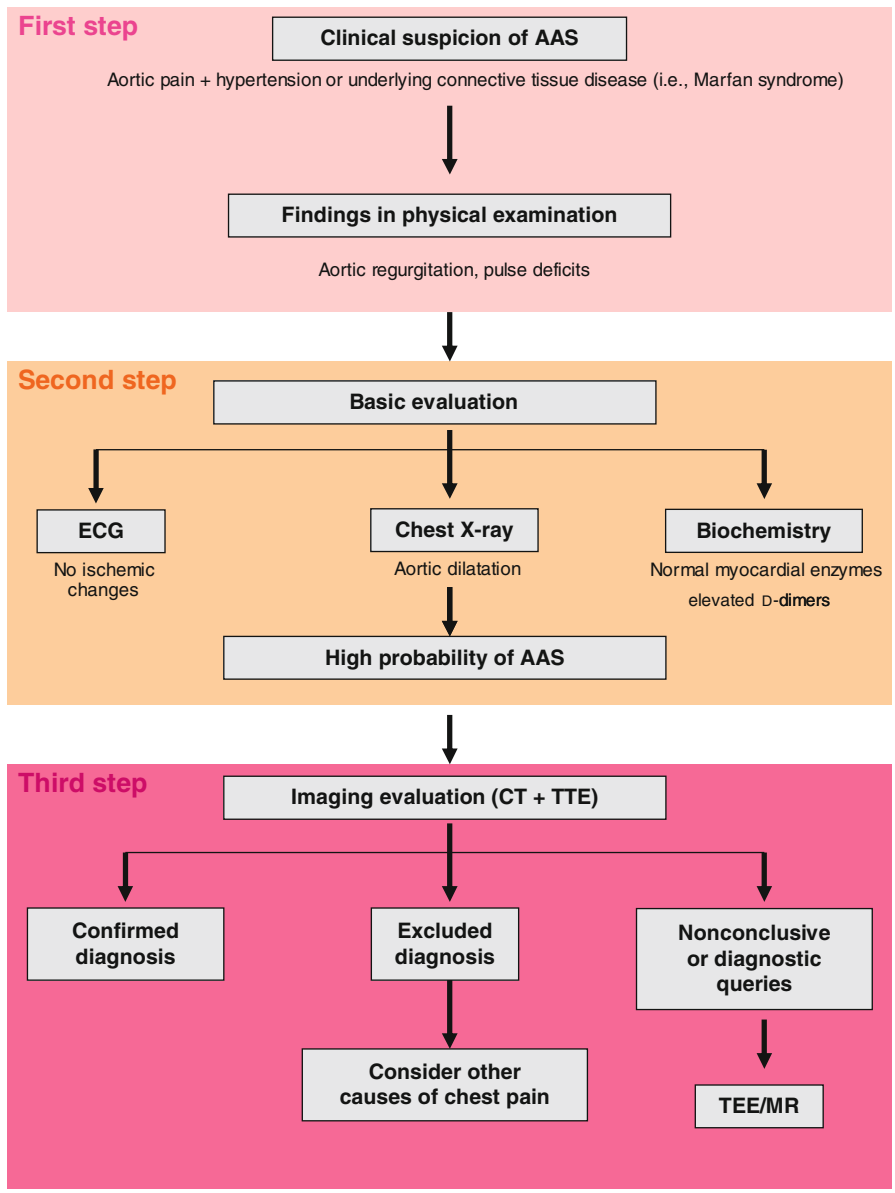

Fig. 20.3 Diagnostic workup for assessing patients with suspected acute aortic syndrome. Abbreviations: *AAS* acute aortic syndrome, *ECG* electrocardiography, *CT* multidetector-row computed tomography, *TTE* transthoracic echocardiography, *TEE* multiplane transesophageal echocardiography, *MR* magnetic resonance imaging

Laboratory tests, electrocardiography, and chest X-ray may help to differentiate AAS from ACS (Fig. 20.3). Increased plasma D-dimer values and an unremarkable electrocardiogram (ECG) are consistent with AAS [16–18]. In contrast, elevated myocardial enzymes and electrocardiographic abnormalities are indicative of ACS. Of note, the conjunction of AAS and ACS is nowadays more frequent than previously reported [8, 19, 20]. Chest radiographs are frequently obtained in patients with acute chest pain. An enlarged mediastinum is associated with a high probability of AAS [20]. Nevertheless, a normal mediastinal contour fails to confidently exclude an underlying aortic disease [21]. After this basic assessment, the patient with suspected AAS has to be evaluated with a reference imaging technique for the diagnosis of acute aortic diseases (Fig. 20.3).

Multidetector-row computed tomography (CT), magnetic resonance imaging (MRI), and multiplane transesophageal echocardiography (TEE) are powerful imaging modalities to accurately identify acute aortic diseases associated with AAS [22, 23]. A definitive diagnosis is required in patients with suspected AAS since false-positive or false-negative results may have dramatic consequences in this clinical setting. Accordingly, some patients often require more than one noninvasive imaging study. In exceptional cases, aortography is necessary. There is no consensus on the best imaging modality to be used for the diagnosis of AAS. In hemodynamically stable patients who can be safely transported to the radiology suite, the choice of imaging technique mainly depends on medical experience and equipment availability in the institution.

Importantly, hypotension or shock may be indicative of acute aortic diseases. In this case, the initial presence of aortic pain occurring in a hypertensive patient is crucial to document because circulatory failure associated with AAS raises the suspicion of blood extravasation. In these patients, lethal aortic rupture is imminent. Hypotension or shock is estimated to be associated with acute aortic dissection in approximately 8% of the cases [24]. Noticeably, circulatory failure is the result of a complicated dissection of the ascending aorta in 95% of the cases [24]. This explains why surface ultrasonography is frequently diagnostic in this specific clinical setting (Fig. 20.4). Transthoracic echocardiography (TTE) has the unparalleled advantage of being safe, rapid to use at bedside, and accurate for the identification of blood extravasation (e.g., hemopericardium with potential tamponade), aortic regurgitation, and enlarged ascending aorta (Fig. 20.5). In hemodynamically unstable patients who cannot be safely transported to the radiology suite, the presence of these TTE findings should prompt surgery without further workup. In this case, TEE has to be performed in the operating room, in an anesthetized patient, to confirm the diagnosis of complicated AAS and precisely identify the nature and characteristics of the underlying acute aortic disease (Fig. 20.6).

20.3 Description of Acute Aortic Diseases Associated with AAS

20.3.1 Classic Aortic Dissection

20.3.1.1 Pathology

Classic aortic dissection is typically characterized by the presence of a so-called intimal flap with an entry tear [25, 26]. Through this tear, blood under pressure dissects the aortic media longitudinally and splits up the aorta into a true (circulating) and a false (poorly or noncirculating) lumen. At pathology, a variable longitudinal and circumferential separation of the aortic media is consistently present (Fig. 20.7). The outer part of the aortic media constitutes with the adventitia the false channel outside wall, whereas the rest of the aortic media constitutes with the intimal layer the dissection flap [1, 26]. Accordingly, the intimal flap is a misnomer because the flap tissue is composed mainly of aortic media delaminated from the aortic wall. The entry tear is most frequently located in the areas of greatest hydraulic stress: the right lateral wall of the ascending aorta or the proximal segment of the descending thoracic aorta (Fig. 20.8). A reentry tear and several communicating points between the true and false lumens may be present along the descending aorta [26]. As a general rule, the true lumen is smaller than the false lumen. The latter is frequently partially covered by yellowish and gelatinous laminated thrombi [25] (Fig. 20.7).

In addition to the location of the entry tear, the extension of the dissecting process allows acute dissections to be distinguished as they involve the ascending aorta or solely the descending aorta (Fig. 20.9). The DeBakey classification distinguishes three types of classic aortic dissection: type I, when both the ascending and descending aorta are involved; type II,

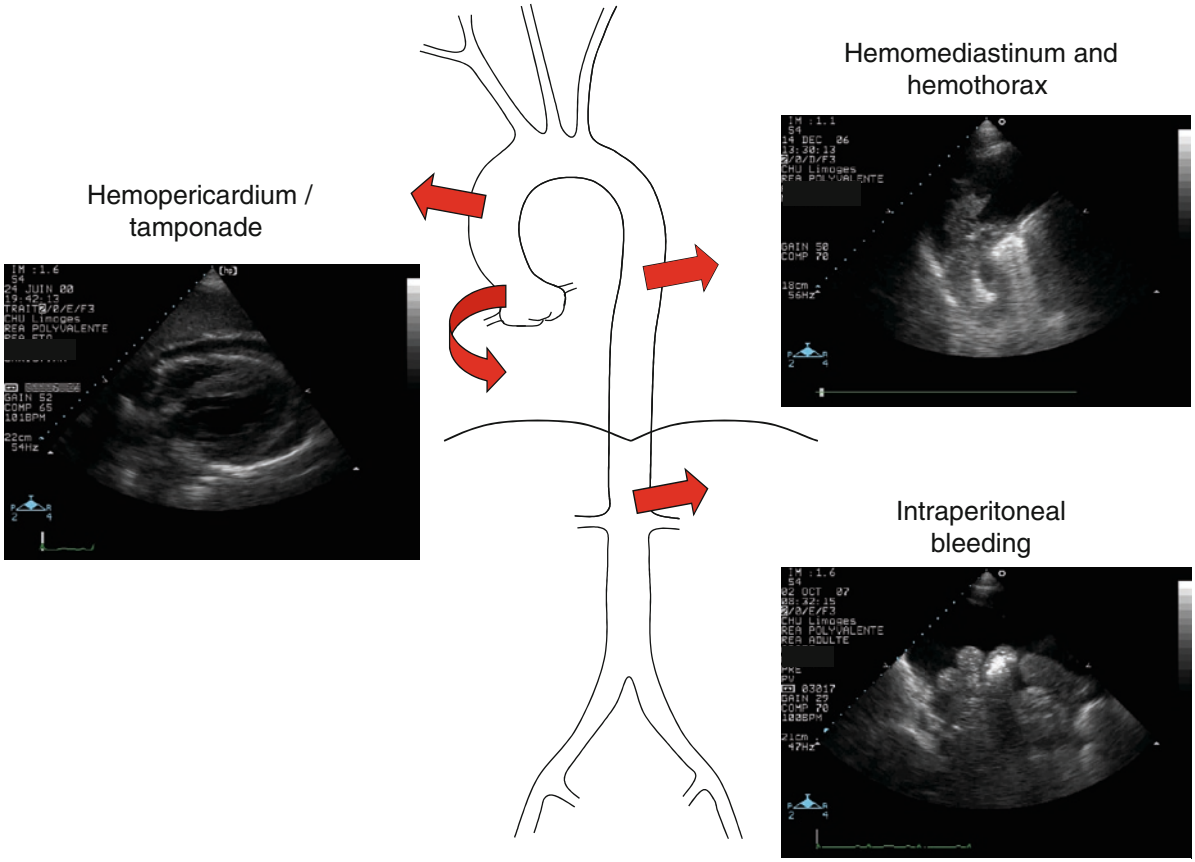

Fig. 20.4 The diagnostic field of surface ultrasonography in patients presenting with circulatory failure associated with acute aortic syndrome. At bedside, ultrasonography can rapidly depict blood extravasation in the pericardial, pleural, or abdominal space secondary to complicated acute aortic disease (*arrows*)

when the ascending aorta alone is involved; and type III, when the dissection is restricted to the descending aorta [27]. The Stanford classification categorizes classic aortic dissections into type A or type B [28], according to the involvement of the ascending aorta (Fig. 20.9).

20.3.1.2 Diagnosis

CT, TEE, and MRI have a similar diagnostic accuracy for the identification of classic aortic dissection (Fig. 20.10) [22, 23].

Echocardiography

TEE provides excellent images of the entire thoracic aorta and may even visualize the upper segment of the abdominal aorta. Currently used multiplane TEE probes reduce the traditional "blind zone," located at the junction of the distal ascending aorta and the proximal segment of the aortic arch. Studies using multiplane TEE for the diagnosis of classic aortic dissection have reported sensitivities and specificities greater than 95% [23, 29]. TEE diagnosis of aortic dissection is based on the depiction of an aortic flap separating a true and a false lumen (Fig. 20.11). The flap associated with aortic dissection typically appears as a thin, linear, intraluminal structure, which is mobile in real time. TEE linear artifacts mimicking an aortic flap are commonly observed in the ascending aorta (Fig. 20.12). They are usually due to ultrasound reverberations within the left atrium or right pulmonary artery [30]. Differential diagnostic criteria to differentiate accurately linear artifacts from true aortic flaps have been previously described [31]. M-mode may help to distinguish between linear artifacts and a true flap within

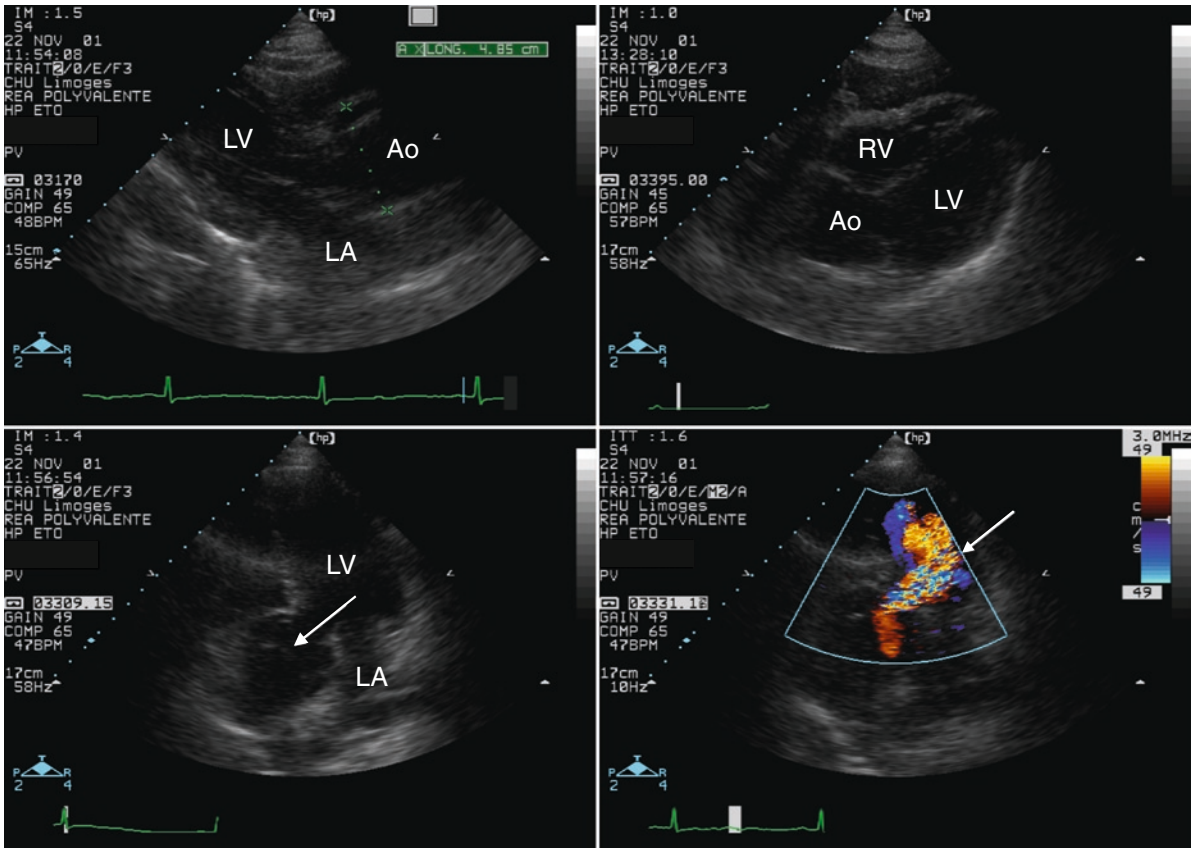

Fig. 20.5 Illustrative example of complicated acute dissection of the ascending aorta (Ao). In this hemodynamically unstable patient with shock potentially related to an acute aortic syndrome, transthoracic echocardiography was immediately performed at bedside in the emergency department. In both the parasternal long-axis (*upper left*) and subcostal four-chamber view (*upper right*), the Ao appears markedly dilated. A flap is evidenced within the dilated aortic root in the apical four-chamber view (*lower left, arrow*). Color Doppler mapping depicts a clinically relevant aortic regurgitation related to the dissected ascending aorta (*lower right, arrow*). The patient was referred for prompt surgery based on this examination. Abbreviations: *LA* left atrium, *LV* left ventricle, *RV* right ventricle

the ascending aorta [32]. A linear artifact remains parallel to the aortic walls throughout the cardiac cycle, whereas the intimal flap oscillates according to instantaneous variations in pressure gradient between the true and false lumen of the aortic dissection (Fig. 20.13). A mirror artifact is frequently observed at the level of the descending thoracic aorta (Fig. 20.14).

The entry tear constitutes a discontinuity of the aortic flap that is best identified in transversal echocardiographic planes. TEE is superior to other imaging modalities in precisely locating the entry tear of a classic aortic dissection, especially when coupling two-dimensional imaging with color Doppler mapping (Fig. 20.15). Blood flow through the entry tear may be uni- or bidirectional, according to variations in instantaneous pressure gradient across the intimal flap throughout the cardiac cycle (Fig. 20.16). Precise identification of the entry tear may help in guiding acute management (e.g., type of surgical approach in dissected ascending aorta, guidance of graft stenting in dissected descending aorta).

With the increasing use of endovascular aortic repair, the differentiation between the true and false lumen is also crucial (Table 20.1). TEE guidance of aortic graft stenting allows adequate positioning of the device in the true lumen.

TEE also allows the evaluation of early complications associated with type-A acute aortic dissection, such as aortic regurgitation or hemopericardium (Fig. 20.17). In precisely assessing both the mechanism and severity of aortic regurgitation, TEE helps in evaluating the possibility of valve repair [33].

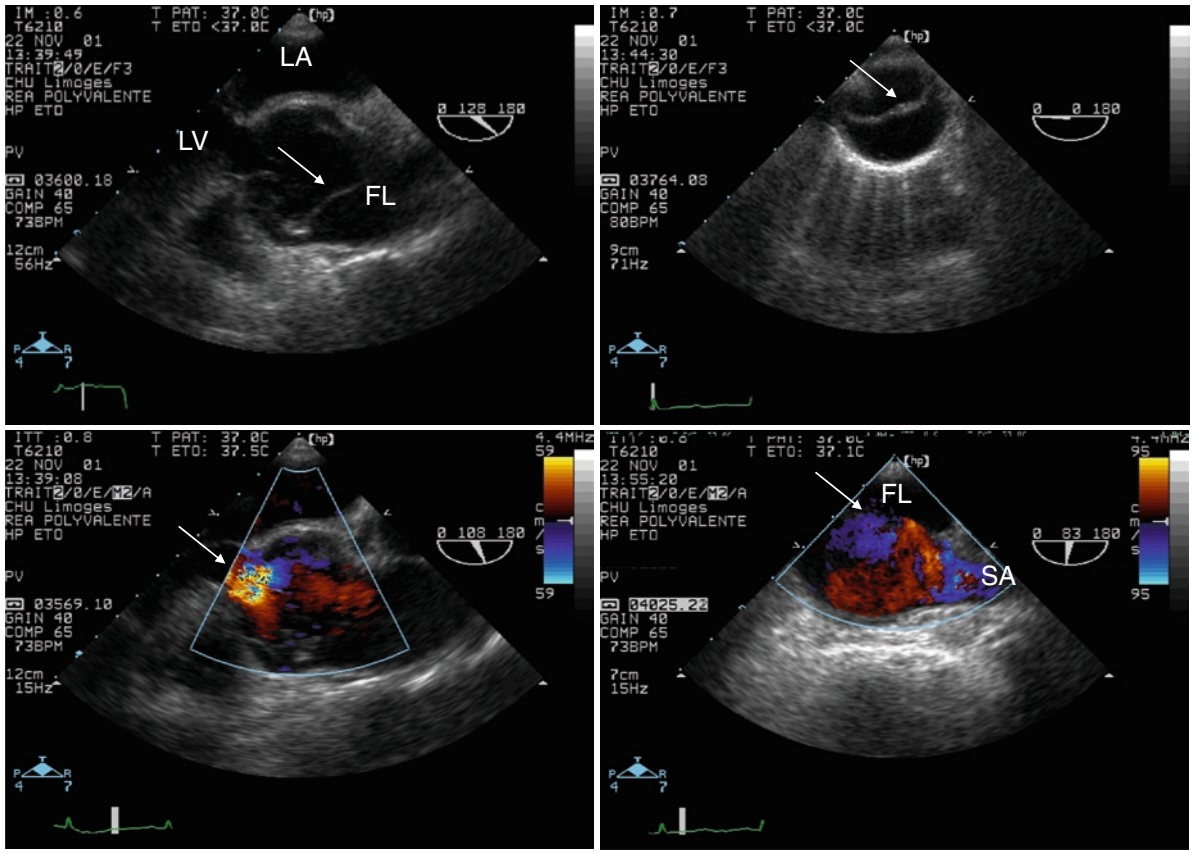

Fig. 20.6 Transesophageal echocardiographic findings obtained in the patient presented in Fig. 20.5. Conventional transesophageal examination was performed under general anesthesia in the operating room for safety. This allowed a comprehensive description of the classic aortic dissection, which helped guide surgical procedure. In the long-axis view of the ascending aorta (*left panels*), the vessel appears dilated secondary to a dissecting process as reflected by the presence of an intimal flap highly mobile in real time (*upper left, arrow*). Color Doppler mapping confirmed the presence of a significant central aortic regurgitation related to aortic dilatation (*lower left, arrow*). This type-A dissection extends up to the descending aorta, where a flap is also evidenced (*upper right, arrow*). The emergence of the left subclavian artery is not dissected and irrigated by the true lumen of the dissection, as depicted by color Doppler mapping (*lower right, arrow*). Abbreviations: *LA* left atrium, *LV* left ventricle, *FL* false lumen, *SA* subclavian artery

Other Imaging Modalities

CT is an accurate alternative imaging modality for the diagnosis of classic aortic dissection (Fig. 20.18). For assessing potential extension of the dissecting process to the aortic branches (Fig. 20.19), CT is currently the best-suited imaging modality in emergency settings (Fig. 20.20) [34, 35]. MRI is less frequently used because of its limited availability, reduced access to the patient, and restricted monitoring possibility [4].

20.3.1.3 Evolutive Patterns

False-channel rupture is the most common mechanism of death in patients with classic aortic dissection. Aortic rupture usually occurs at the level of the ascending aorta in the vicinity of the entry tear. Accordingly, hemopericardium (with potential cardiac tamponade) is a warning sign (blood extravasation) that reflects imminent death [25, 36]. Periaortic hematoma related to the accumulation of blood around the aorta may develop [37]. It is usually located in the vicinity of the entry tear and is due to slow oozing from the dissected and stretched aorta. Accordingly, periaortic hematoma may be attributed to blood extravasation, which reflects impending aortic rupture. Patients with periaortic hematoma frequently present with hemodynamic instability. This complication is an independent predictor of mortality in acute aortic dissection [37].

Acute compression of the true lumen by the false lumen of the dissection also has a bleak prognosis.

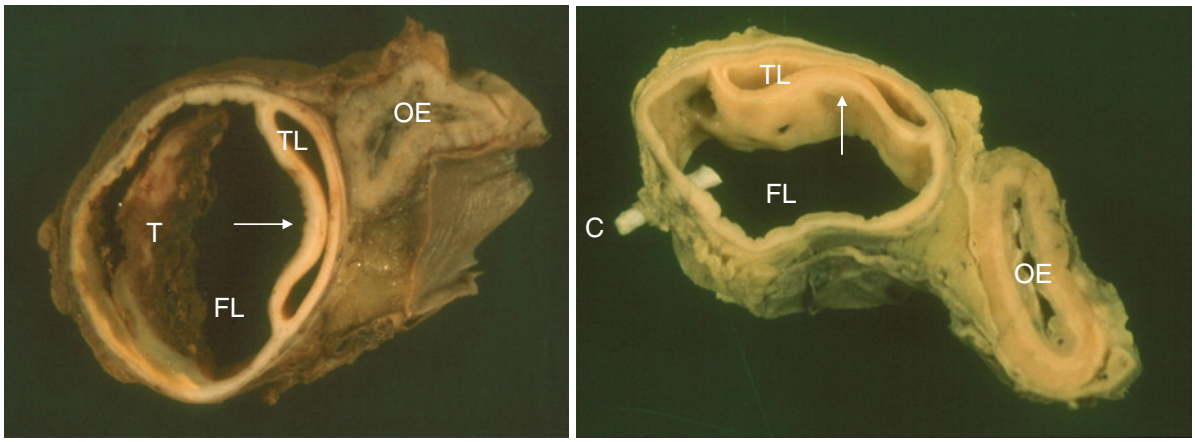

Fig. 20.7 Anatomical specimen of a classic aortic dissection. The location of the echocardiographic probe within the esophagus is anatomically close to the descending aorta, allowing a detailed depiction of its anatomy. A typical "double-barreled" aorta is delimited by an intimomedial flap (*arrows*). The false lumen is larger than the true lumen. A thrombus may develop in the false lumen owing to the absence of flow or extremely low flow (*left panel, T*). A communication point in the center of the dissection flap corresponding to the ostium of an intercostal artery allows flow to cross the dissection flap (*right panel, C*). Abbreviations: *E* esophagus, *TL* true lumen, *FL* false lumen

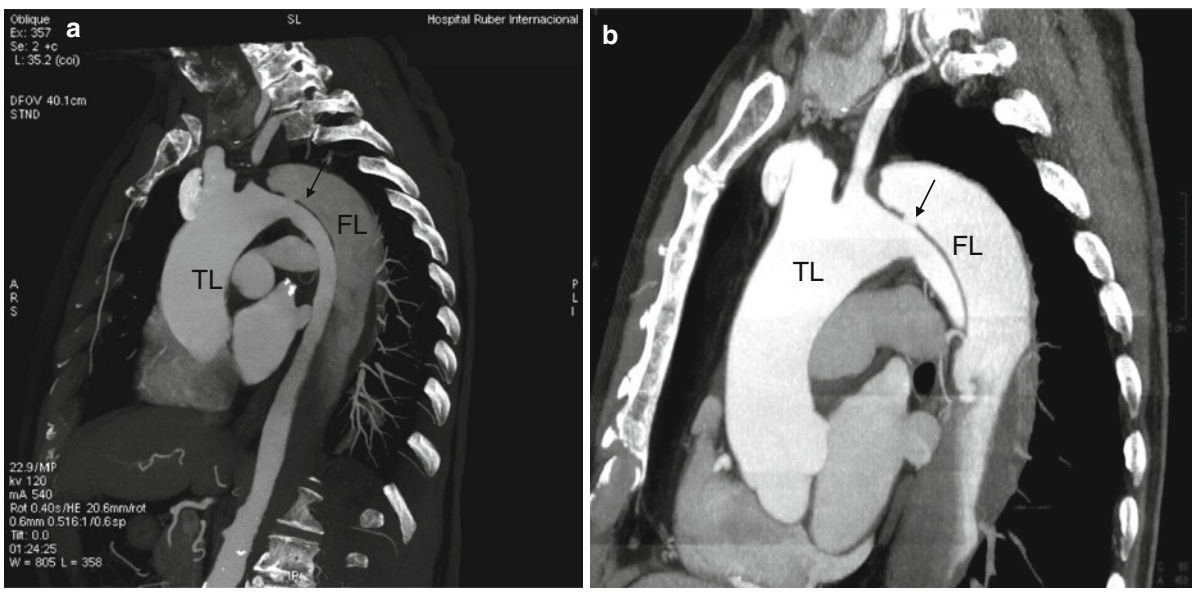

Fig. 20.8 Classic aortic dissection involving solely the descending aorta documented by multidetector-row computed tomodensitometry. Arrows indicate the entry tear. Abbreviations: *TL* true lumen, *FL* false lumen

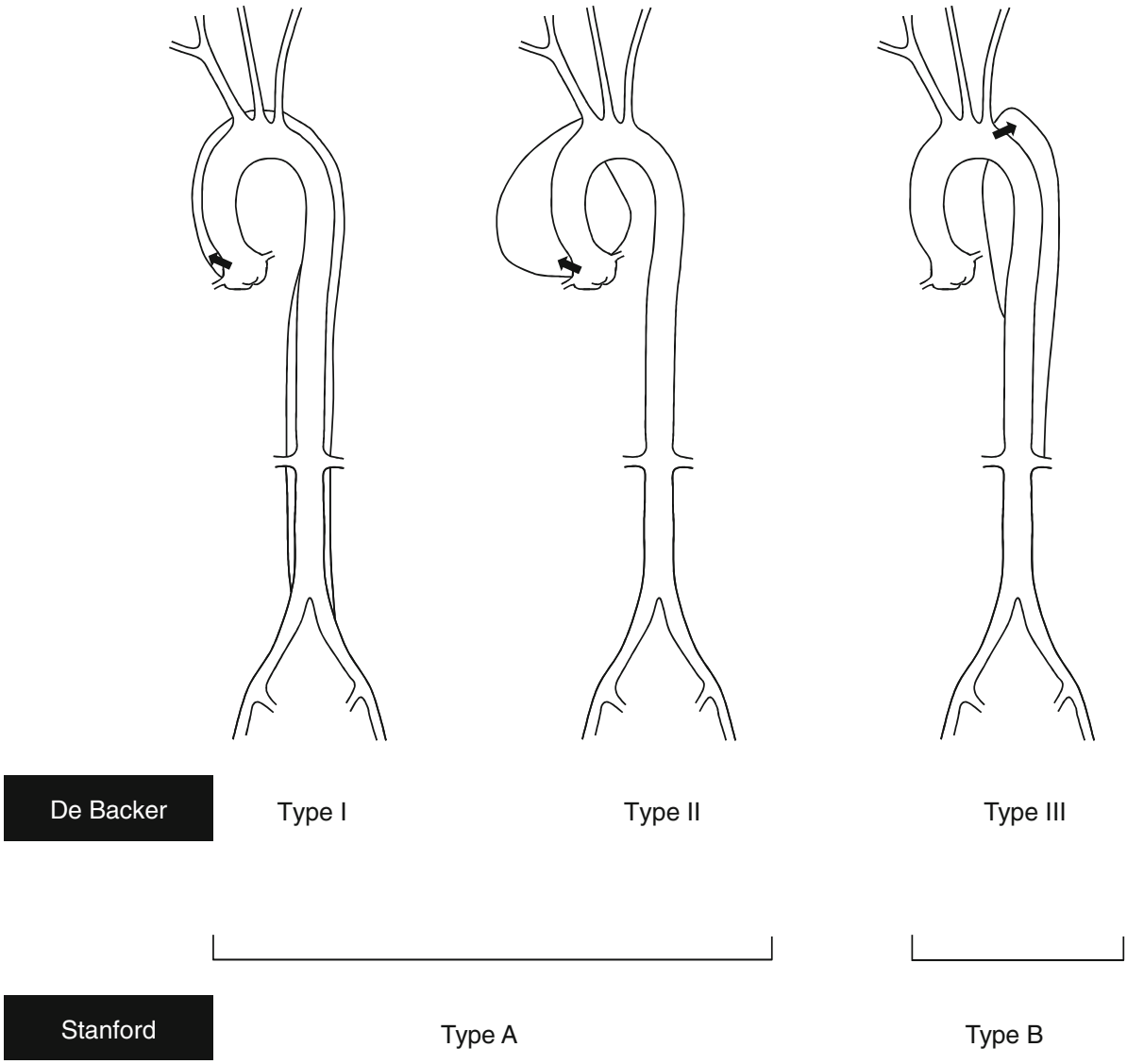

Fig. 20.9 Widely used classifications of classic aortic dissection. Both the location of the entry tear (*arrows*) and extension of the dissecting process allow distinguishing several types of aortic dissection with distinct prognosis and treatment.

In this case, malperfusion of visceral branches of the abdominal aorta or of the iliac axes can occur. Malperfusion of the mesenteric circulation is a risk factor for mortality [38].

20.3.2 Intramural Aortic Hematoma

20.3.2.1 Pathology

IAH is defined as a variant of classic aortic dissection, which is characterized by the absence of an entry tear [11, 39]. It is, therefore, a noncommunicating type of aortic dissection (Fig. 20.21). The hemorrhage into the aortic media may result from the rupture of an abnormal vasa vasorum [1, 2, 40]. IAH may also be secondary to a fractured atherosclerotic plaque [36–38] or a traumatic injury to the aortic wall [41].

IAH is present in 10–30% of patients presenting with AAS [11, 42, 43]. In a recent meta-analysis, IAH involved more frequently the ascending (type-A) than the descending (type-B) aorta (57% vs 43%, respectively) [43]. In other studies, distal IAHs are more frequent than proximal IAH [11, 44]. Necropsy series showed that in 5–13% of patients diagnosed with acute

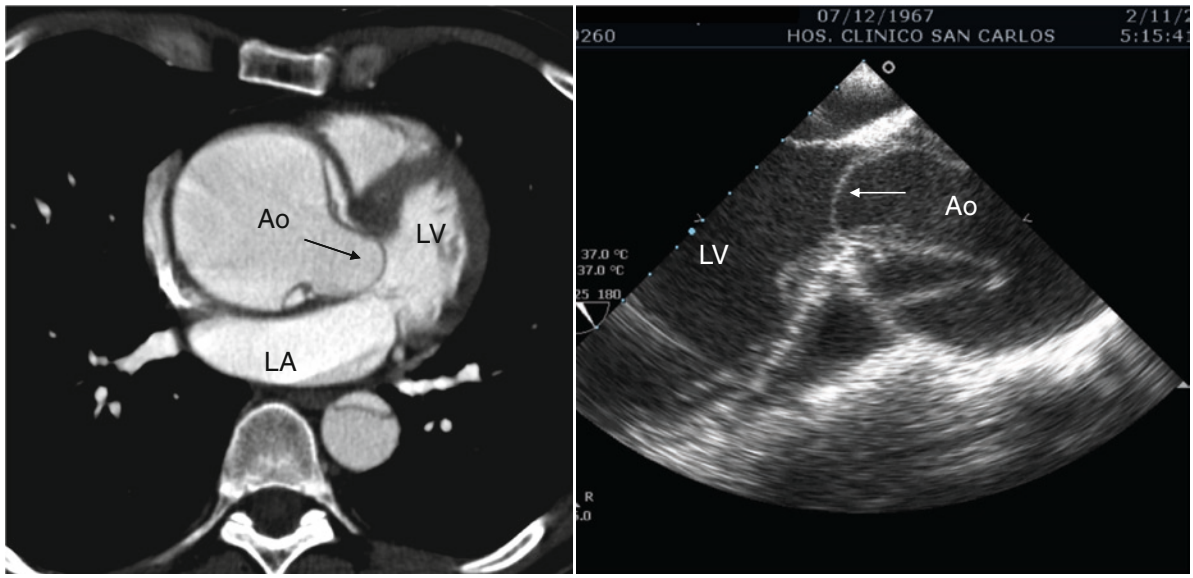

Fig. 20.10 Classic (complete) acute dissection of the ascending aorta (Ao) in a patient presenting with an acute aortic syndrome. Type-A acute aortic dissection is depicted by both contrast-enhanced multidetector-row computed tomography (*left panel*) and multiplane transesophageal echocardiography (*right panel*). The intimal flap prolapsed into the outflow tract of the left ventricle (LV) through the aortic valve (*arrows*). Abbreviation: *LA* left atrium

aortic dissection, the entry tear is not evident [8, 45, 46]. In the presence of a small entry tear, which may not be identified using current imaging modalities, it can be virtually impossible to differentiate an acute aortic dissection from an IAH [47–50].

20.3.2.2 Diagnosis

The diagnostic accuracy of TEE, CT, and MRI for the identification of IAH is similar [22].

Echocardiography

TEE findings associated with IAH are the presence of a semicircular or circular thickening (>5 mm) of the aortic wall with a thrombus-like echodensity, a decreased diameter of the aortic lumen, and a central displacement of intimal calcifications [11, 39]. Importantly, no entry tear or blood flow is evidenced using color Doppler mapping within the aortic wall, as opposed to what is observed in a classic aortic dissection (Fig. 20.22). TEE may identify small echolucent areas within the IAH, which correspond to pools of low blood flow that come from the aortic lumen through limited flap ruptures (Fig. 20.23). Differential diagnosis with classic aortic dissection and thrombosed false lumen, aortic aneurysm with a mural thrombus, and complex atheromatous plaque may be challenging [11, 39, 49]. Evolution of IAH during follow-up may help differentiate this lesion from other acute aortic diseases.

Other Imaging Modalities

Most IAHs can be diagnosed using CT [43]. A thickened, crescentic aortic wall with a high attenuation value is typical for IAH. Since IAH does not communicate directly with the aortic lumen, the thickened aortic wall is not enhanced after the injection of contrast (Fig. 20.24).

On T1-weighted MRI images, IAH appears as a crescentic aortic wall thickening with low-signal intensity in the early acute phase and high-signal intensity after 1 week. The signal intensity on T1- and T2-weighted images differs according to lesion age.

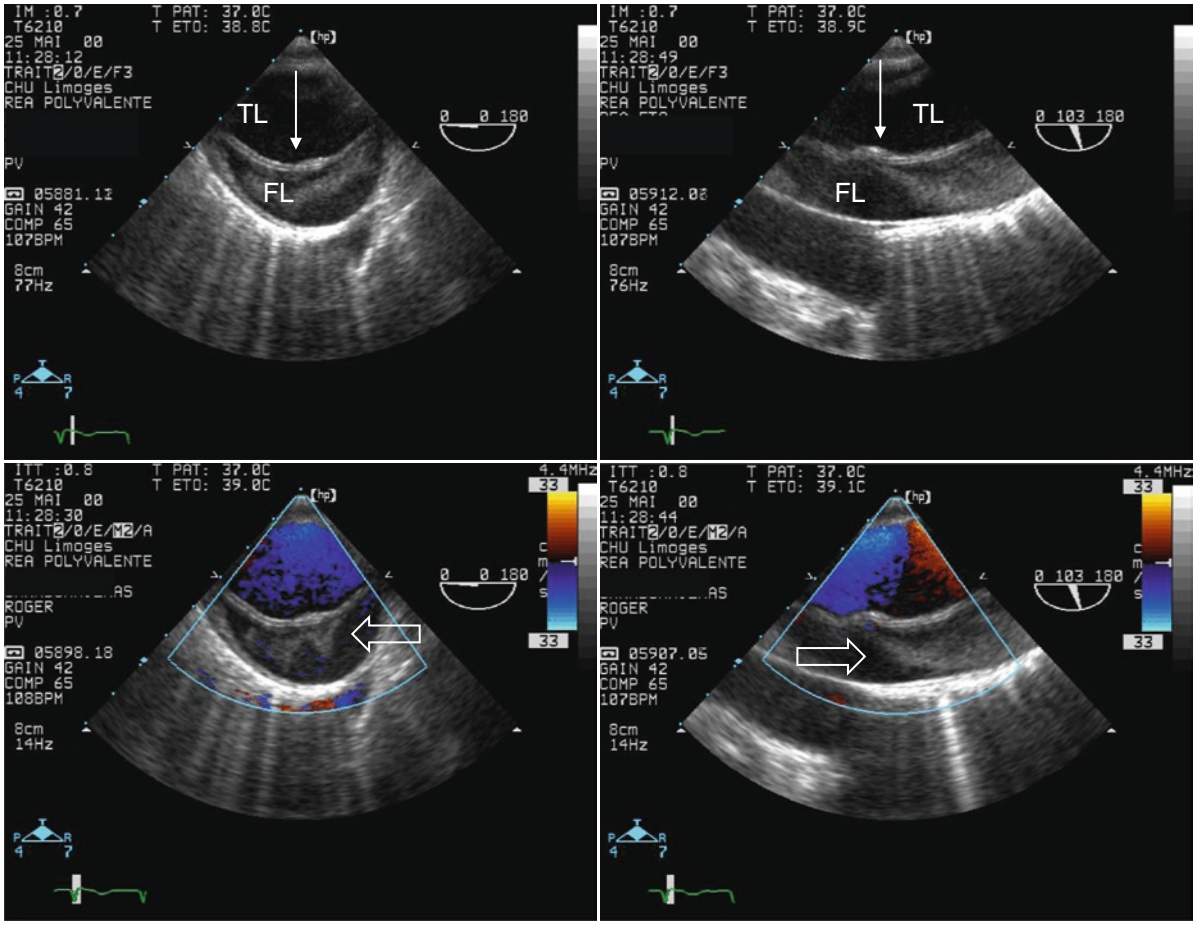

Fig. 20.11 Identification of a type-B acute aortic dissection using multiplane transesophageal echocardiography. The diagnosis of classic dissection relies on the identification of an aortic flap in the transverse (0°) and longitudinal (103°) views (*upper panels, arrows*), which separated the vessel into two distinct channels. Color Doppler mapping typically depicts blood flow within the true lumen and low flow within the false lumen (*lower panels*). Thrombus may rapidly develop in the false lumen (*lower panels, open large arrows*). Abbreviations: *TL* true lumen, *FL* false lumen

20.3.2.3 Evolutive Patterns

IAH consistently evolves with time in an unpredictable manner. It may therefore appear differently according to when the imaging modality is performed. Therefore, patients with IAH have to be carefully monitored using several complementary imaging techniques. As with classic aortic dissection, blood extravasation may complicate the course of IAH (Fig. 20.23) [11, 44]. IAH may also evolve to a classic aortic dissection owing to intimal disruption (Fig. 20.25) [7, 11, 42, 51, 52]. Some patients may simultaneously exhibit an IAH and a classic dissection involving distinct aortic segments [49]. Growing and progression of IAH with increase in the aortic wall thickness may ensue if parietal hemorrhage continues [53]. Conversely, the spontaneous resolution of IAH (i.e., partial or total regression of the aortic wall thickening) is common in distal hematomas (Fig. 20.26) [7, 11, 42, 52]. Currently, the two most important predictors of mortality in patients with IAH are the involvement of the ascending aorta and maximal aortic diameter ≥50 mm [42, 51, 54, 55]. In contrast, the prognostic value of the thickness of the hematoma is low [56].

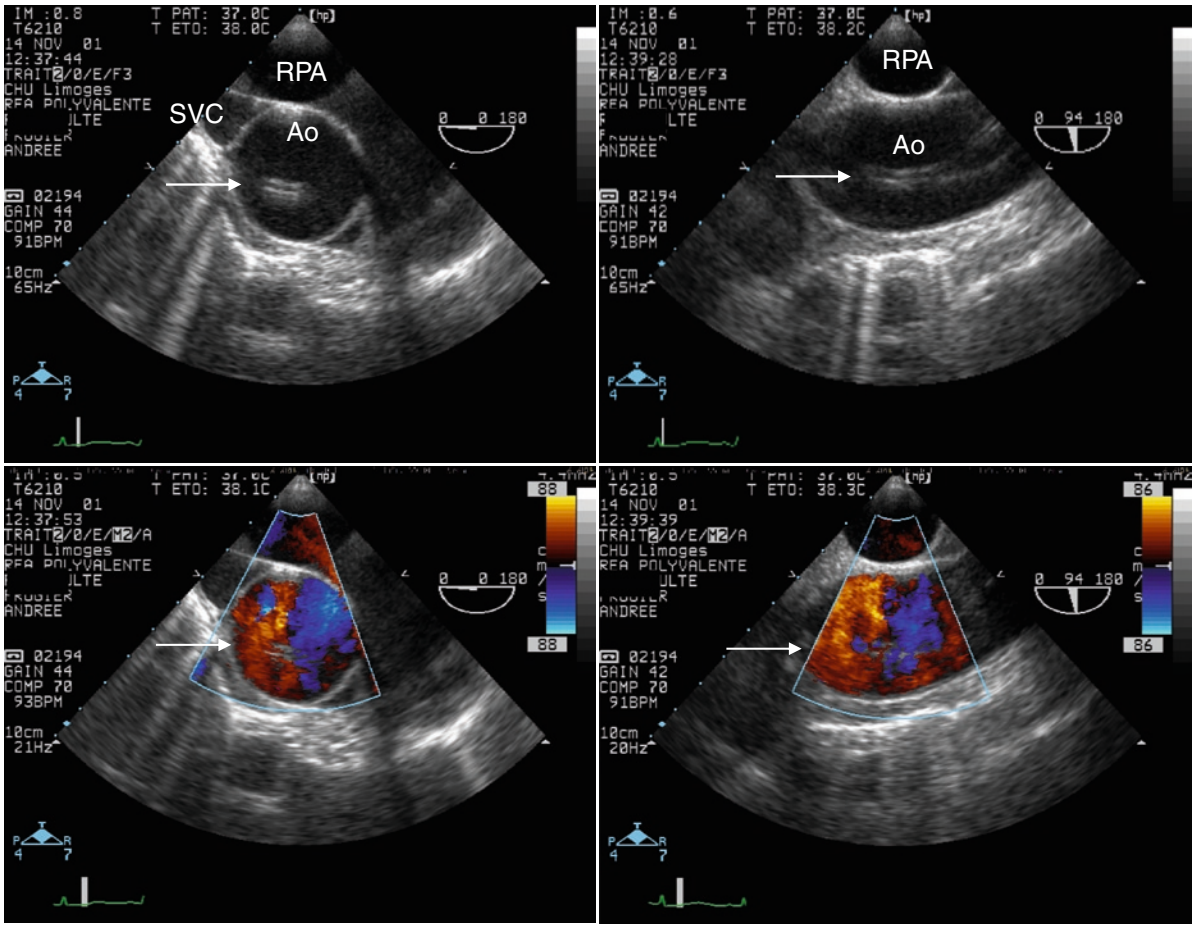

Fig. 20.12 Intraluminal linear artifact identified in the ascending aorta (Ao) with transesophageal echocardiography. The misleading linear image mimicking an aortic flap is evidenced in the transverse (*left panels*) and longitudinal plane (*right panels*) of the ascending aorta (*arrows*). Differential diagnostic criteria with aortic flap are as follows: horizontal orientation, displacement parallel to aortic walls, thickness, and normal color Doppler pattern consistent with laminar flow (*lower panels*). Abbreviations: *RPA* right pulmonary artery, *SVC* superior vena cava

20.3.3 Penetrating Aortic Ulcer

20.3.3.1 Pathology

Most atherosclerotic aortic ulcerations are incidentally discovered stable lesions without clinical expression. PAU refers to atherosclerotic aortic lesions in which ulceration penetrates the internal elastic lamina into the media [12, 57, 58]. Aortic ulcers are usually focal lesions that are most frequently located in the descending thoracic aorta, but they may also develop in other aortic segments. In the excavated area or "crater" of these ulcerated lesions, necrotic debris, foam cells, cholesterol, and thrombotic material can be found. In

Fig. 20.14 Mirror artifact of the descending aorta depicted by transesophageal echocardiography. In the transverse (*left panels*) and longitudinal views (*right panels*), the descending aorta appears duplicated due to ultrasound reverberations on a strong interface (blood-filled aorta and air-filled left lung). Color Doppler mapping may also be misleading (*lower panels*). The pitfall is to misinterpret the duplicated aortic lumen as a double barreled aorta with the normal wall seen as an intimal flap (*arrows*). Abbreviations: *Ao*, descending thoracic aorta; *Ao2*, mirror artifact falsely duplicating the descending aorta

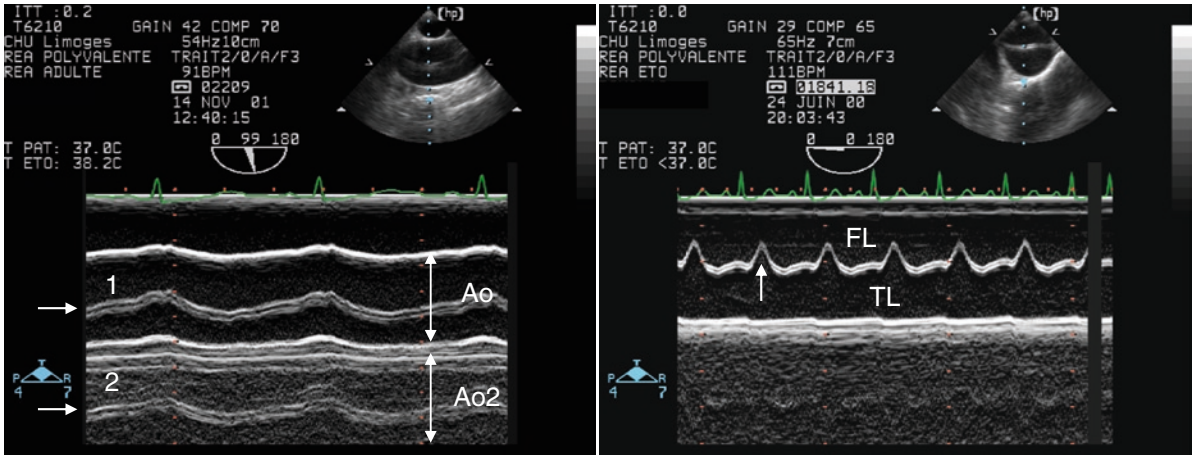

Fig. 20.13 Differential diagnosis between intimal flap and linear artifact of the ascending aorta using M-mode transesophageal echocardiography. The linear artifact is a thick linear image, which appears strictly parallel to aortic walls (*left panel, arrows*). It is the result of ultrasound reverberations, as reflected by a duplicated ascending aorta (double-headed arrows: mirror image). In contrast, the aortic flap exhibits free mobility within the aortic lumen, which directly depends on the variations of pressure gradient during the cardiac cycle between the true and the false lumen (*right panel, arrow*) and Abbreviations: *Ao* normal ascending aorta, *Ao2* duplicated artifactual ascending aorta, *TL* true lumen, *FL* false lumen

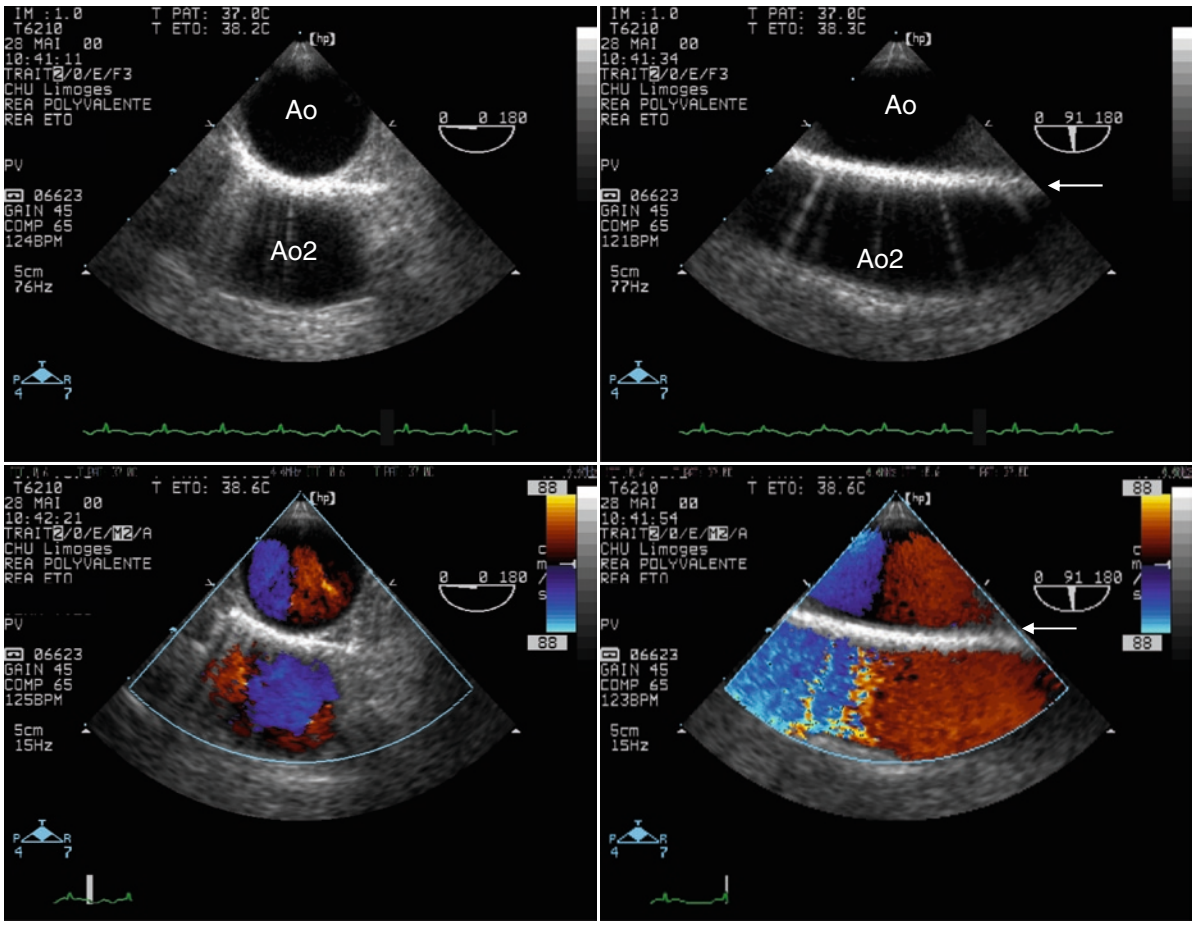

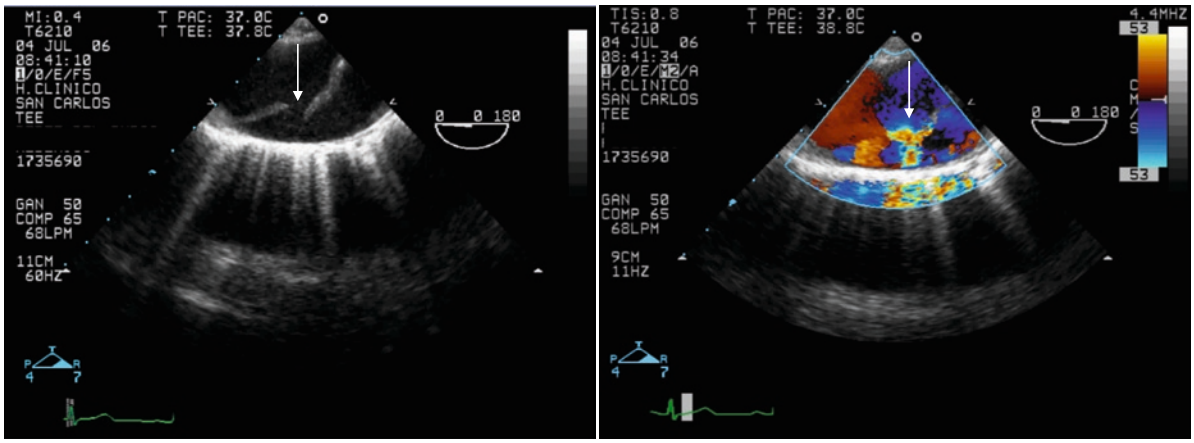

Fig. 20.15 Identification of the entry tear of a classic dissection of the descending aorta using transesophageal echocardiography. The two-dimensional transverse view of the descending aorta depicts an aortic flap with a clear discontinuation corresponding to the entry tear of the dissection (*left panel, arrow*). Color Doppler mapping depicts the presence of a turbulent blood flow through the intimal tear (*right panel, arrow*)

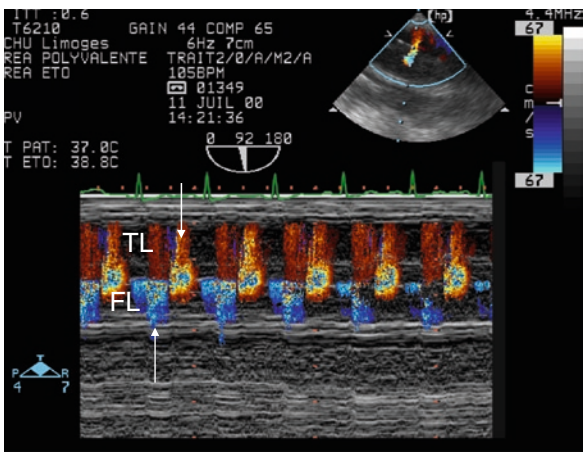

Fig. 20.16 Entry tear diagnosed using color Doppler in a patient with a type-B aortic dissection. M-mode clearly depicts a bidirectional blood flow through the entry tear, according to variations in pressure gradient across the aortic flap throughout the cardiac cycle (*arrows*). Abbreviations: *TL* true lumen, *FL* false lumen

Table 20.1 Distinctive transesophageal echocardiography findings allowing differentiation of the true from the false lumen of classic aortic dissection

	True lumen	False lumen
Global size	Small	Large
Size in systole	Increased	Decreased
Thrombus formation	No	Yes
Spontaneous contrast	No	Yes
Blood flow profile (color Doppler)	Laminar Early in systole	Swirling and turbulent, or absent Late in systole
External wall thickness	Normal	Reduced

addition, PAUs are commonly associated with a variable amount of intramural hemorrhage [58]. Usually, PAUs are associated with other atherosclerotic aortic lesions [49], including aneurysms of the descending aorta [12].

20.3.3.2 Diagnosis

The diagnosis of PAU can accurately be documented by TEE, CT, MRI, or angiography, depicting an outpouching of the aortic wall with jagged edges, usually in the presence of extensive aortic atheroma [57–61].

Fig. 20.18 Type-A acute aortic dissection diagnosed using contrast-enhanced multidetector-row computed tomography in a patient presenting with acute aortic syndrome. Transversal tomographic images (*upper and lower left panels*) clearly depict the presence of an aortic flap (*arrows*), separating a contrast-enhanced true lumen and a poorly circulating false lumen. The dissecting process involves both the ascending and descending aorta. Reconstruction images accurately document the extension of this type-A acute aortic dissection and the relative size of both channels (*lower right*). Abbreviations: *TL* true lumen, *FL* false lumen, *LV* left ventricle

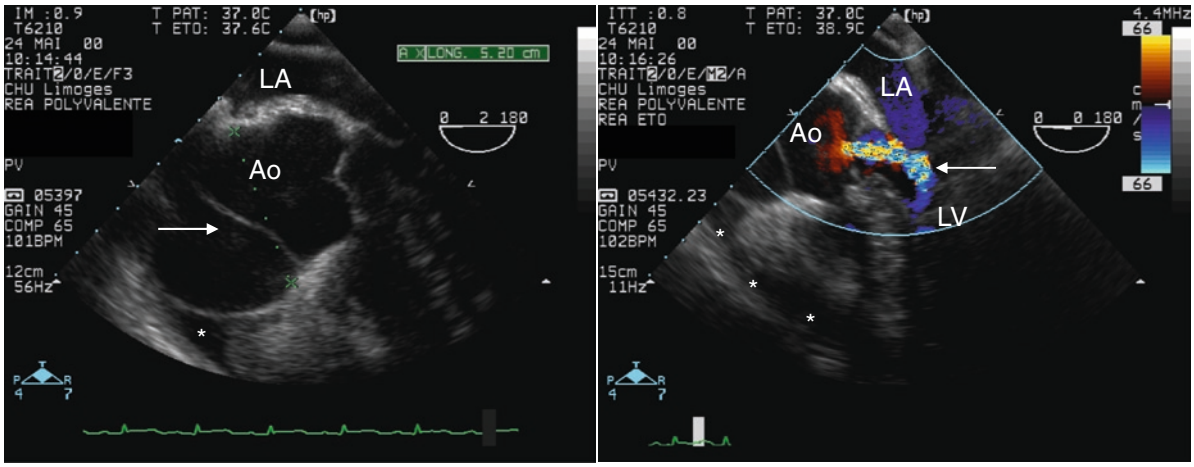

Fig. 20.17 Complicated acute dissection of the ascending aorta (Ao) clearly identified with multiplane transesophageal echocardiography. Two-dimensional imaging discloses the presence of a dilated aortic root and an intraluminal flap consistent with acute aortic dissection (*left panel, arrow*). Color Doppler mapping depicts a mild central aortic regurgitation secondary to aortic annulus dilatation (*right panel, arrow*). Of note, noncompressive hemopericardium is present (*asterisks*). Abbreviations: *LA* left atrium, *LV* left ventricle

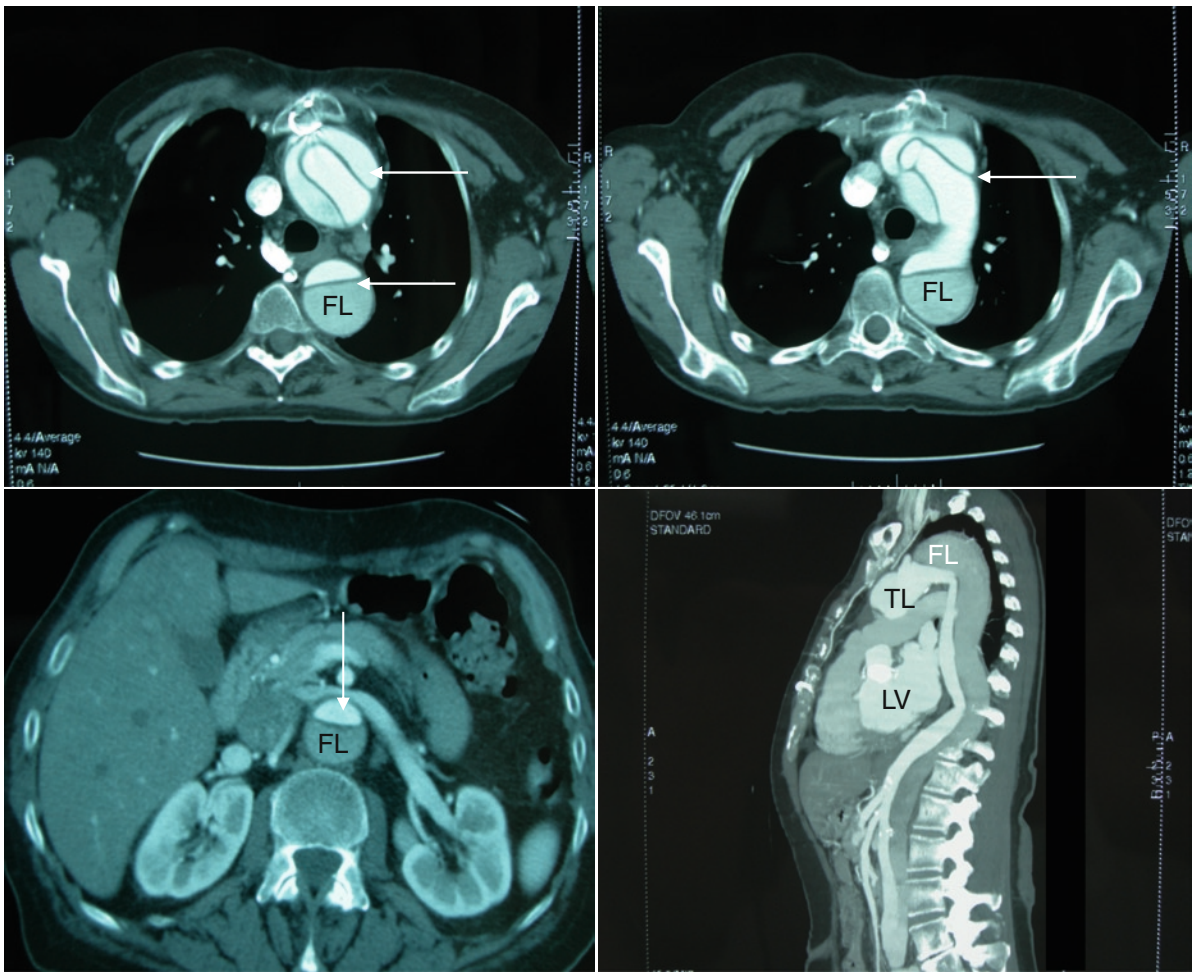

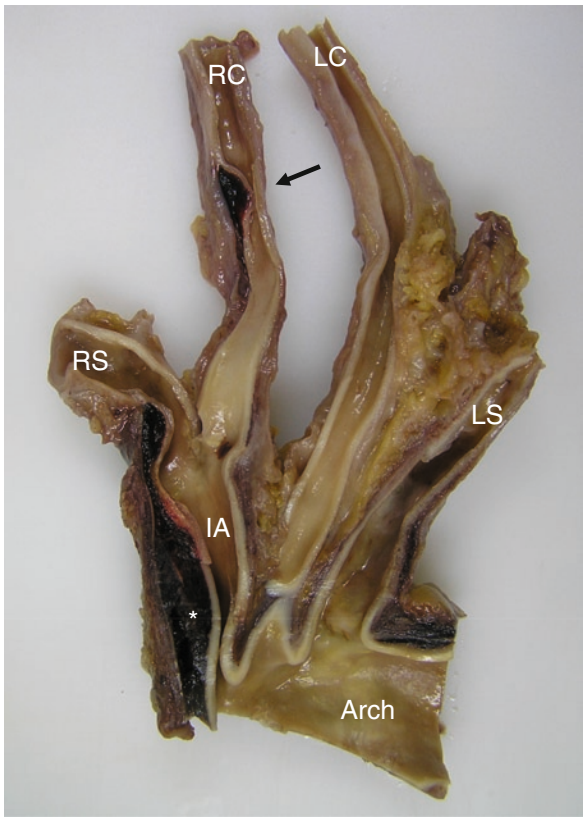

Fig. 20.19 Anatomical specimen of classic aortic dissection extended to the neck vessels and aortic arch (Arch). The dissection of the innominate artery resulted in thrombus formation in the false lumen (*asterisk*), with associated narrowing of the true lumen of the right carotid artery (*arrow*). Abbreviations: *IA* innominate artery, *RC* right carotid artery, *RS* right subclavian artery, *LC* left carotid artery, *LS* left subclavian artery

Echocardiography

TEE typically depicts a deep crater inside the aortic wall; the crater may be partially or totally filled by thrombus formation and associated with intramural hematoma (Fig. 20.27). Color Doppler imaging improves the detection of the atherosclerotic ulcer. Occasionally, an internal displacement of a calcified intima can be observed, indicating the presence of intramural hemorrhage or a localized false lumen.

Other Imaging Modalities

CT and MRI also allow the detection of PAU and associated complications (Figs. 20.28 and 20.29) [62]. Many patients with PAU have severe atherosclerosis and chronic renal failure. In this situation, MRI or TEE is more adequate.

20.3.3.3 Evolutive Patterns

The natural history of PAU is unknown. Most patients with PAU do not need immediate aortic repair but require close follow-up with serial imaging studies to document any progression or complication of aortic disease. PAU may be complicated by slowly progressive aneurysm formation [63], pseudoaneurysm

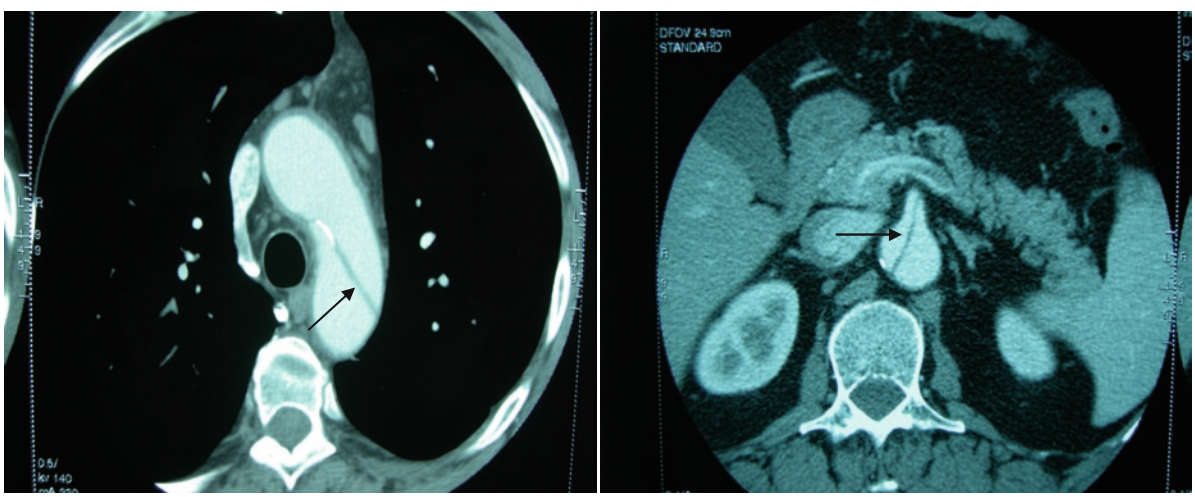

Fig. 20.20 Evaluation of the extension of type-A acute aortic dissection to collaterals using contrast-enhanced multidetector-row computed tomography. An aortic flap (*arrows*) associated with a circulating false lumen is evidenced at the level of the ascending aorta (*upper left*). This type-A aortic dissection involves the supra-aortic arteries (*lower left*) and mesenteric artery (*upper right*), but not the renal arteries (*lower right*)

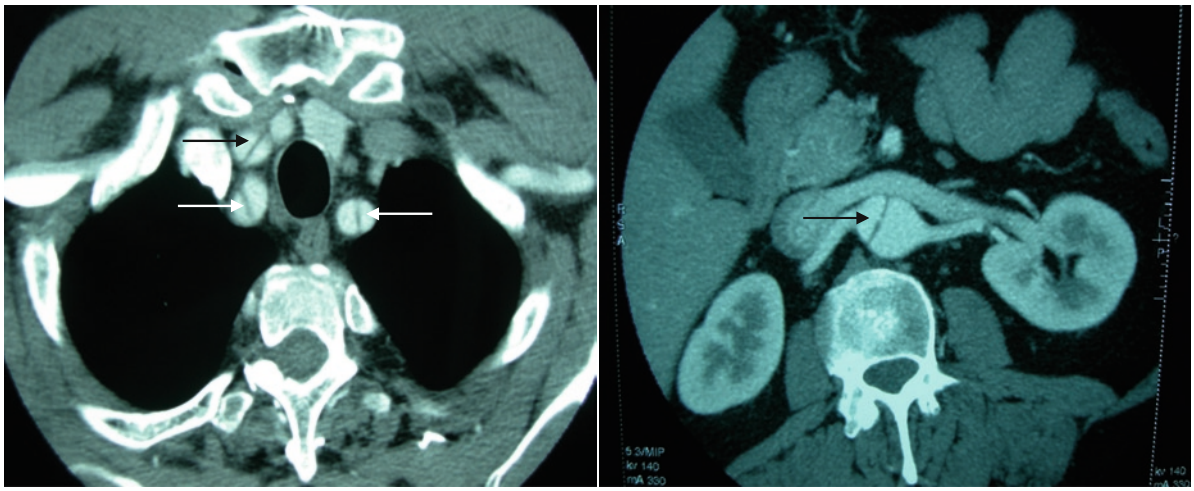

Fig. 20.20 (continued)

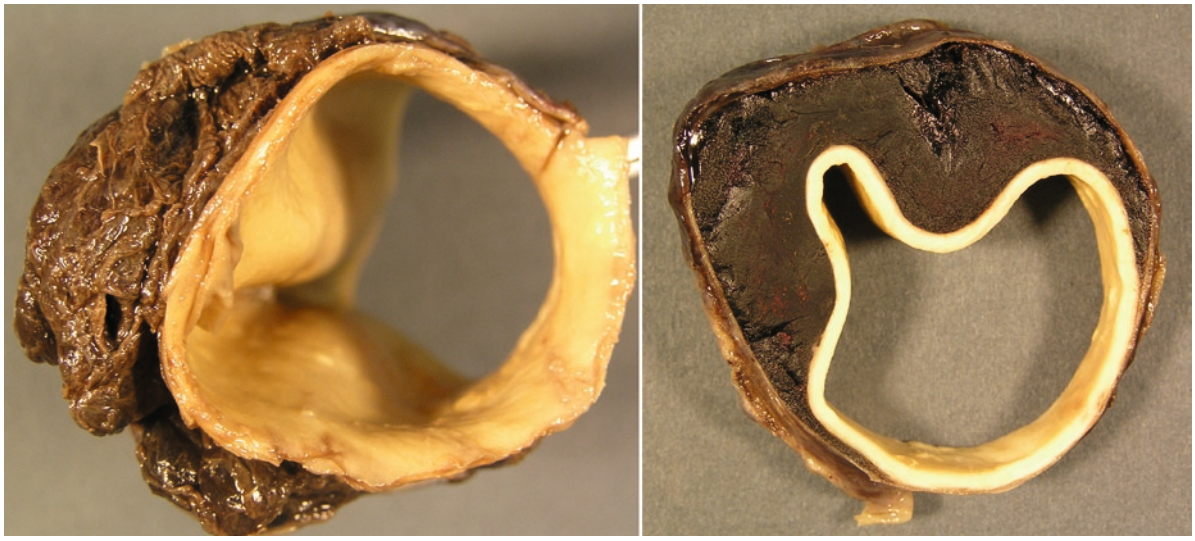

Fig. 20.21 Anatomical specimen of intramural aortic hematoma of the ascending aorta. Note the presence of clotted blood within the aortic wall

formation or "contained aortic rupture" [57, 60], or transmural aortic rupture [64, 65]. PAU may also evolve to aortic dissection [57, 66, 67]. In this case, the entry tear is the ulcerated crater [57]. This specific type-B aortic dissection has distinctive features when compared with classic aortic dissection (Table 20.2).

20.3.4 Incomplete Aortic Dissection

20.3.4.1 Pathology

Incomplete aortic dissection refers to the presence of an intimomedial tear without significant separation of the medial layers [5, 6]. Subadventitial hematoma

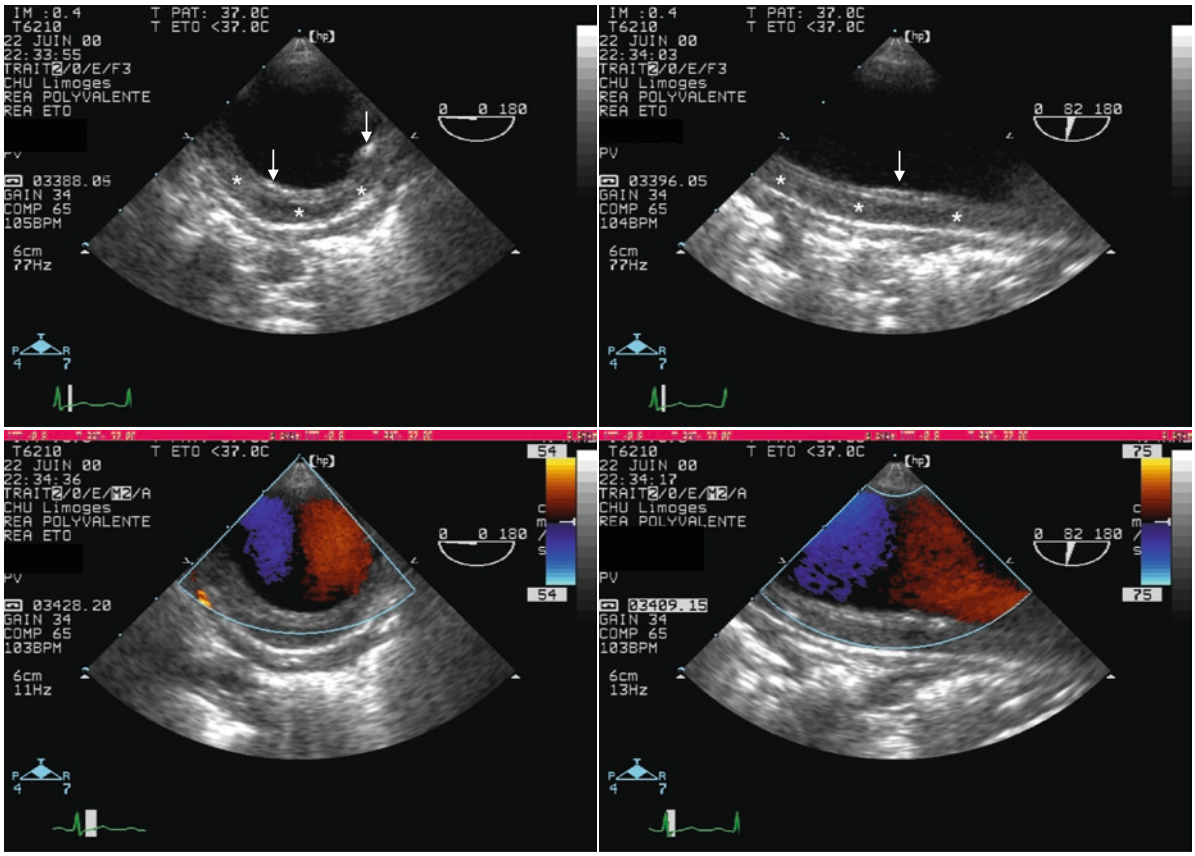

Fig. 20.22 Intramural hematoma of the descending thoracic aorta depicted by multiplane transesophageal echocardiography. In the transverse view (*left panels*), a crescentic echo-dense thickening of the aortic wall is evidenced (*asterisks*) and intimal calcifications are displaced toward the vascular lumen (*arrows*). In the longitudinal view (*right panels*), the hematoma is strictly confined within the aortic wall (*asterisks*) and results in a central displacement of calcified aortic intima (arrows). Noticeably, color Doppler fails to depict any entry tear or blood flow within the aortic wall (*lower panels*)

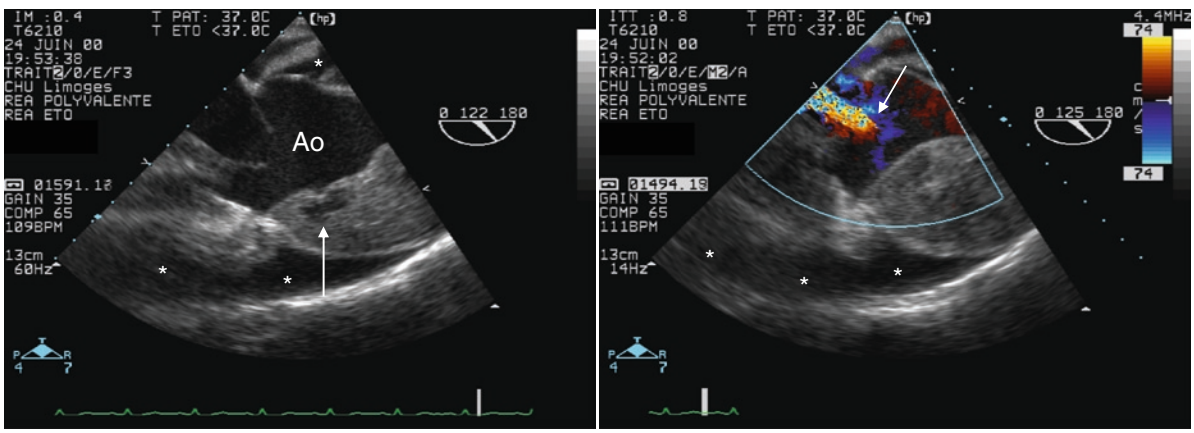

Fig. 20.23 Intramural hematoma of the ascending aorta (Ao) with extravasation signs depicted by multiplane transesophageal echocardiography in a ventilated patient presenting with acute aortic syndrome and shock. In a ~120° transesophageal view of the ascending aorta (*upper panels*), an echo-dense thickening of the aortic wall with echolucent areas (*left, arrow*) is evidenced. Significant aortic regurgitation is depicted by color Doppler mapping (*right, arrow*). Extravasation of blood was present in the pericardial sac (*asterisks*). Prompt surgery revealed the presence of extravasated blood around the distended ascending aorta (*lower left*), and a split aortic wall after evacuation of clotted blood (*lower right, arrow*)

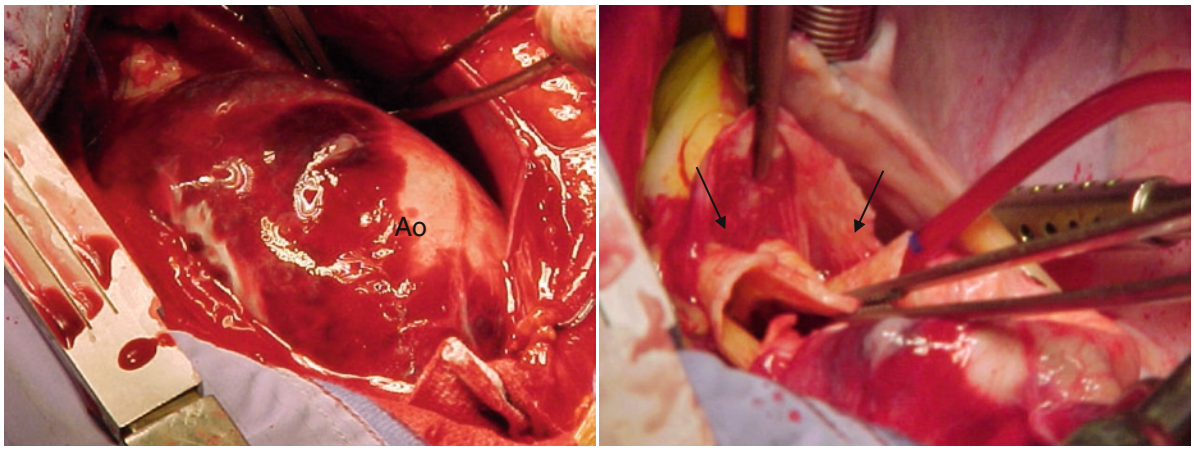

Fig. 20.23 (continued)

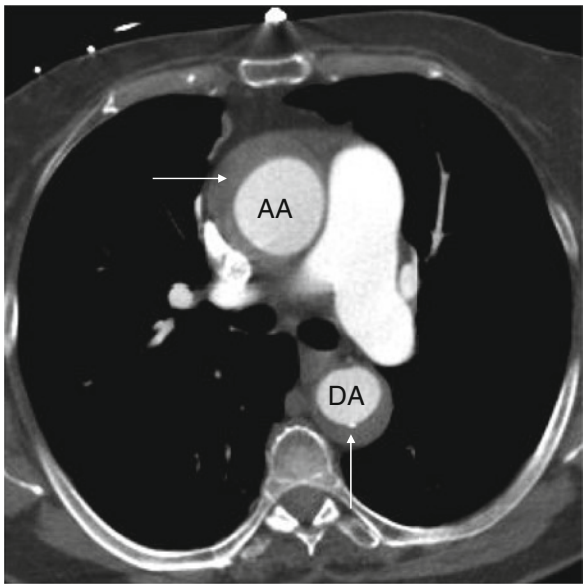

Fig. 20.24 Intramural aortic hematoma depicted by contrast-enhanced multidetector-row computed tomography in the same patient as in Fig. 20.19. Both the ascending (AA) and descending aorta (DA) are involved, as reflected by a crescentic thickening of the aortic wall, which is not enhanced after the contrast injection (*arrows*)

(i.e., collection of blood between the adventitia and media) is frequently present in the acute phase (Fig. 20.30). After the acute phase, the edges of the intimomedial laceration retract, and it is progressively filled by fibrous tissue [5, 68]. Incomplete dissection occurs mostly in the ascending aorta [68, 69]. Tears are usually located on the posterior aspect of the ascending aorta, immediately above the left coronary ostium [69]. This acute aortic lesion may be associated with aortic insufficiency [5, 68].

20.3.4.2 Diagnosis

Diagnosis of incomplete aortic dissection is challenging [6]. Clinical presentation and predisposing factors are similar to any AAS [69]. In contrast to classic (complete) aortic dissection, no flap separating the two aortic channels is evidenced. In addition, the intimomedial laceration is difficult to depict using currently available imaging modalities. In many cases, the ascending aorta is dilated and significant aortic regurgitation is present. The documentation of a subtle eccentric bulge at the tear site is diagnostic [6]. Regardless of the imaging modality used to screen patients with AAS, a meticulous examination has to be performed to detect subtle bulges in the external perimeter of the ascending aorta and minor irregularities in the internal aortic lumen contour.

In patients with incomplete aortic dissection, TEE may depict a stellate or linear discontinuity of the involved aortic wall, small aortic wall fragments oscillating within the aortic lumen, or systolic bulging of the undermined posterior aortic wall [69]. In some patients, TEE may depict an eccentric localized thickening of the aortic wall consistent with a subadventitial hematoma formation [69]. Differential diagnosis between incomplete aortic dissection and IAH may therefore be challenging. Nevertheless, aortic lumen size is usually reduced in the presence of IAH, but not in the case of incomplete dissection (Table 20.3). Blood extravasation signs (echo-free space surrounding the proximal ascending aorta) may also be present [69].

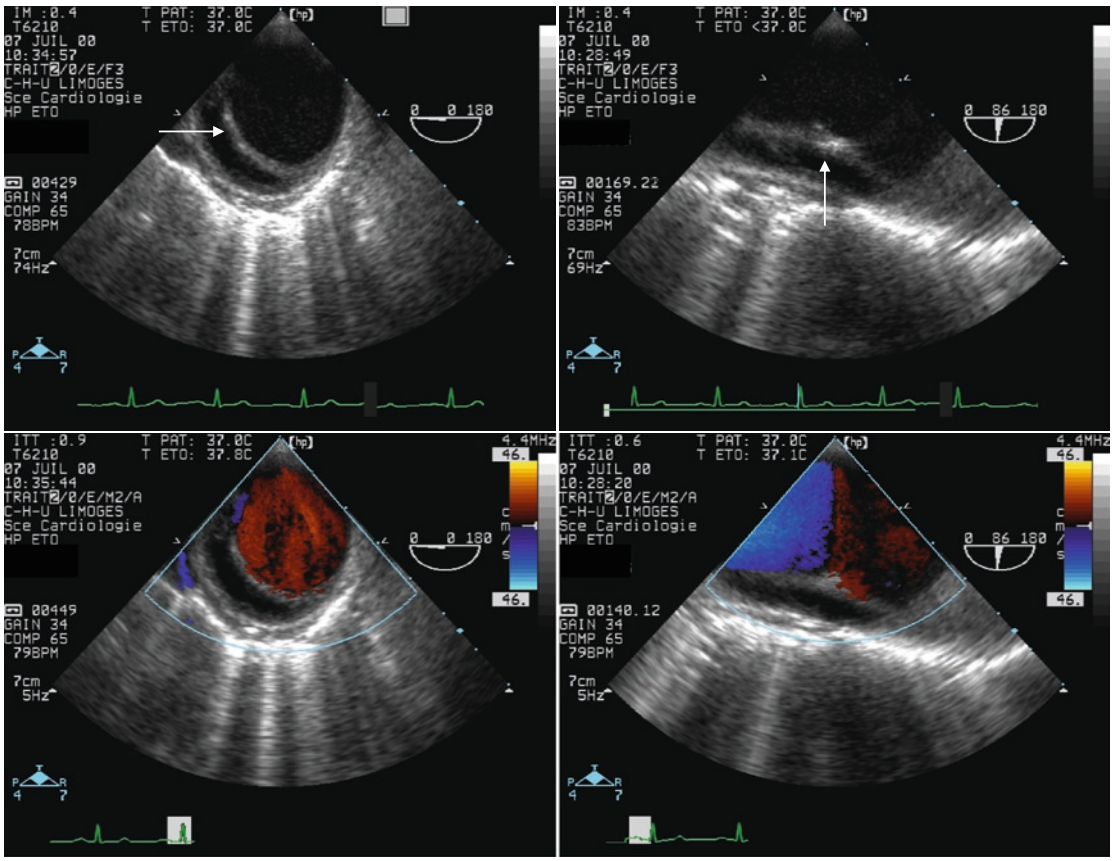

Fig. 20.25 Classic type-B aortic dissection depicted by transesophageal echocardiography in a patient diagnosed with an intramural aortic hematoma medically treated 15 days earlier (see Fig. 20.22). In both the transverse (*left panels*) and longitudinal views (*right panels*), an aortic flap separating two distinct channels is clearly depicted (*arrows*). Color Doppler mapping shows differences in blood-flow velocities between the two aortic channels (*lower panels*)

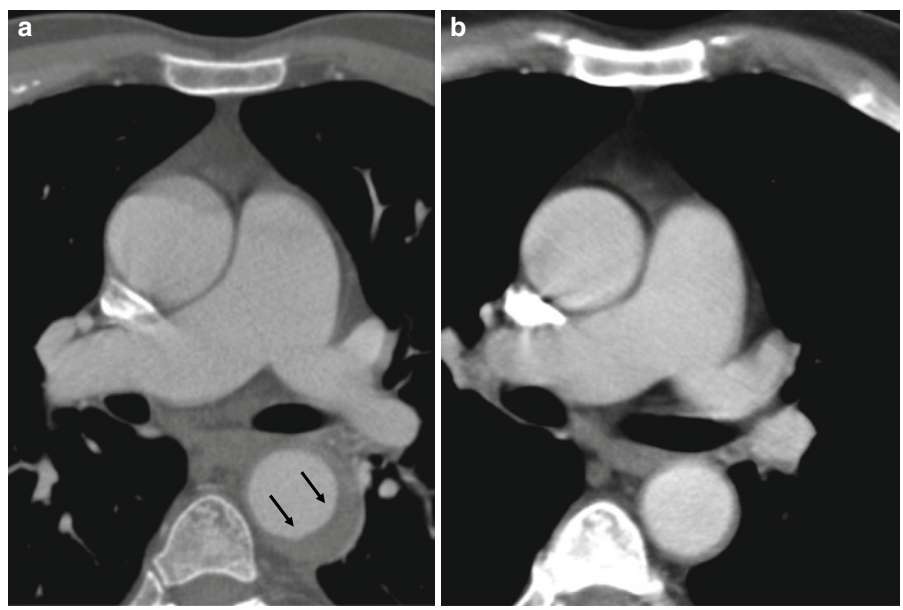

Fig. 20.26 Spontaneous regression of a type-B intramural aortic hematoma documented by serial multidetector-row computed tomographic examinations. On patient admission for acute aortic syndrome, a distal aortic wall hematoma is clearly depicted (*left panel, arrows*). Three months later, the intramural aortic hematoma has totally regressed (*right panel*)

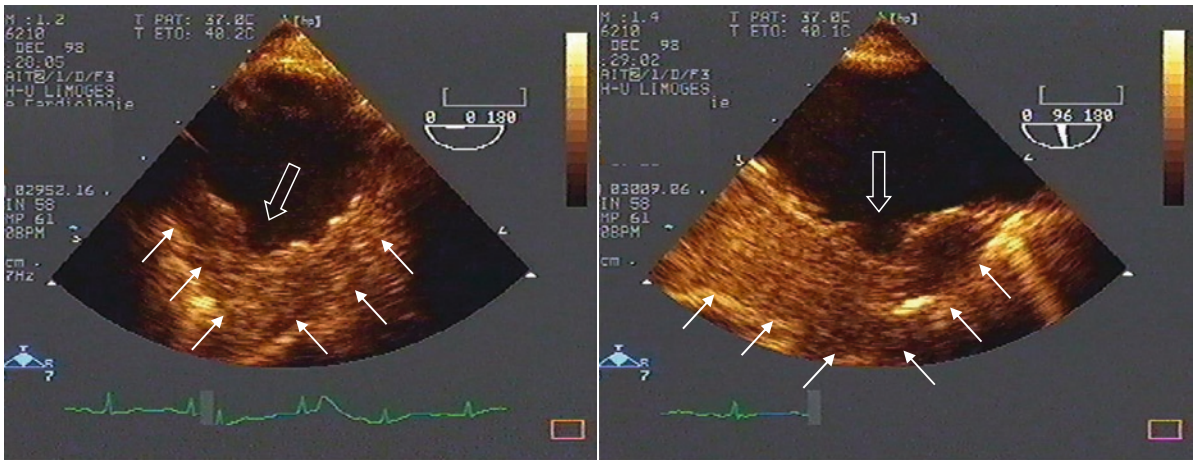

Fig. 20.27 Penetrating atherosclerotic ulcer of the descending aorta documented by transesophageal echocardiography in a patient presenting with acute aortic syndrome. In both the transversal (*left panel*) and longitudinal views (*right panel*), a crater penetrating the aortic media is evidenced (*large open arrows*). Extended hematoma around the penetrating aortic lesion is associated with the atherosclerotic ulcer (*small arrows*)

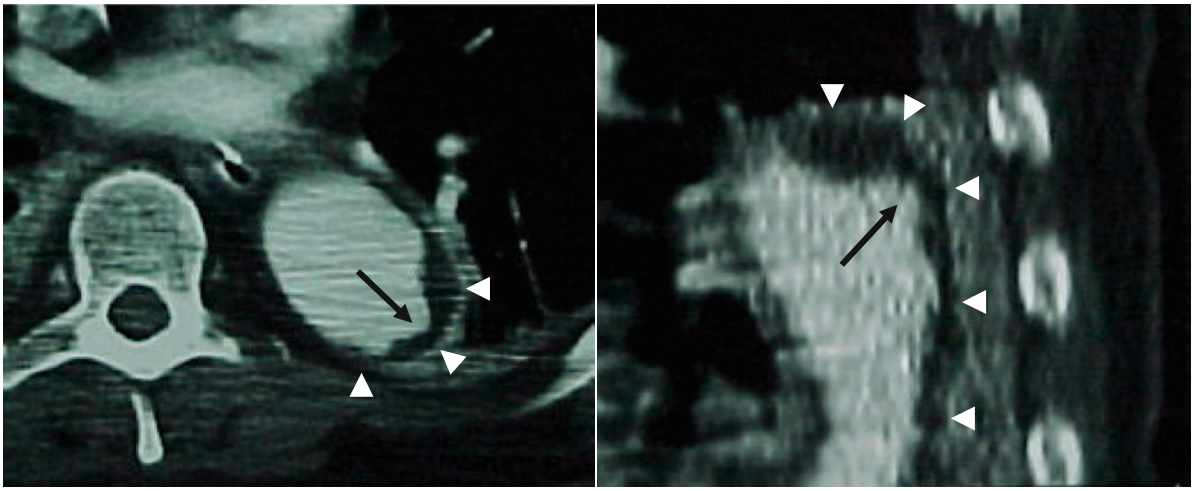

Fig. 20.28 Penetrating atherosclerotic ulcer of the descending aorta documented by contrast-enhanced computed tomography in the same patient as in Fig. 20.27. A clear ulceration of the aortic wall (*arrows*) with associated hematoma (*white arrowheads*) is depicted

20.3.4.3 Evolutive Patterns

Patients who present with incomplete dissection are at high risk of aortic rupture [5, 70], cardiac tamponade [6, 69], and death. Incomplete dissection may also extend and become a classic aortic dissection (Fig. 20.2) [5, 6, 69].

20.4 Management Strategy of Patients with AAS

Early surgery is advocated for patients with proximal (type-A) AAS, including classic (complete) aortic dissection, IAH, PAU, and incomplete aortic dissection [3]. Medical therapy for patients with distal (type-B)

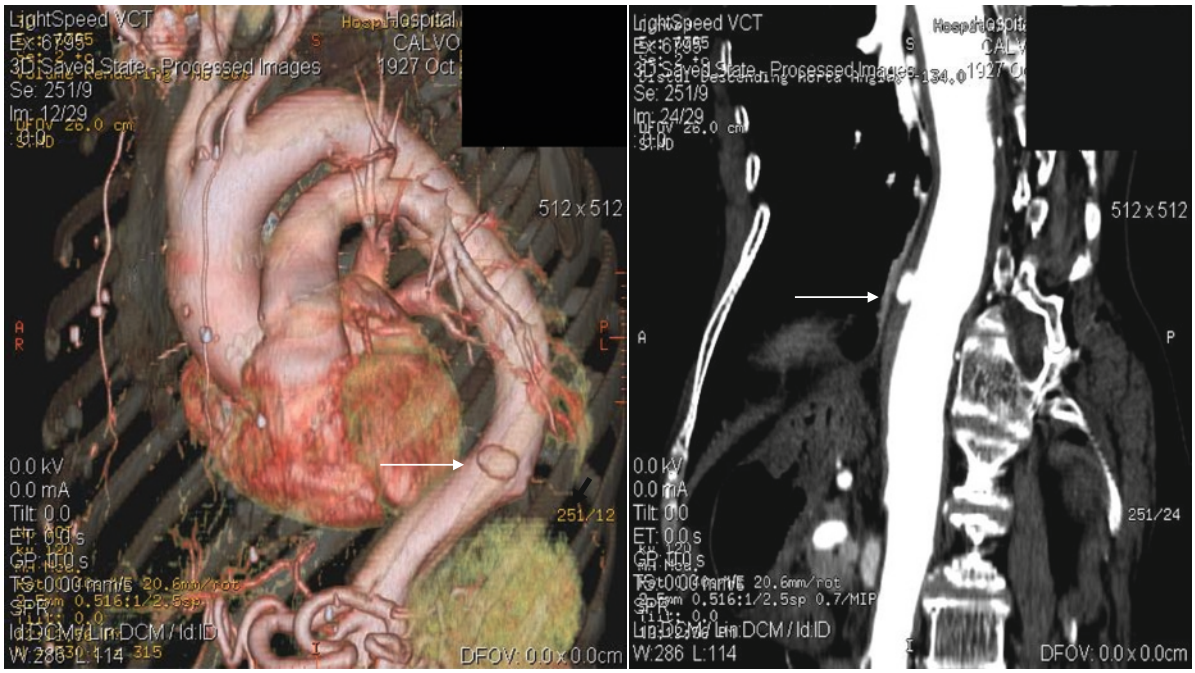

Fig. 20.29 Penetrating atherosclerotic ulcer of the descending thoracic aorta depicted by multidetector-row computed tomography. The ulcer crater is clearly documented after reconstruction (*left panel, arrow*) and contrast-enhancement (*right panel, arrow*)

Table 20.2 Distinctive features of aortic dissections secondary to penetrating atherosclerotic ulcers

Distal (type-B) dissection
Localized dissection (short longitudinal extension)
Entry tear away from typical location
Thick, calcified, and static aortic flap
True lumen equal or larger than the false lumen
Retrograde extension

AAS is currently the widely advocated treatment when the aortic disease is deemed stable based on clinical and imaging criteria. In the presence of unstable or complicated acute aortic disease (e.g., persistent aortic pain, extension of aortic lesions on serial imaging, signs of imminent aortic rupture, end-organ ischemia), surgical or endovascular aortic repair (stenting) is indicated [3].

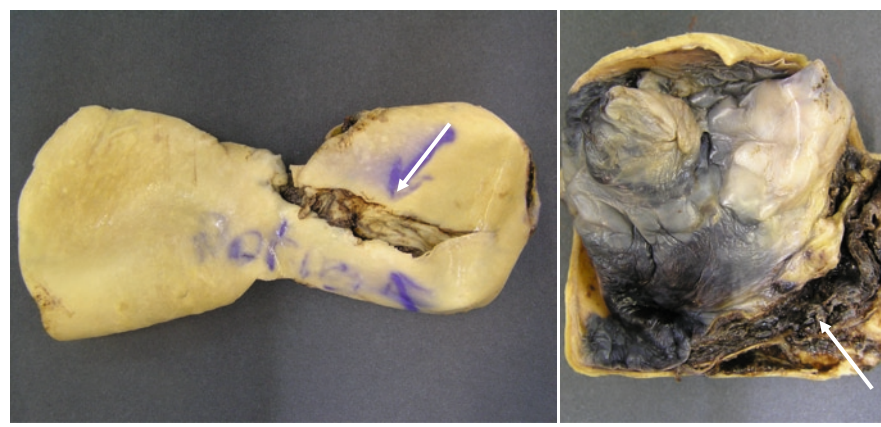

Fig. 20.30 Anatomical specimen of an incomplete aortic dissection. An intimomedial laceration is clearly seen (*left, arrow*). Subadventitial hematoma is also present (*right panel, arrow*)

Table 20.3 Imaging differential diagnosis criteria to distinguish between classic aortic dissection, intramural aortic hematoma, and incomplete dissection

	Classic aortic dissection	Intramural aortic hematoma	Incomplete aortic dissection
Dissection flap	Yes	No	No
Double aortic lumen	Yes	No	No
Entry tear	Yes	No	Yes[a]
Aortic wall thickening	No	Yes	Yes
Decreased aortic lumen	–	Yes	No

[a]An intimomedial tear (stellate or linear discontinuity of the internal aortic layers) or a subtle aortic bulging is frequently identified

20.5 Conclusion

AAS encompasses a broad spectrum of various acute aortic diseases. When AAS involves the ascending aorta, the threat is imminent aortic rupture, leading to blood exsanguination and subsequent death. Accordingly, proximal AAS has to be rapidly treated surgically, whereas distal AAS involving solely the descending thoracic aorta is usually managed conservatively. Signs of blood extravasation (e.g., hemopericardium) accompanying proximal AAS have to prompt surgical repair. Definite diagnosis relying on widely available noninvasive modern imaging modalities is required in any patient with clinically suspected AAS. Improvement of the prognosis of this devastating condition relies on prompt and tailored management.

References

1. Vilacosta I, San Román JA (2001) Acute aortic syndrome. Heart 85:365–368
2. Macura KJ, Corl FM, Fishman EK, Bluemke DA (2003) Pathogenesis in acute aortic syndromes: aortic dissection, intramural hematoma, and penetrating atherosclerotic aortic ulcer. AJR Am J Roentgenol 181:309–316
3. Ahmad F, Cheshire N, Hamady M (2006) Acute aortic syndrome: pathology and therapeutic strategies. Postgrad Med J 82:305–312
4. Khan IA, Nair CK (2002) Clinical, diagnostic, and management perspectives of aortic dissection. Chest 122:311–328
5. Murray CA, Edwards JE (1973) Spontaneous laceration of ascending aorta. Circulation 47:848–859
6. Svensson LG, Labib SB, Eisenhauer AC, Butterly JR (1999) Intimal tear without hematoma. An important variant of aortic dissection that can elude current imaging techniques. Circulation 99:1331–1336
7. Nienaber CA, von Kodolitsch Y, Petersen B, Loose R, Helmchen U, Haverich A, Spielmann RP (1995) Intramural hemorrhage of the thoracic aorta: diagnostic and therapeutic implications. Circulation 92:1465–1472
8. Hirst AE Jr, Johns VJ Jr, Kime SY Jr (1958) Dissecting aneurysm of the aorta: a review of 505 cases. Medicine 37: 217–219
9. Kouchoukos NT, Dougenis D (1997) Surgery of the thoracic aorta. N Engl J Med 336:1876–1888
10. Wooley CF, Sparks EH, Boudoulas H (1998) Aortic pain. Prog Cardiovasc Dis 40:563–589
11. Vilacosta I, San Román JA, Ferreirós J, Aragoncillo P, Méndez R, Castillo JA, Rollán MJ, Batle E, Peral V, Sánchez-Harguindey L (1997) Natural history and serial morphology of aortic intramural hematoma: a novel variant of aortic dissection. Am Heart J 134:495–507
12. Coady MA, Rizzo JA, Hammond GL, Pierce JG, Kopf GS, Elefteriades JA (1998) Penetrating ulcer of the thoracic aorta: what is it? How do we recognize it? How do we manage it? J Vasc Surg 27:1006–1016
13. Svensson LG, Crawford ES, Coselli JS, Safi HJ, Hess KR (1989) Impact of cardiovascular operation on survival in the Marfan patient. Circulation 80(suppl I):I-233–I-242
14. Gott VL, Gillinov AM, Pyeritz RE, Cameron DE, Reitz BA, Greene PS, Stone CD, Ferris RL, Alejo DE, McKusick VA (1995) Aortic root replacement: risk factor analysis of a seventeen-year experience with 270 patients. J Thorac Cardiovasc Surg 109:536–544
15. Von Kodolitsch Y, Schwartz AG, Nienaber CA (2000) Clinical prediction of acute aortic dissection. Arch Intern Med 160:2977–2982
16. Eggebrecht H, Naber CK, Bruch C, Kroger K, Von Birgelen C, Schmermund A, Wichert M, Bartel T, Mann K, Erbel R (2004) Value of plasma fibrin D-dimers for detection of acute aortic dissection. J Am Coll Cardiol 44:804–809
17. Ohlmann P, Faure A, Morel O, Petit H, Kabbaj H, Meyer N, Cheneau E, Jesel L, Epailly E, Desprez D, Grunebaum L, Schneider F, Roul G, Mazzucotteli JP, Eisenmann B, Bareiss P (2006) Diagnostic and prognostic value of circulating D-dimers in patients with acute aortic dissection. Crit Care Med 34:1358–1364
18. Sodeck G, Domanovits H, Schillinger M, Ehrlich MP, Endler G, Herkner H, Laggner A (2007) D-dimer in ruling out acute aortic dissection: a systematic review and prospective cohort study. Eur Heart J 28:3067–3075

19. Nakashima Y, Kurozumi T, Sueishi K, Tanaka K (1990) Dissecting aneurysm: a clinicopathologic and histopathologic study of 111 autopsied cases. Hum Pathol 21:291–296
20. Shirakabe A, Hata N, Yokoyama S, Shinada T, Suzuki Y, Kobayashi N, Kikuchi A, Takano T, Mizuno K (2008) Diagnostic score to differentiate acute aortic dissection in the emergency room. Circ J 72:986–990
21. Von Kodolitsch Y, Nienaber CA, Dieckmann C, Schwartz AG, Hofmann T, Brekenfeld C, Nicolas V, Berger J, Meinertz T (2004) Chest radiography for the diagnosis of acute aortic syndrome. Am J Med 116:73–77
22. Higgins CB (2004) Modern imaging of the acute aortic syndrome. Am J Med 116:134
23. Sommer T, Fehske W, Holzknecht N, Smekal AV, Keller E, Lutterbey G, Kreft B, Kuhl C, Gieseke J, Abu-Ramadan D, Schild H (1996) Aortic dissection: a comparative study of diagnosis with spiral CT, multiplanar transesophageal echocardiography, and MR imaging. Radiology 199: 347–352
24. Hagan PG, Nienaber CA, Isselbacher EM, Bruckman D, Karavite DJ, Russman PL et al (2000) The international registry of acute aortic dissection (IRAD). New insights into an old disease. JAMA 283:897–903
25. Roberts WC (1981) Aortic dissection: anatomy, consequences, and causes. Am Heart J 101:195–214
26. Vilacosta I, Castillo JA, San Román JA, Rollán MJ, Aragoncillo P, Sánchez-Harguindey L (1995) New echoanatomical correlations in aortic dissection. Eur Heart J 16: 126–128
27. DeBakey ME, Henly WS, Cooley DA, Morris GC, Crawford ES, Beall AC (1965) Surgical management of dissecting aneurysms of the aorta. J Thorac Cardiovasc Surg 49: 130–149
28. Daily PO, Trueblood HW, Stinson EB, Wuerflein RD, Shumway NE (1970) Management of acute aortic dissections. Ann Thorac Surg 10:237–247
29. Keren A, Kim CB, Hu BS et al (1996) Accuracy of biplane and multiplane transesophageal echocardiography in diagnosis of typical acute aortic dissection and intramural hematoma. J Am Coll Cardiol 28:627–636
30. Appelbe AF, Walker PG, Yeoh JK, Bonitatibus A, Yoganathan AP, Martin RP (1993) Clinical significance and origin of artifacts in transesophageal echocardiography of the thoracic aorta. J Am Coll Cardiol 21:754–760
31. Vignon P, Spencer KT, Rambaud G, Preux PM, Krauss D, Balasia B, Lang RM (2001) Differential transesophageal echocardiographic diagnosis between linear artifacts and intraluminal flaps of aortic dissection or disruption. Chest 119:1778–1790
32. Evangelista A, Garcia-Del-Castillo H, Gonzalez-Alujas T, Dominguez-Oronoz R, Salas A, Permanyer-Miralda G, Soler-Soler J (1996) Diagnosis of ascending aortic dissection by transesophageal echocardiography: utility of M-mode in recognizing artifacts. J Am Coll Cardiol 27:102–107
33. Movsowitz HD, Levine RA, Hilgenberg AD, Isselbacher EM (2000) Transesophageal echocardiographic description of the mechanisms of aortic regurgitation in acute type A aortic dissection: implication for aortic valve repair. J Am Coll Cardiol 36:884–890
34. Yoshida S, Akiba H, Tamakawa M, Yama N, Hareyama M, Morishita K, Abe T (2003) Thoracic involvement of type A aortic dissection and intramural hematoma: diagnostic accuracy – comparison of emergency helical CT and surgical findings. Radiology 228:430–435
35. Vernhet H, Serfaty JM, Serhal M, McFadden E, Bonnefoy E, Adeleine P, Revel D, Douek P (2004) Abdominal CT angiography before surgery as a predictor of postoperative death in acute aortic dissection. AJR Am J Roentgenol 182:875–879
36. Swaminathan A, Kandaswamy K, Powari M, Mathew J (2007) Dying from cardiac cause. World J Emerg Surg 2:22
37. Mukherjee D, Evangelista A, Nienaber CA, Sechtem U, Suzuki T, Trimarchi S et al (2005) Implications of periaortic hematoma in patients with acute aortic dissection (from the International Registry of Acute Aortic Dissection). Am J Cardiol 96:1734–1738
38. Vilacosta I (2003) Síndrome aórtico agudo. Rev Esp Cardiol 56(supl I):29–39
39. Mohr-Kahaly S, Erbel R, Kearney P, Puth M, Meyer J (1994) Aortic intramural hemorrhage visualized by transesophageal echocardiography: findings and prognostic implications. J Am Coll Cardiol 23:658–664
40. O'Gara PT, DeSanctis RW (1995) Acute aortic dissection and its variants. Toward a common diagnostic and therapeutic approach. Circulation 92:1376–1378
41. Vilacosta I, San Román JA, Peral V, Castillo J, Domínguez L, Batlle E, Rollán MJ, Sánchez-Harguindey L (1995) Imaging aortic intramural hematoma. Identification of two groups of patients. Circulation 92(Suppl I):I307
42. Evangelista A, Dominguez R, Sebastia C, Salas A, Permanyer-Miralda G, Avegliano G, Gómez-Bosch Z, González-Alujas T, García del Castillo H, Soler-Soler J (2004) Prognostic value of clinical and morphologic findings in short-term evolution of aortic intramural haematoma. Eur Heart J 25:81–87
43. Maraj R, Rerkpattanapipat P, Jacobs LE, Makornwattana P, Kotler MN (2000) Meta-analysis of 143 reported cases of aortic intramural hematoma. Am J Cardiol 86:664–668
44. Evangelista A, Mukherjee D, Mehta RH, O'Gara PT, Fattori R, Cooper JV, Smith DE, Oh JK, Hutchison S, Sechtem U, Isselbacher EM, Nienaber CA, Pape LA, Eagle KA (2005) Acute intramural hematoma of the aorta. A mystery in evolution. Circulation 111:1063–1070
45. Gore I (1952) Pathogenesis of dissecting aneurysm of the aorta. Arch Pathol 53:142–153
46. Wilson SK, Hutchins GM (1982) Aortic dissecting aneurysms: causative factors in 204 subjects. Arch Pathol Lab Med 106:175–180
47. Berdat PA, Carret T (1999) Aortic dissection limited to the ascending aorta mimicking intramural hematoma. Eur J Cardiothorac Surg 15:108–109
48. Willens HJ, Kessler KM (1999) Transesophageal echocardiography in the diagnosis of diseases of the thoracic aorta. Part I. Aortic dissection, aortic intramural hematoma, and penetrating atherosclerotic ulcer of the aorta. Chest 166: 1772–1779
49. Vilacosta I, Ferreirós J, Bustos A, San Román JA, Aragoncillo P (2006) Intramural aortic hematoma and aortic ulcers, physiopathology and natural history. In: Rousseau H, Verhoye J-P, Heautot J-F (eds) Thoracic aortic diseases. Springer-Verlag, Berlin, Heidelberg, pp 277–288
50. Vilacosta I, Martín de Dios R, González Pinto A (2000) Aortic intramural hematoma during coronary angioplasty: insights into the pathogenesis of intramedial hemorrhage. J Am Soc Echocardiogr 13:403–406

51. Von Kodolitsch Y, Csösz SK, Koschyk DH, Meinertz T, Nienaber CA (2003) Intramural hematoma of the aorta. Predictors of progression to dissection and rupture. Circulation 107:1158–1163
52. Neri E, Capannini G, Carone E, Diciolla F, Sassic C (1999) Evolution toward dissection of an intramural hematoma of the ascending aorta. Ann Thorac Surg 68:1855–1856
53. Jani S, Liou M, Sibert KA, Stelzer P, Berger M, Hecht SR (2007) Serial images demonstrating proximal extension of an aortic intramural hematoma. Circulation 115:e38–e40
54. Kaji S, Nishigami K, Akasaka T, Hozumi T, Takagi T, Kawamoto T, Okura H, Shono H, Horibata Y, Honda T, Yoshida K (1999) Prediction of progression or regression of type A aortic intramural hematoma by computed tomography. Circulation 100(Suppl II):281–286
55. Moizumi Y, Komatsu T, Motoyoshi N, Tabayashi K (2004) Clinical features and long-term outcome of type A and type B intramural hematoma of the aorta. J Thorac Cardiovasc Surg 127:421–427
56. Sueyoshi E, Imada T, Sakamoto I, Matsuoka Y, Hayashi K (2002) Analysis of predictive factors for progression of type B aortic intramural hematoma with computed tomography. J Vasc Surg 35:1179–1183
57. Vilacosta I, San Román JA, Aragoncillo P, Ferreirós J, Méndez R, Graupner C, Batlle E, Serrano J, Pinto A, Oyonarte JM (1998) Penetrating atherosclerotic aortic ulcer: documentation by transesophageal echocardiography. J Am Coll Cardiol 32:83–89
58. Stanson AW, Kazmier FJ, Hollier LH, Edwards WD, Pairolero PC, Sheedy PF, Joyce JW, Johnson MC (1986) Penetrating atherosclerotic ulcers of the thoracic aorta: natural history and clinicopathologic correlations. Ann Vasc Surg 1: 15–23
59. Yucel EK, Steinberg FL, Egglin TK, Geller SC, Waltman AC, Athanasoulis CA (1990) Penetrating aortic ulcers: diagnosis with MR imaging. Radiology 177:779–781
60. Movsowitz HD, David M, Movsowitz C, Kotler MN, Jacobs LE (1993) Penetrating atherosclerotic aortic ulcers: the role of transesophageal echocardiography in diagnosis and clinical management. Am Heart J 126:745–747
61. Atar S, Nagai T, Birnbaum Y, Harold JG, Luo H, Naqui TZ, Siegel RJ (1999) Transesophageal echocardiographic Doppler findings in patients with penetrating aortic ulcers. Am J Cardiol 83:133–135
62. Chiles C, Carr JJ (2005) Vascular diseases of the thorax: evaluation with multidetector CT. Radiol Clin N Am 43:543–569
63. Harris JA, Bis KG, Glover JL, Bendick PJ, Shetty A, Brown OW (1994) Penetrating atherosclerotic ulcers of the aorta. J Vasc Surg 19:90–99
64. Ando Y, Minami H, Muramoto H, Narita M, Sakai S (1994) Rupture of thoracic aorta caused by penetrating aortic ulcer. Chest 106:624–626
65. Vilacosta I, San Román JA, Aragoncillo P (2001) Atherosclerotic aortic rupture: documentation by transesophageal echocardiography. J Am Soc Echocardiogr 14: 152-–154
66. Tisnado J, Cho SR, Beachley MC, Vines FS (1980) Ulcerlike projections: a precursor angiographic sign to thoracic aortic dissection. AJR Am J Roentgenol 135:719–722
67. Hayashi H, Matsuoka Y, Sakamoto I, Sueyoshi E, Okimoto T, Hayashi K, Matsugana N (2000) Penetrating atherosclerotic ulcer of the aorta: imaging features and disease concept. Radiographics 20:995–1005
68. Vaideeswar P, Dixit V, Butany J, David TE, Feindel C (2008) Surgical Pathology of chronic ascending aortic dissections. Pathology 40:505–512
69. Chirillo F, Salvador L, Bacchion F, Grisolia EF, Valfrè C, Olivari Z (2007) Clinical and anatomical characteristics of subtle-discrete dissection of the ascending aorta. Am J Cardiol 100:1314–1319
70. Comfort SR, Curry RC Jr, Roberts WC (1996) Sudden death while playing tennis due to a tear in the ascending aorta (without dissection) and probable transient compression of the left main coronary artery. Am J Cardiol 78: 493–495

Part VI

Outlook

Learning and Competence in Critical Care Echocardiography

21

Philippe Vignon, Bernard P. Cholley, Daniel De Backer, Michel Slama, and Antoine Vieillard-Baron

Contents

P. Vignon (✉)
Medical-surgical Intensive Care Unit, and
Clinical Investigation Center INSERM 0801,
CHU Dupuytren, 2 Avenue Martin Luther King,
87000, Limoges, France and
Université de Limoges, 2 Ave. Dr. Marcland,
87000, Limoges, France
e-mail: philippe.vignon@unilim.fr

B.P. Cholley
Service d'Anesthésie-Réanimation,
Hôpital Européen Georges Pompidou, 20 rue Leblanc,
75908, Paris cedex 15, France

D. De Backer
Department of Intensive Care, Erasme University Hospital,
Université Libre de Bruxelles, 808 route de Lennik,
B-1070, Brussels, Belgium

M. Slama
Unité de réanimation médicale, service de néphrologie, CHU Sud, 80054, Amiens Cedex 1 and INSERM ERI 12, Faculté de médcine d'Amiens, Universite Jules Verne, France

A. Vieillard-Baron
Intensive Care Unit, University Ambroise Paré Hospital,
Assistance Publique des Hôpitaux de Paris, 9 Avenue Charles de Gaulle, 92104, Boulogne, France and
University Versailles Saint Quentin en Yvelines,
78000, Versailles, France

Echocardiography has gained wide acceptance among the medical community in assessing critically ill patients with circulatory and respiratory compromise. There are several reasons for the rapid diffusion of echocardiography in intensive care unit (ICU) settings: technological advances allowing the miniaturization of systems and improved imaging quality, real-time access to morphological and functional information on the heart and great vessels, minimally invasive assessment of central hemodynamics, and the ability to serially evaluate online both the efficacy and tolerance of therapeutic interventions. The availability of dedicated systems in a growing number of ICUs, time constraints requiring the presence of trained operators around-the-clock, and the accumulated evidence in the literature of the pivotal role of echocardiography in managing ICU patients account for the urgent and growing need for education of the critical care medicine community in this specific field of competence [1, 2]. The current state of this educational process is markedly variable around the world, and for various historical reasons striking differences are noticeable between continents and within European countries [3]. This chapter describes the competence required to perform echocardiography in ICU patients and briefly reviews published studies that evaluate training programs dedicated to intensivists without previous experience in ultrasound.

21.1 What Is Critical Care Echocardiography?

Echocardiography is a powerful imaging modality whose use differs dramatically in cardiology and ICU settings (Table 21.1). Currently, the specific needs of

D. De Backer et al. (eds.), *Hemodynamic Monitoring Using Echocardiography in the Critically Ill*,
DOI: 10.1007/978-3-540-87956-5_21, © Springer-Verlag Berlin Heidelberg 2011

Table 21.1 Specificities of critical care echocardiography when compared to conventional use in cardiology

	Critical care echocardiography	Conventional echocardiography
Clinical setting	Intensive care unit	Cardiology department
Nature of assessment	Focused and functional May be goal-directed[a]	State-of-the-art examination Exhaustive quantitative evaluation
Patient profile	Unstable Frequently ventilated	Stable/stabilized Spontaneously breathing
Condition	Acute/acute-on-chronic	Subacute/chronic
Availability	Around-the-clock	Scheduled assessment
Therapeutic impact	Immediate decision making	Planned therapeutic changes

[a]One straightforward clinical question and one "yes or no" qualitative answer for the basic level in critical care echocardiography

the critical care medicine community are clearly defined and account for the requirement of structured training programs dedicated to intensivists without prior exposure to echocardiography (see Chap. 1). Recently, a roundtable endorsed by the American College of Chest Physicians and the Société de Réanimation de Langue Française defined critical care echocardiography (CCE) as an examination performed and interpreted by the intensivist at the bedside to establish diagnoses and to guide therapy in ICU patients with cardiopulmonary compromise [4]. As with any other diagnostic procedure, intensivists who perform CCE commit themselves to assume the responsibility of image acquisition and interpretation as a guide to patient management. The requirements of CCE, including a specific hemodynamic approach and therapeutic algorithms mostly used in ventilated patients, make the classical "cardiological" diagnostic framework inappropriate. Hence, CCE and conventional cardiological echocardiography demand different teaching programs in accordance with their respective requirements (Table 21.1).

As with other imaging modalities, echocardiography is operator-dependent since both the quality of recorded images and accuracy of their interpretation closely depend on the level of competence of the operator. According to personal needs, the intensivist may invest a variable amount of time in training to reach the desired level of competence [1, 2]. Two distinct levels of competence have recently been defined for intensivists who want to perform CCE on clinical grounds: a basic and an advanced level [4].

Commercially available echocardiographic systems are numerous, with variable technical characteristics and imaging capacities. Importantly, the type of system used has to be in accordance with the level of competence of the operator. Hand-held miniaturized devices frequently have reduced two-dimensional imaging quality and limited Doppler capabilities [5, 6]. They may be adapted to perform basic CCE [7]. In contrast, advanced-level CCE requires a dedicated upper-end platform equipped with a multiplane transesophageal probe [2]. Since such sophisticated equipment has also now been miniaturized, care has to be taken not to confuse new-generation full-feature imaging systems with hand-held devices offering limited capabilities [5].

21.2 Competence Level in CCE

21.2.1 Basic CCE

Basic CCE aims at answering a limited number of specific clinical questions related to the management of ICU patients [4]. It mainly relies on two-dimensional transthoracic echocardiography (TTE) with a qualitative and goal-oriented examination that favors specificity over sensitivity (Table 21.2). Competence in image acquisition includes the parasternal long- and short-axis views, the apical and subcostal four-chamber views, and the inferior vena cava (IVC) view. In basic CCE, competence in image interpretation includes the qualitative assessment of left ventricular (LV) cavity size (small, normal, or severely dilated), LV systolic function (normal, hyperdynamic, mild to moderate dysfunction, or severe dysfunction),

Table 21.2 Main characteristics of basic and advanced levels in critical care echocardiography (CCE)

	Basic level CCE	Advanced level CCE
Addressed clinical questions	Limited	Extended[a]
Nature of the evaluation	Qualitative or semiquantitative Goal-oriented	Quantitative Functional and comprehensive
Field of competence	Limited Call if indeterminate or unexpected findings	Extended Self-sufficient for common indications of CCE[a]
Modality	Transthoracic echocardiography Two-dimensional, color Doppler mapping	Transthoracic and transesophageal echocardiography All modalities including spectral Doppler and tissue Doppler imaging
Diagnostic capacity	Favors specificity over sensitivity	Sensitivity and specificity are required to optimize diagnostic accuracy

[a]In indications other than circulatory or respiratory failure, self-sufficiency of the operator depends on personal medical background, accumulated experience, and level of expertise in echocardiography [1]

homogeneous or inhomogeneous pattern of LV contraction, right ventricular (RV) cavity size (normal or dilated when it exceeds LV size) and function, identification of pericardial fluid (distinguishing pericardial fat, pleural effusion, and ascites) and tamponade physiology (right atrial or RV collapse, dilated and noncollapsible IVC). In addition, the qualitative evaluation of valve function to identify a severe valvular regurgitation using color Doppler mapping is part of basic CCE competence. Overall, competence in basic CCE should be obtained by virtually any intensivist since it allows rapid diagnosis of overt hypovolemia, LV and RV failure, tamponade and acute massive left-sided valvular regurgitation [4]. Importantly, indeterminate results (e.g., doubtful interpretation, unsuspected findings) should lead the intensivist to seek consultation with a more advanced echocardiographer (Table 21.2).

21.2.2 Advanced CCE

Advanced-level CCE allows the intensivist to be self-sufficient in conducting comprehensive, serial hemodynamic assessment of ICU patients in guiding therapeutic management [4]. Competence in image acquisition and interpretation is strongly recommended for both TTE and transesophageal echocardiography (TEE), and all available modalities, including spectral Doppler and tissue Doppler imaging, have to be mastered (Table 21.2). Competence in image acquisition for advanced CCE is similar to that required for cardiologists trained in echocardiography [4]. All TTE and TEE views should be mastered. Competence in image interpretation includes the evaluation of fluid responsiveness (i.e., measurement of dynamic indices), LV ejection performance (i.e., measurement of LV stroke volume, fractional area change, and ejection fraction) and size, identification of LV wall-motion abnormality, assessment of RV size and function (i.e., measurement of RV and LV end-diastolic area ratio, identification of paradoxical septal motion, interpretation of RV outflow Doppler pattern, assessment of systolic pulmonary artery pressure based on tricuspid and pulmonary insufficiency), evaluation of LV filling pressure and LV diastolic function (Doppler indices), assessment of native and prosthetic valve function (recognition and quantification of significant native valve regurgitation and stenosis using color and spectral Doppler), and identification of pericardial effusion with potentially associated hemodynamic burden (identification of pericardial effusion and tamponade physiology using two-dimensional and Doppler imaging). In contrast, certain situations require cardiology consultation, including the assessment of prosthetic valve function, complex congenital heart disease, and the search for a cardiac source of systemic embolism. Importantly, cognitive skills extend beyond image interpretation since the operator has to be trained in critical care medicine, with special reference to the pathophysiology of circulatory and respiratory failure,

in order to integrate the results of CCE functional assessment in the clinical scenario [4].

21.3 Which Curriculum to Reach Competence in CCE?

21.3.1 Basic CCE

The most basic application of echocardiography in the ICU is the goal-directed examination [2]. This focused ultrasonographic examination of the heart and related vasculature is purposely limited to answer specific straightforward clinical questions applicable to the management of ICU patients. It corresponds to basic CCE [4]. Goal-directed echocardiography has been compared to an ultrasonographic extension of physical examination [8, 9]. Its emergence has been facilitated by the recent diffusion of miniaturized hand-held imaging systems in the cardiology community [10]. Only a few training programs dedicated to intensivists with no prior exposure to ultrasound have been established, where the aim is to impart competence in basic CCE. Manasia et al. [11] showed that a formal 10-h training program allowed intensivists to perform successfully a limited TTE in 89 of 90 studied ICU patients and to interpret the examination correctly in 84% of them. Jones et al. [12] reported the efficacy of a 6-h training program (5 h of theory and 1 h of practical) in improving goal-directed TTE performance and interpretation by emergency physicians. Royse et al. [13] organized five supervised examination sessions and five unsupervised practice sessions during a 4-week training program dedicated to third-year medical students with no prior experience in TTE. They recommended a minimum of 20 training studies for novice operators prior to integrating goal-directed TTE in their clinical practice [13]. After a curriculum including 3 h of theory and 5 h of practical, noncardiologist residents adequately appraised LV systolic function ($\kappa = 0.76 \pm 0.09$), LV dilatation ($\kappa = 0.66 \pm 0.12$), RV dilatation ($\kappa = 0.71 \pm 0.12$), and pericardial effusion ($\kappa = 0.68 \pm 0.18$), and pleural effusion ($\kappa = 0.71 \pm 0.09$) in ICU patients [7]. Using a modified curriculum (Table 21.3), the same authors showed that focused training blending theory, practical sessions, and interactive cases was efficient for noncardiologist residents to achieve competence in basic CCE [14]. Noticeably, the trainees adequately answered the clinical questions covered by the basic CCE level with the performance of a mean of 33 TTE during the study period (range, 29–38). Finally, Melamed et al. [15] showed that 2 h of theory and 4 h of practical training in image acquisition and visual estimation of LV function allowed intensivists without previous experience in ultrasound to qualitatively estimate LV function in ICU patients with reasonable accuracy.

Altogether this data clearly shows that basic CCE can be rapidly learned with a curriculum blending theory, clinical cases, and practical training. A recent international roundtable recommended that the training program to reach competence in basic CCE include 10 h of lectures and illustrative case studies, and the performance of 30 fully supervised TTEs [16].

21.3.2 Advanced CCE

Advanced CCE requires mastery of image acquisition and interpretation in all TTE and TEE views, including full Doppler examination, to perform a comprehensive hemodynamic assessment and monitoring in unstable ICU patients [4]. Intensivists who want to attain competence in advanced CCE need an extensive training to become self-sufficient in assessing and monitoring any ICU patient with a circulatory or respiratory compromise [3]. As they accumulate experience, intensivists may extend their advanced CCE competence to other indications of TEE [17], such as assessing patients with severe blunt chest trauma [18], suspected endocarditis or intracardiac shunt [19], and circulatory assistance [20]. A scoring system has been validated to serially assess the learning curve in developing the skills for image acquisition and interpretation using TEE for hemodynamic monitoring [21]. Regardless of the indication, having an accurate grasp of where exactly one stands on the learning curve significantly improves the diagnostic accuracy [22]. Having extended practice of echocardiography in ICU patients and acquiring experience allows a fully trained intensivist to attain expertise in CCE [1]. This intensivist will in turn be able to supervise the training of other intensivists who want to gain competence for advanced CCE (Fig. 21.1).

Table 21.3 Proposed curriculum for basic critical care transthoracic echocardiography[a]

Curriculum for noncardiological intensivists
Theory (4 h)
Ultrasound basics and image optimization, artifacts
Overview on use of echocardiography in ICU settings (indications, contraindications, advantages, limitations)
Standard transthoracic views of the heart: parasternal long- and short-axis views, apical four-chamber view, subcostal four-chamber view, and IVC view
Cardiac anatomy: chambers, valves, pericardium, great vessels, normal variants
Normal color Doppler mapping
Abnormal echocardiographic patterns:
LV global systolic function: normal or increased (hyperdynamic), depressed, or severely depressed
Identification of LV regional wall-motion abnormalities as a heterogeneous pattern of systolic LV wall thickening (precise identification of segmental distribution not required)
LV cavity size: normal, enlarged, or reduced (near obliteration at end systole)
RV size: normal or dilated; paradoxical septal motion (best identified in parasternal short-axis view) consistent with cor pulmonale when associated with a dilated RV
IVC size: small, normal, or dilated vessel; respiratory variations in IVC size (in spontaneously breathing patients): collapsible or noncollapsible vessel
Identification of pericardial fluid and differential diagnoses (fat pad, left pleural effusion, ascites)
Identification of tamponade: pericardial effusion, collapsed (right) cardiac cavities and dilated, noncollapsible IVC
Identification of acute massive left-sided valvular regurgitation using color Doppler mapping (massive regurgitant flow with normal sized hyperdynamic LV)
Interactive clinical cases (2 h)
At least two illustrations of all clinical syndromes covered by basic CCE [4]
Tutored hands-on (6 h)
Hand-held device: operating information and machine settings
Examination of normal volunteers: probe positioning and orientation, normal views, identification of normal anatomical structures and landmarks, normal intracardiac blood flow as assessed by color Doppler mapping
Examination of 10–12 ventilated ICU patients with circulatory or respiratory failure and an abnormal echocardiographic study

Abbreviations: *ICU* intensive care unit, *CCE* critical care echocardiography, *LV* left ventricle, *RV* right ventricle, *IVC* inferior vena cava

[a]Adapted from Vignon et al. [7] with permission

In the absence of official curricular recommendations with regard to competence in advanced CCE, training programs undoubtedly vary widely around the world. An additional crucial issue is the availability of training centers able to provide efficiently a favorable environment for the performance of the required number of tutored TTE and TEE studies. To be accredited as a training center in France, an ICU needs to fulfill the following requirements: (1) dedicated full-feature, high-quality imaging system, available around-the-clock and equipped with a multiplane TEE probe; (2) at least one certified intensivist or anesthesiologist (national diploma) in the medical staff; (3) recognized experience in the routine use of echocardiography in daily care [3]. In certain countries, a national diploma dedicated to intensivists is not yet available. In these instances, intensivists may be integrated in existing structured national training programs driven by cardiologists, with the close collaboration of their institutional cardiology community.

A recent international roundtable recommended that the intensivist who wants to achieve competence

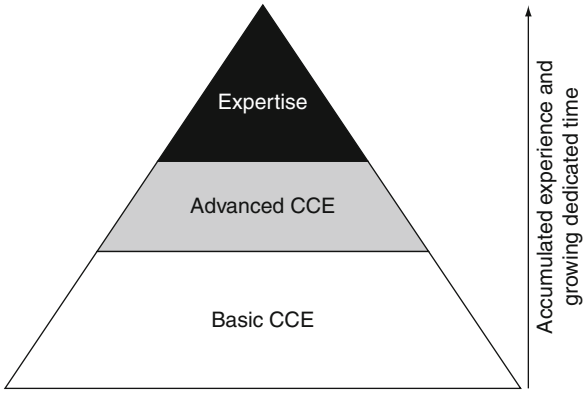

Fig. 21.1 Levels of competence in critical care echocardiography (CCE). With accumulated experience, intensivists with competence in advanced critical care echocardiography may reach expertise and supervise physicians in training. Modified from Cholley et al. [1] with permission

in advanced CCE be already trained in basic CCE [16]. The training program to attain competence in advanced CCE should include a minimum of 40 h of theory with image-based training (lectures and case studies) and the performance of 100 fully supervised TTE and 50 TEE examinations over a maximal 2-year period. Finally, an official recognition of competence (e.g., certification, accreditation, diploma) should be obtained by trained intensivists to allow a clear identification of their specific competence by the medical community and by hospital administration [16].

21.4 Conclusion

Intensivists should achieve competence in basic CCE, since this approach based on a goal-directed TTE examination allows the answering of straightforward clinical questions and improves the diagnostic accuracy of physical examination. Intensivists desiring to reach competence in advanced CCE must dedicate time to follow an extensive training program aimed at acquiring technical and cognitive skills for mastering all aspects of TTE and TEE in the ICU settings. Competence in advanced CCE needs to be officially recognized. As they accumulate experience, intensivists competent in advanced CCE will acquire expertise and may acts as tutors for other physicians in training. To provide an adequate solution to the tremendous need for training in CCE, each country has to establish structured educational programs based on existing international standards.

References

1. Cholley BP, Vieillard-Baron A, Mebazaa A (2005) Echocardiography in the ICU: time for widespread use! Intensive Care Med 32:9–10
2. Poelaert J, Mayo P (2007) Education and evaluation of knowledge and skills in echocardiography: how should we organize? Intensive Care Med 33:1684–1686
3. Vieillard-Baron A, Slama M, Cholley BP, Janvier G, Vignon P (2008) Echocardiography in the intensive care unit: from evolution to revolution? Intensive Care Med 34:243–249
4. Mayo PH, Beaulieu Y, Doelken P, Feller-Kopman D, Harrod C, Kaplan A, Oropello J, Vieillard-Baron A, Axler O, Lichtenstein D, Maury E, Slama M, Vignon Philippe (2009) American College of Chest Physicians/La Société de Réanimation de Langue Française statement on competence in critical care echocardiography. Chest 135:1050–1060
5. Mondillo S, Giannotti G, Innelli P, Ballo PC, Galderisi M (2006) Hand-held echocardiography: which usefulness? Who user? Int J Cardiol 111:1–5
6. Vignon P, Frank MBJ, Lesage J, Mücke F, François B, Normand S et al (2004) Hand-held echocardiography with Doppler capability for the assessment of critically-ill patients: is it reliable? Intensive Care Med 30:718–723
7. Vignon P, Dugard A, Abraham J, Belcour D, Gondran G, Pépino F, Marin B, François B, Gastinne H (2007) Focused training for goal-oriented hand-held echocardiography performed by noncardiologist residents in the intensive care unit. Intensive Care Med 33:1795–1799
8. Popp RL (1998) Perspective – the physical examination of the future: echocardiography as part of the assessment. ACC Curr J Rev 7:79–81
9. Schiller NB (2001) Hand-held echocardiography: revolution or hassle? J Am Coll Cardiol 37:2023–2024
10. Kobal SL, Atar S, Siegel RJ (2004) Hand-carried ultrasound improves the bedside cardiovascular examination. Chest 126:693–701
11. Manasia AR, Nagaraj HM, Kodali RB, Croft LB, Oropello JM, Kohli-Seth R, Leibowitz AB, DelGiudice R, Hufanda JF, Benjamin E, Goldman ME (2005) Feasibility and potential utility of goal-directed transthoracic echocardiography performed by noncardiologist intensivists using a small hand-carried device (SonoHeart) in critically ill patients. J Cardiothorac Vasc Anesth 19:155–159
12. Jones AE, Tayal VS, Kline JA (2003) Focused training of emergency medicine residents in goal-directed echocardiography: a prospective study. Acad Emerg Med 10:1054–1058
13. Royse CF, Seah JL, Donelan L, Royse AG (2006) Point of care ultrasound for basic haemodynamic assessment: novice compared with an expert operator. Anaesthesia 61:849–855

14. Vignon P, Mücke F, Bellec F, Marin B, Croce J, Brouqui T, Palobart C, Senges P, Truffy C, Wachmann A, Dugard A, Amiel JB. Basic critical care echocardiography: validation of a curriculum dedicated to noncardiologist residents. Crit Care Med (in press)
15. Melamed R, Sprenkle MD, Ulstad VK, Herzog CA, Leatherman JW (2009) Assessment of left ventricular function by intensivists using hand-held echocardiography. Chest 135:1416–1420
16. International Consensus Statement on training standards for critical care echocardiography. Vienna, 9–10 October 2009. Submitted to Intensive Care Med
17. Price S, Nicol E, Gibson DG, Evans TW (2006) Echocardiography in the critically ill: current and potential roles. Intensive Care Med 32:48–59
18. Vignon P, Guéret P, Vedrinne JM, Lagrange P, Cornu E, Abrieu O, Gastinne H, Lang RM (1995) Role of transesophageal echocardiography in the diagnosis and management of traumatic aortic disruption. Circulation 92:2959–2968
19. Slama M, Novara A, Van De Putte P, Diebold B, Safavian A, Safar M, Ossart M, Fagon JY (1996) Diagnostic and therapeutic implications of transeosphageal echocardiography in medical ICU patients with unexplained shock, hypoxemia, or suspected endocarditis. Intensive Care Med 22: 916–922
20. Catena E, Paino R, Milazzo F, Colombo T, Marianeschi S, Lanfranconi M, Aresta F, Bruschi G, Russo C, Vitali E (2009) Mechanical circulatory support for patients with fulminant myocarditis: the role of echocardiography to address diagnosis, choice of device, management, and recovery. J Cardiothorac Vasc Anesth 23:87–94
21. Charron C, Prat G, Caille V, Belliard G, Lefèvre M, Aegerter P, Boles JM, Jardin F, Vieillard-Baron A (2007) Validation of a skills assessment scoring system for transesophageal echocardiographic monitoring of hemodynamics. Intensive Care Med 33:1712–1718
22. Vignon P, Rambaud G, Cornu E, François B, Gastinne H (1998) Evaluation des traumatismes thoraciques fermés graves par échocardiographie transœsophagienne: expérience à propos de 150 patients. Ann Fr Anesth Réanim 17:1206–1216

Echocardiography Alone or Coupled with Other Hemodynamic Devices?

22

Gorazd Voga, Daniel De Backer, and Antoine Vieillard-Baron

Contents

22.1 Introduction

In this book, we have amply illustrated the ability of echocardiography, either via transthoracic or transesophageal approaches, to diagnose the different categories of circulatory failure and for proper adjustment of various therapeutic options (volume loading, vasoactive treatment, inotropic support, optimal ventilatory support). However, after initial treatment or even after initial reevaluation of its effects, the hemodynamic situation can evolve and repeated assessment of the hemodynamic condition may be warranted. Echocardiography can be used alone or combined with other hemodynamic devices for this purpose. The goal of this chapter is not to discuss the intrinsic value or reliability of each of these devices, but rather to outline the factors that influence the choice of hemodynamic monitoring device to be used.

Arterial blood pressure is measured invasively in the majority of critically ill patients. An international consensus conference on shock management has recently presented continuous invasive arterial blood pressure recording as mandatory [1]. In 2005, Varpula et al. reported that mean arterial pressure (MAP), especially when it falls below 60 mmHg, is strongly associated with prognosis in patients with septic shock [2]. MAP is thus undoubtedly one of the most important hemodynamic variables, but it gives only limited information on flow and no information on the adequacy of flow with regard to metabolic needs of the tissues. Therefore, using arterial pressure as the only monitored variable can be misleading, and it does not allow proper treatment decisions to be made. Beside blood pressure, we have to estimate preload dependency and measure flow and flow adequacy. Preload assessment is of the utmost importance in critically ill patients as it is usually the first therapeutic option in patients with

G. Voga (✉)
Medical Intensive Care Unit, General Hospital Celje,
Oblakova 5, 3000, Celje, Slovenia
e-mail: gorazd.voga@guest.arnes.si

D. De Backer
Department of Intensive Care, Erasme University Hospital,
Université Libre de Bruxelles, 808 route de Lennik,
B-1070, Brussels, Belgium

A. Vieillard-Baron
Intensive Care Unit, University hospital Ambroise Paré,
Assistance Publique Hôpitaux de Paris,
9 Avenue Charles de Gaulle, 92104,
Boulogne Cedex, France

D. De Backer et al. (eds.), *Hemodynamic Monitoring Using Echocardiography in the Critically Ill*,
DOI: 10.1007/978-3-540-87956-5_22, © Springer-Verlag Berlin Heidelberg 2011

hemodynamic instability. Measurement of flow (cardiac output) is necessary, but it cannot be interpreted without knowledge of its adequacy, which should be assessed in all critically ill patients. Importantly, changes in volume, vasopressor and inotropic drugs, ventilatory support, or other treatment modalities affect preload, preload responsiveness, contractility, and flow and its adequacy. Repeated measurements thus need to be obtained. Finally, the situation may rapidly evolve, and so the time response has to be addressed.

22.2 Methods for Hemodynamic Assessment

Assessments of hemodynamic status based on physical examination and chest roentgenogram alone are frequently inadequate [3]. Experienced physicians achieve the same accuracy in clinical predicting hemodynamic parameters as their less experienced colleagues, although they are significantly more confident [4]. Accordingly, specific monitoring devices are required for accurate hemodynamic assessment.

22.2.1 Merits of Echocardiography

Cardiac function and the circulatory status can be assessed using various noninvasive and invasive methods. The value of every method should be assessed according to its ability and reliability in measuring preload, flow, and flow adequacy. The method also has to be evaluated according to its ability to provide relevant data that can be easily and accurately interpreted by all intensivists. The problem of applicability of these methods in the intensive care unit (ICU) still exists, and the clinician has to be able to select the most appropriate method for a given patient and the specific disease; the method is, of course, also dependent on the skills of the physician. In this selection process, consideration has to be given to the risk/benefit ratio of the technique, its invasiveness, specific diagnosis of the patient, time response of the devices, and the characteristics of the physicians and the ICU. A combination of complementary methods, rather than a single method, should be used in the majority of patients to obtain optimal results. It must be stressed that in critically ill and unstable patients, frequent reassessment has to be performed because of rapid changes in the patient's condition. However, in practice, even though some intensivists always use continuous monitoring tools, hemodynamic monitoring is actually discontinuous in most situations. This is why we believe that, despite the fact it is noncontinuous, echocardiography is a true hemodynamic monitoring tool, provided it is available on a 24-h basis and is performed by the intensivist. According to a European Society of Intensive Care Medicine (ESICM) survey in 2002, permanent access to echocardiography was possible in only 66% of European ICUs and only 20% of ICU staff physicians were properly trained in echocardiography [5]. Despite the relatively rapid increase in the use of echocardiography, the problem of continuous echocardiography availability and possession of proper skills by ICU physicians still exists. The image acquisition usually takes less than 5 min. However, machine displacement and initialization also take time, so a total of 15–20 min can be considered reasonable. Depending on unit staffing, organization, and case mix, this can be afforded or not. In some units, the number of echocardiographic devices or investigators may be insufficient to allow monitoring with echocardiography alone. Under such circumstances, it is advisable to add other techniques. Whatever the technique employed, we consider echocardiography one of the key elements of hemodynamic monitoring and believe that the examination should be repeated if there is deterioration in the clinical condition or an alternative technique indicates a problem not compatible with the initial diagnostic.

Transthoracic echocardiography is the most suitable bedside method. It is noninvasive, can be repeated frequently, and enables a direct, real-time computation of pressures and variables of cardiac contractility (global and regional). However, it has limitations regarding inadequate visualization in some patients, especially the most severe cases with chest edema or patients undergoing ventilation with high positive end-expiratory pressure (PEEP) level. This leads to difficulties in correctly interpreting modifications in cardiac function over time, especially if the examination is performed by different operators or if respiratory condition. Some measurements are more prone to interobserver variability, such as evaluation of mitral flow index, aortic velocity–time integral, and right ventricular size.

For these reasons, transesophageal echocardiography (TEE) is of particular interest in the most severe patients. Most of the time, this provides optimal visualization. Different views are reproducible irrespective of the respiratory condition and operator. TEE can be successfully used as a means of short-term intraoperative continuous monitoring in patients with cardiac or noncardiac surgery during hemodynamic instability [6–8]. However, repeated interventions may be more difficult in the ICU. First, it requires that the patient be still sedated. If this is not a major issue for patients in acute circulatory failure, it may limit the evaluation of patients during weaning procedures [9]. Second, even though the risks of TEE are quite limited, prolonged or repeated insertion of the probe and repeated manipulations may increase the risk of esophageal lesions.

22.2.2 Alternative Hemodynamic Assessments

The alternative hemodynamic measurements include cardiac output from various techniques, venous O_2 saturation, pulmonary artery pressure, and extravascular lung water.

Cardiac output, in particular, can be measured by right-side thermodilution (pulmonary artery catheter; PAC) and arterial blood waveform, calibrated with transpulmonary thermodilution (PiCCO system) or lithium (LiDCO) or even uncalibrated (FloTrac or PRAM). Other noninvasive measurements of cardiac output have been proposed. The intrinsic value of each of these devices will not be discussed here. All the above techniques generally offer a good means of tracking changes in cardiac output, either spontaneously or in the context of a particular therapy. Even though medical skills are mandatory for catheter insertion, most can be nurse driven, and so these monitoring devices can be easily implemented. When abnormal values are detected (values outside predefined goals since a normal value of cardiac output cannot be defined), a more complete hemodynamic assessment should be performed.

Interestingly, stroke volume variation has been reported with techniques determining cardiac output from an arterial pressure trace, and pulse pressure variation can be intermittently measured from an arterial pressure tracing. These represent simple and useful variables that can be used to predict fluid responsiveness in mechanically ventilated patients with preserved sinus rhythm [10–12]. They could be important variables to follow, especially with therapeutic interventions that may affect preload or preload responsiveness.

The adequacy of flow and global tissue perfusion can be continuously assessed only by invasive methods, measuring mixed venous oxygen saturation (SvO_2) with PAC. When other techniques are employed, one may consider using superior vena cava oxygen saturation ($ScvO_2$), which can be measured either by intermittent sampling though a regular central venous catheter or continuously with a specific catheter. Admittedly, the measurements produced are not identical, and some divergences can be observed [13–15], but they are physiologically related, and $ScvO_2$ follows SvO_2 in many instances [16]. It seems reasonable to consider that markedly altered $ScvO_2$ values point to evident inadequacy of tissue perfusion, while normal or close to normal values cannot rule out inadequate perfusion. Some alternatives have been proposed. For instance, base deficit or lactate measurements can be used as potential markers of tissue hypoxia [1, 17], even though these have well-known limitations. Lactate clearance is an excellent marker of the adequacy of resuscitation, which is associated with outcome [18]. The main limitation of this variable is that low lactate clearance may be related to ongoing circulatory failure as well as other factors, such as impaired liver function or aerobic production of lactate under the influence of beta-adrenergic agents. Some teams have proposed adapting therapies in septic shock by combining serial dosages of base deficit and echocardiography [19].

Measurement of pulmonary artery pressure can be obtained only with PAC. This measurement may be useful when it is considered essential to manipulate pulmonary hypertension. Although uncommon, this covers some perioperative complications (like pulmonary artery thromboendarterectomy and pulmonary hypertension complicating cardiac surgery or transplantation) and some specific medical conditions (primary pulmonary hypertension, severe secondary pulmonary hypertension) in which fine-tuning of therapy based on measurements of pulmonary artery pressure can be proposed.

Recent studies have highlighted the role of echocardiography in identifying cardiac dysfunction as a cause of failure in weaning from mechanical ventilation [9, 20]. Indeed, it is not uncommon for signs

of cardiogenic pulmonary edema to develop during weaning from mechanical ventilation as a result of a combined increase in preload and afterload after removal of respiratory positive pressure. As suggested by an accompanying editorial [21], it seems reasonable to propose PAC monitoring for further weaning attempts once a cardiac cause has been identified.

22.3 Choice of Most Appropriate Method

After consideration of the points in the previous sections, it is clear that the use of echocardiography is essential in the hemodynamic assessment of critically ill patients and should be employed immediately after the basic clinical examination. Echocardiography enables rapid diagnosis of the underlying cardiac disorders and allows a reliable, though intermittent, hemodynamic appraisal. The need to assess flow adequacy and, in some cases, measure other variables may prompt the combined use of other hemodynamic techniques. In most cases, specific logistic aspects related to the patient, physician, and/or ICU may also indicate the use of combined hemodynamic monitoring.

The most important problem of echocardiography is the permanent availability of echocardiography in the ICU.

22.4 Conclusions

Echocardiography is an essential, irreplaceable method for hemodynamic assessment and reliable diagnosis of cardiac abnormalities in the critically ill. It is complementary to basic clinical examination and routine ICU procedures. In some conditions specific to the patient, organization of the ICU and skills and/or activities of the physician, it may be useful to combine echocardiography with other hemodynamic devices. The choice of the alternate hemodynamic device should be guided by the variables considered essential to monitor as well as by a risk/benefit evaluation. In all cases, whatever the tools, echocardiography has to be completely mastered by intensivists and integrated into a clear therapeutic management.

References

1. Antonelli M, Levy M, Andrews PJ, et al. Hemodynamic monitoring in shock and implications for management. International Consensus Conference, Paris, France, 27–28 Apr 2006. Intensive Care Med 2007
2. Varpula M, Tallgren M, Saukkonen K et al (2005) Hemodynamic variables related to outcome in septic shock. Intensive Care Med 31:1066–1071
3. Connors AF, McCaffree DR, Gray BA (1983) Evaluation of right-heart catheterization in the critically ill patient without acute myocardial infarction. N Engl J Med 308:263–267
4. Dawson NV, Connors AF, Speroff T et al (1993) Hemodynamic assessment in managing the critically ill: is physician confidence warranted? Med Decis Making 13: 258–266
5. Voga G, Bennett D, Matamis D et al (2002) The use of echocardiography in European intensive care units (ICU's). Intensive Care Med 28:S18
6. Guarracino F, Baldassarri R (2009) Transesophageal echocardiography in the OR and ICU. Minerva Anestesiol 75:518–529
7. Salem R, Vallee F, Rusca M et al (2008) Hemodynamic monitoring by echocardiography in the ICU: the role of the new echo techniques. Curr Opin Crit Care 14:561–568
8. Hunsaker RP (2005) Intraoperative transesophageal echocardiography: standard monitor and diagnostic instrument for difficult situations? J Clin Anesth 17:155–157
9. Lamia B, Maizel J, Ochagavia A et al (2009) Echocardiographic diagnosis of pulmonary artery occlusion pressure elevation during weaning from mechanical ventilation. Crit Care Med 37:1696–1701
10. Slama M, Masson H, Teboul JL et al (2002) Respiratory variations of aortic VTI: a new index of hypovolemia and fluid responsiveness. Am J Physiol 283:H1729–H1733
11. Feissel M, Michard F, Mangin I et al (2001) Respiratory changes in aortic blood velocity as an indicator of fluid responsiveness in ventilated patients with septic shock. Chest 119:867–873
12. De Backer D, Taccone FS, Holsten R et al (2009) Influence of respiratory rate on stroke volume variation in mechanically ventilated patients. Anesthesiology 110:1092–1097
13. Varpula M, Karlsson S, Ruokonen E et al (2006) Mixed venous oxygen saturation cannot be estimated by central venous oxygen saturation in septic shock. Intensive Care Med 32:1336–1343
14. Dueck MH, Klimek M, Appenrodt S et al (2005) Trends but not individual values of central venous oxygen saturation agree with mixed venous oxygen saturation during varying hemodynamic conditions. Anesthesiology 103:249–257
15. Sander M, Spies CD, Foer A et al (2007) Agreement of central venous saturation and mixed venous saturation in cardiac surgery patients. Intensive Care Med 33:1719–1725
16. Reinhart K, Kuhn HJ, Hartog C et al (2004) Continuous central venous and pulmonary artery oxygen saturation monitoring in the critically ill. Intensive Care Med 30: 1572–1578
17. Smith I, Kumar P, Molloy S et al (2001) Base excess and lactate as prognostic indicators for patients admitted to intensive care. Intensive Care Med 27:74–83

18. Arnold RC, Shapiro NI, Jones AE et al (2009) Multicenter study of early lactate clearance as a determinant of survival in patients with presumed sepsis. Shock 32:35–39
19. Vieillard-Baron A, Caille V, Charron C et al (2009) Reversal of refractory septic shock with drotrecogin alpha (activated). Intensive Care Med 35:1204–1209
20. Caille V, Amiel JB, Charron C et al (2010) Echocardiography: a help in the weaning process. Crit Care 14:R120
21. Voga G (2010) Hemodynamic changes during weaning: can we assess and predict cardiac-related weaning failure by transthoracic echocardiography? Crit Care 14:174

Future Applications

23

James N. Kirkpatrick and Roberto M. Lang

Contents

J.N. Kirkpatrick (✉)
Cardiovascular Division, Hospital of the University of Pennsylvania, Center for Bioethics, University of Pennsylvania, 3400 Spruce St., 9021 Gates Pavilion, Philadelphia, PA, 19104, USA
e-mail: James.kirkpatrick@uphs.upenn.edu

R.M. Lang
Noninvasive Cardiac Imaging Laboratories, Cardiology Fellowship Program, University of Chicago Medical Center, 5841 S. Maryland Ave. MC 5084, Chicago, IL, 60637, USA

23.1 Introduction

Standard echocardiography is an established modality for hemodynamic measurement in the critical care setting, but novel Doppler two-dimensional (2D) and three-dimensional (3D) techniques may further improve diagnosis and monitoring in the intensive care unit (ICU). This chapter describes recent developments, limitations, and potential ICU applications of tissue Doppler imaging (TDI), speckle tracking, real-time 3D echocardiography, and emerging applications of intracardiac echo and hand-carried ultrasonography.

23.2 Tissue Doppler Imaging

TDI uses the same principles as spectral Doppler imaging, but instead of blood velocity, it measures the velocity and directionality of tissue motion. The velocity of myocardial tissue is usually much slower, and the amplitude of reflected ultrasound waves much higher, than that of blood. Processing the returning ultrasound signals to register low-velocity, high-amplitude waves while filtering out all other signals yields myocardial velocity profiles when applied to high-frame-rate images (usually >180 frames/s). Pulsed-wave Doppler can interrogate specific regions of the myocardium to measure maximum velocities; color-coded real-time velocities from the entire sector show movement of all of the visualized myocardium toward or away from the transducer as well as mean velocities. Integration of the velocity over time provides a measure of myocardial displacement. Simply measuring myocardial displacement, however, fails to differentiate between motion of the entire heart (as in translational motion due to pericardial effusion, deep

D. De Backer et al. (eds.), *Hemodynamic Monitoring Using Echocardiography in the Critically Ill*,
DOI: 10.1007/978-3-540-87956-5_23, © Springer-Verlag Berlin Heidelberg 2011

respirations, or tethering effects) and motion of a specific segment relative to other segments and to its position at rest (the shortening and relaxing motion of the myocardium). This latter motion is termed deformation and reflects intrinsic properties of myocardial contractility and diastolic function [1].

As an illustration of the difference between displacement and deformation, consider a patient with renal failure in tamponade secondary to a large pericardial effusion who has a large, old, anterior-wall myocardial infarction. The infarcted myocardial segment is scarred and does not contract (there is no deformation); but because of the simultaneous swinging motion of the heart within the large pericardial effusion, this segment is displaced, along with the rest of the heart. TDI velocity imaging cannot differentiate between these two types of motion.

TDI can, however, also measure deformation, which is termed "strain." It does so by measuring the velocities at two different myocardial points and the distance between them to calculate strain rate (SR) as follows:

$$(v_1 - v_2)/L$$

where SR is the strain rate in seconds^{-1}; v_1, velocity at myocardial point 1 in m/s; v_2, velocity at myocardial point 2 in m/s; and L, the length between the points in m. Strain is obtained indirectly by integrating SR over time to yield length:

$$S = L - L_0 / L_0$$

where S is strain (dimensionless or percentage); L_0, initial length between the two myocardial points; and L, the length between the two myocardial points after motion stops.

23.2.1 Limitations of TDI Velocity and Strain

There are several limitations to TDI velocity and strain parameters. As a Doppler-based technique, TDI is angle-dependent and measures velocity at discrete points in the myocardium. If the Doppler beam is not parallel to the direction of the tissue motion, it underestimates tissue velocity. An angle deviation of as little as 15–20° introduces significant inaccuracies. TDI is mostly used in measuring longitudinal (base moving toward and away from apex) velocities in transthoracic echocardiography (TTE) apical views. It cannot measure apical motion, which is relatively fixed in the longitudinal direction. Radial motion (essentially the thickening movement of the myocardium inward) can be measured by TDI, but only of the septal and inferolateral walls in the parasternal views. Limited circumferential velocity of the septal and lateral walls from the parasternal short-axis view can also be measured. Attempting to measure velocities of the septum, however, is complicated by the fact that it is composed of fibers from the left ventricle (LV) and right ventricle (RV), each of which move with different velocities [2].

23.2.2 Current and Future Applications in Critical Care of TDI Velocity and Strain

As discussed in a previous chapter, TDI velocity measurements play a significant role in the echocardiographic determination of diastolic dysfunction and, when coupled with mitral valve spectral Doppler inflow velocities, provide an accurate and reproducible assessment of LV filling pressures. TDI velocity also constitutes a powerful prognostic marker in heart failure patients [3, 4].

TDI can be used to differentiate between constrictive and restrictive cardiomyopathy. Filling pressures are elevated in both of these conditions, but constrictive physiology occurs because of pericardial constraint on LV and RV filling. Restrictive cardiomyopathy usually occurs as a primary myocardial disorder (as from an infiltrative process, ischemia, hypertrophy, or dilated cardiomyopathy), which also limits LV and RV filling. Classically, constrictive pericardiopathy involves early filling followed by rapid equalization of atrial and ventricular pressures (the "dip and plateau" sign on invasive hemodynamics). This rapid early filling correlates with rapid early mitral annular longitudinal diastolic motion (high E' velocity) on TDI, in part because of reduced expansion in other directions from pericardial constraint. Conversely, restrictive filling involves intrinsic myocardial relaxation abnormalities, which are reflected in slow mitral annular diastolic motion (low E' velocity) [5]. Several studies demonstrated that an $E' \geq 8$ cm/s appears to be a highly specific cutoff value for distinguishing constrictive pericarditis from restrictive cardiomyopathy [6, 7].

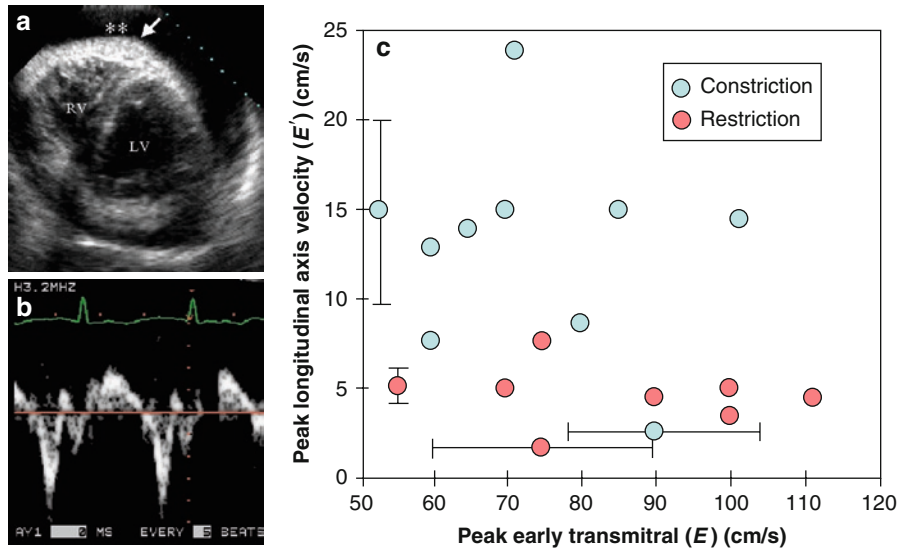

Fig. 23.1 Tissue Doppler imaging assessment of pericardial constriction vs. restriction. (**a**) A short-axis view of a large pericardial effusion (**) with a thickened pericardium (*white arrow*). (**b**) Relatively rapid (10 cm/s) maximal diastolic relaxation velocity (*E′*) of the septal mitral annulus. (**c**) The normal to increased *E′* velocities in pericardial constriction and reduced *E′* velocities seen in restrictive cardiomyopathy. In contrast, E-wave velocity could not distinguish between the two disease states (Adapted from Garcia MJ et al. [5])

E′ < 6 cm/s is usually found in restriction [8]. M-mode-based velocity gradient of the posterior wall has also been shown to differentiate between constriction and restriction [9] (Fig. 23.1).

Dobutamine stress echocardiography is a portable technique for the detection of myocardial ischemia and viability and therefore uniquely useful for patients who cannot be transported out of the ICU setting. Its limitations include dependence on image quality and the subjective nature of wall-motion interpretation. TDI velocity provides a more objective assessment of wall dysfunction, possibly identifiable at an earlier stage of ischemia than would produce a wall-motion abnormality diagnosed by visual inspection. It has been shown to improve the sensitivity, specificity, and accuracy of dobutamine stress testing for the detection of ischemia [10]. Abnormalities in TDI longitudinal, circumferential, and radial strain rates can be diagnosed in coronary artery disease patients at low-dose dobutamine [11]. Longitudinal peak strain demonstrated incremental value over standard wall-motion assessment for the detection of viability, using positron emission tomography (PET) scanning as a gold standard [12]. Strain parameters may be superior to velocity measurements because they can detect post-systolic shortening – the contraction of dysfunctional wall segments during the isovolumic relaxation phase of diastole, when intracavitary pressures (and therefore the pressure the segment must overcome in order to contract) are low [13].

Left ventricular ejection fraction (LVEF), especially by visual assessment, provides prognostic data but lacks accuracy in describing systolic function of the LV. Initial work demonstrated that TDI systolic (*S′*), early-diastolic (*E′*), and late-diastolic (*A′*) velocities were lower in patients with myocardial infarction and cardiogenic shock compared with patients with chronic heart failure, despite similarly reduced LVEF [14]. Better precision is required for early detection and monitoring of subtle changes in LV dysfunction, particularly due to sepsis and toxic-metabolic disturbances, as well as ischemia.

TDI velocities also have been used to demonstrate systolic dysfunction in patients with preserved LVEF. Work by Yu et al. [15, 16] found that peak TDI velocity of <4.4 cm/s detected systolic dysfunction in patients with normal LVEF and evidence of clinical heart failure, and in patients with normal LVEF and no heart failure but evidence of diastolic dysfunction. TDI RV free-wall systolic velocities (S′ wave) demonstrated a good correlation with right ventricular ejection fraction (RVEF) by cardiac magnetic resonance imaging (MRI) and may prove to be an accurate and highly reproducible way to quantify RV function [17].

TDI strain parameters may be an even better way to detect abnormal LV systolic function. In the normal heart, strain correlates with stroke volume, and peak SR correlates with systolic d*P*/d*t* – change in pressure over time (an accurate index of contractile function) [18]. Strain and SR outperformed TDI velocities in differentiating between three groups of patients with

amyloidosis: those with no cardiac involvement, those with cardiac involvement but no symptoms, and those with cardiac involvement with symptoms [19].

Making the important distinction between hypertrophic, nonobstructive cardiomyopathy (HNOCM), and hypertrophy due to hypertension using standard echo techniques is nearly impossible. But the myofibril disarray in HNOCM does produce alterations in myocardial mechanics that can be detected with a TDI systolic strain cutoff of −10.6% [20]. In patients with myocarditis, TDI has been reported to identify myocardial edema before the onset of LV dysfunction [21]. Regional strain assessment may correlate with areas of patchy infiltration on cardiac MRI and may prove beneficial in directing the location of myocardial biopsy or obviating the need for such invasive diagnostics [22].

TDI SR applied to longitudinal RV function demonstrated regional dysfunction in pulmonary hypertension patients, with particularly strong correlations between reduced apical SR and invasively determined pulmonary pressures and pulmonary vascular resistance [23]. TDI has also been shown to correlate with moderate to severe perfusion defects in acute pulmonary embolism, suggesting that it may play a role in determining the severity of embolism in patients who cannot undergo contrast-enhanced computed tomography or ventilation-perfusion scanning [24].

23.3 Speckle Tracking: Multidirectional Measurements

Speckle tracking is a new technique for measuring myocardial motion. It overcomes some of the problems with TDI, specifically angle dependency, since it is based on 2D, rather than Doppler images. It requires a lower frame rate (50–100 frames/s, which is still higher than most standard 2D imaging). Reflected ultrasound waves from the myocardium and adjacent structures interfere with each other to create unique speckled patterns. These patterns are evenly distributed in the myocardium. Specialized software can track the motion of these patterns from frame to frame throughout the cardiac cycle to measure displacement of speckles relative to the transducer and to other speckles. Strain is easily calculated from this displacement data, and velocity and SR can be calculated by adding time data.

Systolic contraction involves longitudinal shortening, in which the base moves toward the apex, radial shortening (inward thickening of the myocardium), and circumferential shortening (motion around the center point) (Fig. 23.2). It also involves a complex rotational motion, in which the apex and base rotate in opposite directions to produce a motion akin to wringing water out of a wet towel. Speckle tracking measures all of these components and is uniquely able to capture rotational motion by measuring the degree of angular displacement and rotational velocity for different myocardial segments as well as for the different layers of the myocardium (Fig. 23.3). Studies have demonstrated excellent correlation of all of these parameters with both cardiac MRI and sonomicrometry, the gold standard technique that involves implanting small crystal markers in the myocardium and tracking their movement [25].

23.3.1 Limitations of Speckle Tracking

Speckle tracking is extremely dependent on image quality. Artifacts, especially dropout, interfere with the software's ability to track speckle motion. Furthermore, speckles can move out of the detection plane, especially secondary to translational motion, and at faster heart rates and lower frame rates. Though technically angle independent, speckle tracking algorithms may be less accurate in following speckle movement perpendicular to the ultrasound beam than movement parallel to the beam [26].

23.3.2 Current and Future Applications of Speckle Tracking in Critical Care

Initial work suggests that speckle tracking strain parameters may provide a superior description of diastolic filling compared with the E/E' index. The ratio of E to SR of isovolumic relaxation discriminated between filling states when the E/E' ratio was indeterminate (between 8 and 15). It proved accurate in patients with preserved systolic function and in patients with regional wall-motion abnormalities [27].

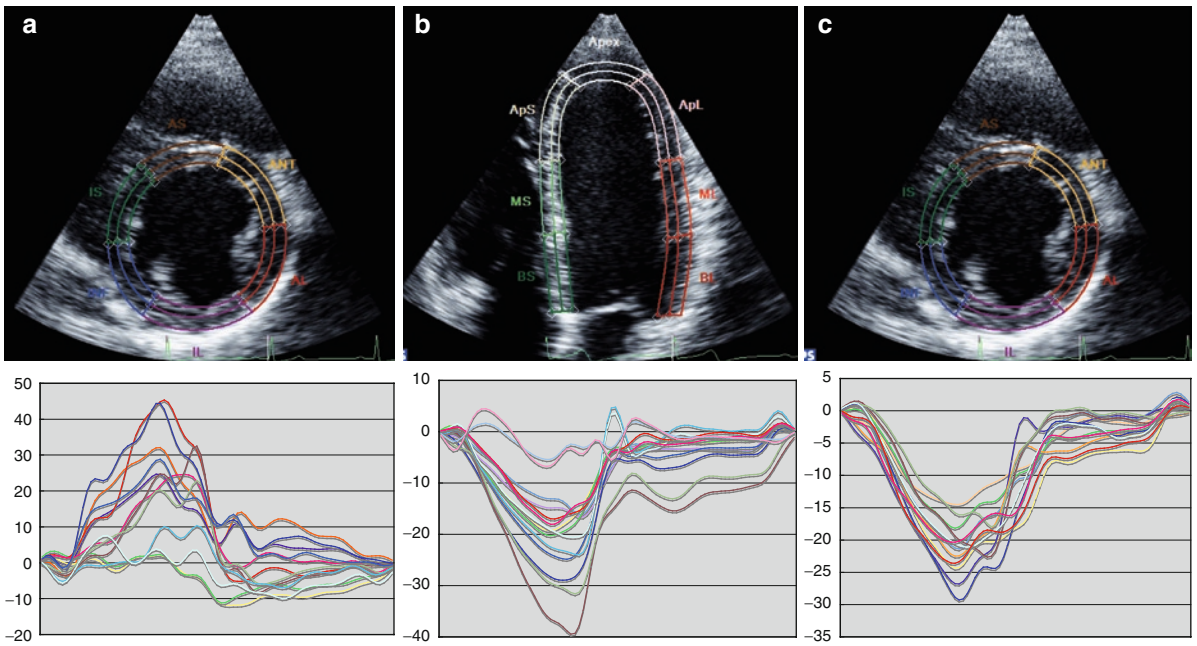

Fig. 23.2 Measurement of left ventricular strain. Using speckle tracking techniques, strain can be calculated in different myocardial segments (*color coded*) and graphically displayed (*bottom parts of panel*). Each color-coded myocardial segment corresponds to the colored line on the graph. (**a**) Radial strain from the parasternal short-axis midventricular view. (**b**) Longitudinal strain from the apical four-chamber view. (**c**) Circumferential strain from the parasternal short-axis midventricular view. Abbreviations: *AS* anteroseptum, *ANT* anterior, *AL* anterolateral, *IL* inferolateral, *INF* inferior, *IS* inferoseptum, *BS* basal septum, *MS* midseptum, *ApS* apical septum, *ApL* apical lateral, *ML* midlateral, *BL* basal lateral

Like TDI strain, speckle tracking strain parameters accurately identify reversible ischemia [28]. In a three-way comparison between speckle tracking, TDI, and visual wall-motion assessment during dobutamine stress testing, there were no significant differences overall in the detection of significant coronary artery disease (>70% stenosis by angiography). Speckle tracking, however, was not as feasible at peak stress as TDI, and it was significantly less accurate in the detection of right coronary artery disease [29].

Speckle tracking techniques allow for the calculation of global strain, a parameter that may prove more sensitive for the detection of LV systolic dysfunction than LVEF, TDI velocity, or TDI strain parameters (which cannot provide a real-time global assessment because of angle dependency). With its improved reproducibility, speckle tracking may prove better than TDI at characterizing both systolic and diastolic myocardial dysfunction in ICU patients as well as characterizing dyssynchronous contraction patterns, which may signify occult ischemia or myocardial dysfunction amenable to treatment with cardiac resynchronization therapy (Fig. 23.4). Improvements over time in global and regional strain may be able to predict which patients with myocardial depression from sepsis, stress-induced cardiomyopathy, tachycardia-medicated cardiomyopathy, early infiltrative diseases, toxic-metabolic disturbances, postpartum cardiomyopathy, myocarditis, and ischemia may be likely to recover or respond to certain interventions and which patients will progress to worsened or persisting degrees of LV dysfunction. In the future, research may demonstrate a subgroup of patients with normal LVEF but reduced global strain who benefit from specific heart failure therapies (e.g., angiotensin-converting enzyme inhibition and beta-blockade).

Global RV strain imaging is also possible by speckle tracking. Initial small studies demonstrate regional and global strain parameters that track the severity of pulmonary hypertension [30, 31].

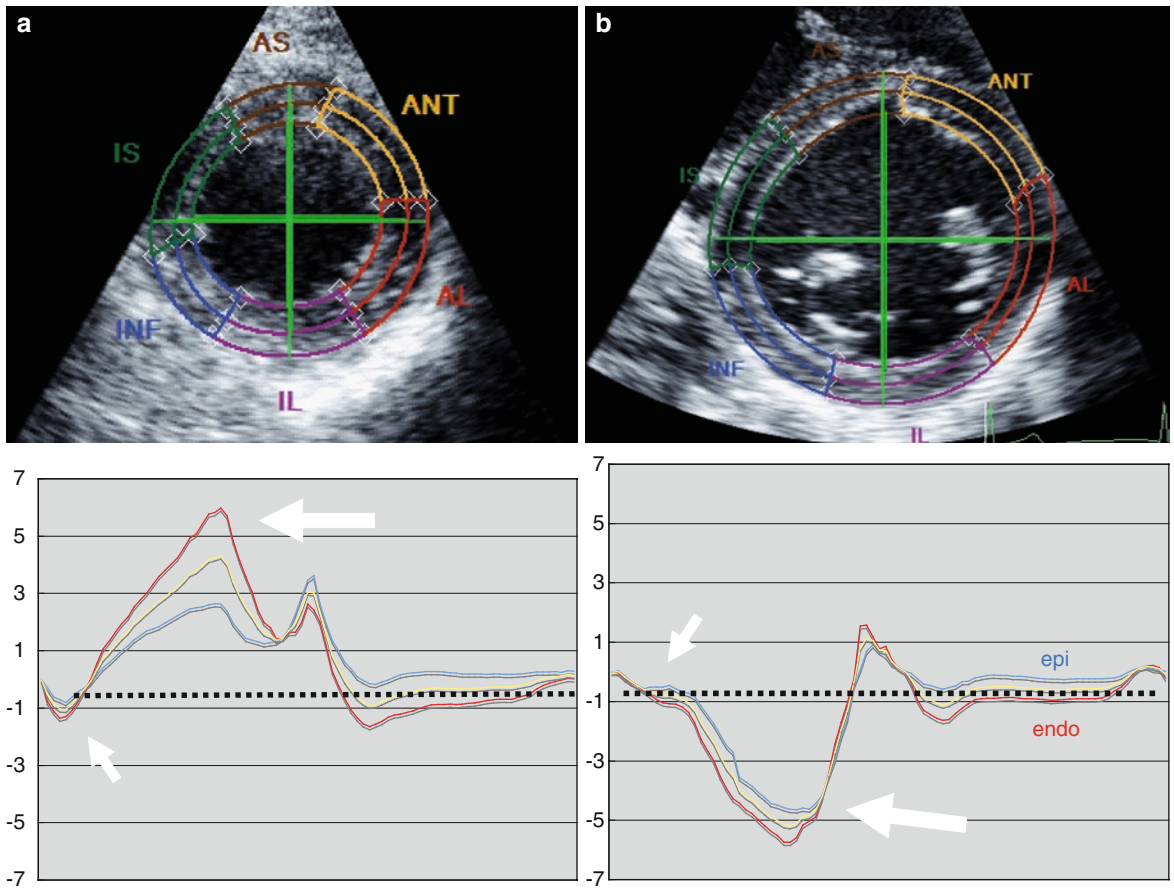

Fig. 23.3 Rotational dynamics of the left ventricle. Speckle tracking can be used to measure and graphically display the rotational motion of the left ventricle over the cardiac cycle. In the graphs, the *y*-axis represents degrees of rotation and the *x*-axis time; the colored lines correspond to different layers of the myocardium (*light blue, epicardium; yellow, midmyocardium; red, endocardium*). From the graphs, both maximal degree of rotation and rate of rotation (*from the slopes of the lines*) can be measured. Panel (**a**) demonstrates apical motion. There is an initial small clockwise twisting motion (*small arrow*), followed by counterclockwise rotation during the majority of systole (*large arrow*). Panel (**b**) shows basal rotation, which is initially in a counterclockwise direction (*small arrow*), followed by clockwise rotation through most of systole (*large arrow*). The net effect of these opposing motions is similar to the motion performed when wringing out a wet towel. Note the differences in degree and speed of rotation in the epicardium vs endocardium, particularly at the apex (both increased in the endocardium relative to the epicardium) Abbreviations: *AS* anteroseptum, *ANT* anterior, *AL* anterolateral, *IL* inferolateral, *INF* inferior, *IS* inferoseptum, *BS* basal septum, *MS* midseptum, *ApS* apical septum, *ApL* apical lateral, *ML* midlateral, *BL* basal lateral

The next horizon in speckle tracking is the implementation of this technique with 3D echocardiography. 3D speckle tracking will eliminate the confounding effect of speckles moving out of the imaging plane owing to translational motion and will allow simultaneous assessment of regional strain in all myocardial segments, including apical segments, calculation of true global strain and real-time imaging of rotational motion at all levels of the LV.

23.4 Real-Time 3D Echocardiography

3D echocardiography has been available for many years, but it consisted of time-consuming, off-line reconstruction of sequentially acquired 2D images. The recent development of ultrasound probes with >3,000 piezoelectric crystals in a matrix array has ushered in a new era of clinical applicability for 3D imaging owing

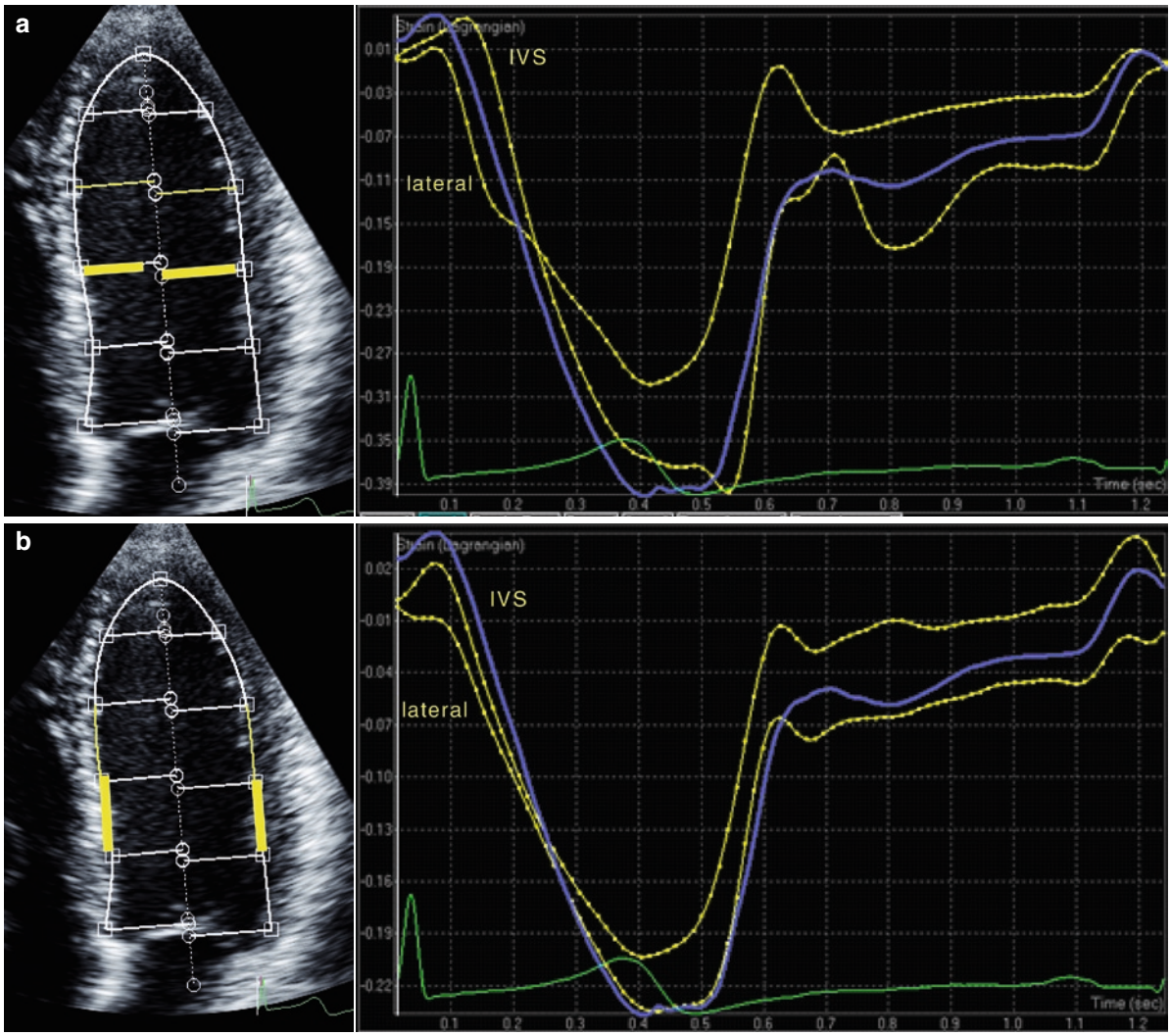

Fig. 23.4 Assessment of left ventricular dyssynchrony by texture tracking. Detection and tracking of the endocardial boarder using speckle tracking can be used to generate strain curves from apical four-chamber images. From these curves, the time to peak maximal strain can be calculated to assess dyssynchrony in opposing wall segments (*yellow lines*). The blue line represents global/average strain. (**a**) Radial shortening strain (measured along the horizontal thick yellow bars) for the mid-interventricular septum (IVS) and lateral wall. Curve separation suggests significant radial dyssynchrony. (**b**) Longitudinal shortening strain (*measured along the vertical thick yellow bars*) for the mid-IVS and lateral wall. Note there appears to be less longitudinal than radial dyssynchrony

to increased practicability. The probes collect and display pyramids of data in real time on the echo machine screen. So-called full-volume data sets can be acquired in a matter of seconds, with instantaneous online reconstruction. These data sets consist of four sequential pyramids of data stitched together to form a larger, 90×90 degree pyramid with a wide 3D sector. From these full-volume datasets, casts of the LV cavity can be generated by software that automatically detects the endocardial-blood interface throughout the cardiac cycle. These casts can be automatically segmented to track regional myocardial motion. Similar, albeit more complex, endocardial-surface detection programs are becoming available for the RV. Real-time 3D echocardiography (RT3DE) and full-volume images of valves, arteries, veins, masses, and septa allow visualization of these structures from orientations not available in standard echocardiographic imaging planes.

23.4.1 Limitations of RT3DE

There are several significant limitations to 3D echocardiography. One involves the large footprint of the transducer, which results in difficult imaging in small intercostal spaces. The frame rate for RT3DE is considerably lower than 2D, leading to reduced image quality. There usually is a relatively steep learning curve for acquiring 3D images and manipulating them so as to visualize the desired structure. These limitations generally ensure that patients with poor 2D imaging windows have even worse 3D windows. In addition, because the acquisition of full-volume data sets requires stitching together four slabs of data to obtain a full-volume data set, arrhythmias, respirations, and other causes of translational motion will introduce "stitching artifacts," which appear as linear discontinuities in the 3D image.

Recently, real-time 3D transesophageal echocardiography (TEE) has become available (see Sect. 23.5 below). While not eliminating problems with low frame rate, it greatly improves 3D image quality. Stitching artifacts and the learning curve for image acquisition and manipulation remain minor limitations of this technique.

23.4.2 Current and Future Applications of RT3DE in Critical Care

Much of the literature on RT3DE to date has demonstrated improved measurements of LV volumes, LV mass, and LVEF [32, 33]. Studies have shown high reproducibility and accuracy, mostly compared with cardiac MRI (Fig. 23.5), in normal hearts [35],

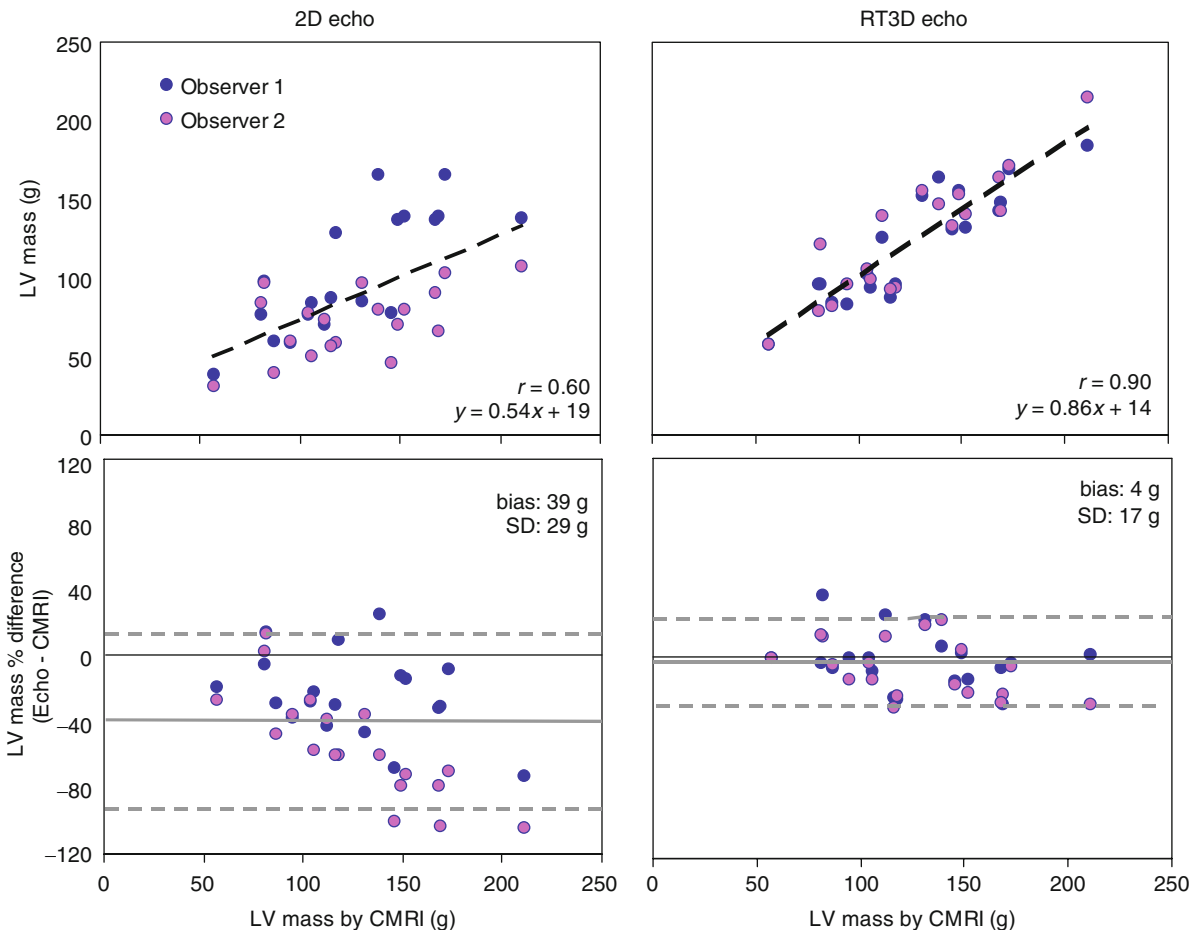

Fig. 23.5 Improved accuracy of real-time 3D (RT3D) echocardiography vs conventional 2D echocardiography when compared with the gold standard of cardiac magnetic resonance imaging (CMRI) for calculation of left ventricular (LV) mass (Reproduced from Mor-Avi et al. [34])

ischemic and nonischemic cardiomyopathy [36], and congenital heart disease [37]. In the ICU setting, the improved accuracy and reproducibility in LVEF measurements compared with 2D echocardiography may improve the tracking of LV function over time, and accurate assessment of LV volumes may provide a better assessment of LV filling (Figs. 23.6 and 23.7). Aside from LVEF determination as a marker of systolic function, RT3DE may improve the noninvasive calculation of stroke volume and cardiac output by providing a more accurate way to measure LVOT area (from the actual short-axis view of the LVOT, rather than measuring the diameter and calculating the area, as is involved in standard 2D techniques). A novel method can also use 3D color Doppler to calculate flow rate, with improved accuracy over 2D techniques [38].

Simultaneous and objective quantification of regional function may provide a more accurate and reproducible measure of regional myocardial ischemia [39]. RT3DE has been used in dobutamine stress testing with good results [40, 41]. The future of dobutamine stress testing and of myocardial mechanics in general will be the combination of RT3DE with speckle tracking. Prototype software is currently under development and has to overcome the significant problems associated with low spatial and temporal resolution of current RT3DE techniques to incorporate the high frame rates necessary for speckle tracking [42].

The RV is a very complex structure, and it becomes even more complex in diseased states. 2D attempts to describe RV structure and function invariably miss certain aspects. Initial studies with 3D RV imaging

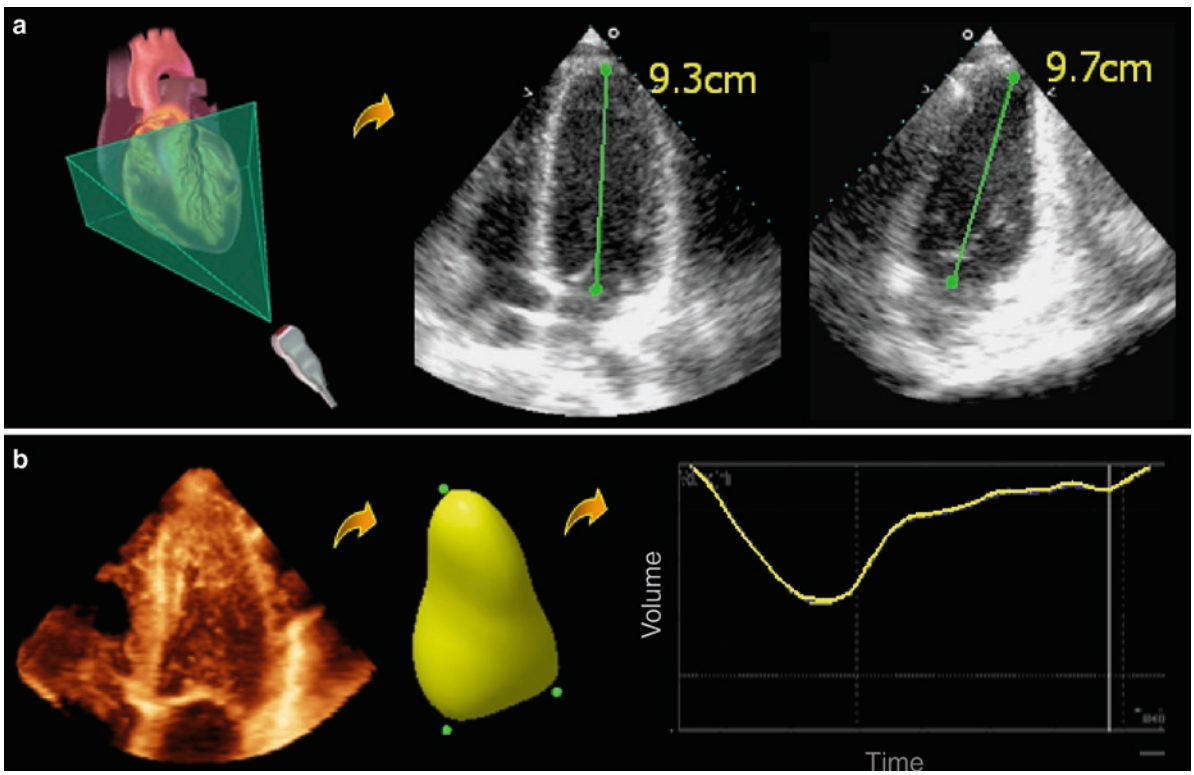

Fig. 23.6 Two uses of 3D datasets to measure left ventricular ejection fraction (LVEF). Conventional 2D volume calculations, from which LVEF is calculated, use potentially foreshortened apical views and rely on geometric modeling of the ventricle. (**a**) The problem of foreshortening can be solved by selecting, from the 3D data pyramid, anatomically correct, nonforeshortened apical views. From these, left ventricular (LV) volumes can then be measured and LVEF calculated according to the traditional manner of tracing the endocardial border in the apical four- and two-chamber views at end systole and end diastole, assuming a bullet shape to the ventricle and calculating volumes (method of disks). (**b**) Alternatively, the endocardial surface can be detected and traced from a full-volume 3D data set. The instantaneous 3D LV volume throughout the cardiac cycle can then be directly measured and displayed graphically. LVEF is easily calculated from end-systolic and end-diastolic values

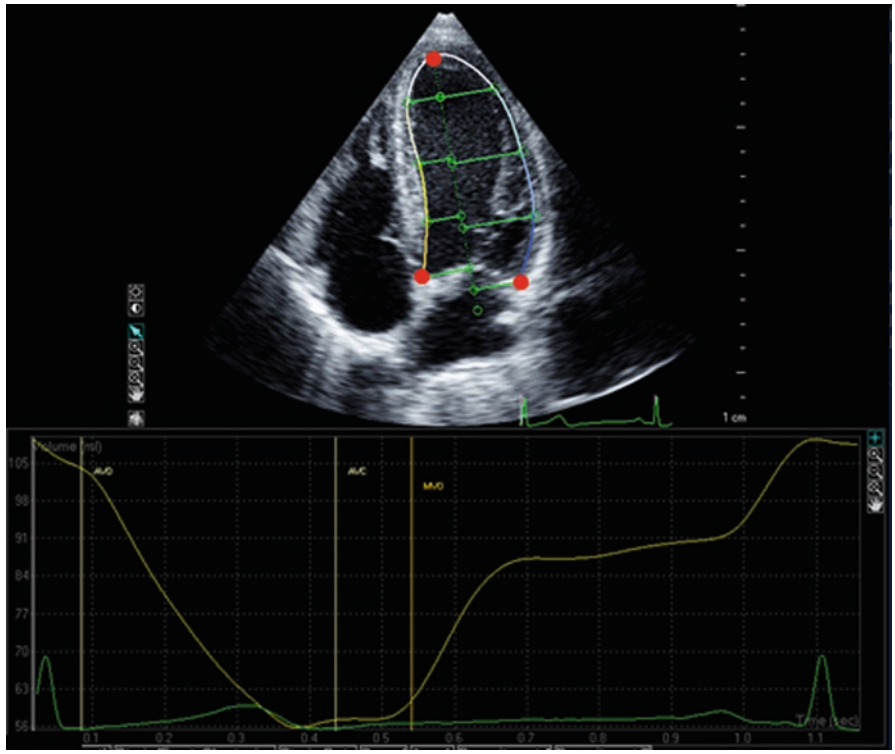

Fig. 23.7 Texture tracking of the left ventricle, apical four-chamber view. Recent advances in speckle tracking have been used to highlight the interface between the endocardial border and the blood pool. This interface can be tracked to measure changes in LV volume throughout the cardiac cycle, from which a volume curve can be constructed. Abbreviations: *AVO* aortic valve opening, *AVC* aortic valve closure *MVO* mitral valve opening

have demonstrated good correlation with cardiac MRI for RV volumes and RVEF in patients with congenital heart disease, arrhythmogenic RV dysplasia, and probable RV infarction [43–45]. RT3DE should constitute a superior method for detecting RV pathology and also in following the dynamic changes in RV size and shape as a result of acute versus chronic insults and their treatments (e.g., RV infarct versus primary pulmonary hypertensive disease), and RT3DE should provide better markers for specific interventions (e.g., thrombolytics in acute massive pulmonary embolism and placement of an RV assist device; Fig. 23.8).

RT3DE affords the opportunity for better detection and characterization of valvulopathy, especially of the mitral and tricuspid valves, which are nonplanar structures and therefore cannot be evaluated in a single 2D imaging plane. Accurate assessment of eccentric mitral regurgitation (MR) is particularly important in postmyocardial infarction and in structural valvular abnormalities, such as prolapsed and flail segments. 2D methods for MR quantification require geometric assumptions that are invalid in eccentric jets. The ability of 3D to better characterize these jets represents a significant advantage over 2D echocardiography [46, 47]. In one study, RT3DE showed improved assessment of MR and mitral valve pathology compared with 2D transesophageal imaging (except for flail segments), using surgical findings as the gold standard [48]. The same may hold true for aortic insufficiency [49]. The use of 3D TTE provides superior information for planning and monitoring of valve surgery or percutaneous valve interventions, especially in allowing visualization from the surgeon's view [50]. Recent developments in mitral valve quantification may inform not only the timing of surgery but also surgical approaches (Figs. 23.9 and 23.10).

The next generation of RT3DE probes should be able to collect a full-volume data set in one cardiac cycle, eliminating the problems associated with stitching artifact. Improvements in frame rate will allow improved endocardial detection as well as more precise measurements of color Doppler jets.

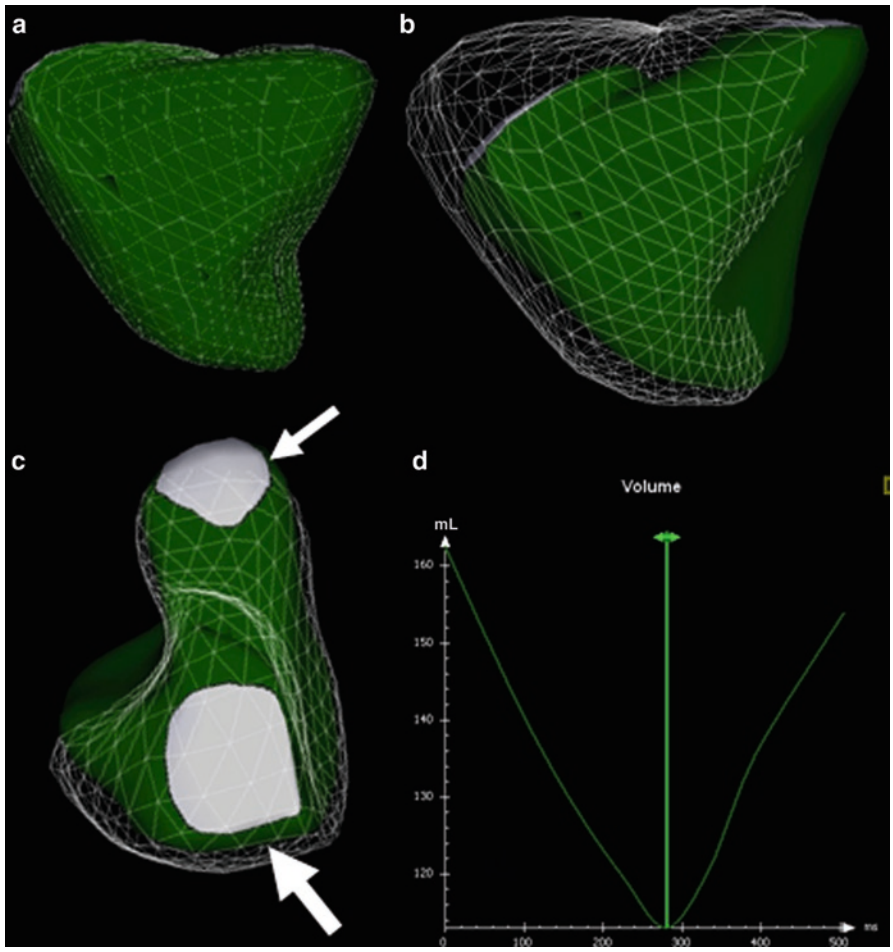

Fig. 23.8 Three-dimensional volumetric rendering of the right ventricle (RV). (**a, b**) The RV as viewed from an anterior perspective: (**a**) end diastole; (**b**) end systole (the white mesh indicates end diastole). Note the very irregular shape of the RV which makes characterization from 2D imaging planes extremely difficult. In (**c**), the 3D dataset has been rotated counterclockwise and to the right; it is viewed from a superior perspective. The white shaded areas denote the inflow/tricuspid valve (*large white arrow*) and outflow/pulmonary valve (*small white arrow*) portions of the RV. (**d**) The volume curve over the cardiac cycle, which can be measured from the 3D dataset (*y*-axis volume in mL; *x*-axis time in ms

23.5 Real-Time 3D TEE

One of the most exciting recent developments in echocardiography is the development of real-time 3D TEE (RT3D TEE). The RT3D TEE probe is approximately the same size as a standard TEE probe, and it can capture real-time or full-volume data sets in a manner analogous to that of transthoracic RT3DE. RT3D TEE eliminates many of the limitations of transthoracic RT3D imaging. The proximity of the probe in the esophagus to cardiac structures dramatically improves image quality, especially of near-field structures, such as the mitral and aortic valves, the interatrial septum, and the aorta (Figs. 23.11 and 23.12). Pepi et al. [51] compared 2D TTE, 2D TEE, RT3D TTE, and RT3D TEE with surgical findings in patients undergoing mitral valve repair. RT3D TEE outperformed the other techniques in accurately assessing mitral morphology, particularly the location of prolapse [51].

RT3D TEE has proven useful in examining ventricular septal defects (VSD). A study by Mercer-Rosa et al. [52] demonstrated the superiority of RT3D TEE over 2D TTE and TEE in displaying the exact morphology of the VSD compared with operative findings.

23.6 ICU Applications of Other Echocardiographic Technologies

23.6.1 Intracardiac Echo

The placement of low-frequency ultrasound transducers on the end of steerable catheters has enabled the imaging of cardiac structures from within the heart, most commonly from the right atrium. Intracardiac echocardiography (ICE) is frequently used in percutaneous

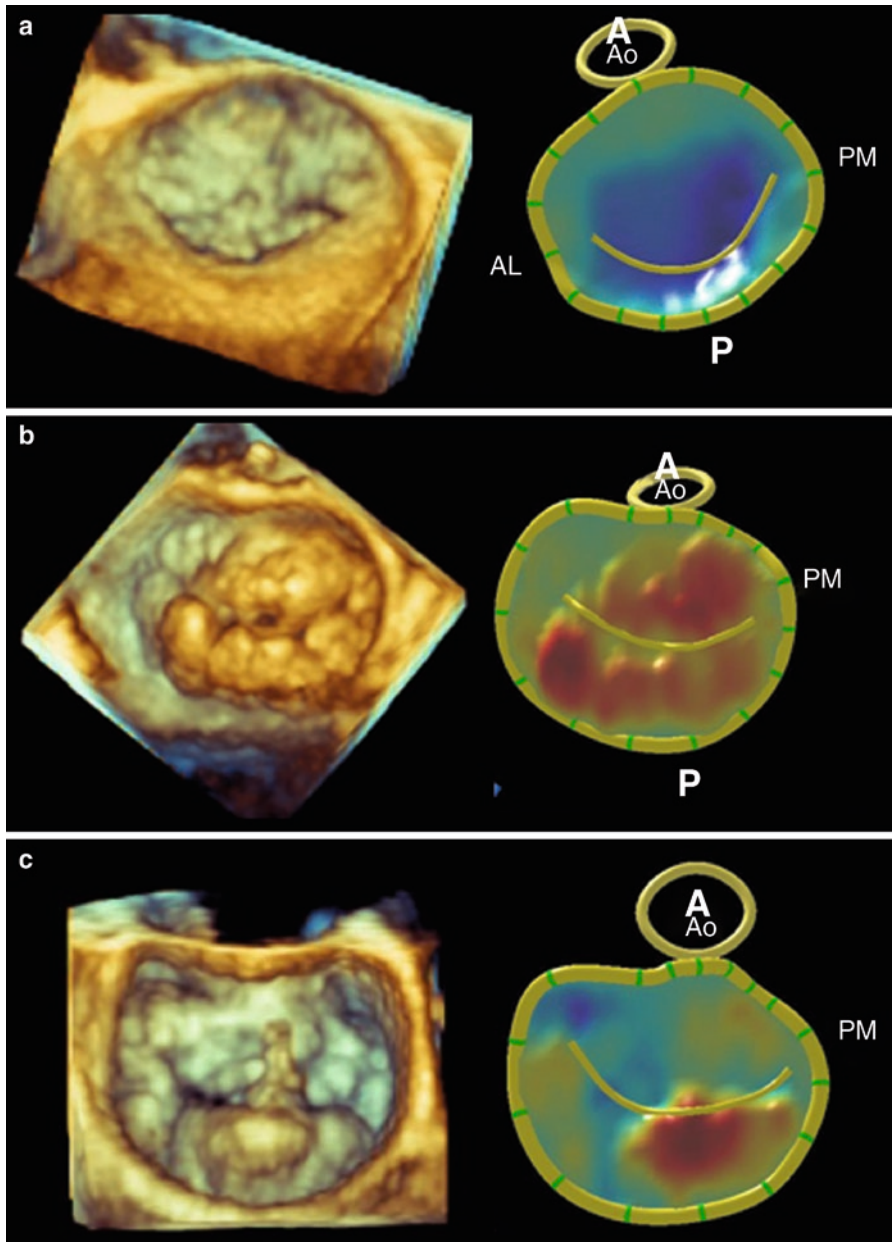

Fig. 23.9 Three-dimensional quantitative, parametric analysis of different mitral valves using 3D transesophageal echocardiography (TEE) datasets with end-systolic reconstructions from the left atrial perspective; 3D TEE images on the left, parametric reconstructions on the right. The orange color indicates the location above the mitral annular plane and in the left atrium; blue denotes the location below the mitral annular plane. (**a**) Normally there is no prolapse of any mitral valve segments above the annular plane. (**b**) Barlow's syndrome, in which there is myxomatous degeneration of both mitral valve leaflets, leading to extensive, "billowing" prolapse of multiple anterior and posterior mitral valve segments. (**c**) Fibroelastic deficiency leading to flail of the second posterior mitral valve leaflet segment (*P2, dark orange*)

cardiovascular procedures to guide puncture of the atrial septum and closely monitor placement of septal occluder devices, ablation catheters, and mitral valvuloplasty balloons (Fig. 23.13) [53, 54]. In each of these applications, ICE has been useful in detecting intracardiac thrombi. It may prove an adequate replacement to TEE-guided cardioversion [55]. Although primarily used for anatomical diagnosis, ICE probes have spectral and color Doppler capabilities, potentially allowing diagnostic evaluation of shunts, regurgitation, and hemodynamics. ICE is an invasive procedure, and the size of the small transducer has limited penetration and a narrow imaging sector. Considerable skill is required to position the catheter to achieve adequate imaging windows. For patients with poor transthoracic windows who have esophageal pathology precluding TEE (e.g., esophagectomy and bleeding esophageal varices), it enables echocardiographic diagnosis of cardiac pathology. ICE catheters are portable and can be inserted at bedside in the ICU under sterile conditions.

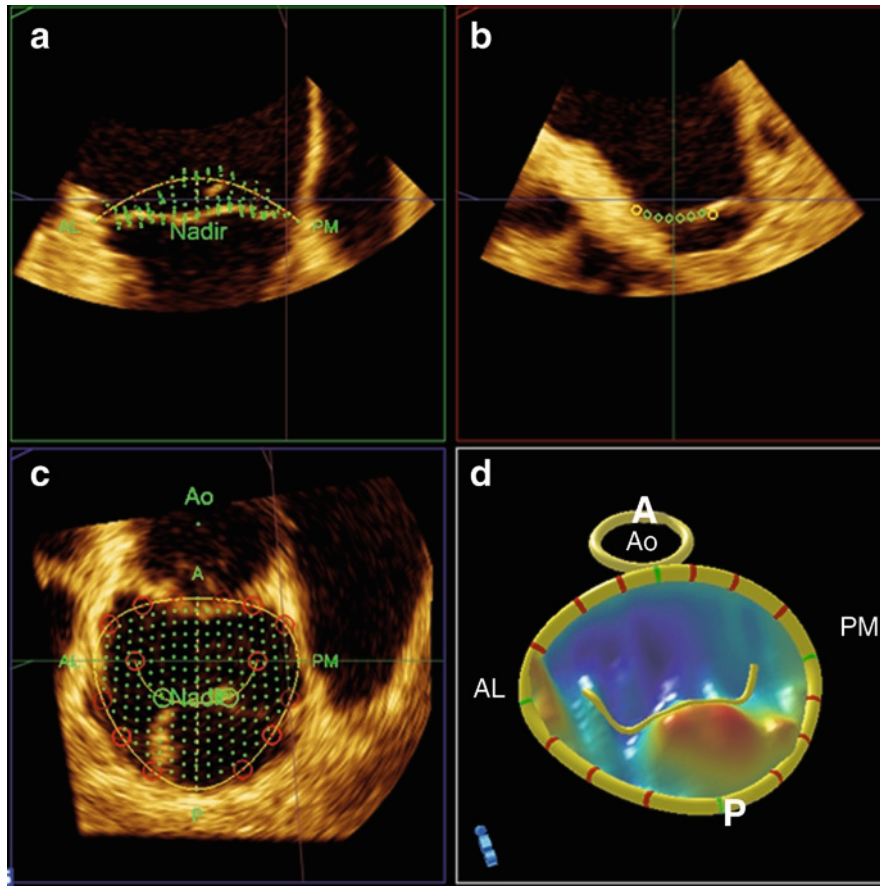

Fig. 23.10 Quantitation of mitral valve (MV) anatomy from 3D transthoracic echocardiography. (**a**) Quantitative software detection of the maximal (*yellow line*) and minimal (Nadir) transverse excursion of the MV. In (**b**), the contour of the MV is defined in an orthogonal plane. (**c**) The en face view of the mitral valve from the surgeon's view of the left atrium (LA) with the aortic root (Ao) situated anteriorly (A). The coaptation line between the anterior and posterior leaflets is denoted by the curved yellow line. The yellow circle outlines the MV annulus. (**d**) The quantitative software automatically tracks and displays MV anatomy in a parametric reconstruction with color coding of excursion (*orange/yellow out of the plane and into the LA; blue at or below the mitral annular plane, into the left ventricle*). Well illustrated is severe prolapse of the second posterior leaflet segment (P2), colored orange. Abbreviations: *A* anterior, *Ao* aorta, *AL* anterorolateral, *PM* posteromedial, *P* posterior

23.6.2 Hand-Carried Ultrasound

Hand-carried ultrasound (HCU) has benefited significantly in recent years by improvements in 2D image quality (primarily from harmonic imaging and phased-array transducer technology) and the introduction of spectral, color, and tissue Doppler. High-end platforms provide features for performing full TTE and TEE. A substantial body of literature now exists to support the use of HCU devices in a variety of clinical settings and the performance of HCU by a variety of clinician sonographers, from nurses to cardiologists [56, 57]. Most of these studies show a relatively favorable accuracy of HCU compared with sonographer-performed and cardiologist-interpreted full-feature echocardiography, along with a substantial improvement of HCU over physical examination in detecting cardiac pathology [58]. Debate continues, however, on the specific clinical applications of HCU and whether or how performance of HCU should be reimbursed [59]. In the ICU setting, several reports have demonstrated significant diagnostic limitations, even when HCU was performed by sonographers or cardiologists and included spectral Doppler capabilities [60, 61]. Poor transthoracic

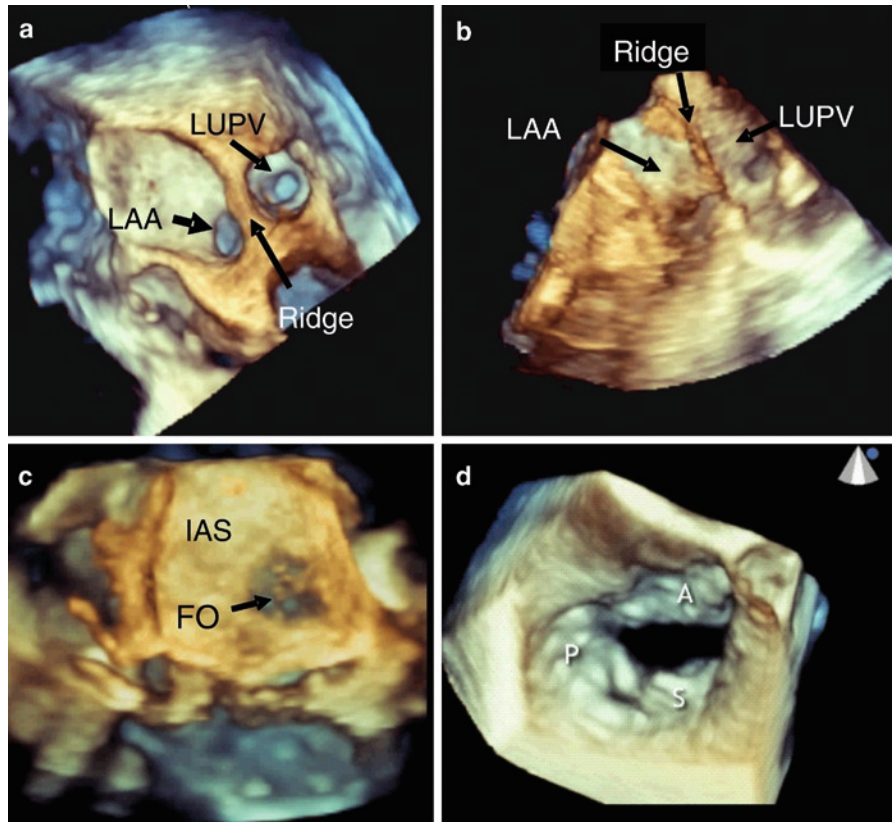

Fig. 23.11 Three-dimensional transesophageal echocardiography provides views of structures not available from 2D imaging planes. In (**a**), the location of the ostia of the left atrial appendage (LAA) relative to the left upper pulmonary vein (LUPV) is clearly demonstrated. (**b**) The same image rotated to a long-axis plane view. (**c**) The fossa ovalis (FO) in the interatrial septum (IAS), as viewed from the right atrium. (**d**) The anterior (A), septal (S), and posterior (P) leaflets of the tricuspid valve

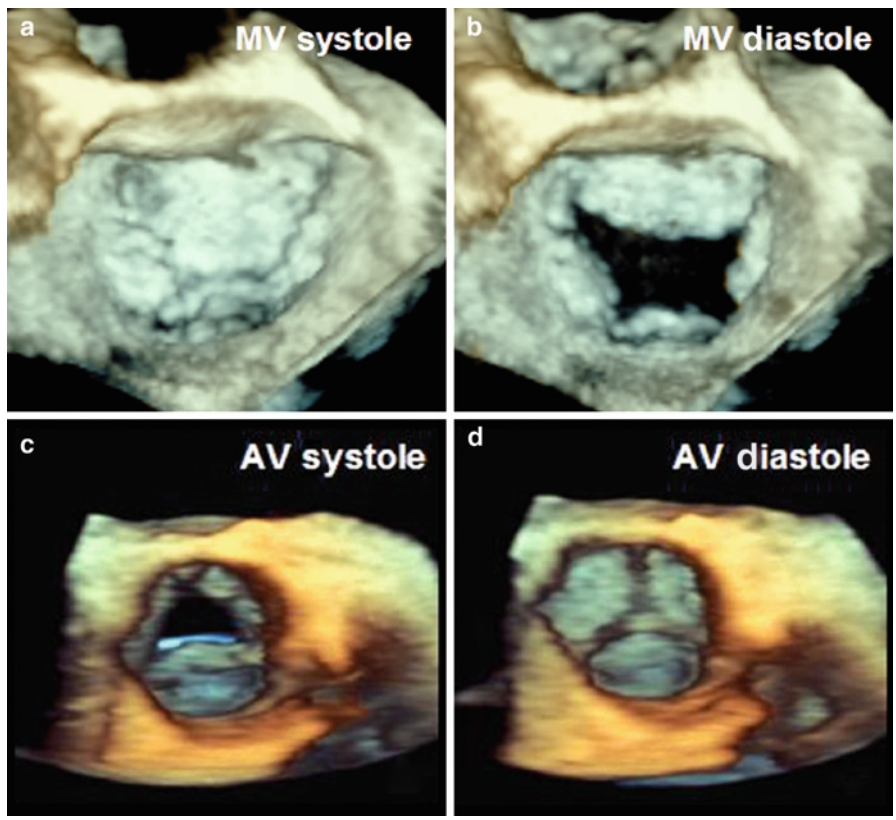

Fig. 23.12 Three-dimensional transesophageal echocardiography: 3D perspective is enhanced by color shading to demonstrate depth. Top panels: superior perspective from the left atrium. Bottom panels: inferior perspective from the left ventricular outflow tract. (**a**) Closure of the mitral valve (MV) during systole. (**b**) Maximal opening of the mitral valve during diastole. (**c**) Maximal opening of the aortic valve. (**d**) Aortic valve closure during diastole

imaging windows limiting full-feature examination by a trained sonographer are common in the ICU setting. Difficult imaging windows will exacerbate the problems experienced by a noncardiologist clinician sonographer using an HCU device. There is some consensus that HCU examination should be brief and focused and not be considered an adequate alternative to full-feature echocardiography. Potential uses in the ICU may include screening patients for cardiovascular disorders in whom there is no clinical indication for full echocardiography [62], rapid identification of cardiac pathology when full echocardiography is not readily available [63], and, potentially, serial monitoring of anatomical and hemodynamic parameters. Studies with newer-model HCU devices suggest excellent accuracy in the monitoring of pulmonary artery systolic pressures, compared with Swan-Ganz catheters [64].

23.7 Key Points

New Doppler 2D and 3D techniques may further improve noninvasive diagnosis and monitoring in ICUs. TDI measures both displacement and deformation of tissue. While limited by angle dependency, TDI provides important information about myocardial mechanics, specifically diastolic and systolic function in patients with preserved LVEF and in RV dysfunction. TDI may improve the sensitivity for detecting ischemia during dobutamine stress testing. Speckle tracking provides detailed characterization of myocardial motion in multiple directions, but it is extremely dependent on adequate frame rate and image quality. Speckle tracking strain coupled with mitral inflow velocity may provide the most accurate noninvasive measure of LV filling pressures. Global systolic

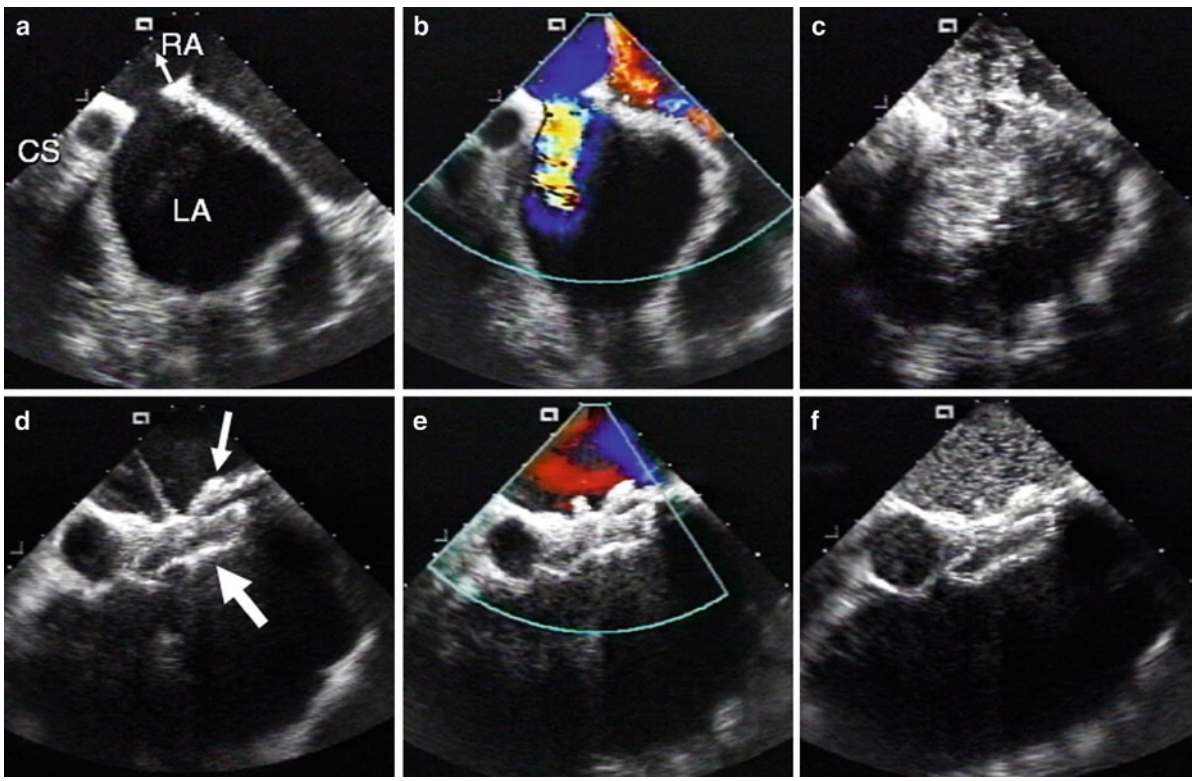

Fig. 23.13 Intracardiac echocardiographic (ICE) views of percutaneous closure of a sinus venosus atrial septal defect (ASD). The ICE catheter with an ultrasound transducer has been introduced via the femoral vein and advanced into the right atrium (RA). Unlike a transesophageal echocardiography view of the atria, in which the left atrium (LA) is in the near field (*top of the screen*) and the RA in the far field, the RA is in the near field in ICE images. (**a**) A sinus venosus ASD between the RA and left atrium (LA) at the level of the inferior vena cava near the coronary sinus (*CS; white arrow*). (**b**) Color flow through the ASD. (**c**) Free flow of agitated saline contrast bubbles from the RA into the LA. (**d**) Placement of a percutaneous closure device across the ASD. After advancing a catheter across the defect, an outer sheath is pulled back, allowing expansion of a disk on the LA side of the defect (*large white arrow*) and a smaller disk on the RA side (*small white arrow*), which is pushed against the defect. Correct positioning is confirmed, then the disk apparatus is released. (**e**) No color flow across the defect. (**f**) No passage of contrast across the closed defect

and diastolic strain may prove to be the most sensitive parameters for detecting and following changes in LV and RV function in various cardiomyopathic states, including sepsis, stress-induced cardiomyopathy, tachycardia-mediated cardiomyopathy, early infiltrative diseases, toxic-metabolic disturbances, postpartum cardiomyopathy, myocarditis, and ischemia. RT3DE improves the measurement of cavity dimensions without relying on geometric assumptions and allows full visualization of nonplanar structures. Although limited by relatively low temporal and spatial resolution, the recent availability of RT3D TEE has brought the benefits of 3D echocardiography to patients with difficult transthoracic imaging windows. The use of RT3DE in the ICU includes improved accuracy in LV volumes and LVEF assessments, accurate global assessment of RV size and function, and characterization of valvular pathology, especially eccentric regurgitant jets. RT3D TEE may provide the most comprehensive morphological assessment of cardiac structures, especially valves and intracardiac shunts. Intracardiac echocardiography, although invasive, provides an important diagnostic option in patients with poor transthoracic windows and contraindications to TEE. HCU devices used by noncardiologist clinician sonographers, though not an adequate replacement for full-feature echocardiography, may prove useful in extremely rapid detection of cardiac pathology or serial measurements of anatomical and hemodynamic parameters.

References

1. Teske AJ, WL De Boeck BWL, Melman PG (2007) Echocardiographic quantification of myocardial function using tissue deformation imaging, a guide to image acquisition and analysis using tissue Doppler and speckle tracking. Cardiovasc Ultrasound 5:27
2. Boettler P, Claus P, Herbots L et al (2005) New aspects of the ventricular septum and its function: an echocardiographic study. Heart 91:1343–1348
3. Redfield MM, Rodeheffer RJ, Jacobsen SJ et al (2004) Plasma brain natriuretic peptide to detect preclinical ventricular systolic or diastolic dysfunction: a community-based study. Circulation 109:3176–3181
4. Dokainish H, Zoghbi WA, Lakkis NM et al (2005) Incremental predictive power of B-type natriuretic peptide and tissue Doppler echocardiography in the prognosis of patients with congestive heart failure. J Am Coll Cardiol 45:1223–1226
5. Garcia MJ, Rodriguez L, Ares M, Griffin BP, Thomas JD, Klein AL (1996) Differentiation of constrictive pericarditis from restrictive cardiomyopathy: Assessment of left ventricular diastolic velocities in longitudinal axis by Doppler tissue imaging. J Am Coll Cardiol 27:108–114
6. Ha JW, Ommen SR, Tajik AJ, Barnes ME, Ammash NM, Gertz MA, Seward JB, Oh JK (2004) Differentiation of constrictive pericarditis from restrictive cardiomyopathy using mitral annular velocity by tissue Doppler echocardiography. Am J Cardiol 94(3):316–319
7. Rajagopalan N, Garcia MJ, Rodriguez L, Murray RD, Apperson-Hansen C, Stugaard M, Thomas JD, Klein AL (2001) Comparison of new Doppler echocardiographic methods to differentiate constrictive pericardial heart disease and restrictive cardiomyopathy. Am J Cardiol 87: 86–94
8. Choi EY, Ha JW, Kim JM, Ahn JA, Seo HS, Lee JH, Rim SJ, Chung N (2007) Incremental value of combining systolic mitral annular velocity and time difference between mitral inflow and diastolic mitral annular velocity to early diastolic annular velocity for differentiating constrictive pericarditis from restrictive cardiomyopathy. J Am Soc Echocardiogr 20(6):738–743
9. Palka P, Lange A, Donnelly JE, Nihoyannopoulos P (2000) Differentiation between restrictive cardiomyopathy and constrictive pericarditis by early diastolic Doppler myocardial velocity gradient at the posterior wall. Circulation 102(6): 655–662
10. Larrazet F, Pellerin D, Daou D et al (1999) Concordance between dobutamine Doppler tissue imaging echocardiography and rest reinjection thallium-201 tomography in dysfunctional hypoperfused myocardium. Heart 82: 432–437
11. Tanaka H, Oishi Y, Mizuguchi Y et al (2007) Three dimensional evaluation of dobutamine induced changes in regional myocardial deformation in ischemic myocardium using ultrasonic strain measurements: the role of circumferencial myocardial shortening. J Am Soc Echocardior 20(11): 1294–1299
12. Hoffmann R, Altiok E, Nowak B et al (2002) Strain rate measurement by Doppler echocardiography allows improved assessment of myocardial viability in patients with depressed left ventricular function. J Am Coll Cariol 6(39): 443–449
13. Voigt JU, Nixdorff U, Bogdan R et al (2004) Comparison of deformation imaging and velocity imaging for detecting regional inducible ischemia during dobutamine stress echocardiography. Eur Heart J 25(17):1477–1479
14. Hameed AK, Gosal T, Fang T, Ahmadie R, Lytwyn M, Barac I, Zieroth S, Hussain F, Jassal DS (2008) Clinical utility of tissue Doppler imaging in patients with acute myocardial infarction complicated by cardiogenic shock. Cardiovasc Ultrasound 6:11
15. Yu CM, Lin H, Yang H et al (2002) Progression of Systolic Abnormalities in Patients With "Isolated" Diastolic Heart Failure and Diastolic Dysfunction. Circulation 105: 1195–1201
16. Yu CM, Wang Q, Lau CP et al (2001) Reversible impairment of left and right ventricular systolic and diastolic function during short-lasting atrial fibrillation in patients with an implantable atrial defibrillator: a tissue Doppler imaging study. Pacing Clin Electrophysiol 24:979–988

17. Wang J, Prakasa K, Bomma C, Tandri H, Dalal D, James C, Tichnell C, Corretti M, Bluemke D, Calkins H, Abraham TP (2007) Comparison of novel echocardiographic parameters of right ventricular function with ejection fraction by cardiac magnetic resonance. J Am Soc Echocardiogr 20(9):1058–1064
18. Weidemann F, Jamal F, Sutherland GR et al (2002) Myocardial function defined by strain rate and strain during alterations in inotropic states and heart rate. Am J Physiol Heart Circ Physiol 283:H792–H799
19. Koyama KMD, Ray-Sequin PA, Falk RH (2003) Longitudinal Myocardial Function Assessed by Tissue Velocity, Strain, and Strain Rate Tissue Doppler Echocardiography in Patients With AL (Primary) Cardiac Amyloidosis. Circulation 107:2446–2452
20. Kato TS, Noda A, Izawa H et al (2004) Discrimination of Nonobstructive Hypertrophic Cardiomyopathy From Hypertensive Left Ventricular Hypertrophy on the Basis of Strain Rate Imaging by Tissue Doppler Ultrasonography. Circulation 110:3808–3814
21. Di Bella G, Coglitore S, Zimbalatti C, Minutoli F, Zito C, Patane' S, Carerj S (2008) Strain Doppler echocardiography can identify longitudinal myocardial dysfunction derived from edema in acute myocarditis. Int J Cardiol 126(2):279–280, 23 May 2008
22. Takamura T, Dohi K, Onishi K, Kurita T, Tanabe M, Tanigawa T, Isaka N, Ito M (2007) Improvement of left ventricular mechanical dyssynchrony associated with restoration of left ventricular function in a patient with fulminant myocarditis and complete left bundle branch block. Int J Cardiol. Apr 11
23. Dambrauskaite V, Delcroix M, Claus P, Herbots L, D'hooge J, Bijnens B, Rademakers F, Sutherland GR (2007) Regional right ventricular dysfunction in chronic pulmonary hypertension. J Am Soc Echocardiogr 20(10):1172–1180
24. Kjaergaard J, Schaadt BK, Lund JO, Hassager C (2008) Quantification of right ventricular function in acute pulmonary embolism: relation to extent of pulmonary perfusion defects. Eur J Echocardiogr. Feb 19. Epub ahead of print
25. Helle-Valle T, Crosby J, Edvardsen T et al (2005) New Noninvasive Method for Assessment of Left Ventricular Rotation Speckle Tracking Echocardiography. Circulation 112:3149–3156
26. Langeland S, Wouters PF, Claus P et al (2006) Experimental assessment of a new research tool for the estimation of two-dimensional myocardial strain. Ultrasound Med Biol 32(10):1509–1513
27. Wang J, Khoury DS, Thohan V et al (2007) Global Diastolic Strain Rate for the Assessment of Left Ventricular Relaxation and Filling Pressures. Circulation 115:1376–1383
28. Becker M, Lenzen A, Ocklenburg C et al (2008) Myocardial deformation imaging based on ultrasonic pixel tracking to identify reversible myocardial dysfunction. J Am Coll Cardiol 51(15):1473–1481
29. Hanekom L, Cho GY, Leano R, Jeffriess L, Marwick TH (2007) Comparison of two-dimensional speckle and tissue Doppler strain measurement during dobutamine stress echocardiography: an angiographic correlation. Eur Heart J 28(14):1765–1772
30. Pirat B, McCulloch ML, Zoghbi WA (2006) Evaluation of global and regional right ventricular systolic function in patients with pulmonary hypertension using a novel speckle tracking method. Am J Cardiol 98(5):699–704
31. Borges AC, Knebel F, Eddicks S, Panda A, Schattke S, Witt C, Baumann G (2006) Right ventricular function assessed by two-dimensional strain and tissue Doppler echocardiography in patients with pulmonary arterial hypertension and effect of vasodilator therapy. Am J Cardiol 98(4):530–534
32. Jenkins C, Bricknell K, Hanekom L, Marwick TH (2004) Reproducibility and accuracy of echocardiographic measurements of left ventricular parameters using real-time three-dimensional echocardiography. J Am Coll Cardiol 44(4):878–886
33. Sugeng L, Mor-Avi V, Weinert L et al (2006) Quantitative assessment of left ventricular size and function: side-by-side comparison of real-time three-dimensional echocardiography and computed tomography with magnetic resonance reference. Circulation 114(7):654–661
34. Mor-Avi V, Sugeng L, Weinert L, et al Fast Measurement of Left Ventricular Mass With Real-Time Three-Dimensional Echocardiography (2004) Circulation 110:1814–1818
35. Gopal AS, Keller AM, Rigling R, King DL Jr, King DL (1993) Left ventricular volume and endocardial surface area by three-dimensional echocardiography: comparison with two-dimensional echocardiography and nuclear magnetic resonance imaging in normal subjects. J Am Coll Cardiol 22:258–270
36. Shiota T, McCarthy PM, White RD et al (1999) Initial clinical experience of real-time three dimensional echocardiography in patients with ischemic and idiopathic dilated cardiomyopathy. Am J Cardiol 84:1068–1073
37. Van den Bosch AE, Robbers-Visser D, Krenning BJ et al (2006) Real-time transthoracic three-dimensional echocardiographic assessment of left ventricular volume and ejection fraction in congenital heart disease. J Am Soc Echocardiogr 19:1–6
38. Pemberton J, Ge S, Thiele K et al (2006) Real-time threedimensional color Doppler echocardiography overcomes the inaccuracies of spectral Doppler for stroke volume calculation. J Am Soc Echocardiogr 19(11):1403–1410
39. Corsi C, Lang RM, Veronesi F et al (2005) Volumetric quantification of global and regional left ventricular function from real-time three-dimensional echocardiographic images. Circulation 112(8):1161–1170
40. Ahmad M, Xie T, McCulloch M, Abreo G, Runge M (2001) Real-time three-dimensional dobutamine stress echocardiography in assessment of ischemia: comparison with two-dimensional dobutamine stress echocardiography. J Am Coll Cardiol 37:1303–1309
41. Takeuchi M, Otani S, Weinert L, Spencer KT, Lang RM (2006) Comparison of contrast-enhanced real-time live 3-dimensional dobutamine stress echocardiography with contrast 2-dimensional echocardiography for detecting stress-induced wall-motion abnormalities. J Am Soc Echocardiogr 19:294–299
42. Song, X, Myronenko, A, Sahn, DJ (2007) Speckle Tracking in 3D Echocardiography with Motion Coherence, CVPR07(1-7)
43. Niemann PS, Pinho L, Balbach T, Galuschky C, Blankenhagen M, Silberbach M, Broberg C, Jerosch-Herold M, Sahn DJ (2007) Anatomically oriented right ventricular volume measurements with dynamic three-dimensional echocardiography validated by 3-Tesla magnetic resonance imaging. J Am Coll Cardiol 50(17):1668–1676
44. Prakasa KR, Dalal D, Wang J, Bomma C, Tandri H, Dong J, James C, Tichnell C, Russell SD, Spevak P, Corretti M, Bluemke DA, Calkins H, Abraham TP (2006) Feasibility and ariability of three dimensional echocardiography in

arrhythmogenic right ventricular dysplasia/cardiomyopathy. Am J Cardiol 97(5):703–709
45. Jenkins C, Chan J, Bricknell K, Strudwick M, Marwick TH (2007) Reproducibility of right ventricular volumes and ejection fraction using real-time three-dimensional echocardiography: comparison with cardiac MRI. Chest 131(6): 1844–1851
46. Sitges M, Jones M, Shiota T et al (2003) Real-time three-dimensional color Doppler evaluation of the flow convergence zone for quantification of mitral regurgitation: validation experimental animal study and initial clinical experience. J Am Soc Echocardiogr 16:38–45
47. Sugeng L, Spencer KT, Mor-Avi V et al (2003) Dynamic three-dimensional color flow Doppler: an improved technique for the assessment of mitral regurgitation. Echocardiography 20:265–273
48. Agricola E, Oppizzi M, Pisani M, Maisano F, Margonato A (2008) Accuracy of real-time 3D echocardiography in the evaluation of functional anatomy of mitral regurgitation. Int J Cardiol 127(3):342–349, Epub 2007 Jul 23
49. Shiota T, Jones M, Tsujino H et al (2002) Quantitative analysis of aortic regurgitation: real-time 3-dimensional and 2-dimensional color Doppler echocardiographic method – a clinical and a chronic animal study. J Am Soc Echocardiogr 15:966–971
50. Macnab A, Jenkins NP, Bridgewater BJ et al (2004) Three-dimensional echocardiography is superior to multiplane transoesophageal echo in the assessment of regurgitant mitral valve morphology. Eur J Echocardiogr 5:212–222
51. Pepi M, Tamborini G, Maltagliati A, Galli CA, Sisillo E, Salvi L, Naliato M, Porqueddu M, Parolari A, Zanobini M, Alamanni F (2006) Head-to-head comparison of two- and three-dimensional transthoracic and transesophageal echocardiography in the localization of mitral valve prolapse. J Am Coll Cardiol 48(12):2524–2530, Dec 19
52. Mercer-Rosa L, Seliem MA, Fedec A, Rome J, Rychik J, Gaynor JW (2006) Illustration of the additional value of real-time 3-dimensional echocardiography to conventional ransthoracic and transesophageal 2-dimensional echocardiography in imaging muscular ventricular septal defects: does this have any impact on individual patient treatment? J Am Soc Echocardiogr 19(12):1511–1519
53. Bruce CJ, Friedman PA (2001) Intracardiac echocardiography. Eur J Echocardiogr 2:234–244
54. Maloney JD, Burnett JM, Dala-Krishna P et al (2005) New directions in intracardiac echocardiography. J Interv Card Electrophysiol 13(Suppl 1):23–29
55. Rao HB, Saksena S, Mitruka R et al (2005) Intracardiac echocardiography guided cardioversion to help interventional procedures (ICE-CHIP) study: study design and methods. J Interv Card Electrophysiol 13(Suppl 1):31–36
56. Kirkpatrick JN, Furlong K, Mugica VL et al (2005) Effectiveness of echocardiographic imaging by nurses to identify left ventricular systolic dysfunction in high-risk patients. Am J Cardiol 95:1271–1272
57. Gorcsan J III, Pandey P, Sade LE (2004) Influence of hand-carried ultrasound on bedside patient treatment decisions for consultative cardiology. J Am Soc Echocardiogr 17: 50–55
58. DeCara JM, Lang RM, Spencer KT (2003) The hand-carried echocardiographic device as an aid to the physical examination. Echocardiography 20:477–485
59. Schiller NB (2001) Hand-held echocardiography: revolution or hassle? J Am Coll Cardiol 37:2023–2024
60. Goodkin GM, Spevack DM, Tunick PA et al (2001) How useful is hand-carried bedside echocardiography in critically ill patients? J Am Coll Cardiol 37:2019–2022
61. Vignon P, Frank MBJ, Lesage J et al (2004) Handheld echocardiography with doppler capability for the assessment of critically ill patients: is it reliable? Intensive Care Med 30:718–723
62. Fedson S, Neithardt G, Thomas P et al (2003) Unsuspected clinically important findings detected with a small portable ultrasound device in patients admitted to a general medicine service. J Am Soc Echocardiogr 16:901–905
63. Breitkreutz R, Walcher F, Seeger FH (May 2007) Focused echocardiographic evaluation in resuscitation management: concept of an advanced life support-conformed algorithm. Crit Care Med 35(5 Suppl):S150–S161
64. Borges AC, Knebel F, Walde T, Sanad W, Baumann G (Mar 2004) Diagnostic accuracy of new handheld echocardiography with Doppler and harmonic imaging properties. J Am Soc Echocardiogr 17(3):234–238

Index

D. De Backer et al. (eds.), *Hemodynamic Monitoring Using Echocardiography in the Critically Ill*,
DOI: 10.1007/978-3-540-87956-5, © Springer-Verlag Berlin Heidelberg 2011